ADVANCES IN NEUROMYELITIS OPTICA SPECTRUM DISORDERS (NMOSD)

EDITED BY: Yu Cai, Yangtai Guan, Wei Qiu, Fu-Dong Shi and Jodie Burton
PUBLISHED IN: Frontiers in Neurology and Frontiers in Immunology

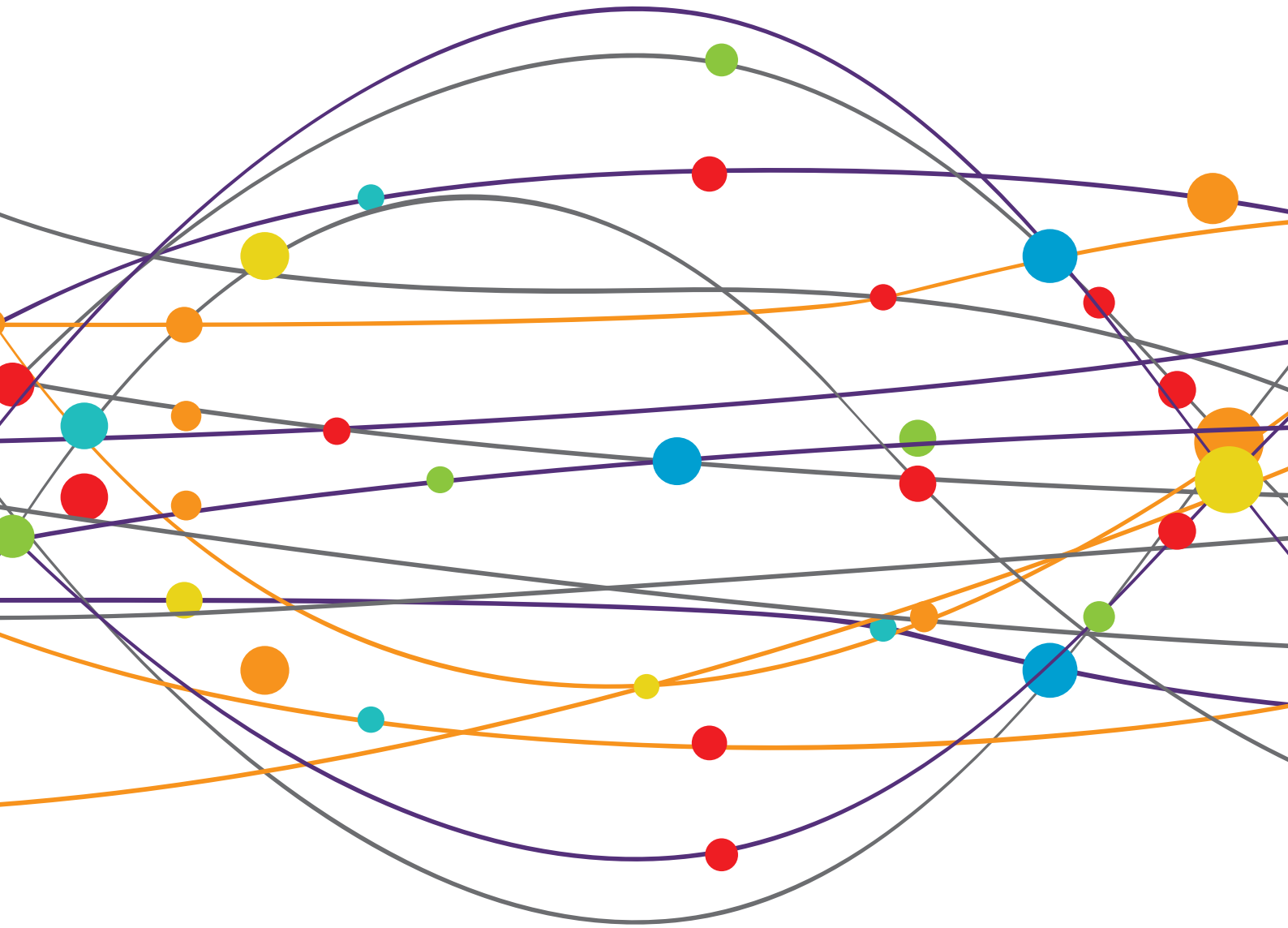

frontiers Research Topics

ISSN 1664-8714
ISBN 978-2-83250-175-7
DOI 10.3389/978-2-83250-175-7

About Frontiers

Frontiers is more than just an open-access publisher of scholarly articles: it is a pioneering approach to the world of academia, radically improving the way scholarly research is managed. The grand vision of Frontiers is a world where all people have an equal opportunity to seek, share and generate knowledge. Frontiers provides immediate and permanent online open access to all its publications, but this alone is not enough to realize our grand goals.

Frontiers Journal Series

The Frontiers Journal Series is a multi-tier and interdisciplinary set of open-access, online journals, promising a paradigm shift from the current review, selection and dissemination processes in academic publishing. All Frontiers journals are driven by researchers for researchers; therefore, they constitute a service to the scholarly community. At the same time, the Frontiers Journal Series operates on a revolutionary invention, the tiered publishing system, initially addressing specific communities of scholars, and gradually climbing up to broader public understanding, thus serving the interests of the lay society, too.

Dedication to Quality

Each Frontiers article is a landmark of the highest quality, thanks to genuinely collaborative interactions between authors and review editors, who include some of the world's best academicians. Research must be certified by peers before entering a stream of knowledge that may eventually reach the public - and shape society; therefore, Frontiers only applies the most rigorous and unbiased reviews.
Frontiers revolutionizes research publishing by freely delivering the most outstanding research, evaluated with no bias from both the academic and social point of view. By applying the most advanced information technologies, Frontiers is catapulting scholarly publishing into a new generation.

What are Frontiers Research Topics?

Frontiers Research Topics are very popular trademarks of the Frontiers Journals Series: they are collections of at least ten articles, all centered on a particular subject. With their unique mix of varied contributions from Original Research to Review Articles, Frontiers Research Topics unify the most influential researchers, the latest key findings and historical advances in a hot research area! Find out more on how to host your own Frontiers Research Topic or contribute to one as an author by contacting the Frontiers Editorial Office: frontiersin.org/about/contact

ADVANCES IN NEUROMYELITIS OPTICA SPECTRUM DISORDERS (NMOSD)

Topic Editors:
Yu Cai, University of Nebraska Medical Center, United States
Yangtai Guan, Shanghai Jiao Tong University, China
Wei Qiu, Third Affiliated Hospital of Sun Yat-sen University, China
Fu-Dong Shi, Tianjin Medical University General Hospital, China
Jodie Burton, University of Calgary, Canada

Citation: Cai, Y., Guan, Y., Qiu, W., Shi, F.-D., Burton, J., eds. (2022). Advances in Neuromyelitis Optica Spectrum Disorders (NMOSD). Lausanne: Frontiers Media SA. doi: 10.3389/978-2-83250-175-7

Table of Contents

frontiers | Frontiers in Neurology

TYPE Editorial
PUBLISHED 26 August 2022
DOI 10.3389/fneur.2022.1005164

OPEN ACCESS

EDITED AND REVIEWED BY
Hans-Peter Hartung,
Heinrich Heine University of Düsseldorf, Germany

*CORRESPONDENCE
Yu Cai
yu.cai.us@gmail.com
Jodie M. Burton
Jodie.Burton@albertahealthservices.ca
Fu-Dong Shi
fshi@tmu.edu.cn
Wei Qiu
qiuwei120@vip.163.com
Yangtai Guan
yangtaiguan@sina.com

SPECIALTY SECTION
This article was submitted to Multiple Sclerosis and Neuroimmunology, a section of the journal Frontiers in Neurology

RECEIVED 28 July 2022
ACCEPTED 10 August 2022
PUBLISHED 26 August 2022

CITATION
Cai Y, Burton JM, Shi F-D, Qiu W and Guan Y (2022) Editorial: Advances in neuromyelitis optica spectrum disorders. *Front. Neurol.* 13:1005164. doi: 10.3389/fneur.2022.1005164

Editorial: Advances in neuromyelitis optica spectrum disorders

Yu Cai[1]*, Jodie M. Burton[2,3]*, Fu-Dong Shi[4,5,6]*, Wei Qiu[7]* and Yangtai Guan[8]*

[1]Department of Pharmacology and Experimental Neuroscience, University of Nebraska Medical Center, Omaha, NE, United States, [2]Department of Clinical Neurosciences, Cumming School of Medicine, University of Calgary, Calgary, AB, Canada, [3]Department of Clinical Neurosciences and Community Health Sciences, University of Calgary, Calgary, AB, Canada, [4]Center for Neuroinflammation, Beijing Tiantan Hospital, Capital Medical University, Beijing, China, [5]China National Clinical Research Center for Neurological Diseases, Beijing, China, [6]Department of Neurology, Tianjin Neurological Institute, Tianjin Medical University General Hospital, Tianjin, China, [7]Department of Neurology, Center for Mental and Neurological Disorders and Diseases, The Third Affiliated Hospital of Sun Yat-sen University, Guangzhou, China, [8]Department of Neurology, Shanghai Jiao Tong University School of Medicine Affiliated Renji Hospital, Shanghai, China

KEYWORDS

NMOSD, MOGAD, molecular mechanism, biomarkers, therapy

Editorial on the Research Topic
Advances in neuromyelitis optica spectrum disorders

This topic issues, Advances in Neuromyelitis Optica Spectrum Disorder, jointly published by Frontiers in Neurology and Frontiers in Immunology represents the contribution and efforts of many individuals over the better part of a year. The co-editors of this issue would like to thank the journal staff and all of those who submitted their manuscripts for consideration. We were encouraged to see 40 submissions during the call for papers, with almost half (19) accepted for publication.

This issue was created to highlight important, new work in the field, both in neuromyelitis optica spectrum disorder (NMOSD) and MOG-associated disease (MOGAD), providing new insights into disease mechanisms, diagnosis, and treatment.

Advances in NMOSD

Formerly known as Devic's disease or neuromyelitis optica (NMO), Neuromyelitis optica spectrum disorders (NMOSD) is an autoimmune demyelinating disease, characterized by demyelination primarily of the optic nerves and spinal cord. The central nervous system (CNS) is more commonly affected in Asian and black patients than in white patients, in whom the age of onset is typically around 40 years (1). Yu et al. reported a higher likelihood of severe disabilities in NMOSD patients with onset after age 40 in central China.

Despite the discovery of autoantibody NMO IgG directed against aquaporin-4 (AQP4), the mechanisms and dynamics of inflammatory degeneration of the CNS in NMOSD, remain elusive. Using a mouse model of spontaneous opticospinal encephalomyelitis (OSE), Petrikowski et al. depicted characteristics of inflammatory and degenerative alterations in both morphology and function of retina and optic nerve with involvement of the complement system. T follicular helper (Tfh) cells derived from germinal center (GC) plays a critical role in promoting pathogenic autoantibody production (2). Cheng et al. demonstrated a correlation of NMOSD recurrence with Tfh cells and CXCL13, in which gut microbiome and bile acid metabolism plays a critical role. These findings lead to the establishment of a gut microbiome–metabolite–Tfh-CXCL13 system to predict the recurrence of NMOSD.

The diagnosis of NMOSD is based on the presence of core clinical manifestation, biomarkers and MRI neuroimaging features (3). AQP4 antibody is a major diagnostic biomarker distinguishing NMOSD from other neuroimmune disorders, but identification of new potential biomarkers also better assist the diagnosis of NMOSD especially in patients with negative AQP4 antibody status (4). Zhang et al. reported a case of NMOSD with similar clinical manifestation of infectious meningomyelitis, highlighting the significant diagnostic and therapeutic importance of biomarker. Based on the expression and clinical correlation analysis, Tang et al. showed the potential of serum repulsive guidance molecules a (RGMa) as a prognostic biomarker of NMOSD. Intriguingly, Shang et al. reported a case of NMOSD with the presence of anti-flotillin, a novel antibody. Kim et al. also review clinical data suggesting glial fibrillary acidic protein (GFAP) as a prospective serum biomarker candidate for NMOSD. Dinoto et al. further summarize current evidence of both CSF and serum biomarkers from the perspectives of antibody titers, cytokine profiles, complement factors and markers of neuronal and astroglial damage. In addition to biomarkers, MRI neuroimaging also plays an indispensable role in diagnosing NMOSD, but it remains a challenge to interpret neuroimaging results for differentiating between neuroimmune disorders in a non-bias manner. Based on the MRI imaging of brain and spinal cord, Huang et al. successfully developed a novel transformer-based deep-learning model for discriminating CNS demyelinating diseases including multiple sclerosis (MS), AQP4-seropositive NMOSD and MOGAD.

Currently, glucocorticoid therapy and adjunctive plasma exchange are the mainstay of the treatment in acute attacks of NMOSD while long-term immunotherapy is recommended to reduce the risk of relapse (5). Deng et al. demonstrated that pregnancy is associated with increased rates of relapse of NMOSD, which can be reduced by prompt immunosuppressive (IS) therapy. Saab et al. reported two cases improved chronic cognitive impairment in AQP4-seropositive NMOSD treated with eculizumab. However, there is still an urgent need for refinement and development of precise therapeutic methods to reduce the rates of long-term disability and mortality while minimizing the adverse effects. Accumulating evidence showed that human umbilical cord mesenchymal stem cells (hUC-MSC) possess differentiation capability, regulate immune response, promote local tissue repair and regeneration, suggesting a therapeutic potential of hUC-MSC in autoimmune disorders (6). Yao et al. thus proposed a study protocol for a prospective multicenter, randomized, placebo-controlled clinical trial for hUC-MSC to treat NMOSD (hUC-MSC-NMOSD).

Advances in MOGAD

MOGAD, a more recently discovered mimic of NMOSD, albeit one with distinct immunopathological, clinical and treatment features, was a common area of research. Sechi et al. provided a detailed update of clinical and MRI features, as well as diagnostic and treatment guidelines in an international and collaborative effort.

Liu et al. submitted a fascinating look at the immune signatures in a small cohort of RRMS and MOG patients using single cell transcriptome profiling, finding that while CD19+ CXCR4+ naive B cell subsets were expanded in both these MS and MOGAD patients, but in RRMS patients, single-cell transcriptomic was characterized by increased naive CD8+ T cells and cytotoxic memory-like NK cells coupled with a decrease in inflammatory monocytes, while MOGAD exhibited increased inflammatory monocytes and cytotoxic CD8 effector T cells, coupled with decreased plasma cells and memory B cells. Such methods could potentially become a diagnostic tool. Lin et al. presented their work providing evidence that the easily measured plasma C3 and C4 were significantly lower in NMOSD vs. MOGAD and controls, raising the possibility it could be a viable, and easily obtained, biomarker for diagnosis. As is now being understood, SARS-CoV-2 infection can lead to possibly immune mediated complications, including cases of MOGAD and NMOSD. Matsumoto et al. provided a fascinating and complex case of such a patient to educate us in recognizing and considering this possibility. Furthermore, Di Pauli et al. review the co-occurrence of MOG and AQP-4 antibodies with another common virus, VZV, finding both are, rare, MOG rarer still.

Neuroimaging also serves as one of the most critical diagnostic methods for MOGAD. Wang et al. showed 4 cases of MOGAD with abnormal signals in cortical or brainstem observed in cranial MRI. Rechtman et al. demonstrated an association between a relapsing disease course and reduced volume in gray matter in cerebrum and hippocampus within the 1st year of diagnosis.

In conclusion, this Research Topic attempts to show the most up-to-date advances in the field of NMOSD and MOGAD, covering a broad range of topics from mechanistic studies, case reports, diagnostic innovations and therapeutic strategies. We hope that these findings could provide insights for both physicians and researchers interested in the CNS demyelinating disorders.

Author contributions

All authors listed have made a substantial, direct, and intellectual contribution to the work and approved it for publication.

Conflict of interest

The authors declare that the research was conducted in the absence of any commercial or financial relationships that could be construed as a potential conflict of interest.

Publisher's note

All claims expressed in this article are solely those of the authors and do not necessarily represent those of their affiliated organizations, or those of the publisher, the editors and the reviewers. Any product that may be evaluated in this article, or claim that may be made by its manufacturer, is not guaranteed or endorsed by the publisher.

References

1. Mealy MA, Wingerchuk DM, Greenberg BM, Levy M. Epidemiology of neuromyelitis optica in the United States: A multicenter analysis. *Arch Neurol.* (2012) 69:1176–80. doi: 10.1001/archneurol.2012.314

2. Simpson N, Gatenby PA, Wilson A, Malik S, Fulcher DA, Tangye SG, et al. Expansion of circulating T cells resembling follicular helper T cells is a fixed phenotype that identifies a subset of severe systemic lupus erythematosus. *Arthritis Rheum.* (2010) 62:234–44. doi: 10.1002/art.25032

3. Wingerchuk DM, Banwell B, Bennett JL, Cabre P, Carroll W, Chitnis T, et al. International consensus diagnostic criteria for neuromyelitis optica spectrum disorders. *Neurology.* (2015) 85:177–89. doi: 10.1212/WNL.0000000000001729

4. Jiao Y, Fryer JP, Lennon VA, Jenkins SM, Quek AM, Smith CY, et al. Updated estimate of Aqp4-Igg serostatus and disability outcome in neuromyelitis optica. *Neurology.* (2013) 81:1197–204. doi: 10.1212/WNL.0b013e3182a6cb5c

5. Sherman E, Han MH. Acute and chronic management of neuromyelitis optica spectrum disorder. *Curr Treat Options Neurol.* (2015) 17:48. doi: 10.1007/s11940-015-0378-x

6. Abbaspanah B, Reyhani S, Mousavi SH. Applications of umbilical cord derived mesenchymal stem cells in autoimmune and immunological disorders: from literature to clinical practice. *Curr Stem Cell Res Ther.* (2021) 16:454–64. doi: 10.2174/1574888X16999201124153000

frontiers in Immunology

ORIGINAL RESEARCH
published: 19 October 2021
doi: 10.3389/fimmu.2021.769653

Myelin Oligodendrocyte Glycoprotein Antibody-Associated Disease and Varicella Zoster Virus Infection - Frequency of an Association

Franziska Di Pauli[1], Paul Morschewsky[1], Klaus Berek[1], Michael Auer[1], Angelika Bauer[1], Thomas Berger[2], Gabriel Bsteh[2], Paul Rhomberg[3], Kathrin Schanda[1], Anne Zinganell[1], Florian Deisenhammer[1], Markus Reindl[1†] and Harald Hegen[1*†]*

[1] Department of Neurology, Medical University of Innsbruck, Innsbruck, Austria, [2] Department of Neurology, Medical University of Vienna, Vienna, Austria, [3] Department of Neuroradiology, Medical University of Innsbruck, Innsbruck, Austria

To determine whether there is a correlation between myelin oligodendrocyte glycoprotein (MOG) antibody-associated diseases and varicella zoster virus (VZV) infection. We provide a case report and performed a study to determine the frequency of MOG antibodies (MOG-IgG) in neurological VZV infections. Patients admitted to the Medical University of Innsbruck from 2008–2020 with a diagnosis of a neurological manifestation of VZV infection (n=59) were included in this study; patients with neuroborreliosis (n=34) served as control group. MOG-IgG was detected using live cell-based assays. In addition, we performed a literature review focusing on MOG and aquaporin-4 (AQP4) antibodies and their association with VZV infection. Our case presented with VZV-associated longitudinally extensive transverse myelitis and had MOG-IgG at a titer of 1:1280. In the study, we did not detect MOG-IgG in any other patient neither in the VZV group (including 15 with VZV encephalitis/myelitis) nor in the neuroborreliosis group. In the review of the literature, 3 cases with MOG-IgG and additional 9 cases with AQP4 IgG associated disorders in association with a VZV infection were identified. MOG-IgG are rarely detected in patients with VZV infections associated with neurological diseases.

Keywords: AQP-4-IgG, MOG-IgG, MOG antibody associated diseases, longitudinally extensive transverse myelitis, varicella zoster virus infection, neuromyelitis optica spectrum disorder

OPEN ACCESS

Edited by:
Jodie Burton,
University of Calgary, Canada

Reviewed by:
Eslam Shosha,
McMaster University, Canada
Yoshiki Takai,
Tohoku University Hospital, Japan

****Correspondence:***
Markus Reindl
markus.reindl@i-med.ac.at
Harald Hegen
harald.hegen@i-med.ac.at

†These authors have contributed equally to this work

Specialty section:
This article was submitted to Multiple Sclerosis and Neuroimmunology, a section of the journal Frontiers in Immunology

Received: *02 September 2021*
Accepted: *05 October 2021*
Published: *19 October 2021*

Citation:
Di Pauli F, Morschewsky P, Berek K, Auer M, Bauer A, Berger T, Bsteh G, Rhomberg P, Schanda K, Zinganell A, Deisenhammer F, Reindl M and Hegen H (2021) Myelin Oligodendrocyte Glycoprotein Antibody-Associated Disease and Varicella Zoster Virus Infection - Frequency of an Association. Front. Immunol. 12:769653. doi: 10.3389/fimmu.2021.769653

1 INTRODUCTION

Varicella zoster virus (VZV) is an exclusively human neurotropic herpes virus, presents with chickenpox (varicella) as inaugural infection, and remains latent in the dorsal root ganglions, cranial nerves, and the autonomic nervous system, and upon reactivation, results in rash and pain in one or more dermatomes, known as shingles (herpes zoster). This would occur often decades after the primary infection, particularly in susceptible immunocompromised patients, and older patients due to immunosenescence (1).

Typical VZV neurological complications include postherpetic neuralgia, VZV vasculopathy, cranial nerve neuropathy, and radiculopathy (2). Central nervous system (CNS) demyelinating-inflammatory diseases, such as myelitis and encephalitis, are rare complications in primary VZV infection and VZV reactivation (3, 4). It has been suggested that VZV myelitis is caused by direct viral invasion of the spinal cord and cell lysis (5). However, there is mounting evidence for an immune-mediated mechanism, as there are several case reports of aquaporin-4 antibody (AQP4-IgG) positive neuromyelitis optica spectrum disorder (NMOSD) following VZV infection (6–13). Recently, in addition to AQP4-IgG associated NMOSD, the identification of myelin oligodendrocyte glycoprotein (MOG) antibodies has broadened the spectrum of antibody-associated CNS demyelinating-inflammatory diseases that are distinct from classical multiple sclerosis (14). Similar to the identification of AQP4-IgG following VZV infection, some case reports described MOG-IgG antibody-associated disease (MOGAD) following VZV, influenza A, or herpes simplex virus infection (15–18).

However, until now, there has been no systematic analysis about the association of MOG-IgG and neurological manifestations of VZV infection. Here, we describe a patient with MOG-IgG positive VZV-associated longitudinally extensive transverse myelitis (LETM), perform a study to determine the MOG-IgG frequencies in patients with VZV infection and neurological involvement and present the results of a literature review.

2. MATERIALS AND METHODS

2.1 Patients and Samples

The retrospective study included 59 patients who were admitted to the Medical University of Innsbruck between 2008 and 2020 with the diagnosis of a neurological manifestation due to VZV infection and had an available serum sample of at least 500 µl. Diagnosis of VZV infection with neurological involvement (i.e., meningitis, encephalitis, myelitis, encephalomyelitis, cranial nerve or/and segmental zoster paresis) was based on the presence of typical dermatomal rash followed by neurological symptoms and supported by laboratory findings (elevated CSF cell count, positive VZV DNA in the cerebrospinal fluid (CSF) as determined by polymerase chain reaction (PCR), or increased CSF VZV-IgG) (19, 20). CNS involvement was defined as encephalitis or myelitis or a combination of both. In the absence of a typical rash, diagnosis was always based on a positive CSF VZV DNA and CSF pleocytosis.

Patients with neuroborreliosis [previously published (21)] were included as control group (n=34), as this is also a disease entity of infectious origin that might affect the CNS as well as the PNS, and also typically shows elevated CSF cell count and disrupted blood-CSF-barrier as indicated by elevated Qalb. In addition, there is no known association of neuroborreliosis with AQP4 or MOG antibodies. Briefly, these patients were admitted to Medical University of Innsbruck between 2009 and 2016 and received diagnosis of neuroborreliosis according to EFNS criteria (22). Diagnosis was based on typical neurological symptoms, appropriate routine CSF findings (pleocytosis, blood-CSF barrier impairment, and/or intrathecal synthesis of immunoglobulins), and intrathecal synthesis of borrelia-specific IgG antibodies [antibody specificity index (ASI) >1.5] (22).

Results of routine diagnostic procedures, clinical, magnetic resonance imaging (MRI), and CSF data were collected. Routine CSF work-up comprised red blood cell (RBC) and white blood cell (WBC) count, CSF total protein concentration, CSF/serum albumin quotient, and CSF and serum IgG, IgM, and IgA concentrations. Intrathecal synthesis of IgG, IgM and IgA were calculated by the Auer and Hegen formula (23) and expressed as percentage intrathecal fraction. IgG index was calculated as [CSF IgG/serum IgG]/[CSF albumin/serum albumin]. CSF was collected by lumbar puncture and blood by simultaneously peripheral venous puncture. Serum was isolated from blood by centrifugation after the blood samples were allowed to clot for ≥30 min. All samples were centrifuged at 2000 g for 10 min at room temperature.

2.2 MOG-IgG Assay

The presence of MOG-IgG was determined by live cell-based immunofluorescence assay with HEK293 cells transfected with full-length human MOG (alpha-1 isoform), as previously described (24). Screening for serum antibodies was performed at 1:20 and 1:40 dilutions by two independent investigators blinded for the clinical diagnosis. An isolated IgM reactivity was excluded by the use of heavy chain-specific secondary antibodies against IgG (Dianova, Hamburg, Germany) (24).

2.3 Ethics

The study was approved by the Ethics Committee of the Medical University of Innsbruck (approval number AM3041A). Written informed consent was obtained from all patients. Authorization has been obtained for disclosure (consent to disclose) from the index case patient.

2.4 Statistics

Statistical analysis was performed using SPSS 26.0 (SPSS Inc, Chicago, IL, USA). Non-parametric data were displayed as median and interquartile range. Categorical variables were reported as frequency and percentage. For group comparisons, Mann-Whitney-U and χ^2 tests were applied, as appropriate. Two-sided P-values <0.05 were considered statistically significant.

2.5 Literature Review

We conducted a literature search in MEDLINE and Google Scholar. Search terms were: VZV AND MOG or AQP4 or NMOSD or LETM; herpes zoster AND MOG or AQP4 or NMOSD or LETM. Abstracts that primarily did not deal with VZV infection and MOGAD or NMOSD or LETM were excluded. In addition, articles identified in reference lists of the individual papers were selected if considered appropriate.

3 RESULTS

3.1 Index Case

A 30-year-old, previously healthy man presented in 2019 with sensomotor paralytic syndrome (sensory level below T6),

subsequent gait ataxia and neurogenic bladder disturbance requiring catheterization at our emergency department. Six days before the first neurological symptoms, the patient had developed herpes zoster infection (dermatome T6 right side) treated by his general practitioner with oral acyclovir (5 days, 3 x 1000 mg per day orally). There was no history of constitutional symptoms or a recent vaccination. A MRI of the spinal cord showed a T2 hyperintense lesion extending from T1 to conus medullaris confined to gray matter (**Figure 1**) with only a very faint contrast enhancement, whereas brain MRI was normal. CSF analysis revealed lymphocytic pleocytosis with a WBC count of 101 cells/µl, and oligoclonal bands were negative. Despite the VZV DNA PCR results being negative, the CSF VZV antibody-specific index (ASI) was highly elevated (9.4). However, in addition, MOG-IgG in serum were positive at high titer (1:1280), while AQP4-IgG were absent. Further diagnostic work-up to determine immune deficiency or a malignancy was negative (including a whole body 18F-fluorodeoxyglucose positron emission tomography-computed tomography, human immunodeficiency virus screening, serum immunoglobulin levels, flow cytometry of peripheral blood). MOG-IgG associated LETM following VZV infection was diagnosed, and the patient was treated with a combination of high-dose methylprednisolone (10 days: 1,000 mg for 3 days, 500mg for 4 days, 250 mg for 3 days) followed by oral tappering and intravenous acyclovir (3 x 750 mg for 10 days, 3 x 500 mg for 8 days followed by oral acyclovir 3 x 1000 mg for 5 days). Thereafter, no further disease-modifying or immunosuppressive therapy was started. After three months, the MOG-IgG titer had decreased to 1:320, and MOG-IgG was undetectable after another five months. Except for mild neurogenic bladder dysfunction, there was complete clinical and imaging remission without further relapses after an 18-month follow-up. EDSS improved from an initial score of 3.5 to 1.0 at 18-month follow-up.

3.2 Retrospective Study

3.2.1 Demographic, Clinical, and Main Cerebrospinal Fluid Characteristics

A total of 59 patients with neurological involvement due to VZV infection and 34 patients with neuroborreliosis were included into this study (**Figure 2**). Demographic and main clinical

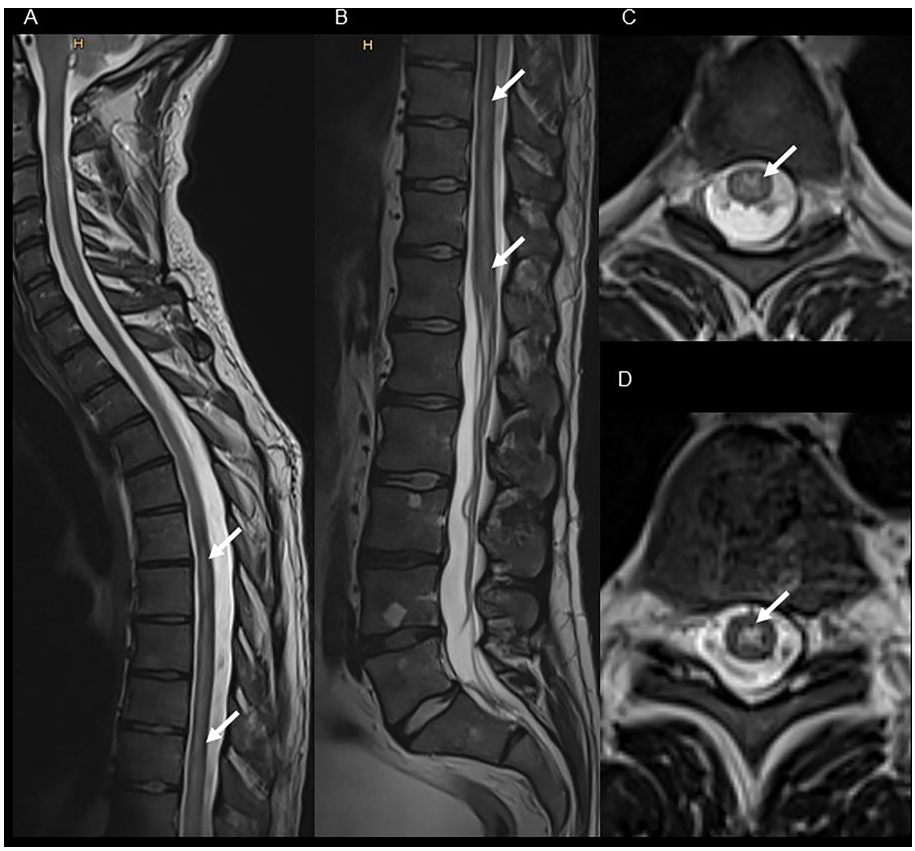

FIGURE 1 | Spinal MRI of the index patient presenting with MOG-IgG associated LETM following VZV infection. T2 weighted cervical, thoracic [panel **(A)**, sagittal view] and lumbar [panel **(B)**, sagittal view] spinal cord MRI shows extensive hyperintense lesion from the level T1 to the conus medullaris [panel **(C)**, axial view of T4; and panel **(D)**, axial view of T9] with only a very faint contrast enhancement (not shown).

characteristics of patients with VZV infection and CNS involvement are shown in **Table 1**, those of patients with neuroborreliosis elsewhere (21). Fifteen patients with a VZV infection (25.4%) presented with either myelitis (n=6; one patient with a LETM), encephalomyelitis (n=1), or encephalitis (n=8). Parenchymal CNS involvement occurred in three (8.8%) of the patients with neuroborreliosis. Patients with neuroborreliosis (median age 46 years, interquartile range [IQR] 10.4–65.6) were younger than patients with VZV infection (median age 63 years, IQR 45.5–76, p<0.001), while males and females were equally distributed in both disease groups (p=0.610). The average interval between typical VZV-associated rashes and neurological symptoms was 7 days (range 2-12). In **Table 2**, the main CSF findings of VZV infection with CNS involvement and neuroborreliosis are shown. In both diseases, the WBC count was increased, although the WBC count was significantly higher in patients with neuroborreliosis. Intrathecal IgG and IgM fraction (%) was significantly elevated in patients with neuroborreliosis compared to patients with VZV infection.

TABLE 1 | Demographic and clinical data of patients with varicella zoster virus infection with central nervous system involvement.

Sex (female), n (%)	**28 (47.5%)**
Age (years), median (IQR)	63 (45.5–76)
Clinical presentation, n (%)	
(Poly)radiculitis or cranial neuritis	32 (54.2%)
Isolated meningitis	12 (20.3%)
Myelitis, encephalomyelitis, or encephalitis	12 (20.3%)
Combination radiculitis or cranial neuritis with myelitis/encephalitis or encephalomyelitis	3 (5.1%)
Days between rash and neurological symptoms, median (IQR)	7 (2–12)
Typical VZV associated rash, n (%)	53 (89.8%)
Diagnosis based on, n (%)	
Positive VZV DNA PCR	44 (74.6%)
Typical clinical features and elevated CSF cell count	3 (5.1%)
Increased CSF VZV IgG	12 (20.3%)

VZV, varicella zoster virus; IQR, interquartile range; n, number.

3.2.2 MOG-IgG in VZV Infection With CNS Involvement

All patients – those with VZV infection with CNS involvement and those with neuroborreliosis – were negative for serum MOG-IgG. One patient with VZV infection and radiculitis had a borderline MOG-IgG positive titer of 1:160. This result was not confirmed by using heavy chain–specific secondary antibodies and was therefore regarded as negative.

3.3 Literature Review

We identified 2 case reports (15, 25) and 1/10 patients in a case series (20) with MOG antibody-associated myelitis in association with a VZV infection; in addition, there are 9 reports of AQP4 antibody-associated CNS disorders in patients with VZV infections (6–13, 20) (**Table 3**).

4 DISCUSSION

Here, we present a case with MOG-IgG associated LETM triggered by VZV infection. In a subsequent retrospective study of 59 patients with VZV infection and neurological involvement; however, we did not found MOG-IgG in any patient (including 15 with VZV encephalitis/myelitis).

MOG-IgG are more often present in children than in adults and are associated with a variable clinical spectrum. Typical clinical presentation of MOGAD, particularly in children, is an acute disseminated encephalomyelitis (approximately 50%), whereas in adults myelitis (up to 30%) or optic neuritis (up to 50%) are more common (14, 26–28). Similar to our case, MOG-IgG associated myelitis is characterized in the MRI by longitudinally extensive T2 hyperintense lesions affecting mainly the grey matter and lack of contrast enhancement (29). MOG-IgG case reports showing an association between MOGAD and VZV infection are rare. Two case reports

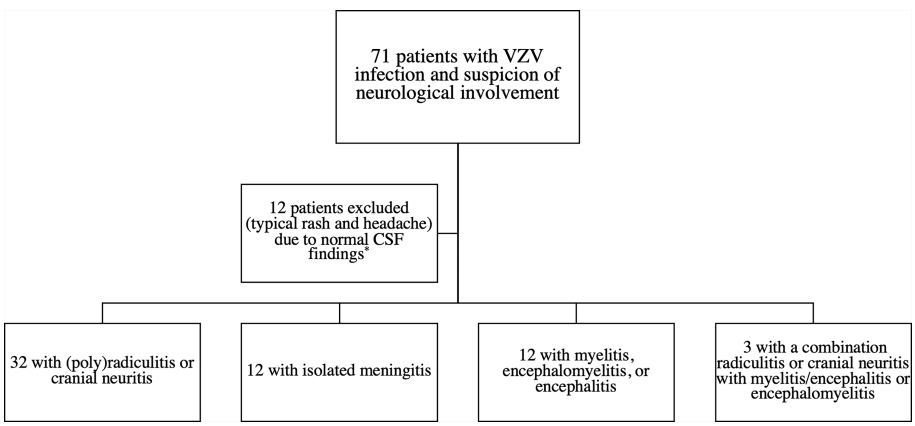

FIGURE 2 | Inclusion flowchart VZV infection with neurological involvement. * Negative CSF VZV specific antibody index, VZV DNA PCR and normal CSF cell count. CSF, cerebrospinal fluid; VZV, varicella zoster virus.

TABLE 2 | Cerebrospinal fluid characteristics of patients with varicella zoster virus infection and neuroborreliosis.

	VZV infection	Neuroborreliosis	p-value[a]
RBC count (cells/μL), median (IQR)	2 (0–21)	4 (0–7)	0.719
WBC count (cells/μL), median (IQR)	99 (18–274)	154 (105–216)	0.037
CSF/serum glucose ratio, median (IQR)	0.55 (0.48–0.67)	0.53 (0.44–0.65)	0.227
CSF total protein (mg/dL), median (IQR)	67 (46–102)	102 (46–179)	0.132
Qalb, median (IQR)	9.44 (6.79–16.22)	14.79 (6.8–28.83)	0.183
IgG index, median (IQR)	0.58 (0.51–0.66)	0.79 (0.62–1.01)	<0.001*
Intrathecal IgG synthesis (%), median (IQR)[1]	0 (0–0)	2.02 (0–25.56)	<0.001*
Intrathecal IgA synthesis (%), median (IQR) [1]	0 (0–0)	0 (0–6.39)	0.059
Intrathecal IgM synthesis (%), median (IQR) [2]	0 (0–0)	42.54 (0–66.4)	<0.001*
VZV antibody index, median (IQR)[3]	2.1 (0.6–3.1)	na	na
Borrelia antibody index, median (IQR)	na	23.6 (7.5–43.8)	na

Data from: [1] 90 cases, [2] 85 cases, [3] 31 cases (18 cases>1.5). CSF WBC and RBC were counted within the Fuchs-Rosenthal chamber (volume of 3.2 μL). Counts are reported as "cells/μL" (correction for a standard volume of 1 μL was achieved by dividing by 3.2). CSF, cerebrospinal fluid; IQR, interquartile range; n, number; na, not applicable; PCR, polymerase chain reaction; RBC, red blood cell; WBC, white blood cell; Qalb, CSF/serum albumin quotient; VZV, varicella zoster virus.

[a]calculated by Mann-Whitney U test, uncorrected p-values are shown, after Bonferroni correction still significant at a level of 0.05.

described the occurrence of LETM after herpes zoster and chicken pox, respectively (15, 25) (**Table 3**). In only one patient, the VZV DNA PCR result was available and reported as positive. In our case, the VZV DNA PCR result was negative, which may have been due to the preceding acyclovir therapy (6 days). However, elevated WBC count and a highly increased VZV ASI confirmed the diagnosis. In a group of 10 immunocompetent patients with VZV infection–related myelitis, MOG-IgG was present in one patient (20). This patient relapsed and fulfilled the seronegative NMOSD criteria during follow-up. In contrast, our patient showed nearly complete recovery without further relapses, and MOG-IgG was undetectable after eight months. Approximately 35% of patients with MOGAD have a relapsing disease (14). Although persistent MOG-IgG positivity is only a moderate marker for relapsing disease with a positive predictive value of approximately 60%, a conversion to undetectable antibody reliably predicted a monophasic disease course in approximately 90% of cases (14). Due to limitations such as a lack of prospective clinical trials in MOGAD and established standard test criteria conversion of detectable to undetectable MOG-IgG is currently not a reliable marker for treatment decisions. However, as a) only approximately one third of the patients with MOG-IgG relapse, b) MOG-IgG was negative during follow-up, and c) due to the known viral trigger, we decided not to start a disease modifying or immunosuppressive treatment. In addition to MOG-IgG, several case reports have described an association of AQP4-IgG with VZV infection (**Table 3**), we identified 9 further reports of AQP4-IgG associated CNS inflammatory demyelinating disorder related to a VZV infection. In synopsis with the MOG-IgG associated cases, eleven patients out of twelve presented with LETM (the one remaining case was MRI-negative myelitis), LETM seems to be a typical clinical presentation of these rare associations. Of particular importance, for eight patients, there was information available that indicated that the NMOSD (1/8 MOG-IgG positive, 7/8 AQP4-IgG positive) criteria were fulfilled, and that relapses occurred in at least six patients. Therefore, in the rare clinical presentation of LETM triggered by a VZV infection, screening for MOG-IgG or AQP4-IgG has therapeutic implications. In contrast to cases in whom MOG-IgG are detected, treatment with a disease-modifying therapy should be considered if AQP4-IgG is detected.

The pathophysiological basis of the association between VZV infection and MOG or AQP4 antibody-associated associated LETM is unclear. In the majority of the reported cases, CSF VZV DNA PCR results were negative (**Table 3**), and a direct viral invasion of the spinal cord seems unlikely, although pathological data are missing. These data are consistent with the retrospective case series of immunocompetent individuals with VZV myelitis published by Wang et al. (20). Four out of 11 patients fulfilled the NMOSD criteria, and despite immunosuppressive treatment in the two relapsing patients, no VZV reactivity was observed. Given the rising number of cases with the presence of MOG-IgG or AQP4-IgG and the typically delayed onset of neurological symptoms (**Table 3**) after the rash, immune-mediated genesis seems likely. The mechanisms suspected to be involved in triggering autoimmunity after infection are molecular mimicry, bystander activation, epitope spreading, and the release of cryptic antigens (30). A possible hypothesis for MOG and AQP4 antibody-associated autoimmunity triggered by a VZV infection is that the VZV infection causes a breakdown of the blood-brain barrier, as indicated by the common finding of an elevated CSF/serum albumin ratio in herpes zoster (31). Subsequently, CNS antigen is released into the periphery, which induces an immune reaction against self-antigens by autoreactive B and T cells.

A limitation of our study is the retrospective design and small number (n=15) of patients with myelitis, encephalomyelitis, or encephalitis. However, data specifically excluded a nonspecific bystander reaction, as patients with VZV infection without parenchymal involvement were negative for MOG-IgG (n=44). As CSF analysis of MOG-IgG improve the sensitivity by 7%, another limitation is that MOG-IgG was only tested in patient sera (32).

Overall, we showed that the presence of MOG-IgG is a rare finding in patients with a VZV infection complicated by CNS demyelinating-inflammatory diseases. Nevertheless, due to

TABLE 3 | Varicella zoster virus infection-associated cases with MOG/AQP4 antibody associated central nervous system disorders.

Case	Clinical phenotype	Neurological symptoms	Presence of rash	Time of onset after Rash in days	Level rash	VZV DNA PCR	Presence/ absence of VZV-IgG/IgM elevation	Imaging findings	Antibody status	Follow-up	Reference#
Cases with MOG IgG											
Male, 69 a	LETM	Paraparesis	+	10	Left L2-3 dermatome	+	nk	Lesion from the bottom of the medulla oblongata to the upper (T2) thoracic region	MOG-IgG +, cell-based-assay		(15)
Female, 34 a	Myelitis	Paraparesis, loss of pain and temperature sensation below her groin, absent vibration sense in both lower limbs	primary VZV infection	21	na	nd	nd	normal	MOG-IgG +	Clinical remission MOG IgG remained positive	(25)
Female, 42 a	LETM	nk	+	1	C dermatome	nk	Increased VZV IgM	Myelitis: C2-4,T 1, Medulla oblongata	MOG-IgG +	Clinical remission (EDSS 6 to 1), relapse, NMOSD criteria fulfilled	(20)
Male, 30 a	LETM	Sensomotor paralytic syndrome (sensory level below T6), subsequent gait ataxia, neurogenic bladder disturbance	+	6	Right T6 dermatome	–	CSF VZV ASI increased (9.4)	Lesion: T1 to the conus medullaris with only a very faint leptomeningeal contrast enhancement	MOG-IgG + (1:1280), cell-based assay	Clinical remission MOG IgG turned negative	Present case
Cases with AQP4 IgG											
Female, 63 a	LETM	Paresis (3–4/5) and mild hypoesthesia of the left leg, sensory impairment for temperature and pain of the right leg and the trunk below level T10, urine incontinence	+	14	Along the lumbar spine	–	CSF VZV ASI normal	Lesion from C7 to Th9 with marked oedema and moderate gadolinium enhancement	AQP4-IgG +, tissue-based indirect immunofluorescence assays	Partial clinical remission (after plasmapheresis) AQP-4 IgG turned negative	(7)
Female, 51 a	LETM,	Decreased power (3/5), hyperreflexia along with sensory loss in the right upper and lower extremity, hyperesthesia in the entire left lower extremity	+	49	Right C5 dermatome	–	nk	Enhancing intramedullary lesion C2 -4, centrally into the right of the midline with signal changes at the T1 level without enhancement or expansive appearance	AQP4-IgG first attack nd, relapse + (>1:160)	Two relapses, diagnosis NMOSD, persistent AQP-4 IgG, clinical remission	(8)
Female, 59 a	LETM	nk	+	15	C dermatome	nk	Increased VZV IgM	Myelitis: C1-6	AQP4-IgG +	Clinical remission (EDSS 2 to 1), no relapse, NMOSD criteria fulfilled	(20)
Female, 29 a	LETM	Acute quadriplegia	+	7	Left T4–6 dermatomes	–	Increased VZV IgM	nk	AQP4-IgG first attack nd, relapse + (1:80), tissue-based indirect immunofluorescence assays	Partial clinical remission, relapse - LETM, NMOSD criteria fulfilled	(9)
Female, 77 a	LETM	Paraparesis, sensory level by L4, urine retention	+	2	Left L4–S1 dermatomes	+	nk	Lesion extending from C2–C3 to T12 with no gadolinium enhancement	AQP4-IgG first attack nd, relapse + indirect immunofluorescence serum assay (1:10)	Severe sequelae, relapse, NMOSD criteria fulfilled	(10)
Female, 48 a	LETM	Right arm abduction paresis, brisk reflexes in the lower limbs, diminished reflexes in the upper limbs, extensor plantar response bilaterally	+	14	Right C6 dermatome	–	nk	Cervical LETM	AQP4-IgG positive, cell-based assay	Fully recovered, except for mild sensory symptoms, NMOSD criteria fulfilled	(11)

(Continued)

TABLE 3 | Continued

Case	Clinical phenotype	Neurological symptoms	Presence of rash	Time of onset after Rash in days	Level rash	VZV DNA PCR	Presence/ absence of VZV-IgG/IgM elevation	Imaging findings	Antibody status	Follow-up	Reference#
Female, 53 a	LETM	Hyperhidrosis of left side of her face, neck, arm and upper chest, muscle weakness of her left leg, sensory impairment for light touch and temperature in her chest and legs	+	7	T5-6 dermatome	nk	CSF VZV IgG index increased (7.9)	Lesion extending from T1-7	AQP4-IgG +	Relapse	(12)
Female, 55 a	LETM	Dysesthesia of the right side of the face, neck, bilateral upper extremities, and T4-T10 levels, urine incontinence	+	14	Left C3-T4 dermatomes	–	CSF VZV ASI increased (4.53)	Lesion extending from the lower part of the medulla oblongata to C5, with marked edema and moderate gadolinium enhancement and abnormal gadolinium enhancement of the left spinal posterior root	AQP4-IgG +, cell-based assay	Mild response to treatment, relapse, NMOSD criteria fulfilled	(6)
Female, 17 a	Area postrema syndrome and LETM	Right eye mydriasis, piloerection, poikilothermia, mild hypoesthesia, and pain in the right arm and trunk in the T2-T3 dermatomes/intractable vomiting	+	21	Right T2 dermatome	–	IgM VZV ASI increased (7.0)	Lesions involved the area postrema, right ventrothalamic area, periaqueductal gray, optic tracts, and cervical and thoracic regions, longitudinally extended from C1-5 and from C6-T6 and axially involving two-thirds of the spinal cord	AQP4-IgG +	NMOSD criteria fulfilled, resolution	(13)

A, age; AQP4, aquaporin-4; ASI, antibody specific index; C, cervica; CSF, cerebrospinal fluid; LETM, longitudinally extensive transverse myelitis; MOG, myelin oligodendrocyte glycoprotein; L, lumbar; MRI, magnetic resonance imaging; not applicable, na; nd, not done; NMOSD, neuromyelitis optica spectrum disease; nk, not known; T, thoracic; VZV, varicella zoster virus; +, positive; -, negative.

therapeutic implications, antibody screening is a useful tool, particularly in patients with a higher pre-test probability, e.g. with LETM. Further prospective larger studies, including children, are required to analyze the frequency of neurological antibody-associated diseases triggered by VZV infection.

DATA AVAILABILITY STATEMENT

The raw data supporting the conclusions of this article will be made available by the authors, without undue reservation.

ETHICS STATEMENT

The studies involving human participants were reviewed and approved by Medical University Innsbruck. Written informed consent to participate in this study was provided by the participants' legal guardian/next of kin. Written informed consent was obtained from the individual(s) for the publication of any potentially identifiable images or data included in this article.

AUTHOR CONTRIBUTIONS

FDP conceptualized the study, collected data, case analysis, statistical analysis, drafted the manuscript, and revised the manuscript for intellectual content. PM collected data and revised the manuscript for intellectual content. KB collected data and revised the manuscript for intellectual content. MA collected data and revised the manuscript for intellectual content. AB collected data and revised the manuscript for intellectual content. TB case analysis and revised the manuscript for intellectual content. GB collected data and revised the manuscript for intellectual content. PR MRI analysis and revised the manuscript for intellectual content. KS collected data and revised the manuscript for intellectual content. AZ collected data and revised the manuscript for intellectual content. FDe case analysis, conceptualized the study, and revised the manuscript for intellectual content. MR conceptualized the study, and revised the manuscript for intellectual content. HH conceptualized the study, collected data, case analysis, statistical analysis, drafted the manuscript, and revised the manuscript for intellectual content. All authors contributed to the article and approved the submitted version.

FUNDING

This study was funded by a research grant from the Austrian Science Fund (FWF projects P32699, MR).

REFERENCES

1. Arvin A. Aging, Immunity, and the Varicella-Zoster Virus. *N Engl J Med* (2005) 352:2266–7. doi: 10.1056/NEJMp058091
2. Kennedy PGE, Gershon AA. Clinical Features of Varicella-Zoster Virus Infection. *Viruses* (2018) 10:609. doi: 10.3390/v10110609
3. Nagel MA, Gilden D. Neurological Complications of Varicella Zoster Virus Reactivation. *Curr Opin Neurol* (2014) 27:356–60. doi: 10.1097/WCO.0000000000000092
4. Bozzola E, Tozzi AE, Bozzola M, Krzysztofiak A, Valentini D, Grandin A, et al. Neurological Complications of Varicella in Childhood: Case Series and a Systematic Review of the Literature. *Vaccine* (2012) 30:5785–90. doi: 10.1016/j.vaccine.2012.05.057
5. Hogan EL, Krigman MR. Herpes Zoster Myelitis. *Evidence Viral Invasion Spinal Cord Arch Neurol* (1973) 29:309–13. doi: 10.1001/archneur.1973.00490290049004
6. Eguchi H, Takeshige H, Nakajima S, Kanou M, Nakajima A, Fuse A, et al. Herpes Zoster Radiculomyelitis With Aquaporin-4 Antibodies: A Case Report and Literature Review. *Front Neurol* (2020) 11:585303. doi: 10.3389/fneur.2020.585303
7. Heerlein K, Jarius S, Jacobi C, Rohde S, Storch-Hagenlocher B, Wildemann B. Aquaporin-4 Antibody Positive Longitudinally Extensive Transverse Myelitis Following Varicella Zoster Infection. *J Neurol Sci* (2009) 276:184–6. doi: 10.1016/j.jns.2008.08.015
8. Jayarangaiah A, Sehgal R, Epperla N. Sjögren's Syndrome and Neuromyelitis Optica Spectrum Disorders (NMOSD)–A Case Report and Review of Literature. *BMC Neurol* (2014) 14:200. doi: 10.1186/s12883-014-0200-5
9. Park JS, Hwang SJ, Shin JH, Kim DS. A Recurrent Longitudinally Extensive Transverse Myelitis With Aquaporin-4(AQP4) Antibody After Herpes Zoster. *J Neurol Sci* (2013) 334:69–71. doi: 10.1016/j.jns.2013.07.2510
10. Machado C, Amorim J, Rocha J, Pereira J, Lourenço E, Pinho J. Neuromyelitis Optica Spectrum Disorder and Varicella-Zoster Infection. *J Neurol Sci* (2015) 358:520–1. doi: 10.1016/j.jns.2015.09.374
11. Mathew T, Thomas K, Shivde S, Venkatesh S, Rockey SM. Post Herpes Zoster Infection Neuromyelitis Optica Spectrum Disorder. *Mult Scler Relat Disord* (2017) 18:93–4. doi: 10.1016/j.msard.2017.09.022
12. Suda M, Tsutsumiuchi M, Uesaka Y, Hayashi N. A Case of Anti Aquapolin-4 Antibody Positive Myelitis With Hyperhidrosis, Following Herpes Zoster. *Rinsho Shinkeigaku* (2017) 57:26–8. doi: 10.5692/clinicalneurol.cn-000820
13. Turco EC, Curti E, Maffini V, Pisani F, Granella F. Neuromyelitis Optica Spectrum Disorder Attack Triggered by Herpes Zoster Infection. *Mult Scler Int* (2020) 2020:6151258. doi: 10.1155/2020/6151258
14. Hegen H, Reindl M. Recent Developments in MOG-IgG Associated Neurological Disorders. *Ther Adv Neurol Disord* (2020) 13:1756286420945135. doi: 10.1177/1756286420945135
15. Shiga Y, Kamimura T, Shimoe Y, Takahashi T, Kaneko K, Kuriyama M. Anti-Myelin Oligodendrocyte Glycoprotein (MOG) Antibody-Positive Varicella-Zoster Virus Myelitis Presenting as Longitudinally Extensive Transverse Myelitis: A Case Report. *Rinsho Shinkeigaku* (2017) 57:579–83. doi: 10.5692/clinicalneurol.cn-001066
16. Amano H, Miyamoto N, Shimura H, Sato DK, Fujihara K, Ueno S, et al. Influenza-Associated MOG Antibody-Positive Longitudinally Extensive Transverse Myelitis: A Case Report. *BMC Neurol* (2014) 14:224. doi: 10.1186/s12883-014-0224-x
17. Vieira JP, Sequeira J, Brito MJ. Postinfectious Anti-Myelin Oligodendrocyte Glycoprotein Antibody Positive Optic Neuritis and Myelitis. *J Child Neurol* (2017) 32:996–9. doi: 10.1177/0883073817724927
18. Nakamura M, Iwasaki Y, Takahashi T, Kaneko K, Nakashima I, Kunieda T, et al. A Case of MOG Antibody-Positive Bilateral Optic Neuritis and Meningoganglionitis Following a Genital Herpes Simplex Virus Infection. *Mult Scler Relat Disord* (2017) 17:148–50. doi: 10.1016/j.msard.2017.07.023
19. Hung CH, Chang KH, Kuo HC, Huang CC, Liao MF, Tsai YT, et al. Features of Varicella Zoster Virus Myelitis and Dependence on Immune Status. *J Neurol Sci* (2012) 318:19–24. doi: 10.1016/j.jns.2012.04.017
20. Wang X, Zhang X, Yu Z, Zhang Q, Huang D, Yu S. Long-Term Outcomes of Varicella Zoster Virus Infection-Related Myelitis in 10 Immunocompetent Patients. *J Neuroimmunol* (2018) 321:36–40. doi: 10.1016/j.jneuroim.2018.05.005
21. Hegen H, Milosavljevic D, Schnabl C, Manowiecka A, Walde J, Deisenhammer F, et al. Cerebrospinal Fluid Free Light Chains as Diagnostic Biomarker in Neuroborreliosis. *Clin Chem Lab Med* (2018) 56:1383–91. doi: 10.1515/cclm-2018-0028
22. Mygland A, Ljøstad U, Fingerle V, Rupprecht T, Schmutzhard E, Steiner I, et al. EFNS Guidelines on the Diagnosis and Management of European Lyme Neuroborreliosis. *Eur J Neurol* (2010) 17:8–16.e1–4. doi: 10.1111/j.1468-1331.2009.02862.x
23. Auer M, Hegen H, Zeileis A, Deisenhammer F. Quantitation of Intrathecal Immunoglobulin Synthesis - a New Empirical Formula. *Eur J Neurol* (2016) 23:713–21. doi: 10.1111/ene.12924
24. Reindl M, Schanda K, Woodhall M, Tea F, Ramanathan S, Sagen J, et al. International Multicenter Examination of MOG Antibody Assays. *Neurology (R) Neuroimmunol Neuroinflamm* (2020) 7:e674. doi: 10.1212/NXI.0000000000000674
25. Viswanathan LG. Post-Varicella Anti-Myelin Oligodendrocyte Glycoprotein Antibody-Associated Magnetic Resonance Imaging-Negative Myelitis. *Clin Exp Neuroimmunol* (2021) 12:122–3. doi: 10.1111/cen3.12618
26. Di Pauli F, Berger T. Myelin Oligodendrocyte Glycoprotein Antibody-Associated Disorders: Toward a New Spectrum of Inflammatory Demyelinating CNS Disorders? *Front Immunol* (2018) 9:2753. doi: 10.3389/fimmu.2018.02753
27. Jarius S, Paul F, Aktas O, Asgari N, Dale RC, de Seze J, et al. MOG Encephalomyelitis: International Recommendations on Diagnosis and Antibody Testing. *J Neuroinflamm* (2018) 15:134. doi: 10.1186/s12974-018-1144-2
28. Wynford-Thomas R, Jacob A, Tomassini V. Neurological Update: MOG Antibody Disease. *J Neurol* (2019) 266:1280–6. doi: 10.1007/s00415-018-9122-2
29. Dubey D, Pittock SJ, Krecke KN, Morris PP, Sechi E, Zalewski NL, et al. Clinical, Radiologic, and Prognostic Features of Myelitis Associated With Myelin Oligodendrocyte Glycoprotein Autoantibody. *JAMA Neurol* (2019) 76:301–9. doi: 10.1001/jamaneurol.2018.4053
30. Ercolini AM, Miller SD. The Role of Infections in Autoimmune Disease. *Clin Exp Immunol* (2009) 155:1–15. doi: 10.1111/j.1365-2249.2008.03834.x
31. Haanpää M, Dastidar P, Weinberg A, Levin M, Miettinen A, Lapinlampi A, et al. CSF and MRI Findings in Patients With Acute Herpes Zoster. *Neurology* (1998) 51:1405–11. doi: 10.1212/WNL.51.5.1405
32. Mariotto S, Gajofatto A, Batzu L, Delogu R, Sechi G, Leoni S, et al. Relevance of Antibodies to Myelin Oligodendrocyte Glycoprotein in CSF of Seronegative Cases. *Neurology* (2019) 93:e1867–72. doi: 10.1212/WNL.0000000000008479

Conflict of Interest: FDP has participated in meetings sponsored by, received honoraria (lectures, advisory boards, consultations) or travel funding from Almirall, Bayer, Biogen, Celgene, Janssen, Merck, Novartis, Sanofi-Genzyme, Roche and Teva. Her institution has received research grants from Roche. KB has participated in meetings sponsored by and received travel funding from Roche. MA received speaker honoraria and/or travel grants from Biogen, Merck, Novartis and Sanofi. AB has participated in meetings sponsored by Merck and Biogen. TB has participated in meetings sponsored by and received honoraria (lectures, advisory boards, consultations) from pharmaceutical companies marketing treatments for multiple sclerosis: Almirall, Biogen, Biologix, Bionorica, Celgene/BMS, GSK, MedDay, Merck, Novartis, Roche, Sandoz, Sanofi/Genzyme, TG Pharmaceuticals, TEVA-ratiopharm and UCB. His institution has received financial support in the last 12 months by unrestricted research grants (Biogen, Bayer, Celgene/BMS, Merck, Novartis, Roche, Sanofi/Genzyme, and TEVA ratiopharm) and for participation in clinical trials in multiple sclerosis sponsored by Alexion, Bayer, Biogen, Merck, Novartis, Roche, Sanofi/Genzyme, and TEVA. GB has participated in meetings sponsored by, received speaker honoraria or travel funding from Biogen, Celgene, Lilly, Merck, Novartis, Roche, Sanofi-Genzyme and Teva, and received honoraria for consulting Biogen, Celgene, Roche and Teva. AZ has participated in meetings sponsored by, received speaking honoraria or travel funding from Biogen, Merck, Sanofi-Genzyme and Teva. FDe has participated in meetings sponsored by or received honoraria for acting as an advisor/speaker for Almirall, Alexion, Biogen, Celgene, Genzyme-Sanofi, Merck, Novartis Pharma, Roche, and TEVA ratiopharm. His institution has received research grants from Biogen and Genzyme Sanofi. He is section editor of the MSARD Journal (Multiple Sclerosis and Related Disorders). MR was supported by a research support from Euroimmun and Roche.

His institution receives payments for antibody assays (MOG, AQP4, and other autoantibodies) and for MOG and AQP4 antibody validation experiments organized by Euroimmun (Lübeck, Germany). HH has participated in meetings sponsored by, received speaker honoraria or travel funding from Bayer, Biogen, Merck, Novartis, Sanofi-Genzyme, Siemens, Teva, and received honoraria for acting as consultant for Biogen and Teva.

The remaining authors declare that the research was conducted in the absence of any commercial or financial relationships that could be construed as a potential conflict of interest.

Publisher's Note: All claims expressed in this article are solely those of the authors and do not necessarily represent those of their affiliated organizations, or those of the publisher, the editors and the reviewers. Any product that may be evaluated in this article, or claim that may be made by its manufacturer, is not guaranteed or endorsed by the publisher.

frontiers in Immunology

CASE REPORT
published: 23 December 2021
doi: 10.3389/fimmu.2021.808420

Case Report: Clinical and Imaging Characteristics of a Patient with Anti-flotillin Autoantibodies: Neuromyelitis Optica or Multiple Sclerosis?

Ke Shang[†], *Chang Cheng*[†], *Chuan Qin*, *Jun Xiao*, *Gang Deng*, *Bi-Tao Bu*, *Sha-Bei Xu*[*] *and Dai-Shi Tian*[*]

Department of Neurology, Tongji Hospital, Tongji Medical College, Huazhong University of Science and Technology, Wuhan, China

OPEN ACCESS

Edited by:
Wei Qiu,
Third Affiliated Hospital of Sun Yat-sen University, China

Reviewed by:
Chao Quan,
Fudan University, China
Jun Guo,
Air Force Medical University, China

***Correspondence:**
Sha-Bei Xu
shabei_xu@163.com
Dai-Shi Tian
tiandaishi@126.com;
tiands@tjh.tjmu.edu.cn

[†]*These authors have contributed equally to this work*

Specialty section:
This article was submitted to Multiple Sclerosis and Neuroimmunology, a section of the journal Frontiers in Immunology

Received: *03 November 2021*
Accepted: *09 December 2021*
Published: *23 December 2021*

Citation:
Shang K, Cheng C, Qin C, Xiao J, Deng G, Bu B-T, Xu S-B and Tian D-S (2021) Case Report: Clinical and Imaging Characteristics of a Patient with Anti-flotillin Autoantibodies: Neuromyelitis Optica or Multiple Sclerosis? Front. Immunol. 12:808420. doi: 10.3389/fimmu.2021.808420

Background: Demyelination diseases are complex puzzles that are not always straightforward to diagnose. Multiple sclerosis and neuromyelitis optica are two that are frequently encountered. Numerous autoantibodies newly discovered in recent years have significantly aided clinical reasoning and diagnosis in differentiating demyelination disorders. Here we report a case of demyelination disease with anti-flotillin autoantibodies positive, which is not common in past references.

Case summary: The patient presented with characteristic neuromyelitis optica symptoms and had remission and relapse. But his images exhibited characteristics of both neuromyelitis optica spectrum illness and multiple sclerosis.

Conclusion: This is the first case report describing the clinical course and imaging characteristics of demyelination illness associated with anti-flotillin autoantibodies. Although so far it appears to be a subtype of multiple sclerosis, there is still a potential that it is separate from MS and NMOSD.

Keywords: demyelination, flotillin, neuromyelitis optica, multiple sclerosis, anti-flotillin autoantibody, case report

INTRODUCTION

Flotillins are considered to be scaffolding proteins of lipid rafts and are reported to participate in axon regeneration, neuronal differentiation, endocytosis, T-lymphocyte activation, membrane protein recruitment, insulin signaling, cell proliferation, and tumor progression (1, 2). As to flotillins' role in diseases, they had been reported in Alzheimer's disease (AD) (1, 3). Serum flotillin levels are significantly decreased in patients with AD and amyloid-positive MCI (Mild cognition impairment) patients compared with age-matched patients with VaD (Vascular dementia) and MCI patients without amyloid. The decrease in flotillin levels may result from reduced exosome secretion caused by Aβ42 oligomers. Hahn et al. reported the presence of autoantibodies against the flotillin-1/2 heterocomplex in the serum and CSF of patients with multiple sclerosis (4). Here, we first described the clinical and imaging characteristics of a patient with anti-flotillin autoantibodies in detail.

CASE PRESENTATION

Patient Presentation

In 2017, a 26-year-old man experienced a sudden reduction of vision in his left eye without eye movement pain or diplopia. Upon presentation to another hospital, he was diagnosed with optic neuritis and underwent treatment with high-dose intravenous methylprednisolone. Two weeks later, his left eye visual acuity returned to normal. In 2020, he was admitted to our hospital because of blurred vision that had been present in the left eye for 3 months and progressive lower limb weakness that had been present for 1 month. He did not exhibit other new symptoms. Cerebral and cervical magnetic resonance imaging in another hospital revealed multiple demyelinating lesions in the brainstem, bilateral insula, corpus callosum, left parietal lobe, and cervical cord (at the level of C3–C5). The patient had a history of 4–5 cigarettes per day for 8 years. He had no history of rheumatic disorders or other systemic disorders; he also had no history of mental or genetic disorders. His parents did not have a consanguineous relationship.

Physical Examinations

Neurological examination revealed horizontal nystagmus and the presence of weakened light perception and limited abduction in the left eye. Muscle strength in the patient's lower limbs was 80% of normal (4/5) under normal muscular tension. The patient's tendon reflexes were brisk in both lower extremities, but normal in the upper limbs. He exhibited bilateral positive Babinski signs, as well as hemi-thermanalgesia immediately below the level of T8. His other physical findings were unremarkable.

Laboratory Findings

Cerebrospinal fluid (CSF) examination revealed pressure of 0.59 kPa and nucleated cell count of $3*10^6$/L (reference: 0–$8*10^6$/L). The patient's immunoglobulin G index was 1.3 (reference: 0.00–0.70). CSF biochemical, immunological, microbiological, and virological tests showed no abnormalities. Complete blood count, biochemical test results, and findings concerning TPPA, HIV, HBV, HCV, tumor markers, thyroid function, and HbA1c were normal. Furthermore, ANA, RF, ANCA, and LA results were in normal ranges. Oligoclonal band and anti-flotillin-1/2 autoantibodies (1:1) were present in CSF but absent from serum; anti-AQP4, anti-MOG, and anti-MBP autoantibodies were absent from both CSF and serum.

Imaging Data

Chest CT findings were normal. Bilateral optic nerves showed strong signals on T2WI with minimal gadolinium enhancement on T1WI. Spinal MRI revealed long-segment extensive lesions without enhancement, extending from C3 to C5 and from Th5 to Th10. Cerebral MRI showed abnormal long T1 and T2 signals at the bilateral frontal parietal lobe, centrum ovale, bilateral lateral ventricle, corpus callosum, hippocampus, and right cerebellar peduncles; these signals did not show mild enhancement or strong signals on DWI.

Other Examinations

The corrected decimal visual acuity values were 0.08 and 0.1 in the patient's left and left eyes, respectively. Fundus examination and OCT indicated retrobulbar neuritis in the left eye. Visual evoked potential analysis confirmed visual pathway impairment in both eyes. Brainstem auditory evoked potential analysis showed relatively low amplitudes with normal latency, which indicated conduction dysfunction in the peripheral segment of bilateral brainstem auditory pathways. Sensory-evoked potential analysis suggested a conduction dysfunction in the central segment of the bilateral lower limb sensory pathway with normal SEP of the upper limbs.

Diagnosis, Treatment, and Follow-Up

Based on the patient's history, symptoms, and signs, including classical demyelination and evidence of anti-flotillin autoantibody, he was diagnosed with NMOSD. **Figure 1** was showcasing a timeline with relevant data from the episode of care. Therefore, he received high-dose intravenous methylprednisolone (initially 1 g per day, then tapering by half at 3-day intervals). He then received oral prednisone acetate 60 mg per day, with tapering. He also received immunosuppressants; tacrolimus was initially used, but azathioprine was subsequently used because the tacrolimus trough level was insufficient. The patient's lower limb muscle strength recovered to 100% (5/5). His visual acuity in the left eye improved, but has not yet returned to normal. In the next face-to-face follow-up, radiological examinations including susceptibility weighted images, retest of CSF and serum autoantibodies, and thorough cognition assessment were scheduled.

DISCUSSION

Flotillins, also called reggies, are considered to be scaffolding proteins of lipid rafts and are generally used as marker proteins of lipid microdomains. They were initially identified as regeneration molecules that demonstrated upregulation in the regenerating axons of goldfish retinal ganglion cells following optic nerve lesion (5). There are two homologous proteins in flotillin family, flotillin-1 and flotillin-2. Flotillin-1 is expressed most abundantly in brain, heart, lung, and placenta, as well as hematopoietic cells; in contrast, flotillin-2 is expressed in all tissues; the expression of one is regulated by the other. These proteins are ubiquitous and highly conserved lipid raft scaffolding proteins (2). Flotillins do not span the membrane, but interact with other proteins on the other side of the membrane (6). Flotillins reportedly participate in axon regeneration, neuronal differentiation, endocytosis, T-lymphocyte activation, membrane protein recruitment, insulin signaling, cell proliferation, and tumor progression (1, 2). In neuronal cells, flotillins might modulate cadherin-mediated cell–cell adhesion, which is important for synapse organization and function, neuron regeneration, and dendritic spine morphogenesis (2). After reviewing basic functions of flotillins, we first went back to the clinical course of this patient.

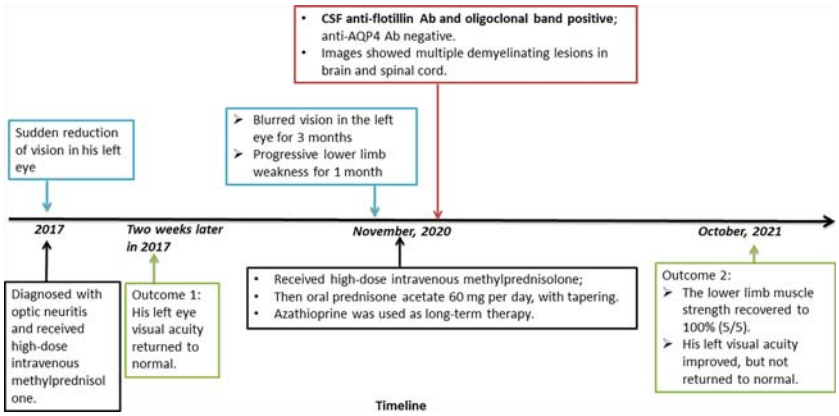

FIGURE 1 | Timeline of the case report.

The patient's first disease onset in 2017 comprised optic neuritis without limb weakness or numbness. Treatment with high-dose methylprednisolone provided rapid remission. It is unclear whether the patient received anti-AQP4 autoantibody detection at the time. In 2020, the patient presented with myelitis, including new symptoms such as lower limb weakness, and sensory disorder below the level of T8. The patient was initially misdiagnosed with NMOSD, on the basis of his disease beginning characteristics (neuritis and myelitis) and imaging findings. The international consensus diagnostic criteria for NMOSD were considered for this patient (7). Although he did not exhibit anti-AQP4, anti-MOG, or anti-MBP autoantibodies in the CSF or serum, he demonstrated two core clinical characteristics: acute optic neuritis and acute myelitis. Furthermore, he had some typical NMOSD lesions on cerebral MRI (**Figure 2**). Nearly symmetrical confluent deep white matter lesions were distributed around bilateral ventricles (red arrows in **Figure 2**); the corpus callosum (blue arrows in **Figure 2**) and associated periependymal brainstem (yellow arrows in **Figure 2**) were also involved.

However, a search of the literature revealed that anti-flotillin autoantibodies were mostly identified in reports of multiple sclerosis patients except for one recent case which reported anti-flotillin 1/2 autoantibody-associated atypical dementia (8). Furthermore, the patient's optic nerve and spinal cord lesions did not clearly meet the diagnostic criteria for NMOSD (7). The T1-weighted gadolinium enhancing lesion in the patient's optic nerve did not extend over more than half of the optic nerve length (red arrows in **Figure 3**); neither cervical nor thoracic lesions extended over three contiguous segments (blue arrows in **Figure 3**). Dawson's fingers (i.e., elongated flame-shaped lesions perpendicular to the lateral ventricle wall) were observed on FLAIR images (yellow arrows in **Figure 3**); in light of the patient's age, his brain displayed slight atrophy. The presence of Dawson's fingers and brain atrophy are considered indicative of multiple sclerosis (9, 10). Consideration of the above posed a difficulty to the diagnosis of NMOSD.

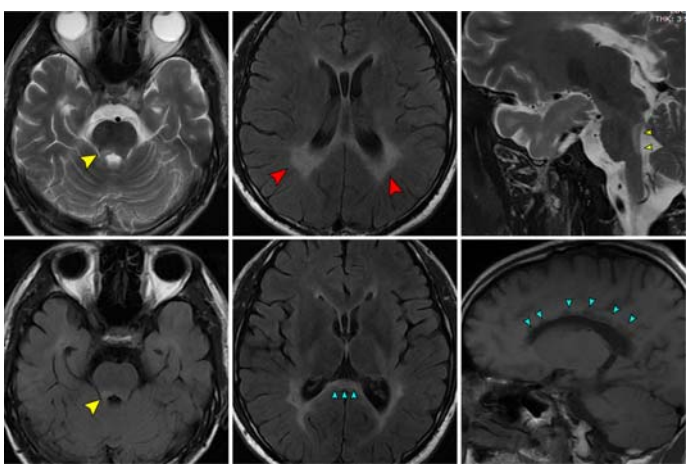

FIGURE 2 | The patient's MR images which mimicking NMOSD.

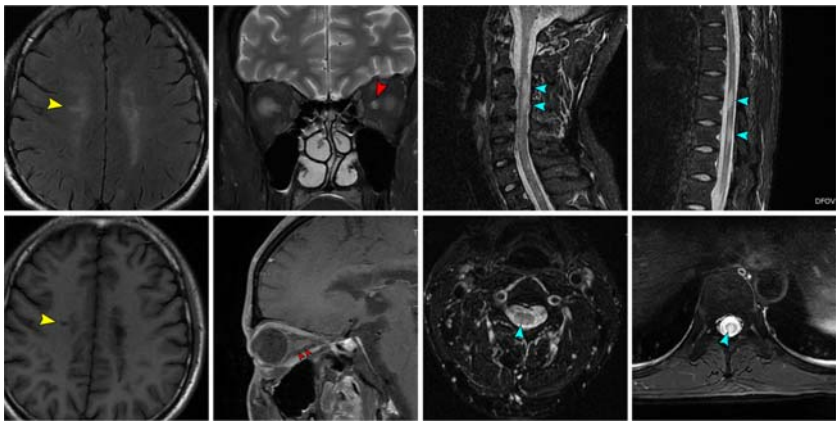

FIGURE 3 | The patient's MR images which mimicking MS.

In Hahn's research (4), most of the anti-flotillin-1/2-positive patients had no evidence for a disorder other than MS. CSF analysis had revealed mild pleocytosis and/or CSF-specific oligoclonal band (OCB) in all patients. Thirteen (93%) patients were female. Nine (64%) patients had a history of optic neuritis. None of the patients displayed anti-AQP4 or anti-MOG antibodies. And none met the latest international consensus criteria for NMOSD and all demonstrated 'red flag' criteria according to that consensus (7). This study did not describe radiological signs of disseminated demyelination in detail, except for those described in the 'red flag' section, such as symmetrical confluent deep white matter lesions surrounding bilateral ventricles, lesions in the corpus callosum, and periependymal brainstem lesions, which were obvious in this case. These lesions, when paired with two key clinical characteristics: acute optic neuritis and acute myelitis, easily misled us into diagnosing NMOSD; nevertheless, a 'red flag' informed us of the need for a correction diagnosis of MS with anti-flotillin autoantibodies positive. Based on Hahn's research (4) in a large cohort of pre-diagnosed MS patients, the flotillin-1/2 heterocomplex seems to be a B cell autoantigen in a subset of about 1–2% of MS patients. We hadn't found studies or cases reporting anti-flotillin autoantibodies positive in Asian population. As more understanding of it and more patients diagnosed, we speculated that it would become a new subtype of MS or a disease distinctive from MS. Since flotillins had been reported as a possible new marker of AD (11, 12) and recently found in a patient of atypical dementia (8), besides classical symptoms and relapses, this patient's cognition function requires further care during long-term follow-up.

Given a deep understanding of flotillins' physiological functions, it's not hard to infer why optic nerves, deep white matter and spinal cord are prone to be impaired by anti-flotillin autoantibodies. In early years, flotillins were found to be unregulated in retinal ganglion cells (RGCs) in fish (5) and the same in mammalian RGCs (13), which might explained vision loss. Munderloh et al. found that downregulation of flotillins triggered a clear reduction (up to 70%) of the number of regenerating axon in zebrafish and the knockdown of flotillins by flotillin-specific siRNAs restrained the axon regeneration (14), indicating that flotillins are indeed necessary for axon regeneration, which might illustrate the deep white matter and spinal cord lesions. Besides, flotillins had been reported to participate in hippocampal neurons differentiation. Downregulation of expression levels of flotillins in mammalian hippocampal neurons caused the neurons failed to differentiate (15). Langhorst et al. reported that expression of a trans-negative flotillin-2 deletion mutant, which interfered the oligomerization of flotillin, could inhibit insulin-like growth factor (IGF)-induced neurite outgrowth in N2a cells and impair differentiation of primary rat hippocampal neurons *in vitro* (16). These clues also reminded us to notice if there exists hippocampal injury and cognition impairment during long-term follow-up of this patient. Therefore, based on flotillins' role in axon regeneration and RGCs, clinical symptoms and imaging characteristics of this patient were reasonable, despite the parallels and contrasts with NMOSD or MS.

This case remained a source of contention. To begin, the titer of anti-flotillin autoantibodies (1:1) was low, and this was the first time anti-flotillin autoantibodies had been found in the laboratory. To validate it, the laboratory conducted tests twice using cell-based assays (CBA) and enzyme-linked immunosorbent assays (ELISA). We addressed it in our department of neurology and determined that it was not a false positive based on the patient's clinical presentations and a review of the literature. In due course, we will follow up on this case and reexamine his anti-flotillin autoantibodies in CSF. Second, long-term immunosuppressive medication requires additional observation. In our discussion, the diagnosis of MS and the subtype of relapse-remission MS (RRMS) are contentious. It is well established that disease modifying therapy is the first line of treatment for remission in RRMS. However, it has been noted that several disease-modifying medicines can exacerbate neuromyelitis optica (17–20). We picked tacrolimus and converted it to azathioprine after extensive consideration. As of last month, there has been no relapse attack.

Finally, given that flotillin-1/2 heterocomplexes have been detected on the cell surfaces of neural cells *in vivo*, mostly present on the intracellular side or temporarily on the extracellular side, corresponding autoantibodies could be pathogenic and contribute to demyelination. Demyelination disorders induced

by anti-flotillin autoantibodies need further investigation and might constitute independent clinical entities that are distinct from NMOSD and MS.

DATA AVAILABILITY STATEMENT

The original contributions presented in the study are included in the article/supplementary material. Further inquiries can be directed to the corresponding authors.

ETHICS STATEMENT

Written informed consent was obtained from the patient for the publication of any potentially identifiable images or data included in the article.

AUTHOR CONTRIBUTIONS

KS and CC equally contributed to the management of the patient and writing of the manuscript. CQ, JX, and GD contributed to a search of relevant references. B-TB raised meaningful opinions on the patient's image features. S-BX and D-ST equally participated in decision of the patient's long-term therapy and the whole design. All authors contributed to the article and approved the submitted version.

ACKNOWLEDGMENTS

We appreciate this patient's willingness to have his case published. We thank Ryan Chastain-Gross, Ph.D., from Liwen Bianji, Edanz Group China (www.liwenbianji.cn/ac), for editing the English text of a draft of this manuscript.

REFERENCES

1. Bodin S, Planchon D, Rios ME, Comunale F, Gauthier-Rouviere C. Flotillins in Intercellular Adhesion - From Cellular Physiology to Human Diseases. *J Cell Sci* (2014) 127(Pt 24):5139–47. doi: 10.1242/jcs.159764
2. Zhao F, Zhang J, Liu YS, Li L, He YL. Research Advances on Flotillins. *Virol J* (2011) 8:479. doi: 10.1186/1743-422X-8-479
3. Zou K, Abdullah M, Michikawa M. Current Biomarkers for Alzheimer's Disease: From CSF to Blood. *J Pers Med* (2020) 10(3):85. doi: 10.3390/jpm10030085
4. Hahn S, Trendelenburg G, Scharf M, Denno Y, Brakopp S, Teegen B, et al. Identification of the Flotillin-1/2 Heterocomplex as a Target of Autoantibodies in Bona Fide Multiple Sclerosis. *J Neuroinflamm* (2017) 14 (1):123. doi: 10.1186/s12974-017-0900-z
5. Schulte T, Paschke KA, Laessing U, Lottspeich F, Stuermer CA. Reggie-1 and Reggie-2, Two Cell Surface Proteins Expressed by Retinal Ganglion Cells During Axon Regeneration. *Development* (1997) 124(2):577–87. doi: 10.1242/dev.124.2.577
6. Bauer M, Pelkmans L. A New Paradigm for Membrane-Organizing and -Shaping Scaffolds. *FEBS Lett* (2006) 580(23):5559–64. doi: 10.1016/j.febslet.2006.08.077
7. Wingerchuk DM, Banwell B, Bennett JL, Cabre P, Carroll W, Chitnis T, et al. International Consensus Diagnostic Criteria for Neuromyelitis Optica Spectrum Disorders. *Neurology* (2015) 85(2):177–89. doi: 10.1212/WNL.0000000000001729
8. Hansen N, Bartels C, Stocker W, Wiltfang J, Timaus C. Case Report: Anti-Flotillin 1/2 Autoantibody-Associated Atypical Dementia. *Front Psychiatry* (2021) 12:626121. doi: 10.3389/fpsyt.2021.626121
9. Filippi M, Rocca MA, Ciccarelli O, De Stefano N, Evangelou N, Kappos L, et al. MRI Criteria for the Diagnosis of Multiple Sclerosis: MAGNIMS Consensus Guidelines. *Lancet Neurol* (2016) 15(3):292–303. doi: 10.1016/S1474-4422(15)00393-2
10. Sastre-Garriga J, Pareto D, Battaglini M, Rocca MA, Ciccarelli O, Enzinger C, et al. MAGNIMS Consensus Recommendations on the Use of Brain and Spinal Cord Atrophy Measures in Clinical Practice. *Nat Rev Neurol* (2020) 16 (3):171–82. doi: 10.1038/s41582-020-0314-x
11. Abdullah M, Kimura N, Akatsu H, Hashizume Y, Ferdous T, Tachita T, et al. Flotillin Is a Novel Diagnostic Blood Marker of Alzheimer's Disease. *J Alzheimers Dis* (2019) 72(4):1165–76. doi: 10.3233/JAD-190908
12. Abdullah M, Takase H, Nunome M, Enomoto H, Ito J, Gong JS, et al. Amyloid-Beta Reduces Exosome Release From Astrocytes by Enhancing JNK Phosphorylation. *J Alzheimers Dis* (2016) 53(4):1433–41. doi: 10.3233/JAD-160292
13. Lang DM, Lommel S, Jung M, Ankerhold R, Petrausch B, Laessing U, et al. Identification of Reggie-1 and Reggie-2 as Plasmamembrane-Associated Proteins Which Cocluster With Activated GPI-Anchored Cell Adhesion Molecules in Non-Caveolar Micropatches in Neurons. *J Neurobiol* (1998) 37(4):502–23. doi: 10.1002/(SICI)1097-4695(199812)37:4<502::AID-NEU2>3.0.CO;2-S
14. Munderloh C, Solis GP, Bodrikov V, Jaeger FA, Wiechers M, Malaga-Trillo E, et al. Reggies/flotillins Regulate Retinal Axon Regeneration in the Zebrafish Optic Nerve and Differentiation of Hippocampal and N2a Neurons. *J Neurosci* (2009) 29(20):6607–15. doi: 10.1523/JNEUROSCI.0870-09.2009
15. Stuermer CA. The Reggie/Flotillin Connection to Growth. *Trends Cell Biol* (2010) 20(1):6–13. doi: 10.1016/j.tcb.2009.10.003
16. Langhorst MF, Reuter A, Jaeger FA, Wippich FM, Luxenhofer G, Plattner H, et al. Trafficking of the Microdomain Scaffolding Protein Reggie-1/Flotillin-2. *Eur J Cell Biol* (2008) 87(4):211–26. doi: 10.1016/j.ejcb.2007.12.001
17. Barnett MH, Prineas JW, Buckland ME, Parratt JD, Pollard JD. Massive Astrocyte Destruction in Neuromyelitis Optica Despite Natalizumab Therapy. *Mult Scler* (2012) 18(1):108–12. doi: 10.1177/1352458511421185
18. Min JH, Kim BJ, Lee KH. Development of Extensive Brain Lesions Following Fingolimod (FTY720) Treatment in a Patient With Neuromyelitis Optica Spectrum Disorder. *Mult Scler* (2012) 18(1):113–5. doi: 10.1177/1352458511431973
19. Shimizu J, Hatanaka Y, Hasegawa M, Iwata A, Sugimoto I, Date H, et al. IFNbeta-1b may Severely Exacerbate Japanese Optic-Spinal MS in Neuromyelitis Optica Spectrum. *Neurology* (2010) 75(16):1423–7. doi: 10.1212/WNL.0b013e3181f8832e
20. Yamout BI, Beaini S, Zeineddine MM, Akkawi N. Catastrophic Relapses Following Initiation of Dimethyl Fumarate in Two Patients With Neuromyelitis Optica Spectrum Disorder. *Mult Scler* (2017) 23(9):1297–300. doi: 10.1177/1352458517694086

Conflict of Interest: The authors declare that the research was conducted in the absence of any commercial or financial relationships that could be construed as a potential conflict of interest.

frontiers in Immunology

ORIGINAL RESEARCH
published: 05 January 2022
doi: 10.3389/fimmu.2021.800666

Pregnancy-Related Attack in Neuromyelitis Optica Spectrum Disorder With AQP4-IgG: A Single-Center Study and Meta-Analysis

Shuwen Deng, Qiang Lei†* and *Wei Lu*†*

Department of Neurology, The Second Xiangya Hospital, Central South University, Changsha, China

OPEN ACCESS

Edited by:
Wei Qiu,
Third Affiliated Hospital of Sun Yat-sen University, China

Reviewed by:
Huaizhang Shi,
First Affiliated Hospital of Harbin Medical University, China
Sara Mariotto,
University of Verona, Italy
Edgar Carnero Contentti,
Hospital Aleman, Argentina

***Correspondence:**
Wei Lu
luwei0338@csu.edu.cn
Qiang Lei
leiqiang18@csu.edu.cn

†*These authors have contributed equally to this work*

Specialty section:
This article was submitted to Multiple Sclerosis and Neuroimmunology, a section of the journal Frontiers in Immunology

Received: *23 October 2021*
Accepted: *20 December 2021*
Published: *05 January 2022*

Citation:
Deng S, Lei Q and Lu W (2022) Pregnancy-Related Attack in Neuromyelitis Optica Spectrum Disorder With AQP4-IgG: A Single-Center Study and Meta-Analysis. Front. Immunol. 12:800666. doi: 10.3389/fimmu.2021.800666

Objective: This study aimed to investigate the demographic characteristic of pregnancy-related attacks (PRAs) in neuromyelitis optica spectrum disorder (NMOSD). In addition, we investigated the predictors of PRAs as well as the effect of immunosuppressive (IS) therapy in patients with pregnancy-related NMOSD.

Method: We retrospectively analyzed data on clinical and diagnostic characteristics, therapeutic management, and pregnancy outcomes for PRAs in AQP4-IgG-positive NMOSD patients admitted to the Second Xiangya Hospital of Central South University. Moreover, we searched the literature (without any temporal restriction) to identify all such similar cohorts and performed a meta-analysis to evaluate the effectiveness and safety of IS therapy on NMOSD patients with PRAs.

Result: We collected clinical data on 117 women with AQP4 antibody-positive NMOSD; we ultimately included 33 patients (34 pregnancies). Ten patients were relapse-free during pregnancy, and 23 (69.7%) had PRA; attacks were most common during the first trimester of the postpartum period. Maintenance of IS treatment during pregnancy was found to greatly reduce PRAs in patients with NMOSD. PRAs were associated with a higher neutrophil-to-lymphocyte ratio (NLR) at relapse during pregnancy and shorter time interval between the last relapse and conception. The meta-analysis suggested that maintenance of IS treatment during pregnancy can significantly reduce the RR of NMOSD (95%CI=0.35-0.62; z=5.18, $p<0.0001$) and had no adverse effect on the miscarriage rate. However, the unhealthy newborn occurrence among those receiving IS treatment was 3.73 times higher than that of those not receiving treatment during pregnancy (95% CI=1.40–9.91; z=2.64, $p=0.008$).

Conclusion: Our study results demonstrates that pregnancy can induce the onset or relapse of attacks in NMOSD patients. The increased NLR value and disease activity may be a predictor for PRAs in patients with NMOSD. Moreover, administration of IS treatment during pregnancy can reduce the relapse rate. However, the dosage of drugs and risks of adverse effects to the fetus need to be considered. Future prospective studies with larger sample sizes are needed to confirm and extend our findings.

Keywords: pregnancy, aquaporin-4, neuromyelitis optica spectrum disorder, neutrophil-to-lymphocyte ratio, autoimmune diseases

1 INTRODUCTION

Neuromyelitis optica spectrum disorder (NMOSD) is a serious, recurrent antibody-mediated inflammatory demyelination disorder that is mainly characterized by optic neuritis and transverse myelitis; however, it can also affect other areas of the central nervous system (e.g., the brainstem and hypothalamus). This disease causes blindness, paralysis, cognitive impairment (1). Several studies have suggested increased relapse rates and a higher risk of disability in patients with NMOSD occurring during pregnancy and the postpartum period (2, 3). Because NMOSD relapse during pregnancy has adverse effects on both the pregnant woman and the fetus, researchers have suggested the maintained administration of immunosuppressive (IS) treatment for NMOSD following pregnancy (4). However, there have been few cohort studies on the curative effect of IS treatment with respect to prognosis and relapse rates in pregnant patients with seropositive NMOSD (5, 6). Until now, cohort studies have been limited by their small number of cases (7). Delgado et al. were the first to retrospectively analyze the obstetric outcome of patients with NMOSD and AQP4-IgG positivity in Latin America, and only one pregnancy was reported after the first manifestation of NMOSD among 50 pregnancies as there was a decrease in the desire for motherhood after the diagnosis of NMOSD (8). Therefore, it is difficult to interpret the results and make clear conclusions as to whether IS treatment during pregnancy can prevent disease relapse.

Aquaporin-4 IgG is a specific diagnostic and serological marker of NMOSD (9) that binds to AQP4 in astrocyte feet and regulates complement recruitment and activation, thereby inducing complement-dependent cytotoxicity and leading to astrocyte damage (10). Additionally, effector neuroinflammatory cells (including eosinophils, neutrophils, and macrophages attracted by proinflammatory cytokines) lead to astrocytic death, secondary oligodendrocyte injury, and axonal injury (11). Substantial sex hormone shifts occur during gestation and puerperium in NMOSD, and this can alter the amount and function of AQP4 IgG and also the activation of effector neuroinflammatory cells (3). Therefore, pregnancy is a risk factor for relapse in NMOSD patients (12). The neutrophil-to-lymphocyte ratio (NLR) is a novel inflammatory marker and an easily obtained parameter (13). The NLR has been used to predict prognosis and disease activity in many neurologic demyelinating diseases, including NMOSD (14) and multiple sclerosis (15), and in other systemic immunologic diseases, such as systemic lupus erythematosus (16), Sjogren's syndrome (SS) (17), and Behçet's disease (18). There are no previous studies on the association between relapse rate (RR) and the NLR in patients with pregnancy-related NMOSD.

Therefore, the primary objective of this cohort study was to summarize the demographic and clinical characteristics of patients with pregnancy-related NMOSD attacks. We analyzed the risk factors for pregnancy-related attacks (PRAs), including IS treatment and NLR. In addition, we performed a meta-analysis to investigate the efficacy of IS treatments in reducing the RR during pregnancy in women with NMOSD.

2 METHODS

2.1 Meta Analysis

2.1.1 Data Sources and Searches

Two reviewers independently searched the PubMed, Embase, and Cochrane Library databases for articles published in English (without any temporal restrictions). A combination search of MeSH terms and keywords related to "pregnancy" and "neuromyelitis optica" was used in our meta-analysis. The studies were read thoroughly in order to evaluate the appropriateness of their inclusion in the meta-analysis. Cohort studies or case series comprising patients diagnosed with NMOSD prior to pregnancy or for the first-time during pregnancy were included. We excluded studies that enrolled fewer than five patients and those that did not examine the main variables of interest. From the 270 studies initially identified, 7 fulfilled the inclusion criteria and were included. The flowchart of the search strategy is shown in **Figure 1**. The RRs, miscarriage rates and occurrence rate of unhealthy newborns for NMOSD patients treated with or without IS during pregnancy were extracted from these studies. Two reviewers independently screened the titles, abstracts, and full texts; any differences in opinion were resolved *via* discussion and consensus.

2.1.2 Statistical Analysis

The data extracted from the included studies were analyzed using Review Manager 5.4 software (RevMan Corp, Houston, TX, USA). Heterogeneity in RRs, miscarriage rates and occurrence rate of unhealthy newborns was determined using the I^2 index, with an I^2 value greater than or equal to 50% indicating moderate or high heterogeneity (19). When $p > 0.1$ and $I^2 \leq 50\%$, we used a fixed-effect model to conduct the meta-analysis; otherwise, a random-effects model was used. Statistical significance was set at $p < 0.05$.

2.2 Retrospective Analysis

2.2.1 Study Population

We collected data on clinical and diagnostic characteristics, therapy management, and pregnancy outcomes of pregnancy-related AQP4 positive NMOSD patients admitted to the Second Xiangya Hospital of Central South University between August 2000 and August 2020. All patients diagnosed with NMOSD met the diagnostic criteria established in 2015 (1), including those admitted before 2015. Cases lost to follow-up were excluded from the study. This study was approved by the Medical Ethics Committee of Second Xiangya Hospital of Central South University, and informed consent was obtained from all participants *via* telephone interview. This study had no adverse influence on the rights or welfare of patients. This study was conducted in accordance with the Declaration of Helsinki and with the utmost respect for patient privacy; we ensured the confidentiality of all patient information.

2.2.2 Clinical Data Collection

We collected medical data for the 33 patients enrolled in this cohort, including age at conception, relapse rate, pregnancy outcomes, clinical manifestations, routine blood test results,

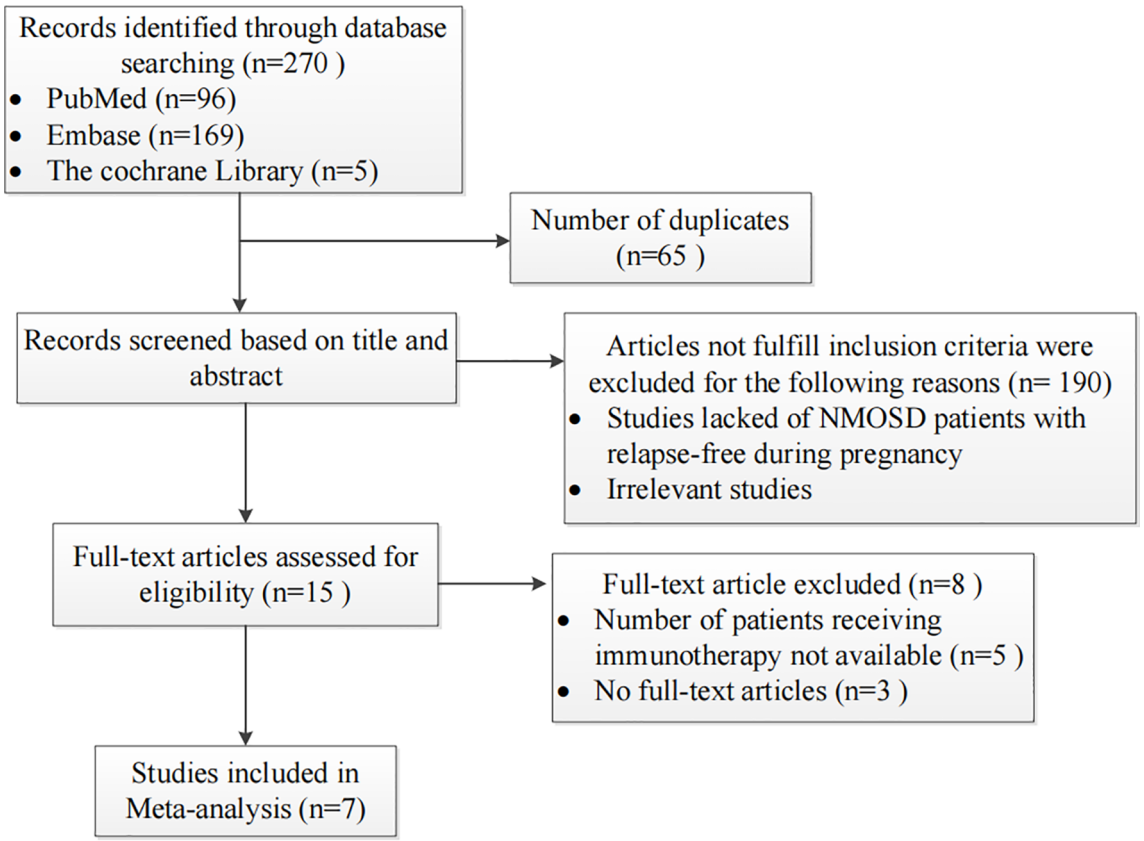

FIGURE 1 | Flow chart presenting the process of study selection for the pregnancy-related neuromyelitis optica spectrum disorder (NMOSD) meta-analysis.

serological analysis of autoantibodies, imaging features, Expanded Disability Status Scale (EDSS) scores, treatment management, and time interval between last relapse and conception. In NMOSD patients who received IS treatment, the blood test results used were those obtained at the beginning of the second trimester of pregnancy (since IS treatment started at the beginning of the second trimester of pregnancy), while in those with PRAs who did not receive IS treatment, these data were obtained at relapse, before IS treatment (intravenous methylprednisolone or intravenous immunoglobulin). Blood test results of NMOSD patients without PRAs who did not receive IS treatment were obtained at the beginning of the second trimester.

Blood sample were tested for analysis of auto-antibodies and NLR. AQP4-IgG was assessed using cell-based transfection immunofluorescence assay (CBA) in a laboratory of neuroimmunology (20). The NLR was calculated as the ratio of absolute neutrophil count to absolute lymphocyte count. This ratio is influenced by different physiological and medical conditions as well as by some medications. Some of the influencing factors include (1) pregnancy; (2) presence of autoimmune (including rheumatoid arthritis, SS, SLE, and inflammatory bowel disease), cardiometabolic (including diabetes mellitus, hypertension, and dyslipidemia) or liver diseases; malignancies; or hematologic conditions; (3) blood transfusions during the last four months, as well as use of antiplatelet medications (such as aspirin and clopidogrel); and (4) treatment with hormones, gamma-globulins, and immunosuppressive drugs in the past 6 months. For the analysis of NLR, we excluded the data of patients who met one or more of the above factors, except for autoimmune diseases and pregnancy. We also excluded those who lacked information on blood counts or had missing follow-up information in the medical records. Those with evidence of other infections were also excluded (13, 17, 21).

The EDSS scores were evaluated by two experienced neurologists to determine the severity of neurological deficits. EDSS scores were assessed at onset or relapse of NMOSD during pregnancy or within 1 year postpartum in patients with PRA, while it was assessed at the first trimester of the postpartum period in patients without PRA. At 1 year after delivery, all patients underwent EDSS evaluation again. Magnetic resonance imaging (MRI) results showing characteristic lesions in the optic nerve, spinal cord, and brain were defined as abnormal, while normal brain images and unspecific demyelinating brain lesions were defined as normal (1, 14).

Referring to previous research (22), the definitions used in the current study were as follows: (1) *informative pregnancies* were

defined as all pregnancies occurring after the onset of NMOSD as well as all patients in whom the disease presented during the pregnancy or within 12 months postpartum; (2) *PRA* was defined as onset or relapse occurring during pregnancy or within 12 months after delivery or abortion; (3) *relapses* were defined as new or substantially worsened neurological symptoms lasting for at least 24 hours and a new or enhancing lesion on MRI so as to exclude pseudorelapses (23); (4) *pregnancy with IS treatment* was defined as a pregnancy in which the patient was on IS treatment (including corticosteroids, azathioprine [AZA], or rituximab) during at least 7 months of the pregnancy; (5) *pregnancy without IS treatment* was defined as a pregnancy in which the patient did not receive any IS treatment before or during pregnancy; and (6) *miscarriage* was defined as a spontaneous loss of intrauterine pregnancy during the first 24 weeks.

2.2.3 Statistical Analysis

All statistical analyses were performed using Statistical Package for Social Sciences software (version 26.0; IBM Corp, Armonk, NY, USA). The Kolmogorov–Smirnov test was used to determine whether sample data were normally distributed. Continuous data conforming to a normal distribution were expressed as means ± standard deviations (SDs). When continuous data were normally distributed, we used Student's t-tests to identify the differences between groups; otherwise, differences were examined using the Mann–Whitney U-test. The between-group differences in categorical variables were analyzed using Fisher's exact tests. The predictive value of NLR for the prognosis of patients with NMOSD was analyzed using receiver-operating characteristic (ROC) curves, and the optimal cut-off point for continuous variables was determined based on the maximum Youden index (21). A P-value <0.05 was considered statistically significant.

3 RESULTS

3.1 Pregnancy Outcomes

We retrospectively screened 117 women with AQP4 antibody-positive NMOSD. Nineteen NMOSD patients were excluded because they were lost to follow-up. Among the 98 informative NMOSD patients, we enrolled 33 patients with informative pregnancies, which included 34 pregnancies in total. Of these, 23 patients (69.7%) had PRAs. **Figure 2** shows the clinical characteristics of the 23 patients who had at least one PRA. Attacks were most common during the first trimester after delivery/abortion (n=21, 65.6%).

3.2 Demographic and Clinical Characteristics

In total, 23 NMOSD patients with 24 informative pregnancies were included in this study. Of these, 12 (50%) were pregnant after NMOSD onset and 12 (50%) were diagnosed with NMOSD during pregnancy or within 1 year postpartum. The disease characteristics of NMOSD with informative pregnancies are presented in **Table 1**. The mean age at conception was 27.75 years, and the mean disease duration at the time of pregnancy was 1.5 months; these results were similar among the two groups. These 24 informative pregnancies included 13 term deliveries, 4 premature deliveries, 6 elective abortions, and 1 spontaneous miscarriage; further, 5 patients had preeclampsia. The reasons for elective abortions were NMOSD attacks resulting in serious neurological impairments during pregnancy (n=5) and concerns over medication side effects (n=1). Patients with single or multiple symptoms underwent disease confirmation using brain MRI-compatible lesions. NMOSD onset during pregnancy or within 1 year of the postpartum period was more likely to present with optic neuritis (p=0.012). The MRI-compatible lesions found in these 24 pregnancies included optic nerve lesions in 13 patients, myelitis lesions in 15 patients, lesions in the dorsal medulla/area postrema associated with area postrema syndrome in 4 patients, and other NMOSD-typical brain lesions in 9 patients. Fifteen patients had complications with other autoimmune diseases/antibodies, and extractable nuclear antigen positivity was the most common presentation in both groups (especially SS A/B-positive cases).

3.3 Effect of Clinical Indicators on the Severity of Neurological Dysfunction

In order to evaluate the effects of the clinical indicators on the severity of neurological impairment at disease onset or relapse in patients with pregnancy-related NMOSD attacks, we grouped the pregnancy-related NMOSD patients into mild-to-moderate and severe groups according to their EDSS scores (≤3 or >3) as previously described (14). **Table 2** shows the comparisons of demographic and clinical features according to EDSS scores during pregnancy based on NMOSD onset or relapse. Compared with patients in the mild-to-moderate group, those in the severe group were more likely to have MRI abnormalities in the spinal cord (p<0.001) or present with combined myelitis and optic neuritis symptoms (p=0.019). Besides, concomitant antibodies were more commonly seen in the severe group (p=0.004).

3.4 IS Treatment During Pregnancy

In our study, all the patients suspended IS treatment six months before pregnancy. Among these, 14 patients were relapse free during the first trimester and started to receive IS treatment at the beginning of the second trimester of pregnancy (to avoid adverse effects of the drugs on the fetus during early pregnancy). Among these 14, 6 patients were treated with 10 mg prednisone, 5 were treated with 40 mg prednisone, 1 received two rituximab injections during the second trimester of pregnancy and one rituximab injection every six months after delivery, and 2 were treated with AZA (at 100 mg) along with 20 mg of prednisone. Ten patients were relapse-free during pregnancy, eight accepted IS treatment, and two received no drug treatment (these patients were diagnosed with optic neuritis before pregnancy). Of the 8 patients who received IS treatment, the pregnancy outcomes included five term deliveries, two premature deliveries, and one elective abortion (due to concerns about the side effects of AZA).

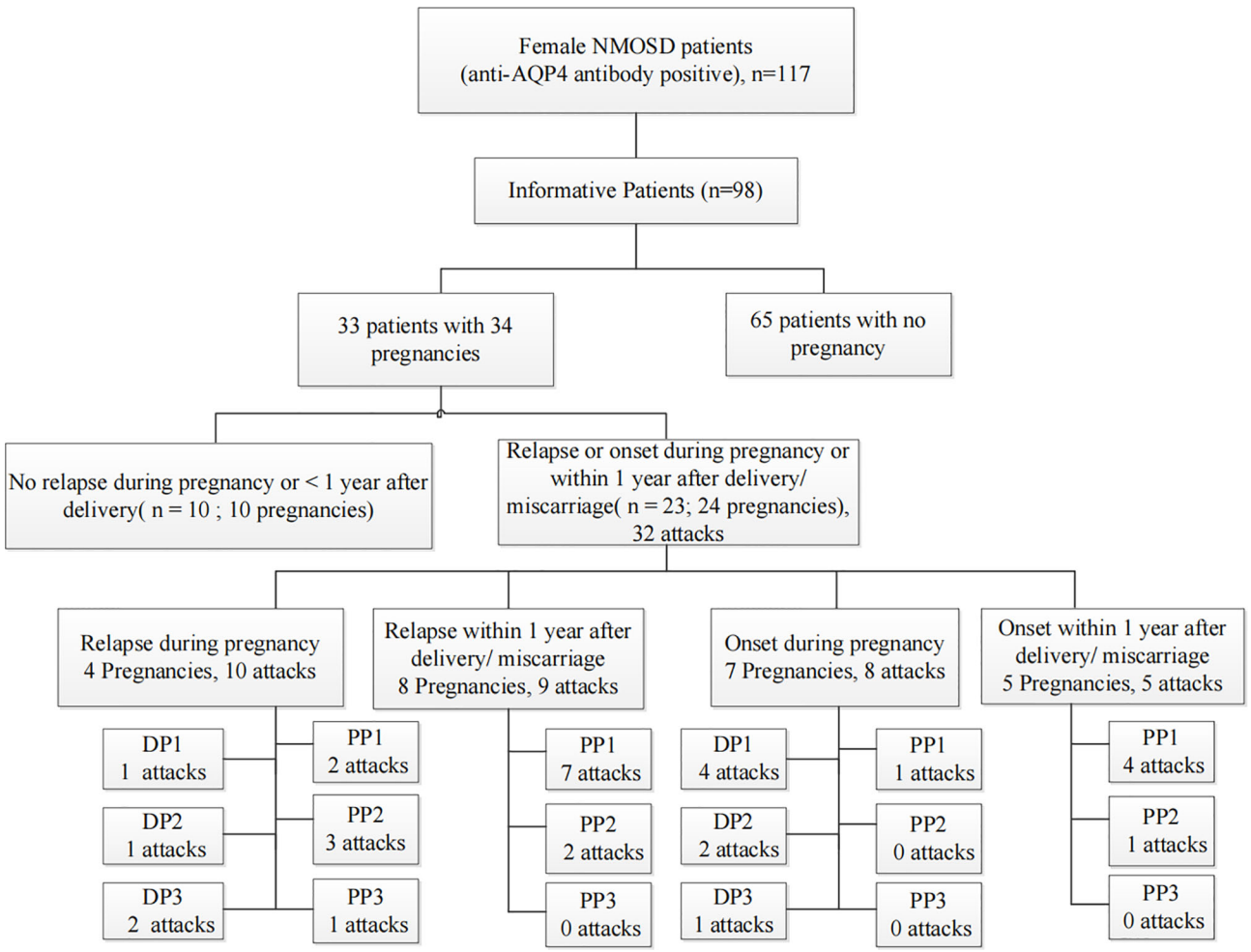

FIGURE 2 | Summative statistics by study population. An informative pregnancy was defined as cases in which an attack occurred during pregnancy or within 1 year after delivery or abortion. DP, the period during pregnancy; DP1, during the first trimester of pregnancy; DP2, during the second trimester of pregnancy; DP3, during the third trimester of pregnancy; PP, within 1 year of the postpartum period; PP1, the first trimester of the postpartum period; PP2, the second trimester of the postpartum period; PP3, 7–12 months of the postpartum period.

Additionally, 6 patients were treated with 10 mg prednisone only; all of these patients had a relapse during pregnancy. Among these 6 patients, the pregnancy outcomes included 1 term delivery, 3 premature deliveries, and 2 elective abortions due to severe neurological dysfunction during pregnancy (n=2).

We compared the RRs of patients treated with and without IS treatment during pregnancy; retrospective studies have been conducted in this regard in eight other study populations, including ours (5, 22, 24–28). The main characteristics of these studies are summarized in **Table 3**. These studies were all retrospective, and 167 patients with 223 PRAs from seven studies were included in the meta-analysis. **Figure 3A** shows a forest plot of the mean differences in the RR ratio before and after IS therapy. Heterogeneity analysis showed results of I=0% and p=0.70 within the Q test, suggesting that there was no heterogeneity among the studies selected for our analysis. Therefore, we decided to use the fixed-effects model to calculate the combined effect quantity. The combined effect RR for the 8 included studies was 0.47 (0.35-0.62; z=5.18, p<0.001). This result indicates that maintenance of IS treatment during pregnancy can significantly reduce the RR of NMOSD. The RR for those receiving IS treatment was 0.47 times that of patients not receiving treatment during pregnancy. Because only eight studies were included, a funnel plot was not constructed.

In addition, we also compared the miscarriage rates and occurrence rate of unhealthy newborns between patients who underwent and did not undergo IS treatment during pregnancy to explore the safety of IS treatment in the abovementioned eight populations. **Figure 3B** shows a forest plot of the mean differences in the miscarriage rate before and after IS therapy. The combined effect of the miscarriage rate for the 8 included studies was 1.29 (95%CI=0.68-2.43; z=0.77, p=0.44). This result indicates that maintenance of IS treatment during pregnancy had no effect on the miscarriage rate for NMOSD. However, the

TABLE 1 | Demographic and clinical characteristics of patients with pregnancy-related NMOSD attacks.

Pregnancies	Pregnancy after NMOSD onset, n=12	NMOSD onset during pregnancy or within 1 year of the postpartum period, n=12	*P*-value
Age at conception, years, mean (SD)	27.75 (5.04)	27.92 (4.74)	0.934
Mean disease duration at time of pregnancy, months, mean (SD)	1.5 (1.0)	2.1 (1.16)	0.198
Pregnancy outcome			
Term delivery	7	6	1.000
Elective abortion	1	5	0.155
Premature delivery	3	1	0.590
Miscarriage	1	0	1.000
Preeclampsia	2	3	1.000
Clinical syndromes, n	12	12	
Myelitis and optic neuritis	8	2	0.036*
Optic neuritis and acute brainstem syndrome	1	1	1.000
Myelitis and area postrema syndrome	1	0	1.000
Optic neuritis and area postrema syndrome	1	0	1.000
Myelitis and acute brainstem syndrome	0	2	0.478
Myelitis and symptomatic cerebral syndrome with NMOSD-typical brain lesions	0	1	1.000
Symptomatic cerebral syndrome with NMOSD-typical brain lesions	0	3	0.217
Acute diencephalic clinical syndrome with NMOSD-typical brain lesions	0	1	1.000
Area postrema syndrome	1	1	1.000
Myelitis	0	1	1.000
MRI Characteristic			
Optic nerve lesion	10	3	0.012*
LETM	9	6	0.400
Dorsal medulla/area postrema lesions	2	2	1.000
Other NMOSD-typical brain lesions	1	8	0.009*
Concomitant with autoimmune diseases/antibodies, n	10	5	0.089
ANA	4	2	0.640
ENA	9	5	0.214
TPO- ab and TG- ab	2	2	1.000

**p < 0.05. ANA, antinuclear antibody; ENA-ab, extractable nuclear antigen antibody; NMOSD, neuromyelitis optica spectrum disorder; TG-ab, thyroglobulin antibody; TPO-ab, thyroid peroxidase antibody; LETM, Longitudinal extensive transverse myelitis; Mean disease duration at time of pregnancy: the time from the symptom onset to alleviation.*

TABLE 2 | Clinical characteristics of patients with pregnancy-related NMOSD attack according to the EDSS score at NMOSD onset or relapse.

Clinical Characteristics	EDSS (≤3), n = 7	EDSS (>3), n = 17	*P*-value
Age at conception, years, mean (SD)	29.57 (4.39)	27.18 (4.84)	0.271
AQP4 IgG titers			1.000
≤1:32	4	8	
>1:32	3	9	
Clinical manifestations, n			
Optic neuritis and acute brainstem syndrome	2	0	0.076
Myelitis and optic neuritis	0	10	0.019*
Myelitis and symptomatic cerebral syndrome	0	1	1.000
Optic neuritis and area postrema syndrome	1	0	0.292
Myelitis and area postrema syndrome	0	1	1.000
Myelitis and acute brainstem syndrome	0	2	1.000
Myelitis	0	1	1.000
Area postrema syndrome	2	0	0.076
Symptomatic cerebral syndrome	1	2	1.000
Acute diencephalic clinical syndrome	1	0	0.292
MRI Characteristic			
Optic nerve lesion	3	10	0.659
LETM	0	15	<0.001*
Dorsal medulla/area postrema lesions	3	1	0.059*
Other NMOSD-typical brain lesions	4	5	0.356
Concomitant with autoimmune diseases/antibodies, n	1	14	0.004*

**p < 0.05. NMOSD, neuromyelitis optica spectrum disorder; LETM, Longitudinal extensive transverse myelitis.*

unhealthy newborn proportions for those receiving IS treatment was 3.73 times that of patients not receiving IS treatment during pregnancy (95%CI=1.40–9.91; z=2.64, p=0.008) (**Figure 3C**), which suggests that IS treatment during pregnancy may have an adverse effect on the health of the neonates. Among the 209 neonates included in this meta-analysis, 13 were unhealthy, with diagnoses of low birth weight (n=7), splenomegaly (n=1), thrombocytopenia (n=1), undeveloped external ear (n=1),

TABLE 3 | Clinical characteristics of 167 patients with 223 pregnancy-related neuromyelitis optica spectrum disorder attacks from 7 studies included in the meta-analysis.

Reference (year)	Type of research	Patient No.	Pregnancies No.	Pregnancy Outcome	AQP4 IgG(+) during pregnancy No.
Kim et al. (5)	Retrospective	29	33	Kim et al. Term delivery and Premature delivery (24) Miscarriage (6)	32
Collongues et al. (22)	Retrospective	28	38	Collongues et al. Term delivery and Premature delivery (28) Miscarriage (9)	38
Wang et al. (24)	Retrospective	60	76	Wang et al. Term delivery and Premature delivery (43) Miscarriage (4)	50
Shi et al. (25)	Retrospective	16	22	Salvador et al. Term delivery (13) Premature delivery (20) Miscarriage (3)	18
Salvador et al. (27)	Retrospective	19	30	Term delivery (1) Premature delivery (5) Miscarriage (3)	30
Wuebbolt et al. (28)	Retrospective	4	12	Term delivery (5) Premature delivery (5) Miscarriage (2)	9
Shimizu et al. (26)	Retrospective	11	12	Term delivery (9) Premature delivery (2) Miscarriage (2)	12

dacrocyte obstruction and scoliosis (n=1), congenital fusion of the syndactyly, and cerebral ischemia(n=1).

3.5 Variables as Predictor of Pregnancy Related Attack in NMOSD

We compared demographic and clinical factors between NMOSD patients with and without PRAs (**Table 4**). The EDSS score at the PRA phase or up to 1 year after pregnancy did not differ between the two groups. However, the EDSS score increased significantly at 1 year after delivery/abortion in pregnancies with PRAs compared with the EDSS score at relapse during pregnancy (p=0.039).

Those with NMOSD with PRAs exhibited a higher NLR at the beginning of the second trimester or at relapse (prior to methylprednisolone therapy or PLEX treatment; p<0.001) as compared to those with NMOSD who were PRA-free (**Figure 4A**). As mentioned before, autoimmune diseases/antibodies and pregnancy status can also influence NLR; therefore, we conducted a subgroup analysis to avoid the influence of the pregnancy and autoimmune antibody status. We first grouped NMOSD patients with PRA into two groups: one group of subjects who had an attack during pregnancy, and a second group comprised of subjects who had an attack within the first year of the postpartum period; we compared the NLR values during pregnancy in NMOSD patients with and without PRAs (**Figure 4C**). Next, we excluded the NLR value in patients with concomitant autoimmune antibodies and performed a comparison to address the confounders of pregnancy status and autoimmune antibody (**Figure 4E**). As can be seen in **Figures 4C, E**, a higher NLR was seen in those with NMOSD with PRAs, and the ROC curve for this is presented in **Figures 4B, D, F**.

The time interval between last relapse (with typical NMOSD-MRI lesions) and conception was shorter in NMOSD patients with PRA compared with NMOSD patients without PRA (**Figure 4G**). Based on the ROC curve, the optimal cut-off values of the time interval for the prediction of the NMOSD relapse during pregnancy was 10.5 months (**Figure 4H**).

4 DISCUSSION

NMOSD is primarily mediated by humoral immunity, and pregnancy plays a regulatory role in the development of NMOSD (25). Pregnancy induces significant changes in the hormonal and immunological environment. The fetoplacental unit synthesizes Th2 cytokines that induce the downregulation of maternal Th1 cytokines, thereby mediating cellular immunity, increasing humoral immunity, and helping maintain a successful pregnancy (30). However, an enhanced generation of autoantibodies is stimulated by increased Th2-mediated immune responses and elevated maternal humoral immunity during pregnancy (31). We analyzed the pregnancy-related characteristics of patients with AQP4-positive NMOSD and found that some cases had disease onset during pregnancy. Among the 23 patients with PRAs, 12 were first diagnosed with NMOSD during pregnancy or within 1 year after delivery/abortion. The onset of NMOSD during pregnancy may result from immunological changes occurring during pregnancy, which may stimulate the production of AQP4-ab. AQP4 is expressed in the human placenta during gestation and plays a regulatory role in the maternal–fetal fluid exchange between placental cells and fetal capillaries in healthy mothers (32, 33). We found increased levels of AQP4 in the placenta and fetal membrane in a patient with acute disseminated encephalomyelitis onset in pregnancy as compared to that in a healthy control; this may be due to the activation of the HMGB1/TLR4/Nf-kB/IL-6 pathway (34). Therefore, we speculate that the increased levels of AQP4 on the placenta were mistakenly identified as "foreign proteins" due to the alteration of the immunological state during pregnancy, leading to the occurrence of autoimmune reactions and stimulating production of AQP4-ab in the serum. However, the miscarriage rate in our study was low (1/3), which is inconsistent with previous findings that NMOSD induces high miscarriage rates (5, 35). Further studies are needed to determine whether anti-AQP4 IgG-mediated pathogenesis increases the miscarriage rate. Additionally, we observed that the attacks commonly occurred in the first trimester of the postpartum period after delivery/abortion (65.6%), which is in accordance with the results of a previous cohort study of pregnancy-related NMOSD (24).

Optic neuritis and myelitis are the most common manifestations of pregnancy-related NMOSD. However, it was interesting to find a slight discrepancy in MRI characteristics between the pregnancy-related NMOSD subgroups. Lesions in the optic nerve are more common in patients who become pregnant after NMOSD onset, whereas patients diagnosed with NMOSD during pregnancy or within 1 year after delivery/abortion more commonly presented with acute

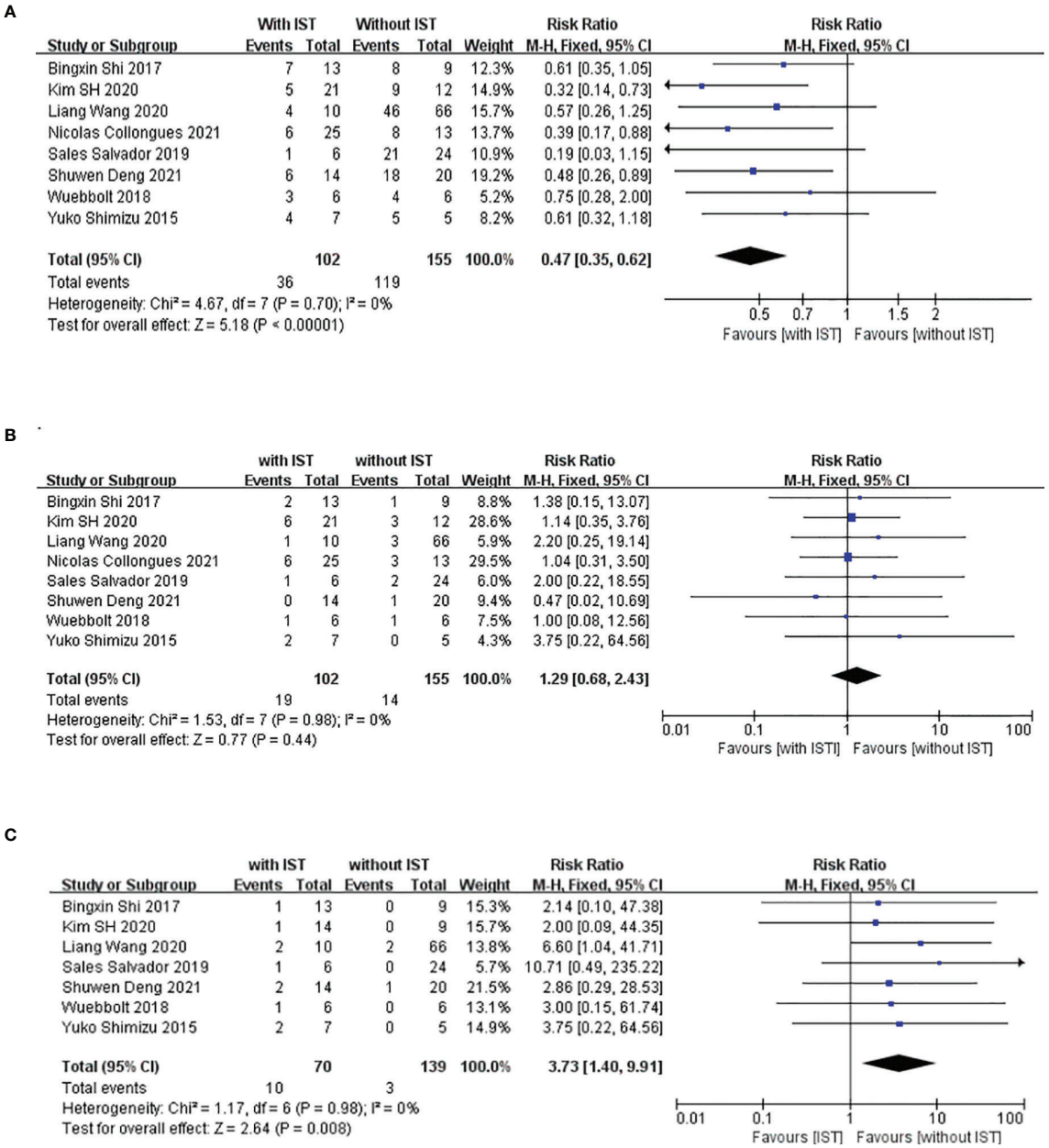

FIGURE 3 | Meta-analysis of immune-suppression treatment during pregnancy and relapse rate (RR), incidence of unhealthy neonates, and miscarriage. This figure presents a meta-analysis of 8 studies (including our study) of the association between maintenance immunosuppression treatment during pregnancy and RR **(A)**, miscarriage rate **(B)** and incidence of unhealthy neonates **(C)**.

encephalic lesions. To our knowledge, this discrepancy was first observed in our study, although these findings require larger cohorts for confirmation.

Attack during pregnancy significantly increased disability in NMOSD patients at 1 year after pregnancy (12). The EDSS score increased significantly at 1 year after delivery or abortion in pregnancies with PRAs, which was also demonstrated in a study by Shi et al. (25). In addition, pregnancy-related NMOSD concomitant with autoimmune diseases/antibodies increased the severity of neurological injury. In our study, the most common autoimmune disease coexisting with NMOSD was SS with SS-A and SS-B positivity. The existence of the SS-A antibody may represent a state of enhanced autoimmune inflammatory response and lead to more severe inflammatory damage. A similar result was found in a study conducted by Akaishi et al, showing that the EDSS score for the acute phase in NMOSD was significantly higher in patients with comorbid SS than in those without comorbid SS (36). Gupta et al.

TABLE 4 | Comparison of clinical characteristics and the outcomes between NMOSD patients with and without pregnancy-related NMOSD attack.

Clinical Characteristics	Pregnancies after NMOSD onset with PRA, n=24	Pregnancies without pregnancy-related attack, n=10	*P*-value
Age at conception, years, mean (SD)	27.88 (4.75)	28.02 (4.76)	0.945
Pregnancy outcome			
Term delivery	13	7	0.467
Elective abortion	6	1	0.644
Premature delivery	4	2	1.000
Miscarriage	1	0	1.000
Preeclampsia	5	1	0.794
NLR at conception or within 1 year of the postpartum period (prior to IS treatment), mean (SD)	7.85 (3.98)	3.98 (1.08)	<0.001*
EDSS score during conception or within 1 year of the postpartum period, mean (SD)	4.84 (1.94)	4.70 (1.23)	0.826
EDSS score at 1 year after delivery, mean (SD)	5.95 (1.61)	4.95 (1.21)	0.086
Unhealthy newborn	1	2	0.201
Concomitant with autoimmune diseases/antibodies, n	15	3	0.134

*$p < 0.05$. NLR, neutrophil-to-lymphocyte ratio; NMOSD, neuromyelitis optica spectrum disorder; EDSS, Expanded Disability Status Scale.

demonstrated that the severity and relapse rates for SS were exacerbated during the period after delivery (37).

Pregnancy without PRAs is associated with IS treatment. We reviewed eight populations (including those from our study) and performed a meta-analysis the results of which demonstrated that IS treatment can reduce the risk of relapse during pregnancy as well as in the postpartum period. Collongues et al. observed a tendency among patients who continued their treatment during pregnancy to have fewer relapses as compared to those who interrupted their treatment before pregnancy (22). Moreover, Wang et al. suggested that maintenance therapy with appropriate immunosuppression or a sufficient dose of oral steroids should be administered during pregnancy as well as during the postpartum period (24).

The maintenance of IS treatment during pregnancy needs to be considered on an individual basis. Previous studies have stated that it is safe to use low-dose prednisone during pregnancy, as the estimated fetal level is only 10% of the maternal level (25, 38). However, chronic use of corticosteroids during pregnancy may result in premature delivery; 2 of 13 patients who received prednisone in our study had premature deliveries, and both of them delivered a baby with low birth weight. Previous studies revealed that daily use of low-dose prednisone does not affect fetal health; however, this type of use does not reduce the RR (25–27). Similar results were found in our study since six patients treated only with 20 mg prednisone had a relapse during pregnancy. Therefore, the literature to date indicates that the dosage of prednisone should be upregulated during single drug maintenance; more studies are needed to identify the specific dose. Although AZA may be a safe therapy for patients with NMOSD occurring during pregnancy (39), many patients in our cohort refused to use AZA during pregnancy because of concerns about the adverse effects of this drug. In relation to this, monoclonal antibodies are increasingly used in pregnancy (40, 41). In our cohort, only one patient, who received rituximab therapy, was relapse-free during pregnancy and delivered a healthy baby. The effectiveness and safety of rituximab for NMSOD, administered in pregnancy, has been rarely reported in cohort studies (29). A cohort study conducted in Germany demonstrated that anti-CD20 mAbs can effectively control progression and relapse in women with NMOSD during pregnancy or after delivery or abortion; moreover, it is safe to use CD20 mAbs within 6 months prior to pregnancy (42). Until now, limited data has been reported on the effectiveness and safety of IS treatment. The meta-analysis conducted in this study showed that the maintenance of IS treatment during pregnancy had no adverse effect on the miscarriage rate among those with NMOSD, while the occurrence rate of unhealthy newborns was elevated. Low birth weight was most common presentation among the unhealthy newborns, based on summarized data from the included studies, despite the fact that this factor has little life-threatening effect for newborns. However, administration of IS treatment during pregnancy still needs careful consideration.

At present, the relevance of the NLR in the recurrence or onset of NMOSD during pregnancy is unclear. Previous studies have observed a correlation between the NLR and RR in NMOSD. Zhou et al. demonstrated that the NLR is an independent risk factor for the severity of neurological dysfunction in patients at the first attack of NMOSD (14). Contentti et al. suggested that the NLR does not appear to act as an independent predictor of worse outcomes and that the NLR may be quite limited as a biomarker of disease activity (13). Therefore, the predictive role of the NLR as an independent predictor of worse outcomes is controversial. To our knowledge, our study is the first to analyze the relationship between the NLR and pregnancy-related NMOSD. We found that pregnancy with a PRA was associated with a higher NLR at relapse during pregnancy and that the value increased significantly compared with that during the remission period. According to our results, the NLR may be an effective predictor of PRAs. In addition, it would be crucial to determine the disease activity prior to pregnancy (the time interval between last relapse and conception) since it can be a predictor of relapse attack during pregnancy.

The primary limitations of our study include its retrospective nature and small sample size. Both the generalizability and robustness of our findings may be affected by these limitations.

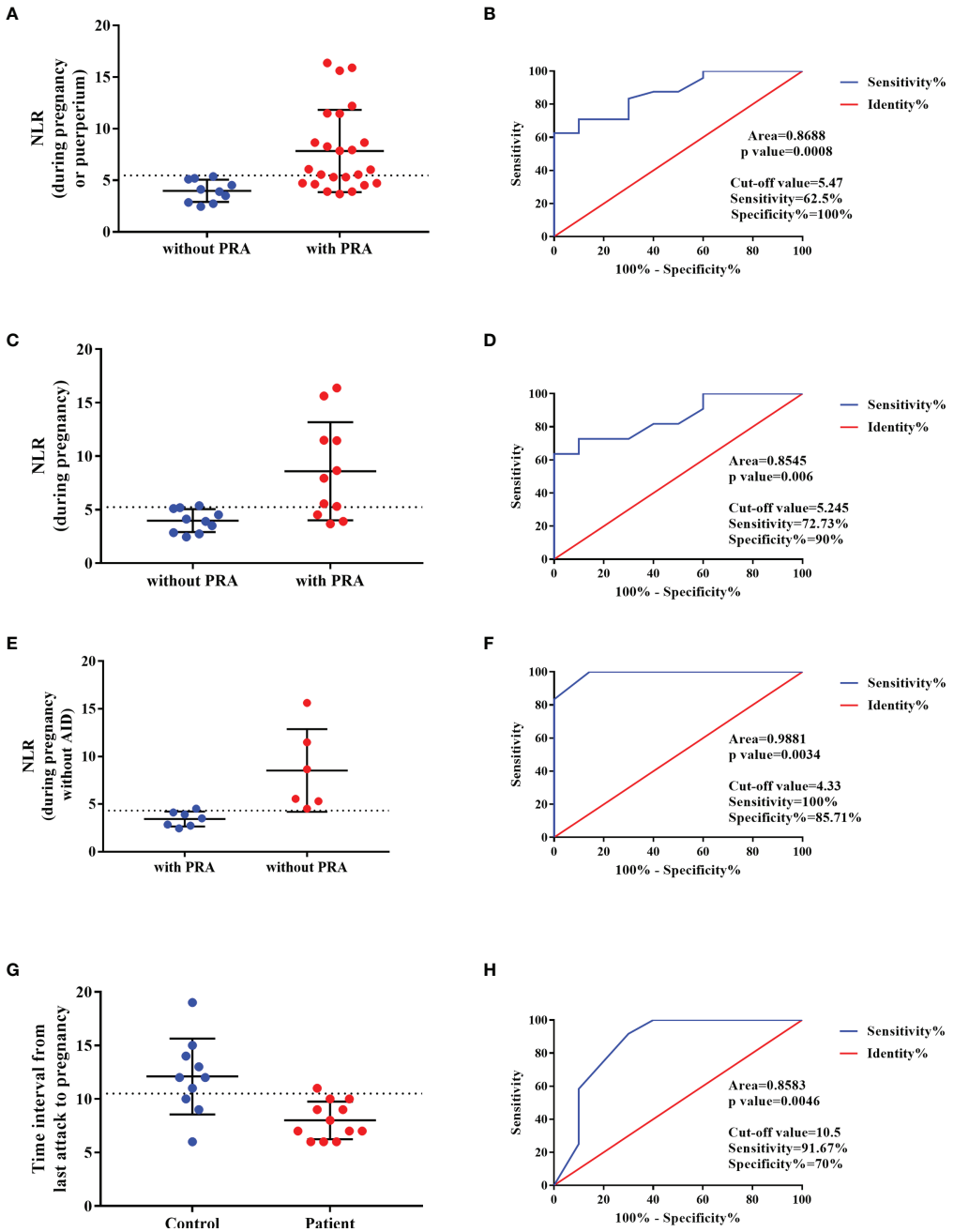

FIGURE 4 | Predictor of the NMOSD relapse during pregnancy. **(A, C, E)** NLR value in NMOSD with pregnancy-related attacks (PRAs) compared to those with NMOSD who were PRA-free, and the ROC curve for this is presented in **(B, D, F)**, respectively. **(G)** The time interval between last relapse and conception in NMOSD patients with PRA compared with NMOSD patients without PRA and the ROC curve was built in **(H)**.

Even though increased NLR may be predictor for PRAs in NMOSD, it is influenced by different physiological and medical conditions as well as pregnancy itself. Further prospective studies with larger sample sizes are needed to clarify our findings. Besides, the EDSS score retrospectively evaluated from the patient chart may influence the result in this study. In addition, relatively few studies were included in our meta-analysis due to the sparsity of the literature; the funnel plot to exclude publication bias was, therefore, not constructed.

Our study demonstrates that pregnancy-related NMOSD attacks occurred mostly in the first trimester after delivery/abortion. Moreover, increased NLR and short time interval between last relapse and conception may be a predictor for PRAs in NMOSD. In addition, maintenance of IS therapy during

pregnancy and after delivery or abortion can reduce the risk of relapse; however, it can also increase the incidence of unhealthy newborns. Therefore, administration of IS treatment during pregnancy to prevent relapse should be done considering the dosage of drugs and after evaluating the risks of adverse effects to the fetus.

DATA AVAILABILITY STATEMENT

The raw data supporting the conclusions of this article will be made available by the authors, without undue reservation.

ETHICS STATEMENT

This study was approved by the Medical Ethics Committee of Second Xiangya Hospital of Central South University, and informed consent was obtained from all participants via telephone interview. This study had no adverse influence on the rights or welfare of patients. This study was conducted in accordance with the Declaration of Helsinki and with the utmost respect for patient privacy; we ensured the confidentiality of all patient information.

AUTHOR CONTRIBUTIONS

SD drafted the manuscript. QL and SD carried out the literature review. WL contributed to and finalized the draft. All authors contributed to the article and approved the submitted version.

FUNDING

This work was funded by the Natural Science Foundation of Hunan Province (#2020JJ4798).

REFERENCES

1. Wingerchuk DM, Banwell B, Bennett JL, Cabre P, Carroll W, Chitnis T, et al. International Consensus Diagnostic Criteria for Neuromyelitis Optica Spectrum Disorders. *Neurology* (2015) 85(2):177–89. doi: 10.1212/WNL.0000000000001729
2. Zare-Shahabadi A, Langroodi HG, Azimi AR, Sahraian MA, Harirchian MH, Baghbanian SM. Neuromyelitis Optica and Pregnancy. *Acta Neurol Belg* (2016) 116(4):431–8. doi: 10.1007/s13760-016-0654-x
3. Davoudi V, Keyhanian K, Bove RM, Chitnis T. Immunology of Neuromyelitis Optica During Pregnancy. *Neurol: Neuroimmunol Neuroinflamm* (2016) 3(6): e288. doi: 10.1212/NXI.0000000000000288
4. Mao-Draayer Y, Thiel S, Mills EA, Chitnis T, Fabian M, Katz Sand I, et al. Neuromyelitis Optica Spectrum Disorders and Pregnancy: Therapeutic Considerations. *Nat Rev Neurol* (2020) 16(3):154–70. doi: 10.1038/s41582-020-0313-y
5. Kim SH, Huh SY, Jang H, Park NY, Kim Y, Jung JY, et al. Outcome of Pregnancies After Onset of the Neuromyelitis Optica Spectrum Disorder. *Eur J Neurol* (2020) 27(8):1546–55. doi: 10.1111/ene.14274
6. Veerachit-O-larn T, Siritho S, Prayoonwiwat N. Retrospective Study of the Adverse Events of the Treatment for an Acute Attack of Neuromyelitis Optica Spectrum Disorder. *Ther Apher Dialysis* (2020) 24(4):453–60. doi: 10.1111/1744-9987.13456
7. D'Souza R, Wuebbolt D, Andrejevic K, Ashraf R, Nguyen V, Zaffar N, et al. Pregnancy and Neuromyelitis Optica Spectrum Disorder - Reciprocal Effects and Practical Recommendations: A Systematic Review. *Front Neurol* (2020) 11:544434. doi: 10.3389/fneur.2020.544434
8. Delgado-García G, Chávez Z, Rivas-Alonso V, Corona T, Flores-Rivera J. Obstetric Outcomes in a Mexican Cohort of Patients With AQP4-Antibody-Seropositive Neuromyelitis Optica. *Mult Scler Relat Disord* (2018) 25:268–70. doi: 10.1016/j.msard.2018.08.015
9. Jarius S, Wildemann B. Aquaporin-4 Antibodies (NMO-IgG) as a Serological Marker of Neuromyelitis Optica: A Critical Review of the Literature. *Brain Pathol* (2013) 23(6):661–83. doi: 10.1111/bpa.12084
10. Papadopoulos MC, Verkman AS. Aquaporin 4 and Neuromyelitis Optica. *Lancet Neurol* (2012) 11(6):535–44. doi: 10.1016/S1474-4422(12)70133-3
11. Wu Y, Zhong L, Geng J. Neuromyelitis Optica Spectrum Disorder: Pathogenesis, Treatment, and Experimental Models. *Mult Scler Relat Disord* (2019) 27:412–8. doi: 10.1016/j.msard.2018.12.002
12. Borisow N, Hellwig K, Paul F. Neuromyelitis Optica Spectrum Disorders and Pregnancy: Relapse-Preventive Measures and Personalized Treatment Strategies. *EPMA J* (2018) 9(3):249–56. doi: 10.1007/s13167-018-0143-9
13. Carnero Contentti E, Delgado-Garcia G, Criniti J, Lopez PA, Pettinicchi JP, Cristiano E, et al. An Abnormally High Neutrophil-To-Lymphocyte Ratio Is Not an Independent Outcome Predictor in AQP4-IgG-Positive NMOSD. *Front Immunol* (2021) 12:628024. doi: 10.3389/fimmu.2021.628024
14. Zhou Y, Xie H, Zhao Y, Zhang J, Li Y, Duan R, et al. Neutrophil-To-Lymphocyte Ratio on Admission is an Independent Risk Factor for the Severity of Neurological Impairment at Disease Onset in Patients With a First Episode of Neuromyelitis Optica Spectrum Disorder. *Neuropsychiatr Dis Treat* (2021) 17:1493–503. doi: 10.2147/NDT.S311942
15. Fahmi RM, Ramadan BM, Salah H, Elsaid AF, Shehta N. Neutrophil-Lymphocyte Ratio as a Marker for Disability and Activity in Multiple Sclerosis. *Mult Scler Relat Disord* (2021) 51:102921. doi: 10.1016/j.msard.2021.102921
16. Li Z, Xiao Y, Zhang L. Application of Procalcitonin, White Blood Cell Count and Neutrophil-to-Lymphocyte Ratio in the Diagnosis of Systemic Lupus Erythematosus With a Bacterial Infection. *Ann Palliat Med* (2020) 9(6):3870–6. doi: 10.21037/apm-20-1777
17. Zhang K, Li W, He C, He X, Hou J. The Ratio of Neutrophil to Lymphocyte Predicts Interstitial Lung Disease and its Prognosis in Patients With Primary Sjögren's Syndrome: A Retrospective Analysis. *Ann Palliat Med* (2021) 10 (6):6493–501. doi: 10.21037/apm-21-1043
18. Shadmanfar S, Masoumi M, Davatchi F, Shahram F, Akhlaghi M, Faezi ST, et al. Correlation of Clinical Signs and Symptoms of Behçet's Disease With Platelet-to-Lymphocyte Ratio (PLR) and Neutrophil-to-Lymphocyte Ratio (NLR). *Immunol Res* (2021) 69(4):363–71. doi: 10.1007/s12026-021-09194-4
19. Gao F, Chai B, Gu C, Wu R, Dong T, Yao Y, et al. Effectiveness of Rituximab in Neuromyelitis Optica: A Meta-Analysis. *BMC Neurol* (2019) 19(1):36–6. doi: 10.1186/s12883-019-1261-2
20. Waters PJ, McKeon A, Leite MI, Rajasekharan S, Lennon VA, Villalobos A, et al. Serologic Diagnosis of NMO: A Multicenter Comparison of Aquaporin-4-IgG Assays. *Neurology* (2012) 78(9):665–671; discussion 669. doi: 10.1212/WNL.0b013e318248dec1
21. Xie H, Zhao Y, Pan C, Zhang J, Zhou Y, Li Y, et al. Association of Neutrophil-to-Lymphocyte Ratio (NLR) With the Prognosis of First Attack Neuromyelitis Optica Spectrum Disorder (NMOSD): A Retrospective Cohort Study. *BMC Neurol* (2021) 21(1):389. doi: 10.1186/s12883-021-02432-0
22. Collongues N, Alves Do Rego C, Bourre B, Biotti D, Marignier R, da Silva AM, et al. Pregnancy in Patients With AQP4-Ab, MOG-Ab, or Double-Negative Neuromyelitis Optica Disorder. *Neurology* (2021) 96(15):e2006–15. doi: 10.1212/WNL.0000000000011744
23. Solomon JM, Paul F, Chien C, Oh J, Rotstein DL. A Window Into the Future? MRI for Evaluation of Neuromyelitis Optica Spectrum Disorder Throughout

the Disease Course. *Ther Adv Neurol Disord* (2021) 14:17562864211014389. doi: 10.1177/17562864211014389
24. Wang L, Zhou L, ZhangBao J, Huang W, Chang X, Lu C, et al. Neuromyelitis Optica Spectrum Disorder: Pregnancy-Related Attack and Predictive Risk Factors. *J Neurol Neurosurg Psychiatry* (2020) 92(1):53–61. doi: 10.1136/jnnp-2020-323982
25. Shi B, Zhao M, Geng T, Qiao L, Zhao Y, Zhao X. Effectiveness and Safety of Immunosuppressive Therapy in Neuromyelitis Optica Spectrum Disorder During Pregnancy. *J Neurol Sci* (2017) 377:72–6. doi: 10.1016/j.jns.2017.03.051
26. Shimizu Y, Fujihara K, Ohashi T, Nakashima I, Yokoyama K, Ikeguch R, et al. Pregnancy-Related Relapse Risk Factors in Women With Anti-AQP4 Antibody Positivity and Neuromyelitis Optica Spectrum Disorder. *Mult Scler* (2016) 22(11):1413–20. doi: 10.1177/1352458515583376
27. Salvador NRS, Brito MNG, Alvarenga MP, Alvarenga RMP. Neuromyelitis Optica and Pregnancy-Puerperal Cycle. *Mult Scler Relat Disord* (2019) 34:59–62. doi: 10.1016/j.msard.2019.05.007
28. Wuebbolt D, Nguyen V, D'Souza R, Wyne A. Devic Syndrome and Pregnancy: A Case Series. *Obstet Med* (2018) 11(4):171–7. doi: 10.1177/1753495X18758868
29. Ciron J, Audoin B, Bourre B, Brassat D, Durand-Dubief F, Laplaud D, et al. Recommendations for the Use of Rituximab in Neuromyelitis Optica Spectrum Disorders. *Rev Neurol* (2018) 174(4):255–64. doi: 10.1016/j.neurol.2017.11.005
30. Tong Y, Liu J, Yang T, Kang Y, Wang J, Zhao T, et al. Influences of Pregnancy on Neuromyelitis Optica Spectrum Disorders and Multiple Sclerosis. *Mult Scler Relat Disord* (2018) 25:61–5. doi: 10.1016/j.msard.2018.07.006
31. Perricone C, de Carolis C, Perricone R. Pregnancy and Autoimmunity: A Common Problem. *Best Pract Res Clin Rheumatol* (2012) 26(1):47–60. doi: 10.1016/j.berh.2012.01.014
32. De Falco M, Cobellis L, Torella M, Acone G, Varano L, Sellitti A, et al. Down-Regulation of Aquaporin 4 in Human Placenta Throughout Pregnancy. *Vivo (Athens Greece)* (2007) 21(5):813–7.
33. Martínez N, Damiano AE. Aquaporins in Fetal Development. *Adv Exp Med Biol* (2017) 969:199–212. doi: 10.1007/978-94-024-1057-0_13
34. Deng S, Qiu K, Tu R, Zheng H, Lu W. Relationship Between Pregnancy and Acute Disseminated Encephalomyelitis: A Single-Case Study. *Front Immunol* (2020) 11:609476. doi: 10.3389/fimmu.2020.609476
35. Nour MM, Nakashima I, Coutinho E, Woodhall M, Sousa F, Revis J, et al. Pregnancy Outcomes in Aquaporin-4-Positive Neuromyelitis Optica Spectrum Disorder. *Neurology* (2016) 86(1):79–87. doi: 10.1212/WNL.0000000000002208
36. Akaishi T, Takahashi T, Fujihara K, Misu T, Fujimori J, Takai Y, et al. Impact of Comorbid Sjogren Syndrome in Anti-Aquaporin-4 Antibody-Positive Neuromyelitis Optica Spectrum Disorders. *J Neurol* (2021) 268(5):1938–44. doi: 10.1007/s00415-020-10377-6
37. Gupta S, Gupta N. Sjögren Syndrome and Pregnancy: A Literature Review. *Permanente J* (2017) 21:16–47. doi: 10.7812/TPP/16-047
38. de Vetten L, van Stuijvenberg M, Kema IP, Bocca G. Maternal Use of Prednisolone Is Unlikely to be Associated With Neonatal Adrenal Suppression-A Single-Center Study of 16 Cases. *Eur J Pediatr* (2017) 176 (8):1131–6. doi: 10.1007/s00431-017-2949-1
39. Gomes SZ, Araujo F, Bandeira CL, Oliveira LG, Hoshida MS, Zugaib M, et al. The Impact of Immunosuppressive Drugs on Human Placental Explants. *Reprod Sci* (2019) 26(9):1225–34. doi: 10.1177/1933719118812739
40. Ciplea AI, Langer-Gould A, de Vries A, Schaap T, Thiel S, Ringelstein M, et al. Monoclonal Antibody Treatment During Pregnancy and/or Lactation in Women With MS or Neuromyelitis Optica Spectrum Disorder. *Neurol(R) Neuroimmunol Neuroinflamm* (2020) 7(4):e723. doi: 10.1212/NXI.0000000000000723
41. Miranda-Acunã J, Rivas-Rodríguez E, Levy M, Ansari M, Stone R, Patel V, et al. Rituximab During Pregnancy in Neuromyelitis Optica: A Case Report. *Neurol: Neuroimmunol Neuroinflamm* (2019) 6(2):e542. doi: 10.1212/NXI.0000000000000542
42. Kümpfel T, Thiel S, Meinl I, Ciplea AI, Bayas A, Hoffmann F, et al. Anti-CD20 Therapies and Pregnancy in Neuroimmunologic Disorders: A Cohort Study From Germany. *Neurol(R) Neuroimmunol Neuroinflamm* (2021) 8(1):e913. doi: 10.1212/NXI.0000000000000913

Conflict of Interest: The authors declare that the research was conducted in the absence of any commercial or financial relationships that could be construed as a potential conflict of interest.

Publisher's Note: All claims expressed in this article are solely those of the authors and do not necessarily represent those of their affiliated organizations, or those of the publisher, the editors and the reviewers. Any product that may be evaluated in this article, or claim that may be made by its manufacturer, is not guaranteed or endorsed by the publisher.

frontiers in Neurology

ORIGINAL RESEARCH
published: 14 January 2022
doi: 10.3389/fneur.2021.807646

Single-Cell Transcriptome Profiling Unravels Distinct Peripheral Blood Immune Cell Signatures of RRMS and MOG Antibody-Associated Disease

*Ju Liu[1], Xiaoyan Yang[1], Jiali Pan[1], Zhihua Wei[1], Peidong Liu[2], Min Chen[1] and Hongbo Liu[1]**

[1] Department of Neurology, The First Affiliated Hospital of Zhengzhou University, Zhengzhou, China, [2] Department of Neurosurgery, The First Affiliated Hospital of Zhengzhou University, Zhengzhou, China

OPEN ACCESS

Edited by:
Yu Cai,
University of Nebraska Medical Center, United States

Reviewed by:
Sonemany Salinthone,
Oregon Health & Science University, United States
Zengmin Miao,
Shandong First Medical University, China
Surendra Sarsaiya,
Zunyi Medical University, China

***Correspondence:**
Hongbo Liu
liuhongbo6279@126.com

Specialty section:
This article was submitted to Multiple Sclerosis and Neuroimmunology, a section of the journal Frontiers in Neurology

Received: *02 November 2021*
Accepted: *16 December 2021*
Published: *14 January 2022*

Citation:
Liu J, Yang X, Pan J, Wei Z, Liu P, Chen M and Liu H (2022) Single-Cell Transcriptome Profiling Unravels Distinct Peripheral Blood Immune Cell Signatures of RRMS and MOG Antibody-Associated Disease. Front. Neurol. 12:807646. doi: 10.3389/fneur.2021.807646

Relapsing-remitting multiple sclerosis (RRMS) and myelin oligodendrocyte glycoprotein (MOG) antibody-associated disease (MOGAD) are inflammatory demyelinating diseases of the central nervous system (CNS). Due to the shared clinical manifestations, detection of disease-specific serum antibody of the two diseases is currently considered as the gold standard for the diagnosis; however, the serum antibody levels are unpredictable during different stages of the two diseases. Herein, peripheral blood single-cell transcriptome was used to unveil distinct immune cell signatures of the two diseases, with the aim to provide predictive discrimination. Single-cell RNA sequencing (scRNA-seq) was conducted on the peripheral blood from three subjects, i.e., one patient with RRMS, one patient with MOGAD, and one patient with healthy control. The results showed that the $CD19^+$ $CXCR4^+$ naive B cell subsets were significantly expanded in both RRMS and MOGAD, which was verified by flow cytometry. More importantly, RRMS single-cell transcriptomic was characterized by increased naive $CD8^+$ T cells and cytotoxic memory-like Natural Killer (NK) cells, together with decreased inflammatory monocytes, whereas MOGAD exhibited increased inflammatory monocytes and cytotoxic CD8 effector T cells, coupled with decreased plasma cells and memory B cells. Collectively, our findings indicate that the two diseases exhibit distinct immune cell signatures, which allows for highly predictive discrimination of the two diseases and paves a novel avenue for diagnosis and therapy of neuroinflammatory diseases.

Keywords: RRMS, MOGAD, peripheral blood, single-cell RNA sequencing, biomarker

INTRODUCTION

Multiple sclerosis (MS) is a common chronic inflammatory demyelinating disease of the central nervous system (CNS) and the leading cause of neurologic disability in young adults (1). Globally, ∼30–300 per 100,000 adults are affected with MS, leading to a substantial economic burden on healthcare systems and societies (2, 3). MS repertoire manifests pathological characteristics of inflammation, demyelination, and axonal damage in the CNS. Among MS, relapsing-remitting MS (RRMS) is the most common type, accounting for nearly 85% of the initial diagnoses (4–6). Myelin oligodendrocyte glycoprotein (MOG) antibody-associated disease (MOGAD) is a newly classified

inflammatory demyelinating disease of CNS that shares clinical manifestations with RRMS (7–10). Hence, the detection of disease-specific serum antibody is currently regarded as the gold standard for their diagnosis, however, the serum antibody levels are unpredictable at different stages of the two diseases (11). Therefore, discovering antibody-independent biomarkers is needed.

Technological advances in single-cell RNA sequencing (scRNA-seq) have improved the understanding of the immunopathology of numerous autoimmune diseases by identifying diagnostic biomarkers (12–14). Hong et al. studied the immune cells of peripheral blood mononuclear cells (PBMCs) of patients with Primary Sjögren's syndrome by using scRNA-seq and identified some disease-specific immune cell subsets (15). Likewise, Ramesh et al. used scRNA-seq to characterize the CNS-specific B cell phenotypes in MS with paired immune repertoires and further confirmed the pathogenic role of B cells in the CNS of patients with MS (16). Schafflick et al. used single-cell transcriptomics to describe the leukocytes of cerebrospinal fluid (CSF) and identified the specific composition and transcriptome of CSF leukocytes (17). In another study, scRNA-seq was conducted on the CSF of patients with RRMS and MOGAD, and the shared myeloid populations were identified (18). However, scRNA-seq has been rarely used to decipher peripheral blood signatures of patients with RRMS or MOGAD.

In this study, peripheral blood single-cell transcriptome was used to identify immune cell signatures of RRMS and MOGAD. Our findings unveil distinct signatures of peripheral blood immune cells of patients with RRMS or MOGAD and provide a reference for diagnostic and therapeutic intervention in neuroinflammatory diseases.

MATERIALS AND METHODS

Subjects

The study was reviewed and approved by the Ethics Committee of the First Affiliated Hospital of Zhengzhou University (2021-KY-0588-002). Before the study, written informed consent was signed by each participant. Patients with RRMS or MOGAD and healthy controls (HCs) were recruited in this study (**Table 1**). The patients with RRMS and MOGAD were confirmed according to the McDonald criteria (19) and MOGAD diagnostic criteria (20), respectively. The exclusion criteria were (1) prior treatment with the immunosuppressants (e.g., azathioprine, mycophenolate mofetil, and even corticosteroids) or disease-modifying therapies (e.g., teriflunomide, fingolimod, and siponimod); (2) coexisting autoimmune disorders (e.g., systemic lupus erythematosus or Sjogren's syndrome); (3) positive with other autoimmune antibodies (e.g., anti-N-methyl D-aspartate (NMDA) receptor antibodies); (4) acute or chronic infections (e.g., respiratory tract infections, hepatitis, or tuberculosis); (5) organ dysfunction; and (6) in stable phase or in remission. The peripheral blood of each participant was collected for subsequent analysis.

Capturing and Sequencing of Single-Cell Data

As previously described (21), the PBMCs were isolated and then resuspended in prechilled phosphate-buffered saline. Trypan blue staining was used to confirm the cell viability. The single-cell suspension with more than 90% of cells was loaded onto 10 × Genomics Chromium Controller using Chromium Single Cell 3' Library and Gel Bead Kit v2 (10 × Genomics). The libraries were constructed according to the guidelines of the manufacturer. The libraries were purified by AMPure beads (Beckman Coulter, Krefeld, Germany) and then sequenced on an Illumina NovaSeq 6000 platform with 150 bp paired-end mode.

Analysis of Single-Cell Sequence Data

Data analysis for single-cell sequencing was performed as previously described (22). Briefly, read files were extracted using the Cell Ranger pipeline v2.2.0 (10 × Genomics) and then aligned to the human GRCh38 genome to generate gene expression data for each cell. Double entries were filtered using Scrublet software (23), followed by exporting the filtered gene expression matrix data into Seurat software v4.0 (24) to perform subsequent analysis. The high-quality single-cell data were normalized using the LogNormalize function, and principal component analysis was carried out. The significant principal component ($p < 1^{e-5}$) was selected to perform cluster analysis. The single cells were clustered by t-Distributed Stochastic Neighbor Embedding (tSNE), and the clusters were classified based on established markers from the CellMarker database (25). Final single-cell data visualization and exploration were generated by tSNE (26). The sequenced data have been deposited into the National Center for Biotechnology Information (NCBI) BioProject database with accession number PRJNA776659.

Flow Cytometry

Fifteen subjects, i.e., five RRMS, five MOGAD, and five HC, were recruited to conduct flow cytometry analysis (27). In brief, after removing erythrocytes using lysing solution (BD Biosciences, San Diego, CA, USA), the staining solution containing ghost dye (Tonbobio, Beijing, China) and human monoclonal specific antibody CD19 was used to stain the samples at 4°C for 30 min, and then the samples were permeated for 30 min at room temperature and then was stained with CXCR4 antibody for 30 min at room temperature. The re-suspended cells were run on a BD FACS Canto II flow cytometer (BD Biosciences, San Diego, CA, USA), and the cells were analyzed using FlowJo software (Tree Star, Ashland, OR, USA).

The antibodies used in this study to stain cells included Allophycocyanin (APC) anti-human CD19 antibody (clone SJ25C1; BioLegend, San Diego, CA, USA) 1:20, and PE anti-human CD184 (CXCR4) antibody (clone 12G5; BioLegend, San Diego, CA, USA) 1:20.

Statistical Analyses

Statistical analysis was done using Graphpad Prism 9 software (GraphPad Software Inc, La Jolla, CA, USA). One-way ANOVA was used to analyze the difference among multiple groups. The

TABLE 1 | Demographic and clinical features of subjects.

Subject	Diagnosis	Sex	Age (years)	Race	Presentation at acute phase	MOG antibody titer (serum)	Cell counts/μl	Protein, mg/dl	OB	Analysis
1	MOGAD	M	53	Han Chinese	Encephalitis and epileptic seizure	1:100	50	44	I	scRNA-seq
2	RRMS	M	37	Han Chinese	Numbness and weakness of limbs	Negative	5	23	II	scRNA-seq
3	HC	M	38	Han Chinese	NA	NA	NA	NA	NA	scRNA-seq
4	MOGAD	F	22	Han Chinese	Optic neuritis	1:10	9	13	I	Flow cytometry
5	MOGAD	M	20	Han Chinese	Encephalitis and seizure	1:1000	29	19	I	Flow cytometry
6	MOGAD	M	49	Han Chinese	ADEM	1:100	10	26	I	Flow cytometry
7	MOGAD	F	50	Han Chinese	Myelitis	1:320	36	43	I	Flow cytometry
8	MOGAD	F	33	Han Chinese	Encephalitis	1:32	32	41	I	Flow cytometry
9	RRMS	F	47	Han Chinese	Left limb weakness	Negative	10	40	I	Flow cytometry
10	RRMS	M	26	Han Chinese	Cerebellar ataxia	Negative	2	18	IV	Flow cytometry
11	RRMS	F	64	Han Chinese	lower-extremity weakness	Negative	4	38	II	Flow cytometry
12	RRMS	M	22	Han Chinese	Left lower-limb numbness and weakness	Negative	4	17	I	Flow cytometry
13	RRMS	F	21	Han Chinese	Diplopia and eye movement disorders	Negative	8	21	II	Flow cytometry
14	HC	M	49	Han Chinese	NA	NA	NA	NA	NA	Flow cytometry
15	HC	M	30	Han Chinese	NA	NA	NA	NA	NA	Flow cytometry
16	HC	F	20	Han Chinese	NA	NA	NA	NA	NA	Flow cytometry
17	HC	F	54	Han Chinese	NA	NA	NA	NA	NA	Flow cytometry
18	HC	F	52	Han Chinese	NA	NA	NA	NA	NA	Flow cytometry

ADEM, acute disseminated encephalomyelitis; HC, healthy control; ON, optic neuritis; OB, oligoclonal band; MOGAD, myelin oligodendrocyte glycoprotein (MOG) antibody-associated disease; NA, not applicable; RRMS, relapsing-remitting multiple sclerosis; scRNA-seq, single-cell RNA sequencing.

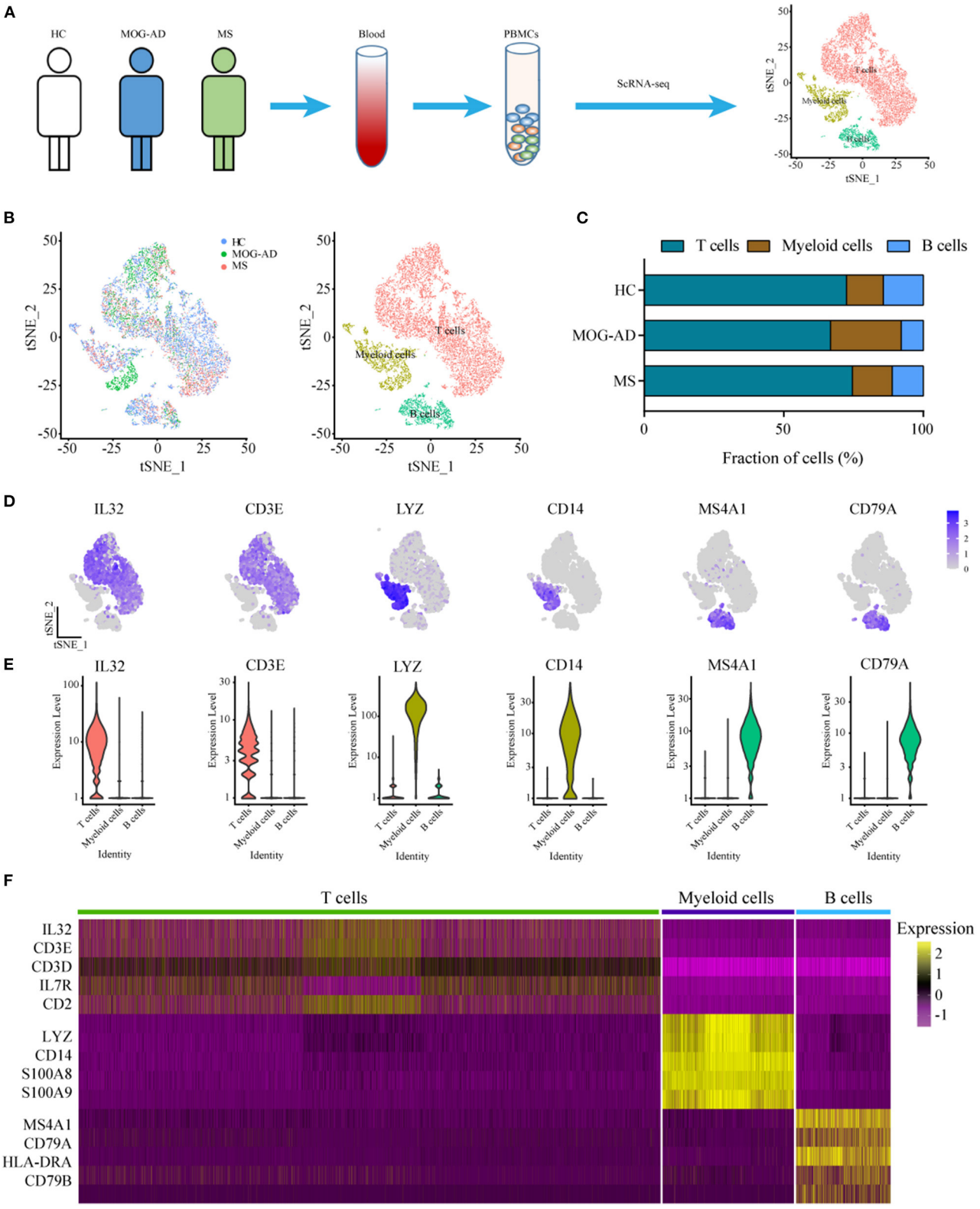

FIGURE 1 | Single-cell transcriptional profiling of PBMCs from HC, RRMS, and MOGAD. **(A)** The experimental workflow for obtaining and analyzing PBMC between all three donor groups. **(B)** The t-Distributed Stochastic Neighbor Embedding (tSNE) was used to visualize cell populations generated by unsupervised cluster analysis of PBMC. **(C)** The percentage of each cell type in HC, MS, and MOGAD. **(D)** The expression level of the marker gene in each cell type was shown. **(E)** Violin illustration shows the expression of marker genes from different known cell types. **(F)** Heatmaps shows the expression of the up- and downregulated genes in T, B, and myeloid

(Continued)

FIGURE 1 | cells. HC, healthy controls; RRMS, relapsing-remitting multiple sclerosis; MOGAD, myelin oligodendrocyte glycoprotein (MOG) antibody-associated disease; PBMC, peripheral blood mononuclear cell.

data represent the mean ± SEM. A $p < 0.05$ was considered statistically significant.

RESULTS

Single-Cell Transcriptomic of Peripheral Blood

To identify the characteristics of immune-cell subsets of peripheral blood of the patients with RRMS or MOGAD, scRNA-seq of PBMCs was performed (**Figure 1A**). A total of 18,016 cells from PBMCs (7,709 cells from HC, 3,969 cells from MOGAD, and 6,338 cells from MS) were isolated and sequenced. After removing the duplicate cells, low-quality, and empty droplets, 15,252 cells were finally collected and used in the subsequent analysis (**Supplementary Figure 1** and **Supplementary Table 1**). Unsupervised clustering analysis identified three distinct immune cell clusters (**Figure 1B** and **Supplementary Table 2**). Cluster 1 (∼72.95%) was identified as T cells based on the expression of marker genes IL32, CD3E, IL7R, CD3D, and CD2 (**Figures 1C–F**). Cluster 2 (∼14.17%) was identified as B cells based on the expression of marker genes MS4A1, CD79A, HLA-DRA, and CD79B (**Figures 1C–F**). Cluster 3 (∼12.87%) was classified as myeloid cells according to the expression of marker genes LYZ, CD14, S100A8, and S100A9 (**Figures 1C–F**). Additionally, a large set of other markers were also identified, such as GIMAP7, CD247, and LCK for T cells, ADAM28, VPREB3, and BANK1 for B cells, LST1, MNDA, FCN1, and SERPINA1 for myeloid cells (**Supplementary Table 3**). We focused on the characteristics of RRMS and MOGAD based on the three immune cell clusters in the above analysis.

Characteristics of Myeloid Cell Subsets Between RRMS and MOGAD

Further unsupervised clustering regarding the myeloid cells was performed to understand the changes of myeloid cell clusters in RRMS and MOGAD. The results showed that three monocyte subsets, classical ($CD14^{++}$ $CD16^{-}$), non-classical ($CD14^{+}$ $CD16^{++}$), and intermediate ($CD14^{++}$ $CD16^{+}$) monocytes, were identified based on the distinct markers, which were observed to be shared among all subjects (**Figures 2A,B**). Among the monocyte subsets, the $CD14^{++}$ $CD16^{-}$ cells were further subdivided into M1 and M2 based on the distinct markers where M1 cells expressed PPBP (CXXL7) and PF4 (CXCL4). In contrast, the M2 subset (inflammatory monocytes) expressed a high level of S100A8, S100A9, and S100A12 (**Figures 2C–E**, **Supplementary Table 4**). $CD14^{+}$ $CD16^{++}$ cells (M3) expressed markers CDKN1C, RHOC, and LYPD2, without S100A12 (**Figures 2C–E** and **Supplementary Table 4**). The intermediate monocytes (M4) expressed high levels of marker HLA-DPB1 and HLA-DPA1.

The percentage of M4 intermediate ($CD14^{++}$ $CD16^{+}$) monocytes was relatively higher in RRMS (2.13%) and MOGAD (1.98%) than in the HCs (1.11%) in the identified myeloid cell subsets. A comparison between RRMS and MOGAD revealed that M1 monocytes were reduced while M2 monocytes were increased in MOGAD (**Figure 2B** and **Supplementary Table 2**). The above-identified four subsets in myeloid cells showed that M4 intermediate ($CD14^{++}$ $CD16^{+}$) monocytes were expanded in RRMS and MOGAD, but M2 inflammatory monocytes were specifically enriched in MOGAD.

Characteristics of T Cell Subsets Between RRMS and MOGAD

The unsupervised clustering of T cells was conducted to understand the differences in T cell clusters between RRMS and MOGAD. Nine sub-clusters (T1-T9) were identified from 10,610 T cells based on the specific markers (**Figures 3A–D** and **Supplementary Table 5**), and 8 clusters (T1–T8) expressed high levels of CD3D and CD3E (**Figures 3D,E**). Two distinct $CD4^{+}$ T cell subsets were identified, such as naive-like CD4 T cells (T2) and T3. T2 was identified based on the expressed marker CCR7, and T3 was based on the expressed marker TNFSF3 (LTβ, an activated CD4 T-cell marker), AQP, GPR183, and LDHB (**Supplementary Table 5**). Six distinct $CD8^{+}$ T cell clusters were identified, such as cytotoxic CD8 effector T cells (T1 and T4: expressed markers FGFBP2, NKG7, and GZMH), transitional CD8 effector T cells (T6: expressed markers GZMK and KLRB1), naive $CD8^{+}$ T cells (T5: expressed markers CD27 and LEF1), and megakaryocyte-like cells (T7 and T8: expressed markers PPBP, PF4, and GNG11) (**Figures 4A–D** and **Supplementary Table 5**). In addition, we can discriminate cluster T9 from T cells based on the lower expression levels of CD3D and CD3E, indicating that cluster T9 may be Natural Killer (NK) cells. Further, the higher levels of FCER1G, GNLY, CD7, KLRF1, and KLRC2 in the T9 were also observed, implying that T9 can be classified as cytotoxic memory-like NK cells (**Figures 3A–E** and **Supplementary Table 5**).

Compared with HCs, the levels of cytotoxic CD8 effector T cells (T4) and cytotoxic memory-like NK cells (T9) were higher in both RRMS and MOGAD, whereas the fraction of megakaryocyte-like cells (T7) was relatively lower. A comparison between RRMS and MOGAD showed that the fraction of T1 subsets was increased while T5 was decreased in MOGAD (**Figure 3B** and **Supplementary Table 2**).

Characteristics of B Cell Subsets in RRMS and MOGAD

The unsupervised clustering on B cells was performed to identify the characteristics of B cell subsets in RRMS and MOGAD. The results showed that four distinct B cell clusters, i.e., plasma (B1), naive B (B2), memory B (B3) cells, and plasmacytoid DCs (B4), were identified from 1,676 B cells based on the

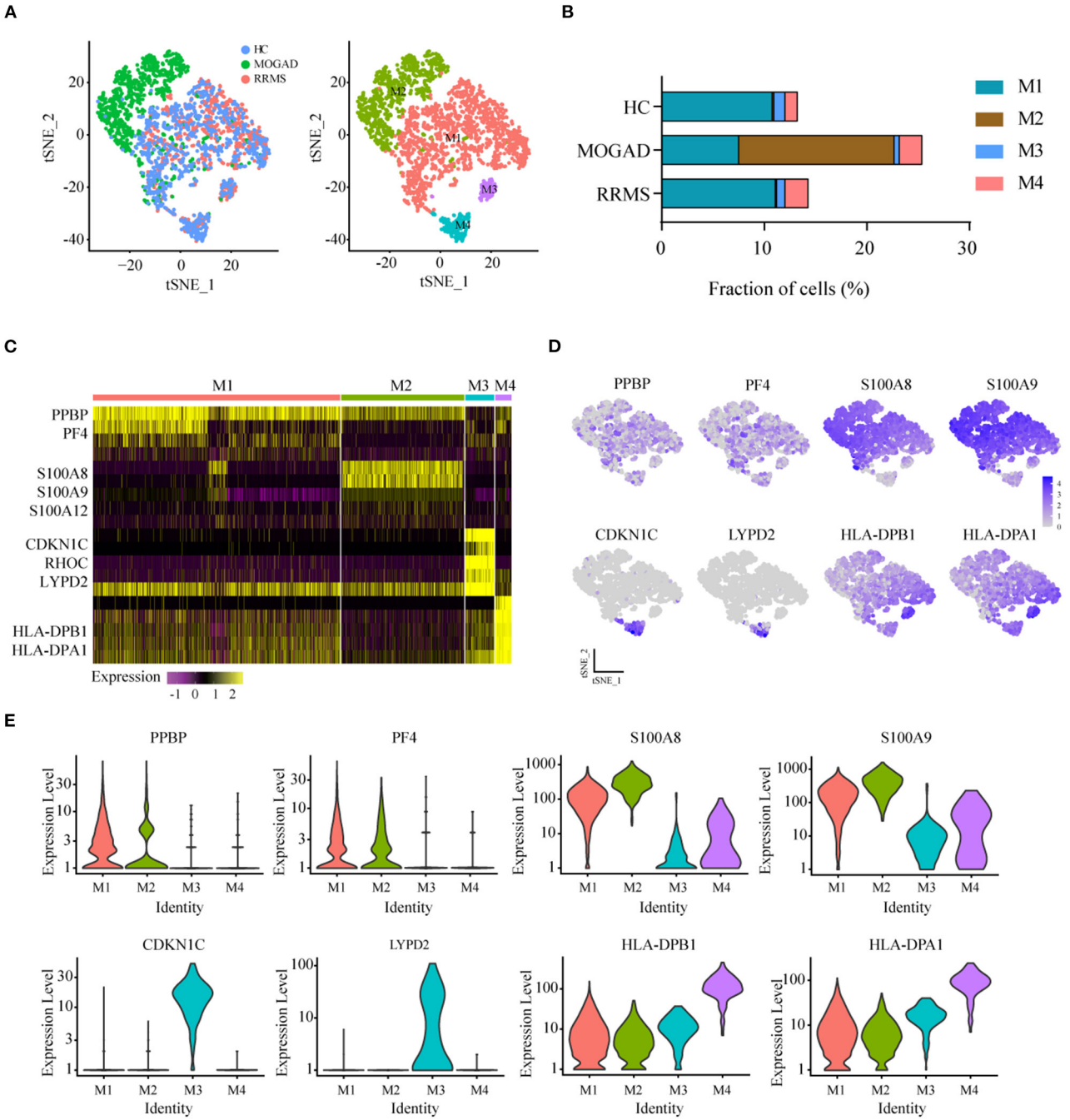

FIGURE 2 | Identification and analysis of myeloid clusters in PBMC from HC, RRMS, and MOGAD. **(A)** tSNE visualization of myeloid cells from HC, RRMS, and MOGAD. **(B)** The percentage of cells for myeloid subsets in HC, RRMS, and MOGAD. **(C)** Heatmaps shows the expression of the up- and downregulated markers in myeloid subsets. **(D)** The expression level of marker gene in each myeloid cell type was shown. **(E)** Violin illustration showed the expression of the marker genes from different myeloid cell types. HC, healthy controls; RRMS, relapsing-remitting multiple sclerosis; MOGAD, myelin oligodendrocyte glycoprotein (MOG) antibody-associated disease; PBMC, peripheral blood mononuclear cell; tSNE, t-Distributed Stochastic Neighbor Embedding.

markers from the CellMarker database (**Figures 4A–C** and **Supplementary Table 6**). Among 4 B cell subsets (**Figures 4C–E** and **Supplementary Table 6**), the B1 subset expressed plasma cell markers IGHA1 and IGHG1, indicating the presence of plasma cells. B2 subset expressed high levels of IL10 (IL10RA) and naive B cell markers IGHD and CXCR4, showing the presence of naive B cells. The B3 cluster with high expression of CD27 was similar to memory B cell, and the B4 subset based on the high expression

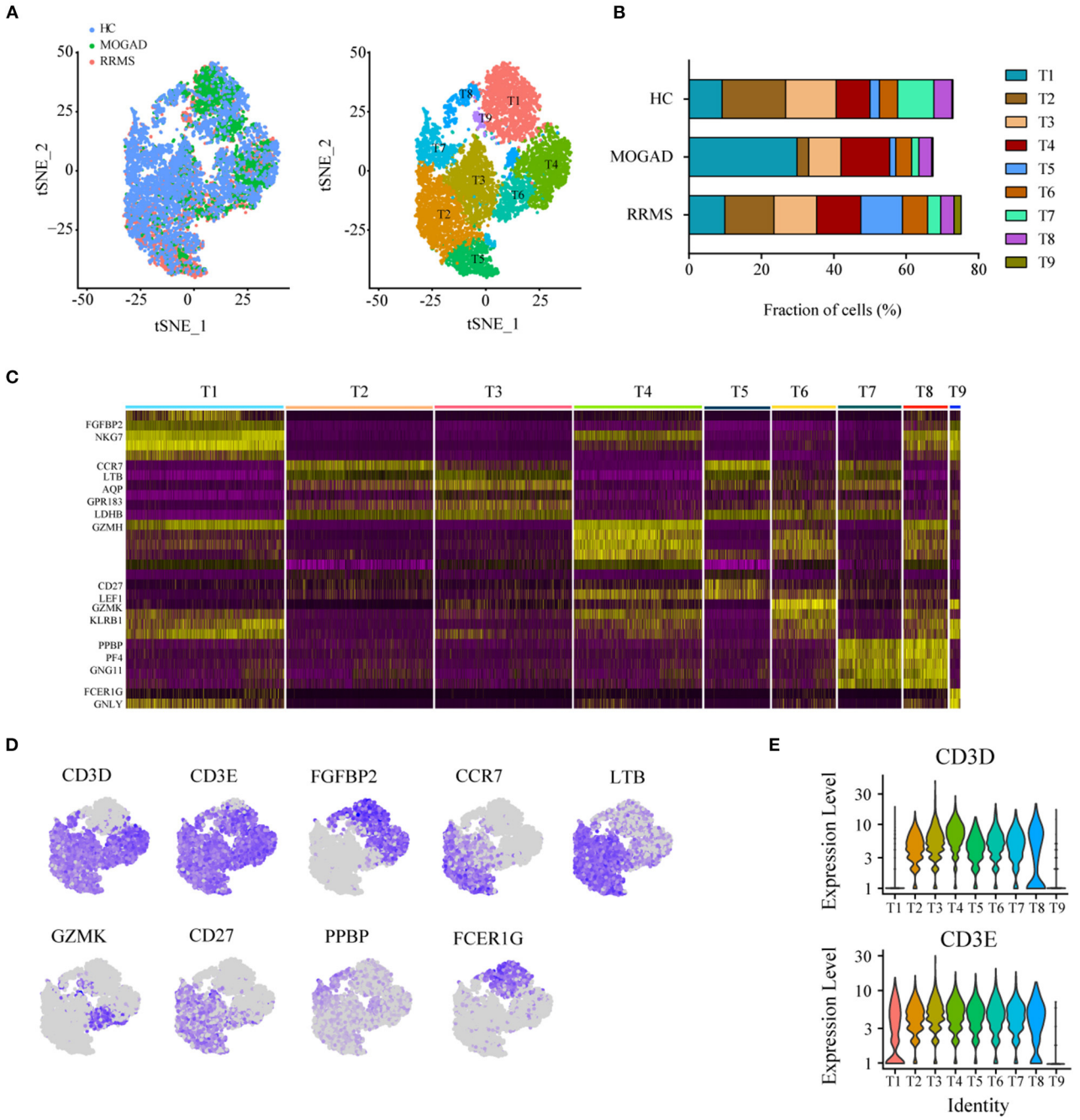

FIGURE 3 | Analysis of T cell clusters from HC, RRMS, and MOGAD. **(A)** tSNE visualization of T cells from HC, RRMS, and MOGAD. **(B)** The percentage of cells for T cell subsets in HC, RRMS, and MOGAD. **(C)** Heatmaps shows the expression of the up- and downregulated markers in T cell subsets. **(D)** The expression level of marker genes in each T cell type was shown. **(E)** Violin illustration shows the expression of the marker genes from different T cell types. HC, healthy controls; RRMS, relapsing-remitting multiple sclerosis; MOGAD, myelin oligodendrocyte glycoprotein (MOG) antibody-associated disease; PBMC, peripheral blood mononuclear cell; tSNE, t-Distributed Stochastic Neighbor Embedding.

of GZMB, CD99, and HSP90B1 was similar to plasmacytoid dendritic cells (pDC)-like cells.

Among four B cell subsets, the naive B cells (B2) were increased in RRMS and MOGAD by ∼4.29 and 5.00%, respectively, compared to HCs (∼2.60%; **Figure 4B** and **Supplementary Table 2**). The increase of naive B cells in these two diseases was confirmed by flow cytometry, which was consistent with single-cell sequencing data (**Figure 5** and **Supplementary Figure 2**). In addition, a comparison between RRMS and MOGAD revealed that the fraction of plasma cells

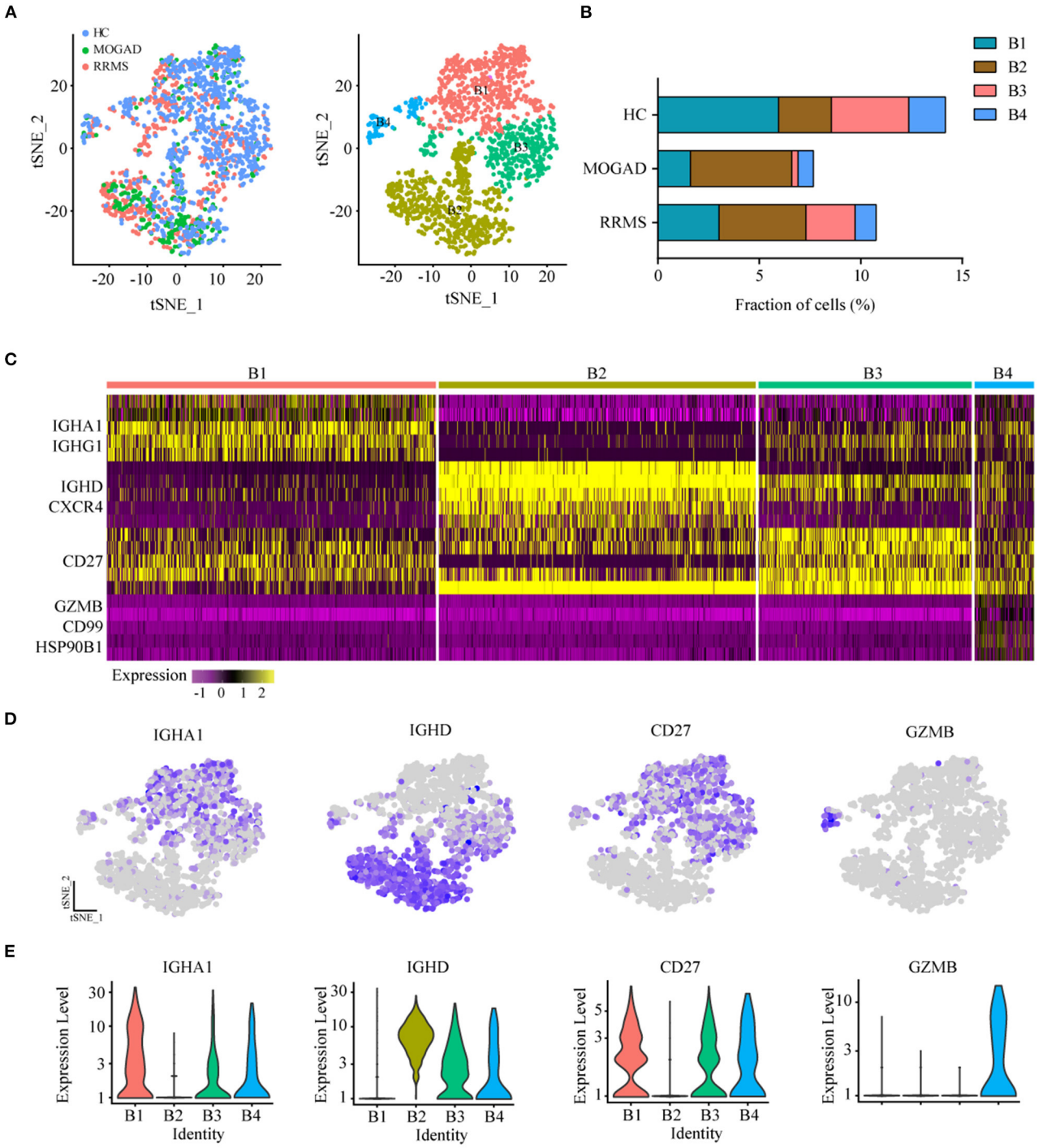

FIGURE 4 | Analysis of B cell clusters from HC, RRMS, and MOGAD. **(A)** tSNE visualization of B cells from HC, RRMS, and MOGAD. **(B)** The percentage of cells for B cell subsets in HC, RRMS, and MOGAD. **(C)** Heatmaps shows the expression of the up- and downregulated markers in B cell subsets. **(D)** The expression level of marker gene in each B cell type was shown. **(E)** Violin illustration shows the expression of the marker genes from different B cell types. HC, healthy controls; RRMS, relapsing-remitting multiple sclerosis; MOGAD, myelin oligodendrocyte glycoprotein (MOG) antibody-associated disease. PBMC, peripheral blood mononuclear cell; tSNE, t-Distributed Stochastic Neighbor Embedding.

(B1) and memory B cells (B3) numerically was reduced in MOGAD. In summary, four different subsets were identified in B cells and further revealed an expansion of naive B cells in both RRMS and MOGAD. The results also showed a reduction in the fraction of plasma and memory B cells in MOGAD than in RRMS.

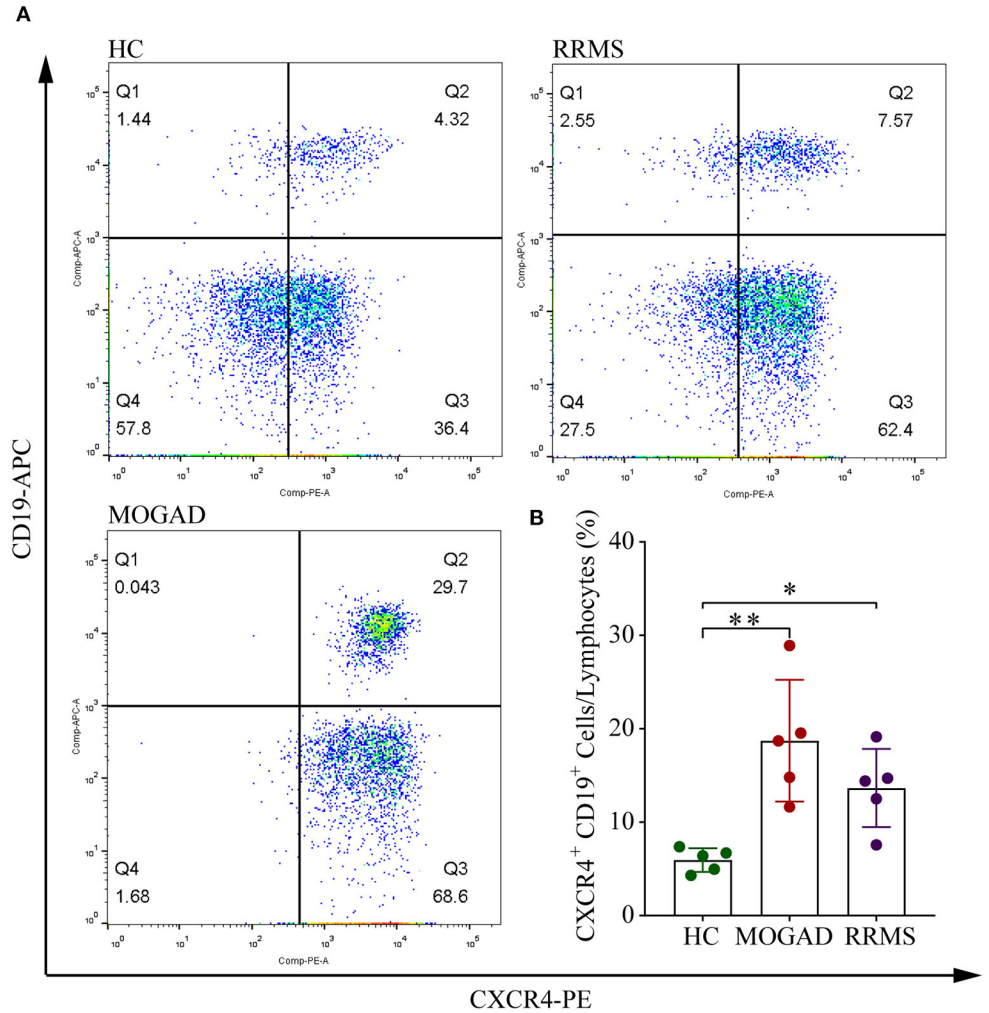

FIGURE 5 | Flow cytometry analysis of CD19$^+$ CXCR4$^+$ B cell subsets in HC, RRMS, and MOGAD. **(A)** Gating strategy of CD19$^+$ CXCR4$^+$ by flow cytometry. **(B)** Percentages of CD19$^+$ CXCR4$^+$ B cells of HC, MOGAD, and RRMS. HC, healthy controls; RRMS, relapsing-remitting multiple sclerosis; MOGAD, myelin oligodendrocyte glycoprotein (MOG) antibody-associated disease; PBMC, peripheral blood mononuclear cell. The data represent the mean ± SEM. *$p < 0.05$, **$p < 0.001$.

DISCUSSION

This study aimed to comprehensively identify the circulating immune-cell subset properties of peripheral blood in the patients with RRMS and MOGAD using scRNA-seq. The results showed the distinct immune cell signatures in RRMS and MOGAD.

Previous studies have shown that myeloid cells play protective roles in neuroinflammation (28–30). In this study, based on the established marker database, four distinct myeloid cell subsets were identified: classical (CD14^{++} CD16$^-$), non-classical (CD14$^+$ CD16^{++}), and intermediate (CD14^{++} CD16$^+$) monocytes. The CD16$^+$ monocytes play key immune surveillance roles in CNS by shifting to the inflammation sites and breaking the blood-brain barrier in neuroinflammation (31). The fraction of intermediate (CD14^{++} CD16$^+$) monocytes was observed to increase in patients with RRMS and MOGAD than in HCs, suggesting that targeting CD16$^+$ monocytes may be a feasible therapeutic strategy for RRMS and MOGAD (32), a finding which is consistent with reports from other studies (33–35). The inflammatory monocytes (M2), specifically enriched in MOGAD, expressed a high level of S100A8, S100A9, and S100A12 in the serum of patients with diverse inflammatory diseases (36, 37). The results above suggest that these inflammatory monocytes may serve as potential diagnostic indicators for MOGAD.

Inflammatory T cells play critical roles in the pathogenesis of neuroinflammatory autoimmune diseases (38, 39). Studies show that CD4$^+$ and CD8$^+$ T cells are associated with demyelinating lesions and axonal damage (40, 41). In this study, a detailed analysis of the T cells identified 2 CD4$^+$ and 6 CD8$^+$ T cell subsets. Previous studies showed that the elevated cytotoxic CD8$^+$ T cells play central roles in MS development

by recognizing myelin basic protein (42). Similarly, increased fractions of cytotoxic $CD8^+$ T cells were present in both RRMS and MOGAD, illustrating that these cells may be an indicator of the disease progression. Cytotoxic NK cells participate in the regulation of immune response and contribute to the pathogenesis of numerous autoimmune diseases (43–46). In this study, the sub-cluster analysis identified the cytotoxic memory-like NK cells, which were markedly expanded in the two diseases, especially RRMS, suggesting that the cells may contribute to disease pathogenesis.

The B cells are important weapons against infectious diseases and also contribute to numerous autoimmune diseases, such as MS (16). Evidence proves that target depletion of $CD20^+$ B cells can effectively suppress inflammatory activities in MS (47–49). After anti-CD20 treatment, the patients with MS demonstrated a reconstituted B cell repertoire different from those not receiving treatment. The reconstituted B cells were naive and can produce less proinflammatory cytokine; for example, an increase in interleukin-10 (IL-10) level may be attributed to the decrease in proinflammatory responses of T cell and myeloid-lineage across the reconstitution phase (50–52). B cells can also weaken the immune response of different stages of CNS inflammation by secreting a set of anti-inflammatory cytokines, namely, IL-10, transforming growth factor beta (TGF-β), and IL-35) (53). In this study, the relative abundance of naive B cells was increased in RRMS and MOGAD, coupled with high levels of IL-10 (54, 55). These results suggest that targeted depletion of B cells could be a feasible strategy on RRMS and MOGAD.

Our findings indicate that the two diseases exhibit distinct immune cell signatures, but several limitations should be mentioned in this study. Due to the fact that some patients were unwilling to take part in this research, the number of subjects was relatively small, which would make the result heavily depend on the specific characteristics of these individuals, such as disease stage, previous infections, other immune-related disorders/conditions, and genetic factors. Last but not least, less-frequent immune-cell populations were not identified and characterized using scRNA-seq in this work, which needs to be further studied.

CONCLUSION

In this study, we described unique peripheral blood single-cell transcriptome profiles in RRMS and MOGAD. RRMS was characterized by increased naive $CD8^+$ T cells and cytotoxic memory-like NK cells, together with decreased inflammatory monocytes, whereas MOGAD exhibited increased inflammatory monocytes and cytotoxic CD8 effector T cells, coupled with decreased plasma cells and memory B cells. These findings allow for highly predictive discrimination of these two diseases and pave a novel avenue for the diagnosis and therapy of neuroinflammatory diseases.

DATA AVAILABILITY STATEMENT

The datasets presented in this study can be found in online repositories. The names of the repository/repositories and accession number(s) can be found in the article/**Supplementary Material**.

ETHICS STATEMENT

The study protocols were approved by the Ethics Committee Board of the First Affiliated Hospital of Zhengzhou University (2021-KY-0588-002). The patients/participants provided their written informed consent to participate in this study.

AUTHOR CONTRIBUTIONS

HL and JL designed the research, contributed valuable advice, and edited the manuscript. JP and XY conducted the research and collected data. ZW and MC analyzed the data and performed the statistical analysis. JL wrote the draft of the main manuscript. All authors drafted the manuscript, performed the revision, and approved the final version of the manuscript.

FUNDING

This work was supported by the Medical Science and Technology Research Project of Henan Province (no. LHGJ20190086) and the National Natural Science Foundation of China (no. U2004128).

ACKNOWLEDGMENTS

We acknowledge assistance with the access of analytic instruments from the Translational Medical Center at The First Affiliated Hospital of Zhengzhou University.

SUPPLEMENTARY MATERIAL

The Supplementary Material for this article can be found online at: https://www.frontiersin.org/articles/10.3389/fneur.2021.807646/full#supplementary-material

Supplementary Figure 1 | Consistency of identification and cell capture in PBMC scRNA-seq. PBMC, peripheral blood mononuclear cells.

Supplementary Figure 2 | Gating strategy of $CD19^+CXCR4^+$ by flow cytometry.

REFERENCES

1. Dobson R, Giovannoni G. Multiple sclerosis-a review. *Eur J Neurol.* (2019) 26:27–40. doi: 10.1111/ene.13819
2. Thompson AJ, Baranzini SE, Geurts J, Hemmer B, Ciccarelli O. Multiple sclerosis. *Lancet.* (2018) 391:1622–36. doi: 10.1016/S0140-6736(18)30481-1
3. Dahham J, Rizk R, Kremer I, Evers S, Hiligsmann M. Economic burden of multiple sclerosis in low- and middle-income countries: a systematic review. *Pharmacoeconomics.* (2021) 39:789–807. doi: 10.1007/s40273-021-01032-7
4. Noseworthy JH. Progress in determining the causes and treatment of multiple sclerosis. *Nature.* (1999) 399:A40–7. doi: 10.1038/399a040
5. Keegan BM, Noseworthy JH. Multiple sclerosis. *Annu Rev Med.* (2002) 53:285–302. doi: 10.1146/annurev.med.53.082901.103909

6. Goodin DS. Therapeutic developments in multiple sclerosis. *Expert Opin Investig Drugs.* (2000) 9:655–70. doi: 10.1517/13543784.9.4.655
7. Ding J, Ren K, Wu J, Li H, Sun T, Yan Y, et al. Overlapping syndrome of MOG-IgG-associated disease and autoimmune GFAP astrocytopathy. *J Neurol.* (2020) 267:2589–93. doi: 10.1007/s00415-020-09869-2
8. Winter A, Chwalisz B. MRI characteristics of NMO, MOG and MS related optic neuritis. *Semin Ophthalmol.* (2020) 35:333–42. doi: 10.1080/08820538.2020.1866027
9. Kim SM, Woodhall MR, Kim JS, Kim SJ, Park KS, Vincent A, et al. Antibodies to MOG in adults with inflammatory demyelinating disease of the CNS. *Neurol Neuroimmunol Neuroinflamm.* (2015) 2:e163. doi: 10.1212/NXI.0000000000000163
10. Kitley J, Woodhall M, Waters P, Leite MI, Devenney E, Craig J, et al. Myelin-oligodendrocyte glycoprotein antibodies in adults with a neuromyelitis optica phenotype. *Neurology.* (2012) 79:1273–7. doi: 10.1212/WNL.0b013e31826aac4e
11. Jurynczyk M, Probert F, Yeo T, Tackley G, Claridge TDW, Cavey A, et al. Metabolomics reveals distinct, antibody-independent, molecular signatures of MS, AQP4-antibody and MOG-antibody disease. *Acta Neuropathol Commun.* (2017) 5:95. doi: 10.1186/s40478-017-0495-8
12. Cao Y, Qiu Y, Tu G, Yang C. Single-cell RNA sequencing in immunology. *Curr Genomics.* (2020) 21:564–75. doi: 10.2174/1389202921999201020203249
13. Selmi C. Autoimmunity in 2019. *Clin Rev Allergy Immunol.* (2020) 59:275–86. doi: 10.1007/s12016-020-08808-3
14. Zhao M, Jiang J, Zhao M, Chang C, Wu H, Lu Q. The application of single-cell RNA sequencing in studies of autoimmune diseases: a comprehensive review. *Clin Rev Allergy Immunol.* (2021) 60:68–86. doi: 10.1007/s12016-020-08813-6
15. Hong X, Meng S, Tang D, Wang T, Ding L, Yu H, et al. Single-cell RNA sequencing reveals the expansion of cytotoxic $CD4^+$ T lymphocytes and a landscape of immune cells in primary Sjogren's syndrome. *Front Immunol.* (2020) 11:594658. doi: 10.3389/fimmu.2020.594658
16. Ramesh A, Schubert RD, Greenfield AL, Dandekar R, Loudermilk R, Sabatino JJ Jr., et al. A pathogenic and clonally expanded B cell transcriptome in active multiple sclerosis. *Proc Natl Acad Sci U S A.* (2020) 117:22932–43. doi: 10.1073/pnas.2008523117
17. Schafflick D, Xu CA, Hartlehnert M, Cole M, Schulte-Mecklenbeck A, Lautwein T, et al. Integrated single cell analysis of blood and cerebrospinal fluid leukocytes in multiple sclerosis. *Nat Commun.* (2020) 11:247. doi: 10.1038/s41467-019-14118-w
18. Esaulova E, Cantoni C, Shchukina I, Zaitsev K, Bucelli RC, Wu GF, et al. Single-cell RNA-seq analysis of human CSF microglia and myeloid cells in neuroinflammation. *Neurol Neuroimmunol Neuroinflamm.* (2020) 7. doi: 10.1212/NXI.0000000000000732
19. Thompson AJ, Banwell BL, Barkhof F, Carroll WM, Coetzee T, Comi G, et al. Diagnosis of multiple sclerosis: 2017 revisions of the McDonald criteria. *Lancet Neurol.* (2018) 17:162–73. doi: 10.1016/S1474-4422(17)30470-2
20. López-Chiriboga AS, Majed M, Fryer J, Dubey D, McKeon A, Flanagan EP, et al. Association of MOG-IgG serostatus with relapse after acute disseminated encephalomyelitis and proposed diagnostic criteria for MOG-IgG-associated disorders. *JAMA Neurol.* (2018) 75:1355–63. doi: 10.1001/jamaneurol.2018.1814
21. Yamagishi M, Kubokawa M, Kuze Y, Suzuki A, Yokomizo A, Kobayashi S, et al. Chronological genome and single-cell transcriptome integration characterizes the evolutionary process of adult T cell leukemia-lymphoma. *Nat Commun.* (2021) 12:4821. doi: 10.1038/s41467-021-25101-9
22. Cai Y, Dai Y, Wang Y, Yang Q, Guo J, Wei C, et al. Single-cell transcriptomics of blood reveals a natural killer cell subset depletion in tuberculosis. *EBioMedicine.* (2020) 53:102686. doi: 10.1016/j.ebiom.2020.102686
23. Wolock SL, Lopez R, Klein AM. Scrublet: computational identification of cell doublets in single-cell transcriptomic data. *Cell Syst.* (2019) 8:281–91.e9. doi: 10.1016/j.cels.2018.11.005
24. Hao Y, Hao S, Andersen-Nissen E, Mauck WM, 3rd, Zheng S, Butler A, et al. Integrated analysis of multimodal single-cell data. *Cell.* (2021) 184:3573–87.e29. doi: 10.1016/j.cell.2021.04.048
25. Zhang X, Lan Y, Xu J, Quan F, Zhao E, Deng C, et al. CellMarker: A manually curated resource of cell markers in human and mouse. *Nucleic Acids Res.* (2019) 47:D721–D8. doi: 10.1093/nar/gky900
26. McDavid A, Finak G, Chattopadyay PK, Dominguez M, Lamoreaux L, Ma SS, et al. Data exploration, quality control and testing in single-cell qPCR-based gene expression experiments. *Bioinformatics.* (2013) 29:461–7. doi: 10.1093/bioinformatics/bts714
27. Biajoux V, Bignon A, Freitas C, Martinez V, Thelen M, Lima G, et al. Expression of CXCL12 receptors in B cells from Mexican Mestizos patients with systemic lupus erythematosus. *J Transl Med.* (2012) 10:251. doi: 10.1186/1479-5876-10-251
28. Herz J, Filiano AJ, Smith A, Yogev N, Kipnis J. Myeloid cells in the central nervous system. *Immunity.* (2017) 46:943–56. doi: 10.1016/j.immuni.2017.06.007
29. Owens T, Benmamar-Badel A, Wlodarczyk A, Marczynska J, Morch MT, Dubik M, et al. Protective roles for myeloid cells in neuroinflammation. *Scand J Immunol.* (2020) 92:e12963. doi: 10.1111/sji.12963
30. Waschbisch A, Schroder S, Schraudner D, Sammet L, Weksler B, Melms A, et al. Pivotal role for $CD16^+$ monocytes in immune surveillance of the central nervous system. *J Immunol.* (2016) 196:1558–67. doi: 10.4049/jimmunol.1501960
31. Mishra MK, Yong VW. Myeloid cells-targets of medication in multiple sclerosis. *Nat Rev Neurol.* (2016) 12:539–51. doi: 10.1038/nrneurol.2016.110
32. Ginhoux F, Jung S. Monocytes and macrophages: developmental pathways and tissue homeostasis. *Nat Rev Immunol.* (2014) 14:392–404. doi: 10.1038/nri3671
33. Gjelstrup MC, Stilund M, Petersen T, Moller HJ, Petersen EL, Christensen T. Subsets of activated monocytes and markers of inflammation in incipient and progressed multiple sclerosis. *Immunol Cell Biol.* (2018) 96:160–74. doi: 10.1111/imcb.1025
34. Kouris A, Pistiki A, Katoulis A, Georgitsi M, Giatrakou S, Papadavid E, et al. Proinflammatory cytokine responses in patients with psoriasis. *Eur Cytokine Netw.* (2014) 25:63–8. doi: 10.1684/ecn.2014.0358
35. Kim YS, Yang HJ, Kee SJ, Choi I, Ha K, Ki KK, et al. The "Intermediate" $CD14^+$ $CD16^+$ monocyte subpopulation plays a role in IVIG responsiveness of children with Kawasaki disease. *Pediatr Rheumatol Online J.* (2021) 19:76. doi: 10.1186/s12969-021-00573-7
36. Foell D, Wittkowski H, Vogl T, Roth J. S100 proteins expressed in phagocytes: a novel group of damage-associated molecular pattern molecules. *J Leukoc Biol.* (2007) 81:28–37. doi: 10.1189/jlb.0306170
37. Kang JH, Hwang SM, Chung IY. S100A8, S100A9 and S100A12 activate airway epithelial cells to produce MUC5AC *via* extracellular signal-regulated kinase and nuclear factor-kappaB pathways. *Immunology.* (2015) 144:79–90. doi: 10.1111/imm.12352
38. Weiss HA, Millward JM, Owens T. $CD8^+$ T cells in inflammatory demyelinating disease. *J Neuroimmunol.* (2007) 191:79–85. doi: 10.1016/j.jneuroim.2007.09.011
39. Chitnis T. The role of CD4 T cells in the pathogenesis of multiple sclerosis. *Int Rev Neurobiol.* (2007) 79:43–72. doi: 10.1016/S0074-7742(07)79003-7
40. Johnson AJ, Suidan GL, McDole J, Pirko I. The CD8 T cell in multiple sclerosis: Suppressor cell or mediator of neuropathology? *Int Rev Neurobiol.* (2007) 79:73–97. doi: 10.1016/S0074-7742(07)79004-9
41. Compston A, Coles A. Multiple sclerosis. *Lancet.* (2002) 359:1221–31. doi: 10.1016/S0140-6736(02)08220-X
42. Zang YC Li S, Rivera VM, Hong J, Robinson RR, Breitbach WT, et al. Increased $CD8^+$ cytotoxic T cell responses to myelin basic protein in multiple sclerosis. *J Immunol.* (2004) 172:5120–7. doi: 10.4049/jimmunol.172.8.5120
43. Kucuksezer UC, Aktas Cetin E, Esen F, Tahrali I, Akdeniz N, Gelmez MY, et al. The role of natural killer cells in autoimmune diseases. *Front Immunol.* (2021) 12:622306. doi: 10.3389/fimmu.2021.622306
44. Zakka LR, Fradkov E, Keskin DB, Tabansky I, Stern JN, Ahmed AR. The role of natural killer cells in autoimmune blistering diseases. *Autoimmunity.* (2012) 45:44–54. doi: 10.3109/08916934.2011.606446
45. Vandenhaute J, Wouters CH, Matthys P. Natural killer cells in systemic autoinflammatory diseases: a focus on systemic juvenile idiopathic arthritis and macrophage activation syndrome. *Front Immunol.* (2019) 10:3089. doi: 10.3389/fimmu.2019.03089
46. Rodriguez-Martin E, Picon C, Costa-Frossard L, Alenda R, Sainz de. la Maza S, Roldan E, et al. Natural killer cell subsets in cerebrospinal fluid of patients with multiple sclerosis. *Clin Exp Immunol.* (2015) 180:243–9. doi: 10.1111/cei.12580

47. Myhr KM, Torkildsen O, Lossius A, Bo L, Holmoy T, B. cell depletion in the treatment of multiple sclerosis. *Expert Opin Biol Ther.* (2019) 19:261–71. doi: 10.1080/14712598.2019.1568407
48. Sabatino JJ, Jr., Zamvil SS, Hauser SL. B-Cell therapies in multiple sclerosis. *Cold Spring Harb Perspect Med.* (2019) 9:a032037. doi: 10.1101/cshperspect.a032037
49. Greenfield AL, Hauser SL. B-cell therapy for multiple sclerosis: Entering an era. *Ann Neurol.* (2018) 83:13–26. doi: 10.1002/ana.25119
50. Duddy M, Niino M, Adatia F, Hebert S, Freedman M, Atkins H, et al. Distinct effector cytokine profiles of memory and naive human B cell subsets and implication in multiple sclerosis. *J Immunol.* (2007) 178:6092–9. doi: 10.4049/jimmunol.178.10.6092
51. Barr TA, Shen P, Brown S, Lampropoulou V, Roch T, Lawrie S, et al. B cell depletion therapy ameliorates autoimmune disease through ablation of IL-6-producing B cells. *J Exp Med.* (2012) 209:1001–10. doi: 10.1084/jem.20111675
52. Li R, Rezk A, Miyazaki Y, Hilgenberg E, Touil H, Shen P, et al. Proinflammatory GM-CSF-producing B cells in multiple sclerosis and B cell depletion therapy. *Sci Transl Med.* (2015) 7:310ra166. doi: 10.1126/scitranslmed.aab4176
53. Shen P, Fillatreau S. Antibody-independent functions of B cells: a focus on cytokines. *Nat Rev Immunol.* (2015) 15:441–51. doi: 10.1038/nri3857
54. Rieger A, Bar-Or A. B-cell-derived interleukin-10 in autoimmune disease: regulating the regulators. *Nat Rev Immunol.* (2008) 8:486–7. doi: 10.1038/nri2315-c1
55. Li R, Patterson KR, Bar-Or A. Reassessing B cell contributions in multiple sclerosis. *Nat Immunol.* (2018) 19:696–707. doi: 10.1038/s41590-018-0135-x

Conflict of Interest: The authors declare that the research was conducted in the absence of any commercial or financial relationships that could be construed as a potential conflict of interest.

frontiers in Immunology

ORIGINAL RESEARCH
published: 20 January 2022
doi: 10.3389/fimmu.2022.827865

Gut Microbiome and Bile Acid Metabolism Induced the Activation of CXCR5+ CD4+ T Follicular Helper Cells to Participate in Neuromyelitis Optica Spectrum Disorder Recurrence

Xi Cheng[1†], Luyao Zhou[1†], Zhibin Li[1], Shishi Shen[1], Yipeng Zhao[1], Chunxin Liu[1], Xiaonan Zhong[1], Yanyu Chang[1], Allan G. Kermode[1,2,3] and Wei Qiu[1*]*

[1] Department of Neurology, Third Affiliated Hospital of Sun Yat-sen University, Guangzhou, China, [2] Centre for Neuromuscular and Neurological Disorders, Perron Institute, The University of Western Australia, Perth, WA, Australia, [3] Institute for Immunology and Infectious Diseases, Murdoch University, Murdoch, WA, Australia

From the perspective of the role of T follicular helper (Tfh) cells in the destruction of tolerance in disease progression, more attention has been paid to their role in autoimmunity. To address the role of Tfh cells in neuromyelitis optica spectrum disorder (NMOSD) recurrence, serum C-X-C motif ligand 13 (CXCL13) levels reflect the effects of the Tfh cells on B-cell-mediated humoral immunity. We evaluated the immunobiology of the CXCR5+CD4+ Tfh cells in 46 patients with NMOSD, including 37 patients with NMOSD with an annual recurrence rate (ARR) of<1 and 9 patients with NMOSD with an ARR of ≥1. Herein, we reported several key observations. First, there was a lower frequency of circulating Tfh cells in patients with an ARR of<1 than in those with an ARR of ≥1 ($P< 0.05$). Second, the serum CXCL13 levels were downregulated in individuals with an ARR<1 ($P< 0.05$), processing the ability to promote Tfh maturation and chemotaxis. Third, the level of the primary bile acid, glycoursodeoxycholic acid (GUDCA), was higher in patients with NMOSD with an ARR of<1 than in those with NMOSD with an ARR of ≥1, which was positively correlated with CXCL13. Lastly, the frequency of the Tfh precursor cells decreased in the spleen of keyhole limpet haemocyanin-stimulated animals following GUDCA intervention. These findings significantly broaden our understanding of Tfh cells and CXCL13 in NMOSD. Our data also reveal the potential mechanism of intestinal microbiota and metabolites involved in NMOSD recurrence.

Keywords: T follicular helper cells, neuromyelitis optica spectrum disorder, CXCL13, bile acid, gut microbiota

OPEN ACCESS

Edited by:
Cristoforo Comi,
University of Eastern Piedmont, Italy

Reviewed by:
Yang Zheng,
Zhejiang University, China
Jinming Han,
Capital Medical University, China

****Correspondence:***
Wei Qiu
qiuwei@mail.sysu.edu.cn
Allan G. Kermode
allan.kermode@uwa.edu.au

[†]These authors share first authorship

Specialty section:
This article was submitted to Multiple Sclerosis and Neuroimmunology, a section of the journal Frontiers in Immunology

Received: *02 December 2021*
Accepted: *03 January 2022*
Published: *20 January 2022*

Citation:
Cheng X, Zhou L, Li Z, Shen S, Zhao Y, Liu C, Zhong X, Chang Y, Kermode AG and Qiu W (2022) Gut Microbiome and Bile Acid Metabolism Induced the Activation of CXCR5+ CD4+ T Follicular Helper Cells to Participate in Neuromyelitis Optica Spectrum Disorder Recurrence. Front. Immunol. 13:827865. doi: 10.3389/fimmu.2022.827865

INTRODUCTION

Neuromyelitis optica spectrum disorder (NMOSD) is an autoimmune disease of the central nervous system that repeatedly involves the optic nerve and spinal cord and is mediated by aquaporin-4 (AQP4) antibodies. The combination of AQP4-Ab with AQP4 expressed on astrocytes of the blood–brain barrier causes complement-dependent cytotoxicity and neutrophil, eosinophil, and cytokine infiltration. Blood-brain barrier destruction results in oligodendrocyte death, myelin loss, and neuronal damage.

Recent data have indicated that the germinal centre (GC) may be a pathogenic hotspot for autoantibody production in autoimmune diseases. In particular, circulating Tfh cells that are derived from GC-Tfh cells shuffle between the peripheral blood and lymphoid tissues (1), and play an important role in the differentiation of B cells into memory B and plasma cells, promoting pathogenic autoantibody production, clinical symptom onset, continued immune responsiveness, and eventually irreversible tissue damage (2). Tfh cells function through chemokine CXC receptor 5 (CXCR5), programmed cell death protein-1 (PD-1), cytokine interleukin-21 (IL-21), and C-X-C motif ligand 13 (CXCL13). Multiple studies have shown that Tfh cells expand in the peripheral blood of humans of systemic autoimmune diseases, including rheumatoid arthritis (3), primary Sjogren's syndrome (4), and immunoglobulin (IgG)-4 related disease (5). Recently, Tfh cells were demonstrated to be reportedly involved in the recurrence of neuroimmune diseases, such as multiple sclerosis (6) and NMOSD (7).

In general, the intestinal microbiota of patients with NMOSD are characterised by lower *Clostridium*, *Parabacteroides*, *Oxalobacter*, and *Burkholderia* and higher *Streptococcus*, *Alistipes*, *Haemophilus*, *Veillonella*, *Butyricimonas*, and *Rothia* abundance than in healthy controls (8, 9). In a previous study, not only did the patients with NMOSD have significantly lower faecal butyrate levels, but the patients with lower Expanded Disability Status Scale (EDSS) scores also showed a major reduction in the butyrate levels (9). The anti-inflammatory effect of short-chain fatty acids is not limited to the intestinal tract; it also increases the Treg level and inhibits Th17 cell differentiation (10). However, limited information is available on the effects of the gut microbiota and metabolites on Tfh and NMOSD recurrence.

Therefore, we assessed the Tfh cell number and frequency in patients with NMOSD with low and high annual recurrence rates (ARRs). We then investigated the effects of the metabolites on the immune system in keyhole limpet haemocyanin (KLH)-stimulated animals. We aimed to provide valuable insights into the causal mechanisms underlying the possible clinical effects of intestinal microbiota and metabolites.

MATERIALS AND METHODS

Clinical Study Design and Population

A total of 109 participants, including 59 patients and 50 age- and sex-matched healthy controls, were enrolled in this study from October 2019 to July 2021 at the Third Affiliated Hospital of Sun Yat-Sen University in southern China. The diagnosis of NMOSD was established based on the International Panel on NMO Diagnosis 2015 criteria (11) and AQP4-IgG seropositivity. We included patients according to the following inclusion criteria: (1) initiation of immunosuppressive treatment as a first-line therapy within 3 years following disease onset and (2) at least 3 months of follow-up. We excluded patients according to the following exclusion criteria: (1) EDSS score ≥ 6.0, (2) body mass index< 20 kg/m^2, (3) a history of cardiovascular or renal disease and other autoimmune diseases, and (4) age< 18 years. The following data were collected from the participants' medical records at the baseline visit: demographics (including age, race/ethnicity, sex, weight, and height), past and present diet attempts, serologic status, date of disease onset (first attack), EDSS scores, and modified Rankin Scale scores. NMOSD data collection included a history of recurrence, past/current immunosuppressive therapies, disease duration, medication history, and reasons for treatment discontinuation. Disease onset was defined as the first recurrence of NMOSD. Attack and recurrence were defined as new symptoms that occurred within at least 24 h and were associated with new magnetic resonance imaging lesions. The ethical committee of the Third Affiliated Hospital of Sun Yat-sen University of Medical Sciences approved the research proposal in 10-15-2019. We have registered our trial before the first participant was enrolled in the clinical trial with a project identification code NCT04101058 that are reported in manuscripts (More information about trial registration see https://register.clinicaltrials.gov/prs/app/action/).

Of the 59 patients with NMOSD, serum samples were collected to measure the cytokine levels, and peripheral blood mononuclear cells (PBMCs) were collected for immunological analysis from the 46 patients, who also provided faecal samples for microbiome analysis and metabolomics. These 46 patients were further categorised into two groups based on the ARR: low ARR group (n = 37, ARR< 1) and high ARR group (n = 9, ARR ≥ 1) (**Table 1**). All the 50 age- and sex-matched healthy controls only supplied stool samples for the microbiome analysis.

Microbiome Analysis

Faecal DNA was isolated using the QIAamp Fast DNA stool Mini Kit (Qiagen, Cat# 51604), and the V3–V4 region of the 16S rRNA bacterial gene was amplified with barcoded specific bacterial primers: forward primer 5′- ACTCCTACGGGA GGCAGCA-3′ and reverse primer 5′-GGACTACHVGGG TWTCTAAT-3′. The 16S rDNA was polymerase chain reaction (PCR) amplified using Q5® High-Fidelity DNA Polymerase (M0491, NEB, USA). The PCR amplicons were quantified using the MiSeq Reagent Kit v3 (MS-102-3003, Illumina Inc., USA) in a MiSeq-PE250 sequencer (Illumina) based on standard protocols. The 16S rDNA amplicon data were analysed using a customised QIIME2 software pipeline (https://qiime2.org). The readings were then processed using the quantitative insights into microbial ecology (QIIME2) analysis. The taxonomy assignment was based on 97% clustered operational taxonomic units of the Greengenes v13.8 database using the naive Bayesian classifier.

TABLE 1 | Baseline characteristics of the study population.

	Low recurrence rate	High recurrence rate	*p*-value (P3 vs. P2)
N	49	10	
Faecal sample	46	10	
Female, n (%)	93.9%	100%	
Age, years	43.0	47.5	0.568
BMI, kg/m^2	22.3	23.9	0.202
Work (2), n (%)	33 (84.6%)	8 (80.0%)	0.659
High-oil diet, n (%)	5 (12.8%)	1 (10.0%)	0.781
High-salt diet, n (%)	11 (38.3%)	2 (20.0%)	0.315
Smoker, n (%)	2 (5.13%)	0 (0.0%)	1
Drink alcohol, n (%)	2 (5.13%)	1 (5.3%)	1
Sports frequency (1, 2) (%)	26 (66.7%)	4 (40.0%)	0.384
Sports strength (1, 2) (%)	7 (17.9%)	0 (0.0%)	0.412
AQP4-IgG, n (%)	49 (100%)	10 (100%)	–
ARR, mean	0.4	1.0	≤0.001
Course of disease, years	6	1.5	0.023
EDSS, mean	3.0	2.75	0.955
mRS, n (%)			0.907
0	2 (5.13%)	1 (10.0%)	
1	26 (66.7%)	7 (70.0%)	
2	9 (23.1%)	2 (20.0%)	
3	2 (5.13%)	0 (0.00%)	
Immunosuppressant			0.419
Azathioprine	11 (22.4%)	2 (20.0%)	
Mycophenolate mofetil	23 (46.9%)	7 (70.0%)	

ARR, annual recurrence rate; EDSS, Expanded Disability Status Scale; mRS, modified Rankin Scale.

Stool Metabolomics

Faecal metabolites were extracted using 50% methanol buffer. Faecal samples (20 μL) were added to 120 μL of pre-cooled 50% methanol, vortexed for 60 s, incubated at 4°C for 10 min, incubated at -20°C for 60 min, centrifuged at 4,000 × g at 4°C for 15 min, transferred to another tube, and then analysed by liquid chromatography-mass spectrometry (LC-MS). Additionally, pooled quench cooled samples were prepared by mixing 10 μL of each extraction mixture. These samples were then processed using an LC-MS system according to the manufacturer's instructions. An LC-MS triple quadrupole mass spectrometer (Shimadzu, LCMS-8050) equipped with LabSolutions was used to collect the primary and secondary mass spectrometry data. The electrospray ionisation ion source parameters for the negative ion mode were set as follows: nebulising gas temperature, 300°C; nebulising gas flow, 3 L/min; heating gas flow, 13 L/min; sheath gas temperature, 350°C; DL temperature, 250°C; heating module temperature, 400°C; and sheath gas flow, 7 L/min. BAs were detected using LabSolutions LCMS software (Shimadzu) to perform peak extraction, peak integration, area calculation on the original file, and quantification using a standard curve.

Measurement of Cytokines

To measure the cytokine levels, blood samples were centrifuged at 2,500 g for 10 min, and the sera were stored at −80°C. The sera were probed for the following 22 markers: interferon-gamma, IL-1beta, IL-10, IL-13, IL-17A, IL-21, IL-6, IL-7, IL-8, nerve growth factor-beta, tumour necrosis factor, vascular endothelial growth factor A, APRIL, B cell-activating factor receptor, CXCL13, granulocyte colony-stimulating factor, macrophage migration inhibitory, interleukin-1 receptor antagonist, metalloproteinase (MMP)-2, MMP-3, MMP-8, MMP-9. The Cytokine/Chemokine/Growth Factor Convenience 45-Plex Human kit (Thermo Fisher Scientific) was allowed to warm at 15°C for 2 h. All the steps were performed according to the manufacturer's recommendations.

Animals

Female BALB/c mice aged 5–6 weeks (15–18 g) were purchased from the Laboratory Animal Center. This study complied with all the relevant ethical regulations and was approved by the Ethics Committee of the South China Agricultural University (ethical number: 2021B002). Animals were housed under specific pathogen-free conditions and maintained over a 12-h light/dark cycle with free access to food and water. Mice received an injection of KLH in both the underarms and groin (100 μg/0.2 mL/site), and the control groups were treated with equal amounts of saline. Mice were then divided into three groups (n = 6 animals per group): control, KLH, and KLH +glycoursodeoxycholic acid (GUDCA) acid groups. Each experimental group was separately gavaged with 50 mg/kg body weight of GUDCA for 4 weeks. The control and KLH groups were treated with equal amounts of saline. After treatment, ileum, spleen, and lymph node samples were collected to analyse the Tfh cell phenotype by fluorescence-activated cell sorting.

Flow Cytometry

FITC-conjugated anti-CD4 (human), BV510-conjugated anti-CXCR5 (human), PE-conjugated anti-CCR7 (human), AF700-conjugated anti-CD4 (mouse), APC-conjugated anti-CXCR5

(mouse), PE-conjugated anti-CCR7 (mouse), and FITC-conjugated-anti-PD-1 (mouse) were purchased from BioLegend (San Diego, CA, USA). PBMCs were separated and frozen at −80°C until phenotypic analysis was performed according to standard protocols. Samples were acquired using a BD LSR II flow cytometer (BD Bioscience) and analysed using FlowJo.

Immunofluorescence

Immunostaining was performed as previously described. For immunostaining, the gut sections were fixed, blocked, and incubated with primary antibodies against CCR7 (BioLegend, 1:200), CXCR5 (BioLegend, 1:200), and PD-1 (BioLegend, 1:200) at 4°C overnight. After washing, the sections were co-stained with 2 μg/mL 4′,6-diamidino-2-phenylindole (nucleus) for 5 min. Fluorescence images were acquired using a confocal microscope (Leica SP8) with a 20× objective.

Statistical Analysis

All the statistical analyses were performed using the Statistical Package for the Social Sciences software version 19.0; the data are presented as mean values with standard deviation. The test of normal distribution was performed before the Student's *t*-test and analysis of variance (ANOVA). Multiple comparisons were performed using one-way ANOVA or Kruskal–Wallis tests between the different groups. The Shapiro-Wilk test was used to assess normality. Inflammatory cytokines levels were $\log_{10}$-transformed when analysed to meet the normal assumption. The correlation between the two variables was assessed using the Spearman rank test. For all analyses, a *p*-value of<0.05 was considered to indicate statistical significance. Correlations between each of the pair of datasets were computed using Pearson correlation coefficients, and visualisations were generated in R (v4.0.0).

RESULTS

CXCL13 Was Significantly Lower in Patients of NMOSD With a Low ARR

The potential value of serum inflammatory cytokine markers was investigated in the diagnosis of NMOSD (**Table 2**). CXCL13 was significantly different between the two groups (51.82 vs. 78.88, $p = 0.019$, **Figure 1A**). The individual simplified signature could discriminate between the two groups based on the area under the curve (AUC) (CXCL13 [AUC = 0.656], **Figure 1B**). We also aimed to explore the correlations between these discriminative inflammatory factors and ARR to identify markers associated with disease recurrence. Spearman's rank correlation analysis showed that CXCL13 ($r = 0.460$, $p = 0.001$) was positively correlated with NMOSD recurrence (**Figure 1C**).

Tfh Cells Were Positively Correlated With NMOSD Recurrence

The frequency of circulating $CXCR5^+CD4^+$ Tfh, $CXCR5^+CCR7^{low}$ Tfh precursor, and CXCR5+$CCR7^{hi}$ resting Tfh cells were analysed using flow cytometry. As shown in **Figure 2A**, the percentage of $CD4^+CXCR5^+$ T cells was significantly higher in the peripheral blood of patients with NMOSD with an ARR of ≥ 1 than in those with an ARR of <1 (24.6% vs. 14.5%, $p < 0.01$). Moreover, the percentage of $CXCR5^+CCR7^{hi}$ Tfh cells among $CD4^+$ T cells was higher in patients

TABLE 2 | Quantitative data of inflammatory cytokines in NMOSD patients.

	Low recurrence rate (range)	High recurrence rate (range)	*p*-value
N	37	9	
IFN-gamma	0.000	0.000	1
IL-1beta	0.12 (0.00–4.69)	0.000	1
IL-10	0.06 (0.00–1.98)	0.000	1
IL-13	0.000	0.000	1
IL-17A	1.06 (0.00–5.78)	0.45 (0.00–4.07)	0.367
IL-21	16.90 (0.00–474.73)	6.41 (0.00–57.67)	0.799
IL-6	0.23 (0.00–8.65)	0.000	1
IL-7	1.30 (0.06–1.62)	1.20 (0.00–1.35)	0.647
IL-8	5.599 (0.00–168.43)	0.93 (0.00–8.38)	0.69
NGF-beta	0.38 (0.00–14.15)	0.000	1
TNF	0.11 (0.00–3.94)	0.000	1
VEGF-A	274.7 (17.64–1284.32)	235.7 (0.00–600.4)	0.792
APRIL	2163 (0.00–9740.55)	3240 (0.00–9880.43)	0.448
BAFF	0.28 (0.00–10.51)	0.00	1
CXCL13	51.82 (0.00–149.08)	78.88 (30.89–181.78)	0.019*
G-CSF	8.09 (0.00–108.58)	1.91 (0.00–17.16)	0.357
MIF	80.32 (49.3–93.6)	73.79 (0.00–218.56)	0.124
IL-1RA	26.48 (0.00–650.43)	0.00	
MMP-2	96.15 (0.00–130)	61.04 (0.00–294.62)	0.355
MMP-3	174.7 (0.00–334)	208.13 (0.00–1053.88)	0.686
MMP-8	7.76 (0.00–226.57)	0.00	1
MMP-9	100.00 (0.00–1340.75)	80.51 (0.00–244.47)	0.572

*$p < 0.05$.

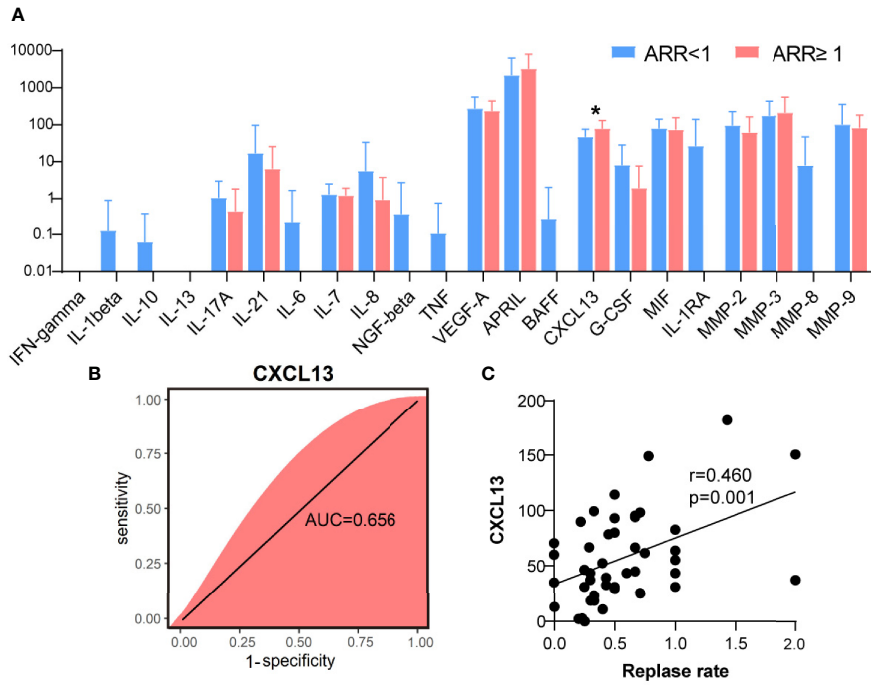

FIGURE 1 | C-X-C motif ligand 13 (CXCL13) as a biological marker for neuromyelitis optica spectrum disorder recurrence. **(A)** Quantification of inflammatory cytokines between two groups of patients with NMOSD (N = 37 in ARR<1 patients, N = 9 in ARR ≥ 1 patients). **(B)** Random forest analysis showed the CXCL13 could discriminate the two groups based on the area under the curve (0.656). **(C)** Using the CXCL13, a relatively poor correlation was achieved with Spearman's correlation analysis (r = 0.460). ARR, annual recurrence rate. *p < 0.05.

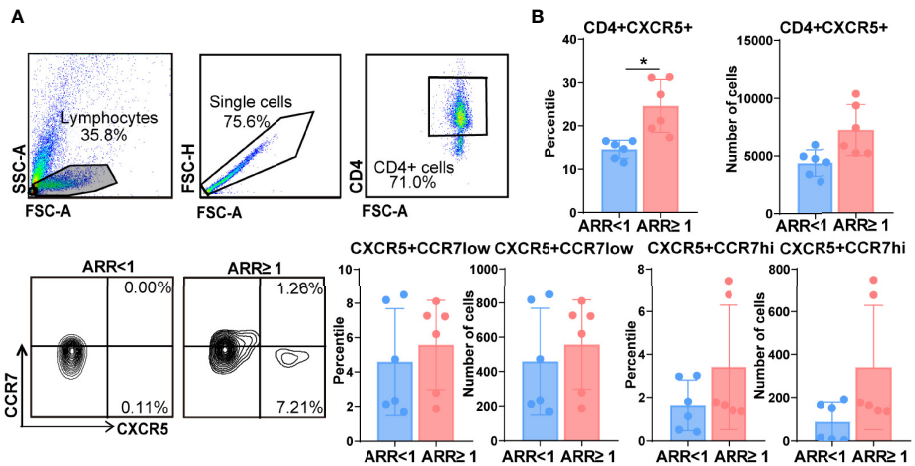

FIGURE 2 | Increased frequency of follicular helper T (Tfh) cells in patients with neuromyelitis optica spectrum disorder (NMOSD) with a high annual recurrence rate. **(A)** Comparison of the frequencies of circulating Tfh cells in patients with two groups patients with NMOSD. Representative expressions of CXCR5+CD4+ T cells, CXCR5+CCR7^{low} Tfh progenitors, and CXCR5+CCR7^{hi} Tfh were detected by flow cytometry. **(B)** Flow cytometric analysis of the different phenotypes of Tfh. N = 6, *$p < 0.05$. ARR, annual recurrence rate.

with NMOSD having an ARR of ≥ 1 than in those with NMOSD having an ARR of <1 (3.4% vs. 1.6%, $p = 0.07$); however, owing to the large individual difference of patients, there was no significant difference between these patients. There were no significant differences in the frequency or number of CXCR5^{+}CCR7^{low} T cells between the two groups of patients, although both showed higher levels in the patients with an ARR of ≥ 1 than in the patients with an ARR of<1 (**Figures 2A, B**). Therefore, we speculated that more

$CXCR5^{+}CCR7^{hi}$ Tfh cells among $CD4^{+}$ T cells in the patients with NMOSD having a higher ARR could explain the higher $CD4^{+}CXCR5^{+}$ T cells in patients with higher ARR, although there was no significant difference between these patients.

Decreased CXCL13 Level Was Associated With GUDCA

The number of CXCR5+CD4+ T cells was significantly higher in the KLH group than in the GUDCA group ($p < 0.001$, **Figures 3A, B**). Further, there was an increasing trend of $CXCR5^{+}CD4^{+}$ Tfh cell count in the GUDCA group ($p = 0.02$, **Figures 3A, B**). In addition, we evaluated the frequency of $CD19^{low}CXCR5^{+}$ Tfh cells, the frequency of $CCR7^{hi}PD\text{-}1^{low}$ resting Tfh and $CCR7^{hi}PD\text{-}1^{hi}$-activated Tfh cells. Tfh cell count did not change significantly, whereas $CCR7^{low}PD\text{-}1^{hi}$ Tfh precursor cells in KLH mice tended to increase following GUDCA supplementation compared with those in the KLH group (**Figures 3A, C**). In addition, a significant increase in the serum CXCL13 level was observed in the GUDCA group compared with that in the KLH group (**Figure 3D**), which supports the immunomodulatory function of GUDCA.

We then analysed the distribution of splenic ($PD\text{-}1^{+}$ and $CXCR5^{+}/CCR7^{+}$ double-positive) Tfh cells with immunohistochemical double staining. Splenic $PD\text{-}1^{+}CCR7^{+}$ and $PD\text{-}1^{+}CXCR5^{+}$ Tfh cells were localised in the T-B cell zone in the control group, whereas they were distributed in the GC-B-cell follicles in the KLH and GUDCA groups (**Figure 3E**). There were barely $PD\text{-}1^{+}CCR7^{+}$ and $PD\text{-}1^{+}CXCR5^{+}$ positive Tfh cells in the intestinal Peyer's patch lymph node of the control group, which accumulated around the margin of Peyer's patch lymph node (**Figure 3F**), supporting the notion that GUDCA supplied a permissive environment for Tfh cell generation.

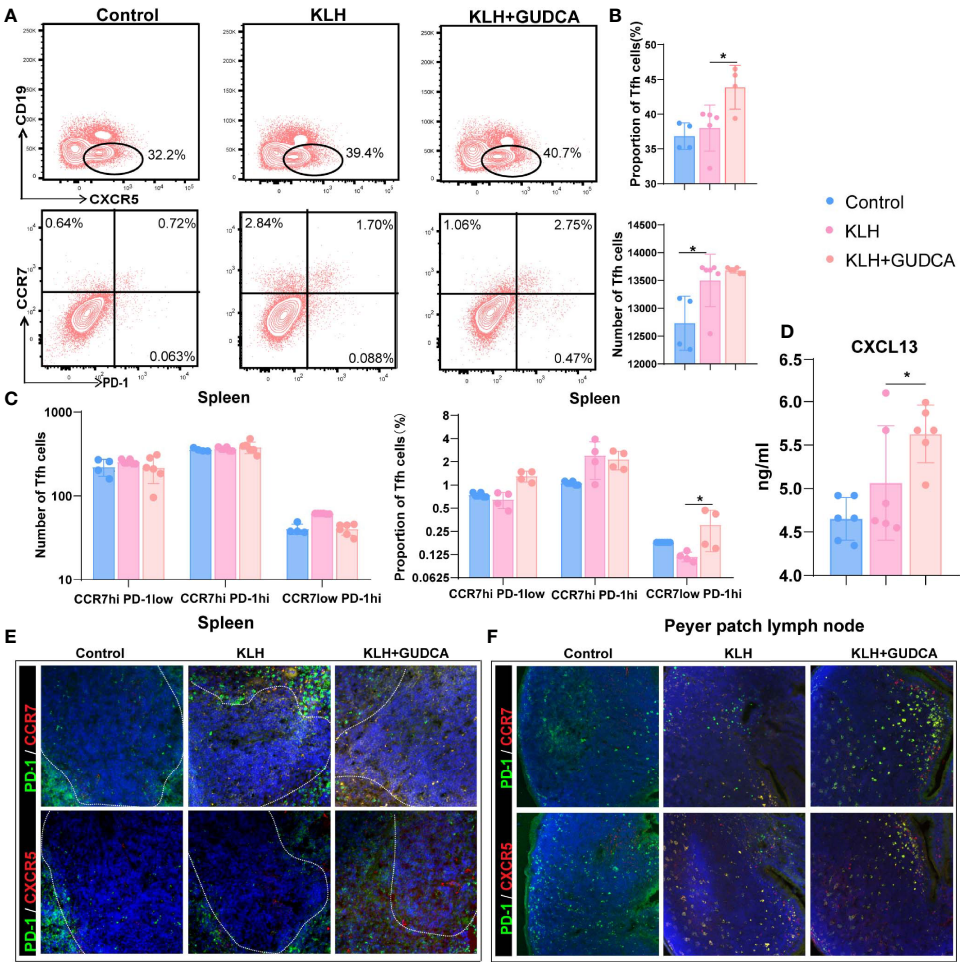

FIGURE 3 | Glycoursodeoxycholic acid administration inhibited the T follicular helper (Tfh) cells in the spleen in KLH-stimulated animals. **(A)** The differentiated plasma cells from B cells were detected using flow cytometry in KLH-stimulated animals. **(B)** Flow cytometric analysis of CD4+CD19-CXCR5+ T cells. **(C)** Flow cytometric analysis of $CCR7^{hi}PD\text{-}1^{low}$ resting Tfh, $CCR7^{hi}PD\text{-}1^{hi}$-activated Tfh, and $CCR7^{low}PD\text{-}1^{hi}$ Tfh cells. **(D)** Expression of CXCL13 in peripheral blood of KLH-stimulated animal using enzyme-link immunosorbent assay. **(E, F)** Representative immunofluorescence image of $CXCR5{+}PD\text{-}1^{hi}$ Tfh and $CCR7{+}PD\text{-}1^{hi}$ Tfh cells in the spleen and Peyer's patch lymph node of the KLH-stimulated animal. N = 6, *$p < 0.05$. KLH, keyhole limpet haemocyanin; GUDCA, glycoursodeoxycholic acid.

Disease Relapse Was Associated With Significant Variations of the Gut Microbiome

Next, we analysed the changes in the stool microbiota of patients with NMOSD using 16S rRNA gene sequencing at the genus taxonomic rank levels (**Figure 4A**). Patients with NMOSD having a high ARR were accompanied by a relatively higher abundance of *Actinomyces* and *Sphingomonas* but a low abundance of *Veillomas*, *Atopobium*, and *Haemophilus* (**Figure 4A**). A higher stool relative abundance of *Actinomycetaceae* (such as *Actinomyces*) and *Mitochondria* predicted a high ARR in these 59 patients, whereas *Bacteroidaceae* (such as *Bacteroides*), *Victivallaceae* (such as *Victivallis*), or *Pasteurellaceae* family members were associated with an optimistic prognosis (**Figure 4B**). Interestingly, *Vagococcus*, *Anaerobiospirillum*, *Stenotrophomonas*, *Veillomas*, *Megasphaera*, *Atopobium*, *VadinCA11*, *Victivallis*, *Haemophilus* and *Bacteroides* were negatively correlated with ARR in NMOSD (**Figure 4C**). Hence, NMOSD recurrence is associated with the local microbiome.

GUDCA Increased the Circulating Tfh Cell and CXCL13 Levels in Mice

Subsequently, we concentrated on the association between CXCL13 and gut microbiota-derived metabolites. Pearson's correlation analysis revealed that GUDCA was positively correlated with the CXCL13 levels (**Figures 5A, B**). A positive correlation between the Taurocholic acid (TCA), LCA ursodesoxycholic acid (UDCA), glycodesoxycholic acid (GDCA) and Taurodeoxycholic acid (TDCA) and the IL-10 levels ($p < 0.001$, $p < 0.001$, $p < 0.001$, $p = 0.006$ and $p = 0.033$, respectively) and a positive correlation between the DCA and LCA, and the IL-17 concentration ($p = 0.005$ and $p = 0.039$, respectively) in NMOSD were also observed (**Figure 5A**). *Anaerobiospirillum* and *Vagococcus* were negatively correlated with GUDCA levels (**Figure 5B**). Using the Virtual Metabolic Human database, we identified that reduced *Veillomas* and *Haemophilus* abundance in Spatients with NMOSD having a high ARR may contribute to decreased cholic acid (CA) and deoxycholic acid (DCA) concentration, which are the metabolites of GUDCA. These data indicate that *Anaerobiospirillum* and *Vagococcus* were the most substantial gut microbiota influencing the levels of GUDCA in the hosts, whereas *Veillomas* and *Haemophilus* were the most substantial gut microbiota in converting GUDCA to DCA (**Figure 5B**).

DISCUSSION

Our findings indicate that the gut microbiota play a crucial role in governing the Tfh immune response induced by CXCL13 in patients with NMOSD. In this study, we analysed the interplay between the stool metabolites and systemic immunomodulation and found significantly downregulated levels of CXCL13 in patients with NMOSD with low ARR. CXCL13 was negatively correlated with GUDCA, which was positively correlated with *Vagococcus and Anaerobiospirillum* abundance, which were negatively correlated with ARR in NMOSD, eliciting CXCL13-induced Tfh cell immune responses possibly dependent on GUDCA and gut microbiota. In this study, we confirmed an increase in the CXCR5+CD4+ T cells in patients with NMOSD with a high ARR. Certainly, serum CXCL13 level reflects the priming and activation of Tfh cells in the spleen. In contrast, GC-Tfh is one of the main producers of plasma CXCL13. There is an increasing number of studies on the Tfh cells in NMO or

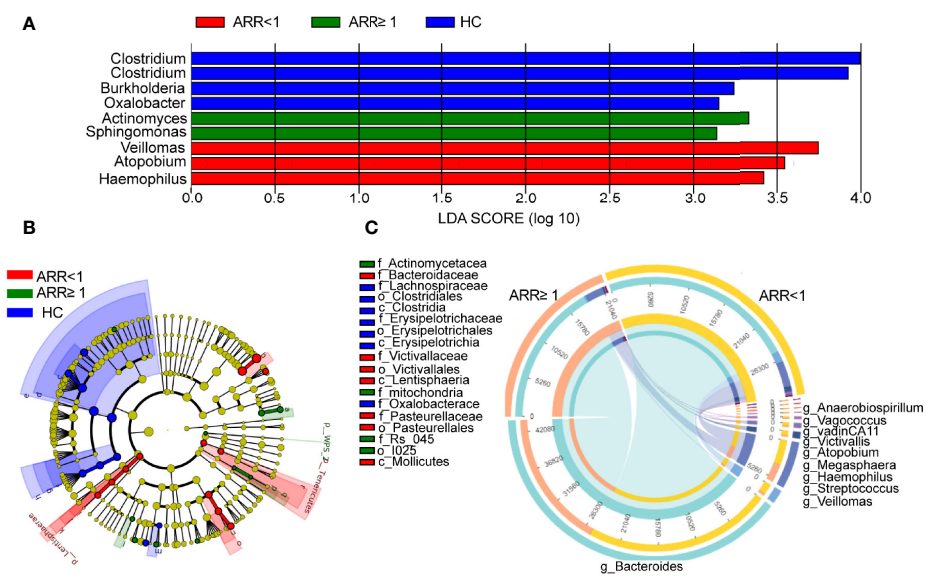

FIGURE 4 | Recurrence-specific changes in bacterial diversities and taxonomic signatures. **(A)** Species were predicted using linear discriminant analysis effect size (LEfSe) at the genus level between two groups patients. **(B)** Cladogram of the LEfSe analysis. **(C)** Correlation detection of ARR-associated gut bacteria in patients with NMOSD. ARR, annual recurrence rate; HC, Healthy controls.

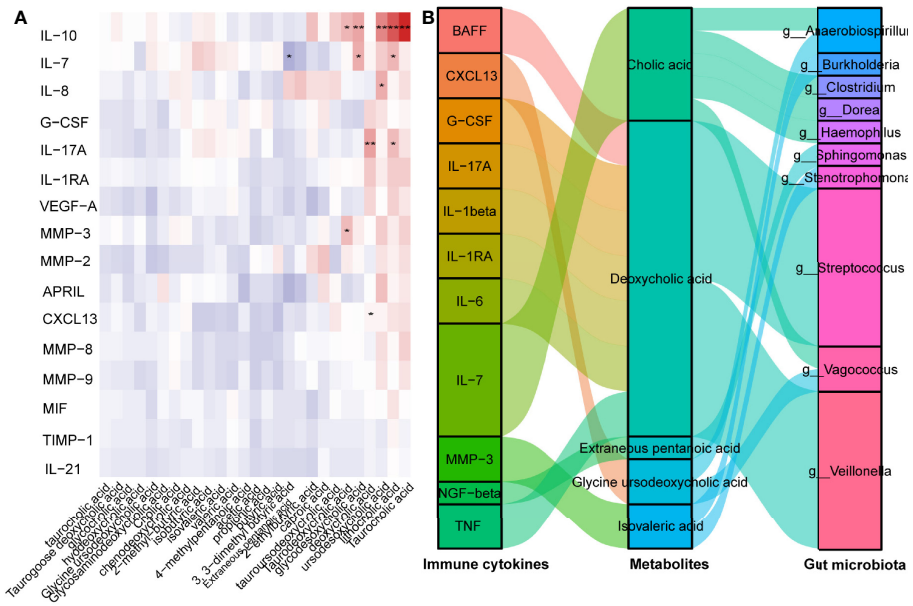

FIGURE 5 | GUDCA increased circulating Tfh cell and CXCL13 levels in mice. **(A)** Correlation between inflammatory factors and metabolites were analysed by Spearman's correlation. Significant changes are denoted as follows: *$^{**}p < 0.01$ and $^{*}p < 0.05$*. **(B)** Spearman's correlation of serum inflammatory cytokines with gut metabolites, gut metabolites and gut bacterial species.

NMOSD. The level of chemokine CXCL13 in the cerebrospinal fluid of patients with NMO is related to the degree of NMO-related nerve defect (7), and patients with recurrence tend to have higher levels of CXCL13 in the serum and cerebrospinal fluid (CSF). The CXCR5 levels in the serum and CSF of patients with NMO are elevated (7). The administration of rituximab (a B-cell depletion therapy) can dramatically reduce the Tfh ratio and re-establish the Tfh subpopulation (12). In summary, the Tfh cells are associated with the disease activity of NMOSD, and could be potential immune markers for disease monitoring, and provide a new direction for NMOSD immunotherapy (13).

Studies have also shown that memory Tfh cells in the circulation express the same surface molecules as effector Tfh cells and can effectively assist B cells in immune responses (14). Therefore, memory Tfh cells can be used as marker cells to monitor the immune activation status of autoimmune diseases. Previous study showed that circulating memory Tfh cells, especially $CCR7^{+}ICOS^{+}$ memory Tfh cells, may be associated with the relapse of MS and the numbers of circulating memory Tfh cells significantly decreased in the remitting stage (15). Among the circulating memory Tfh cells, $CCR7^{+}$ memory Tfh cells can migrate into B cell follicles and promote humoral responses (16, 17), and activated $CCR7^{-}PD\text{-}1^{+}$ memory Tfh cells in the secondary lymphoid tissues also enhance the humoral responses, associated with the development of autoimmune diseases (18). Accordingly, in patients with systemic lupus erythematosus (SLE) and rheumatoid arthritis (RA), increased levels of the $CCR7^{lo}PD\text{-}1^{hi}$ subset correlated with elevated autoantibody profiles and more severe disease activities (18). Intriguingly, our results indicated significantly increased numbers of $CCR7^{-}PD\text{-}1^{+}$ memory Tfh cells in GUDCA-treated KLH mice compared to KLH mice, and the CXCL13 levels were significantly increased in mice sero, Therefore, CXCL13 may participate in the migration of $CCR7^{+}$ and $CCR7^{+}ICOS^{+}$ memory Tfh cells into the secondary lymphoid organs, and consequently, the activated $CCR7^{-}PD\text{-}1^{+}$ memory Tfh cells could enhance the humoral responses associated with the relapse of NMOSD.

Another cytokine, IL-21, also plays a critical role in the survival of Tfh cells and the survival, proliferation, and differentiation of GC B cells. Studies have shown that the frequencies of circulating $CD4^{+}CXCR5^{+}PD\text{-}1^{+}$ T cells and serum IL-21 were higher in patients with NMOSD than in those with MS (19). After glucocorticoid therapy, $CD4^{+}CXCR5^{+}PD\text{-}1^{+}$ T cell count and serum IL-21 levels decreased, suggesting that the Tfh cells and IL-21 are associated with the disease activity of NMOSD (19). A recent study found that the circulating memory Tfh cells ($ICOS^{+}$, $CCR7^{-}$, $CCR7^{-}$, $ICOS^{+}$, $CCR7^{+}$, and $CCR7^{+}ICOS^{+}$ Tfh cells) and serum and cerebrospinal fluid IL-21 levels in patients with NMO/NMOSD significantly increased (7). The proportion of $CCR7^{-}$ and $CCR7^{-}ICOS^{+}$ memory Tfh cells is positively correlated with the ARR, plasma IL-21 level, and AQP-4 antibody levels (7). The proportion of $CCR7^{+}$ and $CCR7^{+}$ $ICOS^{+}$ memory Tfh cells is positively correlated with the number of white blood cells and IL-21 in CSF. After hormone therapy, the levels of $CCR7^{-}ICOS^{+}$, $CCR7^{+}ICOS^{+}$ Tfh cells, and IL-21 reduced in patients with complete remission (7). Hence, IL-21 may participate in the development and relapse of NMO/NMOSD. Although significantly different levels of IL-21 between two groups were not observed in the present study, IL-21 could be utilised as a therapeutic target in NMOSD.

We found that the increased faecal levels of GUDCA induced Tfh activation. Primary BAs in the gut are derived from cholesterol and are synthesised in the liver. BAs are primarily synthesised by the rate-limiting enzyme cholesterol 7α-hydroxylase from the cholesterol in the liver, conjugated with either glycine or taurine (20). Bile salt deconjugation is catalysed by bile salt hydrolase (BSH) and generates free BAs (21), including mainly CDCA and trihydroxy BA CA. The gut microbiome is the only source of enzymes capable of generating hydrophobic SBAs. *Clostridium* and *Desulfovibrio*, which encode the bile acid-inducible operon, convert the host CA to DCA and CDCA and UDCA to LCA (22). In the present study, we found that the *Veillomas* and *Haemophilus* showed the highest increase in patients with NMOSD having an ARR of<1, which could explain the lower levels of GUDCA in the stool. In particular, *Veillomas* and *Haemophilus* spp. were downregulated in patients with NMOSD having a high ARR and negatively correlated with the serum GUDCA levels. The relative abundance of *Veillomas* increased in marathon runners, and inoculation of Veillonella into mice significantly increased the running time (23). Previous studies have reported that the abundance of *Veillonella* increased in patients with cirrhosis (24), whereas the levels of intestinal BAs in patients with liver cirrhosis are frequently insufficient (25). *Haemophilus* displayed a negative correlation with common indicators of dyslipidaemia, such as total cholesterol and high-density lipoprotein cholesterol (26). *Haemophilus* has also been reported to have a negative association with DCA (27). However, the levels of BAs were similar in both groups of NMOSD, ruling out that the discriminant bacteria observed between the two groups were caused by these metabolites. These investigations on the intestinal symbiotic bacteria provide evidence for a precise understanding of the complex interactions between the gut microbiota and host BA metabolites. Our data suggested that the decreased CXCL13 level was associated with GUDCA, $CCR7^{low}PD\text{-}1^{hi}$ Tfh precursor cells in the KLH mice tended to increase following GUDCA supplementation, showing that the levels of CXCL13 and Tfh precursor cells were correlated with the metabolite GUDCA. Meanwhile, *Veillomas* and *Haemophilus* showed the highest increase in patients with NMOSD having an ARR of<1, which could explain the lower levels of GUDCA in the stool. Therefore, our data showed that the recurrence rate correlated with the gut microbiota and their metabolite in NMOSD, whereas the CXCL13-induced activation of the Tfh cells was the possible mechanism.

In addition, recent reports have confirmed that the intestinal microbiota is essential for the local activation of Tfh cells. Immunogenic commensals are distinguishable from tolerogenic bacteria and trigger migratory DCs to release IL-1β and IL-12p70, thereby increasing bacterial or self-antigen-specific Tfh cells or IgG2b responses (28). Various microbial contents can trigger Tfh cell responses, specifically bacterial RNA, which can induce IL-1β-dependent differentiation of Tfh cells and GC B cells (29). After mucosal inoculation with inactivated enterotoxigenic *Escherichia coli*, activated $ICOS^+$ Tfh cells were recirculated in the blood and represented mucosal memory B cell responses (30). Whether antigen-specific Tfh cells are present in NMOSD remains to be defined. Further experiments are needed to address the gut microbiota to detect whether there is a Tfh-specific recognition motif.

In our study, we demonstrated that the gut microbiota and their metabolite correlated to the NMOSD relapse *via* CXCL13-induced activation of Tfh cells. In addition, there was a significant correlation between the multiple microbe metabolites and IL-10 and IL-17A in our study. Previous studies have revealed that the interaction between hosts and their gut bacteria can regulate the host immunological IL10/IL17A homeostasis *via* the BAs. Song et al. have reported that genetic abolition of the BA metabolic pathways in individual gut symbionts significantly decreases this Treg cell population. Restoration of the intestinal BA pool increases the colonic RORγ+ Treg cell counts and ameliorates host susceptibility to inflammatory colitis *via* BA nuclear receptors (31). Campbell et al. found that the secondary bile acid 3β-hydroxydeoxycholic acid (isoDCA) increased the Foxp3 induction by acting on dendritic cells (DCs) to diminish their immunostimulatory properties. Ablating one receptor, the FXR, in DCs enhanced the generation of Treg cells and imposed a transcriptional profile similar to that induced by isoDCA (10). Moreover, IL10/IL17A homeostasis reportedly participates in the pathogenesis of NMOSD (32). Therefore, more research is warranted to better explain the role of gut microbiota and their metabolite in the pathogenesis of NMOSD.

This study has some limitations. Although we noted the accumulation of Tfh cells in the lymph follicle-like structure in the gut and spleen, the origin of Tfh cells remains unclear. We also noted that the number of participants in our cross-sectional analysis was relatively small. We can only verify the role of GUDCA in Tfh activation in the animal experiments. However, there is no direct evidence of whether the gut microbiota affects Tfh activation. In fact, it is not clear if different immunosuppressive treatments and course of disease between the groups may affect Tfh activation.

CONCLUSIONS

In the present study, we demonstrated that the recurrence of NMOSD is correlated with Tfh cells and CXCL13, which is positively correlated with gut GUDCA. These data broaden our understanding of the mechanism of NMOSD and provide intestinal microbiota as a potential therapeutic target. Finally, we established a gut microbiome–metabolite–Tfh-CXCL13 system to predict the recurrence of NMOSD.

DATA AVAILABILITY STATEMENT

The datasets presented in this study can be found in online repositories. The names of the repository/repositories and accession number(s) can be found in the article/**Supplementary Material**.

ETHICS STATEMENT

The studies involving human participants were reviewed and approved by the medical ethics committee of the Third Affiliated Hospital of Sun Yat-sen University. The patients/participants provided their written informed consent to participate in this study. The animal study was reviewed and approved by Medical Ethics Committee of The Third Affiliated Hospital of Sun Yat-sen University.

AUTHOR CONTRIBUTIONS

Conceptualisation, WQ and AK. Methodology, XC. Software, XC. Validation, CL. Formal analysis, XC. Investigation, LZ. Data curation, XZ and YC. Writing—original draft preparation. XC. Writing—review and editing, ZL and LZ. Visualisation, SS. Supervision, YZ. Project administration, XC. Funding acquisition, WQ. All authors have read and agreed to the published version of the manuscript.

FUNDING

Financial support for the research was provided by the National Natural Science Foundation of China (grants. 82001284, 82071344, and 82101418).

SUPPLEMENTARY MATERIAL

The Supplementary Material for this article can be found online at: https://www.frontiersin.org/articles/10.3389/fimmu.2022.827865/full#supplementary-material

REFERENCES

1. Zhang X, Ing S, Fraser A, Chen M, Khan O, Zakem J, et al. Follicular Helper T Cells: New Insights Into Mechanisms of Autoimmune Diseases. *Ochsner J* (2013) 13:131–9.
2. Simpson N, Gatenby PA, Wilson A, Malik S, Fulcher DA, Tangye SG, et al. Expansion of Circulating T Cells Resembling Follicular Helper T Cells is a Fixed Phenotype That Identifies a Subset of Severe Systemic Lupus Erythematosus. *Arthritis Rheum* (2010) 62:234–44. doi: 10.1002/art.25032
3. Ma J, Zhu C, Ma B, Tian J, Baidoo SE, Mao C, et al. Increased Frequency of Circulating Follicular Helper T Cells in Patients With Rheumatoid Arthritis. *Clin Dev Immunol* (2012) 2012:1–7. doi: 10.1155/2012/827480
4. Szabo K, Papp G, Barath S, Gyimesi E, Szanto A, Zeher M. Follicular Helper T Cells may Play an Important Role in the Severity of Primary Sjögren's Syndrome. *Clin Immunol* (2013) 147:95–104. doi: 10.1016/j.clim.2013.02.024
5. Kubo S, Nakayamada S, Zhao J, Yoshikawa M, Miyazaki Y, Nawata A, et al. Correlation of T Follicular Helper Cells and Plasmablasts With the Development of Organ Involvement in Patients With Igg4-Related Disease. *Rheumatol (United Kingdom)* (2018) 57:514–24. doi: 10.1093/rheumatology/kex455
6. Holm Hansen R, Højsgaard Chow H, Sellebjerg F, Rode von Essen M. Dimethyl Fumarate Therapy Suppresses B Cell Responses and Follicular Helper T Cells in Relapsing-Remitting Multiple Sclerosis. *Mult Scler J* (2019) 25:1289–97. doi: 10.1177/1352458518790417
7. Fan X, Jiang Y, Han J, Liu J, Wei Y, Jiang X, et al. Circulating Memory T Follicular Helper Cells in Patients With Neuromyelitis Optica/Neuromyelitis Optica Spectrum Disorders. *Mediators Inflamm* (2016) 2016:1–13. doi: 10.1155/2016/3678152
8. Cui C, Tan S, Tao L, Gong J, Chang Y, Wang Y, et al. Intestinal Barrier Breakdown and Mucosal Microbiota Disturbance in Neuromyelitis Optical Spectrum Disorders. *Front Immunol* (2020) 11:1–15. doi: 10.3389/fimmu.2020.02101
9. Gong J, Qiu W, Zeng Q, Liu X, Sun X, Li H, et al. Lack of Short-Chain Fatty Acids and Overgrowth of Opportunistic Pathogens Define Dysbiosis of Neuromyelitis Optica Spectrum Disorders: A Chinese Pilot Study. *Mult Scler J* (2019) 25:1316–25. doi: 10.1177/1352458518790396
10. Campbell C, McKenney PT, Konstantinovsky D, Isaeva OI, Schizas M, Verter J, et al. Bacterial Metabolism of Bile Acids Promotes Generation of Peripheral Regulatory T Cells. *Nature* (2020) 581:475–9. doi: 10.1038/s41586-020-2193-0
11. Wingerchuk DM, Banwell B, Bennett JL, Cabre P, Carroll W, Chitnis T, et al. International Consensus Diagnostic Criteria for Neuromyelitis Optica Spectrum Disorders. *Neurology* (2016) 86:491–2. doi: 10.1212/WNL.0000000000002366
12. Nicolas P, Ruiz A, Cobo-Calvo A, Fiard G, Giraudon P, Vukusic S, et al. The Balance in T Follicular Helper Cell Subsets Is Altered in Neuromyelitis Optica Spectrum Disorder Patients and Restored by Rituximab. *Front Immunol* (2019) 10:1–7. doi: 10.3389/fimmu.2019.02686
13. Zhao C, Li HZ, Zhao D, Ma C, Wu F, Bai YN, et al. Increased Circulating T Follicular Helper Cells are Inhibited by Rituximab in Neuromyelitis Optica Spectrum Disorder. *Front Neurol* (2017) 8:1–9. doi: 10.3389/fneur.2017.00104
14. Helmold Hait S, Hogge CJ, Rahman MA, Hunegnaw R, Mushtaq Z, Hoang T, et al. TFH Cells Induced by Vaccination and Following SIV Challenge Support Env-Specific Humoral Immunity in the Rectal-Genital Tract and Circulation of Female Rhesus Macaques. *Front Immunol* (2021) 11:1–21. doi: 10.3389/fimmu.2020.608003
15. Fan X, Jin T, Zhao S, Liu C, Han J, Jiang X, et al. Circulating CCR7+ICOS+ Memory T Follicular Helper Cells in Patients With Multiple Sclerosis. *PloS One* (2015) 10:1–14. doi: 10.1371/journal.pone.0134523
16. Morita R, Schmitt N, Bentebibel SE, Ranganathan R, Bourdery L, Zurawski G, et al. Human Blood CXCR5+CD4+ T Cells Are Counterparts of T Follicular Cells and Contain Specific Subsets That Differentially Support Antibody Secretion. *Immunity* (2011) 34:108–21. doi: 10.1016/j.immuni.2010.12.012
17. Breitfeld D, Ohl L, Kremmer E, Ellwart J, Sallusto F, Lipp M, et al. Follicular B Helper T Cells Express CXC Chemokine Receptor 5, Localize to B Cell Follicles, and Support Immunoglobulin Production. *J Exp Med* (2000) 192:1545–51. doi: 10.1084/jem.192.11.1545
18. He J, Tsai LM, Leong YA, Hu X, Ma CS, Chevalier N, et al. Circulating Precursor CCR7loPD-1hi CXCR5+ CD4+ T Cells Indicate Tfh Cell Activity and Promote Antibody Responses Upon Antigen Reexposure. *Immunity* (2013) 39:770–81. doi: 10.1016/j.immuni.2013.09.007
19. Yang X, Peng J, Huang X, Liu P, Li J, Pan J, et al. Association of Circulating Follicular Helper T Cells and Serum CXCL13 With Neuromyelitis Optica Spectrum Disorders. *Front Immunol* (2021) 12:1–8. doi: 10.3389/fimmu.2021.677190
20. Sayin SI, Wahlström A, Felin J, Jäntti S, Marschall HU, Bamberg K, et al. Gut Microbiota Regulates Bile Acid Metabolism by Reducing the Levels of Tauro-Beta-Muricholic Acid, a Naturally Occurring FXR Antagonist. *Cell Metab* (2013) 17:225–35. doi: 10.1016/j.cmet.2013.01.003
21. Jones BV, Begley M, Hill C, Gahan CGM, Marchesi JR. Functional and Comparative Metagenomic Analysis of Bile Salt Hydrolase Activity in the Human Gut Microbiome. *Proc Natl Acad Sci United States America* (2008) 105:13580–5. doi: 10.1073/pnas.0804437105
22. Just S, Mondot S, Ecker J, Wegner K, Rath E, Gau L, et al. The Gut Microbiota Drives the Impact of Bile Acids and Fat Source in Diet on Mouse Metabolism. *Microbiome* (2018) 6:1–18. doi: 10.1186/s40168-018-0510-8
23. Scheiman J, Luber JM, Chavkin TA, MacDonald T, Tung A, Pham LD, et al. Meta-Omics Analysis of Elite Athletes Identifies a Performance-Enhancing Microbe That Functions *via* Lactate Metabolism. *Nat Med* (2019) 25:1104–9. doi: 10.1038/s41591-019-0485-4

24. Chen Y, Ji F, Guo J, Shi D, Fang D, Li L. Dysbiosis of Small Intestinal Microbiota in Liver Cirrhosis and Its Association With Etiology. *Sci Rep* (2016) 6:1–9. doi: 10.1038/srep34055
25. Oh TG, Kim SM, Caussy C, Fu T, Guo J, Bassirian S, et al. A Universal Gut-Microbiome-Derived Signature Predicts Cirrhosis. *Cell Metab* (2020) 32:878–888.e6. doi: 10.1016/j.cmet.2020.06.005
26. Granado-Serrano AB, Martín-Garí M, Sánchez V, Riart Solans M, Berdún R, Ludwig IA, et al. Faecal Bacterial and Short-Chain Fatty Acids Signature in Hypercholesterolemia. *Sci Rep* (2019) 9:1–13. doi: 10.1038/s41598-019-38874-3
27. De Chiara M, Hood D, Muzzi A, Pickard DJ, Perkins T, Pizza M, et al. Genome Sequencing of Disease and Carriage Isolates of Nontypeable Haemophilus Influenzae Identifies Discrete Population Structure. *Proc Natl Acad Sci USA* (2014) 111:5439–44. doi: 10.1073/pnas.1403353111
28. Roberti MP, Yonekura S, Duong CPM, Picard M, Ferrere G, Tidjani Alou M, et al. Chemotherapy-Induced Ileal Crypt Apoptosis and the Ileal Microbiome Shape Immunosurveillance and Prognosis of Proximal Colon Cancer. *Nat Med* (2020) 26:919–31. doi: 10.1038/s41591-020-0882-8
29. Barbet G, Sander LE, Geswell M, Leonardi I, Cerutti A, Iliev I, et al. Sensing Microbial Viability Through Bacterial RNA Augments T Follicular Helper Cell and Antibody Responses. *Immunity* (2018) 48:584–98.e5. doi: 10.1016/j.immuni.2018.02.015
30. Cárdeno A, Magnusson MK, Quiding-Järbrink M, Lundgren A. Activated T Follicular Helper-Like Cells are Released Into Blood After Oral Vaccination and Correlate With Vaccine Specific Mucosal B-Cell Memory. *Sci Rep* (2018) 8:1–15. doi: 10.1038/s41598-018-20740-3
31. Song X, Sun X, Oh SF, Wu M, Zhang Y, Zheng W, et al. Microbial Bile Acid Metabolites Modulate Gut Rorγ+ Regulatory T Cell Homeostasis. *Nature* (2020) 577:410–5. doi: 10.1038/s41586-019-1865-0
32. Varrin-Doyer M, Spencer CM, Schulze-Topphoff U, Nelson PA, Stroud RM, Bruce BA, et al. Aquaporin 4-Specific T Cells in Neuromyelitis Optica Exhibit a Th17 Bias and Recognize Clostridium ABC Transporter. *Ann Neurol* (2012) 72:53–64. doi: 10.1002/ana.23651

Conflict of Interest: The authors declare that the research was conducted in the absence of any commercial or financial relationships that could be construed as a potential conflict of interest.

Publisher's Note: All claims expressed in this article are solely those of the authors and do not necessarily represent those of their affiliated organizations, or those of the publisher, the editors and the reviewers. Any product that may be evaluated in this article, or claim that may be made by its manufacturer, is not guaranteed or endorsed by the publisher.

frontiers in Neurology

CASE REPORT
published: 21 January 2022
doi: 10.3389/fneur.2021.775181

Case Report: Four Cases of Cortical/Brainstem Encephalitis Positive for Myelin Oligodendrocyte Glycoprotein Immunoglobulin G

*Wan Wang[1], Juntao Yin[2], Zhiliang Fan[1], Juxian Kang[1], Jia Wei[1], Xiaoqian Yin[3] and Shaohua Yin[1]**

[1] Department of Neurology, Affiliated Hospital Xingtai People's Hospital, Hebei Medical University, Xingtai, China, [2] Department of Neurology, Xingtai Third Hospital, Xingtai, China, [3] Department of Imaging, Affiliated Hospital Xingtai People's Hospital, Hebei Medical University, Xingtai, China

Aim: Despite a significant improvement in the number of studies on myelin oligodendrocyte glycoprotein (MOG)-immunoglobulin G (IgG)-associated disorder (MOGAD) over the past few years, MOG-IgG-associated cortical/brainstem encephalitis remains a relatively uncommon and less-reported presentation among the MOGAD spectrum. This study aimed to report the clinical course, imaging features, and therapeutic response of MOG-IgG-associated cortical/brainstem encephalitis.

Methods: Data of four patients who suffered from cortical encephalitis with epileptic seizures and/or brainstem encephalitis during the course of the disease were retrospectively collected and analyzed.

Results: In this study, three male patients and one female patient, with a median age of onset of 21 years (ranging 20–51 years) were enrolled. An epileptic seizure was the main symptom of cortical encephalitis in these patients, while the manifestations of brainstem encephalitis were diverse. Cranial MRI demonstrated abnormal signals in unilateral or bilateral cortical or brainstem. Cerebrospinal fluid studies showed normal or mildly elevated leukocyte counts and protein levels, and a cell-based assay detected positive MOG-IgG in the serum of all patients. Two patients were misdiagnosed at the first attack, and both experienced a relapse. All of them accepted the first-line immunotherapy after a confirmed diagnosis and had a good outcome.

Conclusion: Early suspicion of MOG-IgG-associated encephalitis is necessary for any patient with sudden onset of seizures or symptoms of brainstem damage, especially with lesions on unilateral/bilateral cortical or brainstem on brain MRI.

Keywords: brainstem encephalitis, cortical encephalitis, epileptic seizures, myelin oligodendrocyte glycoprotein, neuromyelitis optica spectrum disorder

OPEN ACCESS

Edited by:
Jodie Burton, University of Calgary, Canada

Reviewed by:
Frederic London, Catholic University of Louvain, Belgium
Jefferson Becker, Pontifical Catholic University of Rio Grande do Sul, Brazil

***Correspondence:**
Shaohua Yin
yinsh1012@163.com

Specialty section:
This article was submitted to Multiple Sclerosis and Neuroimmunology, a section of the journal Frontiers in Neurology

Received: *13 September 2021*
Accepted: *20 December 2021*
Published: *21 January 2022*

Citation:
Wang W, Yin J, Fan Z, Kang J, Wei J, Yin X and Yin S (2022) Case Report: Four Cases of Cortical/Brainstem Encephalitis Positive for Myelin Oligodendrocyte Glycoprotein Immunoglobulin G. Front. Neurol. 12:775181. doi: 10.3389/fneur.2021.775181

INTRODUCTION

Myelin oligodendrocyte glycoprotein (MOG) is a myelin protein expressed on the outer surface of myelin sheaths and oligodendrocyte processes in the central nervous system (CNS) (1). Although MOG-immunoglobulin G (IgG)-positive cases account for about 25% of aquaporin-4 (AQP4)-seronegative neuromyelitis optica spectrum disorders (2), the clinical manifestation

is less well-defined. In recent years, an enormous amount of research has been conducted to determine the role of MOG-IgG in a wide clinical spectrum of inflammatory demyelinating CNS disorders, including optic neuritis (ON), myelitis, cortical damage (3), and less commonly, brainstem lesions (4). Compared with ON and myelitis, cortical encephalitis with seizures and brainstem encephalitis are emerging presentations of MOG-IgG-associated disorder (MOGAD), and the related research has been rarely reported. The relationship between MOG-IgG and cortical encephalitis presentation was not recognized until the first case reported in 2017 (5). Subsequent case series further confirmed the association between MOG-IgG, fluid-attenuated inversion recovery (FLAIR)-hyperintense cerebral cortical lesions, and sudden epilepsy. Furthermore, most patients with MOG-IgG-associated cortical encephalitis had a relapsing disease course and experienced other demyelinating events, such as ON, myelitis, or brainstem damage, at a certain stage of the disease (6–10).

In the present study, four cases of MOG-IgG-associated cortical/brainstem encephalitis are reported, providing detailed information on the clinical manifestations, imaging features, disease evolution, and treatment outcomes of this disease.

CASE PRESENTATION

Case 1

A previously healthy 20-year-old male patient presented with a witnessed primary generalized tonic-clonic seizure. After about 10 h in a coma, a nervous system examination revealed no limb weakness or sensory symptoms. Poorly marginated, hyperintense lesions in the left frontotemporal parietal lobe and the right frontal lobe were displayed on both FLAIR (**Figures 1A**, **2A–E**) and T2-weighted images of cranial MRI (**Figure 1C**), which were less evident on T1-weighted (**Figure 1B**) and diffusion-weighted images (**Figure 1D**). No epileptic waves were captured on an electroencephalogram (EEG). Laboratory data revealed an increase in the white blood cell count (17.32×10^9/L). A cerebrospinal fluid (CSF) analysis showed a mild increase in leukocytes (80/μl) and protein (48 mg/dl). CSF cytology suggested lymphocytic reaction. CSF culture was negative. Neither immunoglobulin M (IgM) nor IgG of the herpes simplex virus were tested positive in CSF. The patient was diagnosed with viral encephalitis and treated with dexamethasone and acyclovir combined with antiepileptic drugs (sodium valproate) for 2 weeks. He no longer had epileptic seizures and was advised to continue prednisone [40 mg qd (once a day)] orally for 40 days after discharge. The dosage of prednisone was reduced by 5 mg every 5 days until discontinued. However, he had to be readmitted several times within 4 months because of frequent epileptic seizures and headaches with or without a fever. During this period, seizures occurred in two main forms: primary generalized and focal. He received symptomatic treatment each time. A follow-up brain MRI after 3 months suggested that FLAIR hyperintensities in the bilateral cortical regions were shallow and fewer (**Figures 1E**, **2F**). He was readmitted because of dizziness and unsteady gait 3 years later, and a nervous system examination revealed poor left-side ataxia. Cranial MRI revealed FLAIR-hyperintense (**Figure 1F**), T1-hyperintense (**Figure 1G**), T2-hyperintense (**Figure 1H**), and diffusion-hyperintense (**Figure 1I**) lesions in the pons and left brachium pontis. CSF analysis showed four leukocytes and a mildly increased protein level (51 mg/dl). AQP4-IgG and oligoclonal bands in serum and CSF were negative. The myelin basic protein (MBP) level in the serum and CSF was not elevated. Antibodies of autoimmune encephalitis in the serum and CSF were negative. The cell-based assays (CBAs) revealed that MOG-IgG was positive with titers of 1:10 in the serum. Thus, the diagnosis was corrected to MOG-IgG-associated encephalitis. He received intravenous pulse methylprednisolone (500 mg/day for 3 days), followed by oral prednisone (60 mg qd, with a tapering dose of 5 mg every 1 week) and mycophenolate mofetil [0.75 g bid (twice a day)]. The FLAIR hyperintensities in the brainstem were shallow and smaller after 1 month (**Figure 1J**). The dosage of prednisone was gradually reduced to 10 mg daily and on maintenance for 1 year. He fully recovered, and MOG-IgG in his serum turned negative after 18 months. No recurrent events occurred during a 28-month follow-up.

Case 2

A 20-year-old male patient without any previous medical history was admitted to the hospital with twice primary generalized tonic-clonic seizures in 48 h. The neurological examination was normal. The brain MRI showed FLAIR-hyperintense lesions in the left frontal lobe (**Figures 2G–K**). EEG captured 2- to 3-Hz complex waves of sharp slow frequencies in the right frontal and bilateral occipitotemporal lobes. The laboratory data revealed a normal white blood cell count and blood biochemistry results. The CSF study showed a mild increase in leukocytes (31/μl) and a normal protein level. The antibodies of autoimmune encephalitis and CNS demyelinating disease in the serum and CSF were tested, which indicated non-elevated MBP levels and negative oligoclonal bands and AQP4-IgG. However, a CBA revealed anti-MOG-IgG in his serum (1:100). He was diagnosed with MOG-IgG-associated encephalitis and treated with antiepileptic drugs (levetiracetam) and intravenous pulse methylprednisolone (500 mg/day for 3 days), followed by oral prednisone (60 mg qd) and mycophenolate mofetil (0.5 g bid) induction. The FLAIR hyperintensities in the unilateral cortical regions disappeared after 1 month (**Figure 2L**). With a tapering dose of 5 mg prednisone every 1 week and low-dose prednisone (10 mg daily) for 6 months, the patient did not experience any relapse during the 16-month follow-up.

Case 3

A 51-year-old female patient was admitted to the hospital for left-side facial paralysis and left perioral numbness. Her medical history showed hysterectomy because of uterine fibroids for 15 years. A neurological examination on admission showed left-side peripheral facial paralysis and decreased touch and pain sensation in the left perioral area. Cranial MRI disclosed nodular FLAIR-hyperintense (**Figure 3A**), T1-hypointense (**Figure 3B**), T2-hyperintense (**Figure 3C**), and diffusion-hyperintense (**Figure 3D**) lesions in the left brachium pontis, with an enhanced edge on T1-weighted images (**Figure 3E**). No supratentorial lesion was found. The conventional laboratory tests of blood and serum antineutrophil cytoplasmic antibody and anti-myeloperoxidase antibody were negative. The CSF

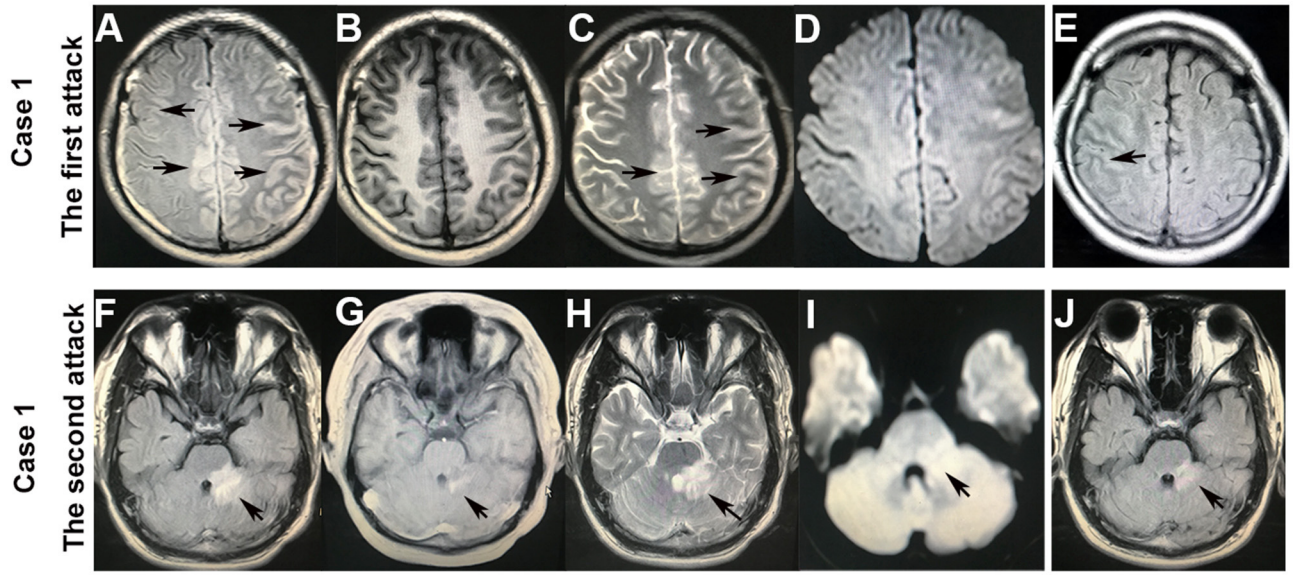

FIGURE 1 | Brain MRI of case 1. After the first attack of an epileptic seizure, the hyperintense lesions with a hazy border in the bilateral cortex on fluid-attenuated inversion recovery (FLAIR) **(A)** and T2-weighted **(C)** images (arrowheads), which were less evident on T1-weighted **(B)** and diffusion-weighted **(D)** images. FLAIR hyperintensities in the cortical regions became shallow and fewer after 3 months **(E)** (arrowheads). After the second attack that presented with dizziness and left-sided ataxia, the hyperintensities in the pons and left brachium pontis on FLAIR **(F)**, T1-weighted **(G)**, T2-weighted **(H)**, and diffusion-weighted **(I)** images (arrowheads). The FLAIR hyperintensities in the brainstem became shallow and smaller after 1 month **(J)**.

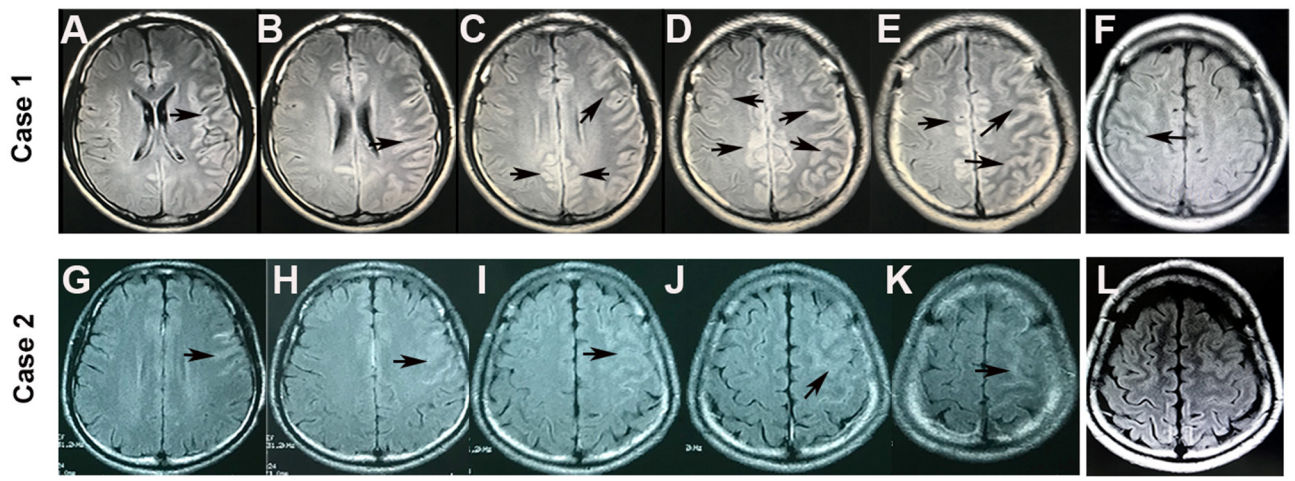

FIGURE 2 | Brain MRI of cortical lesions in cases 1 and 2. FLAIR hyperintensity was seen in the bilateral cerebral cortex in case 1 **(A–E)** and in the left hemispheric cortical region in case 2 **(G–K)** (arrowheads). However, the FLAIR hyperintensities in the cortical regions became shallow and fewer after 3 months in case 1 **(F)** and disappeared after 1 month in case 2 **(L)**.

examination revealed a normal cell count (3/μl) and protein level (31 mg/dl). The tests for oligoclonal bands and AQP4-IgG in both blood and CSF cultures were negative. MBP in the serum and CSF was not elevated. However, a CBA revealed MOG-IgG in her serum (1:10). She was diagnosed with MOG-IgG-associated brainstem encephalitis. After a treatment with intravenous pulse methylprednisolone (500 mg/day for 3 days) followed by oral prednisone (60 mg qd, reduced by 5 mg per week) and mycophenolate mofetil (0.5 g bid), the symptoms gradually improved. The patient was in a stable condition during a 6-month follow-up with 10 mg oral prednisone and 1 g mycophenolate mofetil daily.

Case 4

A 22-year-old male patient presented with dizziness and an unsteady gait. He was admitted to a local hospital and received symptomatic treatment for several days. The symptoms persisted and progressively worsened. He felt weakness in

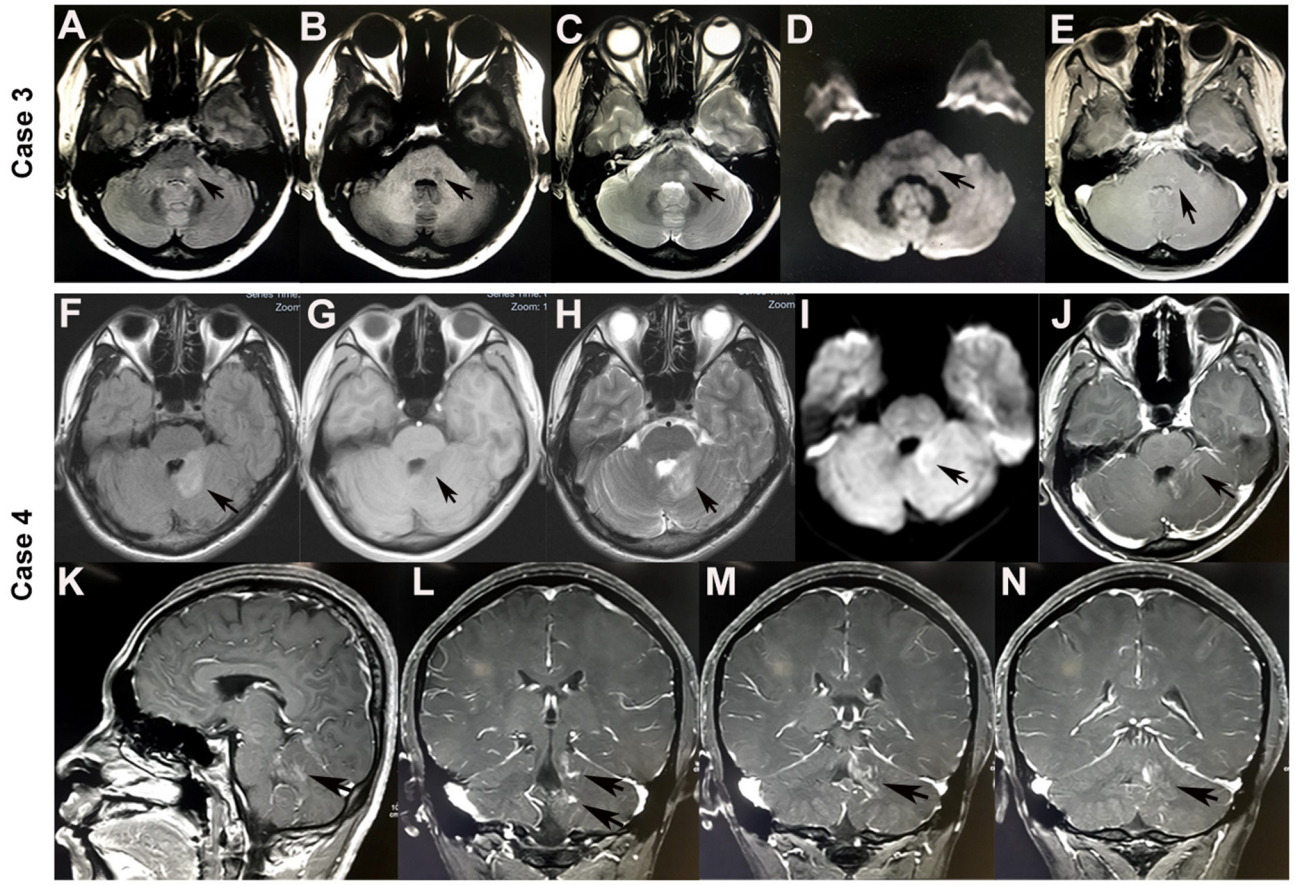

FIGURE 3 | Brain MRI of brainstem lesions in cases 3 and 4. A nodular hyperintense lesion in the left brachium pontis on FLAIR **(A)**, T2-weighted **(C)**, and diffusion-weighted **(D)** images (arrowheads). However, it was hypointense on the T1-weighted image **(B)**, and with a gadolinium-enhanced edge on the T1-weighted image **(E)** (arrowheads). Hyperintense lesions in the left brachium pontis, left cerebellar hemisphere, and cerebellar vermis on FLAIR **(F)**, T2-weighted **(H)**, and diffusion-weighted **(I)** images (arrowheads). However, it was hypointense on the T1-weighted image **(G)**, and with curvilinear post-gadolinium contrast enhancement on the T1-weighted image: axial **(J)**, sagittal **(K)**, and coronal **(L–N)** (arrowheads).

the left-side limbs and was transferred to our hospital. A nervous system examination discovered mild left-side hemiparesis. Cranial MRI revealed T1-hypointense (**Figure 3G**), T2-hyperintense (**Figure 3H**), FLAIR-hyperintense (**Figure 3F**), and diffusion-hyperintense (**Figure 3I**) lesions with curvilinear post-gadolinium contrast enhancement (**Figures 3J–N**) in the left brachium pontis, left cerebellar hemisphere, and cerebellar vermis. The CSF analysis showed a mild increase in leukocytes (55/μl) and normal protein levels. Oligoclonal bands and AQP4-IgG were negative in both blood and CSF. MBP in the serum and CSF was not elevated. However, CBAs detected positive anti-MOG-IgG in CSF (1:1) but negative in serum. Considering the limited reliability of anti-MOG-IgG in CSF and his special image presentation, the patient was diagnosed with probable chronic lymphocytic inflammation with pontine perivascular enhancement responsive to steroids (CLIPPERS) syndrome and received the treatment of high-dose intravenous methylprednisolone (500 mg/day for 3 days), followed by oral prednisone starting at 60 mg daily with a tapering dose of 5 mg every 1 week. His symptoms of dizziness and hemiplegia greatly improved, and he was discharged after 20 days of treatment. After 5 months, when the prednisone was reduced to 5 mg/day, the patient developed a sudden primary generalized tonic-clonic seizure and was readmitted to our hospital. Neither nervous system examination nor cranial MRI revealed any abnormality. Slow waves were seen in the left prefrontal, frontal, and temporal regions in EEG. Although cell counts (2/μL) and biochemistry of CSF were normal this time, the anti-MOG-IgG was positive in both serum (1:32) and CSF (1:1) as detected by CBAs. He was diagnosed with MOG-IgG-associated encephalitis; therefore, azathioprine (50 mg bid) and antiepileptic drugs (levetiracetam 0.5 g bid) were added. The patient remained stable during a 6-month follow-up with 10 mg oral prednisone, 1.0 g levetiracetam, and 100 mg azathioprine daily.

DISCUSSION

Myelin oligodendrocyte glycoprotein (MOG)-IgG–associated disorder (MOGAD) has a specific therapeutic strategy, making early diagnosis and differentiation crucial for developing an

individualized treatment approach. However, diagnosis at the first demyelinating event remains a challenge due to overlapping and fickle clinical features of MOGAD. Among all clinical manifestations, cerebral and brainstem damage were quite rare disease phenotypes (<10%) in both pediatric and adult groups (7, 11, 12). MOG-IgG–positive unilateral or bilateral cortical encephalitis detected as FLAIR-hyperintense cortical lesions (as observed in cases 1 and 2) was first reported by Ogawa et al. (5, 6, 8, 13–17) in 2017 as an emerging phenotype of MOGAD (**Table 1**). Brainstem encephalitis is another infrequent presentation except for cortical encephalitis among the clinical spectrum of MOGAD (7, 13). Patients with brainstem involvement account for about 30% in MOG-IgG-associated encephalomyelitis cases, and isolated brainstem encephalitis that occurs without ON or myelitis is much rarer, accounting for only 1.8% (18).

Cerebral lesions of MOGAD usually look paler, fewer, and less prominent compared with multiple sclerosis cases and can be observed in both T2-weighted and FLAIR images (8, 19, 20). An important basis for diagnosing MOG-IgG cortical encephalitis is unilateral or bilateral cortical lesions on cranial MRI, which are best depicted on FLAIR images (21). In this study, the lesions in case 1 were slightly hyperintense with a hazy border in the bilateral cortical gray matter on FLAIR (**Figures 1A**, **2A–E**) and T2-weighted images (**Figure 1C**); the lesions became lighter and fewer after 3 months and were displayed only on the FLAIR image (**Figures 1E**, **2F**). Similar abnormal lesions located in the unilateral cortical gray matter were observed in case 2 only on the FLAIR image at the beginning of the disease (**Figures 2G–K**) and almost disappeared after a month (**Figure 2L**). Similar to the cortical lesions observed in cases 1 and 2, FLAIR hyperintensity lesions in the cortex or sulcus are also observed in various pathologic conditions, such as meningitis, leptomeningeal metastasis, acute infarction, subarachnoid hemorrhage, and moyamoya disease (22). Thus, patients with MOG-IgG-positive cortical encephalitis, as in cases 1 and 2 in this study, could have been easily misdiagnosed as other diseases.

Brainstem lesions in MOG-IgG-positive cases usually presented a vague, irregularly bordered focus located in different areas of the brainstem, among which the pons was the most commonly involved and accounted for 84.6%. Other common lesions included medulla oblongata (57.1%), cerebellar peduncles (35.7%), and mesencephalon (14.3%) successively (18). The clinical presentations varied according to the areas of brainstem involvement, including cranial nerve palsy, hemiplegia, intractable hiccup, respiratory disturbance, balance difficulties, vertigo, and ataxia. In the present study, case 1 developed brainstem encephalitis 3 years after cortical encephalitis with lesions located in the pons and left brachium pontis, leading to dizziness and left-side ataxia. Lesions limited to the left brachium pontis in case 3 resulted in left-side peripheral facial paralysis and decreased touch and pain sensation in the left perioral area. Positive MOG-IgG in serum and steroid-responsiveness in these two patients confirmed the diagnosis of MOG-IgG-associated brainstem encephalitis. In case 4, diffused lesions in the left brachium pontis, left cerebellar hemisphere, and cerebellar vermis led to multiple neurological deficits, including vertigo and hemiplegia. Curvilinear enhancement signal and negative MOG-IgG in serum led to a misdiagnosis of probable CLIPPERS syndrome. However, with a relapse manifesting as a seizure 5 months later and positive MOG-IgG in serum and CSF, he was eventually diagnosed with MOG-IgG-associated encephalitis. The classical MRI features of CLIPPERS syndrome were punctate or curvilinear gadolinium-enhancing lesions, which were the most prominent in the pons (23). In case 4, the patchy lesions in the left brachium pontis, left cerebellar hemisphere, and cerebellar vermis did not meet the updated CLIPPERS criteria (23). Thus, the presumed diagnosis of CLIPPERS at the first attack was not appropriate. Despite the similar clinical and imaging features of MOG-IgG-related brainstem encephalitis and CLIPPERS (24–26), the diagnostic criteria of CLIPPERS encouraged careful consideration of other possible explanations (23).

Most MOG-IgG are of extrathecal origin; therefore, the presence of MOG-IgG in serum rather than in CSF is recommended as a specific indicator for the diagnosis of MOGAD (4). However, Aoe et al. (27) found that a few patients with MOGAD tested positive for MOG-IgG only in CSF. Patient 4 initially tested positive for MOG-IgG only in CSF, but the detection of MOG-IgG was positive in both serum and CSF when the disease relapsed 5 months later. Thus, we suggest that MOG-IgG should be tested in both serum and CSF simultaneously if possible and re-tested when necessary. Valuable data on regular monitoring of antibody titers in patients of MOGAD are scarce. Nevertheless, disease activity and treatment status may contribute to MOG-IgG titers in serum. Higher median titers were observed during the acute phase rather than the remission stage. Meanwhile, immunotherapy may lead to lower titers (28). In cases 1 and 3, we observed a low titer (1:10) of MOG-IgG during the acute episode, the exact reasons for this are not clear, but several speculations can be offered: first, the effect of glucocorticoid immunotherapy. Second, there may be another unknown pathogenic antibody at the same time. Third, as reported in the literature, some patients have relatively low antibody titers during acute attacks (29).

Cerebrospinal fluid (CSF) findings in our cases presented as pleocytosis of predominant lymphocytes and a normal or mildly elevated protein level around the time of an attack, consistent with previous studies on MOG-IgG-associated encephalitis (5, 6, 8, 13). In an international multicenter study, high MBP levels in the CSF were observed in the MOG-IgG–positive cases, suggesting acute myelin damage during attacks (30). However, the CSF MBP levels were non-elevated in our cases, as observed in patients with MOG-IgG-associated cortical encephalitis in several previous case reports (8, 15, 31). Thus, whether MOG-IgG is directly associated with cortical encephalitis or increased MBP in CSF should be a prerequisite for the diagnosis of MOGAD remains controversial. Notably, positive anti-N-methyl-D-aspartate (NMDA) receptor antibodies were detected in 5/18 of patients in a cohort of MOG-IgG-associated encephalitis (13). This suggested that immune attacks might involve NMDA receptors at the same time. However, antibodies of autoimmune encephalitis in serum and CSF were tested and no

TABLE 1 | Summary of the case reports about MOG-IgG associated cortical encephalitis.

Study	Number of patients (Male: Female)	Mean (median) age of onset	Main clinical manifestations	Abnormal signal in brain MRI	Other antibodies	Disease course
Ogawa et al. (8)	4/ (4:0)	34 (37)	Seizures, ON, encephalophagy	Unilateral cortex	None	2/4 had a relapsing disease
Fujimori et al. (5)	1/ (1:0)	46	Seizures, diziniss, paraparesis	Bilateral cortex	None	relapsing disease
Hamid SHM et al. (6)	5 (3:2)	20(10)	Seizures, ON, encephalophagy	Unilateral cortex	None	5/5 had a relapsing disease
Wang L et al. (13)	18 (10:8)	21.3 (22)	Seizures, ON, encephalophagy	Unilateral cortex	5/18 were NMDAR positive	13/18 had a relapsing disease
Fujimori J et al. (15)	6 (3:3)	34	Fever, headache, seizures, paraparesis, lethargy, memory disturbance	Bilateral cortex ± corpus callosum	No data	No data
Kim KH et al. (16)	2 (1:1)	M44 F52	Fever, aphasia, seizures,	Unilateral cortex	None	Monophase course
Ma GZ et al. (17)	1 (1:0)	39	Fever, headache, seizures	Bilateral cortex	None	relapsing disease
Nie HB et al. (14)	1 (0:1)	19	Fever, headache, seizures	Unilateral cortex	None	Monophase course

sufficient evidence was found that other associated autoimmune antibodies were responsible for the cortical encephalitis and seizures in cases 1 and 2, as observed in many case series/reports (5, 6, 8, 14, 16, 17). The cortical damage in these patients was likely triggered by an episode of demyelination caused by MOG-IgG. Another possibility also existed that an unknown auto-antibody might be involved in disease pathogenesis.

At present, although the long-term prognosis of MOG-IgG-associated encephalitis is not fully understood, the use of corticosteroids and/or plasma exchange or intravenous immunoglobulin remains the current standard treatment in the acute phase (32). Patients with positive MOG-IgG seem to have milder symptoms of neurological impairment (14) and respond more sensitively to corticosteroids than those with positive AQP4 antibodies (33). However, if appropriate treatments are not given in the early course, the symptoms can gradually deteriorate in some MOG-IgG-positive patients (30). Simultaneously, the tapering of oral prednisone slowly following intravenous methylprednisolone is critical on account of a tendency to relapse for rapid withdrawal (28, 34). Long-term immunosuppressive therapy is recommended for patients with recurrence or high risk of recurrence, and mycophenolate mofetil and rituximab are the most commonly used drugs (6). In case 1, the patient did not receive a correct diagnosis and standardized therapy due to limitations in the disease perception and antibody detection methods at the time of the first attack. He also experienced a rapid dose reduction of oral prednisone, leaving intermittent seizures after discharge, and subsequently developed brainstem encephalitis after 3 years. In case 4, the patient was misdiagnosed for the uncertain significance of MOG-IgG in CSF. However, with slow oral prednisone withdrawal, he experienced a relapse representing seizure after 5 months without immunosuppressive agents. Upon experiencing the relapse, cases 1 and 4 were started on mycophenolate mofetil/azathioprine, and they experienced no more events for 28 and 6 months of follow-up, respectively. On the contrary, cases 2 and 3 were diagnosed correctly immediately after the initial attack and recovered completely after the standardized treatment. With the slow oral prednisone and initiation of mycophenolate mofetil, case 2 was stable during 16 months of the follow-up and case 3 remained in clinical remission after 6 months of treatment.

CONCLUSION

In summary, this study reported four adult patients who suffered from cortical encephalitis with epileptic seizures and/or brainstem encephalitis during the course of the disease, all of whom were MOG-IgG positive. The four cases might enhance the understanding of MOG-IgG-related disorders. Although MOG-IgG-associated cortical/brainstem encephalitis occurs infrequently, it should be taken into consideration in patients who experience sudden seizure or symptoms of brainstem damage and when MRI reveals cerebral cortical or brainstem lesions. Currently, research on MOGAD is limited and requires further exploration.

DATA AVAILABILITY STATEMENT

The original contributions presented in the study are included in the article/supplementary material, further inquiries can be directed to the corresponding author/s.

ETHICS STATEMENT

Written informed consent was obtained from the individual(s) for the publication of any potentially identifiable images or data included in this article.

AUTHOR CONTRIBUTIONS

All authors listed have made a substantial, direct, and intellectual contribution to the work and approved it for publication.

FUNDING

This study was supported by the Projects in Science and Technique Plans of Xingtai City (Grant Number 2021ZC152).

REFERENCES

1. Narayan R, Simpson A, Fritsche K, Salama S, Pardo S, Mealy M, et al. MOG antibody disease: A review of MOG antibody seropositive neuromyelitis optica spectrum disorder. *Mult Scler Relat Disord.* (2018) 25:66–72. doi: 10.1016/j.msard.2018.07.025
2. Peschl P, Bradl M, Hftberger R, Berger T, Reindl M. Myelin oligodendrocyte glycoprotein: deciphering a target in inflammatory demyelinating diseases. *Front Immunol.* (2017) 8:529. doi: 10.3389/fimmu.2017.00529
3. Ramanathan S, Dale RC, Brilot F. Anti-MOG antibody: the history, clinical phenotype, and pathogenicity of a serum biomarker for demyelination. *Autoimmun Rev.* (2016) 8:307–24. doi: 10.1016/j.autrev.2015.12.004
4. Jarius S, Paul F, Aktas O, Asgari N, Dale RC, de Seze J, et al. MOG encephalomyelitis: international recommendations on diagnosis and antibody testing. *J Neuroinflammation.* (2018) 15:1–10. doi: 10.1186/s12974-018-1144-2
5. Fujimori J, Takai Y, Nakashima I, Sato DK, Takahashi T, Kaneko K, et al. Bilateral frontal cortex encephalitis and paraparesis in a patient with anti-MOG antibodies. *J Neurol Neurosurg Psychiatry.* (2017) 88:534–6. doi: 10.1136/jnnp-2016-315094
6. Hamid SHM, Whittam D, Saviour M, Alorainy A, Mutch K, Linaker S, et al. Seizures and encephalitis in myelin oligodendrocyte glycoprotein IgG disease vs aquaporin 4 IgG disease. *JAMA Neurol.* (2018) 75:65–71. doi: 10.1001/jamaneurol.2017.3196
7. Cobo-Calvo A, Ruiz A, Maillart E, Audoin B, Zephir H, Bourre B, et al. Clinical spectrum and prognostic value of CNS MOG autoimmunity in adults: The MOGADOR study. *Neurology.* (2018) 90:e1858–69. doi: 10.1212/WNL.0000000000005560
8. Ogawa R, Nakashima I, Takahashi T, Kaneko K, Akaishi T, Takai Y, et al. MOG antibody-positive, benign, unilateral, cerebral cortical encephalitis with epilepsy. *Neurol Neuroimmunol Neuroinflammat.* (2017) 4:e322. doi: 10.1212/NXI.0000000000000322
9. Ikeda T, Yamada K, Ogawa R, Takai Y, Kaneko K, Misu T, et al. The pathological features of MOG antibody-positive cerebral cortical encephalitis as a new spectrum associated with MOG antibodies: a case report. *J Neurol Sci.* (2018) 392:113–5. doi: 10.1016/j.jns.2018.06.028
10. Tao R, Qin C, Chen M, Yu HH, Wu LJ, Bu BT, et al. Unilateral cerebral cortical encephalitis with epilepsy: a possible special phenotype of MOG antibody-associated disorders. *Int J Neurosci.* (2020) 130:1–5. doi: 10.1080/00207454.2020.1720676
11. Jurynczyk M, Messina S, Woodhall MR, Raza N, Everett R, Roca-Fernandez A, et al. Clinical presentation and prognosis in MOG-antibody disease: a UK study. *Brain: J Neurol.* (2017) 140:3128–38. doi: 10.1093/brain/awx276
12. De Mol CL, Wong Y, van Pelt ED, Wokke B, Siepman T, Neuteboom RF, et al. The clinical spectrum and incidence of anti-MOG-associated acquired demyelinating syndromes in children and adults. *Multiple Sclerosis.* (2020) 26:806–14. doi: 10.1177/1352458519845112
13. Wang L, Zhang B, Zhou L, Zhang Y, Li H, Li Y, et al. Encephalitis is an important clinical component of myelin oligodendrocyte glycoprotein antibody associated demyelination: a single-center cohort study in Shanghai China. *Eur J Neurol.* (2019) 26:168–74. doi: 10.1111/ene.13790
14. Nie HB, Gao HF, Li YQ, Shen YY. The clinical features of FLAIR-hyperintense lesions in Anti-MOG antibody associated cerebral cortical encephalitis with seizures: case reports and literature review. *Medicine.* (2021) 100:e26087. doi: 10.1097/MD.0000000000026087
15. Fujimori J, Nakamura M, Yagihashi T, Nakashima I. Clinical and radiological features of adult onset bilateral medial frontal cerebral cortical encephalitis with anti-myelin oligodendrocyte glycoprotein antibody. *Front Neurol.* (2020) 11:600169. doi: 10.3389/fneur.2020.600169
16. Kim KH, Cho J, Cho KH, Shin HY1, Kim SW. Anti-myelin oligodendrocyte glycoprotein antibody-positive encephalitis with seizure and unilateral cortical fluid-attenuated inversion recovery-hyperintense lesions. *J Clin Neurol.* (2021) 17:481–3. doi: 10.3988/jcn.2021.17.3.481
17. Ma GZ, He JZ, Li Y, Xu Y, Hu YX, Cui F. Bilateral meningo-cortical involvement in anti-myelin oligodendrocyte glycoprotein-igg associated disorders: a case report. *Front Neurol.* (2021) 12:670349. doi: 10.3389/fneur.2021.670349
18. Jarius S, Kleiter I, Ruprecht K, Asgari N, Pitarokoili K, Borisow N, et al. MOG-IgG in NMO and related disorders: a multicenter study of 50 patients. Part 3: Brainstem involvement - frequency, presentation and outcome. *J Neuroinflammat.* (2016) 13:1–23. doi: 10.1186/s12974-016-0719-z
19. Akaishi T, Konno M, Nakashima I, Aoki M. Intractable hiccup in demyelinating disease with anti-myelin oligodendrocyte glycoprotein (MOG) antibody. *Internal Med.* (2016) 55:2905–6. doi: 10.2169/internalmedicine.55.7146
20. Akaishi T, Nakashima I, Sato DK, Takahashi T, Fujihara K. Neuromyelitis optica spectrum disorders. *Neuroimaging Clin N Am.* (2017) 27:251–65. doi: 10.1016/j.nic.2016.12.010
21. Kim S-M, Woodhall MR, Kim J-S, Kim S-J, Park KS, Vincent AF, et al. Antibodies to MOG in adults with inflammatory demyelinating disease of the CNS. *Neurol Neuroimmunol Neuroinflamm.* (2015) 2:e163. doi: 10.1212/NXI.0000000000000163
22. Maeda M, Yagishita A, Yamamoto T, Sakuma H, Takeda K. Abnormal hyperintensity within the subarachnoid space evaluated by fluid-attenuated inversion-recovery MR imaging: a spectrum of central nervous system diseases. *Eur Radiol.* (2003) 13:L192–201. doi: 10.1007/s00330-003-1877-9
23. Tobin WO, Guo Y, Krecke KN, Parisi JE, Lucchinetti CF, Pittock SJ. Diagnostic criteria for chronic lymphocytic inflammation with pontine perivascular enhancement responsive to steroids (CLIPPERS). *Brain.* (2017) 140:2415–25. doi: 10.1093/brain/awx200
24. Symmonds M, Waters PJ, Küker W, et al. Anti-MOG antibodies with longitudinally extensive transverse myelitis preceded by CLIPPERS. *Neurology.* (2015) 84:1177–9. doi: 10.1212/WNL.0000000000001370
25. Berzero G, Taieb G, Marignier R, Younan N, Savatovsky J, Leclercq D, et al. CLIPPERS mimickers: relapsing brainstem encephalitis associated with anti-MOG antibodies. *Eur J Neurol.* (2018) 25:e16–7. doi: 10.1111/ene.13483
26. Obeidat AZ, Block AN, Hooshmand SI. Peppering the pons: CLIPPERS or myelin oligodendrocyte glycoprotein associated disease? *Multiple Sclerosis and Relat Disord.* (2021) 51:102874. doi: 10.1016/j.msard.2021.102874
27. Aoe S, Kume K, Takata T, Touge T, Kaneko K, Nakashima I, et al. Clinical significance of assaying anti-MOG antibody in cerebrospinal fluid in MOG-antibody-associated diseases: a case report. *Mult Scler Relat Disord.* (2019) 28:165–6. doi: 10.1016/j.msard.2018.12.035
28. Jarius S, Ruprecht K, Kleiter I, Borisow N, Asgari N, Pitarokoili K, et al. MOG-IgG in NMO and related disorders: a multicenter study of 50 patients. Part 2: Epidemiology, clinical presentation, radiological and laboratory features, treatment responses, and long-term outcome. *J Neuroinflamm.* (2015) 13:280. doi: 10.1186/s12974-016-0718-0
29. Jarius S, Ruprecht K, Kleiter I, Borisow N, Asgari N, Pitarokoili K, et al. MOG-IgG in NMO and related disorders: a multicenter study of 50 patients. Part 1: frequency, syndrome specificity, influence of disease activity, long-term course, association with AQP4-IgG, and origin. *J Neuroinflammation.* (2016) 13:279. doi: 10.1186/s12974-016-0717-1
30. Kaneko1K, Sato DK, Nakashima1 I, Nishiyama1 S, Tanaka S, Marignier R, et al. Myelin injury without astrocytopathy in neuroinflammatory disorders with MOG antibodies. *J Neurol,*

Neurosurg Psychiat. (2016) 87:1257–9. doi: 10.1136/jnnp-2015-312676
31. Katsuse K, Shimizu G, Saito Sato N, Hatano K, Yagi S, Kimura T, et al. Epilepsia partialis continua as an early sign of anti-myelin oligodendrocyte glycoprotein antibody-positive encephalitis. *Internal Med.* (2020) 59:1445–9. doi: 10.2169/internalmedicine.3076-19
32. Sara S, Majid K, Santiago P, Izlem I, Michael L. MOG antibody-associated encephalomyelitis/encephalitis. *Multiple Sclerosis.* (2019) 25:1427–33. doi: 10.1177/1352458519837705
33. Kitley J, Woodhall M, Waters P, Leite MI, Devenney E, Craig J, et al. Myelin-oligodendrocyte glycoprotein antibodies in adults with a neuromyelitis optica phenotype. *Neurology.* (2012) 79:1273–7. doi: 10.1212/WNL.0b013e31826aac4e
34. Chalmoukou K, Alexopoulos H, Akrivou S, Stathopoulos P, Reindl M, Dalakas MC. Anti-MOG antibodies are frequently associated with steroid-sensitive recurrent optic neuritis. *Neurol Neuroimmunol Neuroinflammation.* (2015) 2:e131. doi: 10.1212/NXI.0000000000000131

Conflict of Interest: The authors declare that the research was conducted in the absence of any commercial or financial relationships that could be construed as a potential conflict of interest.

frontiers in Immunology

ORIGINAL RESEARCH
published: 24 January 2022
doi: 10.3389/fimmu.2021.759389

Progressive Retinal and Optic Nerve Damage in a Mouse Model of Spontaneous Opticospinal Encephalomyelitis

Laura Petrikowski[1,2], Sabrina Reinehr[1], Steffen Haupeltshofer[2], Leonie Deppe[1], Florian Graz[1,2], Ingo Kleiter[2], H. Burkhard Dick[1], Ralf Gold[2], Simon Faissner[2†] and Stephanie C. Joachim[1*†]*

[1] Experimental Eye Research Institute, University Eye Hospital, Ruhr-University Bochum, Bochum, Germany, [2] Department of Neurology, Ruhr-University Bochum, St. Josef-Hospital, Bochum, Germany

OPEN ACCESS

Edited by:
Yu Cai,
University of Nebraska Medical Center, United States

Reviewed by:
Sidney Gospe, Duke University, United States
Benjamin Knier, Technical University of Munich, Germany

***Correspondence:**
Simon Faissner
simon.faissner@rub.de
Stephanie C. Joachim
stephanie.joachim@rub.de

†These authors have contributed equally to this work and share senior authorship

Specialty section:
This article was submitted to Multiple Sclerosis and Neuroimmunology, a section of the journal Frontiers in Immunology

Received: *16 August 2021*
Accepted: *29 December 2021*
Published: *24 January 2022*

Citation:
Petrikowski L, Reinehr S, Haupeltshofer S, Deppe L, Graz F, Kleiter I, Dick HB, Gold R, Faissner S and Joachim SC (2022) Progressive Retinal and Optic Nerve Damage in a Mouse Model of Spontaneous Opticospinal Encephalomyelitis. Front. Immunol. 12:759389. doi: 10.3389/fimmu.2021.759389

Neuromyelitis optica spectrum disorder (NMOSD) and myelin oligodendrocyte glycoprotein-antibody-associated disease (MOGAD) are antibody mediated CNS disorders mostly affecting the optic nerve and spinal cord with potential severe impact on the visual pathway. Here, we investigated inflammation and degeneration of the visual system in a spontaneous encephalomyelitis animal model. We used double-transgenic (2D2/Th) mice which develop a spontaneous opticospinal encephalomyelitis (OSE). Retinal morphology and its function were evaluated via spectral domain optical coherence tomography (SD-OCT) and electroretinography (ERG) in 6- and 8-week-old mice. Immunohistochemistry of retina and optic nerve and examination of the retina via RT-qPCR were performed using markers for inflammation, immune cells and the complement pathway. OSE mice showed clinical signs of encephalomyelitis with an incidence of 75% at day 38. A progressive retinal thinning was detected in OSE mice via SD-OCT. An impairment in photoreceptor signal transmission occurred. This was accompanied by cellular infiltration and demyelination of optic nerves. The number of microglia/macrophages was increased in OSE optic nerves and retinas. Analysis of the retina revealed a reduced retinal ganglion cell number and downregulated *Pou4f1* mRNA expression in OSE retinas. RT-qPCR revealed an elevation of microglia markers and the cytokines *Tnfa* and *Tgfb*. We also documented an upregulation of the complement system via the classical pathway. In summary, we describe characteristics of inflammation and degeneration of the visual system in a spontaneous encephalomyelitis model, characterized by coinciding inflammatory and degenerative mechanisms in both retina and optic nerve with involvement of the complement system.

Keywords: Neuromyelitis optica, optic nerve, inflammation, demyelination, myelin oligodendrocyte glycoprotein antibodies (MOG-IgG), retinal ganglion cells, microglia, complement system

BACKGROUND

Chronic inflammatory diseases of the central nervous system (CNS) have profound implications for patients due to the potential development of disability. While Multiple Sclerosis (MS) is the most common cause (1), there is also a spectrum of relatively rare neuroinflammatory and neurodegenerative diseases such as Neuromyelitis optica spectrum disorder (NMOSD) and myelin oligodendrocyte glycoprotein (MOG)-IgG antibody associated disease (MOGAD). 25% of patients with a NMOSD phenotype present with autoantibodies directed against MOG (2). Recently, a robust association of anti-MOG IgG has been found with optic neuritis, myelitis and brainstem encephalitis, as well as with acute disseminated encephalomyelitis (ADEM)-like presentations (3). Hence, MOGAD is now considered as distinct disease entity with differing pathophysiological features compared to NMOSD (3, 4). MOG is located on the outer surface of the oligodendrocytic myelin sheath (5). The target of MOG antibodies are oligodendrocytes; hence the pathogenesis in MOG^+ patients is different from the astrocytopathy in aquaporin4$^+$ ($APQ4^+$) NMOSD (6, 7).

Since loss of vision is perceived as most impairing in daily life (8), further studies regarding the impact of MOG to the visual system, especially the retina, are needed. To better understand the pathogenesis of MOGAD, we took advantage of an animal model of spontaneous opticospinal encephalomyelitis (OSE), characterized by MOG-reactive transgenic T-cells (2D2) and a transgenic B-cell receptor against MOG (Th) (9). OSE mice develop a progressive encephalomyelitis spontaneously, characterized by inflammation and demyelination of the spinal cord and the optic nerve (9, 10). Only few studies investigated retinal damage in NMOSD or MOG models. Zeka et al. observed retinal inflammation in a NMOSD model in rats (11). None of those previous studies focused on the detailed examination of retinal cells in the OSE model, representing MOGAD. Understanding mechanisms of damage in OSE as model of MOGAD is therefore an important step towards identifying potential targets and developing new therapeutic approaches to stop disease progression and avoid loss of vision in affected patients.

In this study, we describe longitudinal dynamics of morphological, functional and structural retinal alterations as well as (immuno-) histochemical changes in the optic nerve in OSE. Data are corroborated by analyses of gene expression alterations of markers of inflammation and complement activation. We show that the retina loses function in accordance with progressive neurodegeneration of retinal ganglion cells (RGCs) in line with inflammation and complement activation, hence informing about potential therapeutic targets in MOGAD.

Abbreviations: AQP4, Aquaporin-4; CNS, Central nervous system; ERG, Electroretinography; GCL, Ganglion cell layer; GFAP, Glial fibrillary acidic protein; H&E, Hematoxylin and eosin; INL, Inner nuclear layer; IPL, Inner plexiform layer; LFB, Luxol fast blue; MAC, Membrane attack complex; MOGAD, Myelin oligodendrocyte glycoprotein-antibody-associated disease; MOG, Myelin oligodendrocyte glycoprotein; MS, Multiple Sclerosis; NMOSD, Neuromyelitis optica spectrum disorder; OCT, Optical coherence tomography; ONL, Outer nuclear layer; OSE, Opticospinal encephalomyelitis; RGC, Retinal ganglion cell; RNFL, Retinal nerve fiber layer; RT-qPCR, Quantitative real-time reverse transcription polymerase chain reaction.

METHODS

Animals and Evaluation of Spontaneous Opticospinal Encephalomyelitis

All experiments involving animals were performed in accordance with the ARVO statement for the Use of Animals in Ophthalmic and Vision Research and approved by the animal care committee of North Rhine-Westphalia, Germany (Landesamt für Natur, Umwelt und Verbraucherschutz Nordrhein-Westfalen, Recklinghausen, Germany; file no. 84-02.04.2016.A062). All animals were bred and housed in the animal facility of the Ruhr-University Bochum under environmentally controlled conditions with free access to food and water *ad libitum* in the absence of pathogens.

Both male and female C57BL/6 mice with either MOG-specific T cells (2D2) (12) or MOG-specific B cells (Th) (13) were used for the study. The double-transgenic (2D2/Th) OSE mice resulting from the intercross of the single-transgenic TCR^{MOG} and MOG-specific Ig heavy-chain knock-in (IgH^{MOG}) animals spontaneously develop an opticospinal encephalomyelitis with an onset four weeks after birth and an incidence of about 50% (9). The OSE model is a suitable model for MOGAD due to the fact that the demyelinating lesions are restricted to the optic nerve and the spinal cord with histological similarity to human lesions (9). Single-transgenic IgH^{MOG} (Th) mice remain healthy and served as age-matched control animals.

Mice were weighted daily and examined for neurological symptoms using an established 10-point score system: 0=healthy animal, 1=flaccid tail, 2= impaired righting reflex or gait, 3=absent righting, 4=ataxic gait, abnormal position, 5=mild paraparesis, 6=moderate paraparesis, 7=severe paraplegia, 8=tetraparesis, 9=moribund, and 10=death (14).

At six and eight weeks of age, *in vivo* experiments using SD-optical coherence tomography (SD-OCT) and electroretinography (ERG) measurements were carried out. Afterwards, the eyes and optic nerves were removed for histological and immunohistochemical analysis or quantitative real-time PCR (RT-qPCR; **Figure 1A**). Subsequent to the preparation, the histological tissues were fixed in 4% paraformaldehyde (Merck, Darmstadt, Germany) for one hour (retina) or two hours (optic nerve), drained in 30% sucrose (VWR, Langenfeld, Germany), embedded in Tissue Tec (Thermo Scientific, Waltham, MA; USA) and frozen at -80°C. While one eye of each animal was used for immunohistological stainings, the other retina was isolated from the surrounding tissue and frozen at -80°C for RT-qPCR.

In Vivo Retinal Imaging Using SD-OCT

We performed SD-OCT measurements in six- and eight-week-old mice (n=8/group) using a Heidelberg Engineering Spectralis OCT device (Heidelberg Engineering, Heidelberg, Germany) which was modified with a +25 dpt lens for murine eyes. The animals were anesthetized with ketamine/xylazine (120/16 mg/kg body weight). Eyes were treated with 5% tropicamide to

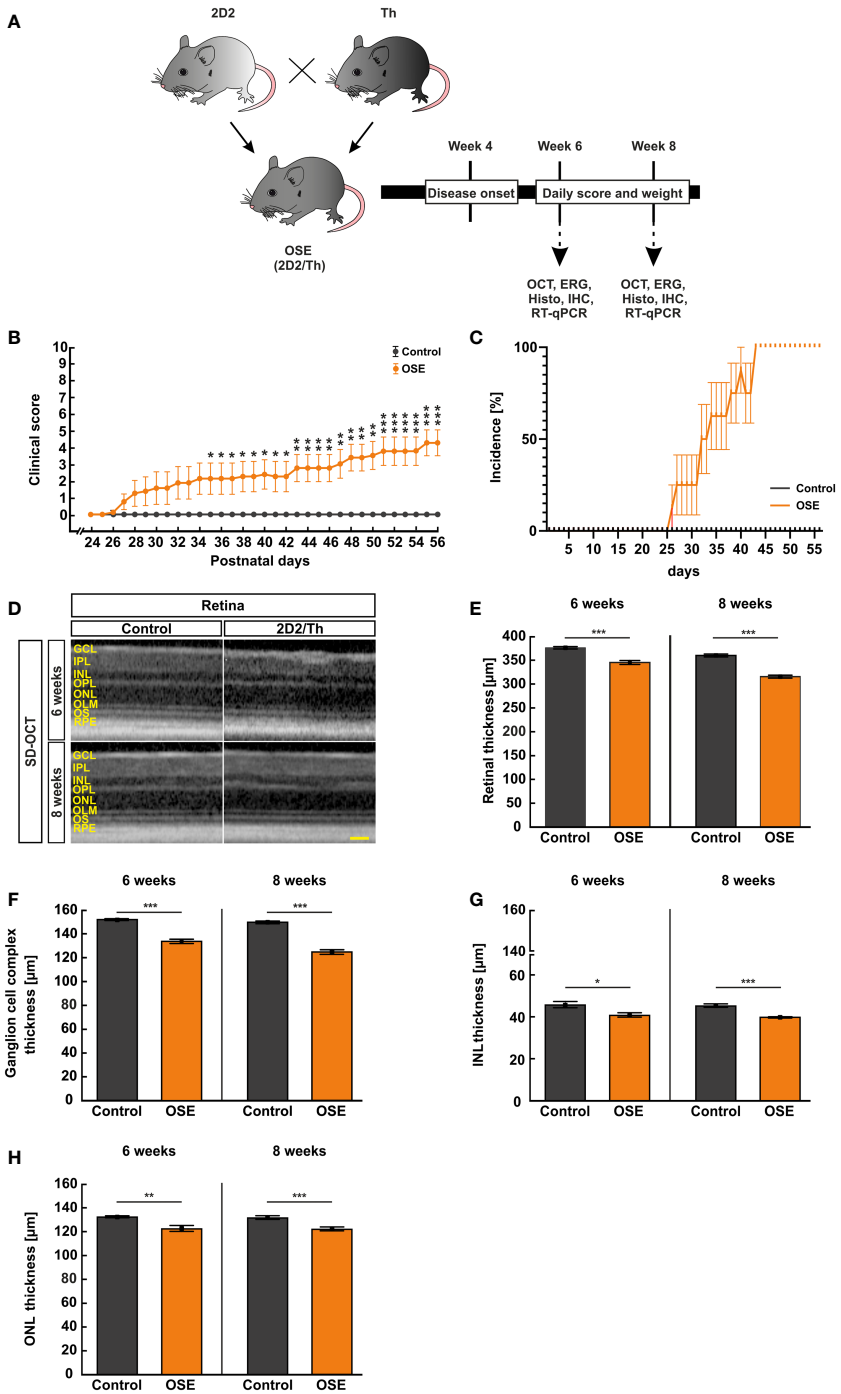

FIGURE 1 | Neurological signs in accordance with structural impairment of the retina. **(A)** Study design. **(B)** OSE mice showed clinical signs of encephalomyelitis with flaccid hind limb paralysis starting at day 26. A significantly higher score was observed in OSE mice while control mice remained healthy. **(C)** Additionally, 50% of OSE mice were affected after 32 days. The incidence increased to 75% at day 38 in OSE mice. **(D)** SD-OCT measurements were performed in six- and eight-week-old mice to evaluate the retinal thickness. **(E)** The morphological analysis of the retina revealed a reduction of the retinal thickness (ganglion cell complex to ONL) in six-week-old OSE animals in comparison to the control group. The reduction of the retinal thickness was also noted after eight weeks. **(F)** The ganglion cell complex thickness (RNFL, GCL and IPL) was reduced by 6.5% in eight-week-old OSE mice. **(G)** The INL thickness decreased by 2.5% between six and eight weeks time point in OSE mice. **(H)** A slight reduction of ONL thickness by 0.4% was seen in OCT analysis in the OSE group. Data are shown as mean ± SEM. ERG, electroretinogram; GCL, ganglion cell layer; Histo, histology; IHC, immunohistochemistry; IPL, inner plexiform layer; INL, inner nuclear layer; OCT, optical coherence tomography; OPL, outer plexiform layer; ONL, outer nuclear layer; OLM, outer limiting membrane; OS, outer segment; RPE, retinal pigment epithelium; RT-qPCR, quantitative real-time polymerase chain reaction. *$p < 0.05$, **$p < 0.01$, ***$p < 0.001$. Scale bar: 200 µm.

induce mydriasis before investigation. Additionally, we applied 0.9% NaCl on the eyes before and during the SD-OCT analysis. The mice were placed in front of the SD-OCT. Three horizontal scans and one ring scan were obtained from both eyes of each animal via the Heyex software (Heidelberg Engineering, Heidelberg, Germany) with the following settings: angle 30°, lens 34.5 dpt., art. frames 100, eye size M. The eyes were treated with eye droplets subsequently to the examination to prevent dehydration. The thickness of the retinal layers was measured manually in an axis perpendicular to the individual layers using ImageJ software (National Institute of Health, Bethesda, MD, USA). The middle of the retina as well as two equidistant measurements per side were performed. Hence, five measurements were used to calculate the mean value for each retina and each layer (15–17). The retinal thickness was measured, the total thickness included the retinal nerve fiber layer (RNFL), ganglion cell layer (GCL), inner plexiform layer (IPL), inner nuclear layer (INL), outer plexiform layer, and the outer nuclear layer (ONL). A separate measurement of the ganglion cell complex (RNFL, GCL, and IPL) as well as separate measurements of the INL and ONL thickness were also carried out.

Electroretinography Recordings

To measure the animals' retinal function, we used full-field flash ERG (HMsERG system; OcuScience, Henderson, NV, USA) as previously described (18). OSE and control mice, six (OSE: n=5; control: n=6) and eight weeks (n=6/group) of age, were dark adapted the day before the ERGs were performed and narcotized with ketamin/xylazin (120/16 mg/kg body weight) prior to the examination. Eyes were dilated with tropicamide (5%) and topically anesthetized using conjuncain (Bausch&Lomb, Berlin, Germany). A feedback temperature controller (TC-1000; CWE Inc., Ardmore, PA, USA) was used to maintain the body temperature at 37°C. Reference electrodes were placed subcutaneously below both ears and a ground electrode was placed in the base of the tail. Contact lenses with silver thread recording electrodes were attached at the center of the cornea after application of methocel (Omni Vision, Puchheim, Germany). Before measurement, the ERG equipment was covered with a Faraday cage. The scotopic ERG measurements were recorded at 0.1, 0.3, 1, 3, 10, and 25 cd.s/m^2. Afterwards, the signals were amplificated, digitalized and averaged to evaluate the a- and b-wave using ERGView software (Version 4.380R; OcuScience). Before evaluating the amplitudes of the a- and b-waves, a 50 hz filtering of the data was applied.

Histopathological Staining and Scoring of the Optic Nerve

We stained longitudinal sections of the optic nerve (4 µm, 3 sections per animal, n=8/group for six and eight weeks) with hematoxylin and eosin (H&E, Merck) or luxol fast blue (LFB; RAL Diagnostics, Martillac Cedex, France). Three images of each cryosection (cranial, medial, caudal) were taken with an Axio Imager M1 microscope (Zeiss, Oberkochen, Germany) at a 400x magnification. The masked pictures were evaluated by two independent examiners regarding cellular infiltration and inflammation using a 4-point scoring system for H&E-stained sections (19): 0=no infiltration, 1=mild infiltration, 2=moderate infiltration, 3=severe infiltration, and 4=massive infiltration with formation of cellular conglomerates. The degree of demyelination in LFB-stained sections was also evaluated by two examiners in 0.5 intervals: 0=no demyelination, 0.5=mild demyelination, 1=moderate demyelination, 1.5=advanced demyelination, and 2=severe demyelination (19).

Immunohistochemistry of the Optic Nerve and the Retina

Immunohistochemical stainings of longitudinal sections of the optic nerve (4 µm, n=8/group) and of retinal cross-sections (10 µm, n=7-8/group) were performed with appropriate primary and secondary antibodies at six and eight weeks (**Table 1**). We used six sections for each animal. First, sections were blocked for 60 min with a solution containing 10-20% donkey serum with or without 1-10% bovine serum albumin and 0.1-0.3% Triton-X in PBS. Primary antibodies were applied and incubated at room temperature overnight. Then, corresponding secondary antibodies were added for 60 min. Nuclear staining with 4',6 diamidino-2-phenylindole (DAPI; Serva Electrophoresis, Heidelberg, Germany) was applied to facilitate orientation on the slides. Negative controls were performed for each staining by using the secondary antibodies only.

Regarding the optic nerve, three pictures were taken of each longitudinal section (cranial, medial, caudal). Six nerve sections per animal were analyzed (24 photographs/animal). Four pictures were taken of each retinal section (two in the peripheral and two in the central retina) via ApoTome.2 microscope (Zeiss) for all stainings with a 400x magnification. Photos of retinal cross-sections were

TABLE 1 | Primary and secondary antibodies used for immunohistochemistry on retina and optic nerve sections.

Primary antibodies			Secondary antibodies		
Antibody	**Company**	**Dilution**	**Antibody**	**Company**	**Dilution**
Anti-C1q	Abcam	1:200	Donkey anti-rabbit Alexa Fluor 555	Invitrogen	1:500
Anti-C3	Cedarlane	1:500	Donkey anti-rabbit Alexa Fluor 555	Invitrogen	1:500
Anti-GFAP	Millipore	1:2000	Donkey anti-chicken Alexa Fluor 488	Jackson Immuno Research	1:500
Anti-Iba1	Synaptic Systems	1:500	Donkey anti-chicken IgG Cy3	Millipore	1:400
Anti-MAC	Thermo Scientific	1:100	Donkey anti-rabbit Alexa Fluor 555	Invitrogen	1:500
Anti-RBPMS	Millipore	1:500	Donkey anti-rabbit Alexa Fluor 555	Invitrogen	1:500
Anti-Tmem119	Abcam	1:200	Donkey anti-rabbit Alexa Fluor 488	Jackson Immuno Research	1:500

taken at a distance of 300 and 3100 µm dorsal and ventral to the optic nerve. Six cross-sections per animal were analyzed in total (24 photographs/animal). Afterwards, all images were masked and cut in a predefined size (Corel Paint Shop Pro, V13; Corel Corporation; Ottawa, Canada).

$RBPMS^+$, $Iba1^+$, $Tmem119^+$, $C1q^+$, $C3^+$, and MAC^+ (membrane attack complex) cells with a co-localization with DAPI (cell nuclei) were counted using ImageJ software. In the retina, $RBPMS^+$ were counted in the GCL. $Iba1^+$, $Tmem119^+$, $C1q^+$, $C3^+$, and MAC^+ cells were quantified in the GCL, IPL, and INL together as well as separately in these three layers.

Regarding GFAP staining, the signal area was measured using an ImageJ macro with the following settings (20): The pictures were transformed into a gray scale (32-bit). After averaging the background subtraction (50 pixel), the lower (14.63) and the upper threshold (252.13) were set. Means per retina were calculated and used for statistical analysis.

Retinal Quantitative Real-Time Reverse Transcription Polymerase Chain Reaction

Two retinas from the same group were pooled for RNA preparation (n=5/group for six weeks, n=5-6/group for eight weeks after pooling) and cDNA synthesis was carried out as previously described (21). The designed oligonucleotides for RT-qPCR are shown in **Table 2**. The RT-qPCR was carried out using DyNAmo Flash SYBR Green (Thermo Scientific) on the PikoReal RT-qPCR Cycler (Thermo Scientific). Primer efficiencies of each primer set were calculated based on a dilution series of 5 to 125 ng cDNA. Ct values of the housekeeping genes *β-actin* (*Actb*) and *Cyclophilin* (*Ppid*) were applied for normalization and relative quantification of gene expressions.

Statistical Analyses

Statistical analyses of clinical scores, SD-OCT, ERG, histology, and immunohistochemistry were performed using Statistica software (Version 13; StatSoft, Tulsa, OK, USA). Groups were compared using Student's *t*-test for each time point. Data are shown as mean ± standard error of the mean (SEM). RT-qPCR data are shown as relative expression values with median ± quartile+minimum/maximum and were assessed *via* Pair Wise Fixed Reallocation Randomisation Test© using REST© software (Qiagen) (22). Incidence and the Spearman correlation coefficient (r, R^2) were calculated for the analyses of the associations between SD-OCT parameters and RGC numbers as well as between clinical scores and RGC numbers/SD-OCT parameters using Prism (Version 9; GraphPad, San Diego, CA, USA). $P<0.05$ was considered as statistically significant, with $^*p<0.05$, $^{**}p<0.01$, and $^{***}p<0.001$.

TABLE 2 | Primer pairs for RT-qPCR analysis.

Gene	Forward (F) and reverse (R) oligonucleotides	GenBank acc. no.	Amplicon size
Actb-F	ctaaggccaaccgtgaaag	NM_007393.5	104 bp
Actb-R	accagaggcatacagggaca		
C1qa-F	cgggtctcaaaggagagaga	NM_007572.2	71 bp
C1qa-R	tcctttaaaacctcggatacca		
C1qb-F	aggcactccagggataaagg	NM_009777.3	80 bp
C1qb-R	ggtccccttttctctccaaac		
C1qc-F	atggtcgttggacccagtt	NM_007574.2	75 bp
C1qc-R	gagtggtagggccagaagaa		
C3-F	accttacctcggcaagtttct	NM_009778.3	75 bp
C3-R	ttgtagagctgctggtcagg		
Cd68-F	tgatcttgctaggaccgctta	NM_001291058.1	66 bp
Cd68-R	taacggccttttgtgagga		
Cfb-F	ctcgaacctgcagatccac	M57890.1	112 bp
Cfb-R	tcaaagtcctgcggtcgt		
Gfap-F	acagactttctccaacctccag	NM_010277.3	63 bp
Gfap-R	ccttctgacacggatttggt		
Hc-F	tgacaccaggcttcagaaagt	XM_017315669.2	69 bp
Hc-R	agttgcgcacagtcagctt		
Iba1-F	ggatttgcagggaggaaaa	D86382.1	92 bp
Iba1-R	tgggatcatcgaggaattg		
Masp2-F	ggcggctactattgctcct	NM_001003893.2	86 bp
Masp2-R	aacacctggcctgaacaaag		
Pou4f1-F	ctccctgagcacaagtaccc	AY706205.1	98 bp
Pou4f1-R	ctggcgaagaggttgctc		
Ppid-F	ttcttcataaccacaagtcaagacc	M60456.1	95 bp
Ppid-R	tccacctccgtaccacatc		
Tgfb-F	aggaggtttataaaatcgacatgc	XM_006497136.3	65 bp
Tgfb-R	tgtaacaactgggcagacagttt		
Tmem119-F	gtgtctaacaggccccagaa	NM_146162.3	110 bp
Tmem119-R	agccacgtggtatcaaggag		
Tnfa-F	ctgtagcccacgtcgtagc	NM_013693.3	97 bp
Tnfa-R	ttgagatccatgccgttg		

The primer pairs listed in the table were used in RT-qPCR experiments. Actin (Actb) and Cyclophilin (Ppid) served as housekeeping genes. F, forward; R, reverse.

RESULTS

OSE Mice Develop Disability in Accordance With Reduced Weight

Single-transgenic control animals (IgH^{MOG}) remained without neurological impairment (mean score 0) over the whole duration of the study, as expected. Contrary, OSE mice developed signs of spontaneous encephalomyelitis, starting at day 26 after birth with an incidence of 25% at day 27 (**Figures 1B, C**). After 32 days, 50% of OSE mice were affected as reflected in a mean score of 1.9 ± 1.0 (p=0.087). The incidence increased to 75% at day 38 in OSE mice (2.3 ± 1.0; p=0.033; **Figure 1C**), reflecting a flaccid tail and an impaired righting reflex or gait. At day 56, the mean EAE score in the OSE group was 4.3 ± 0.8.

Disability in OSE mice was reflected in a 10.8% lower weight (14.1 ± 1.1 g) compared to control mice after six weeks (15.8 ± 0.6 g, p=0.199). Eight-week-old OSE animals weighted significantly less (15.0 ± 1.0 g) than the control group (19.3 ± 0.6 g, p=0.003; **Supplemental Figure 1**).

Retinal Thickness Is Reduced in OSE

To evaluate structural alterations of the retina, we performed SD-OCT after six and eight weeks (**Figure 1D**). The analysis in six weeks old mice showed a significant reduction of the retinal thickness by 8.2% in OSE retinae (345.3 ± 4.2 µm) compared to the control group (376.1 ± 2.5 µm; p<0.001; **Figure 1E**). To investigate whether there was loss of retinal thickness over time, we also performed analyses at eight weeks of age. We found a reduced thickness of 12.3% in OSE animals (314.6 ± 3.1 µm) compared to the control group (358.9 ± 3.1 µm; p<0.001). In addition, we noted a progressive thinning of retina in OSE mice from six to eight weeks (8.9%, p<0.001; **Figure 1E**).

To analyze which layers are affected by the reduction of retinal thickness, separate measurements of the ganglion cell complex (=RNFL, GCL and IPL), the INL, and the ONL were carried out. At 6 weeks, OSE mice had a thinner ganglion cell complex (control: 151.9 ± 0.8 µm, OSE: 133.5 ± 1.8 µm, p<0.001). We found a thinning by 6.5% of the ganglion cell complex in the OSE groups at eight weeks (control: 150.2 ± 1.1 µm, OSE: 124.7 ± 1.9 µm, p<0.001; **Figure 1F**).

A significantly reduced INL (control: 45.6 ± 4.2 µm, OSE: 40.7 ± 1.0 µm, p=0.016; **Figure 1G**) and ONL thickness (control: 132.4 ± 0.7 µm, OSE: 122.4 ± 2.5 µm, p=0.002; **Figure 1H**) was noted at the six weeks´ time point. The INL in the OSE group was also thinner at eight weeks (control: 45.1 ± 0.8 µm, OSE: 39.7 ± 0.3 µm, p<0.001; **Figure 1G**). The ONL thickness at eight weeks was also reduced in the OSE group (control: 131.6 ± 1.5 µm, OSE: 121.9 ± 1.6 µm, p<0.001; **Figure 1H**).

Reduction of Retinal Electrical Output as Marker of Impaired Function

To understand whether loss of retinal thickness is also associated with functional impairment, we performed ERG recordings. In all groups, increased a- and b-wave amplitudes were observed with rising light flash stimuli. At six and eight weeks, ERG waveforms at a flash luminance of 25 cd*s/m^2 showed a decrease in OSE animals compared to controls (**Figure 2A, D**).

The a-wave represents the electrical output of the photoreceptor layer and was significantly reduced at flash intensities of 10 and 25 cd s/m^2 in OSE mice after six weeks (p=0.012 at 10 cd.s/m^2, p=0.032 at 25 cd.s/m^2). At 0.1 and 0.3 cd.s/m^2 flash intensity, the a-wave amplitude of the OSE group was similar to the one of the control group. A non-significant reduction of the a-wave amplitude could be noted at 1 (p=0.059) and 3 cd.s/m^2 (p=0.087) flash intensity (**Figure 2B**).

The b-wave mirrors the electrical conductivity of the inner retinal layers. A non-significant trend for a decreased b-wave amplitude was measured at flash intensities of 0.1 (p=0.051) and 0.3 cd.s/m^2 (p=0.057) in OSE mice in comparison to the control group at six weeks. A significant reduction could be documented at flash intensities of 1 (p=0.034) up to 25 cd.s/m^2 (p=0.03) in OSE mice (**Figure 2C**).

The ERG measurements after eight weeks showed a non-significant reduction of the a-wave amplitude from 0.1 (p=0.566) to 3 cd.s/m^2 (p=0.377). At flash intensities of 10 and 25 cd.s/m^2, a significantly decreased a-wave amplitude was measurable in OSE mice (p=0.013 at 10 cd.s/m^2, p=0.02 at 25 cd.s/m^2; **Figure 2E**). The b-wave amplitude was strongly decreased at all flash intensities in OSE mice after eight weeks (p=0.024 at 0.1 cd.s/m^2, p=0.034 at 0.3 cd.s/m^2, p=0.017 at 1 cd.s/m^2, p=0.04 at 3 cd.s/m^2, p=0.006 at 10 cd.s/m^2, p=0.008 at 25 cd.s/m^2; **Figure 2F**). Those data altogether indicate an impairment of the retinal function, which might be explained by a dysfunction of photoreceptor and bipolar cells in affected mice.

Cellular Infiltration, Inflammation, and Demyelination of Optic Nerves in OSE

We performed histological analyses of optic nerves to investigate the degree of inflammation and demyelination (19). The H&E staining of optic nerve sections was evaluated via scoring the degree of cellular infiltration (**Figure 3A**). After six weeks, OSE mice showed an average score of 2.6 ± 0.1, which was increased compared to the control group (0.6 ± 0.2, p<0.001). The H&E score in the control group increased from six to eight weeks (1.3 ± 0.1; p=0.02). Still, more cellular infiltration and inflammation was also notable in H&E stained OSE nerves at eight weeks of age (2.8 ± 0.2), when compared to controls (p<0.001 **Figure 3B**).

Histopathological stainings with LFB were performed to investigate the degree of demyelination after six and eight weeks (**Figure 3C**). LFB-stained myelin sheaths of the six-week-old control group resembled combed bundles in a parallel arrangement (0.7 ± 0.2). This arrangement was interrupted in the OSE group represented by the brightening of the structure and demyelination (1.4 ± 0.1; p=0.011). At eight weeks of age, demyelination was again significantly higher in the OSE group (1.4 ± 0.1) compared to the control (0.7 ± 0.1; p<0.001; **Figure 3D**).

Increased Infiltration of Activated Microglia in the Optic Nerve of OSE Mice

Iba1 was used to label microglia/macrophages (23, 24). Co-staining with Tmem119, the transmembrane protein which is exclusively expressed by microglia, was used to visualize microglia on optic nerve sections (25) (**Figure 4A**). The results at six weeks display a significantly higher number of $Iba1^+$ cells in

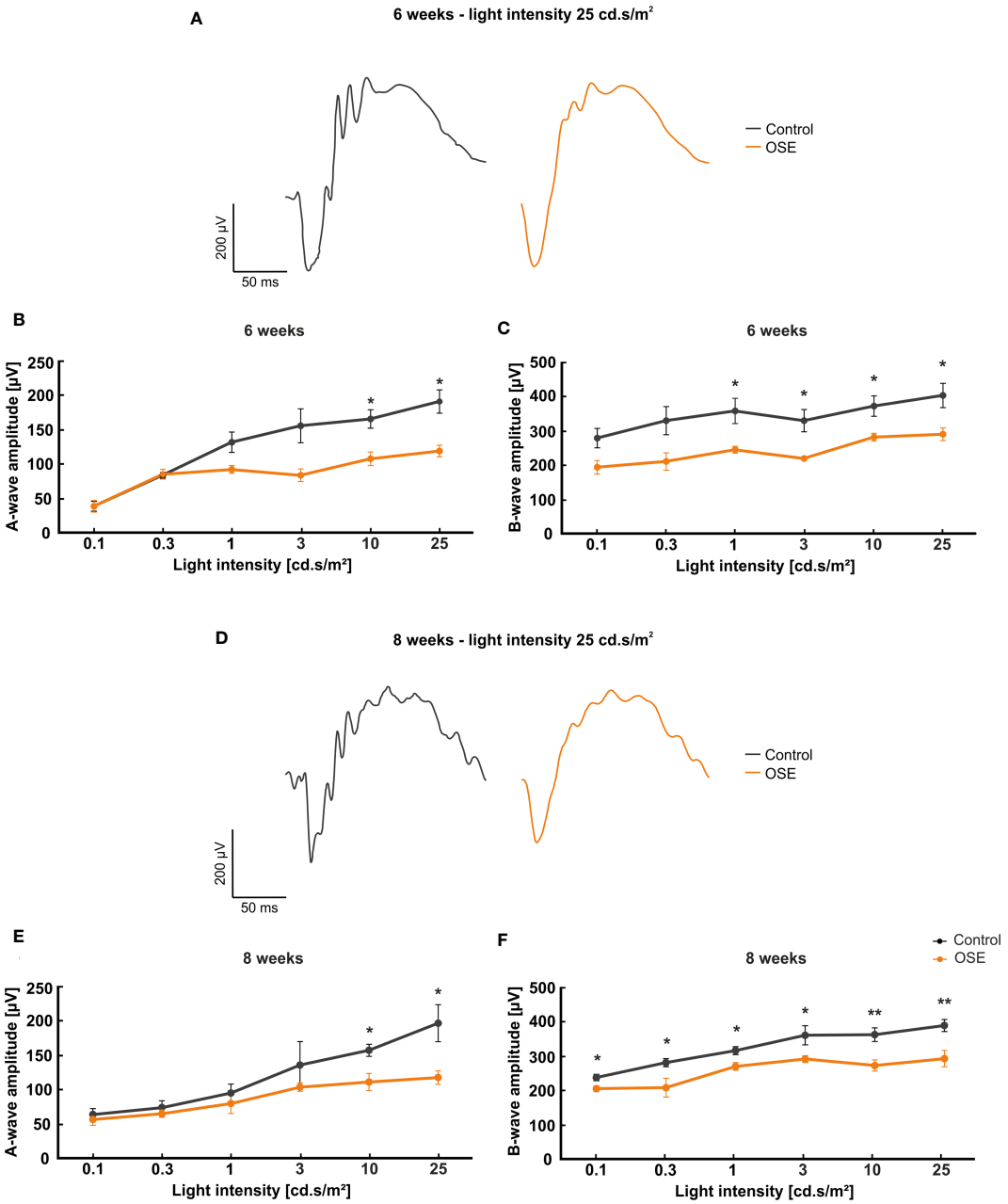

FIGURE 2 | Functional impairment of the retina. **(A)** Exemplary ERG amplitudes at 25 cd.s/m^2 flash luminance at six weeks. **(B)** At six weeks, the a-wave amplitude, representing the photoreceptors, was reduced in the OSE group. **(C)** The b-wave amplitude, which illustrates the conductivity of the inner retinal layers, was significantly reduced in OSE animals in comparison to the control group. **(D)** Exemplary ERG amplitudes at a flash luminance of 25 cd.s/m^2 in eight-week-old mice. **(E)** The ERG measurements after eight weeks again displayed a reduced a-wave amplitude in OSE. **(F)** Also, a loss of the electrical output was noted after eight weeks regarding the b-wave amplitude of OSE mice. Data are shown as mean ± SEM. *p < 0.05, **p < 0.01.

the OSE group (3.1 ± 0.6 cells) in comparison to controls (0.5 ± 0.1 cells, p<0.001). At eight weeks, Iba1$^+$ cell numbers were still increased in OSE mice (6.9 ± 2.4 cells) compared to controls (1.4 ± 0.1 cells, p=0.042; **Figure 4B**).

Tmem119$^+$ cells showed a threefold increase in six-week-old OSE mice (0.8 ± 0.1 cells) compared to controls (0.2 ± 0.1 cells, p=0.007). At eight weeks, the mean Tmem119 cell count in the control group (3.7 ± 0.4 cells) was higher than in younger animals (p<0.001). The number of Tmem119$^+$ cells was similar in the OSE group (5.0 ± 0.8 cells) and the control group at eight weeks (p=0.152; **Figure 4C**).

In addition, a twofold increase in Tmem119$^+$ and Iba1$^+$ cells was noted in OSE mice at the age of six weeks (1.4 ± 0.2 cells) compared to controls (0.7 ± 0.3 cells, p=0.045). The number of

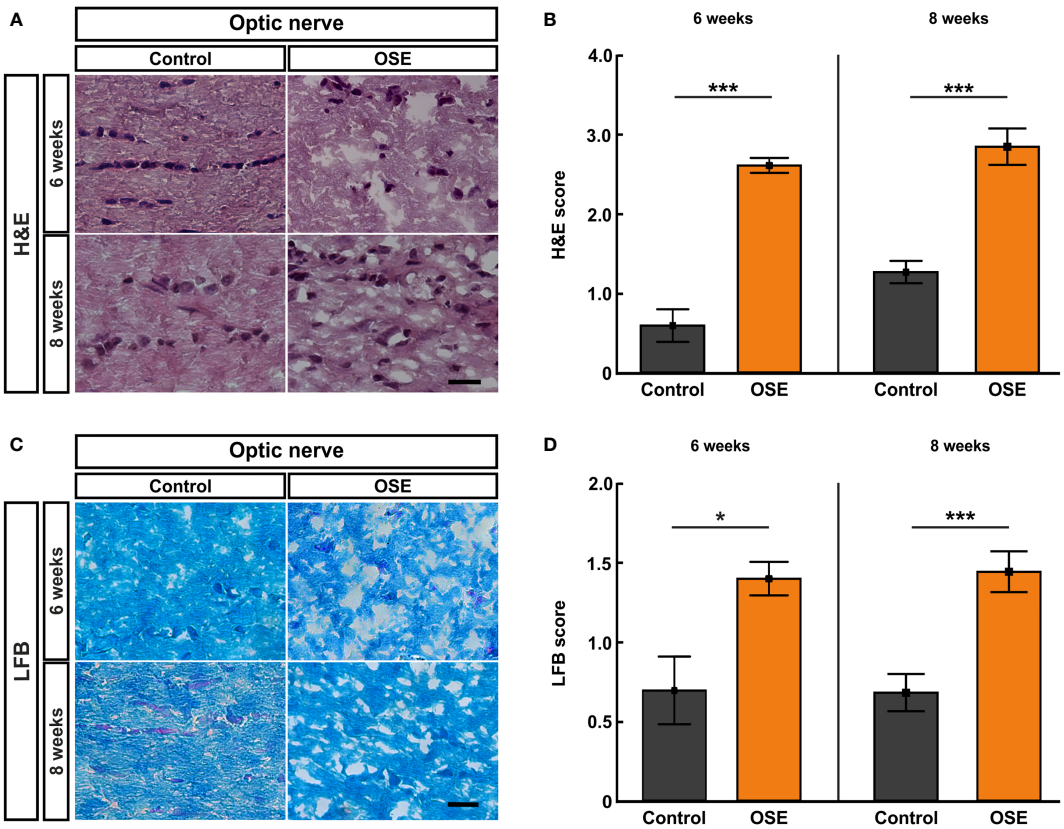

FIGURE 3 | Structural damage and increased demyelination of the optic nerve. **(A)** H&E stainings were performed after six and eight weeks to evaluate the morphology of the optic nerve. **(B)** The optic nerves of OSE mice showed a significantly elevated H&E score compared to the control group at both ages. **(C)** LFB-stained myelin sheaths of the control and OSE group are displayed. **(D)** Demyelination was increased in the OSE group as indicated in a higher LFB score at six as well at eight weeks of age. Data are shown as mean ± SEM. *p < 0.05, ***p < 0.001. Scale bars: 20 µm.

Tmem119$^+$and Iba1$^+$ cells was still significantly increased in OSE (2.5 ± 0.3 cells) at eight weeks (control: 1.2 ± 0.1 cells, p=0.002; **Figure 4D**).

OSE Mice Display a Reduced Number of Retinal Ganglion Cells

We used RBPMS to label RGCs (26) (**Figure 5A**). After six weeks, the number of RGCs was reduced by 37.8% in OSE mice (40.4 ± 1.6 cells/mm) in comparison to the control group (65.0 ± 8.1 cells/mm, p=0.01). A reduction of RGCs by 27.4% was noted in eight-week-old OSE mice (OSE: 42.7 ± 2.6 cells/mm; control: 58.8 ± 4.6 cells/mm, p=0.007; **Figure 5B**).

Additionally, we quantified the *Pou4f1* expression, which is a transcription factor highly expressed in RGCs, using RT-qPCR. In conformity with the immunohistochemical staining, the RT-qPCR displayed a significantly lower *Pou4f1* mRNA expression in the OSE group after six weeks (0.563-fold, p=0.015) in comparison to the control group. The RT-qPCR analyses of the eight-week time point showed a similar result (0.519-fold, p=0.008; **Figure 5C**).

The immunohistological staining with GFAP to analyze macroglia was performed after six and eight weeks (**Figure 5D**), since retinal degeneration is often associated with gliosis (27). The analysis of the GFAP$^+$ area displayed no significant differences between both groups at six (OSE: 2.1 ± 0.4%, control: 2.3 ± 0.3%, p=0.702) and at eight weeks (OSE: 1.7 ± 0.3%, control: 1.7 ± 0.1%, p=0.795; **Figure 5E**). Interestingly, an increased *Gfap* mRNA expression was detectable at six weeks (2.193-fold, p=0.005) whereas no significant changes were notable after eight weeks (1.087-fold, p=0.81, **Figure 5F**).

Increased Number of Microglia/ Macrophages in the Retina

The staining with Iba1 and Tmem119 was likewise performed on retinal cross-sections (**Figure 6A**) and cells were counted in the inner retinal layers (GCL to INL) together as well as separately. The immunohistochemical staining of the retina after six weeks demonstrated a significantly increased number of microglia/ macrophages (Iba1$^+$ cells) in OSE mice (6.4 ± 0.9 cells/mm) compared to the control group (2.9 ± 0.4 cells/mm, p=0.005). After eight weeks, the number of Iba1$^+$ cells was still significantly increased in OSE animals (7.6 ± 0.8 cells/mm) compared to controls (5.5 ± 0.6 cells/mm, p=0.048, **Figure 6B**). Regarding the separate layers, at six weeks, more Iba1$^+$ cells were noted in the

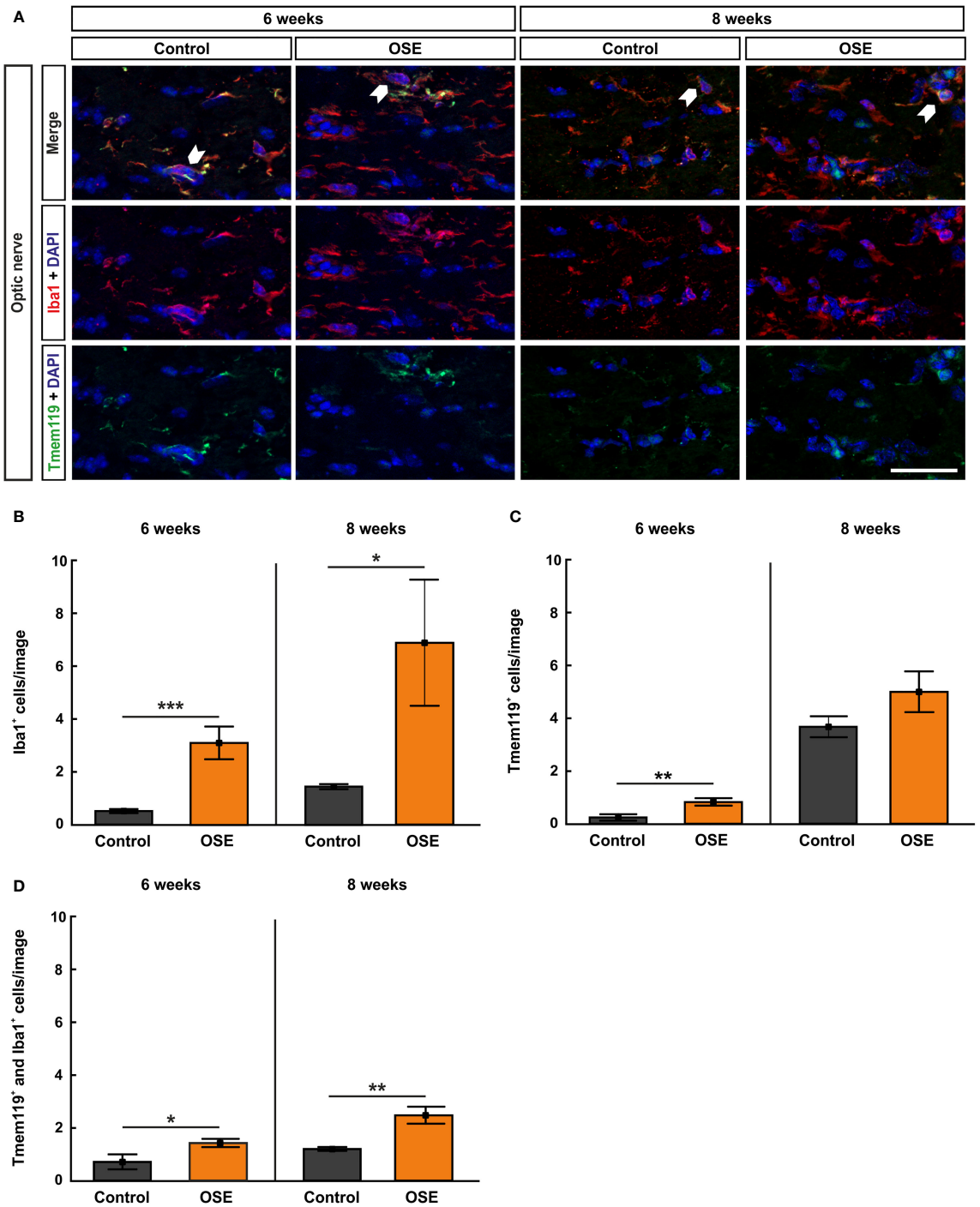

FIGURE 4 | Increased numbers of microglia/macrophages in the optic nerve. **(A)** Optic nerve sections were stained with Iba1 (red, microglia/macrophages) and Tmem119 (green, microglia) at six and after eight weeks. White arrows indicate co-localized Tmem119$^+$ and Iba1$^+$ cells. **(B)** The number Iba1$^+$ cells was significantly increased in the OSE group after six weeks. The staining after eight weeks still displayed an increase of Iba1$^+$ cells among the OSE group. **(C)** Tmem119$^+$ cells were also increased after six weeks. No difference of the number of Tmem119$^+$ cells was measurable between both groups at eight weeks. **(D)** A higher number of microglia (Tmem119$^+$ and Iba1$^+$) was observed at six weeks. This elevation was still noted in the OSE group at eight weeks. Data are shown as mean ± SEM. *$p < 0.05$, **$p < 0.01$, ***$p < 0.001$. Scale bar: 20 μm.

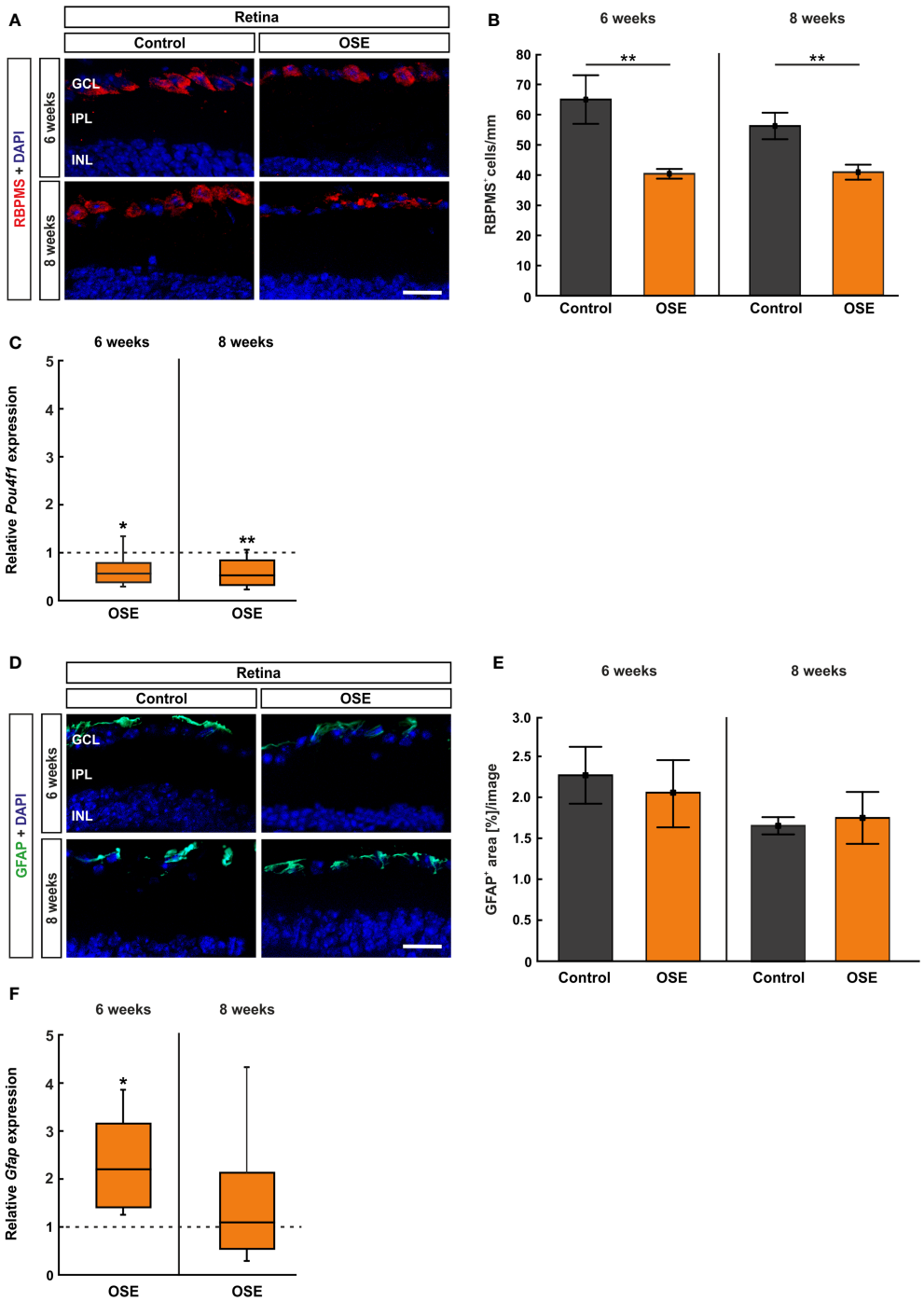

FIGURE 5 | Reduced number of retinal ganglion cells in OSE mice. **(A)** Retinal ganglion cells were stained with RBPMS (red) on retinal cross-sections. Cell nuclei were labeled with DAPI (blue). **(B)** The number of retinal ganglion cells was significantly reduced in the OSE group at six weeks. This reduction was also detectable in eight-week-old animals. **(C)** A significant downregulation of *Pou4f1* mRNA was noted in OSE mice in comparison to the control group at six and eight weeks. **(D)** Immunohistological staining of retinal cross-sections with GFAP (green) and DAPI (blue) was performed to label macroglia. **(E)** The $GFAP^+$ area evaluation revealed no significant differences between both groups at both ages. **(F)** The expression of *Gfap* mRNA was significantly increased in OSE mice at six weeks, but no changes were detectable at eight weeks. Data are mean ± SEM for immunohistochemistry, relative values for RT-qPCR are median ± quartile ± maximum/minimum. The dotted lines in **(C, F)** represent the relative expression level of the control group. GCL, ganglion cell layer; IPL, inner plexiform layer; INL, inner nuclear layer. *$p < 0.05$, **$p < 0.01$. Scale bars: 20 μm.

GCL of OSE mice (3.3 ± 0.7 cells/mm) compared to controls (0.4 ± 0.2 cells/mm, p=0.002), but not at eight weeks (OSE: 2.7 ± 0.4%, control: 1.9 ± 0.4%, p=0.141; **Supplemental Figure 2A**). The number of Iba1$^+$ cells was comparable in both groups in the IPL at six (OSE: 2.4 ± 0.3%, control: 1.4 ± 0.9%, p=0.054) and eight weeks (OSE: 1.3 ± 0.4%, control: 0.7 ± 0.1%, p=0.146; **Supplementary Figure 2B**). Also, no difference between both groups was observed regarding Iba1$^+$ cell counts in the INL at six (OSE: 0.7 ± 0.3%, control: 1.1 ± 0.3%, p=0.187) and eight weeks (OSE: 3.6 ± 0.6%, control: 3.0 ± 0.6%, p=0.469; **Supplemental Figure 2C**).

Additionally, we noted an increase of Tmem119$^+$ cells in the retinae of OSE animals after six weeks (OSE: 0.6 ± 0.2 cells/mm; control: 0.05 ± 0.05 cells/mm, p=0.028). No significant differences regarding Tmem119$^+$ cells were detectable at eight weeks of age (OSE: 23.9 ± 4.0 cells/mm, control: 23.0 ± 5.4 cells/mm, p=0.869; **Figure 6C**). When examining Tmem119$^+$ cells in the retinal layers separately, no differences between the groups could be detected. The number of Tmem119$^+$ cells was similar in the GCL in OSE and control retinas at six (OSE: 2.4 ± 0.3%, control: 1.4 ± 0.9%, p=0.105) and eight weeks (OSE: 1.7 ± 0.5%, control: 1.9 ± 0.5%, p=0.775; **Supplemental Figure 2D**). Also, Tmem119$^+$ cell counts were comparable in the IPL at six (OSE: 0.1 ± 0.1%, control: 0.0 ± 0.0%, p=0.079) and eight weeks (OSE: 1.0 ± 0.2%, control: 0.8 ± 0.3%, p=0.585; **Supplemental Figure 2E**). The same was the case in the INL at six (OSE: 0.3 ± 0.5%, control: 0.06 ± 0.1%, p=0.927) and eight weeks (OSE: 21.2 ± 4.0%, control: 20.7 ± 4.8%, p=0.775; **Supplemental Figure 2F**).

The co-staining of Tmem119 and Iba1 showed significantly more microglia in the retinas of six-week-old OSE mice (4.0 ± 0.7 cells/mm) in comparison to the controls (0.6 ± 0.3 cells/mm, p=0.001). In contrast, no significant changes were detectable at eight weeks (OSE: 3.5 ± 0.9 cells/mm, control: 2.1 ± 0.4 cells/mm, p=0.229; **Figure 6D**). In regard to the cell counts in the separate layers, significant differences were only visible in six-week-old mice. Here, OSE mice (0.7 ± 0.2%) displayed more Tmem119$^+$ and Iba1$^+$ cells in the GCL than control animals (0.1 ± 0.1%, p=0.005). Later on, cell counts were comparable in these groups (OSE: 0.7 ± 0.3%, control: 0.4 ± 0.2%, p=0.336; **Supplemental Figure 2G**). The Tmem119$^+$ and Iba1$^+$ cell numbers in the IPL were higher in OSE mice (2.1 ± 0.4%) than in controls (0.5 ± 0.2%, p=0.003) at six weeks, while at eight weeks, cell counts in this layer were similar in both groups (OSE: 0.6 ± 0.3%, control: 0.2 ± 0.3%, p=0.206; **Supplemental Figure 2H**). In addition, in the INL more, Tmem119$^+$ and Iba1$^+$ cells were counted in the OSE group (4.0 ± 0.7%) than in the control group (2.0 ± 0.7%, p=0.001). At eight weeks, cell counts in both groups in the INL were not different (OSE: 3.5 ± 0.9%, control: 2.1 ± 0.9%, p=0.156; **Supplemental Figure 2I**).

In addition to the immunhistochemical stainings, we also performed RT-qPCR to quantify the expression of the markers *Iba1* (microglia/macrophages), *Tmem119* (microglia), and *CD68* (ED1, macrophages). The analyses via RT-qPCR at six weeks showed a marked increase of the *Iba1* mRNA expression in retinae of OSE mice (6.95-fold, p<0.001). After eight weeks, the expression of *Iba1* mRNA was still increased, though to a lesser extent (1.803-fold, p=0.008; **Figure 6E**). Additionally, we found an increased *Tmem119* mRNA expression in OSE in six- (1.888-fold, p=0.026) and eight-week-old OSE mice (1.963-fold, p=0.016; **Figure 6F**). The expression of *CD68* mRNA was also higher in the OSE group at six weeks (3.877-fold, p=0.002) as well as at eight weeks of age (2.469-fold, p=0.007; **Figure 6G**).

Since microglia are known to be the primary source of proinflammatory cytokines, we analyzed the mRNA expression of *Tnfa* and *Tgfb*. We noted increased mRNA expression levels at both time points regarding *Tnfa* (6 weeks: 2.813-fold, p=0.005; 8 weeks: 2.071-fold, p=0.006; **Figure 6H**). The mRNA expression of *Tgfb* was also upregulated in OSE mice after six (1.682-fold, p=0.003) as well as after eight weeks (1.899-fold, p=0.023, **Figure 6I**).

Activation of the Complement System in the Retina of OSE Mice

Retinal cross-sections were labelled with antibodies against the complement markers C1q, C3, and MAC (**Figure 7A**) and counted in the inner retinal layers (GCL to INL). The staining with C1q at the six weeks´ time point showed a significantly higher number of C1q$^+$ cells in the OSE group (15.8 ± 1.4 cells/mm) in comparison to the control group (2.6 ± 0.3 cells/mm, p<0.001). An increase of 16.5% among C1q$^+$ cells was noted in eight-week-old OSE mice (OSE: 18.4 ± 3.0 cells/mm; control: 2.1 ± 0.3 cells/mm, p<0.001; **Figure 7B**). When looking at the retinal layers separately, at six weeks, we noted a more than 10-fold increase of C1q$^+$ cells in the GCL of OSE animals (7.1 ± 0.9 cells/mm) compared to controls (0.6 ± 0.2 cells/mm, p<0.001). At eight weeks, OSE animals (6.8 ± 1.3 cells/mm) still showed more C1q$^+$ cells in the GCL than controls (0.7 ± 0.2 cells/mm, p<0.001; **Supplemental Figure 3A**). Regarding the IPL, the OSE group (6.0 ± 0.8 cells/mm) displayed more C1q$^+$ cells than controls (1.4 ± 0.3 cells/mm, p<0.001) at six weeks. Similar effects were noted at eight weeks (OSE: 9.5 ± 1.4 cells/mm; control: 1.0 ± 0.2 cells/mm, p<0.001; **Supplemental Figure 3B**). More C1q$^+$ cells were also noted in the INL of OSE retinae at six (OSE: 2.7 ± 0.5 cells/mm; control: 0.5 ± 0.2 cells/mm, p=0.001) and eight weeks (OSE: 2.1 ± 0.4 cells/mm; control: 0.4 ± 0.1 cells/mm, p=0.002; **Supplemental Figure 3C**).

The complement marker C3 was stained on retinal cross-sections (**Figure 7A**). The statistical analysis showed a significant increase of C3$^+$ cells in GCL, IPL, and INL together in the OSE group (7.3 ± 1.1 cells/mm) compared to the control (2.4 ± 0.7 cells/mm, p=0.003) after six weeks. An increase of C3$^+$ cells in GCL, IPL, and INL was notable in eight-week-old OSE mice (10.0 ± 1.7 cells/mm; control: 0.9 ± 0.2 cells/mm, p<0.001; **Figure 7C**). We also investigated the number of C3$^+$ cells in these layers separately. We mainly found an upregulation in the OSE group. The number of C3$^+$ cells in the GCL was higher in OSE retinae at six (OSE: 3.5 ± 0.6 cells/mm; control: 0.9 ± 0.4 cells/mm, p=0.003) and eight weeks (OSE: 2.4 ± 0.9 cells/mm; control: 0.04 ± 0.04 cells/mm, p=0.0147; **Supplemental Figure 3D**). In the IPL, C3$^+$ cell counts were also elevated in OSE animals at six (OSE: 1.7 ± 0.4 cells/mm; control: 0.8 ± 0.2

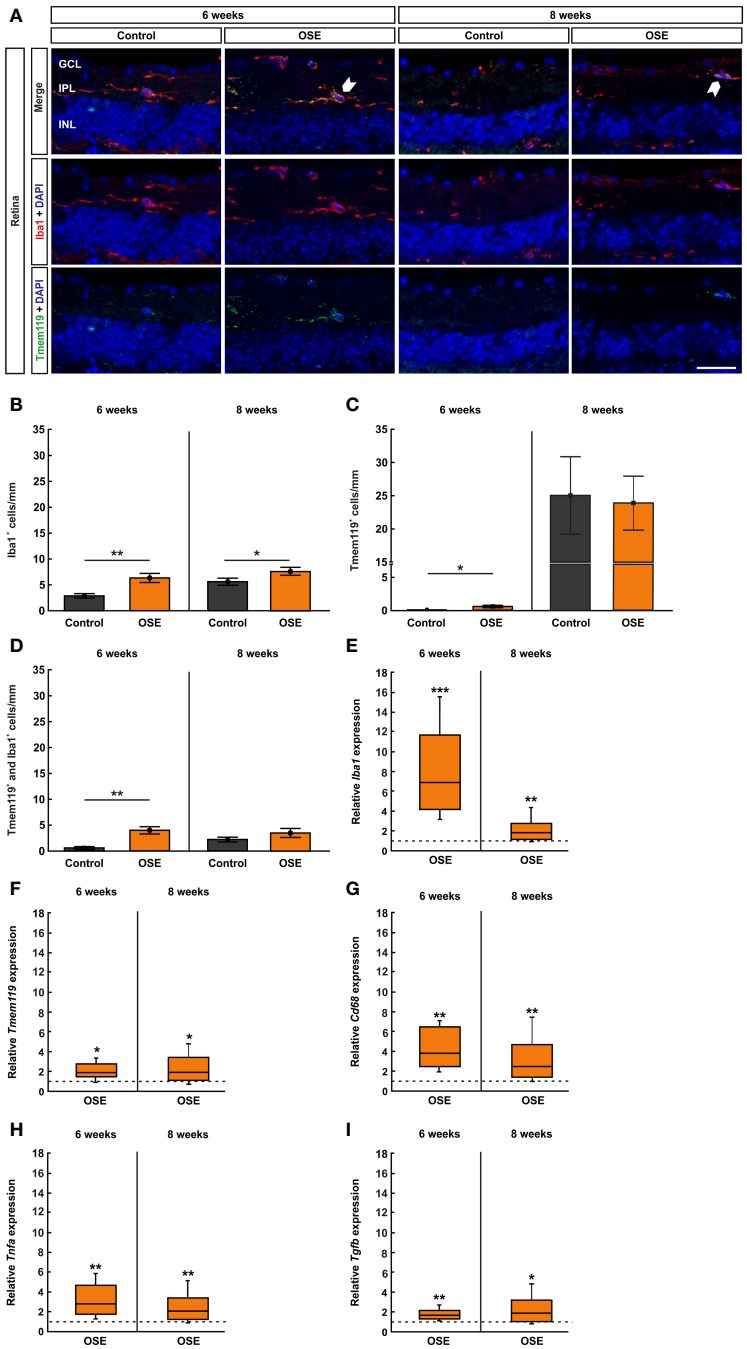

FIGURE 6 | Increased number of microglia/macrophages in OSE retinae. **(A)** Iba1 was used to label microglia/macrophages (red) whereas microglia were co-stained with Tmem119 (green) and Iba1. Iba1$^+$ and Tmem119$^+$ cells were quantified in GCL, IPL, and INL. White arrows point towards co-localized Tmem119$^+$ and Iba1$^+$ cells. **(B)** The immunohistochemical staining of the retina after six weeks demonstrated a significantly increased number of microglia/macrophages (Iba1$^+$) in OSE mice. The number of Iba1$^+$ cells was also significantly increased in eight-week-old OSE mice. **(C)** An increased number of Tmem119$^+$ cells was noted in the retinae of OSE animals at six weeks. Tmem119$^+$ cell counts were comparable in both groups at eight weeks. **(D)** The number of Tmem119$^+$ and Iba1$^+$ cells in the retina was significantly increased in the OSE group at six weeks, which was diminished at eight weeks. **(E)** Using RT-qPCR, a significant upregulation of *Iba1* mRNA was noticed in six-week-old OSE mice. After eight weeks, the expression of *Iba1* mRNA was still significantly increased, though to a lesser extent. **(F)** The expression of *Cd68* mRNA was significantly increased in OSE retinas at both time points. **(G)** The mRNA expression of *Tmem119* was also elevated after six and eight weeks. **(H)** RT-qPCR evaluation of the cytokine *Tnfa* mRNA revealed an increased expression at both ages in OSE mice. **(I)** The *Tgfb* mRNA expression was significantly upregulated at six and eight weeks in the OSE group. Data are shown as mean ± SEM for immunohistochemistry, relative values for RT-qPCR are median ± quartile ± maximum/minimum. The dotted lines in **(E–I)** represent the relative expression level of the control group. GCL, ganglion cell layer; IPL, inner plexiform layer; INL, inner nuclear layer. *p < 0.05, **p < 0.01, ***p < 0.001. Scale bar: 20 µm.

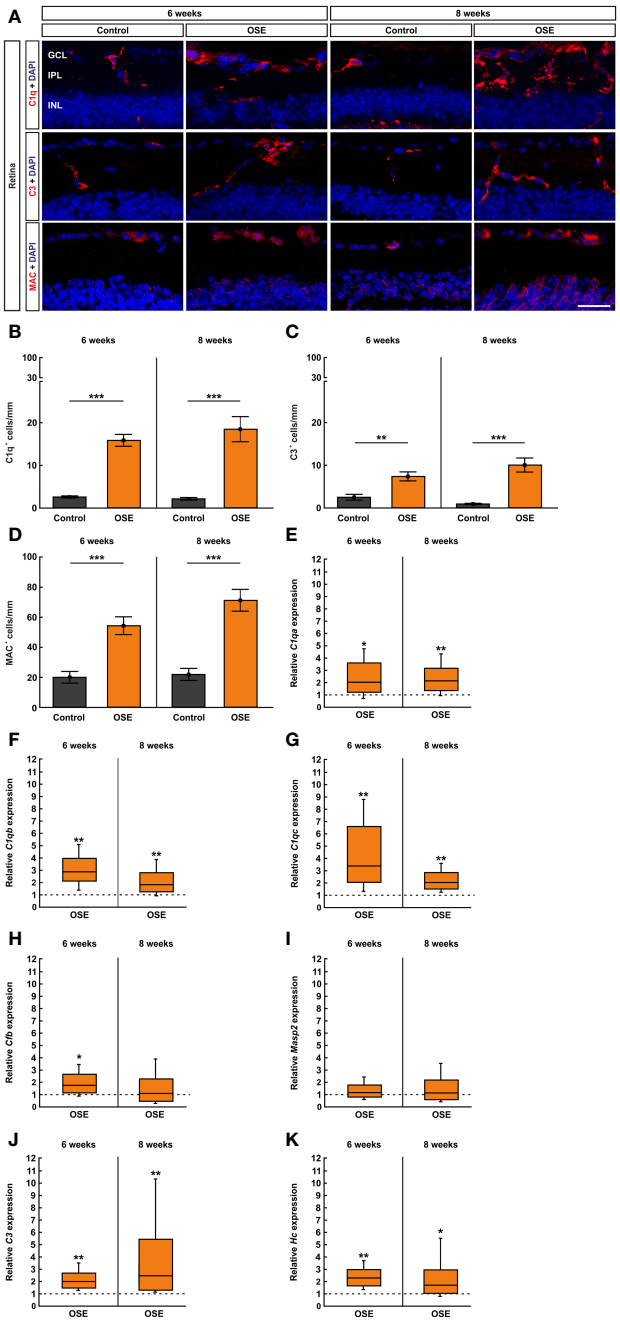

FIGURE 7 | Activation of the classical pathway of the complement system in the retina of OSE mice. **(A)** Staining of retinal cross-sections with the complement markers C1q (red), C3 (red), and MAC (red), while DAPI counterstained cell nuclei (blue). **(B)** A significantly increased number of $C1q^+$ cells was found in the OSE group in the GCL, IPL, and INL after six weeks. An increase of $C1q^+$ cells of 16.5% was noted at the eight weeks´ time point. **(C)** The total number of $C3^+$ cells in GCL, IPL, and INL was significantly elevated in six-week-old OSE mice. After eight weeks, $C3^+$ cells were even further increased. **(D)** The quantification of MAC^+ cells revealed a significant increase among the OSE group at six weeks. A progression of increasing MAC^+ cells in OSE mice was observed after eight weeks. **(E–G)**. Complement pathway factor *C1qa*, *C1qb*, and *C1qc* (classical pathway) mRNA expression were significantly upregulated in six- and eight-week-old OSE mice. **(H)** At six weeks of age, a significant increase of *Cfb* (Factor B, alternative pathway) mRNA expression was noted in OSE retinae, whereas the expression was not significantly altered later on, at eight weeks. **(I)** No significant differences were found in *Masp2* mRNA (lectin pathway) at six and eight weeks. **(J)** An increased *C3* (common pathway) mRNA expression was detected in the OSE group at both ages. **(K)** Likewise, the mRNA level of *Hc* (C5, common pathway) was upregulated at six as well as at eight weeks in OSE retinae. Data are shown as mean ± SEM for immunohistochemistry, relative values for RT-qPCR are median ± quartile ± maximum/minimum. The dotted lines in **(E–K)** represent the relative expression level of the control group. GCL, ganglion cell layer; IPL, inner plexiform layer; INL, inner nuclear layer. *$p < 0.05$, **$p < 0.01$, ***$p < 0.001$. Scale bar: 20 µm.

cells/mm, p=0.050) and eight weeks (OSE: 2.5 ± 0.4 cells/mm; control: 0.4 ± 0.1 cells/mm, p<0.001; **Supplemental Figure 3E**). $C3^+$ cell counts in the INL were similar in both groups at six weeks (OSE: 2.1 ± 0.6 cells/mm; control: 0.8 ± 0.4 cells/mm, p=0.131). At eight weeks, $C3^+$ cell counts were higher in the INL of OSE animals (5.1 ± 0.8 cells/mm) than in controls (0.5 ± 0.2 cells/mm, p<0.001; **Supplemental Figure 3F**).

To complete the immunohistological analyses of the complement system, we used an antibody to label the terminal complex MAC (**Figure 7A**). The results of the six weeks´ time point showed an increase of MAC^+ cells in the retinae of OSE mice (54.2 ± 6.0 cells/mm) compared to the control group (19.8 ± 3.9 cells/mm, p<0.001). The number of MAC^+ cells increased by 31.0% in eight-week-old OSE animals (71.0 ± 7.3 cells/mm; control: 21.7 ± 4.1 cells/mm, p<0.001; **Figure 7D**). In the GCL of six-week-old OSE mice (23.5 ± 3.3 cells/mm) more MAC^+ cells were noted than in controls (11.8 ± 2.9 cells/mm, p=0.020). At eight weeks, counts in both groups were comparable (OSE: 16.1 ± 3.1 cells/mm; control: 10.9 ± 2.4 cells/mm, p=0.208; **Supplemental Figure 3G**). MAC^+ cell numbers were comparable in the IPL of both groups at six (OSE: 0.1 ± 0.1 cells/mm; control: 0.05 ± 0.05 cells/mm, p=0.403) and eight weeks (OSE: 0.0 ± 0.0 cells/mm; control: 0.05 ± 0.05 cells/mm, p=0.337; **Supplemental Figure 3H**). In the INL, the number of MAC^+ cells was significantly higher in the OSE group at six (OSE: 30.6 ± 5.3 cells/mm; control: 8.0 ± 3.1 cells/mm, p=0.003) and eight weeks (OSE: 54.9 ± 7.9 cells/mm; control: 11.5 ± 4.9 cells/mm, p<0.001; **Supplemental Figure 3I**).

In addition, we performed RT-qPCR to quantify the mRNA expression of the complement pathway factors *C1qa*, *C1qb*, *C1qc*, *C3, Hc* (C5), *Masp2* (mannan-binding lectin serine protease 2), *and Cfb* (Factor B). To investigate an involvement of the classical pathway, we analyzed the mRNA levels of *C1qa*, *C1qb*, and *C1qc*. The expression of *C1qa* mRNA was significantly upregulated in six-week-old OSE mice (2.036-fold, p=0.049). At eight weeks, an increase of the *C1qa* mRNA expression was still notable in the OSE group (2.147-fold, p=0.007; **Figure 7E**). The analyses of *C1qb* mRNA showed a significantly increased expression in OSE animals at six weeks (2.892-fold, p=0.004) as well as at eight weeks (1.847-fold, p=0.007; **Figure 7F**). In accordance with the upregulation of *C1qa* and *C1qb*, the expression of *C1qc* mRNA was also upregulated in OSE mice with six weeks of age (3.387-fold, p=0.008). Again, we found an increased expression of *C1qc* mRNA at eight weeks (2.04-fold, p=0.001; **Figure 7G**).

To analyze a potential involvement of the alternative pathway, we quantified the expression of *Cfb* mRNA which encodes Factor B. Indeed, we found a significant upregulation in six-week-old OSE animals in comparison to the control group (1.733-fold, p=0.021). In contrast, we noted no significant alteration of *Cfb* mRNA expression later on, at eight weeks of age (1.077-fold, p=0.834; **Figure 7H**).

The lectin pathway was evaluated via *Masp2*. *Masp2* mRNA expression was similar in both groups at six weeks (1.168-fold, p=0.468) and eight weeks (1.142-fold, p=0.665; **Figure 7I**), indicating that the lectin pathway is not activated in OSE mice.

To evaluate the common pathway which leads to the formation of MAC, we analyzed the expression of *C3* and *Hc*. A significant increase of *C3* mRNA expression was seen in six-week-old OSE mice (2.004-fold, p=0.006). We also found an upregulation of *C3* mRNA in eight-week-old OSE animals (2.465-fold, p=0.001; **Figure 7J**).

In accordance with the increase of *C3* mRNA, the expression of *Hc* mRNA encoding C5 was also upregulated at six weeks, in OSE mice (2.293-fold, p=0.004). At eight weeks, we noted a significantly higher *Hc* mRNA expression in the OSE group (1.711-fold, p=0.035; **Figure 7K**). Those results indicate an activation of the complement system in six- and eight-week-old OSE mice initiated by the classical pathway. Additionally, we noted an activation of the common pathway by the alternative pathway whereas the lectin pathway had no contribution to the activation of the complement system at any time.

Correlation of Evaluated Parameters

Correlation analyses of SD-OCT parameters and RGC counts showed a correlation between ganglion cell complex thickness and RGC numbers at six weeks (r=0.5092; p=0.046; **Supplemental Figure 4A**). A stronger correlation for the same parameters was noted at eight weeks of age (r=0.5825; p=0.016; **Supplemental Figure 4B**). The total retinal thickness, evaluated via SD-OCT, also correlated with the RGC counts at six (r=-0.8211; p<0.001; **Supplemental Figure 4C**) and eight weeks of age (r=-0.8299; p<0.001; **Supplemental Figure 4D**). Regarding the OSE score at 56 days, a negative correlation was noted with RGC numbers at six weeks (r=-0.595; p=0.017; **Supplemental Figure 4E**), but not with RGC numbers at eight weeks (r=-0.3388; p=0.197; **Supplemental Figure 4F**). A strong negative correlation was observed between the clinical score at 56 days and the ganglion cell complex (evaluated *via* SD-OCT) at both time points, six (r=-0.8211; p<0.001; **Supplemental Figure 4G**) and eight weeks (r=-0.8299; p<0.001; **Supplemental Figure 4H**).

DISCUSSION

Understanding mechanisms and dynamics of degeneration of the visual system in chronic inflammatory conditions is a crucial step to implement effective therapeutic approaches, especially in rare conditions with potential devastating effects such as NMOSD or MOGAD. We therefore performed conclusive analyses of function, morphology, and histological alterations as well as changes of gene expression of inflammatory/immune pathways in a model of spontaneous encephalomyelitis. We provide evidence that early on during OSE, mice are affected by severe damage of the visual system with reduced function, retinal thinning, and severe inflammation with involvement of both the adaptive and innate immunity as well as activation of the complement system.

In autoimmune-mediated diseases, like MOGAD, NMOSD, or MS, neurodegeneration is a major component of the pathogenesis. Although the pathology of those diseases is not completely understood, neurodegeneration is mostly seen as secondary response to inflammatory-mediated demyelination (28, 29). Other studies refer to the role of neurodegeneration

as a primary phenomenon occurring in myelin-deficient retina without optic neuritis (30, 31). In our study, OSE mice developed signs of encephalomyelitis after 26 days and 50% had a clinical score after four weeks. Intriguingly, we found indications of degeneration also in clinically unaltered animals without neurological signs.

The clinical analysis of the retina via OCT is frequently used as diagnostic tool in NMOSD and MOGAD (32). It is also applied to monitor disease progress in follow-up investigations (33). NMOSD patients have a significant reduction of the RNFL (34), correlating with the history of optic neuritis (35). In NMOSD, GCL and IPL are significantly more affected compared to MS or patients with isolated optic neuritis (36). Patterns of retinal thinning are, of note, similar in MOGAD and NMOSD (37). In contrast, the visual impairment due to retinal thinning is less severe in MOGAD compared to NMOSD (37–39).

Animal models offer a possibility to study dynamics longitudinally (40, 41). Cruz-Herranz et al. investigated the retinal changes in EAE mice, immunized with myelin oligodendrocyte glycoprotein peptide ($MOG_{35–55}$). They found a thinning of the RNFL, the GCL, and IPL subsequent to the first signs of EAE (42). The reduction of those layers correlated with EAE severity and RGC loss. Another study also showed a significant reduction of the GCL in the EAE model eight weeks after $MOG_{35–55}$ immunization (43). Until now, OCT has not been used in OSE. We showed that within a short time frame retinal thickness was further reduced from 8.2% in six-week-old OSE mice to 12.3% in eight-week-old animals. We especially noted a thinning of the ganglion cell complex via SD-OCT analysis, indicating that ganglion cells are predominantly affected. Also, we observed a strong correlation between retinal thickness and RGC counts. In addition, ganglion cell complex thickness and RGC cell numbers correlated. Our findings concur with the results from previous studies which describe a correlation of retinal thickness with the clinical score was well as with RGC counts (38, 43). This overall supports the use of OCT as marker of degeneration for progression and therapy response in OSE animal models as well as in patients.

Electroretinography is a well-established technique to investigate retinal function. Since retinal function can be impaired in NMO or MS patients with optic neuritis, ERG recordings were previously examined in patient studies (44, 45). ERG recordings were also analyzed in several mouse models for other diseases before (46, 47). We identified an impairment of retinal function correlating with retinal thinning in SD-OCT, suggesting an impairment of both the photoreceptors and the inner retinal layers.

Loss of RGCs correlates with irreversible neurodegeneration. We noted a significant loss of RGCs in the investigated OSE model, correlating with clinical progression. Zhang et al. noted a RGC decline in a rat NMOSD model, where animals were injected with AQP4 IgG-positive serum from NMOSD patients (48). Previous studies have described a significant RGC degeneration in several models of chronic EAE (19, 49–52). In a postmortem study of ocular pathology in MS patients, extensive neurodegeneration of the GCL and INL combined with inflammation of the retina was evident, irrespective of disease duration, while severity of retinal atrophy correlated with brain weight (53). Degeneration could be mediated by apoptosis (14, 19) or as result of inflammation during optic neuritis (54). We showed a reduction of RGCs both at six (37.8% reduction) and eight weeks (27.4% reduction), while OSE progressed further, suggesting that an initial peak of RGC degeneration is followed by rather moderate continuation of cell loss. This is highly relevant since we have shown previously in EAE that only a prophylactic treatment with the immunomodulatory agent laquinimod was able to reduce apoptosis and RGC loss, while a therapeutic approach failed (14).

The activation of macroglia, especially astrocytes, is a crucial factor in chronic inflammation in MS as well as in EAE (55, 56). In MS, an elevated GFAP level in the cerebrospinal fluid points towards severe astrogliosis (57). In contrast to MS, a decreased GFAP immunoreactivity was observed in NMO lesions, whereas the GFAP levels were increased in the cerebrospinal fluid due to the loss of astrocytes (58). The retina contains two types of macroglia, astrocytes and Müller cells (59). Surprisingly, we found no significant increase of the $GFAP^+$ area in the retina at both time points. One possible explanation might be that astrocytic scar formation might happen later during the course of disease. This, however, remains to be proven with longitudinal investigations. Zeka et al. also observed little GFAP response in retinae of a rat model of NMOSD (11).

One hallmark of NMOSD and MOGAD is optic neuritis. The infiltration of the optic nerve with inflammatory cells has been shown in EAE (60) as well as in 12-week-old-mice OSE mice (9). In accordance with the results from these studies, we noted inflammatory infiltrations of the optic nerve, suggestive of optic neuritis, already in six- and eight-week-old-animals associated with demyelination. This was also accompanied by microglial activation, innate immune cells of the CNS important for homeostasis (61), phagocytosis, release of proinflammatory cytokines, and presentation of antigens to T cells (62). Microglia are crucially involved in the pathogenesis of chronic inflammation of the CNS, such as MS, especially during disease progression (63). Moreover, microglial interaction with astrocytes initiated by AQP4 antibodies leads to the formation of lesions in NMO (64). Although antibodies to AQP4 are absent in MOGAD, it is conceivable that microglia are also involved in the early formation of lesions in the OSE model.

In addition to the analyses of microglia in the optic nerve, we investigated microglia in the retina. Microglial activation of the retina was previously observed not only in NMO and MS, but also in EAE (64, 65). In OSE, active microglia and microglia/macrophages were significantly increased in the retina after six weeks. The analyses of the distribution of microglia/macrophages in the retinal layers showed that $Iba1^+$ cells were only significantly increased in the GCL at six weeks whereas no differences were observed in the IPL and INL. In contrast, the number of $Tmem119^+$ and $Iba1^+$ microglia was increased in the GCL, IPL, and INL in the separate cell counts at six, but not at eight weeks suggesting an early peak in microglia response in OSE. In MS,

$CD68^+$ macrophages are upregulated in active white matter lesions in the brain (65). Interestingly, we found significantly upregulated expressions of CD68 and TNFα as well as TGFβ in the retina.

We also investigated the involvement of the complement system, since MOG IgG can induce complement dependent cytotoxicity (66). We showed, for the first time, an activation of the complement system, especially via the classical pathway, on mRNA and protein level. The alternative pathway was involved in the early phase of OSE whereas the lectin pathway was not involved, suggesting that the activation might be induced through antibody/antigen complex recognition. Further, microglia could be the source of complement, especially of C1q, in this model. In a mouse model for Alzheimer's disease, a knock-out of C1q was accompanied by less microglia activation (67). The same group revealed that microglia are the dominant source of C1q in the brain and therefore probably also in the retina (68). The complement activation also supports the theory that neurodegeneration in the retina is not only a secondary phenomenon subsequent to isolated optic neuritis, but at least partly a result of the complement activation in the retina itself. Complement-dependent degeneration was described in the EAE model, while genetic lack of C3 protein protected from signs of EAE and neurodegeneration (69). Anti-complement directed therapeutic approaches such as the anti-C5 monoclonal antibody eculizumab are already in clinical use in NMOSD (70). While we showed an activation of the complement system in OSE, it remains so far unknown, whether activation of the complement system is a primary driver of pathology or rather an epiphenomenon of activated immune cells such as microglia. Hence, complement directed therapies should be investigated in animal models such as OSE to gather more data prior to potential use in MOGAD.

There are some limitations of this study that should be addressed. Only one control group, single-transgenic IgHMOG (Th) mice, was implemented in this study, based on the background of OSE mice. These control animals displayed some subclinical, histopathological alterations in optic nerves without developing neurological signs of EAE. Previous studies found no autoimmunity in the CNS of Th mice even in case of high MOG-autoantibody titers, which was explained by an intact blood-brain barrier (13), hence we suggested that autoimmunity will also be absent in the visual system. The noted subclinical histopathological alterations should be further investigated in future studies. A further limitation of this study is that mice were examined at certain ages and not disease progression stages. This should be addressed in further studies.

In summary, we provide evidence that OSE mice are affected by early damage of the visual system, including the retina and optic nerve, with altered retinal function, morphology, and evidence of inflammation, complement activation as well as degeneration. Since histological analyses of the retina or optic nerve in human are in general only feasible in postmortem tissue, those data help to understand dynamics of degeneration in MOGAD and NMOSD.

DATA AVAILABILITY STATEMENT

The original contributions presented in the study are included in the article/**Supplementary Material**. Further inquiries can be directed to the corresponding authors.

ETHICS STATEMENT

The animal study was reviewed and approved by Landesamt für Natur, Umwelt und Verbraucherschutz Nordrhein-Westfalen (Recklinghausen, Germany; file no. 84-02.04.2016.A062).

AUTHOR CONTRIBUTIONS

LP, SR, SH, LD, and FG performed the experiments. LP, SR, SF, and SJ analyzed data. LP, SF, and SJ wrote the manuscript. SR, SH, FG, IK, HD, and RG critically revised the manuscript. SF and SJ designed and supervised the study. All authors read and approved the final manuscript.

FUNDING

This study was supported by the Hertie Foundation and the FoRUM program of the Medical Faculty of Ruhr-University Bochum. We acknowledge the support by the Open Access Publication Funds of the Ruhr-University Bochum.

ACKNOWLEDGMENTS

We thank Ekaterina Blum, Jasmin Günther, Gesa Stute, and Xiomara Pedreiturria for excellent technical assistance.

SUPPLEMENTARY MATERIAL

The Supplementary Material for this article can be found online at: https://www.frontiersin.org/articles/10.3389/fimmu.2021.759389/full#supplementary-material

REFERENCES

1. Compston A, Coles A. Multiple Sclerosis. *Lancet* (2008) 372:1502–17. doi: 10.1016/S0140-6736(08)61620-7
2. Delarasse C, Daubas P, Mars LT, Vizler C, Litzenburger T, Iglesias A, et al. Myelin/oligodendrocyte Glycoprotein-Deficient (MOG-Deficient) Mice Reveal Lack of Immune Tolerance to MOG in Wild-Type Mice. *J Clin Invest* (2003) 112:544–53. doi: 10.1172/JCI15861
3. Nagireddy RBR, Kumar A, Singh VK, Prasad R, Pathak A, Chaurasia RN, et al. Clinicoradiological Comparative Study of Aquaporin-4-IgG Seropositive Neuromyelitis Optica Spectrum Disorder (NMOSD) and MOG Antibody Associated Disease (MOGAD): A Prospective Observational Study and

Review of Literature. *J Neuroimmunol* (2021) 361:577742. doi: 10.1016/j.jneuroim.2021.577742
4. Weber MS, Derfuss T, Metz I, Bruck W. Defining Distinct Features of Anti-MOG Antibody Associated Central Nervous System Demyelination. *Ther Adv Neurol Disord* (2018) 11:1756286418762083. doi: 10.1177/1756286418762083
5. Clements CS, Reid HH, Beddoe T, Tynan FE, Perugini MA, Johns TG, et al. The Crystal Structure of Myelin Oligodendrocyte Glycoprotein, a Key Autoantigen in Multiple Sclerosis. *Proc Natl Acad Sci USA* (2003) 100:11059–64. doi: 10.1073/pnas.1833158100
6. Kitley J, Waters P, Woodhall M, Leite MI, Murchison A, George J, et al. Neuromyelitis Optica Spectrum Disorders With Aquaporin-4 and Myelin-Oligodendrocyte Glycoprotein Antibodies: A Comparative Study. *JAMA Neurol* (2014) 71:276–83. doi: 10.1001/jamaneurol.2013.5857
7. Ciotti JR, Eby NS, Wu GF, Naismith RT, Chahin S, Cross AH. Clinical and Laboratory Features Distinguishing MOG Antibody Disease From Multiple Sclerosis and AQP4 Antibody-Positive Neuromyelitis Optica. *Mult Scler Relat Disord* (2020) 45:102399. doi: 10.1016/j.msard.2020.102399
8. Optic Neuritis Study G. Visual Function 15 Years After Optic Neuritis: A Final Follow-Up Report From the Optic Neuritis Treatment Trial. *Ophthalmology* (2008) 115:1079–82.e1075. doi: 10.1016/j.ophtha.2007.08.04
9. Krishnamoorthy G, Lassmann H, Wekerle H, Holz A. Spontaneous Opticospinal Encephalomyelitis in a Double-Transgenic Mouse Model of Autoimmune T Cell/B Cell Cooperation. *J Clin Invest* (2006) 116:2385–92. doi: 10.1172/JCI28330
10. Haupeltshofer S, Leichsenring T, Berg S, Pedreiturria X, Joachim SC, Tischoff I, et al. Smad7 in Intestinal CD4(+) T Cells Determines Autoimmunity in a Spontaneous Model of Multiple Sclerosis. *Proc Natl Acad Sci USA* (2019) 116:25860–9. doi: 10.1073/pnas.1905955116
11. Zeka B, Hastermann M, Kaufmann N, Schanda K, Pende M, Misu T, et al. Aquaporin 4-Specific T Cells and NMO-IgG Cause Primary Retinal Damage in Experimental NMO/SD. *Acta Neuropathol Commun* (2016) 4:82. doi: 10.1186/s40478-016-0355-y
12. Bettelli E, Pagany M, Weiner HL, Linington C, Sobel RA, Kuchroo VK. Myelin Oligodendrocyte Glycoprotein-Specific T Cell Receptor Transgenic Mice Develop Spontaneous Autoimmune Optic Neuritis. *J Exp Med* (2003) 197:1073–81. doi: 10.1084/jem.20021603
13. Litzenburger T, Fassler R, Bauer J, Lassmann H, Linington C, Wekerle H, et al. B Lymphocytes Producing Demyelinating Autoantibodies: Development and Function in Gene-Targeted Transgenic Mice. *J Exp Med* (1998) 188:169–80. doi: 10.1084/jem.188.1.169
14. Wilmes AT, Reinehr S, Kuhn S, Pedreiturria X, Petrikowski L, Faissner S, et al. Laquinimod Protects the Optic Nerve and Retina in an Experimental Autoimmune Encephalomyelitis Model. *J Neuroinflamm* (2018) 15:183. doi: 10.1186/s12974-018-1208-3
15. Guo L, Normando EM, Nizari S, Lara D, Cordeiro MF. Tracking Longitudinal Retinal Changes in Experimental Ocular Hypertension Using the cSLO and Spectral Domain-OCT. *Invest Ophthalmol Vis Sci* (2010) 51:6504–13. doi: 10.1167/iovs.10-5551
16. Berger A, Cavallero S, Dominguez E, Barbe P, Simonutti M, Sahel JA, et al. Spectral-Domain Optical Coherence Tomography of the Rodent Eye: Highlighting Layers of the Outer Retina Using Signal Averaging and Comparison With Histology. *PloS One* (2014) 9:e96494. doi: 10.1371/journal.pone.0096494
17. Reinehr S, Gomes SC, Gassel CJ, Asaad MA, Stute G, Schargus M, et al. Intravitreal Therapy Against the Complement Factor C5 Prevents Retinal Degeneration in an Experimental Autoimmune Glaucoma Model. *Front Pharmacol* (2019) 10:1381. doi: 10.3389/fphar.2019.01381
18. Weiss M, Reinehr S, Mueller-Buehl AM, Doerner JD, Fuchshofer R, Stute G, et al. Activation of Apoptosis in a Betab1-CTGF Transgenic Mouse Model. *Int J Mol Sci* (2021) 22(4):1997. doi: 10.3390/ijms.22041997
19. Horstmann L, Schmid H, Heinen AP, Kurschus FC, Dick HB, Joachim SC. Inflammatory Demyelination Induces Glia Alterations and Ganglion Cell Loss in the Retina of an Experimental Autoimmune Encephalomyelitis Model. *J Neuroinflamm* (2013) 10:120. doi: 10.1186/1742-2094-10-120
20. Reinehr S, Kuehn S, Casola C, Koch D, Stute G, Grotegut P, et al. HSP27 Immunization Reinforces AII Amacrine Cell and Synapse Damage Induced by S100 in an Autoimmune Glaucoma Model. *Cell Tissue Res* (2018) 371:237–49. doi: 10.1007/s00441-017-2710-0
21. Reinehr S, Reinhard J, Gandej M, Kuehn S, Noristani R, Faissner A, et al. Simultaneous Complement Response via Lectin Pathway in Retina and Optic Nerve in an Experimental Autoimmune Glaucoma Model. *Front Cell Neurosci* (2016) 10:140. doi: 10.3389/fncel.2016.00140
22. Pfaffl MW, Horgan GW, Dempfle L. Relative Expression Software Tool (REST) for Group-Wise Comparison and Statistical Analysis of Relative Expression Results in Real-Time PCR. *Nucleic Acids Res* (2002) 30:e36. doi: 10.1093/nar/30.9.e36
23. Karlstetter M, Scholz R, Rutar M, Wong WT, Provis JM, Langmann T. Retinal Microglia: Just Bystander or Target for Therapy? *Prog Retin Eye Res* (2015) 45:30–57. doi: 10.1016/j.preteyeres.2014.11.004
24. Li L, Eter N, Heiduschka P. The Microglia in Healthy and Diseased Retina. *Exp Eye Res* (2015) 136:116–30. doi: 10.1016/j.exer.2015.04.020
25. Bennett ML, Bennett FC, Liddelow SA, Ajami B, Zamanian JL, Fernhoff NB, et al. New Tools for Studying Microglia in the Mouse and Human CNS. *Proc Natl Acad Sci USA* (2016) 113:E1738–46. doi: 10.1073/pnas.1525528113
26. Kwong JM, Caprioli J, Piri N. RNA Binding Protein With Multiple Splicing: A New Marker for Retinal Ganglion Cells. *Invest Ophthalmol Vis Sci* (2010) 51:1052–8. doi: 10.1167/iovs.09-4098
27. Bringmann A, Pannicke T, Grosche J, Francke M, Wiedemann P, Skatchkov SN, et al. Muller Cells in the Healthy and Diseased Retina. *Prog Retin Eye Res* (2006) 25:397–424. doi: 10.1016/j.preteyeres.2006.05.003
28. Ferguson B, Matyszak MK, Esiri MM, Perry VH. Axonal Damage in Acute Multiple Sclerosis Lesions. *Brain* (1997) 120(Pt 3):393–9. doi: 10.1093/brain/120.3.393
29. Trapp BD, Peterson J, Ransohoff RM, Rudick R, Mork S, Bo L. Axonal Transection in the Lesions of Multiple Sclerosis. *N Engl J Med* (1998) 338:278–85. doi: 10.1056/NEJM199801293380502
30. Brandt AU, Oberwahrenbrock T, Ringelstein M, Young KL, Tiede M, Hartung HP, et al. Primary Retinal Pathology in Multiple Sclerosis as Detected by Optical Coherence Tomography. *Brain* (2011) 134:e193; author reply e194. doi: 10.1093/brain/awr095
31. Saidha S, Syc SB, Ibrahim MA, Eckstein C, Warner CV, Farrell SK, et al. Primary Retinal Pathology in Multiple Sclerosis as Detected by Optical Coherence Tomography. *Brain* (2011) 134:518–33. doi: 10.1093/brain/awq346
32. Borisow N, Mori M, Kuwabara S, Scheel M, Paul F. Diagnosis and Treatment of NMO Spectrum Disorder and MOG-Encephalomyelitis. *Front Neurol* (2018) 9:888. doi: 10.3389/fneur.2018.00888
33. Zhao G, Chen Q, Huang Y, Li Z, Sun X, Lu P, et al. Clinical Characteristics of Myelin Oligodendrocyte Glycoprotein Seropositive Optic Neuritis: A Cohort Study in Shanghai, China. *J Neurol* (2018) 265:33–40. doi: 10.1007/s00415-017-8651-4
34. Bouyon M, Collongues N, Zephir H, Ballonzoli L, Jeanjean L, Lebrun C, et al. Longitudinal Follow-Up of Vision in a Neuromyelitis Optica Cohort. *Mult Scler* (2013) 19:1320–2. doi: 10.1177/1352458513476562
35. Ratchford JN, Quigg ME, Conger A, Frohman T, Frohman E, Balcer LJ, et al. Optical Coherence Tomography Helps Differentiate Neuromyelitis Optica and MS Optic Neuropathies. *Neurology* (2009) 73:302–8. doi: 10.1212/WNL.0b013e3181af78b8
36. Park KA, Kim J, Oh SY. Analysis of Spectral Domain Optical Coherence Tomography Measurements in Optic Neuritis: Differences in Neuromyelitis Optica, Multiple Sclerosis, Isolated Optic Neuritis and Normal Healthy Controls. *Acta Ophthalmol* (2014) 92:e57–65. doi: 10.1111/aos.12215
37. Sotirchos ES, Filippatou A, Fitzgerald KC, Salama S, Pardo S, Wang J, et al. Aquaporin-4 IgG Seropositivity Is Associated With Worse Visual Outcomes After Optic Neuritis Than MOG-IgG Seropositivity and Multiple Sclerosis, Independent of Macular Ganglion Cell Layer Thinning. *Mult Scler* (2020) 26:1360–71. doi: 10.1177/1352458519864928
38. Filippatou AG, Mukharesh L, Saidha S, Calabresi PA, Sotirchos ES. AQP4-IgG and MOG-IgG Related Optic Neuritis-Prevalence, Optical Coherence Tomography Findings, and Visual Outcomes: A Systematic Review and Meta-Analysis. *Front Neurol* (2020) 11:540156. doi: 10.3389/fneur.2020.540156
39. Wildemann B, Horstmann S, Korporal-Kuhnke M, Viehover A, Jarius S. Aquaporin-4 and Myelin Oligodendrocyte Glycoprotein Antibody-Associated Optic Neuritis: Diagnosis and Treatment. *Klin Monbl Augenheilkd* (2020) 237:1290–305. doi: 10.1055/a-1219-7907
40. Knier B, Rothhammer V, Heink S, Puk O, Graw J, Hemmer B, et al. Neutralizing IL-17 Protects the Optic Nerve From Autoimmune Pathology

and Prevents Retinal Nerve Fiber Layer Atrophy During Experimental Autoimmune Encephalomyelitis. *J Autoimmun* (2015) 56:34–44. doi: 10.1016/j.jaut.2014.09.003
41. Cruz-Herranz A, Oertel FC, Kim K, Canto E, Timmons G, Sin JH, et al. Distinctive Waves of Innate Immune Response in the Retina in Experimental Autoimmune Encephalomyelitis. *JCI Insight* (2021) 6(11). doi: 10.1172/jci.insight.149228
42. Cruz-Herranz A, Dietrich M, Hilla AM, Yiu HH, Levin MH, Hecker C, et al. Monitoring Retinal Changes With Optical Coherence Tomography Predicts Neuronal Loss in Experimental Autoimmune Encephalomyelitis. *J Neuroinflamm* (2019) 16:203. doi: 10.1186/s12974-019-1583-4
43. Nishioka C, Liang HF, Barsamian B, Sun SW. Sequential Phases of RGC Axonal and Somatic Injury in EAE Mice Examined Using DTI and OCT. *Mult Scler Relat Disord* (2019) 27:315–23. doi: 10.1016/j.msard.2018.11.010
44. Forooghian F, Sproule M, Westall C, Gordon L, Jirawuthiworavong G, Shimazaki K, et al. Electroretinographic Abnormalities in Multiple Sclerosis: Possible Role for Retinal Autoantibodies. *Doc Ophthalmol* (2006) 113:123–32. doi: 10.1007/s10633-006-9022-0
45. You Y, Zhu L, Zhang T, Shen T, Fontes A, Yiannikas C, et al. Evidence of Muller Glial Dysfunction in Patients With Aquaporin-4 Immunoglobulin G-Positive Neuromyelitis Optica Spectrum Disorder. *Ophthalmology* (2019) 126:801–10. doi: 10.1016/j.ophtha.2019.01.016
46. Kremers J, Tanimoto N. Measuring Retinal Function in the Mouse. *Methods Mol Biol* (2018) 1753:27–40. doi: 10.1007/978-1-4939-7720-8_2
47. Reinehr S, Koch D, Weiss M, Froemel F, Voss C, Dick HB, et al. Loss of Retinal Ganglion Cells in a New Genetic Mouse Model for Primary Open-Angle Glaucoma. *J Cell Mol Med* (2019) 23:5497–507. doi: 10.1111/jcmm.14433
48. Zhang Y, Bao Y, Qiu W, Peng L, Fang L, Xu Y, et al. Structural and Visual Functional Deficits in a Rat Model of Neuromyelitis Optica Spectrum Disorders Related Optic Neuritis. *Exp Eye Res* (2018) 175:124–32. doi: 10.1016/j.exer.2018.06.011
49. Meyer R, Weissert R, Diem R, Storch MK, De Graaf KL, Kramer B, et al. Acute Neuronal Apoptosis in a Rat Model of Multiple Sclerosis. *J Neurosci* (2001) 21:6214–20. doi: 10.1523/JNEUROSCI.21-16-06214.2001
50. Hobom M, Storch MK, Weissert R, Maier K, Radhakrishnan A, Kramer B, et al. Mechanisms and Time Course of Neuronal Degeneration in Experimental Autoimmune Encephalomyelitis. *Brain Pathol* (2004) 14:148–57. doi: 10.1111/j.1750-3639.2004.tb00047.x
51. Horstmann L, Kuehn S, Pedreiturria X, Haak K, Pfarrer C, Dick HB, et al. Microglia Response in Retina and Optic Nerve in Chronic Experimental Autoimmune Encephalomyelitis. *J Neuroimmunol* (2016) 298:32–41. doi: 10.1016/j.jneuroim.2016.06.008
52. Manogaran P, Samardzija M, Schad AN, Wicki CA, Walker-Egger C, Rudin M, et al. Retinal Pathology in Experimental Optic Neuritis is Characterized by Retrograde Degeneration and Gliosis. *Acta Neuropathol Commun* (2019) 7:116. doi: 10.1186/s40478-019-0768-5
53. Green AJ, Mcquaid S, Hauser SL, Allen IV, Lyness R. Ocular Pathology in Multiple Sclerosis: Retinal Atrophy and Inflammation Irrespective of Disease Duration. *Brain* (2010) 133:1591–601. doi: 10.1093/brain/awq080
54. Shindler KS, Guan Y, Ventura E, Bennett J, Rostami A. Retinal Ganglion Cell Loss Induced by Acute Optic Neuritis in a Relapsing Model of Multiple Sclerosis. *Mult Scler* (2006) 12:526–32. doi: 10.1177/1352458506070629
55. Smith ME, Somera FP, Eng LF. Immunocytochemical Staining for Glial Fibrillary Acidic Protein and the Metabolism of Cytoskeletal Proteins in Experimental Allergic Encephalomyelitis. *Brain Res* (1983) 264:241–53. doi: 10.1016/0006-8993(83)90822-3
56. Halder SK, Milner R. The GFAP Monoclonal Antibody GA-5 Identifies Astrocyte Remodeling and Glio-Vascular Uncoupling During the Evolution of EAE. *Cell Mol Neurobiol* (2021). doi: 10.1007/s10571-021-01049-8
57. Axelsson M, Malmestrom C, Nilsson S, Haghighi S, Rosengren L, Lycke J. Glial Fibrillary Acidic Protein: A Potential Biomarker for Progression in Multiple Sclerosis. *J Neurol* (2011) 258:882–8. doi: 10.1007/s00415-010-5863-2
58. Lucchinetti CF, Guo Y, Popescu BF, Fujihara K, Itoyama Y, Misu T. The Pathology of an Autoimmune Astrocytopathy: Lessons Learned From Neuromyelitis Optica. *Brain Pathol* (2014) 24:83–97. doi: 10.1111/bpa.12099
59. Reichenbach A, Bringmann A. Glia of the Human Retina. *Glia* (2020) 68:768–96. doi: 10.1002/glia.23727
60. Guy J. Optic Nerve Degeneration in Experimental Autoimmune Encephalomyelitis. *Ophthalmic Res* (2008) 40:212–6. doi: 10.1159/000119879
61. Wolf SA, Boddeke HW, Kettenmann H. Microglia in Physiology and Disease. *Annu Rev Physiol* (2017) 79:619–43. doi: 10.1146/annurev-physiol-022516-034406
62. Dong Y, Yong VW. When Encephalitogenic T Cells Collaborate With Microglia in Multiple Sclerosis. *Nat Rev Neurol* (2019) 15:704–17. doi: 10.1038/s41582-019-0253-6
63. Faissner S, Plemel JR, Gold R, Yong VW. Progressive Multiple Sclerosis: From Pathophysiology to Therapeutic Strategies. *Nat Rev Drug Discov* (2019) 18:905–22. doi: 10.1038/s41573-019-0035-2
64. Chen T, Lennon VA, Liu YU, Bosco DB, Li Y, Yi MH, et al. Astrocyte-Microglia Interaction Drives Evolving Neuromyelitis Optica Lesion. *J Clin Invest* (2020) 130:4025–38. doi: 10.1172/JCI134816
65. Plastini MJ, Desu HL, Brambilla R. Dynamic Responses of Microglia in Animal Models of Multiple Sclerosis. *Front Cell Neurosci* (2020) 14:269. doi: 10.3389/fncel.2020.00269
66. Mader S, Gredler V, Schanda K, Rostasy K, Dujmovic I, Pfaller K, et al. Complement Activating Antibodies to Myelin Oligodendrocyte Glycoprotein in Neuromyelitis Optica and Related Disorders. *J Neuroinflamm* (2011) 8:184. doi: 10.1186/1742-2094-8-184
67. Fonseca MI, Zhou J, Botto M, Tenner AJ. Absence of C1q Leads to Less Neuropathology in Transgenic Mouse Models of Alzheimer's Disease. *J Neurosci* (2004) 24:6457–65. doi: 10.1523/JNEUROSCI.0901-04.2004
68. Fonseca MI, Chu SH, Hernandez MX, Fang MJ, Modarresi L, Selvan P, et al. Cell-Specific Deletion of C1qa Identifies Microglia as the Dominant Source of C1q in Mouse Brain. *J Neuroinflamm* (2017) 14:48. doi: 10.1186/s12974-017-0814-9
69. Hammond JW, Bellizzi MJ, Ware C, Qiu WQ, Saminathan P, Li H, et al. Complement-Dependent Synapse Loss and Microgliosis in a Mouse Model of Multiple Sclerosis. *Brain Behav Immun* (2020) 87:739–50. doi: 10.1016/j.bbi.2020.03.004
70. Carpanini SM, Torvell M, Morgan BP. Therapeutic Inhibition of the Complement System in Diseases of the Central Nervous System. *Front Immunol* (2019) 10:362. doi: 10.3389/fimmu.2019.00362

Conflict of Interest: The authors declare that the research was conducted in the absence of any commercial or financial relationships that could be construed as a potential conflict of interest.

frontiers in Immunology

ORIGINAL RESEARCH
published: 03 February 2022
doi: 10.3389/fimmu.2022.766099

Expression and Clinical Correlation Analysis Between Repulsive Guidance Molecule a and Neuromyelitis Optica Spectrum Disorders

Jinhua Tang[1,2†], Xiaopeng Zeng[1†], Jun Yang[1], Lei Zhang[1], Hang Li[1], Rui Chen[1], Shi Tang[1], Yetao Luo[3], Xinyue Qin[1] and Jinzhou Feng[1]*

[1] Department of Neurology, The First Affiliated Hospital of Chongqing Medical University, Chongqing, China, [2] Department of Neurology, People's Hospital of Chongqing Hechuan, Chongqing, China, [3] Department of Biostatistics, School of Public Health and Management, Chongqing Medical University, Chongqing, China

Objectives: This study sought to explore the expression patterns of repulsive guidance molecules a (RGMa) in neuromyelitis optica spectrum disorders (NMOSD) and to explore the correlation between RGMa and the clinical features of NMOSD.

Methods: A total of 83 NMOSD patients and 22 age-matched healthy controls (HCs) were enrolled in the study from October 2017 to November 2021. Clinical parameters, including Expanded Disability Status Scale (EDSS) score, degree of MRI enhancement, and AQP4 titer were collected. The expression of serum RGMa was measured by enzyme-linked immunosorbent assay (ELISA) and compared across the four patient groups. The correlation between serum RGMa levels and different clinical parameters was also assessed.

Results: The average serum expression of RGMa in the NMOSD group was significantly higher than that in the HC group ($p < 0.001$). Among the patient groups, the acute phase group exhibited significantly higher serum RGMa levels than did the remission group ($p < 0.001$). A multivariate analysis revealed a significant positive correlation between RGMa expression and EDSS score at admission, degree of MRI enhancement, and segmental length of spinal cord lesions. There was a significant negative correlation between the expression of RGMa in NMOSD and the time from attack to sampling or delta EDSS.

Conclusions: The current study suggests that RGMa may be considered a potential biomarker predicting the severity, disability, and clinical features of NMOSD.

Keywords: neuromyelitis optica spectrum disorders, repulsive Guidance Molecule a (RGMa), EDSS, AQP4, correlation analysis

OPEN ACCESS

Edited by:
Wei Qiu,
Third Affiliated Hospital of Sun Yat-sen University, China

Reviewed by:
Yoshiki Takai,
Tohoku University Hospital, Japan
Chao Quan,
Fudan University, China

****Correspondence:***
Jinzhou Feng
fengjinzhou@hotmail.com

†These authors have contributed equally to this work

Specialty section:
This article was submitted to Multiple Sclerosis and Neuroimmunology, a section of the journal Frontiers in Immunology

Received: *28 August 2021*
Accepted: *17 January 2022*
Published: *03 February 2022*

Citation:
Tang J, Zeng X, Yang J, Zhang L, Li H, Chen R, Tang S, Luo Y, Qin X and Feng J (2022) Expression and Clinical Correlation Analysis Between Repulsive Guidance Molecule a and Neuromyelitis Optica Spectrum Disorders. Front. Immunol. 13:766099. doi: 10.3389/fimmu.2022.766099

INTRODUCTION

Neuromyelitis optica spectrum disorders (NMOSD) is a rare autoimmune demyelinating disorder of the central nervous system (CNS) associated with aquaporin-4 (AQP4) in which astrocytopathy is the primary pathology followed by neuroaxonal damage (1, 2). The prevalence of NMOSD varies from 0.5 to 4 per 100,000 people worldwide, 1 in 100,000 among Caucasians, 0.278 in 100,000 among Chinese individuals (3), and up to 10 in 100,000 among black individuals (4). Permanent disability rate is high among NMOSD patients, with approximately 35% of patients exhibiting severe visual impairment and 26% suffering from motor impairment (4, 5). Multiple episodes often lead to significant disabilities, incurring a heavy social and family burden. Early treatment can significantly reduce the disability rate and mortality, thus emphasizing the importance of early identification of NMOSD episodes and early treatment (6). AQP4 antibody can help diagnose NMOSD, but its titer level and disease severity do not always show a consistent trend or predict relapse (7–9).

Repulsive guidance molecule a (RGMa) is a glycosylphosphatidylinositol (GPI) anchored protein which guides axons and is widely involved in the development and pathology of the central nervous system (10). The binding of RGMa and its receptor neogenin can regulate axonal guidance, neuronal differentiation, and survival (11). Under pathological conditions, RGMa can affect functional recovery by inhibiting axon growth and participate in the pathogenesis of various CNS diseases, such as multiple sclerosis (MS), NMOSD, cerebral infarction (CI), spinal cord injury (SCI), Parkinson's disease (PD), and epilepsy (12–18). Inhibiting RGMa can enhance the recovery of neural function, suggesting that RGMa may be a potential target for the treatment of CNS disorders (12–17). Humanized monoclonal anti-RGMa antibody has been reported to delay the onset of disease manifestations in rat models of NMOSD and alleviate disease severity (13). Our previous study had demonstrated that RGMa may play a critical role in reactive astrogliosis and glial scar formation (14), indicating that RGMa may be involved in the pathogenesis of NMOSD and may be used as a biomarker of disease activity.

However, the link between clinical parameters and RGMa in patients with NMOSD remains unknown. To assess whether RGMa may reflect the disease activity of NMOSD and the pathogenesis of NMOSD, we analyzed the correlation between serum RGMa levels and the clinical features of NMOSD.

METHODS

Study Population

A total of 83 NMOSD patients and 22 age-matched healthy control patients from October 2017 to November 2021 were enrolled at The First Affiliated Hospital of Chongqing Medical University (Chongqing, China). Serum samples were collected and stored at -80°C. The diagnoses of all patients were reviewed, and only the patients who fulfilled the diagnostic criteria established by Wingerchuk et al. in 2015 were included (1). The following patients were excluded: those with malignant tumors, those with severe hepatic or renal insufficiency, and those without laboratory results of RGMa; the study was approved by the Ethics Committee of the First Affiliated Hospital of Chongqing Medical University. Informed consent was obtained from all the patients and HCs.

Medical records, laboratory data, and MRI findings were retrospectively assessed. Clinical information collected included age, sex, corresponding disease status (early acute phase, acute phase, or remission phase), number of relapses, total disease course, combined autoimmune disorders, Expanded Disability Status Scale (EDSS), serum levels of anti-AQP4 antibody, presentation of optic neuritis (ON), myelitis, magnetic resonance images (characteristic brain lesions on MRI, degree of MRI enhancement, length of spinal lesions, number of lesions on T2), delta EDSS (EDSS at discharge minus EDSS at admission), delta EDSS score after intravenous methylprednisolone (IVMP) (EDSS at the end of IVMP minus EDSS at admission when relapse occurred or first attack), and corticosteroid/immunomodulatory agent treatment history at the time of sampling. Time from attack to sampling refers to the disease duration from the time of the latest attack episode to sampling. According to the attack time, patients were divided into the early acute phase (episode ≤ 7 days), acute phase (7d<episode ≤ 30 days), and remission phase (episode > 30 days) (19). Neurological deficits were assessed using the EDSS score (20). The length of spinal lesions, characteristic brain lesions on MRI, and number of T2 lesions (including brain and spinal cord lesions) were counted using fluid-attenuated inversion recovery MRI scans (15). According to the enhancement degree of MRI lesions, patients were divided into no enhancement, mild enhancement, and marked enhancement groups. All patients underwent an MRI scan of the brain using a 3.0-T system (GE Medical Systems, Milwaukee, WI, USA) using an eight-channel phased-array head coil. Every contrast-enhancing lesion or hyperintensity on T_2WI was delineated manually by two experienced neuroradiologists. The neuroradiologists were blinded to the characteristics of the study population, including brain MRI findings and clinical presentations. Cases in which neuroradiologists disagreed were reviewed and resolved by consensus.

RGMa Measurement

Serum samples were centrifuged at 2500 rpm for 10 min at 4°C and stored thereafter at -80°C within 3 h of collection. The expression of serum RGMa was measured three times and the average value was obtained by enzyme-linked immunosorbent assay (ELISA) (R&D Systems Human RGM-A Assay kit; catalog No. DY2459-05). All sample measurements were carried out in a blinded fashion.

Statistical Analysis

SAS 9.4 (SAS Institute Inc., Cary, North Carolina) was used for data analyses. Quantitative data of the normal distribution are presented as the mean ± SD. Two independent samples/paired t-tests and a variance analysis were used for comparisons

between groups. Quantitative data of skewed distribution are presented as median and quartile intervals, and a Wilcoxon rank sum test was used for comparison between groups. Enumeration data were described by the number of cases and rates, and a chi-squared test was used for comparison between groups. The Pearson correlation coefficient describes the correlation between variables. A linear regression was used to assess the factors influencing the EDSS and RGMa. The mediation model was evaluated using Hayes' model 4 in the PROCESS macro for SPSS, and a bootstrapping method with 2,000 resamples was used. Regression coefficients (βmult) were back-transformed to the original scale, and therefore reflected multiplicative effects. Age and sex were included in all the models for multivariate analysis. Bilateral $p < 0.05$, indicated that the difference was statistically significant.

RGMa expression levels were upregulated in the early acute phase of NMOSD compared to acute phase (25078.83 ± 7649.24 ng/ml vs. 15523.17 ± 7236.70 ng/ml, p=0.008). The expression of RGMa was significantly higher in the acute group than the chronic group (12356.16 ± 4362.56 ng/ml, p=0.002) (**Figure 1**).

NMOSD patients were divided into three groups according to the degree of MRI enhancement, corresponding to the no enhancement group (n=16), mild enhancement group (n=38), and marked enhancement group (n=26). The expression of serum RGMa in marked enhancement group was significantly higher compared to mild enhancement group (26058.91 ± 5593.62 ng/ml vs. 16137.12 ± 5972.77 ng/ml, p<0.001). The expression of serum RGMa in the mild enhancement group was also significantly higher than that in the no enhancement group (16137.12 ± 5972.77 ng/ml vs. 9443.21 ± 2678.64 ng/ml, P<0.001) (**Figure 2**).

RESULTS

Participant Demographic Features and Clinical Data

A total 83 NMOSD patients and 22 healthy controls (HCs) were enrolled in the study. There was no significant difference in gender and age between the NMOSD and HC groups, as well as between the RGMa higher group and the RGMa lower group (all $p>0.05$). A total of 72 of the 83 patients (86.7%) tested positive for serum anti-AQP4 antibody. The median EDSS was 3.80 ± 1.73. Of the 83 patients with NMOSD, 37 had ON and 59 had myelitis.

RGMa Serum Levels in Patients With NMOSD

The mean serum RGMa level was significantly higher in the general NMOSD patients than in the HCs (18800.32±8279.17 ng/ml vs. 8721.72 ± 9090.09 ng/ml, $p < 0.001$). Patients were divided into RGMa higher/lower group equally according to the RGMa level; results showed that RGMa higher group exhibited significantly higher EDSS (4.40 ± 1.64 vs. 3.19 ± 1.62, p <0.001), longer spinal lesion length (5.82 ± 2.08 vs. 3.57 ± 1.30, p<0.001) and higher delta EDSS score (-2.02 ± 1.13 vs. -0.65 ± 0.86, p<0.001) compared to the RGMa lower group (**Table 1**).

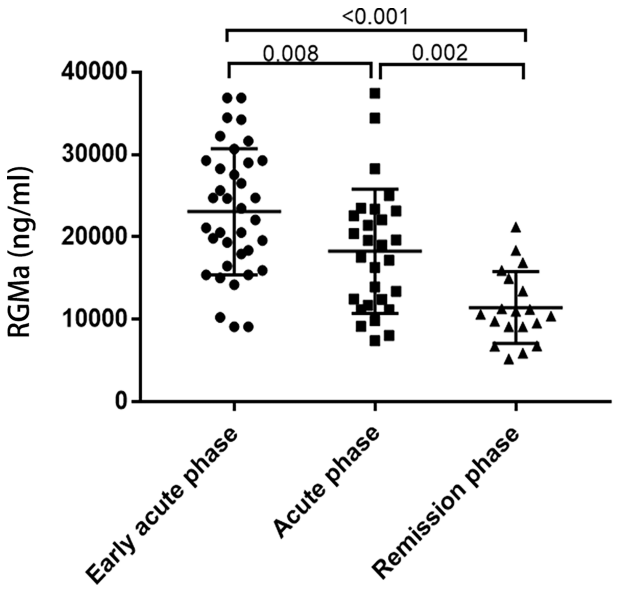

FIGURE 1 | Comparison of serum RGMa levels according to the disease phase.

TABLE 1 | Clinical data of patients with NMOSD.

	NMOSD (N = 83)	RGMa lower group (N = 41)	RGMa higher group (N = 42)	P value
Age (mean±Std)	38.94±15.30	41.97±15.48	35.98±14.70	0.074
Sex (Female,%)	63 (75.9)	32 (73.8)	31 (78)	0.652
Time from attack to sampling (median, IQR, day)	10 (5,26)	25 (7.5,55)	6 (4,10)	<0.001
Number of episodes (median, IQR)	2 (2,3.5)	2 (2,3)	2.5 (1.5,4)	0.009
EDSS at admission(mean±Std)	3.80±1.73	3.19±1.62	4.40±1.64	0.001
EDSS at discharge(mean±Std)	2.46±1.60	2.66±1.63	2.25±1.59	0.275
Delta EDSS	-1.32±1.21	-0.65±0.86	-2.02±1.13	<0.001
Serum levels of RGMa (mean±Std, ng/ml)	18800.32±8279.17	11746.78±3362.01	27382.85±6181.19	0.001
Length of spinal cord lesions (mean±Std)	4.72±2.07	3.57±1.30	5.82±2.08	<0.001
Number of lesions on T2 (median, IQR)	2 (2,6)	3 (1.5,5)	4.5 (3,7.5)	0.241

EDSS, Expanded Disability Status Scale; IQR, interquartile range;
Delta EDSS score (EDSS at discharge minus EDSS at admission).

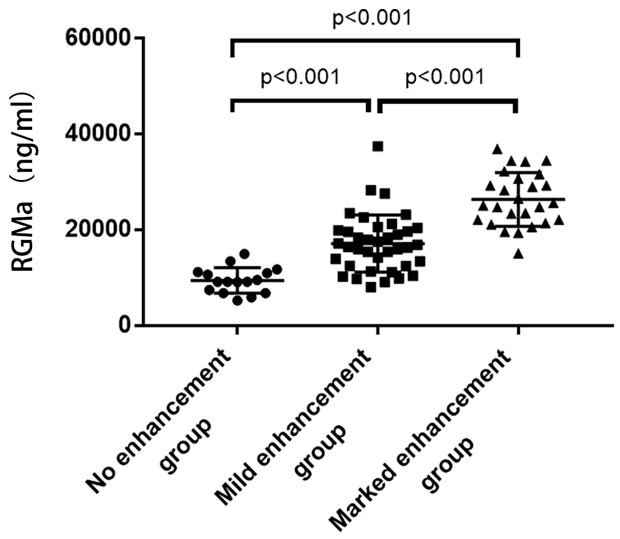

FIGURE 2 | Comparison of serum RGMa levels according to MRI enhancement.

Correlation of Serum Levels of RGMa With Clinical Parameters in NMOSD

As represented in **Table 2**, a significant positive correlation was observed between serum RGMa expression in NMOSD and EDSS at admission (r = 0.521, p <0.001), degree of MRI enhancement (r=0.757, p < 0.001), and length of spinal lesions (r=0.476, p < 0.001). There was a significant negative correlation between the expression of RGMa in NMOSD and time from attack to sampling (r=-0.444, P < 0.001) or delta EDSS (r=-0.640, p<0.001). Moreover, a multivariate model analysis showed that ESDD at admission, delta EDSS, degree of MRI enhancement, and length of spinal lesions were dependent factors that affected RGMa levels after adjusting for age and sex (p=0.035, p=0.009, p<0.001, p=0.014) (**Table 3**).

After adjusting for sex, age, total disease course, time from attack to sampling, number of episodes, the positive correlation observed between the serum RGMa expression in NMOSD and EDSS score at admission or negative correlation between RGMa expression and delta EDSS remained significant (r = 0.406, p <0.001, **Figure 3**; r=-0.568, p<0.001, **Figure 4**).

Paired t-test results demonstrated that RGMa significantly decreased after IVMP compared to before IVMP treatment in early acute phase patients (P=0.02) and was consistent with delta EDSS after IVMP. In terms of relapse, either myelitis or optic neuritis was independently associated with higher serum RGMa levels in the early acute phase (before acute phase treatment). Immunosuppressive/corticosteroid treatment was not an independent factor that influenced the levels of RGMa by comparing the first episode and non-first episode patients in early acute phase patients (**Table 4**).

TABLE 2 | Correlation of serum levels of RGMa with clinical parameters in NMOSD.

Variables	R	P value	R^2
Age	-0.162	0.144	0.0262
Sex	-0.024	0.827	0.0006
Time from attack to sampling	-0.444	<0.001	0.1971
Number of episodes	-0.088	0.436	0.0077
Total disease course	-0.123	0.277	0.0151
EDSS at admission	0.521	<0.001	0.2714
EDSS at discharge (mean±Std)	0.019	0.872	0.0004
Delta EDSS	-0.640	<0.001	0.4096
AQP4 titer	-0.12	0.352	0.0140
Degree of MRI enhancement	0.757	<0.001	0.5731
Number of lesions on T2	0.169	0.179	0.0286
Length of spinal lesions	0.476	<0.001	0.2266

Delta EDSS score (EDSS at discharge minus EDSS at admission).

Mediating Effects of the Degree of MRI Enhancement and Time From Attack to Sampling in NMOSD Patients With Respect to RGMa Serum Levels and EDSS Score at Admission

As **Table 5** represents, for the path analysis of the mediation model, adjusting for age, gender, total disease course, and number of episodes, serum levels of RGMa were directly related to EDSS score at admission (β= 0.209, p < 0.01), and indirectly related to EDSS score at admission *via* degree of MRI enhancement, with indirect effects of β=0.283 (95% CI = [0.123, 0.456], p <0.01). The proportion of the mediating effect in the total effect was 57.52% (0.283/0.492).

As **Table 6** represents, serum levels of RGMa were directly related to EDSS score at admission (β= 0.386, p <0.001), and indirectly related to EDSS score at admission *via* time from attack to sampling, with indirect effects of β=0.127 (95% CI = [0.064,0.204], p <0.05). The proportion of mediating effect in the total effect was 24.76% (0.127/0.513).

DISCUSSION

Scientists have sought to explore biomarkers reflecting the activity of NMOSD, such as neurofilament light (NfL), GFAP, and tau, but none have been generally recognized as biomarkers for predicting disease severity and clinical features. The current study is the first to explore the clinical value of plasma RGMa levels as a biomarker in patients with NMOSD. Enhanced magnetic resonance imaging is widely used to monitor the disease activity of NMOSD, but the accumulation of gadolinium contrast agents has raised safety concerns (21, 22). In addition, some studies have revealed that approximately 50% of patients with NMOSD still present with enhanced lesions one month after the onset of IVMP therapy, thereby suggesting that enhanced magnetic resonance imaging cannot accurately reflect the disease activity of NMOSD patients in the late stage of an attack (23).

Our previous study had demonstrated that RGMa may play a critical role in reactive astrogliosis and glial scar formation (14). This study showed that plasma RGMa levels in NMOSD patients

TABLE 3 | Univariate and multivariate models testing the correlations between RGMa levels and clinical parameters in patients with NMOSD.

	Univariate			Multivariate		
	β	95%CI	p	β	95%CI	p
Age	3.612	(-205.65,30.45)	0.09	3.612	(-76.49,83.71)	0.929
Sex						
Female	–					
Male	-469.02	(-4721.68,3783.64)	0.83	-1683.055	(-4481.19,1115.08)	0.234
EDSS at admission	2503.87	(1585.81,3421.94)	<0.001	906.529	(65.88,1747.18)	0.035
Delta EDSS	-4341.10	(-5574.83,-3107.37)	<0.001	-1902.658	(-3310.286-495.029)	0.009
Time from attack to sampling	-56.20	(-81.27,-31.14)	<0.001	1.711	(-19.48,22.90)	0.872
Degree of MRI enhancement	8546.90	(6882.68,10211.12)	<0.001	6986.044	(4865.71,9106.38)	<0.001
Length of spinal lesions	2191.23	(1376.10,3006.36)	<0.001	861.077	(183.96,1538.20)	0.014

Delta EDSS score (EDSS at discharge minus EDSS at admission).

were significantly higher than those in healthy controls. Considering that NMOSD are primarily astrocytopathy, suggesting that RGMa may be linked to the pathogenesis of NMOSD.

Many studies have demonstrated that RGMa may be involved in the pathogenesis of multiple sclerosis (MS) *via* a variety of mechanisms, such as by promoting demyelination of the central nervous system, inhibiting axon regeneration, resulting in the abnormal signal transduction of immune cells, inhibiting angiogenesis, and regulating BBB permeability (24–33). Fully humanized anti-RGMa mAb are currently being assessed in the context of double-blind, placebo-controlled, randomized clinical trials (34). However, the specific mechanisms by which RGMa affect the pathogenesis of NMOSD patients remain unclear.

Previous studies have reported that plasma RGMa is inversely related to delta EDSS in patients with MS (12). We also found that plasma RGMa levels were negatively correlated with delta EDSS and delta EDSS scores following IVMP in NMOSD. Moreover, the level of RGMa was positively correlated with the admission EDSS score at admission when relapsed, indicating that RGMa is associated with neurological impairment. Even though RGMa higher group showed a higher delta EDSS score compared to RGMa lower group, it still hard to considering RGMa level itself as a dependent predictor to NMOSD prognosis, but the variation of RGMa level related to treatment is more valuable. Those combined results indicate that plasma RGMa may be used as an index to predict therapeutic effects in the acute phase.

Currently, the onset time and degree of MRI enhancement can reflect disease activity to some extent (21–23). The destruction of the blood–brain barrier (BBB) is an important pathological process in the acute phase of NMOSD, and the degree of MRI enhancement can reflect the degree of BBB damage in NMOSD patients (35, 36). We have revealed that RGMa expression consistent with the onset time according to the acute phase group had significantly higher serum RGMa expression level than that in the remission group. Furthermore, RGMa serum expression level in the marked enhancement group was the highest among the mild enhancement group and the lowest in the no enhancement group. We conclude that RGMa expression was negatively correlated with the time from attack to sampling and positively correlated with the degree of magnetic resonance enhancement. These results demonstrate that RGMa may be a relatively useful biomarker for NMOSD disease activity in predicting the treatment of the acute phase. RGMa may be related to BBB permeability damage in NMOSD.

The length of spinal lesions is correlated with inflammatory activity and neurological impairment (21, 37) and is correlated with disease severity based on the admission EDSS score (38, 39). Our study demonstrated for the first time that RGMa levels were positively correlated with the length of spinal lesions on NMOSD MRI scans.

The mediation effect analysis revealed that RGMa was directly related to the admission EDSS score and indirectly related to the admission EDSS score through time from attack to sampling and degree of MRI enhancement. This highlights that RGMa may partially affect the degree of neurological impairment by affecting inflammatory activity and BBB permeability in NMOSD.

Our current study had a number of limitations. First, since it was carried out as a retrospective study, limited clinical data were collected, such as the lack of accurate quantitative indicators for BBB damage. Second, it was carried out as a single-center study with a relatively small sample size. Finally, this study lacked a long-term follow-up period with the patients to assess the relationship between RGMa and long-term prognosis of NMOSD. Last but not the least, MRI enhancement assessments were carried out by individuals instead of by using a more objective, quantitative algorithm, which may have compromised the MRI enhancement correlation analysis to a certain degree. In the future, we will try to carry out a number of multi-center and prospective studies to expand the sample size and further validate our research results. In addition, we will increase the volume of clinical data and carry out proof-of-concept experiments using animal models to further assess the pathogenesis of RGMa in NMOSD to guide clinical diagnosis and treatment.

CONCLUSION

In summary, we found that the serum RGMa levels of NMOSD patients were significantly higher than those of healthy controls. The expression and clinical correlation analysis between RGMa

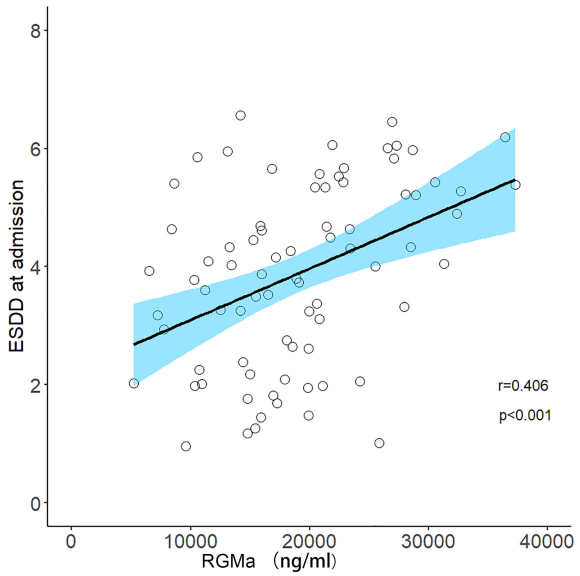

FIGURE 3 | Correlation between serum RGMa level and EDSS score at admission in NMOSD after adjusting for sex, age, total disease course, time from attack to sampling, and number of episodes.

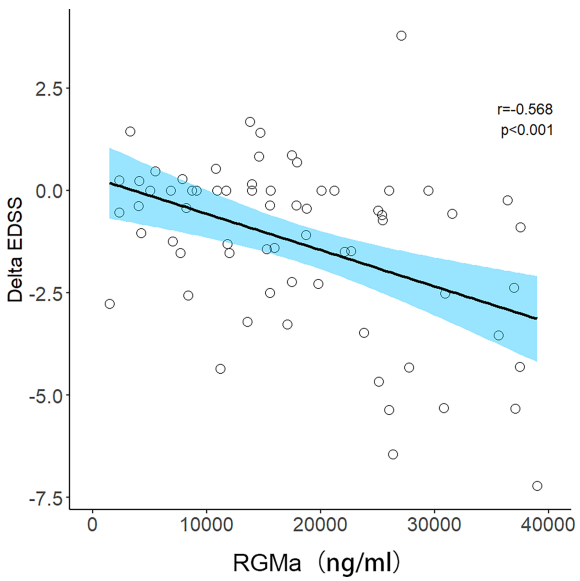

FIGURE 4 | Correlation between serum RGMa level and Delta EDSS score in NMOSD after adjusting for sex, age, total disease course, time from attack to sampling, and number of episodes.

TABLE 4 | Comparison of RGMa level according to different clinical parameters.

	RGMa level	t	*P* value
Relapse in ON (n=9)	19196.78±3871.84	2.942	0.007
Non ON relapse (n=19)	26588.45±7030.32		
Relapse in myelitis (n=15)	29440.35±4123.50	7.078	<0.001
Non myelitis relapse (n=13)	18161.80±4298.86		
Before IVMP (n=20)	23870.2±7769.62	3.993	0.02
After IVMP (n=20)	17545.2±5977.55		
Delta EDSS after IVMP	1.16±1.10	-6.788	<0.01
First episode (n=14)	26747.23±5306.56	1.556	0.133
Non first episode (corticosteroid/ immunosuppressive agent) (n=15)	22676.01±8514.95		

A paired t-test was used for the two groups before and after IVMP treatment in the early acute phase; A independent t-test was performed for the other two groups.

TABLE 5 | The mediating effects of degree of MRI enhancement between serum RGMa level and the EDSS score on admission.

Effect	β	LLCI	ULCI
Direct effect			
Serum levels of RGMa to EDSS at admission	0.240**	0.084	0.396
Serum levels of RGMa to EDSS at admission△	0.209**	0.046	0.373
Indirect effect			
Serum levels of RGMa to degree of MRI enhancement and EDSS at admission	0.258**	0.116	0.405
Serum levels of RGMa to degree of MRI enhancement and EDSS at admission△	0.283**	0.123	0.456
Total effect			
Serum levels of RGMa to EDSS at admission	0.499***	0.298	0.699
Serum levels of RGMa to EDSS at admission†	0.492***	0.284	0.701

†*Adjusted for age, sex, total disease course, and number of episodes.*
β=standardized coefficient; LLCI=lower limit of the 95% confidence interval. ULCI=upper limit at 95% confidence interval.
P < 0.01,P < 0.001.*

TABLE 6 | The mediating effects of time from attack to sampling between serum RGMa level and EDSS score on admission.

Effect	β	LLCI	ULCI
Direct effect			
Serum levels of RGMa to EDSS at admission	0.396***	0.197	0.595
Serum levels of RGMa to EDSS at admission△	0.386***	0.181	0.592
Indirect effect			
Serum levels of RGMa to Time from attack to sampling and EDSS at admission	0.118*	0.064	0.193
Serum levels of RGMa to Time from attack to sampling and EDSS at admission△	0.127*	0.064	0.204
Total effect			
Serum levels of RGMa to EDSS at admission	0.513***	0.317	0.709
Serum levels of RGMa to EDSS at admission†	0.513***	0.311	0.715

†*Adjusted for age, sex, total disease course, and number of episodes.*
β=standardized coefficient; LLCI=lower limit of the 95% confidence interval. ULCI=upper limit at 95% confidence interval.
**P < 0.05, ***P < 0.001.*

suggested that RGMa may be considered as a relatively safe and quantitative potential biomarker for predicting the activity of NMOSD. We demonstrated that higher RGMa levels in patients with NMOSD were associated with more severe neurological deficits, longer segments of spinal cord lesions, shorter onset time, higher plasma AQP4 antibody titers, and more obvious lesion enhancement. This suggests that RGMa can reflect the disease activity of NMOSD and may be involved in the pathogenesis of NMOSD by affecting BBB permeability and AQP4; however, further studies are warranted.

DATA AVAILABILITY STATEMENT

The raw data supporting the conclusions of this article will be made available by the authors, without undue reservation.

ETHICS STATEMENT

The studies involving human participants were reviewed and approved by Ethics Committee of the First Affiliated Hospital of Chongqing Medical University. The patients/participants provided their written informed consent to participate in this study.

AUTHOR CONTRIBUTIONS

All authors contributed to the manuscript and approved the submitted version. JT drafted the manuscript, XZ collected the sample and YL analysis, and interpretation of the data. XQ and JF designed the study and revised the manuscript.

FUNDING

This work was supported by the National Natural Science Foundation of China to Jinzhou Feng (No. 81701191) and the National Key Clinical Specialties Construction Program of China.

ACKNOWLEDGMENTS

We specially appreciate to Yongmei Li and Qiao Zheng for the radiology assistance.

REFERENCES

1. Wingerchuk D, Banwell B, Bennett J, Cabre P, Carroll W, Chitnis T, et al. International Consensus Diagnostic Criteria for Neuromyelitis Optica Spectrum Disorders. *Neurology* (2015) 85(2):177–89. doi: 10.1212/WNL.0000000000001729
2. Paul S, Mondal GP, Bhattacharyya R, Ghosh KC, Bhat IA. Neuromyelitis Optica Spectrum Disorders. *J Neurol Sci* (2020) 420:117225. doi: 10.1016/j.jns.2020.117225
3. Tian DC, Li Z, Yuan M, Zhang C, Gu H, Wang Y, et al. Incidence of Neuromyelitis Optica Spectrum Disorder (NMOSD) in China: A National Population-Based Study. *Lancet Reg Health West Pac* (2020) 2:100021. doi: 10.1016/j.lanwpc.2020.100021
4. Kim SH, Mealy MA, Levy M, Schmidt F, Ruprecht K, Paul F, et al. Racial Differences in Neuromyelitis Optica Spectrum Disorder. *Neurology* (2018) 91 (22):e2089–99. doi: 10.1212/WNL.0000000000006574
5. Kitley J, Leite MI, Nakashima I, Waters P, McNeillis B, Brown R, et al. Prognostic Factors and Disease Course in Aquaporin-4 Antibody-Positive Patients With Neuromyelitis Optica Spectrum Disorder From the United Kingdom and Japan. *Brain* (2012) 135(Pt 6):1834–49. doi: 10.1093/brain/aws109
6. Tugizova M, Vlahovic L, Tomczak A, Wetzel NS, Han MH. New Therapeutic Landscape in Neuromyelitis Optica. *Curr Treat Options Neurol* (2021) 23 (4):13. doi: 10.1007/s11940-021-00667-3
7. Hsu JL, Liao MF, Chang KH, Cheng MY, Ro LS. Correlations Among Disability, Anti-AQP4 Antibody Status and Prognosis in the Spinal Cord Involved Patients With NMOSD. *BMC Neurol* (2021) 21(1):153. doi: 10.1186/s12883-021-02171-2
8. Du Y, Li K, Liu W, Song R, Luo M, He J, et al. Recent Advances in Neuromyelitis Optica Spectrum Disorder: Pathogenesis, Mechanisms and Potential Treatments. *Curr Pharm Des* (2021) 28(4):272–9. doi: 10.2174/1381612827666210329101335
9. Akaishi T, Takahashi T, Himori N, Fujihara K, Misu T, Abe M, et al. Serum AQP4-Igg Level is Associated With the Phenotype of the First Attack in Neuromyelitis Optica Spectrum Disorders. *J Neuroimmunol* (2020) 340:577168. doi: 10.1016/j.jneuroim.2020.577168
10. Monnier P, Sierra A, Macchi P, Deitinghoff L, Andersen JS, Mann M, et al. RGM is a Repulsive Guidance Molecule for Retinal Axons. *Nature* (2002) 419 (6905):392–5. doi: 10.1038/nature01041
11. Rajagopalan S, Deitinghoff L, Davis D, Conrad S, Skutella T, Chedotal A, et al. Neogenin Mediates the Action of Repulsive Guidance Molecule. *Nat Cell Biol* (2004) 6(8):756–62. doi: 10.1038/ncb1156
12. Malekzadeh A, Leurs C, van Wieringen W, Steenwijk MD, Schoonheim MM, Amann M, et al. Plasma Proteome in Multiple Sclerosis Disease Progression. *Ann Clin Transl Neurol* (2019) 6(9):1582–94. doi: 10.1002/acn3.771
13. Harada K, Fujita Y, Okuno T, Tanabe S, Koyama Y, Mochizuki H, et al. Inhibition of Rgma Alleviates Symptoms in a Rat Model of Neuromyelitis Optica. *Sci Rep* (2018) 8(1):34. doi: 10.1038/s41598-017-18362-2
14. Zhang R, Jiang F, Chen CS, Wang T, Feng J, Tao T, et al. Serum Levels of IL-1 Beta, IL-6, TGF- Beta, and MMP-9 in Patients Undergoing Carotid Artery Stenting and Regulation of MMP-9 in a New In Vitro Model of THP-1 Cells Activated by Stenting. *Cell Death Differ* (2018) 25(8):1503–16. doi: 10.1038/s41418-018-0058-y
15. Li M, Wen Y, Zhang R, Xie F, Zhang G, Qin XY, et al. Adenoviral Vector-Induced Silencing of Rgma Attenuates Blood-Brain Barrier Dysfunction in a Rat Model of MCAO/Reperfusion. *Brain Res Bull* (2018) 142:54–62. doi: 10.1016/j.brainresbull.2018.06.010
16. Nakagawa H, Ninomiya T, Yamashita T, Takada M. Treatment With the Neutralizing Antibody Against Repulsive Guidance Molecule-a Promotes Recovery From Impaired Manual Dexterity in a Primate Model of Spinal Cord Injury. *Cereb Cortex (New York N.Y.: 1991)* (2019) 29(2):561–72. doi: 10.1093/cercor/bhx338
17. Korecka J, Moloney E, Eggers R, Hobo B, Scheffer S, Ras-Verloop N, et al. Repulsive Guidance Molecule a (Rgma) Induces Neuropathological and Behavioral Changes That Closely Resemble Parkinson's Disease. *J Neurosci: Off J Soc Neurosci* (2017) 37(39):9361–79. doi: 10.1523/JNEUROSCI.0084-17.2017
18. Song M, Tian F, Xia H, Xie Y. Repulsive Guidance Molecule a Suppresses Seizures and Mossy Fiber Sprouting via the FAK–P120rasgap–Ras Signaling Pathway. *Mol Med Rep* (2019) 19(4):3255–62. doi: 10.3892/mmr.2019.9951
19. Kwon Y, Kim B, Ahn S, Seo J, Kim SB, Yoon SS, et al. Serum Level of IL-1β in Patients With Inflammatory Demyelinating Disease: Marked Upregulation in the Early Acute Phase of MOG Antibody Associated Disease (MOGAD). *J Neuroimmunol* (2020) 348:577361. doi: 10.1016/j.jneuroim.2020.577361
20. Kurtzke JF. Rating Neurologic Impairment in Multiple Sclerosis: An Expanded Disability Status Scale (EDSS). *Neurology* (1983) 33(11):1444–52. doi: 10.1212/WNL.33.11.1444
21. Kuchling J, Paul F. Visualizing the Central Nervous System: Imaging Tools for Multiple Sclerosis and Neuromyelitis Optica Spectrum Disorders. *Front Neurol* (2020) 11:450. doi: 10.3389/fneur.2020.00450
22. Schlemm L, Chien C, Bellmann-Strobl J, Dorr J, Wuerfel J, Brandt AU, et al. Gadopentetate But Not Gadobutrol Accumulates in the Dentate Nucleus of Multiple Sclerosis Patients. *Mult Scler* (2017) 23(7):963–72. doi: 10.1177/1352458516670738
23. Xu Y, Ren Y, Li X, Xu W, Wang X, Duan Y, et al. Persistently Gadolinium-Enhancing Lesion is a Predictor of Poor Prognosis in NMOSD Attack: A Clinical Trial. *Neurotherapeutics* (2021) 18(2):868–77. doi: 10.21203/rs.3.rs-41052/v1
24. Kubo T, Tokita S, Yamashita T. Repulsive Guidance Molecule-a and Demyelination: Implications for Multiple Sclerosis. *J Neuroimmune*

Pharmacol: Off J Soc NeuroImmune Pharmacol (2012) 7(3):524–8. doi: 10.1007/s11481-011-9334-z
25. Franklin RJM, Frisén J, Lyons DA. Revisiting Remyelination: Towards a Consensus on the Regeneration of CNS Myelin. *Semin Cell Dev Biol* (2020) 116:3–9. doi: 10.1016/j.semcdb.2020.09.009
26. Tanabe S, Yamashita T. Repulsive Guidance Molecule-a is Involved in Th17-Cell-Induced Neurodegeneration in Autoimmune Encephalomyelitis. *Cell Rep* (2014) 9(4):1459–70. doi: 10.1016/j.celrep.2014.10.038
27. Fujita Y, Yamashita T. The Roles of Rgma-Neogenin Signaling in Inflammation and Angiogenesis. *Inflammation Regener* (2017) 37(6). doi: 10.1186/s41232-017-0037-6
28. Korn T, Kallies A. T Cell Responses in the Central Nervous System," Nature Reviews. *Immunology* (2017) 17(3):179–94. doi: 10.1038/nri.2016.144
29. Kant R, Halder S, Fernández J, Fernandez JA, Griffin JH, Milner R, et al. Activated Protein C Attenuates Experimental Autoimmune Encephalomyelitis Progression by Enhancing Vascular Integrity and Suppressing Microglial Activation. *Front Neurosci* (2020) 14:333. doi: 10.3389/fnins.2020.00333
30. Novakova L, Axelsson M, Khademi M, Zetterberg H, Blennow K, Malmestrom C, et al. Cerebrospinal Fluid Biomarkers of Inflammation and Degeneration as Measures of Fingolimod Efficacy in Multiple Sclerosis. *Multiple Sclerosis (Houndmills Basingstoke England)* (2017) 23(1):62–71. doi: 10.1177/1352458516639384
31. Bell J, Spencer J, Yates R, DeLuca G. The Cortical Blood-Brain Barrier in Multiple Sclerosis: A Gateway to Progression? *J Neurol* (2018) 265(4):966–7. doi: 10.1007/s00415-017-8727-1
32. Müller T, Barghorn S, Lütge S, Haas T, Mueller R, Gerlach B, et al. Decreased Levels of Repulsive Guidance Molecule a in Association With Beneficial Effects of Repeated Intrathecal Triamcinolone Acetonide Application in Progressive Multiple Sclerosis Patients. *J Neural Transm (Vienna Austria: 1996)* (2015) 122(6):841–8. doi: 10.1007/s00702-014-1308-x
33. Pitarokoili K, Sgodzai M, Grüter T, Bachir H, Motte J, Ambrosius B, et al. Intrathecal Triamcinolone Acetonide Exerts Anti-Inflammatory Effects on Lewis Rat Experimental Autoimmune Neuritis and Direct Anti-Oxidative Effects on Schwann Cells. *J Neuroinflamm* (2019) 16(1):58. doi: 10.1186/s12974-019-1445-0
34. Huang L, Fung E, Bose S, Popp A, Boser P, Memmott J, et al. Elezanumab, A Clinical Stage Human Monoclonal Antibody That Selectively Targets Repulsive Guidance Molecule A to Promote Neuroregeneration and Neuroprotection in Neuronal Injury and Demyelination Models. *Neurobiol Dis* (2021) 159:105492. doi: 10.1016/j.nbd.2021.105492
35. You X, Yan L, Li X, Pang Y, Guo X, Ye J, et al. Disruption of Blood-Brain Barrier Integrity Associated With Brain Lesions in Chinese Neuromyelitis Optica Spectrum Disorder Patients. *Multiple Sclerosis Related Disord* (2019) 27:254–9. doi: 10.1016/j.msard.2018.10.114
36. Zalewski N, Morris P, Weinshenker BG, Lucchinetti CF, Guo Y, Pittock SJ, et al. Ring-Enhancing Spinal Cord Lesions in Neuromyelitis Optica Spectrum Disorders. *J Neurol Neurosurg Psychiatry* (2017) 88(3):218–25. doi: 10.1136/jnnp-2016-314738
37. Yang CS, Zhang QX, Deng Y, Zhou BJ, Zhang LJ, Li LM, et al. Increased Serum IL-36β and IL-36γ Levels in Patients With Neuromyelitis Optica Spectrum Disorders: Association With Disease Activity. *BMC Neurol* (2019) 19(1):185. doi: 10.1186/s12883-019-1415-2
38. Bonnan M, Debeugny S, Mejdoubi M, Cabre P. Predictive Value of Conventional MRI Parameters in First Spinal Attacks of Neuromyelitis Optica Spectrum Disorder. *Mult Scler* (2020) 26(4):468–75. doi: 10.1177/1352458519834857
39. Marrodan M, Gaitán MI, Correale J. Spinal Cord Involvement in MS and Other Demyelinating Diseases. *Biomedicines* (2020) 8(5). doi: 10.3390/biomedicines8050130

Conflict of Interest: The authors declare that the research was conducted in the absence of any commercial or financial relationships that could be construed as a potential conflict of interest.

Publisher's Note: All claims expressed in this article are solely those of the authors and do not necessarily represent those of their affiliated organizations, or those of the publisher, the editors and the reviewers. Any product that may be evaluated in this article, or claim that may be made by its manufacturer, is not guaranteed or endorsed by the publisher.

frontiers in Neurology

CASE REPORT
published: 01 March 2022
doi: 10.3389/fneur.2022.845755

MOG Antibody-Associated Disorders Following SARS-CoV-2 Vaccination: A Case Report and Literature Review

Yuki Matsumoto[1], *Ayane Ohyama*[2], *Takafumi Kubota*[2], *Kensuke Ikeda*[2], *Kimihiko Kaneko*[2], *Yoshiki Takai*[2], *Hitoshi Warita*[2], *Toshiyuki Takahashi*[3], *Tatsuro Misu*[2]* *and Masashi Aoki*[1,2]

[1] *Department of Neurology, Tohoku University Graduate School of Medicine, Sendai, Japan,* [2] *Department of Neurology, Tohoku University Hospital, Sendai, Japan,* [3] *Department of Neurology, National Hospital Organization Yonezawa Hospital, Yonezawa, Japan*

Myelin oligodendrocyte glycoprotein (MOG) antibody-associated disorder (MOGAD) is a newly identified autoimmune demyelinating disorder that is often associated with acute disseminated encephalomyelitis and usually occurs postinfection or postvaccination. Here we report a case of MOGAD after mRNA severe acute respiratory syndrome coronavirus 2 (SARS-CoV-2) vaccination. A previously healthy 68-year-old woman presented to our department with gradually worsening numbness on the right side of her face, which began 14 days after her second dose of an mRNA-1273 vaccination. The patient's brain MRI revealed a right cerebellar peduncle lesion with gadolinium enhancement, a typical finding of MOGAD. A neurological examination revealed paresthesia on her right V2 and V3 areas. Other neurological examinations were unremarkable. Laboratory workups were positive for serum MOG-IgG as assessed by live cell-based assays and the presence of oligoclonal bands in the cerebrospinal fluid (CSF). The patient's serum test results for cytoplasmic-antineutrophil cytoplasmic antibodies, perinuclear-cytoplasmic-antineutrophil cytoplasmic antibodies, GQ1b-antibodies, and aquaporin-4 antibodies (AQP4-IgG) were all negative. Tests for soluble interleukin (IL)-2 receptors in the serum, IL-6 in the CSF and skin pricks, and angiotensin converting enzyme tests were all unremarkable. The patient was diagnosed with MOGAD after receiving an mRNA SARS-CoV-2 vaccination. After two courses of intravenous methylprednisolone treatment, the patient's symptoms improved and her cerebellar peduncle lesion shrunk slightly without gadolinium enhancement. To date, there have only been two cases of monophasic MOGAD following SARS-CoV-2 vaccination, including both the ChAdOx1 nCOV-19 and mRNA-1273 vaccines, and the prognosis is generally similar to other typical MOGAD cases. Although the appearance of MOG antibodies is relatively rare in post-COVID-19–vaccine demyelinating diseases, MOGAD should be considered in patients with central nervous system (CNS) demyelinating diseases after receiving a SARS-CoV-2 vaccine.

Keywords: myelin oligodendrocyte glycoprotein (MOG), SARS-CoV-2, COVID-19, post-vaccination, mRNA vaccine, cerebellar peduncle

OPEN ACCESS

Edited by:
Jodie Burton,
University of Calgary, Canada

Reviewed by:
Markus Reindl,
Medizinische Universität Innsbruck, Austria
Michael Levy,
Massachusetts General Hospital and Harvard Medical School, United States

***Correspondence:**
Tatsuro Misu
misu@med.tohoku.ac.jp

Specialty section:
This article was submitted to Multiple Sclerosis and Neuroimmunology, a section of the journal Frontiers in Neurology

Received: *30 December 2021*
Accepted: *24 January 2022*
Published: *01 March 2022*

Citation:
Matsumoto Y, Ohyama A, Kubota T, Ikeda K, Kaneko K, Takai Y, Warita H, Takahashi T, Misu T and Aoki M (2022) MOG Antibody-Associated Disorders Following SARS-CoV-2 Vaccination: A Case Report and Literature Review. Front. Neurol. 13:845755. doi: 10.3389/fneur.2022.845755

INTRODUCTION

The emergence in December 2019 of a novel coronavirus, the severe acute respiratory syndrome coronavirus 2 (SARS-CoV-2), has had devastating global consequences. To overcome the unprecedented effects of the pandemic, there was a rapid global effort to develop several vaccines against SARS-CoV-2, which resulted in several safe and efficacious immunogenic vaccines including ChAdOx1 nCOV-19 and mRNA-1273 (1, 2). In particular, the ChAdOx1 nCOV-19 vaccine has shown an acceptable safety profile and has demonstrated a 62.1–90% efficacy reduction in COVID-19 infections in a clinical trial involving 23,848 participants (1). In this particular trial, 3 cases of transverse myelitis occurred, of which 1 case was determined to be possibly related to the vaccination as this case occurred 14 days after a ChAdOx1 nCoV-19 second booster vaccination. The remaining 2 cases were determined to be unlikely related to vaccinations as the first case occurred 10 days after the individual received a first vaccine dose and the individual had a preexisting unrecognized condition of multiple sclerosis (MS). The second case was determined not to be related to the vaccination as this individual received a placebo vaccine (1). The mRNA-1273 vaccine, which was developed by Moderna and the Vaccine Research Center at the National Institute of Allergy and Infectious Diseases (NIAID), has demonstrated tremendous clinical efficacy and safety against COVID-19 (2). The common adverse events of the mRNA-1273 vaccine are considered mild, which include transient headache, pain, muscle spasms, and myalgia (2). To date, only several cases of central nervous system (CNS) demyelinating disease occurring after mRNA vaccinations have been reported (3).

Myelin oligodendrocyte glycoprotein (MOG) antibody-associated disease (MOGAD) is a newly identified disease entity that was initially identified mainly in pediatric cases of acute disseminated encephalomyelitis (ADEM), usually in postvaccination or postinfectious circumstances (4, 5). So far, there have been 15 cases of ADEM and acute hemorrhagic leukoencephalitis (AHLE) after COVID-19 infections occurring mainly in adults. Of these 15 cases, there has only been 1 pediatric case involving a 13-month-old female patient with an MOG antibody (6). Furthermore, despite many cases of postvaccination ADEM after SARS-CoV-2 vaccination, MOG antibody–positive cases are rare (7). Here we describe a case of typical cerebellar peduncle lesion with an identified MOG-IgG occurring 2 weeks after an mRNA-1273 vaccination. We also analyzed MOGAD cases following SARS-CoV-2 vaccinations in a literature review.

CASE DESCRIPTION

A 68-year-old Japanese woman presented to our department with a complaint of gradually worsening numbness on the right side of her face 14 days after receiving a second dose of the mRNA-1273 vaccination. The patient developed a slight fever following the second dose of the mRNA-1273 vaccination, but the fever subsequently resolved. The patient had a remote history of well-controlled hypertension and had undergone the removal of the tail of her pancreas because of an intraductal papillary mucinous neoplasm 12 years before. The patient did not have a history of allergies or vaccine-induced side effects. There were no marked related findings in the patient's family's medical history. A neurological examination revealed paresthesia on the patient's right V2 and V3 areas. Other neurological examinations including pyramidal signs and ocular movements were normal. Blood tests showed no abnormal blood counts or abnormal biochemical profiles including those indicating the soluble interleukin (IL)-2 receptor. The patient's lumbar puncture revealed no pleocytosis or elevated proteins but did reveal positive oligoclonal bands. Her serum test results for the cytoplasmic-antineutrophil cytoplasmic antibody, perinuclear-cytoplasmic-antineutrophil cytoplasmic antibody, GQ1b-antibody, and aquaporin-4 IgG (AQP4-IgG) antibody were all negative. However, a live cell-based assay with titers of 1:512 using anti-IgG-Fc and 1:256 using anti-IgG1 as secondary antibodies (cut-off value; 1:128) was positive for MOG-IgG in the patient's serum, but was negative in her cerebrospinal fluid (CSF). Interferon-gamma release assays for tuberculosis were negative. An angiotensin-converting enzyme test, a tuberculosis skin test, and a chest X-ray were all unremarkable, and neurosarcoidosis was also deemed unlikely. A skin prick test was normal, and IL-6 in the CSF was not elevated. Neuro-Behcet's disease was also determined to be unlikely. A screening polymerase chain reaction (PCR) test of SARS-CoV-2 from nasopharyngeal swabs was negative. Brain MRI images showed a hyperintense lesion on the right lateral pontine, trigeminal nerve, and a middle cerebellar peduncle lesion was seen in T2-weighted and fluid-attenuated inversion recovery (FLAIR) images with a T1-gadolinium enhancement (**Figure 1**). The patient was diagnosed with MOGAD and administered 2 courses of intravenous methylprednisolone (IVMP), 1 g/d over 3 days. After two courses of IVMP, the cerebellar peduncle lesion shrunk slightly with a diminishment of the gadolinium enhancement (**Figure 1**). The paresthesia of the patient's face improved, but mild numbness on her right jaw remained at her discharge. The patient did not experience any relapse during the subsequent 6-month period without any treatment. Her MOG-IgG status in 6 months follow-up was positive for anti-IgG-Fc (1:128), but negative for IgG1 as secondary antibody.

We obtained written informed consent from the patient in the case presented. We were able to discover cases of MOGAD following COVID-19 vaccination by utilizing a PubMed search for terms including "COVID-19," "vaccination," and "myelin oligodendrocyte glycoprotein." We also searched "COVID-19," "vaccination," and "neuromyelitis optica spectrum disorder" in order to ensure we had found all the documented cases of MOGAD.

DISCUSSION

We demonstrated a case of brainstem and cerebellar peduncle encephalitis with MOG antibodies developed after the patient's SARS-CoV-2 vaccination. In previous reports, we showed that middle cerebellar peduncle lesions are typical features of

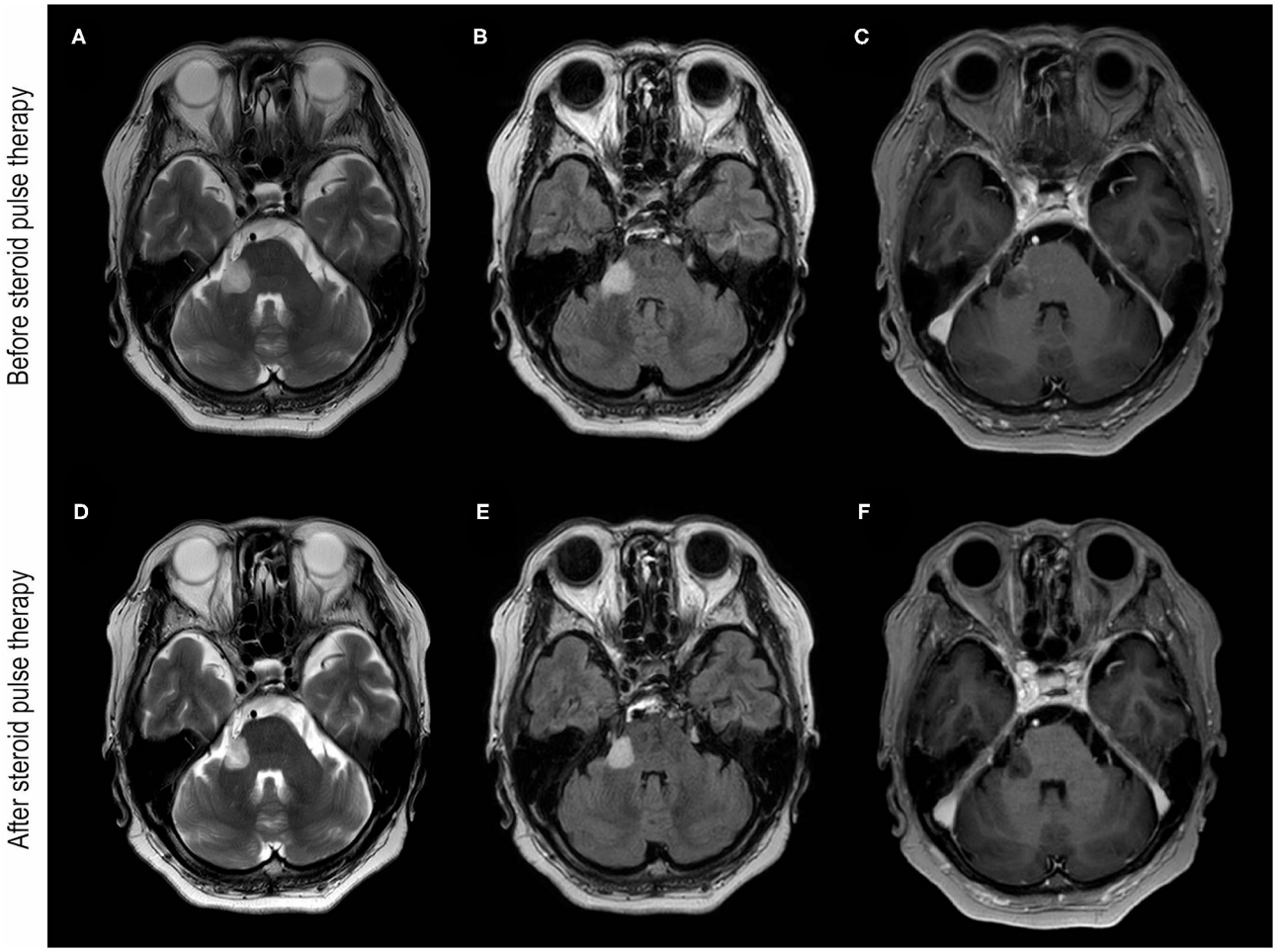

FIGURE 1 | Brain MRI images before and after steroid pulse therapy. **(A–C)** Were obtained before steroid pulse therapy. Brain MRI of T2-weighted (A) and fluid-attenuated inversion recovery (FLAIR) **(B)** images showing hyperintensity of the cerebellar peduncle and the root of trigeminal nerve. **(C)** T1-weighted brain MRI with gadolinium enhancement (T1Gd) showing enhancement around the lesion. **(D–F)** were obtained after steroid pulse therapy. Brain MRI of T2-weighted **(D)** and FLAIR images **(E)** showing the reduction in the hyperintensity lesion of the cerebellar peduncle. **(F)** T1Gd brain MRI showing no gadolinium enhancement after steroid therapy.

MOGAD, and therefore the lesion seen in the present case made a probable diagnosis of MOGAD (8). In contrast, MOGAD is less likely to occur in postvaccination CNS demyelinating diseases, because all cases of testing 10 MOG antibody cases were negative in recent systematic reviewed cases (7). It is possible to develop MOGAD after receiving the COVID-19 vaccination; MOGAD can develop from the postexposure production of pathogenic IgG via the molecular mimicry theory and vaccine-induced bystander inflammation-induced tissue injury and antigen presentation. In addition, the vaccination could simply unmask a potential preexisting autoimmune disease.

After the vaccination campaign during the "swine flu" in 1976, the number of Guillain-Barré syndrome (GBS) cases in the United States increased (9). Although the calculated relative risk was 6.2, an increase in the number of cases of multiple sclerosis was not observed (10). Later studies suggested that influenza vaccines can induce the production of antiganglioside GM1 antibodies in animal models by a molecular mimicry theory (11). It has been reported that the cumulative incidence of confirmed COVID-19 cases in MS patients is two-fold higher when the cases without PCR test in the Barcelona are included (12). However, a systematic review analysis has suggested that having MS does not significantly increase the mortality rate of COVID-19 (13). A pilot study, focused on the cross-reactivity between SARS-CoV-2 spike proteins and 50 different tissues using enzyme-linked immunosorbent assays, has indicated that SARS-CoV-2 spike proteins show the strongest immunoreactions with transglutaminases, myelin basic proteins, mitochondria, nuclear antigens, myosin, collagen, claudin5/6, and S100B (14). Furthermore, by analyzing the cross-reactions between host and microbial proteins using the Protein Data Bank, we found that SARS-CoV-2 proteins were found to possibly interact with many kinds of proteins including proteins involved in synaptic vesicle trafficking, endocytosis, axonal transport, neuronal transmission, thrombosis, inflammation, and the mitochondrial and blood brain barrier as well as protein growth factors (15). Although

TABLE 1 | A summary of case reports of MOG-IgG-associated disorders after COVID-19 vaccination.

References	Age	Sex	Vaccine	Interval between vaccination and onset	Symptoms	MRI findings	CSF cell count (/μl)	CSF Protein (mg/dl)	OCBs	Treatment	Outcome
Mumoli et al. (19)	43	Male	ChAdOx1 nCOV-19	7 days after first dose	Bilateral lower limbs weakness urinary retention	Multiple brain white matter lesion and LETM	43	40.6	(+)	IVMP	Mostly recovered
Dams et al. (20)	59	Male	ChAdOx1 nCOV-19	14 days after first dose	paresthesia, gait disturbance, urinary and rectal dysfunction	LETM	110	n.d.	(-)	IVMP and PLEX	Partially recovered
Our case	68	Female	mRNA-1273	14 days after second dose	Paresthesia on her right V2 and V3 area	Cerebellar peduncle lesion	0	32	(+)	IVMP	Partially recovered

MOGAD, MOG antibody associated disorders; CSF, cerebrospinal fluid; OCB, oligoclonal band; LETM, longitudinally extensive transverse myelitis; n.d., not described; IVMP, intravenous methylprednisolone; PLEX, plasma exchange.

molecular mimicry between SARS-CoV-2 spike proteins and MOG is unclear, these cross-reaction theories show a potential correlation between CNS inflammation and demyelinating diseases including MOGAD and COVID-19.

In the current case report, the patient developed MOGAD 2 weeks after receiving an mRNA vaccination containing the SARS-CoV-2 spike protein, which is considered sufficient time for the creation of autoantibodies (16). Initially, the vaccinated antigen is taken up by dendritic cells, then trafficked to the draining lymph node, and interacted with activated T and B cells. T cell-dependent B cell maturation results in specific antibody production by plasma cells, which could induce a rapid rise in serum antibody levels over a subsequent 2-week period. Therefore, in the present case, detecting the antibody 2 weeks after an immunization with the antigen is reasonable (16). Previous to this present case report, there were reports of two MOGAD cases, one involving a 19-year-old male and another a 47-year-old female, both developing 2 weeks after revaccination against diphtheria, tetanus, pertussis, polio, and influenza. In these two cases, both patients had recurrent episodes of demyelinating diseases with frequent relapses that were refractory to treatment (17). Another reported case involved a 37-year-old female, who had transiently tested positive for an MOG antibody with monophasic symptoms of myelitis a few weeks before receiving measles, mumps, rubella, and tetanus vaccinations (18). Therefore, it is possible that MOG antibodies may be produced by several kinds of vaccines, and some vaccines may cause a vaccine-induced unveiling of multiphasic disease or a transient induction of antibody production in monophasic disease.

Including our case, during the current COVID-19 pandemic, there have been three cases of MOGAD occurring after SARS-CoV-2 vaccinations (19, 20). In these cases, the patients developed their neurological symptoms at various times throughout their vaccinations, from 1 to 2 weeks after the first or second vaccine doses (**Table 1**). In a systematic review analysis of 32 cases of CNS demyelinating diseases after COVID-19 vaccinations, it was reported that 71.8% of CNS demyelinating diseases occurred after the first dose of any of the COVID-19 vaccines. Furthermore, the interval from vaccination to disease onset was usually 3 weeks, but this time interval was dependent on the existence of preexisting conditions in each case. Of these 32 cases, there were 17 cases involving preexisting immune-mediated diseases, including MS ($n = 7$), a clinically isolated syndrome suggestive of MS ($n = 1$), transverse myelitis ($n = 1$), recurrent neurologic diseases ($n = 2$), and other immune or autoimmune diseases ($n = 6$). In three postvaccination MOGAD cases, neurological symptoms were relatively mild and responded well to intravenous prednisolone treatment. Furthermore, all these cases were monophasic without recurrence, although they were observed carefully for the appearance of oligoclonal bands in two cases and continuous MOG-antibody positivity in our case. Especially, as MOG-IgG was positive but the antibody titer was gradually declining, we should observe the clinical relapse and check the positivity of MOG-IgG carefully. A recent report suggested that the risk of transverse myelitis associated with COVID-19 represents 1.2% of all neurological complications

(21). However, the risk of developing demyelinating disease following vaccination for COVID-19 is far less than the risk of contracting COVID-19. We therefore do not hesitate to recommend receiving COVID-19 vaccinations in this report.

Vaccines may trigger a preexisting latent autoimmune disease as was seen in a previous case of neuromyelitis optica spectrum disorder (NMOSD) (22) involving a patient that was found to be seropositive for the AQP4-IgG over 10 years before the onset of NMOSD. There have been new reports of onset cases of MS and NMOSD in addition to prediagnosed cases with vaccine-induced recurrence in MS (7). In such cases, the mRNA vaccination may cause the activation of nonspecific or specific cellular immunity and elevated cytokines, which could induce the breakdown of the blood brain barrier leading to the entry of antibodies and unveil the potential for MOG-IgG pathogenesis (23).

Although the present case involved a rare condition of MOGAD after the COVID-19 mRNA vaccination, detailed studies of additional clinical cases are necessary to determine the causation and the risk of developing MOGAD. It is premature to discuss the causal relationship of demyelinating disease MOGAD following COVID-19 vaccination. We have revealed, however, MOGAD's rarity and relatively benign course after vaccination compared with refractory cases of COVID-19-related ADEM and AHLE. It is important to note that the public should not avoid being vaccinated for COVID-19 for fear of developing MOGAD.

DATA AVAILABILITY STATEMENT

The raw data supporting the conclusions of this article will be made available by the authors, without undue reservation.

ETHICS STATEMENT

The studies involving human participants were reviewed and approved by the Ethical Committee of Tohoku University Hospital. The patients/participants provided their written informed consent to participate in this study. Written informed consent was obtained from the individual(s) and/or minor(s)' legal guardian/next of kin for the publication of any potentially identifiable images or data included in this article.

AUTHOR CONTRIBUTIONS

YM, AO, and TM contributed to conception and design of the study. YM wrote the first draft of the manuscript. TM wrote the additional sections of the manuscript. AO, TK, KI, and HW contributed to the clinical analysis. KK and YT assessed the patient. TT did the diagnostic test. TM and MA supervised this report. All authors contributed to the manuscript's revision, and read and approved the submitted version.

FUNDING

This work was supported by JSPS KAKENHI grant no. 19K07953 and the MEXT/JSPS WISE Program: Advanced Graduate Program for Future Medicine and Health Care, Tohoku University.

ACKNOWLEDGMENTS

We would like to thank Ms. Mayu Atsumi for testing MOG-IgG.

REFERENCES

1. Voysey M, Clemens SAC, Madhi SA, Weckx LY, Folegatti PM, Aley PK, et al. Safety and efficacy of the ChAdOx1 nCoV-19 vaccine (AZD1222) against SARS-CoV-2: an interim analysis of four randomised controlled trials in Brazil, South Africa, and the UK. *Lancet.* (2021) *397*:99–111. doi: 10.1016/S0140-6736(20)32661-1
2. Baden LR, El Sahly HM, Essink B, Kotloff K, Frey S, Novak R, et al. Efficacy and safety of the mRNA-1273 SARS-CoV-2 vaccine. *N Engl J Med.* (2021) 384:403–16. doi: 10.1056/NEJMoa2035389
3. Khayat-Khoei M, Bhattacharyya S, Katz J, Harrison D, Tauhid S, Bruso P, et al. COVID-19 mRNA vaccination leading to CNS inflammation: a case series. *J Neurol.* (2021) 1–14. doi: 10.1007/s00415-021-10780-7
4. Pröbstel AK, Dornmair K, Bittner R, Sperl P, Jenne D, Magalhaes S, et al. Antibodies to MOG are transient in childhood acute disseminated encephalomyelitis. *Neurology.* (2011) 77:580–8. doi: 10.1212/WNL.0b013e318228c0b1
5. Baumann M, Sahin K, Lechner C, Hennes EM, Schanda K, Mader S, et al. Clinical and neuroradiological differences of paediatric acute disseminating encephalomyelitis with and without antibodies to the myelin oligodendrocyte glycoprotein. *J Neurol Neurosurg Psychiatry.* (2015) 86:265–72. doi: 10.1136/jnnp-2014-308346
6. Manzano GS, McEntire CRS, Martinez-Lage M, Mateen FJ, Hutto SK. Acute disseminated encephalomyelitis and acute hemorrhagic leukoencephalitis following COVID-19: systematic review and meta-synthesis. *Neurol Neuroimmunol Neuroinflamm.* (2021) 8:6. doi: 10.1212/NXI.0000000000001080
7. Ismail II, Salama S. A systematic review of cases of CNS demyelination following COVID-19 vaccination. *J Neuroimmunol.* (2022) 362:577765. doi: 10.1016/j.jneuroim.2021.577765
8. Matsumoto Y, Misu T, Mugikura S, Takai Y, Nishiyama S, Kuroda H, et al. Distinctive lesions of brain MRI between MOG-antibody-associated and AQP4-antibody-associated diseases. *J Neurol Neurosurg Psychiatry.* (2020) 92:682–84. doi: 10.1136/jnnp-2020-324818
9. Schonberger LB, Bregman DJ, Sullivan-Bolyai JZ, Keenlyside RA, Ziegler DW, Retailliau HF, et al. Guillain-Barre syndrome following vaccination in the national influenza immunization program, United States, 1976-1977. *Am J Epidemiol.* (1979) 110:105–23. doi: 10.1093/oxfordjournals.aje.a112795
10. Kurland LT, Molgaard CA, Kurland EM, Wiederholt WC, Kirkpatrick JW. Swine flu vaccine and multiple sclerosis. *JAMA.* (1984) 251:2672–5. doi: 10.1001/jama.1984.03340440030022
11. Israeli E, Agmon-Levin N, Blank M, Chapman J, Shoenfeld Y. Guillain-Barré syndrome-a classical autoimmune disease triggered by infection or vaccination. *Clin Rev Allergy Immunol.* (2012) 42:121–30. doi: 10.1007/s12016-010-8213-3
12. Sepúlveda M, Llufriu S, Martínez-Hernández E, Català M, Artola M, Hernando A, et al. Incidence and impact of COVID-19 in MS: a survey from a Barcelona MS unit. *Neurol Neuroimmunol Neuroinflamm.* (2021) 8:e954. doi: 10.1212/NXI.0000000000000954
13. Barzegar M, Mirmosayyeb O, Gajarzadeh M, Afshari-Safavi A, Nehzat N, Vaheb S, et al. COVID-19 among patients with multiple sclerosis: a systematic review. *Neurol Neuroimmunol Neuroinflamm.* (2021) 8:e1001. doi: 10.1212/NXI.0000000000001001

14. Vojdani A, Kharrazian D. Potential antigenic cross-reactivity between SARS-CoV-2 and human tissue with a possible link to an increase in autoimmune diseases. *Clin Immunol.* (2020) 217:108480. doi: 10.1016/j.clim.2020.108480
15. Yapici-Eser H, Koroglu YE, Oztop-Cakmak O, Keskin O, Gursoy A, Gursoy-Ozdemir Y. Neuropsychiatric symptoms of COVID-19 explained by SARS-CoV-2 proteins' mimicry of human protein interactions. *Front Hum Neurosci.* (2021) 15:656313. doi: 10.3389/fnhum.2021.656313
16. Pollard AJ, Bijker EM. A guide to vaccinology: from basic principles to new developments. *Nat Rev Immunol.* (2021) 21:83–100. doi: 10.1038/s41577-020-00479-7
17. Jarius S, Ruprecht K, Kleiter I, Borisow N, Asgari N, Pitarokoili K, et al. MOG-IgG in NMO and related disorders: a multicenter study of 50 patients. Part 2: Epidemiology, clinical presentation, radiological and laboratory features, treatment responses, and long-term outcome. *J Neuroinflammation.* (2016) 13:280. doi: 10.1186/s12974-016-0718-0
18. Kumar N, Graven K, Joseph NI, Johnson J, Fulton S, Hostoffer R, et al. Case report: postvaccination anti-myelin oligodendrocyte glycoprotein neuromyelitis optica spectrum disorder: a case report and literature review of postvaccination demyelination. *Int J MS Care.* (2020) 22:85–90. doi: 10.7224/1537-2073.2018-104
19. Mumoli L, Vescio V, Pirritano D, Russo E, Bosco D. ADEM anti-MOG antibody-positive after SARS-CoV2 vaccination. *Neurol Sci.* (2021) 43:763–6. doi: 10.1007/s10072-021-05761-7
20. Dams L, Kraemer M, Becker J. MOG-antibody-associated longitudinal extensive myelitis after ChAdOx1 nCoV-19 vaccination. *Mult Scler.* (2021) :13524585211057512. doi: 10.1177/13524585211057512
21. Román GC, Gracia F, Torres A, Palacios A, Gracia K, Harris D. Acute transverse myelitis (ATM): clinical review of 43 patients with COVID-19-associated ATM and 3 post-vaccination ATM serious adverse events with the ChAdOx1 nCoV-19 vaccine (AZD1222). *Front Immunol.* (2021) 12:653786. doi: 10.3389/fimmu.2021.653786
22. Nishiyama S, Ito T, Misu T, Takahashi T, Kikuchi A, Suzuki N, et al. A case of NMO seropositive for aquaporin-4 antibody more than 10 years before onset. *Neurology.* (2009) 72:1960–1. doi: 10.1212/WNL.0b013e3181a82621
23. Bradl M, Misu T, Takahashi T, Watanabe M, Mader S, Reindl M, et al. Neuromyelitis optica: pathogenicity of patient immunoglobulin in vivo. *Ann Neurol.* (2009) 66:630–43. doi: 10.1002/ana.21837

Conflict of Interest: The authors declare that the research was conducted in the absence of any commercial or financial relationships that could be construed as a potential conflict of interest.

Publisher's Note: All claims expressed in this article are solely those of the authors and do not necessarily represent those of their affiliated organizations, or those of the publisher, the editors and the reviewers. Any product that may be evaluated in this article, or claim that may be made by its manufacturer, is not guaranteed or endorsed by the publisher.

frontiers in Neurology

MINI REVIEW
published: 17 March 2022
doi: 10.3389/fneur.2022.865730

Glial Fibrillary Acidic Protein in Blood as a Disease Biomarker of Neuromyelitis Optica Spectrum Disorders

Hyunjin Kim[1], *Eun-Jae Lee*[1,2]*, *Young-Min Lim*[1] and *Kwang-Kuk Kim*[1]

[1] Department of Neurology, Asan Medical Center, University of Ulsan College of Medicine, Seoul, South Korea, [2] Department of Medicine, Asan Medical Institute of Convergence Science and Technology, Seoul, South Korea

Glial fibrillary acidic protein (GFAP) is a type III intermediate filament protein found in astrocytes in the brain. Damaged astrocytes release GFAP into cerebrospinal fluid and blood. Thus, GFAP levels in these body fluids may reflect the disease state of neuromyelitis optica spectrum disorder (NMOSD), which includes astrocytopathy, characterized by pathogenic antibodies against aquaporin 4 located on astrocytes. Recently, single-molecule array technology that can detect these synaptic proteins in blood, even in the subfemtomolar range, has been developed. Emerging evidence suggests that GFAP protein is a strong biomarker candidate for NMOSD. This mini-review provides basic information about GFAP protein and innovative clinical data that show the potential clinical value of blood GFAP levels as a biomarker for NMOSD.

Keywords: glial fibrillary acidic protein, neuromyelitis optica spectrum disorder, blood, biomarker, anti-aquaporin-4 antibodies, GFAP, NMOSD

OPEN ACCESS

Edited by:
Yangtai Guan,
Shanghai Jiao Tong University, China

Reviewed by:
Katsuhisa Masaki,
University of Chicago Medical Center, United States
Xia Wu,
Peking Union Medical College Hospital (CAMS), China

***Correspondence:**
Eun-Jae Lee
eunjae.lee@amc.seoul.kr

Specialty section:
This article was submitted to Multiple Sclerosis and Neuroimmunology, a section of the journal Frontiers in Neurology

Received: *30 January 2022*
Accepted: *21 February 2022*
Published: *17 March 2022*

Citation:
Kim H, Lee E-J, Lim Y-M and Kim K-K (2022) Glial Fibrillary Acidic Protein in Blood as a Disease Biomarker of Neuromyelitis Optica Spectrum Disorders. Front. Neurol. 13:865730. doi: 10.3389/fneur.2022.865730

INTRODUCTION

Neuromyelitis optica spectrum disorder (NMOSD) is a chronic inflammatory disease of the central nervous system (CNS) (1, 2). The main pathogenesis of NMOSD is autoimmune channelopathy/astrocytopathy that targets the water channel aquaporin-4 (AQP4) on perivascular astrocytic endfeet, and antibodies against AQP4 (AQP4-Ab) have been established as a diagnostic biomarker (3–5). Because NMOSD is a lifelong disease characterized by unpredictable attacks, subsequent severe neurological disability, and variable responses to treatments, blood biomarkers for monitoring and predicting the course of the disease would be useful (6–8). Serum AQP4-Ab titers may serve as such a disease biomarker; however, they have failed to show consistent results regarding their correlations with disease activity, severity, outcome, or responses to therapy (9–14). Currently, no blood biomarkers for monitoring are available in clinical practice.

Glial fibrillary acidic protein (GFAP) is the specific intermediate filament protein that constitutes the cytoskeleton of astrocytes (15). Damaged astrocytes release GFAP into interstitial fluid, cerebrospinal fluid (CSF), and finally the blood. Because NMOSD is an astrocytopathy, GFAP blood levels may be a useful biomarker for NMOSD. The recent development of ultrasensitive single-molecule array (Simoa) technology has expedited the realization of the potential of GFAP as a biomarker for NMOSD (16, 17).

In this review article, we will first briefly provide basic information about GFAP protein and its function in the brain. Then, we will review detection methods for GFAP protein in the blood and the recent evidence for the potential of GFAP as a blood biomarker for NMOSD. Finally, we will discuss several considerations in using GFAP as a disease biomarker and future directions.

GFAP

GFAP, a type III intermediate filament protein that was discovered by Dr. Eng in 1969 (18, 19), is responsible for the main cytoskeletal structure of astrocytes (19, 20). Apart from being present in the CNS, GFAP is also present in non-myelinated Schwann cells in the peripheral nervous system (PNS) and in enteric glia cells, which constitute the enteric nervous system (21, 22).

The human GFAP gene consists of nine exons and is located on chromosome 17 (17q21), spanning 10 kb (23). Alternative splicing occurs, and several GFAP isoforms have been identified (**Figure 1A**) (24). The three major domains of GFAP protein are the head, rod, and tail domains. The head domain is followed by the rod domain, which is composed of four α-helical coils. The N-terminal head domain is crucial for filament assembly, the rod domain plays a role in filament formation by coiling between polypeptides, and the C-terminal tail domain is important for stabilizing intermediate filaments (25). GFAP-α is the most abundant isoform in the brain and spinal cord but is also present in the PNS (26). This is the most commonly detected and analyzed isoform in the literature (20). GFAP-β is primarily expressed in non-myelinated Schwann cells in the PNS and has an alternate N-terminal (27). GFAP-γ also has an alternative N-terminal and is mainly located in the corpus callosum (28). GFAP-δ/ε is specifically expressed in neurogenic niches, such as the subventricular zone, and has an alternate C-terminal known to interact with presenilin (29–31). In addition, GFAP-δ/ε plays a role in modulating intermediate filament network dynamics (24, 32). GFAP-κ and GFAP-ζ also have distinct alternative C-terminals, which can modulate the properties of intermediate filaments (31, 33). Furthermore, an additional four isoforms of GFAP are collectively called GFAP+1, indicating isoform formation by a single nucleotide frameshift. GFAP+1 is found in a limited number of astrocytes in patients with Alzheimer's disease, Down syndrome, and chronic epilepsy; however, its implications remain to be elucidated (34–36). Although the precise functions of the different isoforms are not well-known, these isoforms seem to play a role in modulating intermediate filament networks during physiological and pathological states (37).

GFAP serves numerous pivotal functions in the CNS. GFAP is important for maintaining the mechanical strength of astrocytes and supporting neighboring neurons (38). In addition, GFAP participates in astrocytic motility and mitosis (39–41), maintains the integrity of the blood-brain barrier (BBB) and myelination (42, 43), protects neurons against neurotransmitter excess (44, 45) and injury (46, 47), regulates vesicle trafficking and autophagy (48, 49), and promotes synaptic plasticity (50, 51). Because GFAP is a major structural scaffold of astrocytes, damaged astrocytes release GFAP into their environment, e.g., interstitial fluid and CSF. Such released GFAP finally reaches the blood through an impaired BBB and/or glymphatic efflux (**Figure 1B**) (52–56). As such, blood GFAP exhibits much potential as a biomarker reflecting the state of NMOSD.

ULTRASENSITIVE DETECTION OF GFAP: SINGLE-MOLECULE ARRAY

GFAP concentrations can be detected with immunoassays such as enzyme-linked immunosorbent assay (ELISA) (57, 58). Conventional ELISA typically measures proteins at concentrations above 10^{-12} M (16). However, its sensitivity may be insufficient to reliably measure GFAP in the blood, of which concentrations in most patients with neurological disorders range from 10^{-14} to 10^{-10} M (0.5–5,000 pg/mL) (59–64). In patients with demyelinating diseases, the median CSF GFAP level is 8,601 pg/mL and the median serum GFAP level is 167 pg/mL from NMOSD and MS patient (59). The limit of quantification of commercial ELISA varies from 62.5 pg/mL (Eagle Biosciences, NH, USA) to 1,500 pg/mL (MilliporeSigma, MA, USA). Accordingly, although conventional ELISA measured CSF GFAP levels that showed promise as a potential biomarker for NMOSD (65–67), the blood GFAP levels demonstrated inconsistent results, indicating little clinical value for NMOSD (68, 69).

Recently, an ultrasensitive digital ELISA technology, Simoa, has been developed (16). The technique detects fluorescent signals from each single protein molecule by using femtoliter-volume chambers that isolate a single bead holding an immuno-complex with an enzymatic reporter generating fluorescence. High sensitivity to enzyme labeling and low background signals due to digitizing the detection of proteins has enabled the technology to detect blood proteins at subfemtomolar concentrations ($<10^{-15}$ M) (16). There are also other quantifying methods for GFAP such as electrochemiluminescence-based immunoassays and mass spectrometry (70). However, Simoa not only requires the smallest amount (only femtoliters) of blood for testing, but also shows the best analytical sensitivity with the limit of quantification of serum GFAP of 0.467 pg/mL (71). The reliability of Simoa for detecting blood neuronal and glial proteins is also high, as shown by the strong correlations between CSF and serum levels measured by Simoa technology (59, 72).

GFAP IN BLOOD AS A BIOMARKER FOR NMOSD

Recently, several studies have demonstrated that blood GFAP levels measured by Simoa have potential as a useful NMOSD biomarker for (1) differentiating NMOSD from other demyelinating diseases, (2) identifying and predicting clinical attacks, (3) monitoring disease disability and progression, and (4) evaluating treatment effects (59, 71, 73–78) (**Table 1**).

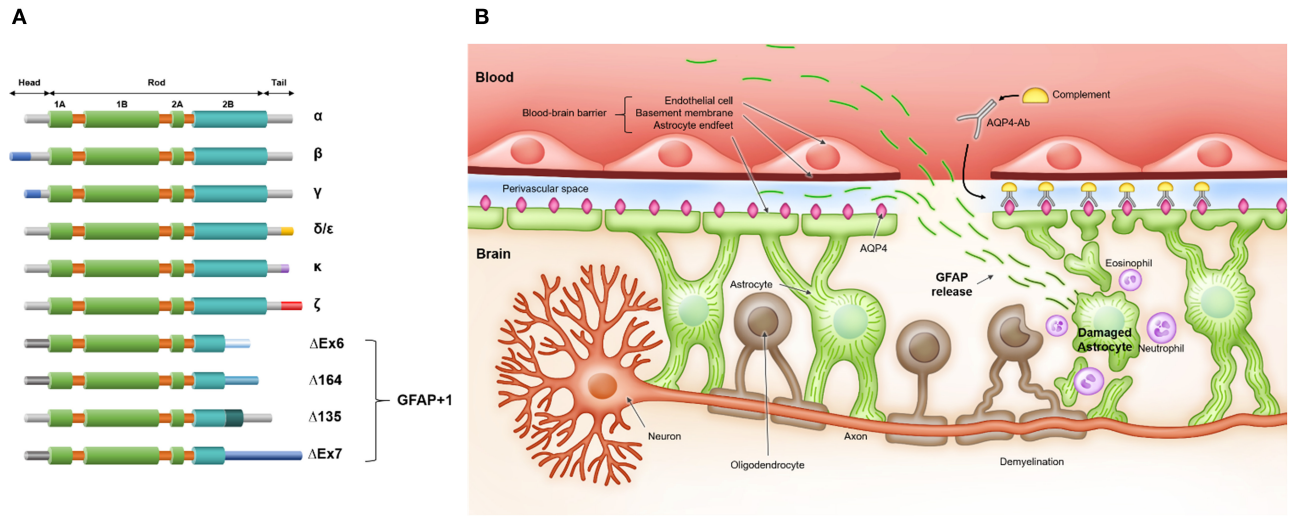

FIGURE 1 | (A) Glial fibrillary acid protein (GFAP) isoforms and **(B)** release of GFAP after astrocyte injury in neuromyelitis optica spectrum disorder. **(A)** GFAP protein consists of three domains: N-terminal head, central rod, and C-terminal tail. The head domain is crucial for filament assembly, the rod domain has a role in filament formation by coiling between polypeptides, and the tail domain is important in stabilizing the intermediate filament. **(B)** Serum anti-aquaporin-4 antibodies (AQP4-Ab) penetrate the blood-brain barrier and bind to aquaporin-4 (AQP4) on astrocyte endfeet. Antibody- and complement-dependent cellular cytotoxicity results in inflammatory cell recruitment, astrocyte damage, demyelination, and neuronal loss. After astrocyte damage, GFAP, an astrocytic scaffold protein, is released into interstitial and cerebrospinal fluid and finally reaches the blood through an impaired blood-brain barrier and/or glymphatic efflux.

TABLE 1 | GFAP in blood as a biomarker for NMOSD.

Author	Comparison of levels*			Attack vs. remission*	Correlation with		Prediction for future attack	Treatment effect
	vs. HC	vs. MS	vs. MOGAD		Age	EDSS	(Elevated vs. non-elevated)	
Watanabe et al. (59)	↑ (207.7 vs. 97.2)	↑ (207.7 vs. 121.1)	N/A	↑ (540.9 vs. 152.9)	NS	+	N/A	N/A
Kim et al. (73)	N/A	N/A	↑ (123.1 vs. 90.2)	↑ (253.8 vs. 104.4)	NS	+	N/A	N/A
Aktas et al. (75)	↑ (128.3 vs. 71.3)	↑ (128.3 vs. 97.5)	N/A	↑ (2,160 vs. 168.4)	+	N/A	Hazard ratio 3.09	Inebilizumab†
Schindler et al. (76)	NS (109.2 vs. 67.7)	N/A	NS (109.2 vs. 81.1)	N/A	+	+	Hazard ratio 11.6	N/A
Kim et al. (71)	↑ (154.1 vs. 98.9)	N/A	N/A	↑ (275.5 vs. 153.7)	NS	N/A	N/A	Rituximab¶
Chang et al. (77)	↑ (274.1 vs. 61.4)	↑ (274.1 vs. 66.5)	NS (274.1 vs. 136.7)	↑ (284.4 vs. 147.1)	NS	+	N/A	N/A
Zhang et al. (78)	↑ (149.7 vs. 68.7)	N/A	N/A	↑ (2,691 vs. 114.0)	NS	+	N/A	Tocilizumab, rituximab§

EDSS, expanded disability status scale; GFAP, glial fibrillary acidic protein; HC, healthy control; MOGAD, myelin oligodendrocyte glycoprotein antibody-associated disease; MS, multiple sclerosis; N/A, not available; NMOSD, neuromyelitis optica spectrum disorder; NS, not significant.

**The unit for GFAP levels is pg/mL. The figures in parentheses are median level of blood GFAP of each group.*

†Inebilizumab attenuated the attack-related increase in serum GFAP levels [inebilizumab, median fold change (FC): 1.1 vs. placebo, median FC: 20.2], and decreased serum GFAP levels in patients who did not experience attacks (inebilizumab, −12.9% vs. placebo, +2.9% at week 16).

¶Rituximab-treated patients manifested stable serum GFAP levels over time, but other immunosuppressant-treated patients, treated with corticosteroids and/or immunosuppressants (azathioprine, mycophenolate mofetil, or methotrexate), showed significantly increased serum GFAP levels over time (rituximab: baseline 145.6 pg/mL → follow-up 168.1 pg/mL, $p = 0.433$; immunosuppressant: baseline 128.6 pg/mL → follow-up 153.0 pg/mL, $p < 0.001$).

§Tocilizumab and rituximab decreased plasma GFAP levels by 36 and 23%, respectively, compared to the change between baseline and follow up of the prednisone-treated group.

Differentiating NMOSD From Other Demyelinating Diseases

It is important in clinical practice to differentiate NMOSD from other demyelinating diseases, including multiple sclerosis (MS) and myelin oligodendrocyte glycoprotein antibody-associated disease (MOGAD), because treatments for these diseases differ considerably. Inappropriate treatments may result in poor outcomes. For example, treating NMOSD patients with therapies for MS could worsen the disease (79–81). Although the testing of AQP4-Ab is essential for the diagnosis of NMOSD, differentiation of the diseases remains crucial. Contrary to the high specificity of the AQP4-Ab assay (96.6–99.8%), the sensitivity of the AQP4-Ab assay (48.7–76.7%) varies according to the assay methodology, indicating a high risk of false-negative results (82). In addition, a patient's treatment and clinical status can affect the result of an antibody assay (83, 84).

Serum GFAP levels could be used as a diagnostic marker for NMOSD, as they are significantly higher in NMOSD patients compared to those in healthy controls (59, 71, 75, 77, 78) and patients with other demyelinating diseases (MS or MOGAD) (59, 73, 75, 77). These findings are in line with immunopathological studies which showed that GFAP-positive astrocytes are highly destroyed only in active lesions of NMOSD but not in those of MS (85–90). Neurofilament light chain (NfL), a scaffolding protein of the neuronal cytoskeleton that is released upon axonal damage, may represent another diagnostic biomarker because it is also elevated in the blood of NMOSD patients, compared to healthy controls (59, 71, 75, 77, 78). However, serum NfL levels do not differ between NMOSD patients and MS or MOGAD patients (59, 73, 77), suggesting that NfL lacks specificity as a biomarker for NMOSD. A recent study proposed that the serum GFAP/NfL quotient at attack state could be a useful biomarker that differentiates NMOSD from MS with a sensitivity of 73.0% and a specificity of 75.8% (59). The serum GFAP/NfL quotient also distinguished AQP4-Ab-seropositive NMOSD from MOGAD and MS (77).

Identifying and Predicting Clinical Attacks

Identifying and predicting clinical attacks in NMOSD patients would be useful. Attack or relapse is defined as new or worsening neurological symptoms with an objective sign on neurological examination correlating with new or aggravating magnetic resonance image (MRI) lesions (91). However, pseudo-attacks or pseudo-relapses, i.e., clinical exacerbations with similar symptoms and signs but without true lesions, also occur in NMOSD patients, and clinically distinguishing between the two conditions can be difficult (91). Furthermore, although currently no method can predict future clinical attacks, a recent report revealed that clinically silent MRI lesions may represent a high risk of relapse (92). However, clinically silent brain or spinal cord lesions are rare in NMOSD patients, and thus performing regular MRI to predict future relapses would be inefficient.

Serum GFAP levels may help identify and predict clinical attacks in NMOSD patients, as they are higher in the attack state than in the remission state, and their elevation is associated with recent relapses (59, 71, 73–75, 77, 78). In a longitudinal NMOSD cohort (median follow up: 17 months), serum GFAP levels alone successfully discriminated clinical attacks from remission with a sensitivity of 94.7% and a specificity of 74.6% (area under the receiver characteristic curve = 0.876). Remarkably, this performance was better than that of other blood biomarkers, such as NfL and the GFAP/NfL quotient (71). In line with this, another study on a longitudinal NMOSD cohort (median follow up: 12 months) showed that plasma GFAP levels were the most powerful contributor in a random forest model to differentiate relapses from remissions, compared to other biomarkers (NfL, GFAP, and GFAP/NfL) and clinical variables [age, annual relapse rates, expanded disability status scale (EDSS) score, disease duration, and treatment status] (78). After relapse, serum GFAP levels decrease over time, and most patients show reduced serum GFAP levels below the predefined cut-off value ($\geq$3 standard deviations of mean levels in age-/sex-matched healthy controls) within 3 months (71, 74).

Notably, increased serum GFAP levels may indicate forthcoming clinical relapses. In a substudy of the N-MOmentum study, significantly increased serum GFAP levels were already observed 1 week before a clinical attack (93), and serum GFAP levels were linearly correlated with the risk of an upcoming attack (75). Additionally, patients with elevated serum GFAP levels at baseline ($\geq$2 standard deviations of the mean level of healthy controls) showed a 3-fold higher risk of having future NMOSD attacks than patients without elevated serum GFAP levels at baseline (75). Similar results were shown by another study on a prospective longitudinal cohort. NMOSD patients with high serum GFAP levels (>90 pg/mL, the cut-off value was derived from the 75th percentile of serum GFAP levels in healthy controls) at baseline had a shorter time to a future attack than those without [adjusted hazard ratio (95% confidence interval):11.6 (1.3–105.6)] (76). Conversely, in the same NMOSD cohort, baseline serum NfL levels were not significantly associated with a risk of future attack (76).

Monitoring Disease Disability and Progression

Monitoring disease disability is necessary to determine the severity and track the progression of the disease, and to assess treatment effectiveness (94). The most popular and widely used instrument is the EDSS. However, considering that the inter-rater variability of EDSS is as high as 30%, establishing an objective and easily measurable biomarker would be preferable (95). Many studies have demonstrated that blood GFAP concentration is independently associated with EDSS score in NMOSD patients (59, 73, 76–78, 96). Serum GFAP levels are also correlated with other clinical disability parameters, including the MS functional composite score, 9-Hole Peg Test, and paced auditory serial addition test (76). Blood NfL levels also tend to increase with EDSS score in NMOSD patients. However, the degree of association is not as strong as that of blood GFAP levels; positive correlations were significant in some studies (59, 77, 78, 96) but not in others (73, 76).

Serum GFAP levels may also be useful to monitor disease progression. NMOSD is considered to lack subclinical disease activity, and all disabilities are related to attacks (97, 98). Conversely, MS exhibits subclinical progression (99, 100). However, recent optical coherent tomography and visual evoked potential studies suggested subclinical neurodegeneration in NMOSD patients (101, 102). More recently, silent progression of brain atrophy was documented in NMOSD patients, even in clinically inactive patients (103). Additional studies on blood GFAP levels further support the concept of ongoing subclinical neurodegeneration in NMOSD. First, median blood GFAP levels during remission periods are significantly higher in NMOSD patients than those in healthy controls (59, 71, 75, 77, 78). Second, blood GFAP levels gradually increase over time even in patients with no clinical relapse, and the rate of increase of GFAP levels is faster than that related to normal aging (71). Third, monoclonal antibody treatments such as inebilizumab, tocilizumab, and rituximab decrease serum GFAP levels more than treatments with placebo or prednisolone (75, 78). This

indicates that gradual increases in GFAP levels may reflect ongoing pathological processes and may be alleviated by active treatment. However, it should be noted that most of these findings have been derived from small studies conducted at single centers or from substudies of clinical trials that may be different from real clinical situations. Future larger studies are warranted to confirm these findings.

Evaluating Treatment Effects

It would be useful to have blood markers as objective endpoints in determining therapeutic effects, as shown in a recent clinical trial (104), or as index markers for selecting optimal personalized treatments (105). Recent data suggest that blood GFAP levels may represent such markers. In a longitudinal follow-up study, rituximab (anti-CD20 monoclonal antibody)-treated NMOSD patients exhibited stable serum GFAP levels over time, in contrast to patients with other immunosuppressant treatments who showed significantly increased serum GFAP levels during the same period (71). Inebilizumab, an anti-CD19 monoclonal antibody, also prevented increases in serum GFAP levels. It attenuated the attack-related increase in serum GFAP levels (75) and significantly decreased serum GFAP levels in patients who did not experience an attack, as compared to placebo treatment (75). Tocilizumab, an anti-IL6 monoclonal antibody, also significantly reduced plasma GFAP levels in NMOSD patients, as compared to prednisolone (78). These findings are remarkable because they indicate that blood GFAP levels can reflect treatment responses during silent periods without clinical relapses.

SPECIAL CONSIDERATIONS

Age

Physiological aging gradually affects the brain (106), and serum GFAP levels increase with aging in healthy controls (59, 71, 75, 77). However, this positive association has not been consistently demonstrated in NMOSD patients (59, 71, 73, 75–78). One explanation for such inconsistent GFAP–age correlations could be that NMOSD patients tend to have high serum GFAP levels even at a young age. Furthermore, aging-related processes, such as increased astrogliosis, also appear to affect the clinical implication of GFAP in elderly patients. In a study that analyzed the effect of age on serum biomarkers in NMOSD patients, positive GFAP–EDSS correlations were distinctively stronger in the youngest ($\leq$45 years) compared to the oldest ($\geq$55 years) group (96). The association between GFAP levels and disease severity may have been compromised in elderly patients due to increased astrogliosis following neurodegeneration (96). Therefore, age should be considered when interpreting blood levels of neuronal and glial proteins in NMOSD patients.

Temporal Trajectories

The temporal dynamics of GFAP and date of blood sampling are also important. After brain injury, the serum GFAP levels peak at 20 h and decline over 72 h, indicating estimated half-life as 24–48 h (107, 108). It should also be noted that GFAP levels increases from 1 week before the advent of clinical symptoms (75). Even detected during the remission state, GFAP levels in NMOSD patients are still higher than healthy controls (59, 77, 78). In reflecting acute NMOSD attacks, GFAP may represent the event most appropriately within 7 days after attack, since 92% samples drawn within 1–7 days following attacks showed elevated level of blood GFAP ($\geq$2 standard deviations of mean level of healthy controls) (75).

Specificity

Blood GFAP levels increase not only in NMOSD but in various neurological diseases (109), thus the specificity of GFAP as an NMOSD biomarker should be discussed. Blood GFAP levels in patients with NMOSD, which often increase more than 1,000 pg/mL during relapses, tend to be higher than in patients with other diseases such as relapsing remitting MS (59, 60, 77), progressive MS (59–61), and even ischemic stroke (62). This is because patients with NMOSD are accompanied by direct damage of astrocytes. However, blood GFAP levels can also increase very high in glioblastoma, traumatic brain injury, and hemorrhagic stroke, as the level of NMOSD during relapses (63, 64, 110, 111). Therefore, it is difficult to regard that blood GFAP levels alone are a pathognomonic biomarker for NMOSD. Another parameter like GFAP/NfL ratio may enhance the specificity in terms of discriminating NMOSD from other diseases (59). However, it should also be emphasized that GFAP alone reflects well the longitudinal disease course of NMOSD and may be the most appropriate marker to monitor the disease changes within the NMOSD cohort (71).

NfL

As a representative biomarker of neuronal damage, serum NfL has also demonstrated disease association with NMOSD as well as MS (59, 71, 73, 76–78, 112, 113). However, serum NfL was not useful to distinguish NMOSD from other demyelinating diseases, and less sensitive and specific than serum GFAP in identifying and predicting NMOSD relapses (59, 71, 76–78). The value of NfL may be more pronounced elsewhere. Given that NfL is a neuronal structural component, serum NfL might be a better biomarker for monitoring the degree of neurodegeneration of NMOSD (101–103) and associated cognitive impairment (113) than serum GFAP. This possibility should be elucidated in future studies.

OUTLOOK

For GFAP to be used as a biomarker in clinical practice, several limitations that hinder the applicability of blood GFAP in clinical settings should be addressed. First, standard protocols and quality control criteria should be established across different laboratories (113). In addition, age-specific and sex-specific reference should also be developed. The dynamics of GFAP after releases upon NMOSD attacks should be explored to determine accurate blood GFAP half-life. This work should be paralleled with unraveling mechanisms and pathways of GFAP released from brain into the blood. Finally, the intervals for testing blood GFAP levels and guidelines for biomarker-based decision making should also be established.

Clinically, management strategies could be available by stratifying the risk of future attack based on both age-adjusted cut-off values and intraindividual changes in blood GFAP levels. Based on an individual's different strata of attack risk, clinicians could decide treatment initiation, continuation, and escalation/de-escalation of NMOSD patients. For example, it could be possible to set a serum GFAP range for the treatment response of patients and classify patients into treatment-responsive and treatment-resistant groups. This classification would enable precision treatment strategies that quickly change from one option to another suitable before it is too late (e.g., the advent of clinical relapses).

CONCLUSIONS

Although more than 50 years have passed since GFAP was first discovered, only recently has GFAP been suggested as a reliable blood biomarker in clinical practice. The role of GFAP as a biomarker for NMOSD shows promise because GFAP not only has pathophysiological specificity that can reflect astrocytopathy as much as AQP4-Ab, but it also has the advantage of being quantifiable with much more sensitivity than AQP4-Ab. After several clinical and technical issues are resolved, blood GFAP levels may expedite the process of personalized care of NMOSD patients.

AUTHOR CONTRIBUTIONS

HK and E-JL contributed to conception and design of the review. HK wrote the manuscript. E-JL acquired funding. Y-ML, K-KK, and E-JL supervised the study and revised the manuscript. All authors contributed to manuscript revision, read, and approved the submitted version.

FUNDING

This study was supported by grants from the Ministry of Science and ICT, South Korea (NRF−2018R1C1B6008884).

REFERENCES

1. Papadopoulos MC, Verkman AS. Aquaporin 4 and neuromyelitis optica. *Lancet Neurol.* (2012) 11:535–44. doi: 10.1016/S1474-4422(12)70133-3
2. Fujihara K. Neuromyelitis optica spectrum disorders: still evolving and broadening. *Curr Opin Neurol.* (2019) 32:385–94. doi: 10.1097/WCO.0000000000000694
3. Lennon VA, Kryzer TJ, Pittock SJ, Verkman AS, Hinson SR. IgG marker of optic-spinal multiple sclerosis binds to the aquaporin-4 water channel. *J Exp Med.* (2005) 202:473–7. doi: 10.1084/jem.20050304
4. Lennon VA, Wingerchuk DM, Kryzer TJ, Pittock SJ, Lucchinetti CF, Fujihara K, et al. A serum autoantibody marker of neuromyelitis optica: distinction from multiple sclerosis. *Lancet.* (2004) 364:2106–12. doi: 10.1016/S0140-6736(04)17551-X
5. Papadopoulos MC, Bennett JL, Verkman AS. Treatment of neuromyelitis optica: state-of-the-art and emerging therapies. *Nat Rev Neurol.* (2014) 10:493–506. doi: 10.1038/nrneurol.2014.141
6. Melamed E, Levy M, Waters PJ, Sato DK, Bennett JL, John GR, et al. Update on biomarkers in neuromyelitis optica. *Neurol Neuroimmunol Neuroinflamm.* (2015) 2:e134. doi: 10.1212/NXI.0000000000000134
7. Lee EJ, Lim YM, Kim SY, Lee J, Kim H, Jin JY, et al. The clinical and prognostic value of antinuclear antibodies in NMO-IgG seropositive neuromyelitis optica spectrum disorder. *J Neuroimmunol.* (2019) 328:1–4. doi: 10.1016/j.jneuroim.2018.11.012
8. Kim S, Lee EJ, Kim KW, Seo D, Moon S, Kim KK, et al. Quality of life of patients with multiple sclerosis and neuromyelitis optica spectrum disorders: cross-sectional and longitudinal analysis. *Mult Scler Relat Disord.* (2022) 58:103500. doi: 10.1016/j.msard.2022.103500
9. Jitprapaikulsan J, Fryer JP, Majed M, Smith CY, Jenkins SM, Cabre P, et al. Clinical utility of AQP4-IgG titers and measures of complement-mediated cell killing in NMOSD. *Neurol Neuroimmunol Neuroinflam.* (2020) 7:e727. doi: 10.1212/NXI.0000000000000727
10. Takahashi T, Fujihara K, Nakashima I, Misu T, Miyazawa I, Nakamura M, et al. Anti-aquaporin-4 antibody is involved in the pathogenesis of NMO: a study on antibody titre. *Brain.* (2007) 130:1235–43. doi: 10.1093/brain/awm062
11. Akaishi T, Takahashi T, Nakashima I, Abe M, Ishii T, Aoki M, et al. Repeated follow-up of AQP4-IgG titer by cell-based assay in neuromyelitis optica spectrum disorders (NMOSD). *J Neurol Sci.* (2020) 410:116671. doi: 10.1016/j.jns.2020.116671
12. Jarius S, Aboul-Enein F, Waters P, Kuenz B, Hauser A, Berger T, et al. Antibody to aquaporin-4 in the long-term course of neuromyelitis optica. *Brain.* (2008) 131:3072–80. doi: 10.1093/brain/awn240
13. Dujmovic I, Mader S, Schanda K, Deisenhammer F, Stojsavljevic N, Kostic J, et al. Temporal dynamics of cerebrospinal fluid anti-aquaporin-4 antibodies in patients with neuromyelitis optica spectrum disorders. *J Neuroimmunol.* (2011) 234:124–30. doi: 10.1016/j.jneuroim.2011.01.007
14. Takahashi T, Miyazawa I, Misu T, Takano R, Nakashima I, Fujihara K, et al. Intractable hiccup and nausea in neuromyelitis optica with anti-aquaporin-4 antibody: a herald of acute exacerbations. *J Neurol Neurosurg Psychiatry.* (2008) 79:1075–8. doi: 10.1136/jnnp.2008.145391
15. Brenner M, Johnson AB, Boespflug-Tanguy O, Rodriguez D, Goldman JE, Messing A. Mutations in GFAP, encoding glial fibrillary acidic protein, are associated with Alexander disease. *Nat Genet.* (2001) 27:117–20. doi: 10.1038/83679
16. Rissin DM, Kan CW, Campbell TG, Howes SC, Fournier DR, Song L, et al. Single-molecule enzyme-linked immunosorbent assay detects serum proteins at subfemtomolar concentrations. *Nat Biotechnol.* (2010) 28:595–9. doi: 10.1038/nbt.1641
17. Chang L, Rissin DM, Fournier DR, Piech T, Patel PP, Wilson DH, et al. Single molecule enzyme-linked immunosorbent assays: theoretical considerations. *J Immunol Methods.* (2012) 378:102–15. doi: 10.1016/j.jim.2012.02.011
18. Eng L, Gerstl B, Vanderhaeghen J. A study of proteins in old multiple sclerosis plaques. *Trans Am Soc Neurochem.* (1970) 1:42.
19. Eng LF, Ghirnikar RS, Lee YL. Glial fibrillary acidic protein: GFAP-thirty-one years (1969-2000). *Neurochem Res.* (2000) 25:1439–51. doi: 10.1023/A:1007677003387
20. Hol EM, Capetanaki Y. Type III intermediate filaments desmin, glial fibrillary acidic protein (GFAP), vimentin, and peripherin. *Cold Spring Harb Perspect Biol.* (2017) 9:a021642. doi: 10.1101/cshperspect.a021642
21. Gulbransen BD, Sharkey KA. Novel functional roles for enteric glia in the gastrointestinal tract. *Nat Rev Gastroenterol Hepatol.* (2012) 9:625–32. doi: 10.1038/nrgastro.2012.138
22. Laranjeira C, Sandgren K, Kessaris N, Richardson W, Potocnik A, Vanden Berghe P, et al. Glial cells in the mouse enteric nervous system can undergo neurogenesis in response to injury. *J Clin Invest.* (2011) 121:3412–24. doi: 10.1172/JCI58200
23. Blechingberg J, Lykke-Andersen S, Jensen TH, Jørgensen AL, Nielsen AL. Regulatory mechanisms for 3'-end alternative splicing and polyadenylation of the Glial Fibrillary Acidic Protein, GFAP, transcript. *Nucleic Acids Res.* (2007) 35:7636–50. doi: 10.1093/nar/gkm931

24. Moeton M, Stassen OM, Sluijs JA, van der Meer VW, Kluivers LJ, van Hoorn H, et al. GFAP isoforms control intermediate filament network dynamics, cell morphology, and focal adhesions. *Cell Mol Life Sci.* (2016) 73:4101–20. doi: 10.1007/s00018-016-2239-5
25. Ralton JE, Lu X, Hutcheson AM, Quinlan RA. Identification of two N-terminal non-alpha-helical domain motifs important in the assembly of glial fibrillary acidic protein. *J Cell Sci.* (1994) 107:1935–48. doi: 10.1242/jcs.107.7.1935
26. Reeves SA, Helman LJ, Allison A, Israel MA. Molecular cloning and primary structure of human glial fibrillary acidic protein. *Proc Natl Acad Sci USA.* (1989) 86:5178–82. doi: 10.1073/pnas.86.13.5178
27. Galea E, Dupouey P, Feinstein DL. Glial fibrillary acidic protein mRNA isotypes: expression *in vitro* and *in vivo*. *J Neurosci Res.* (1995) 41:452–61. doi: 10.1002/jnr.490410404
28. Zelenika D, Grima B, Brenner M, Pessac B. A novel glial fibrillary acidic protein mRNA lacking exon 1. *Brain Res Mol Brain Res.* (1995) 30:251–8. doi: 10.1016/0169-328X(95)00010-P
29. Roelofs RF, Fischer DF, Houtman SH, Sluijs JA, Van Haren W, Van Leeuwen FW, et al. Adult human subventricular, subgranular, and subpial zones contain astrocytes with a specialized intermediate filament cytoskeleton. *Glia.* (2005) 52:289–300. doi: 10.1002/glia.20243
30. Nielsen AL, Holm IE, Johansen M, Bonven B, Jørgensen P, Jørgensen AL. A new splice variant of glial fibrillary acidic protein, GFAP epsilon, interacts with the presenilin proteins. *J Biol Chem.* (2002) 277:29983–91. doi: 10.1074/jbc.M112121200
31. Kamphuis W, Mamber C, Moeton M, Kooijman L, Sluijs JA, Jansen AH, et al. GFAP isoforms in adult mouse brain with a focus on neurogenic astrocytes and reactive astrogliosis in mouse models of Alzheimer disease. *PLoS ONE.* (2012) 7:e42823. doi: 10.1371/journal.pone.0042823
32. Perng MD, Wen SF, Gibbon T, Middeldorp J, Sluijs J, Hol EM, et al. Glial fibrillary acidic protein filaments can tolerate the incorporation of assembly-compromised GFAP-delta, but with consequences for filament organization and alphaB-crystallin association. *Mol Biol Cell.* (2008) 19:4521–33. doi: 10.1091/mbc.e08-03-0284
33. Blechingberg J, Holm IE, Nielsen KB, Jensen TH, Jørgensen AL, Nielsen AL. Identification and characterization of GFAPkappa, a novel glial fibrillary acidic protein isoform. *Glia.* (2007) 55:497–507. doi: 10.1002/glia.20475
34. Kamphuis W, Middeldorp J, Kooijman L, Sluijs JA, Kooi EJ, Moeton M, et al. Glial fibrillary acidic protein isoform expression in plaque related astrogliosis in Alzheimer's disease. *Neurobiol Aging.* (2014) 35:492–510. doi: 10.1016/j.neurobiolaging.2013.09.035
35. Hol EM, Roelofs RF, Moraal E, Sonnemans MA, Sluijs JA, Proper EA, et al. Neuronal expression of GFAP in patients with Alzheimer pathology and identification of novel GFAP splice forms. *Mol Psychiatry.* (2003) 8:786–96. doi: 10.1038/sj.mp.4001379
36. Boer K, Middeldorp J, Spliet WG, Razavi F, van Rijen PC, Baayen JC, et al. Immunohistochemical characterization of the out-of frame splice variants GFAP Delta164/Deltaexon 6 in focal lesions associated with chronic epilepsy. *Epilepsy Res.* (2010) 90:99–109. doi: 10.1016/j.eplepsyres.2010.03.014
37. Middeldorp J, Hol EM. GFAP in health and disease. *Prog Neurobiol.* (2011) 93:421–43. doi: 10.1016/j.pneurobio.2011.01.005
38. Yang Z, Wang KK. Glial fibrillary acidic protein: from intermediate filament assembly and gliosis to neurobiomarker. *Trends Neurosci.* (2015) 38:364–74. doi: 10.1016/j.tins.2015.04.003
39. Elobeid A, Bongcam-Rudloff E, Westermark B, Nister M. Effects of inducible glial fibrillary acidic protein on glioma cell motility and proliferation. *J Neurosci Res.* (2000) 60:245–56. doi: 10.1002/(SICI)1097-4547(20000415)60:2<245::AID-JNR14>3.0.CO;2-1
40. Triolo D, Dina G, Lorenzetti I, Malaguti M, Morana P, Del Carro U, et al. Loss of glial fibrillary acidic protein (GFAP) impairs Schwann cell proliferation and delays nerve regeneration after damage. *J Cell Sci.* (2006) 119:3981–93. doi: 10.1242/jcs.03168
41. Rutka JT, Smith SL. Transfection of human astrocytoma cells with glial fibrillary acidic protein complementary DNA: analysis of expression, proliferation, and tumorigenicity. *Cancer Res.* (1993) 53:3624–31.
42. Pekny M, Stanness KA, Eliasson C, Betsholtz C, Janigro D. Impaired induction of blood-brain barrier properties in aortic endothelial cells by astrocytes from GFAB-deficient mice. *Glia.* (1998) 22:390–400. doi: 10.1002/(SICI)1098-1136(199804)22:4<390::AID-GLIA8>3.0.CO;2-7
43. Liedtke W, Edelmann W, Bieri PL, Chiu F-C, Cowan NJ, Kucherlapati R, et al. GFAP is necessary for the integrity of CNS white matter architecture and long-term maintenance of myelination. *Neuron.* (1996) 17:607–15. doi: 10.1016/S0896-6273(00)80194-4
44. Lieth E, Barber AJ, Xu B, Dice C, Ratz MJ, Tanase D, et al. Glial reactivity and impaired glutamate metabolism in short-term experimental diabetic retinopathy. Penn State Retina Research Group. *Diabetes.* (1998) 47:815–20. doi: 10.2337/diabetes.47.5.815
45. Pekny M, Eliasson C, Siushansian R, Ding M, Dixon SJ, Pekna M, et al. The impact of genetic removal of GFAP and/or vimentin on glutamine levels and transport of glucose and ascorbate in astrocytes. *Neurochem Res.* (1999) 24:1357–62. doi: 10.1023/A:1022572304626
46. Nawashiro H, Messing A, Azzam N, Brenner M. Mice lacking GFAP are hypersensitive to traumatic cerebrospinal injury. *Neuroreport.* (1998) 9:1691–6. doi: 10.1097/00001756-199806010-00004
47. Otani N, Nawashiro H, Fukui S, Ooigawa H, Ohsumi A, Toyooka T, et al. Enhanced hippocampal neurodegeneration after traumatic or kainate excitotoxicity in GFAP-null mice. *J Clin Neurosci.* (2006) 13:934–8. doi: 10.1016/j.jocn.2005.10.018
48. Bandyopadhyay U, Sridhar S, Kaushik S, Kiffin R, Cuervo AM. Identification of regulators of chaperone-mediated autophagy. *Molecular Cell.* (2010) 39:535–47. doi: 10.1016/j.molcel.2010.08.004
49. Potokar M, Kreft M, Li L, Daniel Andersson J, Pangršič T, Chowdhury HH, et al. Cytoskeleton and vesicle mobility in astrocytes. *Traffic.* (2007) 8:12–20. doi: 10.1111/j.1600-0854.2006.00509.x
50. McCall M, Gregg R, Behringer R, Brenner M, Delaney C, Galbreath E, et al. Targeted deletion in astrocyte intermediate filament (Gfap) alters neuronal physiology. *Proc Natl Acad Sci.* (1996) 93:6361–6. doi: 10.1073/pnas.93.13.6361
51. Shibuki K, Gomi H, Chen L, Bao S, Kim JJ, Wakatsuki H, et al. Deficient cerebellar long-term depression, impaired eyeblink conditioning, and normal motor coordination in GFAP mutant mice. *Neuron.* (1996) 16:587–99. doi: 10.1016/S0896-6273(00)80078-1
52. Chodobski A, Zink BJ, Szmydynger-Chodobska J. Blood-brain barrier pathophysiology in traumatic brain injury. *Transl Stroke Res.* (2011) 2:492–516. doi: 10.1007/s12975-011-0125-x
53. Obermeier B, Daneman R, Ransohoff RM. Development, maintenance and disruption of the blood-brain barrier. *Nature Medicine.* (2013) 19:1584–96. doi: 10.1038/nm.3407
54. Da Mesquita S, Fu Z, Kipnis J. The meningeal lymphatic system: a new player in neurophysiology. *Neuron.* (2018) 100:375–88. doi: 10.1016/j.neuron.2018.09.022
55. Mestre H, Mori Y, Nedergaard M. The brain's glymphatic system: current controversies. *Trends Neurosci.* (2020) 43:458–66. doi: 10.1016/j.tins.2020.04.003
56. Plog BA, Dashnaw ML, Hitomi E, Peng W, Liao Y, Lou N, et al. Biomarkers of traumatic injury are transported from brain to blood via the glymphatic system. *J Neurosci.* (2015) 35:518–26. doi: 10.1523/JNEUROSCI.3742-14.2015
57. Petzold A, Keir G, Green AJ, Giovannoni G, Thompson EJ. An ELISA for glial fibrillary acidic protein. *J Immunol Methods.* (2004) 287:169–77. doi: 10.1016/j.jim.2004.01.015
58. Rosengren LE, Wikkelsø C, Hagberg L. A sensitive ELISA for glial fibrillary acidic protein: application in CSF of adults. *J Neurosci Methods.* (1994) 51:197–204. doi: 10.1016/0165-0270(94)90011-6
59. Watanabe M, Nakamura Y, Michalak Z, Isobe N, Barro C, Leppert D, et al. Serum GFAP and neurofilament light as biomarkers of disease activity and disability in NMOSD. *Neurology.* (2019) 93:e1299–e311. doi: 10.1212/WNL.0000000000008160
60. Abdelhak A, Huss A, Kassubek J, Tumani H, Otto M. Serum GFAP as a biomarker for disease severity in multiple sclerosis. *Sci Rep.* (2018) 8:14798. doi: 10.1038/s41598-018-33158-8
61. Ayrignac X, Le Bars E, Duflos C, Hirtz C, Maleska Maceski A, Carra-Dallière C, et al. Serum GFAP in multiple sclerosis: correlation with

disease type and MRI markers of disease severity. *Sci Rep.* (2020) 10:10923. doi: 10.1038/s41598-020-67934-2
62. Kalra LP, Khatter H, Ramanathan S, Sapehia S, Devi K, Kaliyaperumal A, et al. Serum GFAP for stroke diagnosis in regions with limited access to brain imaging (BE FAST India). *Eur Stroke J.* (2021) 6:176–84. doi: 10.1177/23969873211010069
63. Jung CS, Foerch C, Schänzer A, Heck A, Plate KH, Seifert V, et al. Serum GFAP is a diagnostic marker for glioblastoma multiforme. *Brain.* (2007) 130:3336–41. doi: 10.1093/brain/awm263
64. Czeiter E, Amrein K, Gravesteijn BY, Lecky F, Menon DK, Mondello S, et al. Blood biomarkers on admission in acute traumatic brain injury: relations to severity, CT findings and care path in the CENTER-TBI study. *EBioMedicine.* (2020) 56:102785. doi: 10.1016/j.ebiom.2020.102785
65. Uzawa A, Mori M, Sawai S, Masuda S, Muto M, Uchida T, et al. Cerebrospinal fluid interleukin-6 and glial fibrillary acidic protein levels are increased during initial neuromyelitis optica attacks. *Clin Chim Acta.* (2013) 421:181–3. doi: 10.1016/j.cca.2013.03.020
66. Misu T, Takano R, Fujihara K, Takahashi T, Sato S, Itoyama Y. Marked increase in cerebrospinal fluid glial fibrillar acidic protein in neuromyelitis optica: an astrocytic damage marker. *J Neurol Neurosurg Psychiatry.* (2009) 80:575–7. doi: 10.1136/jnnp.2008.150698
67. Takano R, Misu T, Takahashi T, Sato S, Fujihara K, Itoyama Y. Astrocytic damage is far more severe than demyelination in NMO: a clinical CSF biomarker study. *Neurology.* (2010) 75:208–16. doi: 10.1212/WNL.0b013e3181e2414b
68. Storoni M, Verbeek MM, Illes Z, Marignier R, Teunissen CE, Grabowska M, et al. Serum GFAP levels in optic neuropathies. *J Neurol Sci.* (2012) 317:117–22. doi: 10.1016/j.jns.2012.02.012
69. Storoni M, Petzold A, Plant GT. The use of serum glial fibrillary acidic protein measurements in the diagnosis of neuromyelitis optica spectrum optic neuritis. *PLoS ONE.* (2011) 6:e23489. doi: 10.1371/journal.pone.0023489
70. Petzold A. Glial fibrillary acidic protein is a body fluid biomarker for glial pathology in human disease. *Brain Res.* (2015) 1600:17–31. doi: 10.1016/j.brainres.2014.12.027
71. Kim H, Lee EJ, Kim S, Choi LK, Kim HJ, Kim HW, et al. Longitudinal follow-up of serum biomarkers in patients with neuromyelitis optica spectrum disorder. *Mult Scler.* (2021) 0:13524585211024978. doi: 10.1177/13524585211024978
72. Högel H, Rissanen E, Barro C, Matilainen M, Nylund M, Kuhle J, et al. Serum glial fibrillary acidic protein correlates with multiple sclerosis disease severity. *Mult Scler.* (2020) 26:210–9. doi: 10.1177/1352458518819380
73. Kim H, Lee EJ, Kim S, Choi LK, Kim K, Kim HW, et al. Serum biomarkers in myelin oligodendrocyte glycoprotein antibody-associated disease. *Neurol Neuroimmunol Neuroinflamm.* (2020) 7:e708. doi: 10.1212/NXI.0000000000000708
74. Hyun J-W, Kim Y, Kim SY, Lee MY, Kim S-H, Kim HJ. Investigating the presence of interattack astrocyte damage in neuromyelitis optica spectrum disorder. Longitudinal analysis of serum glial fibrillary acidic protein. *Neurol Neuroimmunol Neuroinflamm.* (2021) 8:e965. doi: 10.1212/NXI.0000000000000965
75. Aktas O, Smith MA, Rees WA, Bennett JL, She D, Katz E, et al. Serum glial fibrillary acidic protein: a neuromyelitis optica spectrum disorder biomarker. *Ann Neurol.* (2021) 89:895–910. doi: 10.1002/ana.26067
76. Schindler P, Grittner U, Oechtering J, Leppert D, Siebert N, Duchow AS, et al. Serum GFAP and NfL as disease severity and prognostic biomarkers in patients with aquaporin-4 antibody-positive neuromyelitis optica spectrum disorder. *J Neuroinflamm.* (2021) 18:105. doi: 10.1186/s12974-021-02138-7
77. Chang X, Huang W, Wang L, ZhangBao J, Zhou L, Lu C, et al. Serum neurofilament light and GFAP are associated with disease severity in inflammatory disorders with aquaporin-4 or myelin oligodendrocyte glycoprotein antibodies. *Front Immunol.* (2021) 12:647618. doi: 10.3389/fimmu.2021.647618
78. Zhang T-X, Chen J-S, Du C, Zeng P, Zhang H, Wang X, et al. Longitudinal treatment responsiveness on plasma neurofilament light chain and glial fibrillary acidic protein levels in neuromyelitis optica spectrum disorder. *Ther Adv Neurol Disord.* (2021) 14:17562864211054952. doi: 10.1177/17562864211054952
79. Kleiter I, Hellwig K, Berthele A, Kümpfel T, Linker RA, Hartung H-P, et al. Failure of natalizumab to prevent relapses in neuromyelitis optica. *Arch Neurol.* (2012) 69:239–45. doi: 10.1001/archneurol.2011.216
80. Min J-H, Kim BJ, Lee KH. Development of extensive brain lesions following fingolimod (FTY720) treatment in a patient with neuromyelitis optica spectrum disorder. *Multiple Sclerosis J.* (2012) 18:113–5. doi: 10.1177/1352458511431973
81. Palace J, Leite MI, Nairne A, Vincent A. Interferon beta treatment in neuromyelitis optica: increase in relapses and aquaporin 4 antibody titers. *Arch Neurol.* (2010) 67:1016–7. doi: 10.1001/archneurol.2010.188
82. Waters PJ, Pittock SJ, Bennett JL, Jarius S, Weinshenker BG, Wingerchuk DM. Evaluation of aquaporin-4 antibody assays. *Clin Exp Neuroimmunol.* (2014) 5:290–303. doi: 10.1111/cen3.12107
83. Waters PJ, McKeon A, Leite MI, Rajasekharan S, Lennon VA, Villalobos A, et al. Serologic diagnosis of NMO: a multicenter comparison of aquaporin-4-IgG assays. *Neurology.* (2012) 78:665–71. doi: 10.1212/WNL.0b013e318248dec1
84. Cohen M, De Sèze J, Marignier R, Lebrun C. False positivity of anti aquaporin-4 antibodies in natalizumab-treated patients. *Mult Scler.* (2016) 22:1231–4. doi: 10.1177/1352458516630823
85. Takai Y, Misu T, Suzuki H, Takahashi T, Okada H, Tanaka S, et al. Staging of astrocytopathy and complement activation in neuromyelitis optica spectrum disorders. *Brain.* (2021) 144:2401–15. doi: 10.1093/brain/awab102
86. Misu T, Höftberger R, Fujihara K, Wimmer I, Takai Y, Nishiyama S, et al. Presence of six different lesion types suggests diverse mechanisms of tissue injury in neuromyelitis optica. *Acta Neuropathol.* (2013) 125:815–27. doi: 10.1007/s00401-013-1116-7
87. Masaki K, Suzuki SO, Matsushita T, Matsuoka T, Imamura S, Yamasaki R, et al. Connexin 43 astrocytopathy linked to rapidly progressive multiple sclerosis and neuromyelitis optica. *PLoS ONE.* (2013) 8:e72919. doi: 10.1371/journal.pone.0072919
88. Lucchinetti CF, Mandler RN, McGavern D, Bruck W, Gleich G, Ransohoff RM, et al. A role for humoral mechanisms in the pathogenesis of Devic's neuromyelitis optica. *Brain.* (2002) 125:1450–61. doi: 10.1093/brain/awf151
89. Hayashida S, Masaki K, Yonekawa T, Suzuki SO, Hiwatashi A, Matsushita T, et al. Early and extensive spinal white matter involvement in neuromyelitis optica. *Brain Pathol.* (2017) 27:249–65. doi: 10.1111/bpa.12386
90. Brück W, Popescu B, Lucchinetti CF, Markovic-Plese S, Gold R, Thal DR, et al. Neuromyelitis optica lesions may inform multiple sclerosis heterogeneity debate. *Ann Neurol.* (2012) 72:385–94. doi: 10.1002/ana.23621
91. Kessler RA, Mealy MA, Levy M. Early indicators of relapses vs pseudorelapses in neuromyelitis optica spectrum disorder. *Neurol Neuroimmunol Neuroinflamm.* (2016) 3:e269. doi: 10.1212/NXI.0000000000000269
92. Camera V, Holm-Mercer L, Ali AAH, Messina S, Horvat T, Kuker W, et al. Frequency of new silent MRI lesions in myelin oligodendrocyte glycoprotein antibody disease and aquaporin-4 antibody neuromyelitis optica spectrum disorder. *JAMA Network Open.* (2021) 4:e2137833–e. doi: 10.1001/jamanetworkopen.2021.37833
93. Cree BAC, Bennett JL, Kim HJ, Weinshenker BG, Pittock SJ, Wingerchuk DM, et al. Inebilizumab for the treatment of neuromyelitis optica spectrum disorder (N-MOmentum): a double-blind, randomised placebo-controlled phase 2/3 trial. *Lancet.* (2019) 394:1352–63. doi: 10.1016/S0140-6736(19)31817-3
94. Meyer-Moock S, Feng Y-S, Maeurer M, Dippel F-W, Kohlmann T. Systematic literature review and validity evaluation of the expanded disability status scale (EDSS) and the multiple sclerosis functional composite (MSFC) in patients with multiple sclerosis. *BMC Neurol.* (2014) 14:58. doi: 10.1186/1471-2377-14-58
95. Cohen M, Bresch S, Thommel Rocchi O, Morain E, Benoit J, Levraut M, et al. Should we still only rely on EDSS to evaluate disability in multiple sclerosis patients? A study of inter and intra rater reliability. *Multiple Sclerosis Relat Disord.* (2021) 54:103144. doi: 10.1016/j.msard.2021.103144
96. Lee EJ, Lim YM, Kim S, Choi L, Kim H, Kim K, et al. Clinical implication of serum biomarkers and patient age in inflammatory demyelinating diseases. *Ann Clin Transl Neurol.* (2020) 7:992–1001. doi: 10.1002/acn3.51070
97. Akaishi T, Takahashi T, Misu T, Abe M, Ishii T, Fujimori J, et al. Progressive patterns of neurological disability in multiple sclerosis

and neuromyelitis optica spectrum disorders. *Sci Rep.* (2020) 10:13890. doi: 10.1038/s41598-020-70919-w
98. Wingerchuk DM, Pittock SJ, Lucchinetti CF, Lennon VA, Weinshenker BG. A secondary progressive clinical course is uncommon in neuromyelitis optica. *Neurology.* (2007) 68:603–5. doi: 10.1212/01.wnl.0000254502.87233.9a
99. Correale J, Gaitán MI, Ysrraelit MC, Fiol MP. Progressive multiple sclerosis: from pathogenic mechanisms to treatment. *Brain.* (2017) 140:527–46. doi: 10.1093/brain/aww258
100. Cree BAC, Hollenbach JA, Bove R, Kirkish G, Sacco S, Caverzasi E, et al. Silent progression in disease activity-free relapsing multiple sclerosis. *Ann Neurol.* (2019) 85:653–66. doi: 10.1002/ana.25463
101. Ringelstein M, Harmel J, Zimmermann H, Brandt AU, Paul F, Haarmann A, et al. Longitudinal optic neuritis-unrelated visual evoked potential changes in NMO spectrum disorders. *Neurology.* (2020) 94:e407–18. doi: 10.1212/WNL.0000000000008684
102. Pisa M, Ratti F, Vabanesi M, Radaelli M, Guerrieri S, Moiola L, et al. Subclinical neurodegeneration in multiple sclerosis and neuromyelitis optica spectrum disorder revealed by optical coherence tomography. *Mult Scler.* (2020) 26:1197–206. doi: 10.1177/1352458519861603
103. Masuda H, Mori M, Hirano S, Uzawa A, Uchida T, Muto M, et al. Silent progression of brain atrophy in aquaporin-4 antibody-positive neuromyelitis optica spectrum disorder. *J Neurol Neurosurg Psychiatry.* (2022) 93:32–40. doi: 10.1136/jnnp-2021-326386
104. Hauser SL, Bar-Or A, Cohen JA, Comi G, Correale J, Coyle PK, et al. Ofatumumab versus teriflunomide in multiple sclerosis. *New Engl J Med.* (2020) 383:546–57. doi: 10.1056/NEJMoa1917246
105. Landeck L, Kneip C, Reischl J, Asadullah K. Biomarkers and personalized medicine: current status and further perspectives with special focus on dermatology. *Exp Dermatol.* (2016) 25:333–9. doi: 10.1111/exd.12948
106. Khalil M, Pirpamer L, Hofer E, Voortman MM, Barro C, Leppert D, et al. Serum neurofilament light levels in normal aging and their association with morphologic brain changes. *Nat Commun.* (2020) 11:812. doi: 10.1038/s41467-020-14612-6
107. Papa L, Brophy GM, Welch RD, Lewis LM, Braga CF, Tan CN, et al. Time course and diagnostic accuracy of glial and neuronal blood biomarkers GFAP and UCH-L1 in a large cohort of trauma patients with and without mild traumatic brain injury. *JAMA Neurol.* (2016) 73:551–60. doi: 10.1001/jamaneurol.2016.0039
108. Thelin EP, Zeiler FA, Ercole A, Mondello S, Büki A, Bellander BM, et al. Serial sampling of serum protein biomarkers for monitoring human traumatic brain injury dynamics: a systematic review. *Front Neurol.* (2017) 8:300. doi: 10.3389/fneur.2017.00300
109. Abdelhak A, Foschi M, Abu-Rumeileh S, Yue JK, D'Anna L, Huss A, et al. Blood GFAP as an emerging biomarker in brain and spinal cord disorders. *Nat Rev Neurol.* (2022) 18:158–72. doi: 10.1038/s41582-021-00616-3
110. Huebschmann NA, Luoto TM, Karr JE, Berghem K, Blennow K, Zetterberg H, et al. Comparing glial fibrillary acidic protein (GFAP) in serum and plasma following mild traumatic brain injury in older adults. *Front Neurol.* (2020) 11:1054. doi: 10.3389/fneur.2020.01054
111. Shahim P, Gren M, Liman V, Andreasson U, Norgren N, Tegner Y, et al. Serum neurofilament light protein predicts clinical outcome in traumatic brain injury. *Sci Rep.* (2016) 6:36791. doi: 10.1038/srep36791
112. Disanto G, Barro C, Benkert P, Naegelin Y, Schädelin S, Giardiello A, et al. Serum neurofilament light: a biomarker of neuronal damage in multiple sclerosis. *Ann Neurol.* (2017) 81:857–70. doi: 10.1002/ana.24954
113. Bittner S, Oh J, Havrdová EK, Tintoré M, Zipp F. The potential of serum neurofilament as biomarker for multiple sclerosis. *Brain.* (2021) 144:2954–63. doi: 10.1093/brain/awab241

Conflict of Interest: The authors declare that the research was conducted in the absence of any commercial or financial relationships that could be construed as a potential conflict of interest.

Publisher's Note: All claims expressed in this article are solely those of the authors and do not necessarily represent those of their affiliated organizations, or those of the publisher, the editors and the reviewers. Any product that may be evaluated in this article, or claim that may be made by its manufacturer, is not guaranteed or endorsed by the publisher.

frontiers in Neurology

REVIEW
published: 23 March 2022
doi: 10.3389/fneur.2022.866824

Serum and Cerebrospinal Fluid Biomarkers in Neuromyelitis Optica Spectrum Disorder and Myelin Oligodendrocyte Glycoprotein Associated Disease

Alessandro Dinoto[1], *Elia Sechi*[2], *Eoin P. Flanagan*[3,4], *Sergio Ferrari*[1], *Paolo Solla*[2], *Sara Mariotto*[1]* *and John J. Chen*[5]

[1] Neurology Unit, Department of Neuroscience, Biomedicine and Movement Sciences, University of Verona, Verona, Italy, [2] Department of Medical, Surgical and Experimental Sciences, University of Sassari, Sassari, Italy, [3] Department of Neurology, Mayo Clinic College of Medicine and Science, Rochester, MN, United States, [4] Department of Laboratory Medicine and Pathology, Mayo Clinic College of Medicine and Science, Rochester, MN, United States, [5] Departments of Ophthalmology and Neurology, Mayo Clinic College of Medicine and Science, Rochester, MN, United States

OPEN ACCESS

Edited by:
Yu Cai,
University of Nebraska Medical Center, United States

Reviewed by:
Tetsuya Akaishi,
Tohoku University, Japan
Dandan Chang,
Diagnostic Radiology Department in The First Affiliated Hospital of Sun Yat-sen University, China

***Correspondence:**
Sara Mariotto
sara.mariotto@gmail.com

Specialty section:
This article was submitted to Multiple Sclerosis and Neuroimmunology, a section of the journal Frontiers in Neurology

Received: 31 January 2022
Accepted: 28 February 2022
Published: 23 March 2022

Citation:
Dinoto A, Sechi E, Flanagan EP, Ferrari S, Solla P, Mariotto S and Chen JJ (2022) Serum and Cerebrospinal Fluid Biomarkers in Neuromyelitis Optica Spectrum Disorder and Myelin Oligodendrocyte Glycoprotein Associated Disease. Front. Neurol. 13:866824. doi: 10.3389/fneur.2022.866824

The term neuromyelitis optica spectrum disorder (NMOSD) describes a group of clinical-MRI syndromes characterized by longitudinally extensive transverse myelitis, optic neuritis, brainstem dysfunction and/or, less commonly, encephalopathy. About 80% of patients harbor antibodies directed against the water channel aquaporin-4 (AQP4-IgG), expressed on astrocytes, which was found to be both a biomarker and a pathogenic cause of NMOSD. More recently, antibodies against myelin oligodendrocyte glycoprotein (MOG-IgG), have been found to be a biomarker of a different entity, termed MOG antibody-associated disease (MOGAD), which has overlapping, but different pathogenesis, clinical features, treatment response, and prognosis when compared to AQP4-IgG-positive NMOSD. Despite important refinements in the accuracy of AQP4-IgG and MOG-IgG testing assays, a small proportion of patients with NMOSD still remain negative for both antibodies and are called "seronegative" NMOSD. Whilst major advances have been made in the diagnosis and treatment of these conditions, biomarkers that could help predict the risk of relapses, disease activity, and prognosis are still lacking. In this context, a number of serum and/or cerebrospinal fluid biomarkers are emerging as potentially useful in clinical practice for diagnostic and treatment purposes. These include antibody titers, cytokine profiles, complement factors, and markers of neuronal (e.g., neurofilament light chain) or astroglial (e.g., glial fibrillary acidic protein) damage. The aim of this review is to summarize current evidence regarding the role of emerging diagnostic and prognostic biomarkers in patients with NMOSD and MOGAD.

Keywords: NMOSD, MOGAD, AQP4, biomarkers, neurofilament light chain, glial fibrillary acid protein, cytokines, complement

INTRODUCTION

The term neuromyelitis optica (NMO) was first used in 1894 by Devic and his fellow, Fernand Gault, to propose a distinct disease entity characterized by simultaneous myelitis and bilateral optic neuritis (1). From Devic's first report until 2004, NMO remained an elusive condition that many thought was a monophasic, more aggressive variant of multiple sclerosis (MS). A major landmark in NMO history was the discovery, by Lennon et al. (2), that sera from patients with NMO outlined microvessels, pia, subpia, and Virchow-Robin spaces when tested on tissue-based indirect immunofluorescence. The putative agent of NMO, aquaporin-4 antibodies (AQP4-IgG), was subsequently found to bind the AQP4 water channel (3). AQP4 is highly expressed in the foot processes of astrocytes, particularly in the domains that interacts with dystrophin-associated proteins and microvessels. The discovery of AQP4-IgG led to the evidence that (1) NMO with positivity for AQP4-IgG is a predominantly an astrocytopathy, and (2) AQP4-IgG is both the pathogenetic cause and the biomarker that defines a distinct disorder which differs from MS.

Whilst NMO was initially defined by the occurrence of longitudinally extensive transverse myelitis (LETM) and optic neuritis, the development of more specific assays, particularly cell-based assays (CBAs) with transfected HEK-293 cells expressing AQP4 (4), led to the realization that the spectrum of disorders associated with AQP4-IgG was broader than previously thought, encompassing limited forms of the disease (e.g., isolated optic neuritis or isolated myelitis), and also brain and brainstem involvement (previously regarded as an exclusion criteria for NMO). These concepts were reflected by the evolution of the diagnostic criteria in 2006 (5) and 2015 (6), the latter emphasizing the importance of AQP4-IgG serostatus, and the adoption of the new nomenclature of "neuromyelitis optica spectrum disorder" (NMOSD) including both AQP4-IgG seropositive and seronegative cases.

About 20% of patients who are diagnosed with NMOSD according to the 2015 NMOSD criteria are seronegative for AQP4-IgG, and among these seronegative patients, about 30% will bear antibodies directed against myelin oligodendrocyte glycoprotein (MOG), which is predominantly expressed in oligodendrocytes or, more rarely, in soluble isoforms (7). The biological role of MOG is still unclear and may represent an adhesion molecule. MOG was initially detected by enzyme-linked immunosorbent assay (ELISA) and immunoblotting, but these assays recognized non-native and non-pathogenic MOG epitopes, probably due to missing glycosylation and incorrect antigen structure. Consequently, MOG antibodies were detected on these older assays with great heterogeneity in patients with MS and were initially thought to represent a biomarker of demyelination (8, 9). The development of CBAs that recognize the native MOG conformation allowed to define the distinct phenotype of this condition, in particular when a high titer cut-off value is used (10–13). These advances have led to the development of specific diagnostic criteria that required both the presence of a compatible clinical phenotype including myelitis, optic neuritis, acute disseminated encephalomyelitis (ADEM) or brainstem syndromes and MOG-IgG positivity tested through a conformational assay (14, 15). The accumulating evidence of differences in clinical-MRI features, relapse risk, treatment, and outcome led to the concept that patients with MOG antibodies are affected by a distinct syndrome that differs from MS and AQP4-IgG-seropositive NMOSD. The term MOG antibody-associated disease (MOGAD) was thus coined to characterize these patients with autoimmune oligodendrocytopathy (16).

Despite advances in MOG and AQP4 antibody testing, up to 30% of patients with NMOSD remain seronegative for these antibodies. Seronegative NMOSD remains an elusive condition that poses relevant challenges to clinicians in terms of diagnosis and treatment because of its variable prognosis and outcomes (**Figure 1**).

Over the last few years, different studies have focused on the clinical and paraclinical characterization of NMOSD and MOGAD as distinct demyelinating disorders, but, despite the recent advances, many questions still remain unanswered. The disease course of these conditions, particularly of seronegative NMOSD and MOGAD patients, is unpredictable, with 50% of patients having a monophasic course. There are currently no clinical, paraclinical, or radiological markers that can predict a monophasic or relapsing disease course, which could require different therapeutic choices. In a similar yet different perspective, although the relapsing course of AQP4-IgG seropositive NMOSD always requires immunosuppressive drugs, there are no clinical predictors of treatment response.

In this uncertain setting, the identification of reproducible, repeatable, and easily accessible biomarkers could be of utmost relevance to guide clinicians in these diagnostic and therapeutical challenges.

DIAGNOSTIC CRITERIA AND ASSAYS FOR DIAGNOSING NMOSD AND MOGAD

Neuromyelitis Optica Spectrum Disorder

Based on the most recent 2015 NMOSD diagnostic criteria, the diagnosis of AQP4-IgG NMOSD requires the presence of (i) 1 clinical core feature including optic neuritis, acute transverse myelitis, APS, acute brainstem syndrome, narcolepsy or acute diencephalic lesion or symptomatic cerebral syndrome with typical NMOSD brain lesions, (ii) positive testing for AQP4-IgG (CBAs are recommended), and (iii) the exclusion of alternative diagnoses such as MS, sarcoidosis, infections, neoplasms, and paraneoplastic disorders. The diagnosis of seronegative NMOSD relies on the presence of at least two different clinical manifestations of NMOSD, one being ON, transverse myelitis or AP, with evidence of consistent demyelinating lesions on MRI and negativity of AQP4-IgG tested with the best available assay (6). CSF analysis usually demonstrates pleocytosis (observed in up to 51% of cases), whereas CSF restricted oligoclonal bands are found in only about 16% of patients (17).

AQP4-IgG can be detected using different laboratory techniques such as live- or fixed-CBAs revealed using immunofluorescence or flow-cytometry/fluorescence-activated-cell-sorting (FACS), ELISA or tissue-based assays. These assays,

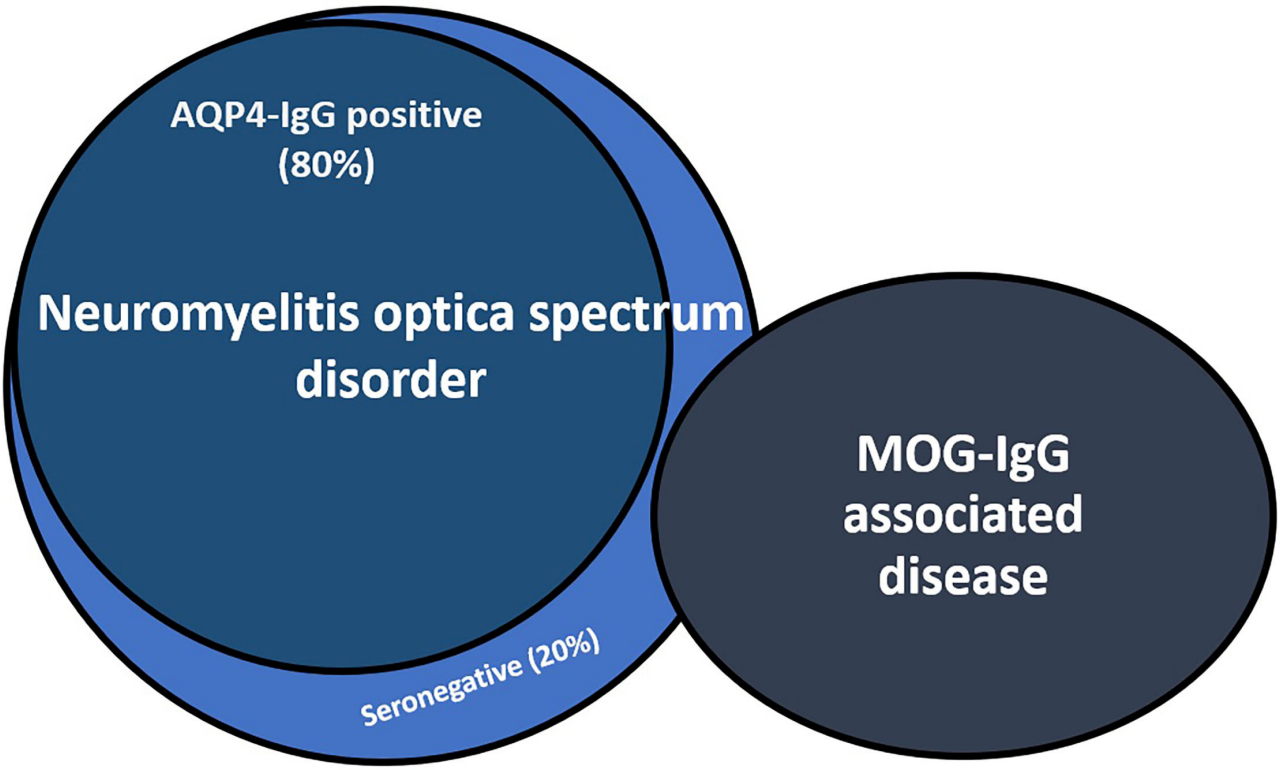

FIGURE 1 | Relationship between aquaporin-4-IgG seropositive and seronegative neuromyelitis optica spectrum disorder (NMOSD) and myelin oligodendrocyte glycoprotein antibody-associated disease (MOGAD). About 30% of NMOSD seronegative patients results positive for MOG-IgG. AQP4-IgG, aquaporin-4 antibodies; MOG-IgG, myelin oligodendrocyte glycoprotein antibodies.

with the exception of tissue-based assays, recognize one of the two isoforms of AQP4, i.e., M1 or M23. The presence of antibodies against each specific isoform has not been associated with different clinical features or outcomes (18). The comparison between diagnostic assays have proved that CBAs, either live or fixed, are the most accurate test for the detection of AQP4-IgG (accuracy: 99.3%) and that M23 expressing cells may perform better than M1-based assays (4, 19). Therefore, live CBAs which use the M1 isoform are the most accurate diagnostic test.

Since the detection of AQP4-IgG is fundamental for treatment decisions, assays such as tissue-based assays and ELISA, whose sensitivity ranges between 60 and 78% and may lead to false negative results (20), are not preferred. Indeed, some patients that tested positive on ELISA but negative with CBA had alternative diagnoses identified suggesting a potential for false positivity (21). Even though early reports preferred immunofluorescence over FACS (19), live cell-based assays (either live or fixed) either detected by FACS or by visual immunofluorescence have very high specificity (22). Immunohistochemistry may be useful to detect the typical AQP4-IgG staining patterns on rodent tissue composite, but then AQP4-IgG presence should be confirmed using CBAs (23).

Finally, CSF testing for AQP4-IgG is not routinely recommended since it is less sensitive than serum testing (24). Indeed, almost all CSF positive patients are positive in serum at high titers (24).

Myelin-Oligodendrocyte Glycoprotein Antibody-Associated Disease

The diagnosis of MOGAD relies on MOG-IgG detection by CBA in patients with compatible clinical-MRI phenotypes, including ADEM or encephalitis, brainstem syndromes, transverse myelitis (often longitudinally extensive with central gray and conus involvement), and ON (typically longitudinally extensive with >50% of the optic nerve length affected often accompanied by perioptic gadolinium enhancement on MRI). The ON attacks are usually associated with optic disc edema and can be bilateral, recurrent, and show steroid dependence. Pleocytosis is found in 38–55% of patients while CSF restricted oligoclonal bands are rarely detected in this condition (6–12% of patients) (25–28).

Testing for MOG-IgG in serum through CBAs, both with FACS or visual based indirect immunofluorescence, using full-length human MOG and Fc or IgG1 as secondary antibodies is recommended, although CSF testing may help in cases of patients with a negative serum test and phenotype suggestive of MOGAD (14, 15, 29).

The diagnosis of MOGAD strongly relies on MOG-IgG detection so that the accuracy of diagnostic assays is of utmost importance. According to a multicenter international

comparative study (30), live-CBAs (with either FACS or immunofluorescence detection) have the greatest concordance (96%), while fixed-CBAs show a slightly lower value (90%) for the diagnosis of MOGAD. ELISA showed no concordance and was unable to distinguish positive and negative patients and thus this method should not be used for diagnostic purposes of MOGAD. Unfortunately, concordance was overall low even for CBAs for sera with borderline/low positivity, which highlights the importance of testing MOG-IgG only when the pre-test probability is high, in order to avoid false-positive results (31). Although diagnostic criteria do not recommend testing MOG-IgG in CSF, some recent studies have reported some patients with MOG-IgG positivity only in the CSF (not serum) who had a clinical and neuropathological MOGAD phenotype (29, 32). Therefore, seronegative patients whose clinical phenotypes are strongly suspicious for MOGAD may benefit from MOG-IgG testing in the CSF, because up to 4–7% of these patients may harbor CSF-restricted antibodies. Patients with CSF restricted MOG-IgG have similar clinical phenotype in comparison with seropositive ones, with the notable exception of isolated optic neuritis, which is uncommon in patients with CSF-restricted MOG-IgG (29, 33, 34). Finally, MOG isoforms (7) and IgG subclasses (35) binding analysis have been performed, but they are currently used for research purposes only.

POTENTIAL BIOMARKERS OF NMOSD AND MOGAD

The role of biomarkers in NMOSD and MOGAD is vital to 1. Aid clinicians in differentiating these conditions from typical MS; 2. Determine the relapse risk; 3. Define disease prognosis; 4. Assist treatment choices.

Current biomarkers are related to different pathogenetic aspects of the diseases and may be broadly classified into these 4 groups (**Figure 2**):

- Antibody titers and persistence
- Complement proteins
- Cytokines and other immunological markers
- Markers of neuronal and astroglial damage.

Antibody Titers and Persistence

Antibody titers reflect antibody concentration and thus may represent a useful biomarker for CNS disorders associated with pathogenic antibodies. Indeed, in other conditions such as NMDA-R encephalitis, higher titers at diagnosis predict a worst outcome and increases in titer in the CSF are associated with relapses (36). MOG-IgG titers have also an important diagnostic role because only high titers have been consistently associated with a defined phenotype, whilst low positive titers me be found in other neurological conditions and they be also found in atypical phenotypes which are not related to MOGAD (31, 37).

However, the role of antibody titers in patients with AQP4-IgG-NMOSD and MOGAD as a prognostic and predictive factor is still debated and differences exist in the potential role of these titers as biomarkers, reflecting the heterogeneity of the underlying biology.

Regarding AQP4-IgG-NMOSD, AQP4-IgG serum titer at the time of attack has been found to be higher in patients presenting with ON (38) and to be associated with the severity and outcome of the event (blindness, length of myelitis on MRI) (39, 40), however these findings were not consistently replicated in other studies (41, 42) and therefore the utility of AQP4-IgG titers in predicting disease is unclear. Furthermore, antibody titers may fluctuate during disease course, particularly during the relapse and remission phase. Several studies demonstrated that patients have higher AQP4-IgG titers at the time of relapse when compared to the remission phase (39, 43–45) however this difference was not seen in all studies (42, 46). An increase of antibody titers may precede relapses, but it is important to note that some patients with high or increasing titers may not experience relapses (43–45, 47). Similarly, patients with low or stable titers, initially thought to be predictive of monophasic disease (39, 48), may also experience relapses (43, 45, 46). Intriguingly, up to 55% of patients may become seronegative during their disease course and experience subsequent relapses with a concomitant increase of AQP4-IgG titers (45), limiting the prognostic role of seronegative conversion after onset.

AQP4-IgG titer in the CSF may have a different dynamic when compared to serum titer. CSF levels of AQP4-IgG are mainly related to the antibody leak in the CNS due to an increased permeability of the blood-brain barrier (49). AQP4-IgG in the CSF may be more frequently detected during attacks (85%) rather than during remission (49) and their ratio to serum titers is also increased in the acute stage (50). CSF titers may decrease after a relapse, whilst serum titers remain stable, and their reduction has been reported to be associated with clinical improvement (51). However, there are less studies on the prognostic utility of AQP4-IgG in the CSF because the difficulty in obtaining CSF and the observation that serum is more sensitive than CSF as a biomarker of NMOSD.

Finally, some studies have found that antibody titers may decrease after immunotherapy (39, 43) and may increase when treatment is suspended (43). The reduction of antibody titers after treatment has been reported to help predict responders to rituximab (44). However, these findings have not been consistently replicated across different studies (41, 46), which limits the use of AQP4-IgG as a clinical biomarker to monitor treatment efficacy.

MOG-IgG titers represent a complex biomarker, influenced by several factors including age and clinical presentation at onset. Studies have suggested that MOG-IgG titers are higher during relapses (13, 26) and may be highest in patients presenting with myelitis (12) or ADEM (10, 52). A study by Cobo-Calvo et al. found that antibody titers at the first episode was related with acute disability at onset, but not with long-term outcome or a predictor of relapse (53). In contrast, a study by Hennes et al. found a high titer at onset predicted a relapsing course in a pediatric cohort (54), and therefore usefulness of the initial MOG-IgG titer level in prognostication remains unclear.

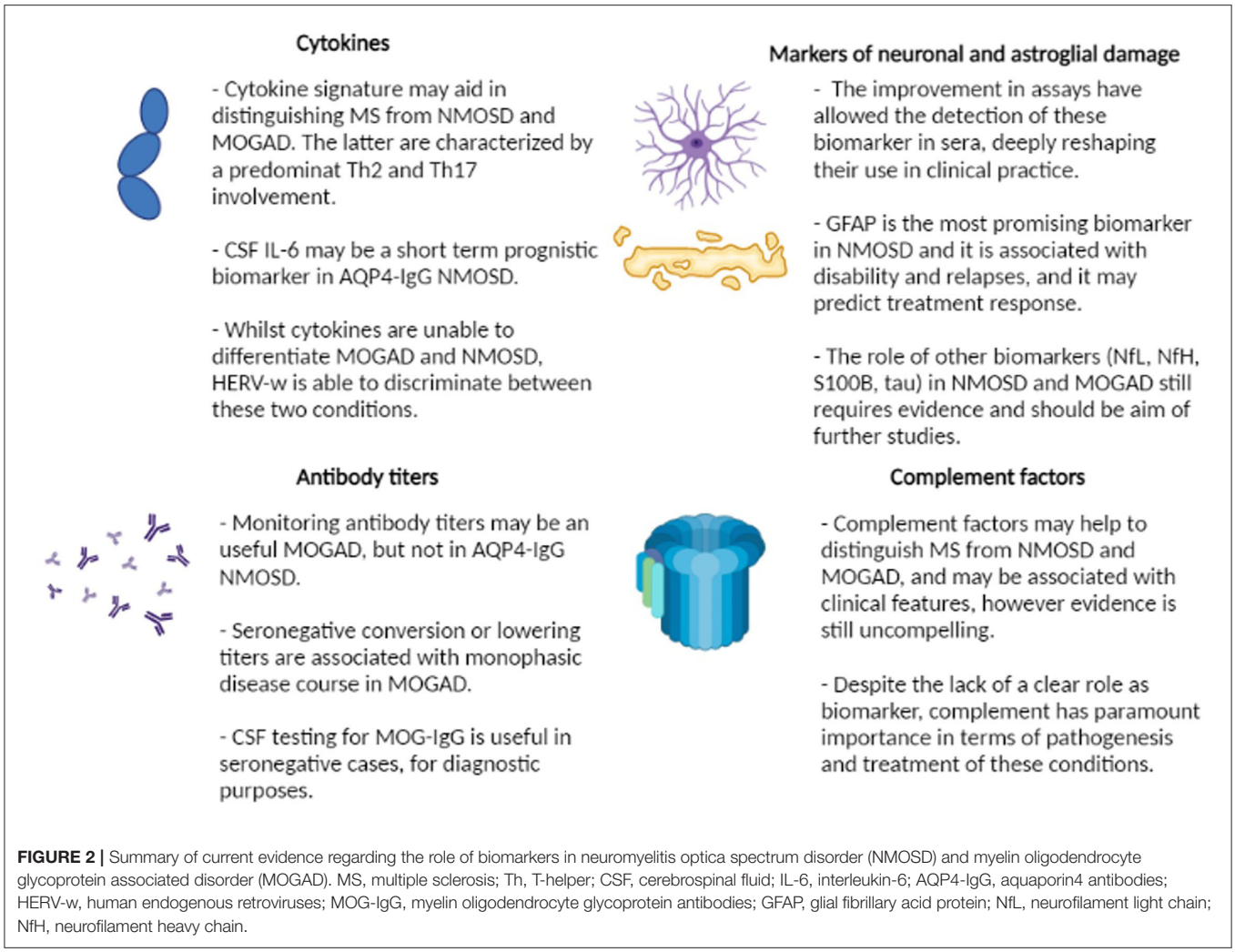

FIGURE 2 | Summary of current evidence regarding the role of biomarkers in neuromyelitis optica spectrum disorder (NMOSD) and myelin oligodendrocyte glycoprotein associated disorder (MOGAD). MS, multiple sclerosis; Th, T-helper; CSF, cerebrospinal fluid; IL-6, interleukin-6; AQP4-IgG, aquaporin4 antibodies; HERV-w, human endogenous retroviruses; MOG-IgG, myelin oligodendrocyte glycoprotein antibodies; GFAP, glial fibrillary acid protein; NfL, neurofilament light chain; NfH, neurofilament heavy chain.

MOG-IgG titer often declines over time after the first demyelinating attack. In pediatric patients with ADEM, MOG-IgG titers are usually high at onset, and may subsequently decline or become seronegative, in about 50% of patients regardless of the onset titer (52, 55). This may have important clinical relevance because seronegative pediatric patients have been shown to have a significantly lower risk of relapse (55, 56). The persistence of high MOG-IgG titers may predict relapses in this setting (54), but up to 72% of persistently positive pediatric ADEM patients will also remain monophasic. When including both adult and pediatric ADEM patients, Lopez et al. found that only 12% of patients that became seronegative experience relapses, compared to 88% of persistently seropositive ones (15). Several other studies, including both pediatric and adult MOGAD patients with a variety of phenotypes, have found that seronegative conversion is associated with a lower relapse risk in MOGAD patients (25, 26, 35, 57). While 50% of pediatric MOGAD patients become seronegative, only roughly 25% of adults become seronegative. It should be noted that while persistent seropositivity may be associated with an increased risk of relapse, not all patients with persistent seropositivity will inevitably experience relapses. Indeed, Juryncyzk et al. found that among 72% of patients that remained persistently seropositive after the first attack, only 59% experienced further relapses (25), thus proving that persistently MOG-IgG seropositivity is not always associated with further clinical events. In addition, some patients that become seronegative can rarely relapse and become seropositive at the time of the relapse (55).

The role of antibody titers in AQP4-IgG-NMOSD and MOGAD is extremely complex and likely differs in the two conditions. The predicting role of AQP4-IgG titers regarding outcomes, disease course or relapses is vastly controversial due to the inconsistency of the results, which may potentially be explained by the different methods used to determine the titer of AQP4-IgG. Some studies used CBAs (39), while others used fluorescence-based immunoprecipitation assay (FIPA) (49) or ELISA (45). Beside methodological differences, it is clear that some relapses in patients with AQP4-IgG-NMOSD occur regardless of AQP4-IgG titer at onset and its fluctuation during the disease course does not always correlate with disease activity.

These features make AQP4-IgG titer a non-optimal biomarker for this condition.

On the contrary, in patients with MOGAD the dynamics of MOG-IgG titers may be helpful in identifying patients that will experience a monophasic disease course since patients that become seronegative will more frequently be monophasic. On the other hand, persistently positive MOG-IgG patients may have a higher chance of relapse, but can also have a monophasic disease course, and therefore, in this setting, antibody titers are less helpful as predictors. Of note, the results found in patients with MOGAD may be more consistent because all recent studies use MOG-IgG testing with conformational CBAs.

Complement Proteins

Both AQP4-IgG and MOG-IgG predominantly belong to the IgG1 subclass and thus may activate the complement cascade. The role of complement activation was noticed even before the discovery of AQP4-IgG (58) and it is now clearly demonstrated (59).

Complement activation and complement-associated cell killing (60) have relevant therapeutic implications in AQP4-IgG NMOSD, including the successful randomized clinical trial of eculizumab in prevention of relapses (61).

On the other hand, the role complement in patients with MOGAD is still a matter of debate (62, 63).

Complement proteins are a potential biomarker of AQP4-IgG NMOSD and have been proposed to be useful to distinguish NMOSD from other demyelinating disorders, such as MS. Indeed, many studies used patients with MS as controls along with patients without inflammatory neurological disorders. The comparison of complement proteins between these groups have regrettably led to inconsistent results. Indeed, an initial study found that C4d and sC5-C9 complex were higher in NMOSD patients in comparison with healthy controls and MS patients (64). Similar results regarding the increase of sC5b-9 complex in serum and CSF were replicated in other studies (65, 66), which failed to give consistent results regarding C3 and C4 proteins. C3 was found to be equal (66, 67) or increased when compared to healthy controls (65). Similarly, C4 was reported to be increased (64) and decreased (65) in NMOSD patients. Kuroda et al. found that CSF concentrations of C3 and C4 did not segregate in the different groups (67). Hoellou et al. found that CSF C3 and C4 were similar in pediatric MS and MOGAD, but C5a was higher in the latter group (68).

More recent studies have systemically assessed complement proteins, activation products and regulators in patients with NMOSD in serum (69) and CSF (70). These studies highlighted that plasmatic C1Inh, C5 may be helpful to distinguish NMOSD vs. healthy controls, whilst C1Inh and C5b–C9 could segregate MS and NMOSD (69). Finally, CSF levels of C3, C4, C5, C9, FH, FHR, and C1Inh may be used to differentiate the two inflammatory conditions (70).

Some studies have reported an association between complement levels and disease activity in patients with AQP4-IgG NMOSD. In particular, serum C3 levels were found to correlate with EDSS (65) and CSF C5a values were associated with MRI activity and delta EDSS (67). In addition, a study by Veszeli et al. suggests complement may be altered, although not activated, even in patients in remission and under disease-modifying treatment (71).

Recent studies have tried to distinguish specific complement signatures in AQP4-IgG NMOSD compared to MOGAD patients. Patients with AQP4-IgG NMOSD had lower (72) or comparable (73) levels of C3 and lower concentration of C4 when compared to patients with MOGAD (72, 73). According to a different study by Hakobayn et al. Bb, C4a and C5a components were higher in AQP4-IgG NMOSD patients, while iC3b and C5b–C9 were higher in MOGAD patients (69). On the contrary, Keller and colleagues surprisingly found that all complement levels with the exception of C3a were higher in patients with MOGAD when compared to NMOSD (63). These discordant findings may be related to the fact that samples were obtained during remission (73) or at first event (72). This study also found that patients with MOGAD have higher complement levels when compared to healthy controls and MS (63). However, the complement levels did not differ between patients with a monophasic or relapsing disease course and did not differ between patients during relapse or in remission (63). Therefore, its role as a biomarker of disease is limited. Future studies are required to confirm complement's role in MOGAD (74).

Overall, complement may be a useful biomarker to discriminate patients with MS, MOGAD, and NMOSD, but studies have been mixed and larger prospective studies are required. Some studies have also demonstrated that complement may be associated with some clinical and radiological indexes of disease activity and severity. However, results among different studies have led to discordant findings, probably due to methodological and sampling issues (e.g., use of CSF or serum, sampling during remission or active disease). Despite these inconsistencies, these studies show that complement may play a key role in the pathogenesis of these disorders and may represent a potential therapeutic target.

Cytokines and Other Immunological Biomarkers

The different pathogenesis between MS and other antibody-mediated demyelinating disorders has led to the question whether cytokine signatures could differ in these conditions, and thus whether cytokines could represent a useful tool in the differential diagnosis.

The importance of studies on cytokines, and in particular interleukin-6 (IL-6), underlies the success of the recent randomized clinical trial on satralizumab, which was found to be more effective in AQP4-IgG NMOSD, but less effective for seronegative NMOSD (75). Similarly, tocilizumab was found to reduce the risk of relapses in both in AQP4-IgG NMOSD and MOGAD (76, 77).

Early studies on "opticospinal multiple sclerosis" (OSMS), which likely were cases of NMOSD, have demonstrated that a discrete number of cytokines, in particular T-helper 2 (Th2) and T-helper 17 (Th17) related ones, could differentiate OSMS from both unaffected patients and patients with other forms of acute myelitis (78) or MS (79).

Among these cytokines, CSF levels of Th2-related IL-6 seem to have a prominent role in patients with NMOSD. Indeed, IL-6 is increased during relapses (80) and it may be a useful biomarker to discriminate between MS and NMOSD (81–85). IL-6 has been shown to correlate with the length of myelitis (83), EDSS (82), particularly in untreated patients (86), and correlate with markers of glial and myelin damage [as glial fibrillary acid protein (GFAP) (84, 86, 87) and myelin basic protein (MBP) (87)]. CSF IL-6 levels may also predict the outcome after a relapse and the occurrence of further short-term relapses (88). Of note, AQP4-IgG seropositive and seronegative NMOSD patients have different concentrations of IL-6 (80, 84), with seropositive patients harboring the highest concentration. In contrast to CSF testing, several studies have shown that measuring IL-6 in serum/plasma is not useful in discriminating between NMOSD and other conditions (84, 85, 89). However, Monteiro et al. (90) demonstrated that plasma concentrations of IL-6 and interleukin-17 (IL-17) are associated with relapses and disability measured with the EDSS score in patients with NMOSD.

Other relevant cytokines analyzed in NMOSD include the Th17 related-ones -IL-8 (85, 86) and IL-17 (82, 86, 89, 90)- and the T-helper regulatory interleukin-10 (IL-10) (84, 87). Individual reports have also highlighted that other chemokines or related molecules, such as CXCL8, CXCL10 (82), CXCL13 (91), BAFF, and APRIL (92), could be useful biomarkers in NMOSD. However, they have been analyzed in only few studies and further evidence is required.

As for MOGAD, studies on cytokines have demonstrated that patients with MOGAD share a similar cytokine signature to that observed in patients with NMOSD, with a predominant involvement of IL-6, IL-8, IL-10, and IL-17 (68, 85, 87, 93) that may be used to distinguish MOGAD from MS but not from NMOSD. Intriguingly, human endogenous retroviruses (HERVs), a novel biomarker that has been studied mainly in MS (94), has shown promising results in terms of differentiating among demyelinating diseases. HERV-w peptides have been found in 78% of patients with MS and in 8% of patients with NMOSD, regardless of AQP4-IgG serostatus (95), suggesting a potential role in differentiating these entities. Moreover, a recent study by Arru et al. found HERV-w peptides in 91% of patients with MOGAD compared to only 32% in AQP4-IgG NMOSD, which suggests it may be a helpful diagnostic biomarker to distinguish between these two conditions (96).

Taken together, the role of cytokines and immunological markers may be useful in NMOSD and MOGAD to predict the short-term outcome and to identify patients that will experience a new attack. However, the role of cytokines, and in particular of IL-6 which has the most solid evidence as a biomarker, is limited by the fact that most of the clinical and prognostic correlations are found with CSF rather than serum IL-6 levels. This limitation is relevant because it prevents monitoring cytokines levels over time and the use of these biomarkers in longitudinal studies.

On the other hand, cytokines levels may be useful to distinguish NMOSD from MS, which has relevant clinical and therapeutical implications. MOGAD and NMOSD share similar cytokines signature and therefore cytokines may not be useful in the differential diagnosis. However, HERV-w peptides have shown promising results in differentiating the two conditions.

Markers of Neuronal and Astroglial Damage

Markers of neuronal and astroglial damage represent a broad spectrum of molecules that are released in the CSF after CNS injury. The two main molecules that have been the most studied within this category are neurofilament light chain (NfL) and GFAP, although other molecules such as astrocytic marker S100B, MBP, neurofilament heavy chain (NfH), and tau proteins have also been analyzed in a few studies in patients with NMOSD and MOGAD.

Briefly, neurofilaments are intracellular proteins involved in radial growth and stability of axons that are released, together with other axonal cytoskeletal proteins, into the CSF after neuroaxonal damage. NfL has been demonstrated to be a promising biomarker (97), useful in different neurological conditions such as MS, dementia, stroke, traumatic brain injury, Parkinson's disease, Huntington disease, encephalitis, peripheral neuropathies, and amyotrophic lateral sclerosis (98–102). On the other hand, GFAP represents the main cytoskeletal protein of mature astrocytes, and it is also involved in regeneration, plasticity, and reactive gliosis (103). GFAP is a promising biomarker in the setting of traumatic brain injury, MS, frontotemporal dementia, and other diseases (104, 105).

Both NfL and GFAP are released in the CSF after axonal or astroglial injury, respectively, and a small proportion of these proteins can also be detected, at lower concentration, in the blood. First- and second-generation assays such as ELISA or immunoblot could detect these biomarkers properly only in the CSF because of the lack of sensitivity. New generation assays (such as electrochemiluminescence and, particularly, single-molecule array -SIMOA-) are able to detect these molecules in the blood with high sensitivity, thus allowing the conduction of longitudinal studies and monitoring of their values over time (99).

Initial studies on patients with NMOSD were performed with ELISA on CSF samples and were thus limited by the lack of longitudinal follow-up or remission phase data, given the difficulties in repeating lumbar punctures outside the setting of an acute event. There are only two studies using ELISA in serum, which provided conflicting results. In particular, Storoni et al. found higher concentrations of serum GFAP in patients with AQP4-IgG related ON (106), while this was not found by Fuji and colleagues (107). Most of these earlier studies, predominantly performed on CSF, showed that the makers of astrocytic damage, GFAP and S100B, were higher in patients with NMOSD when compared to patients with MS or healthy controls (84, 87, 107–112). One recent study that combined GFAP and glutamine synthetase (GS) analyses found that markers of astrocytic damage were higher in patients with AQP4-IgG NMOSD when compared to MS, but also found some seronegative NMOSD patients with high levels of GFAP and GS (113). Other studies have demonstrated that the values of GFAP and S100B are lower

in seronegative patients when compared to AQP4-IgG positive NMOSD patients (87). Given the ability of GFAP to discriminate between NMOSD and MS (112), the increase of GFAP values was proposed as a supportive criterion for NMOSD diagnosis (110). However, the utility of GFAP and S100B in discriminating among MOGAD, AQP4-IgG NMOSD, and double seronegative patients was not consistent according to the few studies which tried to address this issue (111, 112).

Regarding the associations with clinical features, GFAP levels in the CSF have been found to be related to EDSS on relapse (108, 109), EDSS during remission (112), EDSS at 6 months follow-up (109), and the number of spinal cord segments involved (108, 109). S100B values have been associated with the number of spinal cord segments involved (108, 109) and EDSS on relapse (109, 112) and on remission (112). GFAP have been shown to be more elevated in patients with myelitis when compared to those with brain lesions and ON (109, 112) and reduces after treatment (108, 109).

Evidence regarding other biomarkers tested with ELISA on CSF is more limited. MBP was found to be higher in both MOGAD and AQP4-IgG NMOSD patients when compared to MS (87, 111), although this association was not consistent with a previous study (109) showing MBP correlation with EDSS and length of myelitis. NfH values were found to be higher in NMOSD when compared to controls patients (110, 114), but similar to those detected in patients with MS (115). On the other hand, NfL levels were higher in NMOSD in comparison to both healthy controls and patients with MS (115). NfL values correlated with disability in both NMOSD and MS, whilst NfH was associated with disability in MS only. Despite the lack of association with disability, the increase of NfH concentration persisted after relapses in NMOSD (114). Intriguingly, one study analyzing NfL concentration in seronegative NMOSD patients failed to detect differences in comparison with non-inflammatory controls, in contrast to results found in AQP4-IgG NMOSD patients (84).

The advent of next-generation assays, particularly SIMOA, have reshaped the analysis of these biomarkers by allowing a more consistent and reproducible measure in serum, which has the clear advantage of being more accessible than CSF. Recent studies focused on the role of serum GFAP (sGFAP) and NfL (sNfL) during the relapse and remission phase of AQP4-IgG-NMOSD and MOGAD, their association with clinical and paraclinical variables and their role in predicting further relapses.

Most of studies have found higher levels of sGFAP and sNfL in patients with NMOSD and MOGAD compared to healthy controls (116–121), although one study which analyzed samples obtained in sustained clinical remission failed to confirm this finding (122). Intriguingly the few studies which included seronegative NMOSD patients did not find differences of sNfL concentration between seronegative NMOSD patients and healthy controls (116), thus suggesting a different underlying biology.

The role of biomarkers of tissue damage in differentiating MS and other demyelinating disorders is still a matter of debate and data are likely influenced by the timing of sampling (relapse vs. remission). For example, Mariotto et al. found higher concentrations of sNfL in patients with MOGAD and NMOSD when compared to MS in samples obtained mostly during disease activity (116), while Watanabe et al. did not find a difference in sNfL values between MS and NMOSD when samples were obtained during remission (118). Other studies found discordant results with similar levels of sNfL between the two conditions (123) or even higher values in patients with MS (124). On the other hand, most studies have found that sGFAP concentration is higher in NMOSD (118, 124).

As for the difference between patients with NMOSD and MOGAD, one study found that GFAP levels are higher in patients with NMOSD (125), whilst tau and sNfL were comparable. However, other reports did not find any differences between the two conditions in terms of sNfL levels (116, 124) or sGFAP (124). Samples obtained during relapses may help to differentiate between MOGAD and NMOSD. For example, Kim et al. found that tau protein was increased during MOGAD relapses, while sGFAP and sNfL levels were increased during AQP4-IgG NMOSD relapses (125). In addition, the relationship between sGFAP and sNfL (i.e., the sGFAP/sNfL ratio) may be a more specific index of astrocytic damage and may be able to better differentiate these conditions (118, 119, 124) but future larger studies are required to confirm these findings.

Regarding prognosis, sGFAP plays a key role in patients with AQP4-IgG NMOSD and the dynamics of this molecule has been elucidated by a prospective study conducted during the NMO-Momentum trial for inebiliziumab (126). Higher sGFAP levels were found in patients with AQP4-IgG NMOSD, which was also related with age and EDSS. The NMO-Momentum trial found that higher baseline levels of sGFAP was associated with a 3-fold increased risk of subsequent relapses, and within 1 week from a relapse, sGFAP concentration increased and started to decline 5 weeks after the event. The severity of relapse was correlated with the sGFAP concentration. However, it was noted that patients may experience an increase of sGFAP without concomitant relapses, though in these cases minor neurological symptoms (not defined as relapses) or asymptomatic MRI lesions may be detected. The NMO-Momentum trial also showed that treatment with inebilizumab reduced the concentration of sGFAP in treated patients and reduced the risk of relapse. Intriguingly, patients may experience relapses during treatment with inebilizumab, however sGFAP concentrations do not significantly increase, suggesting that relapses on treatment may induce less astrocytic damage or may be a reflection of inebilizumab stabilizing the blood-brain barrier (126).

Other studies in AQP4-IgG NMOSD have also demonstrated that sGFAP is higher during relapses (118, 119, 121, 124, 125), that higher concentration of sGFAP may predict the occurrence of relapses (118, 122), and that sGFAP concentration may discriminate between stable and active disease (119, 121, 125). sGFAP concentrations decrease over time after a relapse (119) but may remain elevated during the remission stage (118, 121) and then normalize after 3–4 months (122, 127). Of note, sGFAP levels may subtly increase during inter-attack periods (127) or may

increase over time in absence of immunotherapy (119), suggesting possible subclinical ongoing astrocytic damage in AQP4-IgG NMOSD.

Regarding the role of sNfL in AQP4-IgG NMOSD, most studies have found that serum sNfL to be increased during relapses (121, 125) and to slowly decrease over time (119, 127) or normalize after treatment (118, 121), reaching comparable levels to that observed in healthy controls in sustained remission (122). However, one single study detected stable sNfL values during relapses (124).

Finally, serum sGFAP values have been associated with EDSS score (118, 121–125), Multiple Sclerosis Composite Scale (122), the occurrence of myelitis (118, 124), and a recent relapse (118, 121). Conversely, serum sNfL have been associated with EDSS only (118, 121, 123, 124).

The role of these biomarkers in patients with MOGAD is less defined. sNfL and sGFAP may increase during relapses (124) and the increase of sNfL is more marked in severe attacks (117). In patients with multiple relapses, sNfL have been found to be increased only during the first relapse and then remain stable, supporting the role of the first attack in determining long-term disability (128). On the contrary, one aforementioned study has demonstrated that only serum tau, and not sGFAP or sNfL, increases during relapses (119). Another study found that sNfL increases during relapses among patients with MOGAD, but sGFAP did not increase (129). As in NMOSD, sNfL levels reduce over time after an acute attack (128) and during remission they may be similar to controls (122, 129).

In MOGAD, sNfL values are associated with EDSS (117, 124, 125), are higher in pediatric patients presenting with encephalopathy (130) and both sGFAP and sNfL have been found to be associated with a recent brain lesion (124). In addition, tau concentration has been found to be associated with EDSS (125). Serum biomarkers may also have a diagnostic role when associated with neuroradiological findings: indeed, the ratio between sNfL and the T2 lesion area on MRI (neurofilament light chain/area ratio) may discriminate between spinal cord infarction and other acute myelopathies, such as NMOSD or MOGAD (131).

Overall, current evidence shows that molecules related to neuronal and astroglial damage are promising biomarkers in NMOSD, and particularly GFAP seems to be a reliable marker of disease activity. The improvements in the diagnostic assays have allowed to study the dynamics of these molecules in the serum during and after relapses, and even in remission. The presence of baseline elevated concentrations of GFAP predicts the occurrence of relapses in NMOSD and thus it may be used to identify patients that may require more aggressive treatment. Similarly, GFAP could be used as a marker of treatment response to promptly identify non-responders. On the other hand, the increase of GFAP before a relapse may be useful to monitor patients without therapy and to promptly treat them when increasing concentrations of this biomarker are detected. Finally, GFAP may be useful to determine subclinical progression in patients with NMOSD. Despite these promising studies, the role of GFAP in clinical practice has not been established and reliable cut-offs are not yet available to determine remission and relapses. Although some studies tried to determine clear cut-offs for disease status, the included populations were small and methodological issues may hinder the reproducibility of these values.

The role of these biomarkers in patients with MOGAD is still uncertain and requires more clinical evidence, although tau and NfL may be promising molecules, given their association with disability, even though their association with relapses is still unclear and deserves further study. Finally, GFAP and NfL may be useful markers to differentiate MS from MOGAD and NMOSD, although studies have been mixed. The adoption of the GFAP/NfL ratio, which represent a marker of astrocytic damage that accounts for both NfL and GFAP, may better discriminate among different demyelinating disorders, but needs to be explored in future studies.

CONCLUSIONS

Ideal biomarkers should be precise, easily accessible, reproducible, and most importantly be able to predict the disease course and aid in the differential diagnosis. Biomarkers are an emerging and promising field that may help clinicians in the management of patients with MOGAD and NMOSD, and their incorporation as surrogate endpoints in clinical trials is warranted.

Regarding the application of biomarkers in the clinical practice, this review has shown that (a) seronegative conversion of MOG-IgG may be helpful in MOGAD to distinguish monophasic and relapsing patients, so that monitoring MOG-IgG titer over time is recommended. On the contrary, evidence does not support monitoring in AQP4-IgG in NMOSD. Even if CSF testing of AQP4-IgG and MOG-IgG is not routinely indicated, there is growing evidence that evaluating for MOG-IgG in the CSF may be useful to identify rare patients with MOGAD when serum is unrevealing; (b) complement proteins shed light on the pathogenesis of antibody-mediated demyelinating disorders and may support the use of complement-directed therapies, but their role as biomarkers has yet to be defined; (c) cytokines, and in particular IL-6, may be useful to distinguish NMOSD/MOGAD from MS, and may be useful as a short-term prognostic factor; (d) given the advances in assay sensitivity allowing evaluation of proteins released after astroglial or neuronal damage in the serum, these markers of injury are becoming promising biomarkers in these conditions. In particular, serum levels of GFAP have a strong association with AQP4-IgG NMOSD disease course, whilst the contrasting data related to MOGAD and seronegative NMOSD patients warrants additional future studies.

AUTHOR CONTRIBUTIONS

AD wrote the first draft of the manuscript. SM and JC performed the first revision of the manuscript including critical additional data. All the authors performed additional

revision to the manuscript and gave critical intellectual content. All authors contributed to the article and approved the submitted version.

FUNDING

This study was supported by personal research funds of the SM.

REFERENCES

1. Devic E. *Myélite aiguë dorse-lombaire avec névrite optique, autopsie*. Congrés français de médecine (Premiere Session, Lyon). Lyon (1895). p. 434–9.
2. Lennon PVA, Wingerchuk DM, Kryzer TJ, Pittock SJ, Lucchinetti CF, Fujihara K, et al. A serum autoantibody marker of neuromyelitis optica: distinction from multiple sclerosis. *Lancet.* (2004) 364:2106–12. doi: 10.1016/S0140-6736(04)17551-X
3. Lennon VA, Kryzer TJ, Pittock SJ, Verkman AS, Hinson SR. IgG marker of optic-spinal multiple sclerosis binds to the aquaporin-4 water channel. *J Exp Med.* (2005) 202:473–7. doi: 10.1084/jem.20050304
4. Waters PJ, Pittock SJ, Bennett JL, Jarius S, Weinshenker BG, Wingerchuk DM. Evaluation of aquaporin-4 antibody assays. *Clin Exp Neuroimmunol.* (2014) 5:290–303. doi: 10.1111/cen3.12107
5. Wingerchuk DM, Lennon VA, Pittock SJ, Lucchinetti CF, Weinshenker BG. Revised diagnostic criteria for neuromyelitis optica. *Neurology.* (2006) 66:1485–9. doi: 10.1212/01.wnl.0000216139.44259.74
6. Wingerchuk DM, Banwell B, Bennett JL, Cabre P, Carroll W, Chitnis T, et al. International consensus diagnostic criteria for neuromyelitis optica spectrum disorders. *Neurology.* (2015) 85:177–89. doi: 10.1212/WNL.0000000000001729
7. Schanda K, Peschl P, Lerch M, Seebacher B, Mindorf S, Ritter N, et al. Differential binding of autoantibodies to MOG isoforms in inflammatory demyelinating diseases. *Neurol Neuroimmunol Neuroinflam.* (2021) 8:1–13. doi: 10.1212/NXI.0000000000001027
8. Berger T, Rubner P, Schautzer F, Egg R, Ulmer H, Mayringer I, et al. Antimyelin antibodies as a predictor of clinically definite multiple sclerosis after a first demyelinating event. *N Engl J Med.* (2003) 349:139–45. doi: 10.1056/NEJMoa022328
9. O'Connor KC, Appel H, Bregoli L, Call ME, Catz I, Chan JA, et al. Antibodies from inflamed central nervous system tissue recognize myelin oligodendrocyte glycoprotein. *J Immunol.* (2005) 175:1974–82. doi: 10.4049/jimmunol.175.3.1974
10. Di Pauli F, Mader S, Rostasy K, Schanda K, Bajer-Kornek B, Ehling R, et al. Temporal dynamics of anti-MOG antibodies in CNS demyelinating diseases. *Clin Immunol.* (2011) 138:247–54. doi: 10.1016/j.clim.2010.11.013
11. Waters P, Woodhall M, O'Connor KC, Reindl M, Lang B, Sato DK, et al. MOG cell-based assay detects non-MS patients with inflammatory neurologic disease. *Neurol Neuroimmunol NeuroInflammation.* (2015) 2:e89. doi: 10.1212/NXI.0000000000000089
12. Jarius S, Ruprecht K, Kleiter I, Borisow N, Asgari N, Pitarokoili K, et al. MOG-IgG in NMO and related disorders: a multicenter study of 50 patients. Part 2: epidemiology, clinical presentation, radiological and laboratory features, treatment responses, long-term outcome. *J Neuroinflammation.* (2016) 13:280. doi: 10.1186/s12974-016-0718-0
13. Jarius S, Ruprecht K, Kleiter I, Borisow N, Asgari N, Pitarokoili K, et al. MOG-IgG in NMO and related disorders: a multicenter study of 50 patients. Part 1: Frequency, syndrome specificity, influence of disease activity, long-term course, association with AQP4-IgG, and origin. *J Neuroinflammation.* (2016) 13:279. doi: 10.1186/s12974-016-0717-1
14. Jarius S, Paul F, Aktas O, Asgari N, Dale RC, De Seze J, et al. Mog encephalomyelitis: international recommendations on diagnosis and antibody testing. *Nervenarzt.* (2018) 89:1388–99. doi: 10.1007/s00115-018-0607-0
15. Lopez-Chiriboga AS, Majed M, Fryer J, Dubey D, McKeon A, Flanagan EP, et al. Association of MOG-IgG serostatus with relapse after acute disseminated encephalomyelitis and proposed diagnostic criteria for MOG-IgG-associated disorders. *JAMA Neurol.* (2018) 75:1355–63. doi: 10.1001/jamaneurol.2018.1814
16. Marignier R, Hacohen Y, Cobo-Calvo A, Pröbstel AK, Aktas O, Alexopoulos H, et al. Myelin-oligodendrocyte glycoprotein antibody-associated disease. *Lancet Neurol.* (2021) 20:762–72. doi: 10.1016/S1474-4422(21)00218-0
17. Jarius S, Paul F, Franciotta D, Ruprecht K, Ringelstein M, Bergamaschi R, et al. Cerebrospinal fluid findings in aquaporin-4 antibody positive neuromyelitis optica: results from 211 lumbar punctures. *J Neurol Sci.* (2011) 306:82–90. doi: 10.1016/j.jns.2011.03.038
18. Kitley J, Woodhall M, Leite MI, Palace J, Vincent A, Waters P. Aquaporin-4 antibody isoform binding specificities do not explain clinical variations in NMO. *Neurol Neuroimmunol Neuroinflammation.* (2015) 2:e121. doi: 10.1212/NXI.0000000000000121
19. Waters P, Reindl M, Saiz A, Schanda K, Tuller F, Kral V, et al. Multicentre comparison of a diagnostic assay: aquaporin-4 antibodies in neuromyelitis optica. *J Neurol Neurosurg Psychiatry.* (2016) 87:1005–15. doi: 10.1136/jnnp-2015-312601
20. Prain K, Woodhall M, Vincent A, Ramanathan S, Barnett MH, Bundell CS, et al. AQP4 antibody assay sensitivity comparison in the era of the 2015 diagnostic criteria for NMOSD. *Front Neurol.* (2019) 10:1028. doi: 10.3389/fneur.2019.01028
21. Williams JP, Abbatemarco JR, Galli JJ, Rodenbeck SJ, Peterson LK, Haven TR, et al. Aquaporin-4 autoantibody detection by ELISA: a retrospective characterization of a commonly used assay. *Mult Scler Int.* (2021) 2021:8692328. doi: 10.1155/2021/8692328
22. Redenbaugh V, Montalvo M, Sechi E, Buciuc M, Fryer JP, McKeon A, et al. Diagnostic value of aquaporin-4-IgG live cell based assay in neuromyelitis optica spectrum disorders. *Mult Scler.* (2021) 7:20552173211052656. doi: 10.1177/20552173211052656
23. Sechi E, Addis A, Batzu L, Mariotto S, Ferrari S, Conti M, et al. Late presentation of NMOSD as rapidly progressive leukoencephalopathy with atypical clinical and radiological findings. *Mult Scler J.* (2018) 24:685–8. doi: 10.1177/1352458517721661
24. Majed M, Fryer JP, McKeon A, Lennon VA, Pittock SJ. Clinical utility of testing AQP4-IgG in CSF: guidance for physicians. *Neurol Neuroimmunol NeuroInflammation.* (2016) 3:e231. doi: 10.1212/NXI.0000000000000231
25. Jurynczyk M, Messina S, Woodhall MR, Raza N, Everett R, Roca-Fernandez A, et al. Clinical presentation and prognosis in MOG-antibody disease: a UK study. *Brain.* (2017) 140:3128–38. doi: 10.1093/brain/awx276
26. Cobo-Calvo A, Ruiz A, Maillart E, Audoin B, Zephir H, Bourre B, et al. Clinical spectrum and prognostic value of CNS MOG autoimmunity in adults: the MOGADOR study. *Neurology.* (2018) 90:e1858–69. doi: 10.1212/WNL.0000000000005560
27. Sechi E, Buciuc M, Flanagan EP, Pittock SJ, Banks SA, Lopez-Chiriboga AS, et al. Variability of cerebrospinal fluid findings by attack phenotype in myelin oligodendrocyte glycoprotein-IgG-associated disorder. *Mult Scler Relat Disord.* (2021) 47:102638. doi: 10.1016/j.msard.2020.102638
28. Jarius S, Pellkofer H, Siebert N, Korporal-Kuhnke M, Hümmert MW, Ringelstein M, et al. Cerebrospinal fluid findings in patients with myelin oligodendrocyte glycoprotein (MOG) antibodies. Part 1: results from 163 lumbar punctures in 100 adult patients. *J Neuroinflammation.* (2020) 17:261. doi: 10.1186/s12974-020-01824-2
29. Mariotto S, Gajofatto A, Batzu L, Delogu R, Sechi G, Leoni S, et al. Relevance of antibodies to myelin oligodendrocyte glycoprotein in CSF of seronegative cases. *Neurology.* (2019) 93:e1867–72. doi: 10.1212/WNL.0000000000008479
30. Reindl M, Schanda K, Woodhall M, Tea F, Ramanathan S, Sagen J, et al. International multicenter examination of MOG antibody assays. *Neurol Neuroimmunol Neuroinflammation.* (2020) 7:e674. doi: 10.1212/NXI.0000000000000674
31. Sechi E, Buciuc M, Pittock SJ, Chen JJ, Fryer JP, Jenkins SM, et al. Positive predictive value of myelin oligodendrocyte glycoprotein autoantibody testing. *JAMA Neurol.* (2021) 78:741–6. doi: 10.1001/jamaneurol.2021.0912

32. Carta S, Höftberger R, Bolzan A, Bozzetti S, Bonetti B, Scarpelli M, et al. Antibodies to MOG in CSF only: pathological findings support the diagnostic value. *Acta Neuropathol.* (2021) 141:801–4. doi: 10.1007/s00401-021-02286-3
33. Akaishi T, Takahashi T, Misu T, Kaneko K, Takai Y, Nishiyama S, et al. Difference in the source of anti-AQP4-IgG and Anti-MOG-IgG antibodies in CSF in patients with neuromyelitis optica spectrum disorder. *Neurology.* (2021) 97:e1–12. doi: 10.1212/WNL.0000000000012175
34. Kwon YN, Kim B, Kim JS, Mo H, Choi K, Oh S, et al. Myelin oligodendrocyte glycoprotein-immunoglobulin G in the CSF. *Neurol Neuroimmunol Neuroinflammation.* (2022) 9:e1095. doi: 10.1212/NXI.0000000000001095
35. Mariotto S, Ferrari S, Monaco S, Benedetti MD, Schanda K, Alberti D, et al. Clinical spectrum and IgG subclass analysis of anti-myelin oligodendrocyte glycoprotein antibody-associated syndromes: a multicenter study. *J Neurol.* (2017) 264:2420–30. doi: 10.1007/s00415-017-8635-4
36. Gresa-Arribas N, Titulaer MJ, Torrents A, Aguilar E, McCracken L, Leypoldt F, et al. Antibody titres at diagnosis and during follow-up of anti-NMDA receptor encephalitis: a retrospective study. *Lancet Neurol.* (2014) 13:167–77. doi: 10.1016/S1474-4422(13)70282-5
37. Held F, Kalluri SR, Berthele A, Klein AK, Reindl M, Hemmer B. Frequency of myelin oligodendrocyte glycoprotein antibodies in a large cohort of neurological patients. *Mult Scler J.* (2021) 7:20552173211022767. doi: 10.1177/20552173211022767
38. Akaishi T, Takahashi T, Himori N, Fujihara K, Misu T, Abe M, et al. Serum AQP4-IgG level is associated with the phenotype of the first attack in neuromyelitis optica spectrum disorders. *J Neuroimmunol.* (2020) 340:577168. doi: 10.1016/j.jneuroim.2020.577168
39. Takahashi T, Fujihara K, Nakashima I, Misu T, Miyazawa I, Nakamura M, et al. Anti-aquaporin-4 antibody is involved in the pathogenesis of NMO: a study on antibody titre. *Brain.* (2007) 130:1235–43. doi: 10.1093/brain/awm062
40. Kessler RA, Mealy MA, Jimenez-Arango JA, Quan C, Paul F, López R, et al. Anti-aquaporin-4 titer is not predictive of disease course in neuromyelitis optica spectrum disorder: a multicenter cohort study. *Mult Scler Relat Disord.* (2017) 17:198–201. doi: 10.1016/j.msard.2017.08.005
41. Akaishi T, Takahashi T, Nakashima I, Abe M, Ishii T, Aoki M, et al. Repeated follow-up of AQP4-IgG titer by cell-based assay in neuromyelitis optica spectrum disorders (NMOSD). *J Neurol Sci.* (2020) 410:116671. doi: 10.1016/j.jns.2020.116671
42. Isobe N, Yonekawa T, Matsushita T, Kawano Y, Masaki K, Yoshimura S, et al. Quantitative assays for anti-aquaporin-4 antibody with subclass analysis in neuromyelitis optica. *Mult Scler J.* (2012) 18:1541–51. doi: 10.1177/1352458512443917
43. Jarius S, Aboul-Enein F, Waters P, Kuenz B, Hauser A, Berger T, et al. Antibody to aquaporin-4 in the long-term course of neuromyelitis optica. *Brain.* (2008) 131:3072–80. doi: 10.1093/brain/awn240
44. Valentino P, Marnetto F, Granieri L, Capobianco M, Bertolotto A. Aquaporin-4 antibody titration in NMO patients treated with rituximab: a retrospective study. *Neurol Neuroimmunol NeuroInflammation.* (2017) 4:1–10. doi: 10.1212/NXI.0000000000000317
45. Kim W, Lee JE, Li XF, Kim SH, Han BG, Lee B, et al. Quantitative measurement of anti-aquaporin-4 antibodies by enzyme-linked immunosorbent assay using purified recombinant human aquaporin-4. *Mult Scler J.* (2012) 18:578–86. doi: 10.1177/135245851 1424590
46. Jitprapaikulsan J, Fryer JP, Majed M, Smith CY, Jenkins SM, Cabre P, et al. Clinical utility of AQP4-IgG titers and measures of complement-mediated cell killing in NMOSD. *Neurol Neuroimmunol Neuroinflammation.* (2020) 7:e727. doi: 10.1212/NXI.0000000000000727
47. Isobe N, Yonekawa T, Matsushita T, Masaki K, Yoshimura S, Fichna J, et al. Clinical relevance of serum aquaporin-4 antibody levels in neuromyelitis optica. *Neurochem Res.* (2013) 38:997–1001. doi: 10.1007/s11064-013-1009-0
48. Weinshenker BG, Wingerchuk DM, Vukusic S, Linbo L, Pittock SJ, Lucchinetti CF, et al. Neuromyelitis optica IgG predicts relapse after longitudinally extensive transverse myelitis. *Ann Neurol.* (2006) 59:566–9. doi: 10.1002/ana.20770
49. Jarius S, Franciotta D, Paul F, Ruprecht K, Bergamaschi R, Rommer PS, et al. Cerebrospinal fluid antibodies to aquaporin-4 in neuromyelitis optica and related disorders: frequency, origin, diagnostic relevance. *J Neuroinflammation.* (2010) 7:1–8. doi: 10.1186/1742-2094-7-52
50. Sato DK, Callegaro D, De Haidar Jorge FM, Nakashima I, Nishiyama S, Takahashi T, et al. Cerebrospinal fluid aquaporin-4 antibody levels in neuromyelitis optica attacks. *Ann Neurol.* (2014) 76:305–9. doi: 10.1002/ana.24208
51. Dujmovic I, Mader S, Schanda K, Deisenhammer F, Stojsavljevic N, Kostic J, et al. Temporal dynamics of cerebrospinal fluid anti-aquaporin-4 antibodies in patients with neuromyelitis optica spectrum disorders. *J Neuroimmunol.* (2011) 234:124–30. doi: 10.1016/j.jneuroim.2011.01.007
52. Pröbstel AK, Dornmair K, Bittner R, Sperl P, Jenne D, Magalhaes S, et al. Antibodies to MOG are transient in childhood acute disseminated encephalomyelitis. *Neurology.* (2011) 77:580–8. doi: 10.1212/WNL.0b013e318228c0b1
53. Cobo-Calvo A, Sepúlveda M, d'Indy H, Armangué T, Ruiz A, Maillart E, et al. Usefulness of MOG-antibody titres at first episode to predict the future clinical course in adults. *J Neurol.* (2019) 266:806–15. doi: 10.1007/s00415-018-9160-9
54. Hennes EM, Baumann M, Schanda K, Anlar B, Bajer-Kornek B, Blaschek A, et al. Prognostic relevance of MOG antibodies in children with an acquired demyelinating syndrome. *Neurology.* (2017) 89:900–8. doi: 10.1212/WNL.0000000000004312
55. Waters P, Fadda G, Woodhall M, O'Mahony J, Brown RA, Castro DA, et al. Serial anti-myelin oligodendrocyte glycoprotein antibody analyses and outcomes in children with demyelinating syndromes. *JAMA Neurol.* (2020) 77:82–93. doi: 10.1001/jamaneurol.2019.2940
56. Armangue T, Olivé-Cirera G, Martínez-Hernandez E, Sepulveda M, Ruiz-Garcia R, Muñoz-Batista M, et al. Associations of paediatric demyelinating and encephalitic syndromes with myelin oligodendrocyte glycoprotein antibodies: a multicentre observational study. *Lancet Neurol.* (2020) 19:234–46. doi: 10.1016/S1474-4422(19)30488-0
57. Hyun JW, Woodhall MR, Kim SH, Jeong IH, Kong B, Kim G, et al. Longitudinal analysis of myelin oligodendrocyte glycoprotein antibodies in CNS inflammatory diseases. *J Neurol Neurosurg Psychiatry.* (2017) 88:811–7. doi: 10.1136/jnnp-2017-315998
58. Lucchinetti CF, Mandler RN, McGavern D, Bruck W, Gleich G, Ransohoff RM, et al. A role for humoral mechanisms in the pathogenesis of Devic's neuromyelitis optica. *Brain.* (2002) 125:1450–61. doi: 10.1093/brain/awf151
59. Asavapanumas N, Tradtrantip L, Verkman AS. Targeting the complement system in neuromyelitis optica spectrum disorder. *Expert Opin Biol Ther.* (2021) 21:1073–86. doi: 10.1080/14712598.2021.1884223
60. Hinson SR, McKeon A, Fryer JP, Apiwattanakul M, Lennon VA, Pittock SJ. Prediction of neuromyelitis optica attack severity by quantitation of complement-mediated injury to aquaporin-4 -expressing cells. *Arch Neurol.* (2009) 66:1164–7. doi: 10.1001/archneurol.2009.188
61. Pittock SJ, Berthele A, Fujihara K, Kim HJ, Levy M, Palace J, et al. Eculizumab in aquaporin-4–positive neuromyelitis optica spectrum disorder. *N Engl J Med.* (2019) 381:614–25. doi: 10.1056/NEJMoa1900866
62. Höftberger R, Guo Y, Flanagan EP, Lopez-Chiriboga AS, Endmayr V, Hochmeister S, et al. The pathology of central nervous system inflammatory demyelinating disease accompanying myelin oligodendrocyte glycoprotein autoantibody. *Acta Neuropathol.* (2020) 139:875–92. doi: 10.1007/s00401-020-02132-y
63. Keller CW, Lopez JA, Wendel EM, Ramanathan S, Gross CC, Klotz L, et al. Complement activation is a prominent feature of MOGAD. *Ann Neurol.* (2021) 90:976–82. doi: 10.1002/ana.26226
64. Tüzün E, Kürtüncü M, Türkoglu R, Içöz S, Pehlivan M, Birişik Ö, et al. Enhanced complement consumption in neuromyelitis optica and Behçet's disease patients. *J. Neuroimmunol.* (2011) 233:211–5. doi: 10.1016/j.jneuroim.2010.11.010
65. Nytrova P, Potlukova E, Kemlink D, Woodhall M, Horakova D, Waters P, et al. Complement activation in patients with neuromyelitis optica. *J Neuroimmunol.* (2014) 274:185–91. doi: 10.1016/j.jneuroim.2014.07.001
66. Wang H, Wang K, Wang C, Qiu W, Lu Z, Hu X. Increased soluble C5b-9 in CSF of neuromyelitis optica. *Scand J Immunol.* (2014) 79:127–30. doi: 10.1111/sji.12132
67. Kuroda H, Fujihara K, Takano R, Takai Y, Takahashi T, Misu T, et al. Increase of complement fragment C5a in cerebrospinal fluid during

exacerbation of neuromyelitis optica. *J Neuroimmunol.* (2013) 254:178–82. doi: 10.1016/j.jneuroim.2012.09.002
68. Horellou P, Wang M, Keo V, Chrétien P, Serguera C, Waters P, et al. Increased interleukin-6 correlates with myelin oligodendrocyte glycoprotein antibodies in pediatric monophasic demyelinating diseases and multiple sclerosis. *J Neuroimmunol.* (2015) 289:1–7. doi: 10.1016/j.jneuroim.2015.10.002
69. Hakobyan S, Luppe S, Evans DR, Harding K, Loveless S, Robertson NP, et al. Plasma complement biomarkers distinguish multiple sclerosis and neuromyelitis optica spectrum disorder. *Mult Scler J.* (2017) 23:946–55. doi: 10.1177/1352458516669002
70. Zelek WM, Fathalla D, Morgan A, Touchard S, Loveless S, Tallantyre E, et al. Cerebrospinal fluid complement system biomarkers in demyelinating disease. *Mult Scler J.* (2020) 26:1929–37. doi: 10.1177/1352458519887905
71. Veszeli N, Füst G, Csuka D, Trauninger A, Bors L, Rozsa C, et al. A systematic analysis of the complement pathways in patients with neuromyelitis optica indicates alteration but no activation during remission. *Mol Immunol.* (2014) 57:200–9. doi: 10.1016/j.molimm.2013.09.010
72. Qin C, Chen B, Tao R, Chen M, Ma X, Shang K, et al. The clinical value of complement proteins in differentiating AQP4-IgG-positive from MOG-IgG-positive neuromyelitis optica spectrum disorders. *Mult Scler Relat Disord.* (2019) 35:1–4. doi: 10.1016/j.msard.2019.06.035
73. Pache F, Ringelstein M, Aktas O, Kleiter I, Jarius S, Siebert N, et al. C3 and C4 complement levels in AQP4-IgG-positive NMOSD and in MOGAD. *J Neuroimmunol.* (2021) 360:577699. doi: 10.1016/j.jneuroim.2021.577699
74. McCombe JA, Flanagan EP, Chen JJ, Zekeridou A, Lucchinetti CF, Pittock SJ. Investigating the immunopathogenic mechanisms underlying MOGAD. *Ann Neurol.* (2021) 91:299–300. doi: 10.1002/ana.26279
75. Cree BAC, Bennett JL, Kim HJ, Weinshenker BG, Pittock SJ, Wingerchuk DM, et al. Inebilizumab for the treatment of neuromyelitis optica spectrum disorder (N-MOmentum): a double-blind, randomised placebo-controlled phase 2 / 3 trial. *Lancet.* (2019) 394:1352–63. doi: 10.1016/S0140-6736(19)31817-3
76. Araki M, Matsuoka T, Miyamoto K, Kusunoki S, Okamoto T, Murata M, et al. Efficacy of the anti-IL-6 receptor antibody tocilizumab in neuromyelitis optica. *Neurology.* (2014) 82:1302–6. doi: 10.1212/WNL.0000000000000317
77. Ringelstein M, Ayzenberg I, Lindenblatt G, Fischer K, Gahlen A, Novi G, et al. Interleukin-6 receptor blockade in treatment-refractory MOG-IgG–associated disease and neuromyelitis optica spectrum disorders. *Neurol Neuroimmunol Neuroinflammation.* (2022) 9:e1100. doi: 10.1212/NXI.0000000000001100
78. Tanaka M, Matsushita T, Tateishi T, Ochi H, Kawano Y, Mei FJ, et al. Distinct CSF cytokine/chemokine profiles in atopic myelitis and other causes of myelitis. *Neurology.* (2008) 71:974–81. doi: 10.1212/01.wnl.0000326589.57128.c3
79. Ishizu T, Osoegawa M, Mei FJ, Kikuchi H, Tanaka M, Takakura Y, et al. Intrathecal activation of the IL-17/IL-8 axis in opticospinal multiple sclerosis. *Brain.* (2005) 128:988–1002. doi: 10.1093/brain/awh453
80. Uzawa A, Mori M, Ito M, Uchida T, Hayakawa S, Masuda S, et al. Markedly increased CSF interleukin-6 levels in neuromyelitis optica, but not in multiple sclerosis. *J. Neurol.* (2009) 256:2082–4. doi: 10.1007/s00415-009-5274-4
81. Uzawa A, Mori M, Sawai S, Masuda S, Muto M, Uchida T, et al. Cerebrospinal fluid interleukin-6 and glial fibrillary acidic protein levels are increased during initial neuromyelitis optica attacks. *Clin Chim Acta.* (2013) 421:181–3. doi: 10.1016/j.cca.2013.03.020
82. Matsushita T, Tateishi T, Isobe N, Yonekawa T, Yamasaki R, Matsuse D, et al. Characteristic cerebrospinal fluid cytokine/chemokine profiles in neuromyelitis optica, relapsing remitting or primary progressive multiple sclerosis. *PLoS ONE.* (2013) 8:2–9. doi: 10.1371/journal.pone.0061835
83. Kimura A, Takemura M, Saito K, Serrero G, Yoshikura N, Hayashi Y, et al. Increased cerebrospinal fluid progranulin correlates with interleukin-6 in the acute phase of neuromyelitis optica spectrum disorder. *J Neuroimmunol.* (2017) 305:175–81. doi: 10.1016/j.jneuroim.2017.01.006
84. Wei Y, Chang H, Li X, Wang H, Du L, Zhou H, et al. Cytokines and tissue damage biomarkers in first-onset neuromyelitis optica spectrum disorders: significance of interleukin-6. *Neuroimmunomodulation.* (2019) 25:215–24. doi: 10.1159/000494976
85. Hofer LS, Mariotto S, Wurth S, Ferrari S, Mancinelli CR, Delogu R, et al. Distinct serum and cerebrospinal fluid cytokine and chemokine profiles in autoantibody-associated demyelinating diseases. *Mult Scler J.* (2019) 5:205521731984846. doi: 10.1177/2055217319848463
86. Uzawa A, Mori M, Arai K, Sato Y, Hayakawa S, Masuda S, et al. Cytokine and chemokine profiles in neuromyelitis optica: significance of interleukin-6. *Mult Scler.* (2010) 16:1443–52. doi: 10.1177/1352458510379247
87. Kaneko K, Sato DK, Nakashima I, Ogawa R, Akaishi T, Takai Y, et al. CSF cytokine profile in MOG-IgG+ neurological disease is similar to AQP4-IgG+ NMOSD but distinct from MS: a cross-sectional study and potential therapeutic implications. *J Neurol Neurosurg Psychiatry.* (2018) 89:927–36. doi: 10.1136/jnnp-2018-317969
88. Uzawa A, Mori M, Sato Y, Masuda S, Kuwabara S. CSF interleukin-6 level predicts recovery from neuromyelitis optica relapse. *J Neurol Neurosurg Psychiatry.* (2012) 83:339–40. doi: 10.1136/jnnp.2011.241760
89. Wang HH, Dai YQ, Qiu W, Lu ZQ, Peng FH, Wang YG, et al. Interleukin-17-secreting T cells in neuromyelitis optica and multiple sclerosis during relapse. *J Clin Neurosci.* (2011) 18:1313–7. doi: 10.1016/j.jocn.2011.01.031
90. Monteiro C, Fernandes G, Kasahara TM, Barros PO, Dias ASO, Araújo CRA, et al. The expansion of circulating IL-6 and IL-17-secreting follicular helper T cells is associated with neurological disabilities in neuromyelitis optica spectrum disorders. *J Neuroimmunol.* (2019) 330:12–8. doi: 10.1016/j.jneuroim.2019.01.015
91. Zhong X, Wang H, Dai Y, Wu A, Bao J, Xu W, et al. Cerebrospinal fluid levels of CXCL13 are elevated in neuromyelitis optica. *J Neuroimmunol.* (2011) 240–1:104–8. doi: 10.1016/j.jneuroim.2011.10.001
92. Wang H, Wang K, Zhong X, Qiu W, Dai Y, Wu A, et al. Cerebrospinal fluid BAFF and APRIL levels in neuromyelitis optica and multiple sclerosis patients during relapse. *J Clin Immunol.* (2012) 32:1007–11. doi: 10.1007/s10875-012-9709-9
93. Kothur K, Wienholt L, Tantsis EM, Earl J, Bandodkar S, Prelog K, et al. B cell, Th17, and neutrophil related cerebrospinal fluid cytokine/chemokines are elevated in MOG antibody associated demyelination. *PLoS ONE.* (2016) 11:e0149411. doi: 10.1371/journal.pone.0149411
94. Arru G, Leoni S, Pugliatti M, Mei A, Serra C, Delogu LG, et al. Natalizumab inhibits the expression of human endogenous retroviruses of the W family in multiple sclerosis patients: a longitudinal cohort study. *Mult Scler.* (2014) 20:174–82. doi: 10.1177/1352458513494957
95. Arru G, Sechi E, Mariotto S, Farinazzo A, Mancinelli C, Alberti D, et al. Antibody response against HERV-W env surface peptides differentiates multiple sclerosis and neuromyelitis optica spectrum disorder. *Mult Scler J.* (2017) 3:2055217317742425. doi: 10.1177/2055217317742425
96. Arru G, Sechi E, Mariotto S, Zarbo IR, Ferrari S, Gajofatto A, et al. Antibody response against HERV-W in patients with MOG-IgG associated disorders, multiple sclerosis and NMOSD. *J Neuroimmunol.* (2020) 338:577110. doi: 10.1016/j.jneuroim.2019.577110
97. Mariotto S, Sechi E, Ferrari S. Serum neurofilament light chain studies in neurological disorders, hints for interpretation. *J Neurol Sci.* (2020) 416:116986. doi: 10.1016/j.jns.2020.116986
98. Mariotto S, Farinazzo A, Magliozzi R, Alberti D, Monaco S, Ferrari S. Serum and cerebrospinal neurofilament light chain levels in patients with acquired peripheral neuropathies. *J Peripher Nerv Syst.* (2018) 23:174–7. doi: 10.1111/jns.12279
99. Khalil M, Teunissen CE, Otto M, Piehl F, Sormani MP, Gattringer T, et al. Neurofilaments as biomarkers in neurological disorders. *Nat Rev Neurol.* (2018) 14:577–89. doi: 10.1038/s41582-018-0058-z
100. Mariotto S, Gajofatto A, Zuliani L, Zoccarato M, Gastaldi M, Franciotta D, et al. Serum and CSF neurofilament light chain levels in antibody-mediated encephalitis. *J Neurol.* (2019) 266:1643–8. doi: 10.1007/s00415-019-09306-z
101. Mangesius S, Mariotto S, Ferrari S, Pereverzyev S, Lerchner H, Haider L, et al. Novel decision algorithm to discriminate parkinsonism with combined blood and imaging biomarkers. *Park Relat Disord.* (2020) 77:57–63. doi: 10.1016/j.parkreldis.2020.05.033
102. Mariotto S, Carta S, Bozzetti S, Zivelonghi C, Alberti D, Zanzoni S, et al. Sural nerve biopsy: current role and comparison with serum neurofilament light chain levels. *J Neurol.* (2020) 267:2881–7. doi: 10.1007/s00415-020-09949-3
103. Middeldorp J, Hol EM. GFAP in health and disease. *Prog Neurobiol.* (2011) 93:421–43. doi: 10.1016/j.pneurobio.2011.01.005

104. Papa L, Brophy GM, Welch RD, Lewis LM, Braga CF, Tan CN, et al. Time course and diagnostic accuracy of glial and neuronal blood biomarkers GFAP and UCH-L1 in a large cohort of trauma patients with and without mild traumatic brain injury. *JAMA Neurol.* (2016) 73:551–60. doi: 10.1001/jamaneurol.2016.0039
105. Katisko K, Cajanus A, Huber N, Jääskeläinen O, Kokkola T, Kärkkäinen V, et al. GFAP as a biomarker in frontotemporal dementia and primary psychiatric disorders: diagnostic and prognostic performance. *J Neurol Neurosurg Psychiatry.* (2021) 92:1305–12. doi: 10.1136/jnnp-2021-326487
106. Storoni M, Petzold A, Plant GT. The use of serum glial fibrillary acidic protein measurements in the diagnosis of neuromyelitis optica spectrum optic neuritis. *PLoS ONE.* (2011) 6:e023489. doi: 10.1371/journal.pone.0023489
107. Fujii C, Tokuda T, Ishigami N, Mizuno T, Nakagawa M. Usefulness of serum S100B as a marker for the acute phase of aquaporin-4 autoimmune syndrome. *Neurosci Lett.* (2011) 494:86–8. doi: 10.1016/j.neulet.2011.02.063
108. Misu T, Takano R, Fujihara K, Takahashi T, Sato S, Itoyama Y. Marked increase in cerebrospinal fluid glial fibrillar acidic protein in neuromyelitis optica: an astrocytic damage marker. *J Neurol Neurosurg Psychiatry.* (2009) 80:575–7. doi: 10.1136/jnnp.2008.150698
109. Takano R, Misu T, Takahashi T, Sato S, Fujihara K, Itoyama Y. Astrocytic damage is far more severe than demyelination in NMO: a clinical CSF biomarker study. *Neurology.* (2010) 75:208–16. doi: 10.1212/WNL.0b013e3181e2414b
110. Petzold A, Marignier R, Verbeek MM, Confavreux C. Glial but not axonal protein biomarkers as a new supportive diagnostic criteria for devic neuromyelitis optica? Preliminary results on 188 patients with different neurological diseases. *J Neurol Neurosurg Psychiatry.* (2011) 82:467–9. doi: 10.1136/jnnp.2009.196550
111. Kaneko K, Sato DK, Nakashima I, Nishiyama S, Tanaka S, Marignier R, et al. Myelin injury without astrocytopathy in neuroinflammatory disorders with MOG antibodies. *J Neurol Neurosurg Psychiatry.* (2016) 87:1257–9. doi: 10.1136/jnnp-2015-312676
112. Wei Y, Chang H, Li X, Du L, Xu W, Cong H, et al. CSF-S100B is a potential candidate biomarker for neuromyelitis optica spectrum disorders. *Biomed Res Int.* (2018) 2018:5381239. doi: 10.1155/2018/5381239
113. Kleerekooper I, Herbert MK, Kuiperij HB, Sato DK, et al. CSF levels of glutamine synthetase and GFAP to explore astrocytic damage in seronegative NMOSD. *J Neurol Neurosurg Psychiatry.* (2020) 91:605–11. doi: 10.1136/jnnp-2019-322286
114. Miyazawa I, Nakashima I, Petzold A, Fujihara K, Sato S, Itoyama Y. High CSF neurofilament heavy chain levels in neuromyelitis optica. *Neurology.* (2007) 68:865–7. doi: 10.1212/01.wnl.0000256820.26489.17
115. Wang H, Wang C, Qiu W, Lu Z, Hu X, Wang K. Cerebrospinal fluid light and heavy neurofilaments in neuromyelitis optica. *Neurochem Int.* (2013) 63:805–8. doi: 10.1016/j.neuint.2013.10.008
116. Mariotto S, Farinazzo A, Monaco S, Gajofatto A, Zanusso G, Schanda K, et al. Serum neurofilament light chain in NMOSD and related disorders: comparison according to aquaporin-4 and myelin oligodendrocyte glycoprotein antibodies status. *Mult Scler.* (2017) 3:2055217317743098. doi: 10.1177/2055217317743098
117. Mariotto S, Ferrari S, Gastaldi M, Franciotta D, Sechi E, Capra R, et al. Neurofilament light chain serum levels reflect disease severity in MOG-Ab associated disorders. *J Neurol Neurosurg Psychiatry.* (2019) 90:1293–6. doi: 10.1136/jnnp-2018-320287
118. Watanabe M, Nakamura Y, Michalak Z, Isobe N, Barro C, Leppert D, et al. Serum GFAP and neurofilament light as biomarkers of disease activity and disability in NMOSD. *Neurology.* (2019) 93:E1299–311. doi: 10.1212/WNL.0000000000008160
119. Kim H, Lee EJ, Kim S, Choi LK, Kim HJ, Kim HW, et al. Longitudinal follow-up of serum biomarkers in patients with neuromyelitis optica spectrum disorder. *Mult Scler J.* (2021) 13524585211024978. doi: 10.1177/13524585211024978
120. Liu C, Zhao L, Fan P, Ko H, Au C, Ng A, et al. High serum neurofilament levels among Chinese patients with aquaporin-4-IgG-seropositive neuromyelitis optica spectrum disorders. *J Clin Neurosci.* (2021) 83:108–11. doi: 10.1016/j.jocn.2020.11.016
121. Zhang TX, Chen JS, Du C, Zeng P, Zhang H, Wang X, et al. Longitudinal treatment responsiveness on plasma neurofilament light chain and glial fibrillary acidic protein levels in neuromyelitis optica spectrum disorder. *Ther Adv Neurol Disord.* (2021) 14:1–13. doi: 10.1177/17562864211054952
122. Schindler P, Grittner U, Oechtering J, Leppert D, Siebert N, Duchow AS, et al. Serum GFAP and NfL as disease severity and prognostic biomarkers in patients with aquaporin-4 antibody-positive neuromyelitis optica spectrum disorder. *J Neuroinflammation.* (2021) 18:1–14. doi: 10.1186/s12974-021-02138-7
123. Liu C, Lu Y, Wang J, Chang Y, Wang Y, Chen C, et al. Serum neurofilament light chain and glial fibrillary acidic protein in AQP4-IgG-seropositive neuromyelitis optica spectrum disorders and multiple sclerosis: a cohort study. *J Neurochem.* (2021) 159:913–22. doi: 10.1111/jnc.15478
124. Chang X, Huang W, Wang L, ZhangBao J, Zhou L, Lu C, et al. Serum neurofilament light and GFAP are associated with disease severity in inflammatory disorders with aquaporin-4 or myelin oligodendrocyte glycoprotein antibodies. *Front Immunol.* (2021) 12:647618. doi: 10.3389/fimmu.2021.647618
125. Kim H, Lee EJ, Kim S, Choi LK, Kim K, Kim HW, et al. Serum biomarkers in myelin oligodendrocyte glycoprotein antibody-associated disease. *Neurol Neuroimmunol Neuroinflammation.* (2020) 7:e708. doi: 10.1212/NXI.0000000000000708
126. Aktas O, Smith MA, Rees WA, Bennett JL, She D, Katz E, et al. Serum glial fibrillary acidic protein: a neuromyelitis optica spectrum disorder biomarker. *Ann Neurol.* (2021) 89:895–910. doi: 10.1002/ana.26067
127. Hyun JW, Kim Y, Kim SY, Lee MY, Kim SH, Kim HJ. Investigating the presence of interattack astrocyte damage in neuromyelitis optica spectrum disorder: longitudinal analysis of serum glial fibrillary acidic protein. *Neurol Neuroimmunol Neuroinflammation.* (2021) 8:e965. doi: 10.1212/NXI.0000000000000965
128. Mariotto S, Gastaldi M, Grazian L, Mancinelli C, Capra R, Marignier R, et al. NfL levels predominantly increase at disease onset in MOG-Abs-associated disorders. *Mult Scler Relat Disord.* (2021) 50:102833. doi: 10.1016/j.msard.2021.102833
129. Hyun JW, Kim SY, Kim Y, Park NY, Kim KH, Kim SH, et al. Absence of attack-independent neuroaxonal injury in MOG antibody-associated disease: Longitudinal assessment of serum neurofilament light chain. *Mult Scler J.* (2021) 30:135245852110637. doi: 10.1177/13524585211063756
130. Simone M, Palazzo C, Mastrapasqua M, Bollo L, Pompamea F, Gabellone A, et al. Serum neurofilament light chain levels and myelin oligodendrocyte glycoprotein antibodies in pediatric acquired demyelinating syndromes. *Front Neurol.* (2021) 12:754518. doi: 10.3389/fneur.2021.754518
131. Sechi E, Mariotto S, McKeon A, Krecke KN, Pittock SJ, Ferrari S, et al. Serum neurofilament to magnetic resonance imaging lesion area ratio differentiates spinal cord infarction from acute myelitis. *Stroke.* (2021) 52:645–54. doi: 10.1161/STROKEAHA.120.031482

Conflict of Interest: JC is a consultant to UCB and Roche.

The remaining authors declare that the research was conducted in the absence of any commercial or financial relationships that could be construed as a potential conflict of interest.

Publisher's Note: All claims expressed in this article are solely those of the authors and do not necessarily represent those of their affiliated organizations, or those of the publisher, the editors and the reviewers. Any product that may be evaluated in this article, or claim that may be made by its manufacturer, is not guaranteed or endorsed by the publisher.

frontiers in Neurology

ORIGINAL RESEARCH
published: 24 March 2022
doi: 10.3389/fneur.2022.867190

Volumetric Brain Loss Correlates With a Relapsing MOGAD Disease Course

*Ariel Rechtman[1], Livnat Brill[1], Omri Zveik[1], Benjamin Uliel[1], Nitzan Haham[1], Atira S. Bick[2], Netta Levin[2] and Adi Vaknin-Dembinsky[1]**

[1] Department of Neurology and Laboratory of Neuroimmunology and the Agnes-Ginges Center for Neurogenetics, Hadassah-Medical Center, Ein–Kerem, Faculty of Medicine, Hebrew University of Jerusalem, Jerusalem, Israel, [2] Functional Imaging Unit, Department of Neurology, Hadassah-Hebrew University Medical Center, Jerusalem, Israel

Background: Myelin oligodendrocyte glycoprotein antibody disorders (MOGAD) have evolved as a distinct group of inflammatory, demyelinating diseases of the CNS. MOGAD can present with a monophasic or relapsing disease course with distinct clinical manifestations.However, data on the disease course and disability outcomes of these patients are scarce. We aim to compare brain volumetric changes for MOGAD patients with different disease phenotypes and HCs.

Methods: Brain magnetic resonance imaging (MRI) scans and clinical data were obtained for 22 MOGAD patients and 22 HCs. Volumetric brain information was determined using volBrain and MDbrain platforms.

Results: We found decreased brain volume in MOGAD patients compared to HCs, as identified in volume of total brain, gray matter, white matter and deep gray matter (DGM) structures. In addition, we found significantly different volumetric changes between patients with relapsing and monophasic disease course, with significantly decreased volume of total brain and DGM, cerebellum and hippocampus in relapsing patients during the first year of diagnosis. A significant negative correlation was found between EDSS and volume of thalamus.

Conclusions: Brain MRI analyses revealed volumetric differences between MOGAD patients and HCs, and between patients with different disease phenotypes. Decreased gray matter volume during the first year of diagnosis, especially in the cerebrum and hippocampus of MOGAD patients was associated with relapsing disease course.

Keywords: MOGAD, brain MRI, relapsing MOGAD, brain volume, brain atrophy

OPEN ACCESS

Edited by:
Yu Cai,
University of Nebraska Medical Center, United States

Reviewed by:
Rinze Neuteboom,
Erasmus Medical Center, Netherlands
Tetsuya Akaishi,
Tohoku University, Japan

****Correspondence:***
Adi Vaknin-Dembinsky
adembinsky@gmail.com

Specialty section:
This article was submitted to Multiple Sclerosis and Neuroimmunology, a section of the journal Frontiers in Neurology

Received: *31 January 2022*
Accepted: *24 February 2022*
Published: *24 March 2022*

Citation:
Rechtman A, Brill L, Zveik O, Uliel B, Haham N, Bick AS, Levin N and Vaknin-Dembinsky A (2022) Volumetric Brain Loss Correlates With a Relapsing MOGAD Disease Course. Front. Neurol. 13:867190. doi: 10.3389/fneur.2022.867190

INTRODUCTION

Myelin oligodendrocyte glycoprotein (MOG) antibody disorders (MOGAD) are a newly recognized group of inflammatory demyelinating diseases of the central nervous system (CNS), characterized by the presence of immunoglobulin G (IgG) antibodies against MOG presented on myelin sheaths (1, 2). MOGAD are predominantly associated with acute disseminated

encephalomyelitis (ADEM) in young children and with optic neuritis (ON) and myelitis in adults, and have lower prevalence in cases of encephalitis and seizures. This has evolved into a new inflammatory CNS disease entity that is distinct from both multiple sclerosis (MS) and neuromyelitis optica spectrum disorders (NMOSD), and is characterized by younger age at onset, equal frequency in males and females, and an optic nerve preference (3, 4).

MOGAD occurs in all decades of life and can present with a monophasic or relapsing course. A relapse pattern has been reported in 44–83% of adults with MOGAD (5). Young adults mostly present with relapsing disease course, while early and late-onset MOGAD mainly presents with a monophasic disease course (6). Children that experience a relapsing course (20-34%) usually present as ADEM, followed by one or multiple episodes of ON, multiphasic disseminated encephalomyelitis, or relapsing NMOSD-like syndromes (7). The current evidence is controversial regarding whether higher MOG antibody levels predict a relapsing course (6). Predicting the disease course will dictate the patient's management (8).

MOGAD lesions are characterized by demyelination, MOG loss, and relative preservation of axons and oligodendrocytes. The cellular infiltrates consist of macrophages/microglia, T-cells (CD4 dominance), and granulocytes. Humoral immunity, evidenced by B cells, IgG and perivascular deposits of activated complement, was observed, although in lower levels than in AQP4 antibody-positive NMOSD (9). Cortical demyelination occurs relatively frequently in MOGAD patients with brain involvement and is often topographically associated with meningeal infiltration (10).

Magnetic resonance imaging (MRI) is a critically important tool for diagnosis and differentiation of demyelinating disorders. Prognosis, disease monitoring and treatment changes are based on clinical symptoms and neuroimaging findings (11). MRI allows whole-brain volume to be measured, as well as the volume of brain lobes and gyri. In MS, whole brain atrophy is considered a good predictor of long-term clinical disability (12). Two-thirds of MOGAD cases have normal brain MRI, however, when lesions exist, they tend to be with a predilection for the brainstem and infratentorial regions. The lesions are mostly bilateral, affecting the deep white matter (13). MRI findings in MOG encephalomyelitis/encephalitis are usually described as an ADEM-like pattern with diffuse signal changes noted in the cortical gray matter/subcortical white matter, and deep white and gray matter (4). In the majority of cases, following clinical recovery there is complete resolution of all MRI abnormalities (14). Extensive lesions can be seen in the optic nerve, predominantly involving the anterior segments of the optic nerve, sparing chiasm and optic tracts (14).

So far, few studies have examined brain volumes of patients with MOGAD. In this study, we analyzed high-resolution MRI data of MOGAD patients with different disease phenotypes and HCs using volBrain and MDbrain analysis software.

METHODS

Approvals

The study was approved by Hadassah Medical Organization's Ethics Committee (reference no. HMO-20-0644). Given the study design, the Hadassah Medical Organization's Ethics Committee has determined that written consent wasn't required. We confirm that all experiments were performed in accordance with relevant guidelines and regulations.

MOG Antibody Testing

Serum samples were tested for MOG-IgG using the Euroimmun commercial biochip immunofluorescence cell-based assay [IIFT: Myelin-oligodendrocyte glycoprotein (MOG) product numb 1156]. Briefly, specific antibodies from the diluted patient sample bind to the solid-phase MOG-bound antigens. In the next step, a fluorescein (FITC)-labeled antibody (conjugate) binds to the specific antibodies from the patient sample. By excitation with the respective wavelength, the complex can be made visible at the fluorescence microscope (15).

MRI Data Acquisition, Processing, and Analysis

Three-dimensional T1-weighted images were acquired mainly using 3 Tesla MRI scanner. Eight of the patients were obtained with 1.5 Tesla. All the MRIs of MOGAD patients were acquired using Demyelination protocol (16). Volumetric data were extracted using the volBrain (http://volbrain.upv.es) and MDbrain (https://grand-challenge.org/aiforradiology/product/mediaire-mdbrain/) platforms. volBrain software contains advanced pipelines and automatically provides volumetric information of the brain MR images at different scales (17). Validation analysis was performed using MDbrain software, an artificial intelligence-based software tool for volumetric brain analysis and characterization of white matter lesions. It quantifies volumetric values and codes deviations from a normal database. MDbrain analysis calculates the coded deviations from normal database, and is available for total brain, white and gray matter, cerebrum, hippocampus and cerebellum.

Cerebellar gray matter was determined using the multi-atlas segmentation tool CEREbellum Segmentation (CERES) (18). HIPS is a pipeline of volBrain for segmenting the hippocampus and its subfields (19).

No differences were found when comparing brain volume levels between the two MRI scanners (**Supplementary Table S1**).

Statistical Analysis

Distribution was tested using the Kolmogorov–Smirnov test. Due to the normal distribution, we used Student's *t*-test to assess differences between two independent variables.

Spearman correlation study was used to assess the correlation between EDSS levels, and number of relapses to brain volume. Differences were considered significant at $P \leq 0.05$.

RESULTS

Patients

The patient cohort included 22 patients [18 females, 4 males; average age: 33.10 ± 17.19 years; mean disease duration 3.51 ± 3.24 years; mean Expanded Disability Status Scale (EDSS), 1.10 ± 1.30; average relapse number: 1.62 ± 1.07; mean duration between first episode and MRI scan: 2.01 ± 2.89 years]. All patients are MOG-IgG seropositive (Demographic and clinical data are presented at **Table 1A**). A group of 22 healthy individuals served as controls (average age: 38.23 ± 12.58; Female:Male ratio: 17:5).

The patient cohort composed of 8 monophasic patients, 8 relapsing patients and 6 patients classified as unknown (disease duration <2.5 years with one relapse). Patients were classified as having a monophasic course after at least 2.5 years of follow-up without relapse (20).

There were no significant differences between the monophasic and relapsing group in regards to age (36.50 ± 15.46 vs. 32.88 ± 20.29, $p = 0.69$), gender (Female:Male ratio: 6:2 vs. 7:1, $p = 0.52$), disease duration at MRI scan (2.16 ± 2.61 vs. 3.19 ± 3.70, $p = 0.53$), EDSS (1.13 ± 1.64 vs. 1.25 ± 1.28, $p = 0.87$), and scans performed in 1.5 vs. 3 Tesla (4:4 vs. 3:5, $p = 0.61$) (Demographic and clinical data of the patients are presented at **Table 1B**).

Brain Volume Loss in MOGAD Patients During the First Year After Diagnosis

We analyzed brain MRI scans of 22 MOGAD patients and 22 HCs and found a significant decreased total brain volume in MOGAD patients compared to HCs (1,214.14 ± 105.65 vs. 1,139.91 ± 135.15, $p = 0.048$). Specifically, there was a significant decrease in white matter volume in MOGAD patients (512.56 ± 57.33 vs. 458.68 ± 89.60, $p = 0.018$) (**Figure 1A**). Looking at the deep gray matter structures of MOGAD patients we observed significant decrease volume in the cerebellum (134.64 ± 10.28 vs. 124.17 ± 12.42, $p = 0.007$), brainstem (23.96 ± 2.55 vs. 21.61 ± 2.45, $p = 0.003$), caudate (7.46 ± 0.79 vs. 6.56 ± 1.03, $p = 0.001$), thalamus (11.97 ± 0.98 vs. 10.74 ± 1.72, $p = 0.008$), hippocampus (7.78 ± 0.83 vs. 6.86 ± 1.27, $p = 0.011$), and amygdala (1.60 ± 0.27 vs. 1.37 ± 0.36, $p = 0.024$) compared to HCs (**Figures 1B–G**).

Limiting the analyses to 15 brain MRI scans of MOGAD patients performed during the first year after diagnosis yielded similar results. Significantly decreased volume of deep gray matter structures compare to HCs: brainstem (23.96 ± 2.49 vs. 22.13 ± 2.48, $p = 0.035$), caudate (7.46 ± 0.79 vs. 6.68 ± 1.03, $p = 0.010$), thalamus (11.92 ± 0.99 vs. 10.99 ± 1.67, $p = 0.040$), hippocampus (7.78 ± 0.83 vs. 6.82 ± 1.41, $p = 0.021$), and amygdala (1.60 ± 0.27 vs. 1.32 ± 0.41, $p = 0.021$) (**Figures 2A–E**) (Volumetric MRI parameters are presented in **Supplementary Table S2,3**) .

Volumetric Brain Loss Evident at Diagnosis Correlates With Relapsing MOGAD Disease Course

MOGAD can follow a monophasic or relapsing course. Volumetric analysis of brain MRI scans revealed significant differences between patients presented with relapsing ($n = 8$) vs. monophasic disease course ($n = 8$). Patients with relapsing disease course presented with a significant decrease in brain volume (1,034.07 ± 88.93 vs. 1,223.45 ± 86.84, $p < 0.001$), gray matter volume (620.94 ± 73.22 vs. 747.28 ± 68.61, $p = 0.003$) and a trend toward a decreased white matter volume (413.63 ± 62.74 vs. 476.17 ± 74.35, $p = 0.088$) (**Figure 3A**). In addition, analysis of brain structures revealed significantly increased volume loss in the cerebellum (114.95 ± 12.81 vs. 130.48 ± 7.08, $p = 0.010$), cerebrum (899.04 ± 88.93 vs. 1,070.78 ± 86.84, $p < 0.001$), putamen (7.02 ± 0.94 vs. 8.04 ± 0.96, $p = 0.051$), thalamus (9.88 ± 1.30 vs. 11.45 ± 1.19, $p = 0.024$), hippocampus (6.72 ± 0.86 vs. 7.79 ± 0.68, $p = 0.015$), and amygdala (1.33 ± 0.21 vs. 1.63 ± 0.15, $p = 0.005$) in patients with relapsing disease course compared to monophasic disease course (**Figures 3A–G**) (Volumetric MRI parameters according to disease course are presented in **Supplementary Table S4**).

The differences between relapsing and monophasic patients were validated using the MDbrain program. MDbrain analysis calculates the coded deviations from normal database. In line with our findings in volBrain analysis, relapsing patients had decreased total brain volume (85.15 ± 14.49 vs. 30.79 ± 36.84, $p = 0.021$), white matter volume (91.90 ± 8.98 vs. 38.03 ± 39.19, $p = 0.024$), and hippocampus (70.00 ± 30.25 vs. 21.60 ± 15.83, $p = 0.006$) compared to monophasic patients (**Supplementary Figures S1A–C**).

Analysis of MRIs performed during the first year of diagnosis revealed significant changes between MOGAD disease phenotypes (10 MRI scans were available from the first year following diagnosis: 5 monophasic and 5 relapsing disease course). Patients that will develop a relapsing MOGAD disease course had decreased whole brain (1,235.95 ± 64.17 vs. 1,041.76 ± 105.77, $p = 0.010$), along with gray matter volume (724.63 ± 61.14 vs. 598.34 ± 83.82, $p = 0.038$), cerebrum (1,080.29 ± 61.15 vs. 907.26 ± 92.98, $p = 0.010$), and hippocampus (7.83 ± 0.70 vs. 6.87 ± 0.96, $p = 0.044$) at diagnosis compared to patients who exhibit a monophasic disease course (**Figures 4A–D**). No significant changes were seen between the monophasic group and HCs.

Additional analysis revealed that patients who experienced more than one relapse during the first 3 years after diagnosis showed significantly decreased volume of total brain (1,025.55 ± 102.59 vs. 1,190.69 ± 103.66, $p = 0.008$), gray matter (602.60 ± 75.69 vs. 733.02 ± 68.23, $p = 0.003$), cerebrum (891.53 ± 91.65 vs. 1,040.94 ± 95.94, $p = 0.008$), cerebellum (113.92 ± 14.69 vs. 127.99 ± 8.45, $p = 0.028$), and thalamus (9.72 ± 1.50 vs. 11.23 ± 1.15, $p = 0.040$) compared to those who had only one relapse (**Supplementary Figures S2A–E**).

Increased Deep Gray Matter Volume Loss in MOGAD Patients

Cerebellar Volume in MOGAD

Pursuant to our findings, we studied volume loss in the cerebellum and hippocampus in depth in MOGAD patients compared to HCs. The cerebellum is a major structure of the hindbrain that has an important role in motor control. The cerebellum lobules are divided into 3 functional divisions from

TABLE 1A | Clinical and imaging data of MOGAD patients.

#	Myelitis	ON	EDSS	Number of relapses	Number of relapses before MRI	Brain MRI	Disease duration (months)	Duration from first episode to MRI (months)	Treatment	OCB
1	No	BIL ON	1	2	2	Encephalitis-like[a]	48	30	B-cell depletion	Negative
2	No	Uni ON	1	2	1	Normal	30	11	Prednisone	Positive
3	Yes	Uni ON	0	3	2	NMO-like[b]	42	11	Methotrexate	Negative
4	Yes	No	0	1	1	Normal	36	3	No Treatment	Negative
5	No	BIL ON	2	4	2	MS-like[c]	24	12	B-cell depletion	Positive
6	No	No	0	1	1	Non-specific lesions[d]	18	18	No Treatment	Positive
7	Yes	No	5	1	1	Normal	72	58	No Treatment	Negative
8	Yes	Uni ON	4	2	2	Normal	18	11	No Treatment	Negative
9	No	Uni ON	1	1	1	Normal	42	9	No Treatment	Negative
10	Yes	No	1	1	1	Normal	54	33	No Treatment	Negative
11	No	BIL ON	1	2	1	Non-specific lesions[e]	30	6	Prednisone	Negative
12	No	BIL ON	1	1	1	NMO-like[f]	132	84	No Treatment	NA
13	No	BIL ON	0	1	1	Normal	30	At first episode	No Treatment	Negative
14	No	Uni ON	1	2	2	Normal	120	120	B-cell depletion Prednisone	NA
15	Yes	No	0	1	1	Area postrema lesion	42	11	No Treatment	NA
16	No	Uni ON	0	4	4	Normal	132	96	Cellcept	NA
17	No	BIL ON	1	1	1	Normal	8	At first episode	No Treatment	Negative
18	No	Uni ON	1	1	1	Normal	5	At first episode	No Treatment	Negative
19	No	Uni ON	2	1	1	Normal	5	At first episode	No Treatment	Negative
20	No	Uni ON	0	1	1	Normal	4	At first episode	No Treatment	Negative
21	Yes	No	2	1	1	Normal	3	At first episode	No Treatment	Positive
22	No	Uni ON	0	1	1	Normal	108	At first episode	No Treatment	Negative

Uni ON, unilateral optic neuritis; BIL ON, bilateral optic neuritis; NMO, neuromyelitis optica; OCB, oligoclonal bands; NA, data not aviable; EDSS, estimated disability status scale.
[a] *Prolongation of MRI signal at frontal, parietal and temporal cortex. In addition, prolongation of MRI signal in pons and brain stem.*
[b] *Abnormal signal intensity involving the medulla and pons.*
[c] *Multiple white matter lesion within the white matter of the cerebral hemispheres. One lession located in the periventricular white matter of the occipital lobe.*
[d] *Multiple bilateral hyperintense non-enhancing T2/Flair Foci involving the supratentorial periventricular and centrum locations.*
[e] *Non-specific lesions at subcortical frontal white matter.*
[f] *Prolongation of T2/Flair in subcortical supratentorial deep white matter.*

TABLE 1B | Clinical and demographic data of monophasic and relapsing MOGAD patients.

	Monophasic	Relapsing	*P*-value
Age (years)	36.50 ± 15.46	32.88 ± 20.29	0.69
Gender (female:male ratio)	6:2	7:1	0.52
Disease duration at MRI scan (years)	2.16 ± 2.61	3.19 ± 3.70	0.53
EDSS	1.13 ± 1.64	1.25 ± 1.28	0.87
Relapse number	1	2.75 ± 1.04	<0.001

EDSS, estimated disability status scale.

motor (lobules I-VI, VIII) to attentional (VI, VIIB, IX) to default-mode processing (Crus I, Crus II and X).

In our cohort of MOGAD patients we found a decreased volume of total cerebellum gray matter (96.23 ± 6.89 vs. 90.66 ± 10.43, $p = 0.050$) in addition to decreased volumes of the cerebellum lobules: I.II (0.12 ± 0.03 vs. 0.09 ± 0.05, $p = 0.009$), Crus II (17.33 ± 2.18 vs. 14.39 ± 1.75, $p < 0.001$), and VIIB (9.70 ± 1.24 vs. 8.26 ± 1.09, $p < 0.001$) compared to HCs (**Figures 5A–D**).

Relapsing MOGAD patients showed a significant decrease volume of total cerebellum gray matter (83.14 ± 10.78 vs. 95.34 ± 8.52, $p = 0.047$), and cerebellar lobule VIIIA (9.87 ± 0.97 vs. 12.09 ± 1.03, $p = 0.002$) compared to monophasic MOGAD patients (**Figures 5E,F**) (Volumetric cerebellar parameters are presented in **Supplementary Tables S5,6**).

Hippocampal Volume in MOGAD

The hippocampus is a complex, heterogeneous structure in the medial temporal lobe that plays an important role in the limbic system. Typically, it is divided into the subiculum, presubiculum, parasubiculum, the cornu ammonis (CA) fields 1–4 and the dentate gyrus (DG) (21). The CA can also be differently divided to 6 strata; stratum oriens (SO), stratum pyramidale (SP), stratum

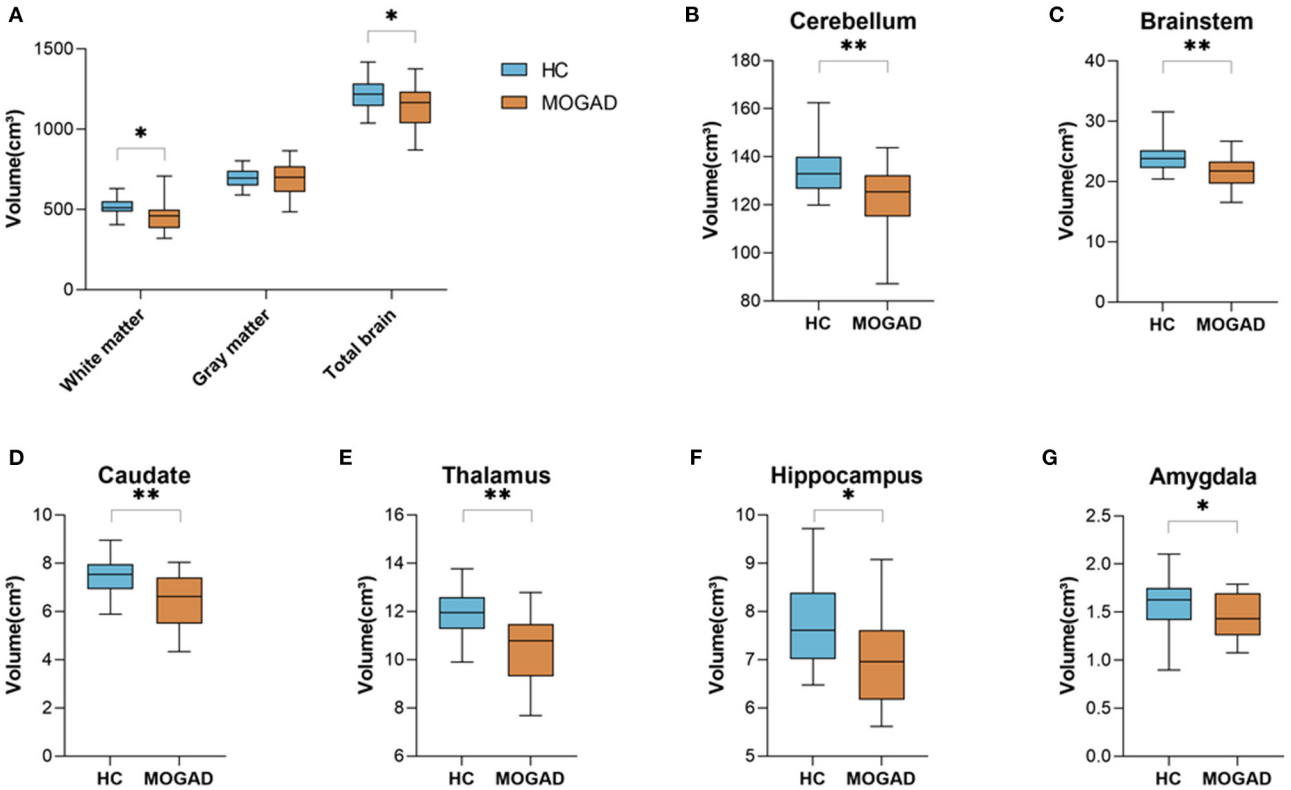

FIGURE 1 | Decreased brain volume in MOGAD patients compare to HCs. Brain volume of HCs ($n = 22$) and MOGAD patients ($n = 22$) analyzed by Volbrain software. **(A)** Volume of white matter (512.56 ± 57.33 vs. 458.68 ± 89.60, $p = 0.018$), gray matter (699.97 ± 59.45 vs. 681.66 ± 106.70, $p = 0.476$) and total brain (1,214.14 ± 105.65 vs. 1,139.91 ± 135.15, $p = 0.048$), and volume of **(B)** cerebellum (134.64 ± 10.28 vs. 124.17 ± 12.42, $p = 0.007$), **(C)** brainstem (23.96 ± 2.55 vs. 21.61 ± 2.45, $p = 0.003$), **(D)** caudate (7.46 ± 0.79 vs. 6.56 ± 1.03, $p = 0.001$), **(E)** thalamus (11.97 ± 0.98 vs. 10.74 ± 1.72, $p = 0.008$), **(F)** hippocampus (7.78 ± 0.83 vs. 6.86 ± 1.27, $p = 0.011$), and **(G)** amygdala (1.60 ± 0.27 vs. 1.37 ± 0.36, $p = 0.024$) of MOGAD patients and HCs. MOGAD, Myelin oligodendrocyte glycoprotein antibody disorders; HCs, healthy controls. p * ≤ 0.05, ** ≤ 0.01.

lucidum (SLU), stratum radiatum (SR), stratum lacunosum (SL) and the stratum molecuare (SM).

We assessed specific subregions of the hippocampus using the HIPS pipeline to determine the extent and pattern of hippocampal atrophy. Subregional analysis of MOGAD patients revealed increased volume loss in CA4/DG (1.31 ± 0.18 vs. 1.14 ± 0.21, $p = 0.009$) and in SR/SL/SM (0.98 ± 0.14 vs. 0.82 ± 0.22, $p = 0.008$) subfields in MOGAD patients compared to HCs (**Figures 6A,B**). In addition, patients with a relapsing disease course showed a significantly decreased volume in CA4/DG (0.98 ± 0.24 vs. 1.23 ± 0.14, $p = 0.028$) compared to patients with monophasic disease (**Figure 6C**) (Volumetric hippocampal parameters of MOGAD patients with different phenotypes are presented in **Supplementary Tables S7,8**).

Brain Atrophy in MOGAD Patients Correlates With Disease Severity

We then studied the correlation between disease severity (EDSS) and volumetric analysis. The median (range) EDSS in the cohort was 1 (0–5). Analysis of EDSS data showed a significant negative correlation between EDSS level and the volume of the white matter ($r = -0.501$, $p = 0.021$) and thalamus ($r = -0.476$, $p = 0.029$). In addition, there is a trend toward a negative correlation between EDSS and the volume of cerebellum ($r = -0.389$, $p = 0.082$), and brainstem ($r = -0.393$, $p = 0.078$) (**Figures 7A–D**). No differences in brain volume were found between patients with ON or those with myelitis. In addition, we found that relapse number, but not disease duration at the time of MRI performing significantly correlated to decreased total brain volume ($r = -0.573$, $p = 0.007$, **Supplementary Figure S3**).

DISCUSSION

Volumetric analysis of brain MRI scans revealed significantly increased brain volume loss in MOGAD patients compared to HCs, with significantly decreased volume of deep gray matter structures: cerebellum, brainstem, caudate, thalamus, hippocampus and amygdala. Moreover, we found a strong association between brain volume loss and disease phenotype. In our cohort of MOGAD, patients with relapsing disease course presented with increased total brain volume loss early after diagnosis, with specifically increased atrophy of the cerebellum and hippocampus compared to patients with monophasic disease course.

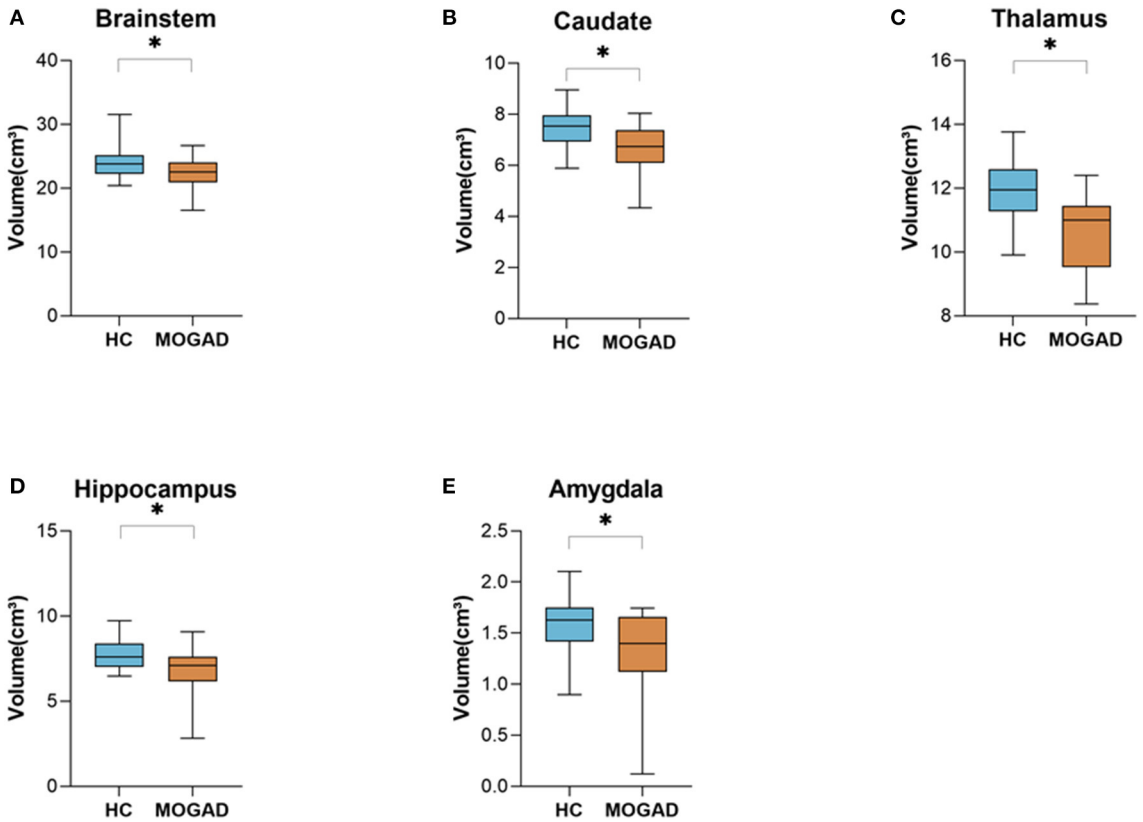

FIGURE 2 | Decrease brain volume of MOGAD patients during the first year of diagnosis. Brain volume of HCs ($n = 22$) and MOGAD patients during the first year of diagnosis ($n = 15$) analyzed by Volbrain software. **(A)** Volume of brainstem (23.96 ± 2.49 vs. 22.13 ± 2.48, $p = 0.035$), **(B)** caudate (7.46 ± 0.79 vs. 6.68 ± 1.03, $p = 0.010$), **(C)** thalamus (11.92 ± 0.99 vs. 10.99 ± 1.67, $p = 0.040$), **(D)** hippocampus 7.78 ± 0.83 vs. 6.82 ± 1.41, $p = 0.021$), and **(E)** amygdala (1.60 ± 0.27 vs. 1.32 ± 0.41, $p = 0.021$) of MOGAD patients during the first year of diagnosis and HCs. MOGAD, Myelin oligodendrocyte glycoprotein antibody disorders; HCs, healthy controls. $p * \leq 0.05$.

According to recent publications, MOGAD patients tend to present with lesions in the cortical and subcortical deep gray matter, white matter, brainstem, cerebellum, and spinal cord (13). MOGAD pathology is dominated by coexistence of both perivenous and confluent white matter demyelination, with an overrepresentation of intracortical demyelinated lesions compared to typical MS (10). To date, there are few works studying brain volume of MOGAD patients (22–24). Zhuo et al. described gray matter atrophy in both the frontal and temporal lobes, insula, thalamus, and hippocampus, and white matter fiber disruption in the optic radiation and anterior/posterior corona radiate (22). Messina et al. showed decreased deep gray matter volume in MS and MOGAD patients, compared to HCs (24). In contrast, Schmidt et al. did not identify significant differences in brain volume between MOGAD patients and HCs (23). In accordance with the former groups, in our cohort of MOGAD patients, we found decreased total brain, white matter, cerebellum, brainstem, caudate, thalamus, hippocampus and amygdala volume compared to HCs. Increased brain volume loss is known to occur in other demyelinating diseases, including in both MS and NMOSD, with increased severity in MS (25).

Deep gray matter atrophy was observed in all MOGAD patients in our cohort, with significant increases in patients with a relapsing phenotype. In MS patients, the involvement of the gray matter, particularly of the thalamus, has been linked to a wide range of clinical manifestations including cognitive decline, motor deficits, fatigue, painful syndromes, and ocular motility disturbances (26). Gray matter atrophy has been identified, particularly in patients with secondary-progressive MS compared to relapsing-remitting MS, is associated with T2 and T1 lesion volume, and correlates with physical and cognitive impairment (27). The volumes of the deep gray matter were reduced in MS compared to NMOSD (28), and in NMOSD deep gray matter atrophy is restricted to the thalamus (although broadly distributed in MS). In the current study we found that, as in MS and NMOSD, there is significant thalamic atrophy in MOGAD patients. In addition, the thalamic atrophy correlated with EDSS, as described in MS and NMOSD (29, 30). Suggesting that gray matter atrophy could be a possible biomarker for disease severity in inflammatory demyelinating diseases.

To date, we still do not have a reliable biomarker to predict disease course of MOGAD. About 40–55% of patients will

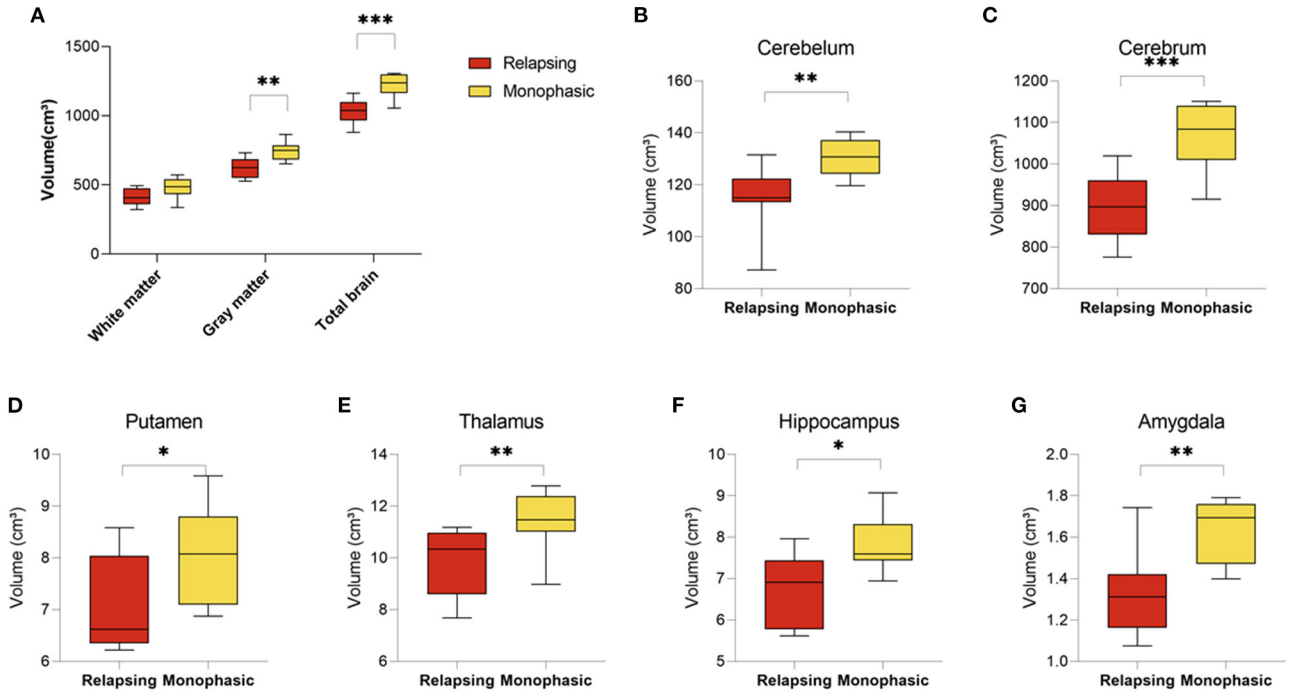

FIGURE 3 | Decreased brain volume in relapsing compared to monophasic MOGAD patients. Brain volume of relapsing ($n = 8$) and monophasic MOGAD patients ($n = 8$) analyzed by Volbrain software. **(A)** White matter (413.63 ± 62.74 vs. 476.17 ± 74.35, $p = 0.088$), gray matter (620.94 ± 73.22 vs. 747.28 ± 68.61, $p = 0.003$) and whole brain volumes (1,034.07 ± 88.93 vs. 1,223.45 ± 86.84, $p < 0.001$), **(B)** cerebellum (114.95 ± 12.81 vs. 130.48 ± 7.08, $p = 0.010$), **(C)** cerebrum (899.04 ± 88.93 vs. 1,070.78 ± 86.84, $p < 0.001$), **(D)** Putamen (7.02 ± 0.94 vs. 8.04 ± 0.96, $p = 0.051$), **(E)** thalamus (9.88 ± 1.30 vs. 11.45 ± 1.19, $p = 0.024$), **(F)** hippocampus (6.72 ± 0.86 vs. 7.79 ± 0.68, $p = 0.015$), and **(G)** amygdala (1.33 ± 0.21 vs. 1.63 ± 0.15, $p = 0.005$) of monophasic and relapsing MOGAD patients. MOGAD, Myelin oligodendrocyte glycoprotein antibody disorders. $p * \leq 0.05$, ** ≤ 0.01, *** ≤ 0.001.

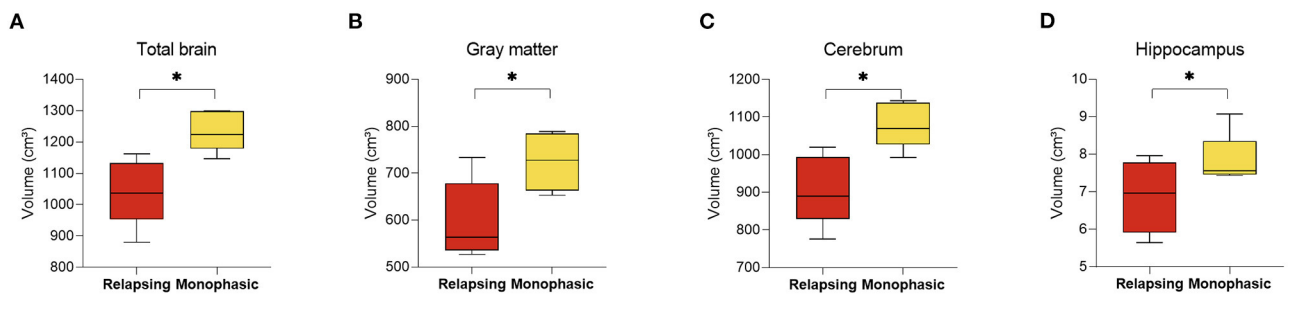

FIGURE 4 | Decreased brain volume in relapsing compared to monophasic MOGAD patients during the first year of diagnosis. Brain volume of relapsing ($n = 5$) and monophasic MOGAD patients ($n = 5$) during the first year of diagnosis analyzed by Volbrain software. Volume of **(A)** total brain (1,235.95 ± 64.17 vs. 1,041.76 ± 105.77, $p = 0.010$), **(B)** gray matter volume (724.63 ± 61.14 vs. 598.34 ± 83.82, $p = 0.038$), **(C)** cerebrum (1,080.29 ± 61.15 vs. 907.26 ± 92.98, $p = 0.010$), and **(D)** hippocampus (7.83 ± 0.70 vs. 6.87 ± 0.96, $p = 0.044$) of monophasic and relapsing course MOGAD patients during the first year of diagnosis. MOGAD, Myelin oligodendrocyte glycoprotein antibody disorders. $p * \leq 0.05$.

follow a monophasic course and might not need preventive therapy (31). In this study we found significant volumetric changes between disease phenotypes, early during the first year after diagnosis. Relapsing patients presented with significantly decreased total brain volume and deep gray matter (cerebrum, putamen, thalamus, hippocampus, and amygdala) in the first year compared to monophasic MOGAD patients. Identifying disease course early after diagnosis will allow for optimized treatment. Suggesting a potential use of MRI volumetry as a biomarker for predicting a relapse course and/or a short interval between the first and second relapse in patients with MOGAD.

In our cohort we found that there is a negative correlation between number of relapses and brain volume, without correlation to disease duration. A recent study shows that new remission silent lesions are found only in 3% of MOGAD patients (27). It is therefore possible that brain atrophy in MOGAD

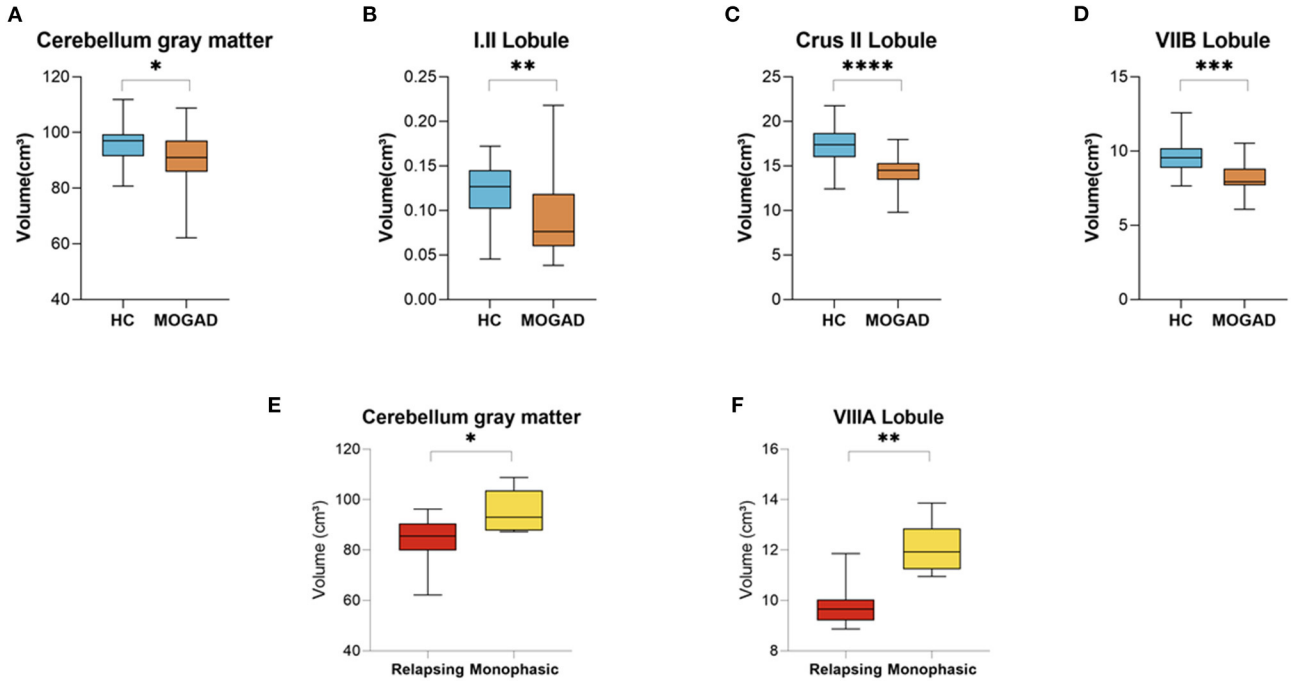

FIGURE 5 | Decrease volume of cerebellar lobules at MOGAD patients compared to HCs and decreased volume of cerebellar lobules at relapsing MOGAD patients compared to monophasic MOGAD patients. **(A–D)** Volume of cerebellar lobules of HCs ($n = 22$) and MOGAD patients ($n = 20$) analyzed by CERES pipeline of Volbrain software. Volume of **(A)** total cerebellum gray matter (96.23 ± 6.89 vs. 90.66 ± 10.43, $p = 0.050$), **(B)** cerebellar lobules I.II (0.12 ± 0.03 vs. 0.09 ± 0.05, $p = 0.009$), **(C)** Crus II (17.33 ± 2.18 vs. 14.39 ± 1.75, $p < 0.001$), and **(D)** VIIB (9.70 ± 1.24 vs. 8.26 ± 1.09, $p < 0.001$) of MOGAD patients and HCs. **(E,F)** Volume of cerebellar lobules of monophasic ($n = 6$) and relapsing ($n = 6$) MOGAD patients analyzed by CERES pipeline of Volbrain software. Volume of **(E)** total cerebellum gray matter (83.14 ± 10.78 vs. 95.34 ± 8.52, $p = 0.047$) and **(F)** cerebellar lobule VIIIA (9.87 ± 0.97 vs. 12.09 ± 1.03, $p = 0.002$) of monophasic and relapsing MOGAD patients. MOGAD, Myelin oligodendrocyte glycoprotein antibody disorders; HCs, healthy controls. p * ≤ 0.05, ** ≤ 0.01, *** ≤ 0.001, **** ≤ 0.0001.

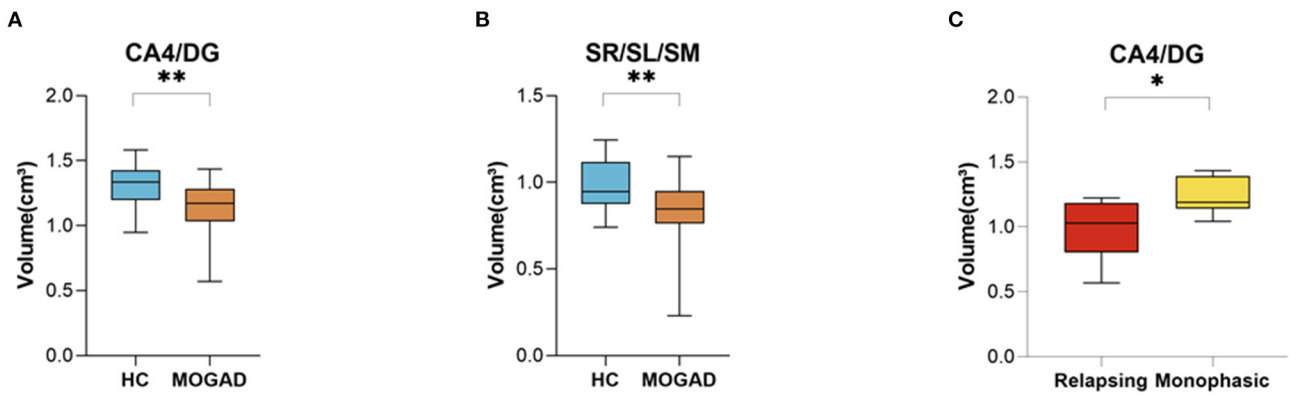

FIGURE 6 | Decreased Volume of CA4/DG at MOGAD patients compare to HCs. **(A,B)** Volume of hippocampal subfields of HCs ($n = 21$) and MOGAD patients ($n = 18$) analyzed by HIPS pipeline of Volbrain software. **(A)** Volumes of CA/DG4 (1.31 ± 0.18 vs. 1.14 ± 0.21, $p = 0.009$) and **(B)** SR/SL/SM (0.98 ± 0.14 vs. 0.82 ± 0.22, $p = 0.008$). **(C)** Volume of hippocampal subfields of monophasic ($n = 6$) and relapsing patients ($n = 6$), analyzed by HIPS pipeline of Volbrain software. **(C)** CA4/DG (0.98 ± 0.24 vs. 1.23 ± 0.14, $p = 0.03$) volume of MOGAD monophasic and relapsing course patients. MOGAD, Myelin oligodendrocyte glycoprotein antibody disorders; HCs, healthy controls. p * ≤ 0.05, ** ≤ 0.01.

patients might be a result of multiple relapses rather than disease progression over time.

Due to its multiple connections to the forebrain, the thalamus and the spinal cord, the cerebellum is not only affected by focal white and gray matter lesions but also by the secondary degeneration of multiple afferent and efferent connections to the supratentorial brain areas and to the spinal cord. Hence, cerebellar atrophy might occur at a significant rate with higher

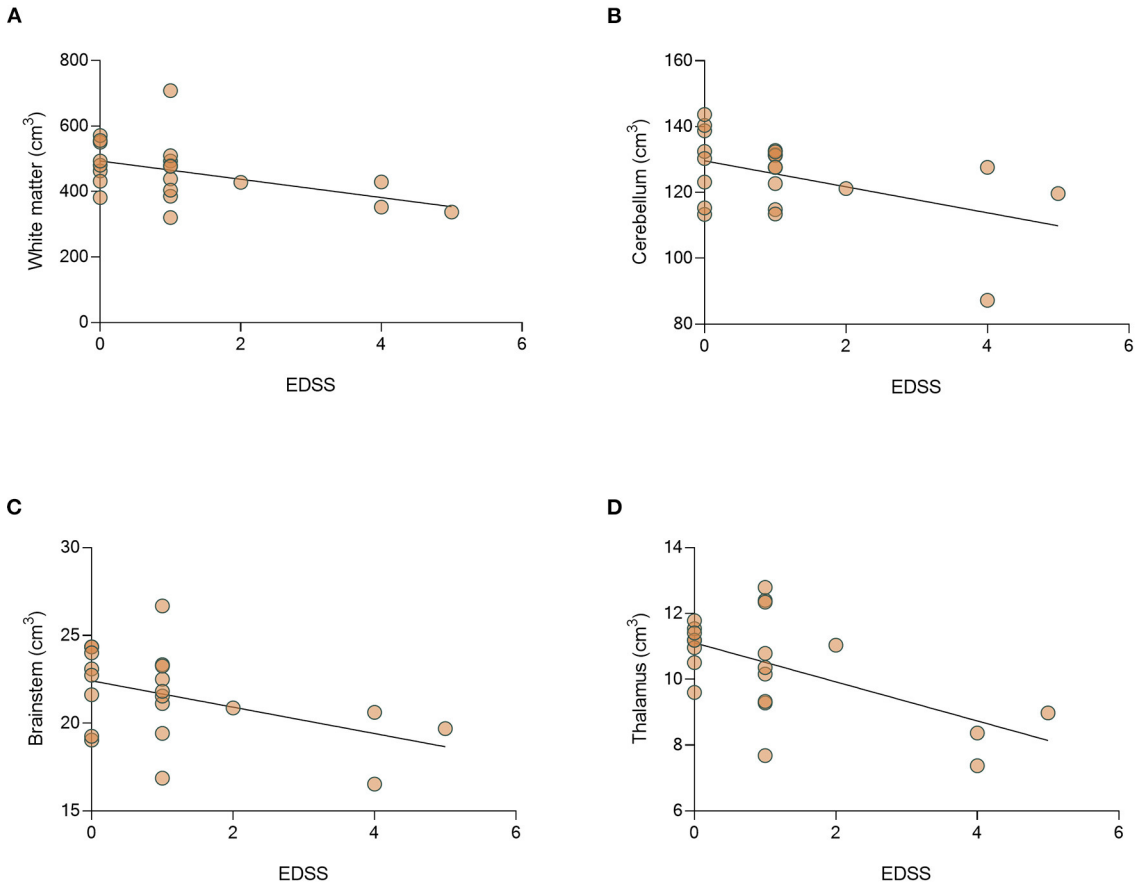

FIGURE 7 | There is a significant correlation between EDSS and decrease volume of thalamus of MOGAD patients. Correlation between EDSS and brain volumes. Correlation between EDSS and volumes of **(A)** white matter ($r = -0.051$, $p = 0.021$), **(B)** cerebellum ($r = -0.389$, $p = 0.082$), **(C)** brainstem ($r = -0.393$, $p = 0.078$), and **(D)** thalamus ($r = -0.476$, $p = 0.029$) in MOGAD patients ($n = 22$). MOGAD, Myelin oligodendrocyte glycoprotein antibody disorders.

chances of affecting the patient's clinical outcome due to the cerebellar strategic position in the motor, coordination, and cognitive networks (32). Damage to the cerebellum is associated with dysdiadokokinesia, ataxia, tremors, loss of balance, muscle weakness, dysarthria, and loss of postural tone. There is also evidence supporting cognitive function of the cerebellum (32).

In MS, tissue damage within the cerebellum is thought to contribute to disability (33). Cerebellar atrophy has been found to be more extensive in patients with secondary progressive MS and correlates with disease duration and disability (33). Hippocampal atrophy also begins early in MS, as shown in MRI studies, and this atrophy has been correlated with impaired performance on visuospatial memory testing, commonly affected in MS patients (34). In NMO, the MRI predictor of cognitive functions is the hippocampal volume (35).

The hippocampus is located in the medial temporal lobe at both sides of the brainstem near to the cerebellum, and is critical for memory functions (21). CA4/DG subfield is the first subfield to be atrophied across the course of MS, at the stage of clinical isolate syndrome; atrophy then spreads to CA1 (34). Furthermore, the CA/DG subfield is significantly decreased in NMO and anti-N-methyl-D-aspartate receptor encephalitis patients compared to HCs (36, 37). Interestingly, in our cohort of total MOGAD patients, and specifically in relapsing patients, the most affected subfield of the hippocampus is the CA4/DG subfield.

Limitations of this study include the small sample size due to the low incidence of the disease, and short follow-up time. Despite these limitations, our findings show for the first-time volumetric brain differences between the monophasic and relapsing MOGAD patients.

In conclusion, in the current study, we found volumetric differences between MOGAD patients that present with relapsing and monophasic disease course. In addition, we identified correlations between disease severity and thalamus atrophy. As early as the first year after diagnosis, patients with relapsing disease course have significant decreased total brain and lower cerebrum and hippocampus volume compared to patients with monophasic disease course. Differences between MOGAD

patients and HCs were found, especially at the deep gray matter structures.

DATA AVAILABILITY STATEMENT

The raw data supporting the conclusions of this article will be made available by the authors, without undue reservation.

ETHICS STATEMENT

The studies involving human participants were reviewed and approved by Hadassah Medical Organization's Ethics Committee (reference no. HMO-20-0644). Written informed consent from the participants was not required to participate in this study in accordance with the national legislation and the institutional requirements.

AUTHOR CONTRIBUTIONS

AR contributed to study design, clinical and MRI data acquisition, data analysis and interpretation, and manuscript preparation. LB and AV-D contributed to study design, data analysis and interpretation, and manuscript preparation. OZ and NH contributed to data acquisition. BU contributed to clinical data acquisition and patient recruitment. AB and NL contributed to MRI data acquisition. All authors read and approved the final manuscript.

SUPPLEMENTARY MATERIAL

The Supplementary Material for this article can be found online at: https://www.frontiersin.org/articles/10.3389/fneur.2022.867190/full#supplementary-material

REFERENCES

1. Kitley J, Woodhall M, Waters P, Leite MI, Devenney E, Craig J, et al. Myelin-oligodendrocyte glycoprotein antibodies in adults with a neuromyelitis optica phenotype. *Neurology.* (2012) 79:1273–7. doi: 10.1212/WNL.0b013e31826aac4e
2. Reindl M, Di Pauli F, Rostásy K, Berger T. The spectrum of MOG autoantibody-associated demyelinating diseases. *Nat Rev Neurol.* (2013) 9:455–61. doi: 10.1038/nrneurol.2013.118
3. Ramanathan S, Mohammad S, Tantsis E, Nguyen TK, Merheb V, Fung VSC, et al. Clinical course, therapeutic responses and outcomes in relapsing MOG antibody-associated demyelination. *J Neurol Neurosurg Psychiatry.* (2018) 89:127–37. doi: 10.1136/jnnp-2017-316880
4. Ogawa R, Nakashima I, Takahashi T, Kaneko K, Akaishi T, Takai Y, et al. MOG antibody-positive, benign, unilateral, cerebral cortical encephalitis with epilepsy. *Neurol Neuroimmunol NeuroInflammation.* (2017) 4:1–10. doi: 10.1212/NXI.0000000000000322
5. Wynford-Thomas R, Jacob A, Tomassini V. Neurological update: MOG antibody disease. *J Neurol.* (2019) 266:1280–6. doi: 10.1007/s00415-018-9122-2
6. Hennes EM, Baumann M, Schanda K, Anlar B, Bajer-Kornek B, Blaschek A, et al. Prognostic relevance of MOG antibodies in children with an acquired demyelinating syndrome. *Neurology.* (2017) 89:900–8. doi: 10.1212/WNL.0000000000004312
7. Bruijstens AL, Lechner C, Flet-Berliac L, Deiva K, Neuteboom RF, Hemingway C, et al. E.U. paediatric MOG consortium consensus: Part 1 – Classification of clinical phenotypes of paediatric myelin oligodendrocyte glycoprotein antibody-associated disorders. *Eur J Paediatr Neurol.* (2020) 29:2–13. doi: 10.1016/j.ejpn.2020.10.006
8. Hacohen Y, Banwell B. Treatment approaches for MOG-Ab-associated demyelination in children. *Curr Treat Options Neurol.* (2019) 21. doi: 10.1007/s11940-019-0541-x
9. Takai Y, Misu T, Kaneko K, Chihara N, Narikawa K, Tsuchida S, et al. Myelin oligodendrocyte glycoprotein antibody-associated disease: an immunopathological study. *Brain.* (2020) 143:1431–46. doi: 10.1093/brain/awaa102
10. Höftberger R, Guo Y, Flanagan EP, Lopez AS, Verena C, Hochmeister S, et al. The pathology of central nervous system inflammatory demyelinating disease accompanying myelin oligodendrocyte glycoprotein autoantibody. *Acta Neuropathol.* (2020) 139:875–92. doi: 10.1007/s00401-020-02132-y
11. Tillema JM, Pirko I. Neuroradiological evaluation of demyelinating disease. *Ther Adv Neurol Disord.* (2013) 6:249–68. doi: 10.1177/1756285613478870
12. Popescu V, Agosta F, Hulst HE, Sluimer IC, Knol DL, Sormani MP, et al. Brain atrophy and lesion load predict long term disability in multiple sclerosis. *J Neurol Neurosurg Psychiatry.* (2013) 84:1082–91. doi: 10.1136/jnnp-2012-304094
13. Ramanathan S, Prelog K, Barnes EH, Tantsis EM, Reddel SW, Henderson APD, et al. Radiological differentiation of optic neuritis with myelin oligodendrocyte glycoprotein antibodies, aquaporin-4 antibodies, and multiple sclerosis. *Mult Scler.* (2016) 22:470–82. doi: 10.1177/1352458515593406
14. Kitley J, Waters P, Woodhall M, Leite MI, Murchison A, George J, et al. Neuromyelitis optica spectrum disorders with aquaporin-4 and myelin-oligodendrocyte glycoprotein antibodies a comparative study. *JAMA Neurol.* (2014) 71:276–83. doi: 10.1001/jamaneurol.2013.5857
15. Reindl M, Schanda K, Woodhall M, Tea F, Ramanathan S, Sagen J, et al. International multicenter examination of MOG antibody assays. *Neurol Neuroimmunol Neuroinflamm.* (2020) 7:e674. doi: 10.1212/NXI.0000000000000674
16. Li D, Traboulsee A, Coyle PK, Arnold DL, Barkhof F, Grossman R, et al. STATEMENT standardized MR imaging protocol for multiple sclerosis : consortium of MS centers consensus. *Am J Neuroradiol.* (2006) 27:455—61.
17. Manjón JV, Coupé P. Volbrain: an online MRI brain volumetry system. *Front Neuroinform.* (2016) 10:1–14. doi: 10.3389/fninf.2016.00030
18. Romero JE, Coupé P, Giraud R, Ta VT, Fonov V, Park MTM, et al. CERES: a new cerebellum lobule segmentation method. *Neuroimage.* (2017) 147:916–24. doi: 10.1016/j.neuroimage.2016.11.003
19. Romero JE, Coupé P, Manjón J V. HIPS: a new hippocampus subfield segmentation method. *Neuroimage.* (2017) 163:286–95. doi: 10.1016/j.neuroimage.2017.09.049
20. Cobo-Calvo A, Ruiz A, Maillart E, Audoin B, Zephir H, Bourre B, et al. Clinical spectrum and prognostic value of CNS MOG autoimmunity in adults: the MOGADOR study. *Neurology.* (2018) 90:e1858–69. doi: 10.1212/WNL.0000000000005560
21. Aanes S, Bjuland KJ, Sripada K, Sølsnes AE, Grunewaldt KH, Håberg A, et al. Reduced hippocampal subfield volumes and memory function in school-aged children born preterm with very low birthweight (VLBW). *NeuroImage Clin.* (2019) 23:101857. doi: 10.1016/j.nicl.2019.101857
22. Zhuo Z, Duan Y, Tian D, Wang X, Gao C, Ding J, et al. Brain structural and functional alterations in MOG antibody disease. *Mult Scler J.* (2020) 27:1350–63. doi: 10.1177/1352458520964415
23. Schmidt FA, Chien C, Kuchling J, Bellmann-Strobl J, Ruprecht K, Siebert N, et al. Differences in advanced magnetic resonance imaging in MOG-IgG and AQP4-IgG seropositive neuromyelitis optica spectrum disorders: a comparative study. *Front Neurol.* (2020) 11:1–8. doi: 10.3389/fneur.2020.499910
24. Messina S, Mariano R, Roca-fernandez A, Cavey A, Leite MI, Calabrese M, et al. Contrasting the brain imaging features of MOG-antibody disease, with

AQP4-antibody NMOSD and multiple sclerosis. *Mult Scler*. (2020) 28:217–27. doi: 10.1177/13524585211018987
25. Fisher E, Rudick RA, Simon JH, Cutter G, Baier M, Lee JC, et al. Eight-year follow-up study of brain atrophy in patients with MS. *Neurology*. (2002) 59:1412–20. doi: 10.1212/01.WNL.0000036271.49066.06
26. Minagar A, Barnett MH, Benedict RHB, Pelletier D, Pirko I, Sahraian MA, et al. The thalamus and multiple sclerosis: modern views on pathologic, imaging, and clinical aspects. *Neurology*. (2013) 80:210–9. doi: 10.1212/WNL.0b013e31827b910b
27. Anderson VM, Wheeler-Kingshott CAM, Abdel-Aziz K, Miller DH, Toosy A, Thompson AJ, et al. A comprehensive assessment of cerebellar damage in multiple sclerosis using diffusion tractography and volumetric analysis. *Mult Scler J*. (2011) 17:1079–87. doi: 10.1177/1352458511403528
28. Eshaghi A, Wottschel V, Cortese R, Calabrese M, Sahraian MA, Thompson AJ, et al. Gray matter MRI differentiates neuromyelitis optica from multiple sclerosis using random forest. *Neurology*. (2016) 87:2463–70. doi: 10.1212/WNL.0000000000003395
29. Rocca MA, Mesaros S, Pagani E, Sormani MP, Comi G, Filippi M. Thalamic damage and long-term progression of disability in multiple sclerosis. *Radiology*. (2010) 257:463–9. doi: 10.1148/radiol.10100326
30. Hyun JW, Park G, Kwak K, Jo HJ, Joung A, Kim JH, et al. Deep gray matter atrophy in neuromyelitis optica spectrum disorder and multiple sclerosis. *Eur J Neurol*. (2017) 24:437–45. doi: 10.1111/ene.13224
31. Brill L, Ganelin-cohen E, Dabby R, Rabinowicz S, Zohar-dayan E, Vaknin-dembinsky A. Age-related clinical presentation of MOG-IgG seropositivity in Israel. *Front Neurol*. (2021) 11:612304. doi: 10.3389/fneur.2020.612304
32. Inglese M, Petracca M, Mormina E, Achiron A, Straus-Farber R, Miron S, et al. Cerebellar volume as imaging outcome in progressive multiple sclerosis. *PLoS ONE*. (2017) 12:1–11. doi: 10.1371/journal.pone.0176519
33. Weier K, Penner IK, Magon S, Amann M, Naegelin Y, Andelova M, et al. Cerebellar abnormalities contribute to disability including cognitive impairment in multiple sclerosis. *PLoS ONE*. (2014) 9:e86916. doi: 10.1371/journal.pone.0086916
34. Sicotte NL, Kern KC, Giesser BS, Arshanapalli A, Schultz A, Montag M, et al. Regional hippocampal atrophy in multiple sclerosis. *Brain*. (2008) 131:1134–41. doi: 10.1093/brain/awn030
35. Liu Y, Fu Y, Schoonheim MM, Zhang N, Fan M, Su L, et al. Structural MRI substrates of cognitive impairment in neuromyelitis optica. *Neurology*. (2015) 85:1491–9. doi: 10.1212/WNL.0000000000002067
36. Chen X, Fu J, Luo Q, Han Y, Zheng Q, Xie M, et al. Altered volume and microstructural integrity of hippocampus in NMOSD. *Mult Scler Relat Disord*. (2019) 28:132–7. doi: 10.1016/j.msard.2018.12.009
37. Finke C, Kopp UA, Pajkert A, Behrens JR, Leypoldt F, Wuerfel JT, et al. Structural hippocampal damage following anti-N-methyl-D-aspartate receptor encephalitis. *Biol Psychiatry*. (2016) 79:727–34. doi: 10.1016/j.biopsych.2015.02.024

Conflict of Interest: The authors declare that the research was conducted in the absence of any commercial or financial relationships that could be construed as a potential conflict of interest.

Publisher's Note: All claims expressed in this article are solely those of the authors and do not necessarily represent those of their affiliated organizations, or those of the publisher, the editors and the reviewers. Any product that may be evaluated in this article, or claim that may be made by its manufacturer, is not guaranteed or endorsed by the publisher.

frontiers | Frontiers in Neurology

ORIGINAL RESEARCH
published: 14 April 2022
doi: 10.3389/fneur.2022.859276

Relatively Early and Late-Onset Neuromyelitis Optica Spectrum Disorder in Central China: Clinical Characteristics and Prognostic Features

Jinbei Yu[1], *Shuai Yan*[2], *Pengpeng Niu*[1] *and Junfang Teng*[1]*

[1] *Department of Neurology, The First Affiliated Hospital of Zhengzhou University, Zhengzhou, China,* [2] *Department of Neurology, Affiliated Hospital of Hebei University, Baoding, China*

Background: We aimed to analyze the clinical characteristics and prognostic features of Chinese patients with relatively late-onset neuromyelitis optica spectrum disorder (RLO-NMOSD>40 years of age at disease onset), compared with patients with relatively early onset NMOSD (REO-NMOSD, ≤ 40 years of age at disease onset).

Methods: We retrospectively reviewed the medical records of patients with NMOSD in central China (with disease courses longer than 3 years) between January 2012 and January 2021. We further analyzed the clinical and prognostic differences between patients with REO-NMOSD and RLO-NMOSD.

Results: A total of 71 patients were included in this study. The results showed that 39 (54.9%) of the patients had RLO-NMOSD. The patients with RLO-NMOSD had higher expanded disability status scale (EDSS) scores than patients with REO-NMOSD at the initial (5.0 *vs.* 3.0, $p = 0.01$), 3-month (4.0 *vs.* 2.5, $p = 0.001$), 1-year (4.0 *vs.* 2.5, $p = 0.003$), 3rd-year (3.5 *vs.* 3.0, $p = 0.0017$), and final follow-up (4.0 *vs.* 2.5, $P = 0.002$) time points. The EDSS scores of visual function were 2.0 (1.0–3.0) in REO-NMOSD and 3.0 (2.0–3.0) in RLO-NMOSD ($p = 0.038$) at the final follow-up time point. The locations of spinal cord lesions at transverse myelitis (TM) onset were prone to cervical cord in patients with REO-NMOSD. There were no between-group treatment differences. The risk of requiring a cane to walk (EDSS score of 6.0) increased as the age of disease onset increased: for every 10-year increase in the age of disease onset, the risk of needing a cane to walk increased by 65% [hazard ratio (*HR*) = 1.65, 95% *CI* 1.15–2.38, $p = 0.007$]. Another significant predictor identified in the multivariate analysis was annualized relapse rate (ARR) (*HR* = 2.01, 95% *CI* 1.09–3.71, $p = 0.025$). In addition, we observed a positive correlation between age at onset and EDSS scores at the final follow-up (Spearman's $r = 0.426$, $p < 0.0001$) time point. EDSS scores at different periods were significantly different between patients with RLO-NMOSD and REO-NMOSD with anti-aquaporin-4 (AQP4) IgG positive.

OPEN ACCESS

Edited by:
Fu-Dong Shi,
Tianjin Medical University General Hospital, China

Reviewed by:
Alessandra Lugaresi,
University of Bologna, Italy
Omid Mirmosayyeb,
Isfahan University of Medical Sciences, Iran

***Correspondence:**
Junfang Teng
tengjf_doc@163.com

Specialty section:
This article was submitted to Multiple Sclerosis and Neuroimmunology, a section of the journal Frontiers in Neurology

Received: *21 January 2022*
Accepted: *17 March 2022*
Published: *14 April 2022*

Citation:
Yu J, Yan S, Niu P and Teng J (2022) Relatively Early and Late-Onset Neuromyelitis Optica Spectrum Disorder in Central China: Clinical Characteristics and Prognostic Features. Front. Neurol. 13:859276. doi: 10.3389/fneur.2022.859276

Conclusion: The patients with RLO-NMOSD developed more severe disabilities than patients with REO-NMOSD at a variety of time periods. All of the patients may experience recurrent aggravated symptoms after their first year, with only patients with REO-NMOSD partly recovering from the 3rd year. The age at onset and ARR were the main predictors of outcomes.

Keywords: neuromyelitis optica spectrum disorder, relatively-late onset, disability, expanded disability status scale scores, disease course, annualized relapse rate, enlarged perivascular space

INTRODUCTION

Neuromyelitis optica spectrum disorder (NMOSD) is an autoimmune disease of the central nervous system that preferentially affects the optic nerve and spinal cord (1, 2). NMOSD was initially considered to be a special type of multiple sclerosis (MS). However, it is a different disease condition characterized by serum antibodies against anti-aquaporin-4 (AQP4)-IgG. NMOSD usually presents between the ages of 30 and 40 years (3).

The onset age of NMOSD is an important factor that can affect the disease relapse and severity (4, 5). Previous studies have reported that the rates of disability and mortality are different among early-onset NMOSD (EO-NMOSD<50 years at onset), late-onset NMOSD (LO-NMOSD, 50–70 years at onset), and very late-onset NMOSD (VLO-NMOSD, >70 years at onset) (5–9). The spinal cord may have increased the vulnerability to inflammation in LO-NMOSD, whereas the optic nerves are more susceptible in EO-NMOSD (7). Patients with LO-NMOSD had higher expanded disability status scale (EDSS) scores during remission and poorer prognoses, indicating that the age of onset is an important factor that affects the disease prognosis (6, 10, 11).

Currently, there are no clear definitions of the terms and cut-off values that are used for the age of onset. Most previous studies used a stratification of 50 years. Since the typical onset age is approximately 40 years, we compared the clinical characteristics of patients with NMOSD using an age stratification of 40 years (1, 3). We hoped that this age stratification would allow us to recommend suitable preventive treatments and improve the prognoses of patients. Most previous studies analyzed EDSS at onset and at the final follow-up time point (5, 7, 8, 12, 13). Although a few studies have analyzed EDSS throughout the long-term follow-up periods, some data suggest that the disease duration may vary between the two groups (5, 7, 13), while some studies only in patients with LO-NMOSD (12), or only in AQP4-Ab patients with NMOSD (8). We first performed a dynamic analysis of EDSS scores at the onset, 3-month, 1-year, 3-year, and final follow-up (∼5-year) time points in patients with NMOSD who had disease courses >3 years. We hope that this approach will help us better understand the characteristics of the disease at different ages of onset, especially high paroxysmal ages.

Some studies have focused on differences in radiological features (i.e., brain lesions) between EO-NMOSD and LO-NMOSD (7, 8, 13–15). They found that NMO-typical brain lesions were common in patients with EO-NMOSD (7, 13), while non-specific white lesions were more frequently noted in patients with LO-NMOSD (8, 13). AQP4 is a water channel expressed in astrocyte endfeet, which wrap around capillaries (16). Thus, AQP4 lines central nervous system microvessels, pia, subpia, and perivascular spaces (17). In addition, they found that perivascular spaces (PVS) can be increased in MS (18). Enlarged PVS (EPVS) may serve as neurodegenerative markers in MS (18). However, there is little data on AQP4 and perivascular spaces in NMOSD (19). Here, we aimed to explore the characteristics of EPVS in REO-NMOSD and RLO-NMOSD.

METHODS

Participants

This study was approved by the Medical Ethics Committee of the First Affiliated Hospital of Zhengzhou University (2021-KY-1103). We retrospectively screened the medical records of patients with NMOSD who came into contact with our healthcare system between January 2012 and January 2021 and had disease courses that were longer than 3 years. All patients were diagnosed with NMOSD based on the 2015 international diagnostic criteria for NMOSD (2, 20). In our study, MS had been ruled out according to the 2017 McDonald criteria (21). Patients with incomplete clinical data, who were lost to follow-up, had poor treatment compliance or had severe comorbidities, such as cerebrovascular diseases or tumors were excluded.

Data Collection

Basic information, such as the age of onset, sex, disease duration, first symptoms (optic neuritis, myelitis, encephalopathy, and/or various combinations of these symptoms), EDSS scores were collected at baseline (at the time of the first attack) and at 3-month, 1-year, 3-year, and final follow-up time points. Additionally, we collected additional data, such as the time interval for the first relapse, the annualized relapse rate (ARR), the time to reach an EDSS score of 6.0, serum AQP4-IgG levels, cerebrospinal fluid (CSF) specific oligoclonal band (OCB), magnetic resonance images (MRIs) of the spinal cord and brain, visual EPVS rating scores in the basal ganglia (BG) and centrum semiovale (CS), treatments, and coexisting autoimmune disorders. Relapse was defined as an acute episode of neurologic symptoms that lasted over 24 h and occurred at least 30 days after the previous attack. An EDSS score of 6.0 was defined as "unilateral assistance needed to walk without wheelchair."

Enlarged perivascular spaces are defined as linear-sharped or dot-like lesions with signal intensities similar to cerebrospinal

fluid that are visible on T2-weighted MRI sequences (22). EPVS are distinguished from lacunes by having diameters lower than 3 mm and no hyperintense rims on the fluid-attenuated inversion recovery (FLAIR) sequences. We counted the number of EPVS in the CS and BG, and rated them with a validated 4-point semiquantitative scale (0 = no EPVS; 1 = 1–10 EPVS; 2 = 11–20 EPVS; 3 = 21–40 EPVS, and 4 ≥ 40 EPVS) (16). We included T1-weighted, T2-weighted, FLAIR, and Diffusion-Weighted Imaging (DWI) sequences. All MRI scans were evaluated by a neurologist who was blind to the clinical information.

Patients were divided into two groups: those with relatively-early onset NMOSD (REO-NMOSD; age at onset = 14–40 years) and those with relatively-late onset NMOSD (RLO-NMOSD; age at onset >40 years). Onset age refers to the age at which symptoms first appeared.

Statistical Analysis

Statistical analyses were performed using SPSS 22.0. Continuous data were described as means ± standard deviation (SD) or as medians with inter-quartile range (IQR). Characteristics were compared between patients with LO-NMOSD and EO-NMOSD using χ^2 (or Fisher's exact) tests for categorical data and Student's *t*-tests (or Wilcoxon rank-sum test) for continuous data. The Kaplan–Meier method was used to estimate the time between disease onset and reaching EDSS scores of 6.0/4.0. Predictive factors for disability were assessed using the Cox proportional hazards regression models. We compared the EPVS degree between the two groups using χ^2 tests. The BG-EPVS and CS-EPVS degrees were dichotomized as high (score > 1) or low (score ≤ 1) (23, 24). The values of $p < 0.05$ were considered to be statistically significant.

RESULTS

Demographic Data and Clinical Characteristics in REO-and RLO-NMOSD

A total of 71 patients (mean age: 39 ± 14 years) were enrolled in the study. The female:male ratio≈11:1. Among these patients, 32 patients were classified as having REO-NMOSD. The mean age of onset was 25.5 ± 6.7 years in the REO-NMOSD group and 50.8 ± 8.1 years in the RLO-NMOSD group. Compared with the RLO-NMOSD group, optic neuritis (ON) was more frequently observed at the time of initial attack in the REO-NMOSD group (43.8 vs. 30.8%), but there were no statistically significant differences. There were no significant between-group differences in the number of patients with at least one ON (REO-NMOSD 21/32, 65.6%; RLO-NMOSD 26/39, 66.7%, $p = 0.926$). The involvements of transverse myelitis (TM) were more common in the RLO-NMOSD group (48.7 vs. 25.0%, $p = 0.041$). Overall, the chance of having the initial symptoms of area postrema syndrome (APS) was significantly higher in the REO-NMOSD group compared with the RLO-NMOSD group (6/32 vs. 1/39, $p = 0.04$). APS was more common in the REO-NMOSD group, while TM was more frequent in the RLO-NMOSD group. Moreover, we found that EDSS scores at the initial and 3-month time points were significantly higher in the REO-NMOSD group (**Table 1**). ARR and duration to relapse were not significantly different between the groups. EDSS scores in the RLO-NMOSD group were significantly higher at the 1-year time point ($p = 0.003$). At the 3-year time point, the EDSS scores were 3.0 (1.5–4.0) for the REO-NMOSD group and 3.5 (2.9–5.1) for the RLO-NMOSD group ($p = 0.017$). This difference persisted to the last

TABLE 1 | The demographic and clinical characteristics of patients with neuromyelitis optica spectrum disorder (NMOSD) according to age group (<40 or ≥40 years).

Characteristic	REO-NMOSD (*n* = 32)	RLO-NMOSD (*n* = 39)	*P*-value
Female: male (ratio)	29:3 (9.7:1)	36:3 (12:1)	1.000
Age at onset, years, IQR	25 (21.3–31.8)	50 (45.0–56.0)	NA
Disease duration (months) IQR	56.5 (43.2–81.0)	63 (46–75)	0.977
Onset attack type, *n* (%)			
Optic neuritis	14 (43.7%)	12 (30.8%)	0.259
Transverse myelitis only	8 (25.0%)	19 (48.7%)	0.041
Area postrema syndrome	6 (18.8%)	1 (2.6%)	0.041
Other	4 (12.5%)	7 (17.9%)	0.763
Time to first relapse, months	7.0 (3.0–16.8)	10.5 (5.0–16.8)	0.339
Annualized relapse rate	1.0 (0–1.0)	1.0 (0–1.0)	0.772
EDSS score, IQR			
At initial	3.0 (2.6–5.8)	5.0 (3.0–7.0)	0.010
Third month follow-up	2.5 (2.0–3.5)	4.0 (3.0–5.5)	0.001
First year follow-up	2.5 (2.0–3.5)	3.0 (2.5–4.5)	0.003
Third year follow-up	3.0 (1.5–4.0)	3.5 (2.9–5.1)	0.017
Latest follow-up	2.5 (1.1–4.9)	4.0 (3.0–6.9)	0.002
EDSS score of visual acuity, IQR			
At initial	3.0 (2.0–3.0)	3.0 (2.0–3.0)	0.466
Nadir	3.0 (2.5–3.5)	3.0 (2.0–4.0)	0.716
Final follow-up	2.0 (1.0–3.0)	3.0 (2.0–3.0)	0.038
Time to EDSS score 6, weeks (IQR)	146 (5.5–273)	74.0 (2.0–196.0)	0.116
Coexisting autoimmune disorders	14 (43.8%)	12 (30.8%)	0.259
Immunosuppressant therapy (IST)	28 (87.5%)	34 (87.2%)	1.000
Time from onset to IST	8 (4–28.5)	9.5 (1–22.2)	0.644
Azathioprine	14	24	0.135
Mycophenolate mofetil	11	8	0.189
Other (MTX/RTX)	3	2	0.652
Without IST	4	5	1.000
Serostatus, *n* (%)			
AQP4-IgG positive	25 (78.1%)	26 (66.7%)	0.302
CS EPVS, *n* (%)			0.329
High degree-CS EPVS (score > 1)	16 (50.0%)	24 (61.5%)	
Low degree-CS EPVS (score≤1)	16 (50.0%)	17 (38.5%)	
BG EPVS, *n* (%)			0.086
High degree-BG EPVS (score > 1)	7 (21.9%)	16 (41.0%)	
Low degree-BG EPVS (score≤1)	25 (78.1%)	23 (59.0%)	

MTX, methotrexate; RTX, rituximab; CS, centrum semiovale; BG, basal ganglia.

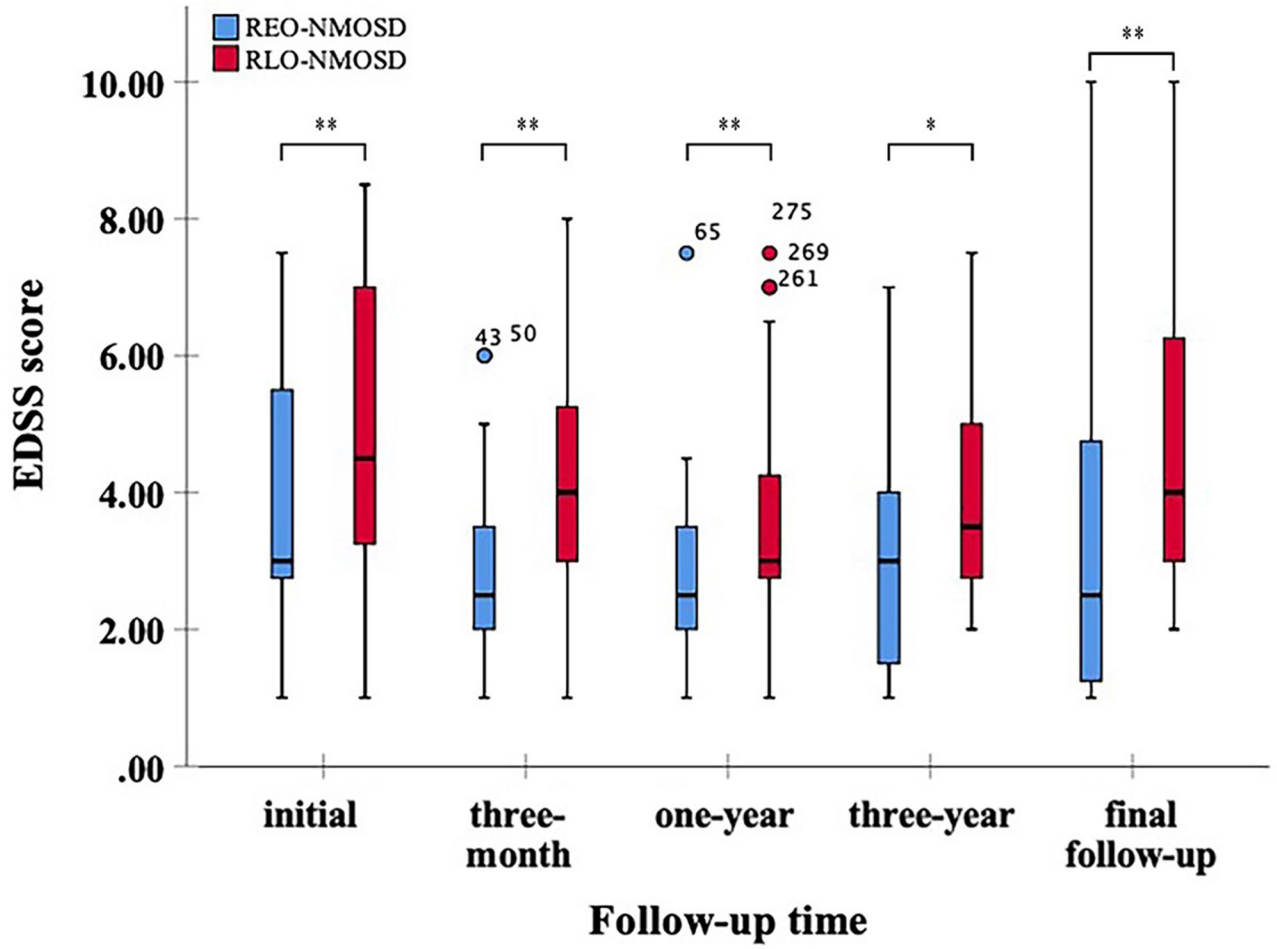

FIGURE 1 | Expanded disability status scale (EDSS) scores at different time periods between patients with relatively early-onset neuromyelitis optica spectrum disorder (REO-NMOSD) and relatively late-onset neuromyelitis optica spectrum disorder (RLO-NMOSD) patients. (*p<0.05,**p<0.01).

follow-up time point ($p = 0.002$; **Figure 1**). We further compared the EDSS scores of visual functioning in patients with ON occurrence. EDSS scores were not significantly different between the two groups at initial attack ($p = 0.466$). The nadir EDSS scores showed no between-group differences ($p = 0.716$). Surprisingly, however, patients with RLO-NMOSD had more serious visual sequelae than patients with REO-NMOSD (**Table 1**). EDSS scores averaged 2.0 (1.0–3.0) in the REO-NMOSD group and 3.0 (2.0–3.0) in the RLO-NMOSD group at the final follow-up time period ($p = 0.038$). No significant between-group differences were found in the rates of coexisting autoimmune disorders (43.8 vs. 30.8%, p>0.05). There were no differences in treatments between the two groups (**Table 1**). Serum AQP4-IgG was observed in a large proportion of patients with REO-NMOSD (25, 78.1%) as well as patients with RLO-NMOSD (26, 66.7%). In serum AQP4-IgG negative patients, CSF-specific OCB markers were negative. Representative examples of EPVS are illustrated in **Figure 2**. There were no differences in BG-EPVS and CS-EPVS scores between the two groups (**Table 1**). For spine MRI findings, 29 patients (29/32, 90.6%) in the REO-NMOSD group and 37 patients (37/39, 94.9%) in the RLO-NMOSD group suffered from at least one TM disease. The median lesion length was 6.0 vertebral segments (IQR, 4.0–7.4) in the REO-NMOSD group and 7.0 (4.5–11.5) in the RLO-NMOSD group at TM onset, which was not a significant difference (**Supplementary Table 1**). The longest segments during disease course showed no differences between the two groups ($p = 0.521$). The locations of spinal cord lesions included the cervical cord, thoracic spine, lumbar spine, and/or both. The locations of spinal cord lesions at TM onset were prone to cervical cord in patients with REO-NMOSD (10/29 vs. 4/37, $p = 0.032$). There were no between-group differences in the distribution of longest lesion locations (**Supplementary Table 1**).

Predictors of the Development of Disability in REO-and RLO-NMOSD

We investigated whether age, disease duration, EDSS scores at the time of disease onset, serostatus, initial attack type, ARR,

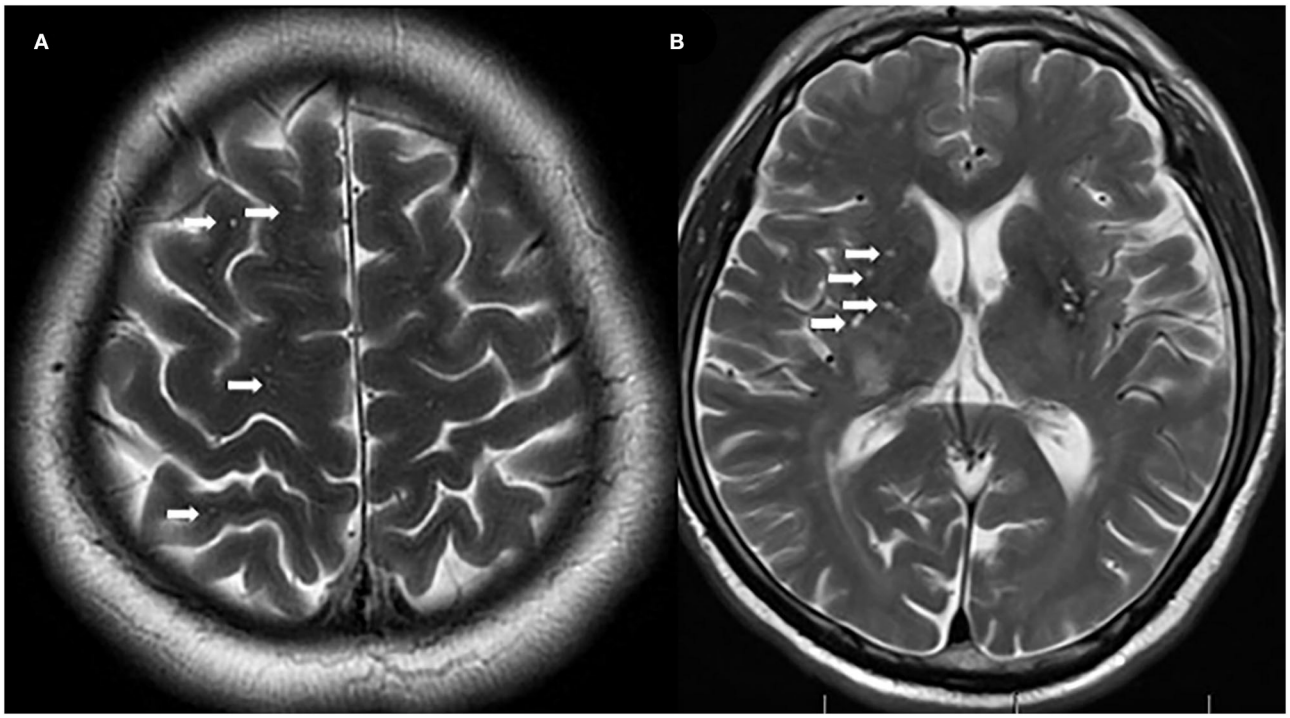

FIGURE 2 | Representative examples of centrum semiovale-enlarged perivascular spaces (CS-EPVS) **(A)** and basal ganglia (BG)-EPVS **(B)**. Arrowheads point to individual EPVS. EPVS, enlarged perivascular spaces; BG, basal ganglia; CS, centrum semiovale.

and immunosuppressant therapies affected the development of disabilities in NMOSD. We found that the risk of needing a cane to walk (EDSS score of 6.0) increased with an older age of disease onset. For every 10-year increase, the risk of needing a cane to walk increased by 65% [hazard ratio (*HR*) = 1.65, 95% *CI* 1.15–2.38, $p = 0.007$]. Another significant predictor identified in the multivariate analysis was ARR (*HR* = 2.01, 95% *CI* 1.09–3.71, $p = 0.025$).

Consistent with reaching an EDSS score of 6.0, we found that for every 10-year increase in the age of disease onset, the risk of reaching an EDSS score of 4.0 increased by 51.9% (*HR* 1.51, 95% *CI* 1.14–2.02, $p = 0.004$). ARR was another significant predictor (*HR* 1.71 95% *CI* 1.06–2.74, $p = 0.027$). The risk of reaching an EDSS score of 6.0 with RLO-NMOSD was three times higher than with EO-NMOSD (*HR* 3.06, 95% *CI* 1.01–9.29, $p = 0.049$). The time to reach the EDSS scores of 6.0 and 4.0 in the two groups was shown in **Figures 3A,B**. EDSS score at the final follow-up time point was also significantly correlated with the age of disease onset (**Figure 4**).

Demographic Data and Clinical Characteristics in REO-and RLO-NMOSD With AQP4-Ab Positive

There were 51 (70.83%) patients whose serum AQP4-Ab was positive. Among these, 25 patients (49.02%) were REO-NMOSD, and 26 patients (50.98%) were RLO-NMOSD (**Table 2**). In AQP4-Ab positive NMOSD, RLO-NMOSD patients' EDSS scores were significantly higher than the score of patients with REO-NMOSD at the time of disease onset ($p = 0.039$); **Figure 5**, and 3 months after treatment ($p = 0.004$). EDSS scores at the 1-year time points were also different between groups ($p = 0.032$). At the 3-year time points, the average EDSS score was 3.0 (1.0–4.0) in the REO-NMOSD group and 3.0 (2.88–5.63) in the RLO-NMOSD group ($p = 0.046$). Differences in EDSS scores also persisted at the final follow-up time point ($p = 0.008$). Although the proportion of EDSS scores >6 at the final follow-up time point was higher in the RLO-NMOSD group (34.6 *vs.* 16.0%), it did not differ significantly between the two groups ($p = 0.199$). The percentage of EDSS scores >4.0 was significantly different between the two groups ($p = 0.032$). The degrees of BG-EPVS and CS-EPVS showed no differences between the two groups (**Table 2**). Other factors, such as sex, ARR, type of onset, coexisting autoimmune disorders, and chronic immunosuppressant therapy, were not significantly different between the two groups.

DISCUSSION

All participants enrolled in our study had long disease courses and were followed-up for at least 3 years, which is different than the varied lengths of follow-up in previous studies (5, 7, 13). Patients with RLO- and REO-NMOSD had similar sex ratios, treatments, and serologic features. However, patients with RLO-NMOSD had higher EDSS scores than patients with REO-NMOSD at various time points. These patients might partly

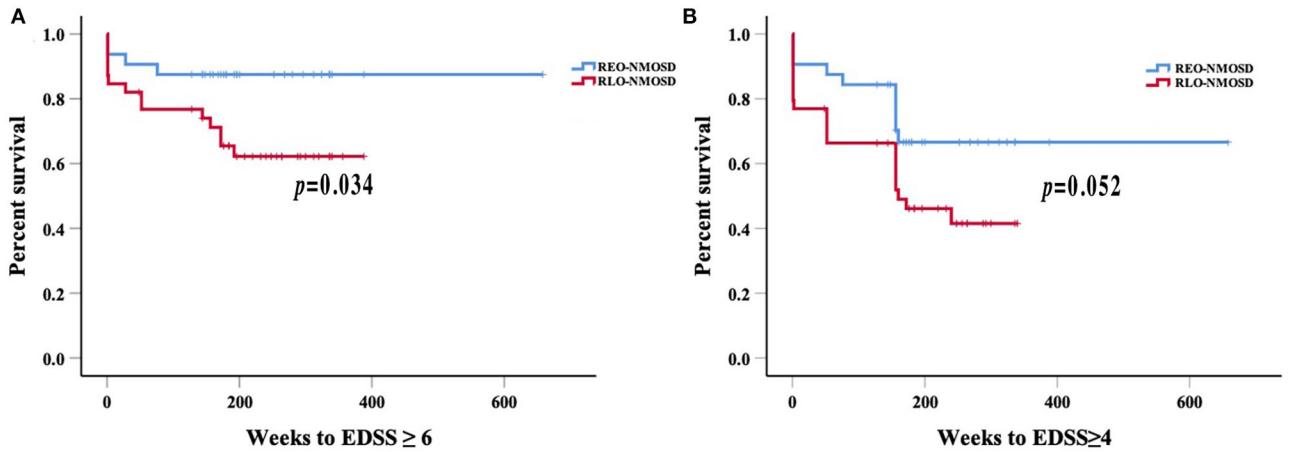

FIGURE 3 | Weeks from onset to reach the EDSS scores of 6.0 and 4.0, stratified by the age of disease onset: **(A)** Patients with RLO-NMOSD reached EDSS scores of 6.0 sooner than patients with REO-NMOSD ($p = 0.034$); **(B)** Time to EDSS score of 4.0 between the two groups ($p = 0.052$).

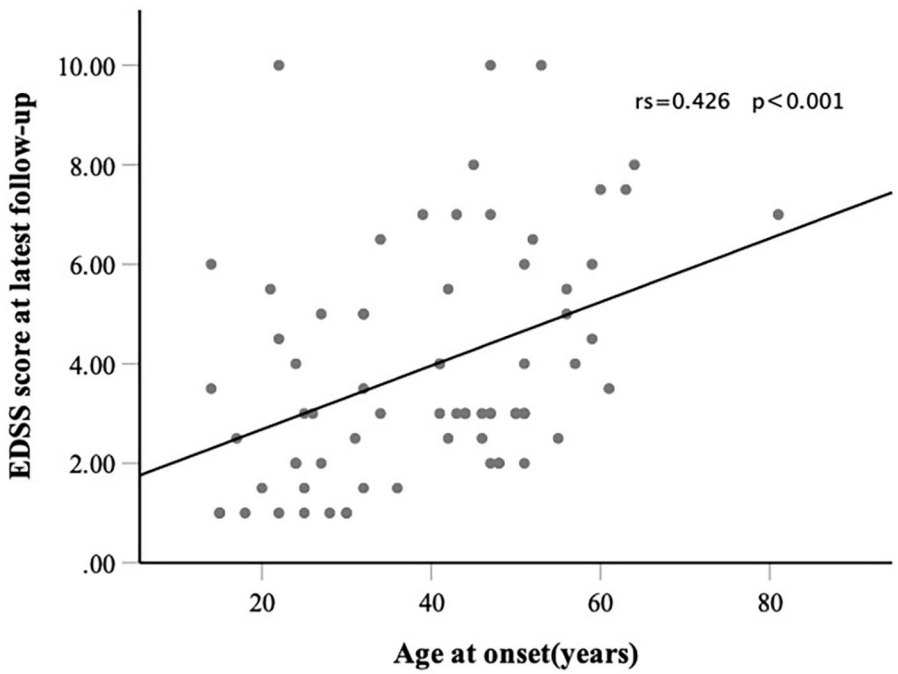

FIGURE 4 | Correlation between onset age and EDSS at the final follow-up time point.

recover after the acute phase but then experience symptom aggravation in the following years. They had more serious visual sequelae than patients with REO-NMOSD. A similar phenomenon was noted in AQP4-Ab positive patients with NMOSD. EDSS at the final follow-up time point was significantly correlated with the age of disease onset. The risk of needing a cane to walk was also correlated with onset age and ARR.

The proportion of female in our study is higher than previous studies, which were about (6–9):1 (1, 7, 13, 15, 25). It may be related to relapsing NMOSD being prone to female (3). Another factor to consider is that a relatively small sample was enrolled in our singer center. Previous studies have identified the effect of age at the disease onset on motor disability and prognosis, suggesting that older patients are more susceptible to disability over short-time courses (5, 7, 8, 13). Previous work showed that the late age onset (i.e., >50 years) was associated with higher EDSS scores at remission, the higher rates of mortality, and the higher rates of motor disability. Pediatric patients with NMOSD predominantly present with ON (7, 26). In some previous LO-NMOSD cohorts, an average EDSS score of 3.0 (2.0–5.0) was reported at the final follow-up time point (7, 12, 13). However, the follow-up time varied between groups (7, 12, 13, 27). The onset age of NMOSD

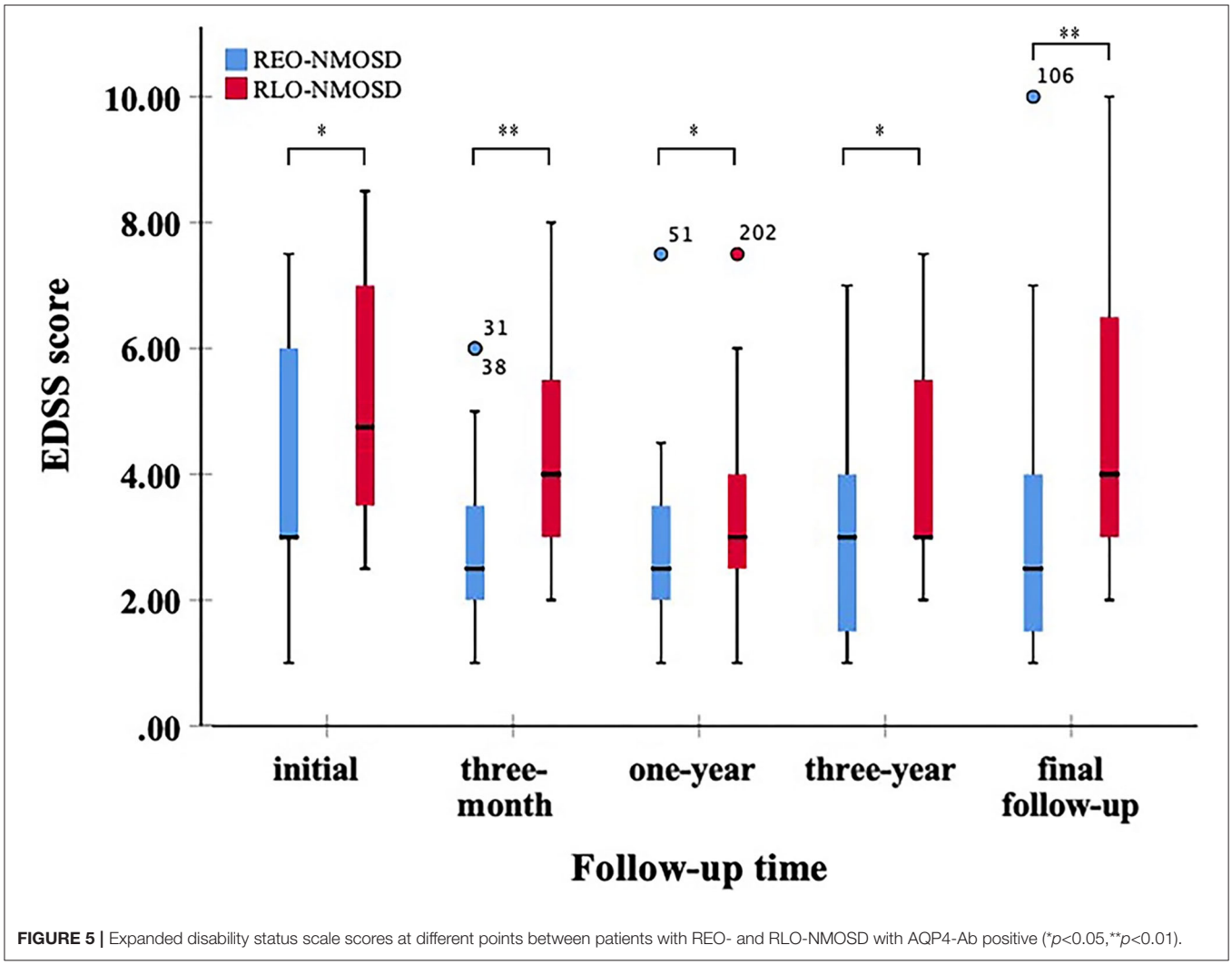

FIGURE 5 | Expanded disability status scale scores at different points between patients with REO- and RLO-NMOSD with AQP4-Ab positive (*p<0.05,**p<0.01).

usually presents in the 40 years, especially in Blacks and Asians (Blacks: ∼28–33 years, Asians: 35–40 years, vs. Whites: 44 years) (1, 3, 25–28). We aimed to investigate the characteristic and prognostic features of NMOSD under the stratification of 40 years old. Previous studies that focused on AQP4-Ab-positive patients found that the LO-NMOSD group had severer disability at 2 or 5 years than patients with EO-NMOSD (27). Here, we selected patients who had disease courses more than 3 years and found that EDSS scores were significantly higher in patients with RLO-NMOSD at different time periods (the onset, 3-month, 1-year, 3-year, and the latest follow-up time points). Patients can partly recover from the first episode after treatment, while could be worse after 3 years. Only patients with REO-NMOSD can partly recover again from 3 years. These results had not been reported in previous studies. The latest EDSS score was 2.5 (1.1–4.9) in the REO-NMOSD group and 4.0 (3.0–6.9) in the RLO-NMOSD group after about 5 years of follow-up. Unlike the previous study (29), the severity of visual acuity showed no between-group differences no matter at onset or the nadir status. However, patients with RLO-NMOSD suffered from more serious sequelae than patients with REO-NMOSD. Additionally, in AQP4-Ab positive patients with NMOSD who had the disease for at least 3 years, the RLO-NMOSD group had higher EDSS scores than the REO-NMOSD group at different time points. The patients with REO-NMOSD who were AQP4-Ab positive could partly recover after the 3rd year, but the patients with RLO-NMOSD could not. We further validated that the onset age was a crucial determinant of disease severity. In addition, the risk of needing a cane to walk increased with the increased age at disease onset and ARR.

Neuromyelitis optica spectrum disorder is an astrocytopathy that mainly affects the spinal cord, optic nerves, and area postrema. Previous studies showed that TM at the onset was more frequently observed in the LO-NMOSD group than in the EO-NMOSD group, while the proportion of patients with at least one ON was higher in the EO-NMOSD group (7, 8, 26, 30, 31). In our study, we found that TM was more common in patients with RLO-NMOSD, while the proportion of ON showed no significant differences between the two groups. Additionally, the media spine cord lesion length at initial attack or the longest segments during disease course also had no significant differences between the two groups. Simialr to previous studies (9, 32), we found that

TABLE 2 | The comparison of demographic and clinical features between patients with REO-NMOSD and RLO-NMOSD with AQP4-IgG.

Characteristic	REO-NMOSD ($n = 25$)	RLO-NMOSD ($n = 26$)	P-value
Female: male (ratio)	24:1 (24:1)	12:1 (24:2)	1.000
Age at onset, years, mean (SD)	26.9 (6.6)	51.9 (8.5)	NA
Disease duration (months) IQR	67.0 (44.5–82.5)	62.5 (44.8–76.3)	0.644
Onset attack type, *n* (%)			
Optic neuritis	10 (40.0%)	10 (38.5%)	0.910
Transverse myelitis only	8 (32.0%)	10 (38.5%)	0.447
Area postrema syndrome	4 (16.0%)	1 (3.8%)	0.191
Other	3 (12.0%)	5 (19.2%)	0.703
Time to first relapse, months	9.0 (3.0–21.0)	9.0 (5.0–20.5)	0.634
Annualized relapse rate	1.0 (0.0–1.0)	1.0 (0.0–1.0)	0.843
EDSS score, IQR			
At initial	3.0 (2.8–6.3)	4.8 (3.5–7.0)	0.039
Third month follow-up	2.5 (2.0–4.0)	4.0 (3.0–5.5)	0.004
First year follow-up	2.5 (1.8–3.5)	3.0 (2.5–4.0)	0.032
Third year follow-up	3.0 (1.5–4.0)	3.0 (2.9–5.6)	0.046
Latest follow-up	2.5 (1.5–4.5)	3.8 (3.0–6.6)	0.010
EDSS score≥6 *n* (%)	4 (16.0%)	9 (34.6%)	0.127
EDSS score≥4 *n* (%)	7 (28.0%)	15 (57.7%)	0.032
Coexisting autoimmune disorders	13 (52.0%)	10 (38.5%)	0.331
Immunosuppressant therapy (IST)	22 (88.0%)	23 (88.5%)	1.000
Time from onset to IST	9.5 (2.5–25.5)	9.0 (1.0–28.0)	0.663
Azathioprine	12 (48.0%)	15 (57.7%)	0.488
Mycophenolate mofetil	9 (36.0%)	7 (26.9%)	0.485
Other (MTX/RTX)	1 (4.0%)	1 (3.8%)	0.745
Without IST	3 (12.0%)	3 (11.4%)	1.000
CS EPVS, *n* (%)			0.867
High degree-CS EPVS (score > 1)	15 (60.0%)	15 (57.7%)	-
Low degree-CS EPVS (score≤1)	10 (40.0%)	11 (42.3%)	-
BG EPVS, *n* (%)			0.406
High degree-BG EPVS (score > 1)	6 (24.0%)	9 (34.6%)	-
Low degree-BG EPVS (score≤1)	19 (76.0%)	17 (65.4%)	-

MTX, methotrexate; RTX, rituximab; CS, centrum semiovate; BG, basal ganglia.

the location of spine cord lesions were mainly at cervical cord and/or thoracic cord. However, patients with REO-NMOSD were more likely to have cervical cord involvement than patients with RLO-NMOSD at TM initial attack. APS is one of the core clinical symptoms of NMOSD (20), and is characterized by intractable nausea, vomiting, and hiccups. APS occurred during disease onset in 7.1–10.3% of patients with NMOSD (33). Here, we found that APS incidence in patients with REO-NMOSD was significantly higher than in patients with RLO-NMOSD. The disability causes poor recovery from attacks (34).

Brain MRI lesions identified in NMOSD included typical brain lesions, peri ependymal lesions surrounding the third ventricles and lateral ventricles, and extensive hemispheric lesions (7, 8, 13). Mao et al. found that the differing characteristics of brain lesions between patients with EO-NMOSD and LO-NMOSD may reflect inflammatory processes (8). AQP4 is a perivascular astrocyte channel protein that regulates glymphatic function (35) and facilitates CSF flow. Convective interstitial fluid (ISF) propels waste products toward veins where they enter the PVS for efflux out of the central nervous system (36). The PVS is lined by astrocytic endfeet which have AQP4 water channels on the exteriors that abutting abluminal vessel walls at the inner boundaries (37). PVS visibility increases with age (i.e., is strongest in the BG) (16, 38, 39). Additionally, it is associated with hypertension and inflammation (16, 38, 40). In this study, we compared the degrees EPVS between patients with REO-NMOSD and RLO-NMOSD. We found that the degrees of CS-EPVS were not significantly different between the two groups, which was the same as in BG-EPVS. In AQP4-Ab positive NMOSD, EPVS degrees were also similar between the REO-NMOSD and RLO-NMOSD groups. In the future, we hope to compare EPVS in NMOSD patients with EPVS in a matched healthy control group and to investigate the PVS kinetics in the two groups.

Our study has limitations: it is a retrospective study and contained a small number of patients from a single center.

In conclusion, for patients with REO- and RLO-NMOSD with disease courses longer than 3 years, those with disabilities can partly recover from their initial attacks during the first year. Patients with RLO-NMOSD become worse throughout time until the final follow-up time points, while patients with REO-NMOSD partly recovered after their third year. Patients with RLO-NMOSD had a worse final visual acuity than patients with REO-NMOSD, while the lengths of spinal cord involvement showed no difference between the two groups. Besides, patients with REO-NMOSD were more likely to have cervical cord involvement than patients with RLO-NMOSD at TM onset. Similar features were reflected in AQP4-Ab positive NMOSD. The age of onset and ARR were the main predictors for disability.

DATA AVAILABILITY STATEMENT

The original contributions presented in the study are included in the article/**Supplementary Material**, further inquiries can be directed to the corresponding author.

ETHICS STATEMENT

The studies involving human participants were reviewed and approved by Medical Ethics Committee of the First Affiliated Hospital of Zhengzhou University (2021-KY-1103). Written informed consent from the participants' legal guardian/next of kin was not required to participate in this study in accordance with the national legislation and the institutional requirements.

AUTHOR CONTRIBUTIONS

JY conceived and designed the study, involved in the acquisition of data, and writing the original draft. SY contributed in the data analysis and editing of the review. PN and JT provided critical revisions to the article. All authors contributed to the article and approved the submitted version.

FUNDING

This work was supported by the Program of Science and Technology Development of Henan Province of China [NO. 2018020108].

SUPPLEMENTARY MATERIAL

The Supplementary Material for this article can be found online at: https://www.frontiersin.org/articles/10.3389/fneur.2022.859276/full#supplementary-material

REFERENCES

1. Wingerchuk DM, Lennon VA, Lucchinetti CF, Pittock SJ, Weinshenker BG. The spectrum of neuromyelitis optica. *Lancet Neurol.* (2007) 6:805–15. doi: 10.1016/S1474-4422(07)70216-8
2. Wingerchuk D, Lennon V, Pittock S, Lucchinetti C, Weinshenker B. Revised diagnostic criteria for neuromyelitis optica. *Neurology.* (2006) 66:1485–9. doi: 10.1212/01.wnl.0000216139.44259.74
3. Pandit L, Asgari N, Apiwattanakul M, Palace J, Paul F, Leite M, et al. Demographic and clinical features of neuromyelitis optica: a review. *Mult Scler*. (2015) 21:845–53. doi: 10.1177/1352458515572406
4. Ma X, Kermode A, Hu X, Qiu W. Risk of relapse in patients with neuromyelitis optica spectrum disorder: Recognition and preventive strategy. *Mult Scler Relat Disord.* (2020) 46:102522. doi: 10.1016/j.msard.2020.102522
5. Sepulveda M, Delgado-García G, Blanco Y, Sola-Valls N, Martinez-Lapiscina E, Armangué T, et al. Late-onset neuromyelitis optica spectrum disorder: The importance of autoantibody serostatus. *Neurol Neuroimmunol Neuroinflamm.* (2019) 6:e607. doi: 10.1212/NXI.0000000000000607
6. Cai L, Zhang Q, Zhang Y, Chen H, Shi Z, Du Q, et al. Clinical characteristics of very late-onset neuromyelitis optica spectrum disorder. *Mult Scler Relat Disord.* (2020) 46:102515. doi: 10.1016/j.msard.2020.102515
7. Seok J, Cho H, Ahn S, Cho E, Park M, Joo I, et al. Clinical characteristics of late-onset neuromyelitis optica spectrum disorder: a multicenter retrospective study in Korea. *Mult Scler.* (2017) 23:1748–56. doi: 10.1177/1352458516685416
8. Mao Z, Yin J, Zhong X, Zhao Z, Qiu W, Lu Z, et al. Late-onset neuromyelitis optica spectrum disorder in AQP4-seropositivepatients in a Chinese population. *BMC Neurol.* (2015) 15:160. doi: 10.1186/s12883-015-0417-y
9. Nakahara K, Nakane S, Nagaishi A, Narita T, Matsuo H, Ando Y. Very late onset neuromyelitis optica spectrum disorders. *Eur J Neurol.* (2021) 28:2574–81. doi: 10.1111/ene.14901
10. Zhang L, Yang L, Li T, Wang J, Qi Y, Zhang D, et al. Distinctive characteristics of early-onset and late-onset neuromyelitis optica spectrum disorders. *Int J Neurosci.* (2017) 127:334–8. doi: 10.1080/00207454.2016.1254630
11. Margoni M, Carotenuto A. Very late-onset recurrent myelitis in a patient diagnosed with antiphospholipid syndrome: a puzzle of autoimmunity. *J Neuroimmunol.* (2019) 337:577051. doi: 10.1016/j.jneuroim.2019.577051
12. Collongues N, Marignier R, Jacob A, Leite MI, Siva A, Paul F, et al. Characterization of neuromyelitis optica and neuromyelitis optica spectrum disorder patients with a late onset. *Mult Scler.* (2014) 20:1086–94. doi: 10.1177/1352458513515085
13. Carnero Contentti E, Daccach Marques V, Soto de. Castillo I, Tkachuk V, Ariel B, Castillo MC, et al. Clinical features and prognosis of late-onset neuromyelitis optica spectrum disorders in a Latin American cohort. *J Neurol.* (2020) 267:1260–8. doi: 10.1007/s00415-020-09699-2
14. Nagaishi A, Takagi M, Umemura A, Tanaka M, Kitagawa Y, Matsui M, et al. Clinical features of neuromyelitis optica in a large Japanese cohort: comparison between phenotypes. *J Neurol Neurosurg Psychiatry.* (2011) 82:1360–4. doi: 10.1136/jnnp-2011-300403
15. Jarius S, Ruprecht K, Wildemann B, Kuempfel T, Ringelstein M, Geis C, et al. Contrasting disease patterns in seropositive and seronegative neuromyelitis optica: A multicentre study of 175 patients. *J Neuroinflammation.* (2012) 9:14. doi: 10.1186/1742-2094-9-14
16. Wardlaw JM, Benveniste H, Nedergaard M, Zlokovic BV, Mestre H, Lee H, et al. Perivascular spaces in the brain: anatomy, physiology and pathology. *Nat Rev Neurol.* (2020) 16:137–53. doi: 10.1038/s41582-020-0312-z
17. Lennon V, Wingerchuk D, Kryzer T, Pittock S, Lucchinetti C, Fujihara K, et al. A serum autoantibody marker of neuromyelitis optica: distinction from multiple sclerosis. *Lancet.* (2004) 364:2106–12. doi: 10.1016/S0140-6736(04)17551-X
18. Kilsdonk ID, Steenwijk MD, Pouwels PJ, Zwanenburg JJ, Visser F, Luijten PR, et al. Perivascular spaces in MS patients at 7 Tesla MRI: a marker of neurodegeneration? *Mult Scler.* (2015) 21:155–62. doi: 10.1177/1352458514540358
19. Chen A, Akinyemi RO, Hase Y, Firbank MJ, Ndung'u MN, Foster V, et al. Frontal white matter hyperintensities, clasmatodendrosis and gliovascular abnormalities in ageing and post-stroke dementia. *Brain.* (2016) 139(Pt 1):242–58. doi: 10.1093/brain/awv328
20. Wingerchuk D, Banwell B, Bennett J, Cabre P, Carroll W, Chitnis T, et al. International consensus diagnostic criteria for neuromyelitis optica spectrum disorders. *Neurology.* (2015) 85:177–89. doi: 10.1212/WNL.0000000000001729
21. Thompson AJ, Banwell BL, Barkhof F, Carroll WM, Coetzee T, Comi G, et al. Diagnosis of multiple sclerosis: 2017 revisions of the McDonald criteria. *Lancet Neurol.* (2018) 17:162–73. doi: 10.1016/S1474-4422(17)30470-2
22. Potter GM, Chappell FM, Morris Z, Wardlaw JM. Cerebral perivascular spaces visible on magnetic resonance imaging: development of a qualitative rating scale and its observer reliability. *Cerebrovasc Dis.* (2015) 39:224–31. doi: 10.1159/000375153
23. Huo Y, Huang S, Li R, Gong X, Zhang W, Zhang R, et al. Elevated hemoglobin is independently associated with enlarged perivascular spaces in the central semiovale. *Sci Rep.* (2021) 11:2820. doi: 10.1038/s41598-021-82327-9
24. Del Brutto O, Mera R. Enlarged perivascular spaces in the basal ganglia are independently associated with intracranial atherosclerosis in the elderly. *Atherosclerosis.* (2017) 267:34–8. doi: 10.1016/j.atherosclerosis.2017.10.024
25. Hor JY, Asgari N, Nakashima I, Broadley SA, Leite MI, Kissani N, et al. Epidemiology of neuromyelitis optica spectrum disorder and its prevalence and incidence worldwide. *Front Neurol.* (2020) 11:501. doi: 10.3389/fneur.2020.00501
26. Kitley J, Leite MI, Nakashima I, Waters P, McNeillis B, Brown R, et al. Prognostic factors and disease course in aquaporin-4 antibody-positive patients with neuromyelitis optica spectrum disorder from the United Kingdom and Japan. *Brain.* (2012) 135(Pt 6):1834–49. doi: 10.1093/brain/aws109
27. Wang L, Tan H, Huang W, Chang X, ZhangBao J, Zhou L, et al. Late onset neuromyelitis optica spectrum disorder with anti-aquaporin 4 and anti-myelin oligodendrocyte glycoprotein antibodies. *Eur J Neurol.* (2021) 29:1128–35. doi: 10.1111/ene.15239
28. Kim SH, Mealy MA, Levy M, Schmidt F, Ruprecht K, Paul F, et al. Racial differences in neuromyelitis optica spectrum disorder. *Neurology.* (2018) 91:e2089–99. doi: 10.1212/WNL.0000000000006574
29. Thongmee W, Narongkhananukul C, Padungkiatsagul T, Jindahra P, Vanikieti K. Comparison of early- and late-onset NMOSD-related optic neuritis in Thai patients: clinical characteristics and long-term visual outcomes. *Clin Ophthalmol.* (2021) 15:419–29. doi: 10.2147/OPTH.S295769
30. Absoud M, Lim MJ, Appleton R, Jacob A, Kitley J, Leite MI, et al. Paediatric neuromyelitis optica: clinical, MRI of the brain and prognostic features. *J Neurol Neurosurg Psychiatry.* (2015) 86:470–2. doi: 10.1136/jnnp-2014-308550
31. Palace J, Lin DY, Zeng D, Majed M, Elsone L, Hamid S, et al. Outcome prediction models in AQP4-IgG positive neuromyelitis optica spectrum disorders. *Brain.* (2019) 142:1310–23. doi: 10.1093/brain/awz054

32. Clarke L, Arnett S, Bukhari W, Khalilidehkordi E, Jimenez Sanchez S, O'Gorman C, et al. MRI patterns distinguish AQP4 antibody positive neuromyelitis optica spectrum disorder from multiple sclerosis. *Front Neurol.* (2021) 12:722237. doi: 10.3389/fneur.2021.722237
33. Shosha E, Dubey D, Palace J, Nakashima I, Jacob A, Fujihara K, et al. Area postrema syndrome: frequency, criteria, and severity in AQP4-IgG-positive NMOSD. *Neurology*. (2018) 91:e1642–51. doi: 10.1212/WNL.0000000000006392
34. Wingerchuk DM, Pittock SJ, Lucchinetti CF, Lennon VA, Weinshenker BG. A secondary progressive clinical course is uncommon in neuromyelitis optica. *Neurology.* (2007) 68:603–5. doi: 10.1212/01.wnl.0000254502.87233.9a
35. Mestre H, Kostrikov S, Mehta R, Nedergaard M. Perivascular spaces, glymphatic dysfunction, and small vessel disease. *Clin Sci.* (2017) 131:2257–74. doi: 10.1042/CS20160381
36. Iliff J, Wang M, Liao Y, Plogg B, Peng W, Gundersen G, et al. A paravascular pathway facilitates CSF flow through the brain parenchyma and the clearance of interstitial solutes, including amyloid β. *Sci Transl Med*. (2012) 4:147ra11. doi: 10.1126/scitranslmed.3003748
37. Nedergaard M, Goldman S. Glymphatic failure as a final common pathway to dementia. *Science.* (2020) 370:50–6. doi: 10.1126/science.abb8739
38. Francis F, Ballerini L, Wardlaw JM. Perivascular spaces and their associations with risk factors, clinical disorders and neuroimaging features: a systematic review and meta-analysis. *Int J Stroke.* (2019) 14:359–71. doi: 10.1177/1747493019830321
39. Yao M, Hervé D, Jouvent E, Duering M, Reyes S, Godin O, et al. Dilated perivascular spaces in small-vessel disease: a study in CADASIL. *Cerebrovasc Dis.* (2014) 37:155–63. doi: 10.1159/000356982
40. Wuerfel J, Haertle M, Waiczies H, Tysiak E, Bechmann I, Wernecke KD, et al. Perivascular spaces–MRI marker of inflammatory activity in the brain? *Brain*. (2008) 131(Pt 9):2332–40. doi: 10.1093/brain/awn171

Conflict of Interest: The authors declare that the research was conducted in the absence of any commercial or financial relationships that could be construed as a potential conflict of interest.

Publisher's Note: All claims expressed in this article are solely those of the authors and do not necessarily represent those of their affiliated organizations, or those of the publisher, the editors and the reviewers. Any product that may be evaluated in this article, or claim that may be made by its manufacturer, is not guaranteed or endorsed by the publisher.

frontiers | Frontiers in Neurology

STUDY PROTOCOL
published: 25 April 2022
doi: 10.3389/fneur.2022.860083

Human Umbilical Cord Mesenchymal Stem Cells to Treat Neuromyelitis Optica Spectrum Disorder (hUC–MSC–NMOSD): A Study Protocol for a Prospective, Multicenter, Randomized, Placebo-Controlled Clinical Trial

Xiao-Ying Yao[1†], Li Xie[2†], Yu Cai[1†], Ying Zhang[1], Ye Deng[1], Mei-Chun Gao[1], Yi-Shu Wang[1], Hui-Ming Xu[3], Jie Ding[1], Yi-Fan Wu[1], Nan Zhao[1], Ze Wang[1], Ya-Ying Song[1], Li-Ping Wang[1], Chong Xie[1], Ze-Zhi Li[1], Wen-Bin Wan[1], Yan Lin[1], Hai-Feng Jin[1], Kan Wang[1], Hui-Ying Qiu[1], Lei Zhuang[1], Yan Zhou[1], Yu-Yan Jin[1], Li-Ping Ni[1], Jia-Li Yan[1], Quan Guo[1], Jia-Hui Xue[1], Bi-Yun Qian[2,4] and Yang-Tai Guan[1]**

[1] Department of Neurology, Ren Ji Hospital, School of Medicine, Shanghai Jiao Tong University, Shanghai, China, [2] Clinical Research Center, School of Medicine, Shanghai Jiao Tong University, Shanghai, China, [3] State Key Laboratory of Oncogenes and Related Genes, Renji-Med-X Clinical Stem Cell Research Center, Renji Hospital, School of Medicine, Shanghai Jiao Tong University, Shanghai, China, [4] Shanghai Clinical Research Promotion and Development Center, Shanghai Hospital Development Center, Shanghai, China

Background: Neuromyelitis Optica spectrum disorder (NMOSD) is severe relapsing and disabling autoimmune disease of the central nervous system. Its optimal first-line treatment to reduce relapse rate and ameliorate neurological disability remains unclear. We will conduct a prospective, multicenter, randomized, placebo-controlled clinical trial to study the safety and effectiveness of human umbilical cord mesenchymal stem cells (hUC–MSCs) in treating NMOSD.

Methods: The trial is planned to recruit 430 AQP4-IgG seropositive NMOSD patients. It consists of three consecutive stages. The first stage will be carried out in the leading center only and aims to evaluate the safety of hUC—MSCs. Patients will be treated with three different doses of hUC–MSCs: 1, 2, or 5 × 10^6 MSC/kg·weight for the low-, medium-, and high-dose group, respectively. The second and third stages will be carried out in six centers. The second stage aims to find the optimal dosage. Patients will be 1:1:1:1 randomized into the low-, medium-, high-dose group and the controlled group. The third stage aims to evaluate the effectiveness. Patients will be 1:1 randomized into the optimal dose and the controlled group. The primary endpoint is the first recurrent time and secondary endpoints are the recurrent times, EDSS scores, MRI lesion numbers, OSIS scores, Hauser walking index, and SF-36 scores. Endpoint events and side effects will be evaluated every 3 months for 2 years.

Discussion: Although hUC–MSC has shown promising treatment effects of NMOSD in preclinical studies, there is still a lack of well-designed clinical trials to evaluate the safety

OPEN ACCESS

Edited by:
Philipp Albrecht, Heinrich Heine University of Düsseldorf, Germany

Reviewed by:
Mahdi Barzegar, Isfahan University of Medical Sciences, Iran
Joachim Havla, Ludwig Maximilian University of Munich, Germany

***Correspondence:**
Yang-Tai Guan
yangtaiguan@sina.com
Bi-Yun Qian
qianbiyun@sjtu.edu.cn

† These authors have contributed equally to this work and share first authorship

Specialty section:
This article was submitted to Multiple Sclerosis and Neuroimmunology, a section of the journal Frontiers in Neurology

Received: *22 January 2022*
Accepted: *21 March 2022*
Published: *25 April 2022*

Citation:
Yao X-Y, Xie L, Cai Y, Zhang Y, Deng Y, Gao M-C, Wang Y-S, Xu H-M, Ding J, Wu Y-F, Zhao N, Wang Z, Song Y-Y, Wang L-P, Xie C, Li Z-Z, Wan W-B, Lin Y, Jin H-F, Wang K, Qiu H-Y, Zhuang L, Zhou Y, Jin Y-Y, Ni L-P, Yan J-L, Guo Q, Xue J-H, Qian B-Y and Guan Y-T (2022) Human Umbilical Cord Mesenchymal Stem Cells to Treat Neuromyelitis Optica Spectrum Disorder (hUC–MSC–NMOSD): A Study Protocol for a Prospective, Multicenter, Randomized, Placebo-Controlled Clinical Trial. Front. Neurol. 13:860083. doi: 10.3389/fneur.2022.860083

and effectiveness of hUC–MSC among NMOSD patients. As far as we know, this trial will be the first one to systematically demonstrate the clinical safety and efficacy of hUC–MSC in treating NMOSD and might be able to determine the optimal dose of hUC–MSC for NMOSD patients.

Trial registration: The study was registered with the Chinese Clinical Trial Registry (CHICTR.org.cn) on 2 March 2016 (registration No. ChiCTR-INR-16008037), and the revised trial protocol (Protocol version 1.2.1) was released on 16 March 2020.

Keywords: neuromyelitis optica spectrum disorder (NMOSD), human umbilical cord mesenchymal stem cell (hUC-MSC), multicenter trial, randomized controlled trial, study protocol

INTRODUCTION

Neuromyelitis Optica spectrum disorder (NMOSD) is a severe disabling inflammatory autoimmune disease of the central nervous system (CNS) featured with recurrent relapses of optic neuritis and longitudinally extensive transverse myelitis (1). Autoantibodies against the water channel protein aquaporin-4 (AQP4) are the diagnostic markers of the disorder and more than two-thirds of patients meeting clinical criteria for NMOSD are AQP4-IgG seropositive (2, 3). Frequent relapses are associated with a stepwise accumulation of neurological disability. Therefore, relapse prevention is particularly important to reduce the risk of a systemic disability over time (4). Azathioprine and mycophenolate mofetil are the most commonly used therapies for patients with NMOSD (5, 6). Recently, some randomized clinical trials show that the use of B-cell depletion (rituximab, inebilizumab), interleukin-6 signaling blockade (tocilizumab, satralizumab), and complement inhibition (eculizumab) can reduce the risk of relapses in NMOSD (7–11). However, still, some patients who have had these therapies have relapsed. So far, the optimal first-line treatment to reduce relapse rate remains unclear. Furthermore, no drug has been proved to improve neurological disability in NMOSD patients.

Stem cells are a group of cells that are immortal and have unlimited renewal abilities. The types of stem cells usually used in the registered clinical trials include multipotent stem cells, hematopoietic stem cells, and mesenchymal stem cells. There are some pilot trials and cohort studies assessing the therapeutic effect of stem cell transplantation in NMOSD patients (12–14). Recently, autologous nonmyeloablative hematopoietic stem cell transplantation showed to be effective on prolonged drug-free remission with AQP4-IgG seroconversion to negative (12).

Mesenchymal stem cells (MSCs) are stromal precursor cells residing in many tissues, including bone marrow, umbilical cord (UC), fetal liver, and adipose tissue (15–17). MSCs are considered to be multipotent and have anti-inflammatory, immune regulation, and paracrine effects, and also regenerative properties (18). MSCs derived from the human umbilical cord (hUC–MSCs) are more primitive, and possess multiple advantages including ethical agreeableness, a less-invasive procedure for isolation, low immunogenicity, high-proliferation capacity, and multi-lineage differentiation capability (19, 20). Therefore, hUC–MSCs are a promising candidate for cell-based therapy.

Treatment with MSC improves the course of the preclinical model of multiple sclerosis, experimental autoimmune encephalomyelitis (EAE) when administered at the early stages. In EAE, MSC has a profound anti-inflammatory and immune-modulating effect, but they also exhibit neuroprotective features and foster remyelination endogenous neurogenesis with scarce evidence of differentiation in neural cells (21–23). A pilot clinical trial showed that infusion of autologous MSC derived from bone marrow is safe, can reduce the relapse frequency, and mitigates neurological disability with the recovery of neural structures in the optic nerve and spinal cord in NMOSD patients (24).

Human umbilical cord–MSCs can regulate the immune response, promote tissue repair, and increase regeneration both *in vitro* and *in vivo* (25). Therefore, we suggest that hUC–MSCs can prevent relapses and ameliorate disability in NMOSD. However, as far as we know, there are very few reports on the use of hUC–MSCs in NMOSD patients. Here, we present the protocol of Human Umbilical Cord Mesenchymal Stem Cells to Treat Neuromyelitis Optica Spectrum Disorder (hUC–MSC–NMOSD), a prospective, multicenter, randomized, and placebo-controlled clinical trial. The main aims of the study are to verify that the hUC–MSCs can prolong the relapse interval, reduce the relapse times and ameliorate the neurological disability in NMOSD patients.

METHODS AND ANALYSIS

Setting and Participants

The study will be conducted in six clinical centers in Shanghai, China. The leading center is Shanghai Ren Ji Hospital, which is one of the main teaching hospitals of the Shanghai Jiao Tong University School of medicine. Ren Ji Hospital is also one of the biggest clinical centers of neuroimmunological disorders in China. The five branch centers are Shanghai Rui Jin Hospital, Shanghai Xin Hua Hospital, Shanghai General Hospital, Shanghai Sixth People's Hospital, and Shanghai Ninth People's Hospital. In this study protocol, only the patients who fulfilled the diagnostic criteria of NMOSD established by Wingerchuk et al. (26) will be included.

The study protocol has been approved by the Ethics Committees of Ren Ji Hospital (2016-071K).

Patients will be recruited from those neuro-immunological centers of Neurology departments in China. Eligible patients will

TABLE 1 | Schedule of activities of human umbilical cord mesenchymal stem cells (hUC–MSCs) to treat neuromyelitis optica spectrum disorder (hUC–MSC–NMOSD) study.

Follow-up Period	V0 (Screening)	V1 (Baseline)	V2	V3	V4	V5	V6	V7	V8	V9
Time	−30∼−1d	0	3M ± 7d	6M ± 7d	9M ± 7d	12M ± 7d	15M ± 7d	18M ± 7d	21M ± 7d	24M ± 7d
General characteristics	√									
Inclusion and exclusion criteria	√									
Informed consent	√									
Physical examination	√		√	√	√	√	√	√	√	√
EDSS score	√		√	√	√	√	√	√	√	√
OSIS score	√		√	√	√	√	√	√	√	√
Hauser walking index	√		√	√	√	√	√	√	√	√
SF-36 score	√		√	√	√	√	√	√	√	√
Exploratory endpoints associated tests	√		√	√	√	√	√	√	√	√
Complete blood counts	√		√	√	√	√	√	√	√	√
Urinalysis	√		√	√	√	√	√	√	√	√
Coagulation function	√		√	√	√	√	√	√	√	√
Liver and kidney function	√		√	√	√	√	√	√	√	√
Serum glucose	√		√	√	√	√	√	√	√	√
Serum electrolyte	√		√	√	√	√	√	√	√	√
Thyroid function	√									
Urine HCG	√		√	√	√	√	√	√	√	√
Tests for infective diseases	√				√					√
Tumor markers	√		√	√	√	√	√	√	√	√
EKG	√		√	√	√	√	√	√	√	√
Abdominal ultrasound.	√		√	√	√	√	√	√	√	√
Chest X-ray or CT	√		√	√	√	√	√	√	√	√
MRI (head)	√					√				√
MRI (spinal cord)	√					√				√
MRI (optical nerve)	√					√				√
OCT	√					√				√
Primary treatment	√	√	√	√	√	√	√	√	√	√
hUC-MSC or placebo treatment		√	√	√	√					
Record of AE		√	√	√	√	√	√	√	√	√
Record of combined medications	√		√	√	√	√	√	√	√	√

be invited to participate. All the participants will receive adequate information about the nature, purpose, possible risk, and benefits of the trial, and about alternative therapeutic choices. A signed written informed consent form will be obtained from all the participants before enrollment.

The clinical study will be conducted in accordance with all the national regulations and complies with the principles of the World Medical Association Declaration of Helsinki—Ethical Principles for Medical Research Involving Human Subjects, with all its amendments, and also with the principles of Good Clinical Practice.

The clinical information collected including age, sex, past medical history, NMOSD attack time and frequency, corrected visual acuity by standard logarithmic visual acuity chart, Expanded Disability Status Scale (EDSS) score, Opticospinal Impairment Scale (OSIS) score, Hauser walking index, quality of life short Form-36 (SF-36) score, serum status of anti-AQP4 antibody (tested in a cell-based assay), laboratory tests as listed in **Table 1**, electrocardiogram, abdominal ultrasound, chest X-ray or computed tomography, optical coherence tomography, number of brain and spinal cord lesions on MR images, immunomodulatory drugs used in the past 6 months, etc.

Study Design

This is a prospective study for an open-labeled, prospective, multicenter, randomized, placebo-controlled clinical trial. The estimated study period is from March 2019 to March 2025. The NMOSD patients in the remission phase will be randomized into two groups: the treatment group (hUC–MSC infusion plus regular treatment) and the controlled group (stem cell base solution infusion plus regular treatment). All the patients will be treated and followed up for 2 years.

The whole clinical trial includes three consecutive stages.

The first stage of the trial, which will last 24 months, is an open-labeled study and will be carried out in the leading center only. The first stage aims to evaluate the safety of the infusion of

hUC–MSC in NMOSD patients. Patients ($n = 30$) will be treated with three different doses of hUC–MSC. According to the process of enrollment, the first to the tenth participant is in the low-dose group ($n = 10$, 1×10^6 MSC / kg·weight); the eleventh to the twentieth participant is in the medium-dose group ($n = 10$, 2×10^6 MSC / kg·weight); the twenty-first to the thirtieth participant are in the high-dose group ($n = 10$, 5×10^6 MSC / kg·weight). The study starts from the low dose. Only when the lower dose group ends the observation period of 3 months, the study will proceed to a higher dose group. In case of unacceptable toxic reaction occurs in the dose escalation, the study will be ended immediately. In relation to safety considerations, before enrolling the patients in the low-dose group, we will give a single medium dose of hUC–MSC to one patient and follow-up the therapy for one year. The outcome of this dosage will be used only for safety evaluation, not to evaluate the therapy's effectiveness.The second and third stages of the study protocol are part of the multi-center double-blinded randomized clinical trial. The second stage, which aims to screen out the optimal dosage, will last for 24 months and will be carried out in six centers (one leading center and five branch centers). Patients ($n = 160$) will be randomized into four groups: the low-, medium-, high-dose groups, and the controlled group ($n = 40$, respectively). In the second stage, we were seeking to determine the 'optimal biological dose.' The dose that allows reaching the optimal efficacy-toxicity trade-off is further selected and recommended to stage 3. The third stage, which aims to evaluate the effectiveness, will last for 24 months and will be developed in six centers. Patients ($n = 320$) will be randomized into two groups: the optimal dose group ($n = 160$) and the controlled group ($n = 160$). The third stage aims to evaluate the effectiveness and safety of hUC–MSC for NMOSD patients. The study flow chart is shown in **Figure 1**.

Inclusion Criteria

1) 18–75 years of age;
2) Met the diagnostic criteria of NMOSD (established by the International Panel for NMOSD in 2015) (26), and serum AQP4-antibody-positive;
3) In the remission phase, defined as no new or worsening of neurological symptoms and signs in the last 30 days;
4) EDSS (Expanded Disability Status Scale) score $\leq$8;
5) Taking azathioprine or mycophenolate mofetil as ongoing treatment for NMOSD;
6) The results of the hepatic and renal function tests, complete blood count, and urinalysis are unremarkable;
7) The coagulation tests are unremarkable;
8) Be able to end the follow-up period;
9) Signed the informed consent (by patients or their families).

Exclusion Criteria

1) Patients with language dysfunction, disturbance of consciousness, or unstable vital signs;
2) With thyroid dysfunction or other endocrine dysfunction which cannot be controlled by treatment;
3) With severe psychiatric disorders, thus unable to cooperate during the study;
4) With severe hepatic or renal disorders: the results of hepatic function >2 upper limits; the creatinine clearance rate calculated by Cockcroft–Gault equation <60 ml/min; or with severe systematic wasting diseases;
5) Scoring complete blood count test, white blood cell count test $<3.0 \times 10^9$/L or $>12 \times 10^9$/L, or hemoglobin level $<$ 80% lower limits, or platelet counts $<100 \times 10^9$/L;
6) Scoring coagulation tests, one or multiple indicators (TT, APTT, PT, FIB, TDP, and DD) >2 upper limits;
7) Gastrointestinal bleeding or other severe bleeding disorders in the last month;
8) Had allergic history to the study-related drugs;
9) Had major surgeries in the last week;
10) Pregnant or breastfeeding;
11) With a history of hepatitis B, hepatitis C, HIV infection, syphilis, or malignancies;
12) With other rheumatic diseases (such as Sjogren's syndrome, systematic lupus erythematosis), who need to use other immunodepressants other than azathioprine or mycophenolate mofetil;
13) With other situations that may affect the patient's engagement in the study.

Withdrawal Criteria

Withdrawal criteria are as follows: (1) patient withdraws consent; (2) newly find misdiagnosis at baseline; (3) patients are lost to follow-up; (4) investigator's decision to withdraw the subject.

For any subject withdrawal, the reasons for withdrawal will be documented.

Intervention

The Isolation and Culture of hUC–MSCs

The hUC–MSCs are isolated from Wharton's jelly (WJ) of the umbilical cord (UC). The parents who donated signed the informed consent. After aseptically collecting the samples of UC, scrape the WJ away from the blood vessels and inner epithelium of the subamnion. Then WJ is mechanically cut into small pieces of no more than a few millimeters in length. The pieces were transferred to culture flasks, which contained Dulbecco's Modified Eagle Medium-F12 (DMEM-F12) and 10% FBS (Fetal Bovine Serum), then it was incubated in a humidified atmosphere containing 5% CO2 at 37°C. The cells migrate from the explant to medium margins.

The Transportation and Storage of hUC–MSCs

The hUC–MSCs will be immersed in liquid nitrogen, carried in a portable liquid nitrogen container, and will be transported to the research centers by a cold chain logistic company. There will be a real-time recording of the temperature inside the liquid nitrogen container. The hUC–MSCs will be stored in liquid nitrogen until resuscitation and infusion.

Resuscitation of hUC–MSCs

A thermostat water bath will be preheated to 37°C. A metal clip will be precooled in liquid nitrogen and then the freezing bags of MSCs will be extracted. The freezing bags will be quickly dropped

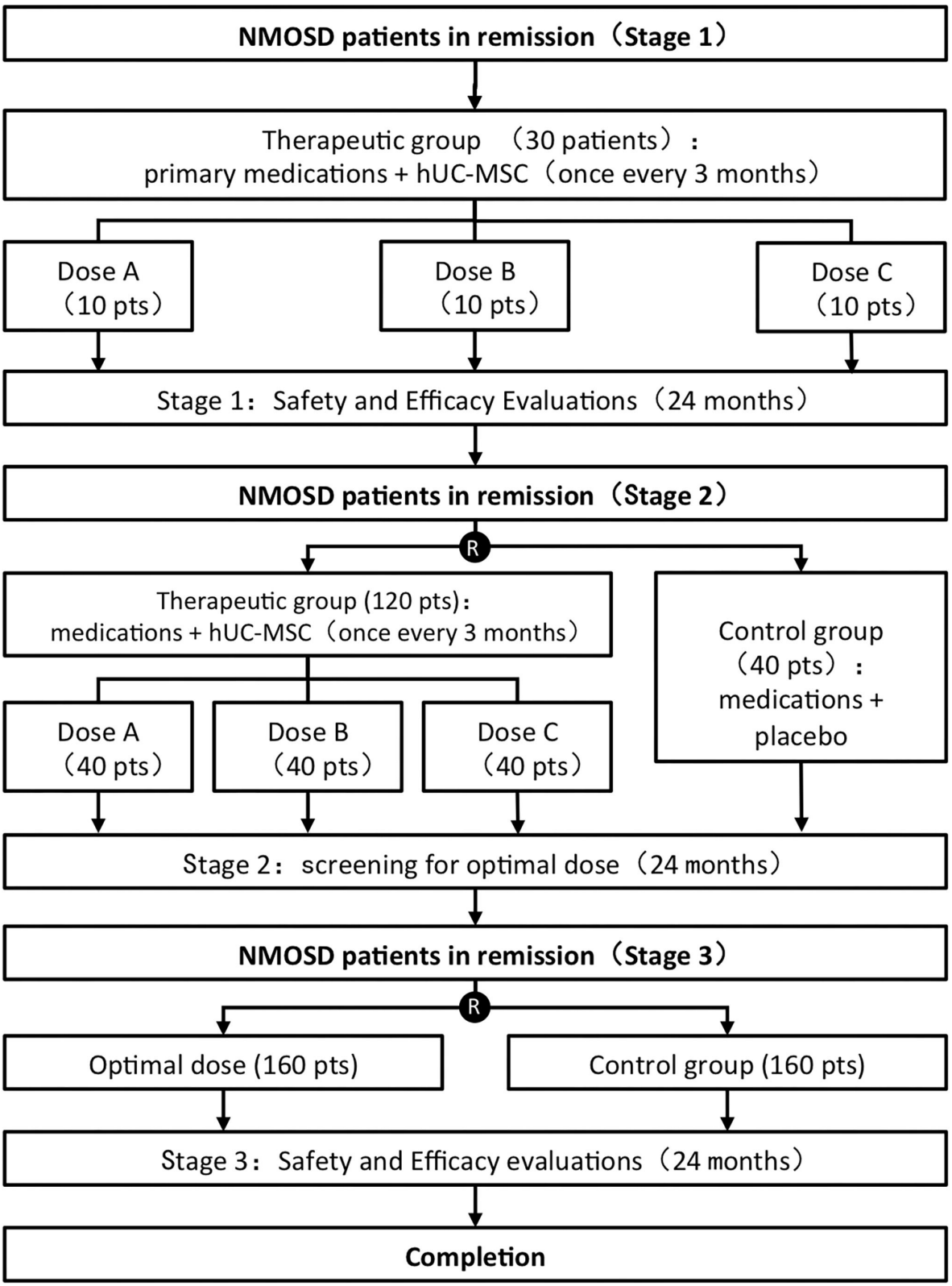

FIGURE 1 | Study flow chart of human umbilical cord mesenchymal stem cells to treat neuromyelitis optica spectrum disorder (hUC-MSC-NMOSD) study.

into the water bath and swayed back and forth gently until totally melting (time duration: 2 min).

Inspections of hUC–MSCs

The subjects can be infused hUC–MSCs only after the sample tests meets the following requirements:

(1) Total cell amount $5 \times 10^7 \pm 10\%$ per package; cell viability over 85%;
(2) Bacterial endotoxin test negative; gram-staining negative.

Transfusion of hUC–MSCs

Subjects in the intervention groups will receive four hUC–MSC infusions every 3 months besides the primary drugs. The dosages are 1, 2, or 5×10^6 MSCs per kg of body weight. The hUC–MSCs will be infused *via* the subjects' peripheral veins. The drip rate is 30 drops per min in the first 15 min of infusion and 45 drops per min in the next 15 min. If there are no adverse effects, the drip rate can be gradually increased, but never exceed 70 drops per min. The time of infusion should last no more than 1 h. After the infusion of MSCs, subjects will be infused with 500 ml normal saline.

Subjects in the control group will receive four stem cell base solution infusions (the same packaging bag as hUC–MSCs) every 3 months besides the primary drugs.

Participant Safety Protection Measures

(1) Subjects will be admitted to the hospital when receiving the infusion;
(2) Intravenous infusion of dexamethasone of 5 mg will be given to subjects 15 min before the infusion of hUC–MSCs;
(3) Subjects will have electrocardiogram monitoring during the whole process of infusion;
(4) Subjects will be discharged after a 2–4 days observation period after the infusion.

Group Allocation, Randomization, and Blinding

The first phase of the trial is an open-label, dose-escalation study that will be performed in a leading center, the Shanghai Ren Ji Hospital. For stages 2 and 3, allocation sequences were generated by an independent statistician by permuted blocks randomization method (block sizes of four or eight). The conceal of allocation sequences were performed by using an integrated web response system (IWRS). The research physician will enroll participants and then assign participants to interventions according to allocation results from IWRS. In stage 2, there are four arms, which are the low dose group (1×10^6 MSC / kg·weight), the medium dose group (2×10^6 MSC / kg·weight), the high dose group (5×10^6 MSC / kg·weight), and the control group (stem cell base solution). Patients will be assigned randomly in a 1:1:1:1 ratio to hUC–MSC groups and control group, respectively. In stage 3, there are two treatment arms. Patients will be assigned randomly in a 1:1 ratio to the hUC–MSC group and control group, respectively. To avoid ethical problems, we designed an add-on trial. Patients in the placebo-controlled group will receive a placebo while they already receive an established regular treatment (azathioprine or mycophenolate mofetil). Therefore, the allocation ratio of 1:1 was based on optimal statistical power and add-on trial design. In stages 2 and 3, all the participants, investigators, and statistician are blinded to group allocation until the end of the study and data analysis. Only pharmacists who are in charge of preparing study drugs are not blinded. Double-blinding will be performed *via* a centralized randomization system. Subjects who leave the study after random allocation will not be replaced.

Sample Size Estimation

Based on previous epidemiology studies on NMOSD among Asians, the replacing rate for the patients in the first year of the onset event is estimated at 55% (27). In this study, we expected that the relapsing rate could be reduced to 40% in the MSC group, according to our preliminary data. In the first stage of an exploratory study, each dosage cohort will include 10 patients to meet the safety evaluation goal, which are 30 patients in total. In the adaptive design stages 2 and 3, a total sample size of 400 patients would have 80% power to detect 15% relapsing rate reduction at a two-sided 5% significant level, with a 20% expected loss to follow-up rate. Therefore, we expected to enroll a total number of 430 subjects in this study. The sample size of this study was determined according to the stage of trial by R software (Version 4.0.3).

Discontinuation of Study Intervention

Unexpected discontinuation of study intervention criteria is (1) deterioration of symptoms leading to MSC infusion intolerance; (2) occurrence of adverse events or abnormal laboratory test results leading to MSC infusion intolerance; (3) individual wishes of the subjects; (4) any reasonable situations that require the clinical trial to be halted; (5) researchers' decisions to halt the clinical trial.

Expulsion criteria are (1) non-compliance to the study protocol; (2) other reasons.

Primary and Secondary Efficacy Endpoints

The primary study endpoint is defined as the first time of recurrence. The recurrence should meet all the following four requirements: occurrence of new symptoms or deterioration of original symptoms; symptoms lasting for more than 24 h; more than 30 days from the last recurrence; no other reasons to explain the recurrence.

Secondary endpoints include the times of recurrence, EDSS scores, MRI lesion numbers, OSIS (Opticospinal Impairment Scale) scores, Hauser walking index, and SF-36 (quality of life short Form-36) scores. MRI lesion numbers refer to the total numbers of the lesions on T2-weighted images of the brain, the cervical, and the thoracic spinal cord, respectively. The SF-36 questionnaire is one of the most widely used qualities of life measures and it has been translated and validated in China (28). It has eight multi-item domains including physical functioning, social function, role limitations related to physical problems, role limitations related to emotional problems, mental health, vitality, bodily pain, and general health perceptions. SF-36 results are presented in two categories of physical component summary (PCS) and mental component summary (MCS). EDSS scores,

OSIS scores, Hauser walking index, and SF-36 scores will be assessed every 3 months.

Exploratory endpoints include: serum lymphocyte subsets (T helper cells, T suppressor cells, Natural Killer cells, and B lymphocytes), cytokines (Interleukin-2,4,6,10,17A, TNF-α, and IFN-γ), complements, serum anti-AQP4 antibody titers, average retinal nerve fiber layer (RNFL) thickness, etc.

Adverse Events

Adverse events (AEs) refer to any unwanted symptoms or signs in a clinical investigation subject and do not necessarily have a causal relationship with the applied intervention (29). All AEs will be coded according to the WHO's Adverse Reactions Terminology. At the end of the clinical trial, the intensity and relationship of any AEs with the study intervention will be identified.

If any severe AE (SAE) is encountered, even with extremely low incidence, it will be reported to the trial's principal investigator, the stem cell research ethics committee, and the state supervision agency within 24 h of its occurrence.

There are two types of side effects that need intensive monitoring, side effects during infusion and long-term side effects.

Side effects during infusion include allergic reactions (such as fever, tachycardia, dyspnea) and systematic complications (infection, embolism, and multiple organ failure);

While monitoring long-term side effects, the following items will be tested every 3 months: tumor markers (AFP, CEA, CA199, CA125, CA153, and CA242); complete blood count and urinalysis, liver and kidney function, blood glucose and electrolyte, coagulation tests, tests for infective diseases (HIV, RPR, hepatitis B, and C; tested at baseline, 9 months and 2 years of follow-up), urine HCG; electrocardiogram, chest X-ray or CT, and abdominal ultrasound.

Follow-Up

Primary, secondary, exploratory endpoint events, and side effects will be evaluated in all participating subjects at baseline and every 3 months. Magnetic resonance scans and optical coherence tomography (OCT) will be evaluated at baseline, year 1, and year 2 of follow-up.

For safety consideration, during stage one of the trial, all the subjects will receive a telephone interview within 1 week after hUC–MSC infusion and then every 2 weeks until the second infusion. The telephone interview will include information on symptoms' change and side effects.

The study schedule is shown in **Table 1**.

Data Management

All the study documents from all the centers will be considered highly confidential and will be stored in locked filing cabinets in a room with restricted access. All data will be translated into electronic format and stored in a database. Access to the database will be strongly restricted. The principal investigator and the biostatistician will be able to log into the data set and get full access to the information only upon permission from the head of this study. Data backups will be performed regularly by trial coordinators. If required, data transfer between centers will be encrypted, and any information capable of identifying individuals will be removed.

Trial Quality Assurance

This study will be implemented according to high-quality standards and will be delivered in accordance with the present trial protocol, which will not be amended unless any SAE occurs during its implementation. All the research staff, including investigators, research assistants, and outcome evaluators, will be trained in advance to be able to competently administer all the items as per the protocol. Once the clinical trial begins, an independent trial inspector will visit each study site monthly and will be responsible for reviewing the following: overall research progress and integrity, adherence to the selection criteria for all the included subjects, compliance with the scheduled intervention for each participant, compliance with national regulations, and the handling of practical problems. Moreover, this trial inspector may occasionally provide suggestions to the principal investigator, who will make any final decisions about trial modifications, continuation, or termination.

Statistical Analysis

The Kolmogorov–Smirnov Z test will be used for checking data normality. Categorical variables will be summarized as counts (percentage) and continuous variables as the means (standard error, SE) or medians (interquartile ranges, IQR), if not normally distributed. For the primary endpoint of the first time of recurrence, survival analysis will be conducted to analyze between-group differences. The Kaplan–Meier estimates for time of recurrence are presented for all groups. Hazard ratios for the comparison of between groups and 95% CIs were calculated with the Cox proportional-hazards model. Prespecified subgroup analyses of the primary outcome were stratified by, EDSS score at baseline, disease duration, age at randomization, the total number of previous relapses, number of relapses 2 years before randomization, and regular treatment. For secondary outcomes, statistical comparisons between the groups will be performed using Student's *t*-test or the Mann–Whitney U test for continuous variables, as well as the chi-square and Fisher's exact tests for categorical variables, as deemed appropriate. Correlations between continuous variables will be assessed by Pearson's correlation coefficient or Spearman's correlation coefficient. All missing data were not imputed in this study.

In this study, two analysis sets will be required. For the safety set (SS) analysis, all safety indicators will be obtained from those who have undergone at least one dose of hUC–MSC infusions. For the effectiveness analysis set, the intention to treat (ITT) analysis set will be used.

Lan–DeMets alpha-spending function with an O'Brien–Fleming boundary will be used to control the family-wise of type I error. Inverse normal combination test will be used to combine data from stages 2 and 3 in the final analysis. An independent Data and Safety Monitoring Board (DSMB) will review and evaluate the accumulated study data for participant safety, study conduct, and progress at each stage of the study. Only members of DSMB could have access to the data and results of the analysis.

The Ethics Committee will be notified of any amendment to the study protocol. DSMB can make recommendations to terminate the study based on one of the following conditions: a significant difference in terms of effectiveness between groups; a significant risk-benefit ratio in one group; low degree of success in a reasonable period (such as poor compliance, low incidence of endpoint events). The advice of the DSMB meeting will be shared with the steering committee of the trial.

DISCUSSION

To the best of our knowledge, this study will be the first one to systematically demonstrate the clinical safety and efficacy of hUC–MSC in treating NMOSD, which leads to severe neurological disability in the young population. Several studies have reported preliminary results on the efficacy of hUC–MSC in treating different types of diseases, such as stroke, spinal cord injury, hereditary spinocerebellar ataxia, multiple system atrophy, multiple sclerosis, and other systemic diseases such as hematological diseases, immunological diseases, etc. (30–36). Toxicity is rarely reported in these studies. In addition, these studies have a small number of subjects, lack control, and are not well-designed. Therefore, there is a need for high-quality evidence on the efficacy of hUC–MSC transfusion.

Some studies with small sample sizes have reported the efficacy of stem cells in treating NMOSD, but they use invasive methodologies in performing stem cell transplantation (12–14). As far as we know, there was only one study using hUC–MSC to treat NMO till the present day. This study was published in 2012. In this study, hUC–MSCs transplantation was used to treat five NMO patients with a follow-up period of 18 months. Among the five cases, four showed therapeutic improvement after hUC–MSCs treatment. Both symptoms and signs improved and relapse frequencies were reduced (37).

The majority of previous studies only tested one dose of hUC–MSCs (36). Therefore, the optimal transfusion dose of hUC–MSC has not been determined till now. We use three different doses (1, 2, or 5×10^6 MSC per kg of body weight) in stages 1 and 2 of the trial in order to determine the optimal dose of hUC–MSC in NMOSD patients, balancing both efficacy and safety.

The route of administration of hUC–MSCs also needs to be determined. The rationale for intrathecal management is the transportation of cells directly into the central nervous system (CNS). However, intrathecal injection of hUC–MSCs does not affect cytokine dissimilarity in peripheral blood (38). Besides, intrathecal administration in humans may lead to meningeal irritation, likely related to CNS inflammation, which can cause headache, seizures, acute encephalomyelitis, etc (39, 40). On the contrary, intravenous administration of hUC–MSCs is not invasive and has very mild self-limited adverse events (39, 40). Therefore, it should be considered as a preferred route.

This study is a well-designed protocol for a clinical trial, and it includes a variety of safety indicators, functional assessments, imaging evaluations, and humoral indicators. We believe that this study protocol will allow us to elucidate the therapeutic efficacy and safety concerns of hUC–MSC in treating AQP4-positive NMOSD and finally to determine the best dosage to be used.

CONCLUSION

In summary, hUC–MSC holds great promise for an effective treatment of NMOSD.

The results of this study may represent a milestone and may be used for future revisions of NMOSD guidelines.

ETHICS STATEMENT

The studies involving human participants were reviewed and approved by the Ethics Committees of Ren Ji Hospital. The patients/participants provided their written informed consent to participate in this study.

AUTHOR CONTRIBUTIONS

Y-TG, B-YQ, X-YY, LX, YC, YD, Z-ZL, CX, W-BW, and YZha: conception and design. Y-TG and B-YQ: administrative support. X-YY, M-CG, Y-FW, NZ, ZW, Y-YS, H-MX, Y-SW, JD, L-PW, KW, H-YQ, LZ, YZho, Y-YJ, L-PN, J-LY, QG, J-HX, YL, and H-FJ: provision of study materials or patients. X-YY, M-CG, Y-FW, NZ, ZW, Y-YS, L-PW, and JD: collection and assembly of data. X-YY and LX: data analysis and interpretation. All authors: manuscript writing and final approval of manuscript.

FUNDING

This study was supported by the National Key Research and Development Project of Stem Cell and Translational Research by the Ministry of Science and Technology (Project No. 2020YFA0113100), National Natural Science Foundation of China (Project Nos. 81771295 and 81801211), and the Funding of Multicenter clinical research projects of School of Medicine, Shanghai Jiao Tong University (Project No. DLY201605).

ACKNOWLEDGMENTS

We would thank all the staff and patients involved with the study at the 6 research sites. We would acknowledge the role of the Clinical Research Center, Ren Ji Hospital, in supporting the ongoing delivery of the trial at the sites. We are grateful to all the staff of the Clinical Research Center of the School of Medicine, Shanghai Jiao Tong University for their support in designing this study protocol.

REFERENCES

1. Wingerchuk DM, Lennon VA, Pittock SJ, Lucchinetti CF, Weinshenker BG. Revised diagnostic criteria for neuromyelitis optica. *Neurology.* (2006) 66:1485–9. doi: 10.1212/01.wnl.0000216139.44259.74
2. Lennon VA, Wingerchuk DM, Kryzer TJ, Pittock SJ, Lucchinetti CF, Fujihara K, et al. A serum autoantibody marker of neuromyelitis optica: distinction from multiple sclerosis. *Lancet.* (2004) 364:2106–12. doi: 10.1016/S0140-6736(04)17551-X
3. Wingerchuk DM, Lennon VA, Lucchinetti CF, Pittock SJ, Weinshenker BG. The spectrum of neuromyelitis optica. *Lancet Neurol.* (2007) 6:805–15. doi: 10.1016/S1474-4422(07)70216-8
4. Papadopoulos MC, Bennett JL, Verkman AS. Treatment of neuromyelitis optica: state-of-the-art and emerging therapies. *Nat Rev Neurol.* (2014) 10:493–506. doi: 10.1038/nrneurol.2014.141
5. Sellner J, Boggild M, Clanet M, Hintzen RQ, Illes Z, Montalban X, et al. EFNS guidelines on diagnosis and management of neuromyelitis optica. *Eur J Neurol.* (2010) 17:1019–32. doi: 10.1111/j.1468-1331.2010.03066.x
6. Mealy MA, Wingerchuk DM, Palace J, Greenberg BM, Levy M. Comparison of relapse and treatment failure rates among patients with neuromyelitis optica: multicenter study of treatment efficacy. *JAMA Neurol.* (2014) 71:324–30. doi: 10.1001/jamaneurol.2013.5699
7. Tahara M, Oeda T, Okada K, Kiriyama T, Ochi K, Maruyama H, et al. Safety and efficacy of rituximab in neuromyelitis optica spectrum disorders (RIN-1 study): a multicentre, randomised, double-blind, placebo-controlled trial. *Lancet Neurol.* (2020) 19:298–306. doi: 10.1016/S1474-4422(20)30066-1
8. Zhang C, Zhang M, Qiu W, Ma H, Zhang X, Zhu Z, et al. TANGO study investigators. Safety and efficacy of tocilizumab vs. azathioprine in highly relapsing neuromyelitis optica spectrum disorder (TANGO): an open-label, multicentre, randomised, phase 2 trial. *Lancet Neurol.* (2020) 19:391–401. doi: 10.1016/S1474-4422(20)30070-3
9. Pittock SJ, Berthele A, Fujihara K, Kim HJ, Levy M, Palace J, et al. Eculizumab in Aquaporin-4-positive neuromyelitis optica spectrum disorder. *N Engl J Med.* (2019) 381:614–25. doi: 10.1056/NEJMoa1900866
10. Cree BAC, Bennett JL, Kim HJ, Weinshenker BG, Pittock SJ, Wingerchuk DM, et al. N-MOmentum study investigators. Inebilizumab for the treatment of neuromyelitis optica spectrum disorder (N-MOmentum): a double-blind, randomised placebo-controlled phase 2/3 trial. *Lancet.* (2019) 394:1352–63. doi: 10.1016/S0140-6736(19)31817-3
11. Traboulsee A, Greenberg BM, Bennett JL, Szczechowski L, Fox E, Shkrobot S, et al. Safety and efficacy of satralizumab monotherapy in neuromyelitis optica spectrum disorder: a randomised, double-blind, multicentre, placebo-controlled phase 3 trial. *Lancet Neurol.* (2020) 19:402–12. doi: 10.1016/S1474-4422(20)30078-8
12. Burt RK, Balabanov R, Han X, Burns C, Gastala J, Jovanovic B, et al. Autologous non-myeloablative hematopoietic stem cell transplantation for neuromyelitis optica. *Neurology.* (2019) 93:e1732–41. doi: 10.1212/WNL.0000000000008394
13. Greco R, Bondanza A, Oliveira MC, Badoglio M, Burman J, Piehl F, et al. Autologous hematopoietic stem cell transplantation in neuromyelitis optica: a registry study of the EBMT autoimmune diseases working party. *Mult Scler.* (2015) 21:189–97. doi: 10.1177/1352458514541978
14. Hoay KY, Ratnagopal P. Autologous hematopoietic stem cell transplantation for the treatment of neuromyelitis optica in Singapore. *Acta Neurol Taiwan.* (2018) 27:26–32.
15. Zannettino AC, Paton S, Arthur A, Khor F, Itescu S, Gimble JM, et al. Multipotential human adipose-derived stromal stem cells exhibit a perivascular phenotype *in vitro* and *in vivo*. *J Cell Physiol.* (2008) 214:413–21. doi: 10.1002/jcp.21210
16. Hoogduijn MJ, Crop MJ, Peeters AM, Van Osch GJ, Balk AH, Ijzermans JN, et al. Human heart, spleen, and perirenal fat-derived mesenchymal stem cells have immunomodulatory capacities. *Stem Cells Dev.* (2007) 16:597–604. doi: 10.1089/scd.2006.0110
17. He Q, Wan C, Li G. Concise review: multipotent mesenchymal stromal cells in blood. *Stem Cells.* (2007) 25:69–77. doi: 10.1634/stemcells.2006-0335
18. Carrion FA, Figueroa FE. Mesenchymal stem cells for the treatment of systemic lupus erythematosus: is the cure for connective tissue diseases within connective tissue? *Stem Cell Res Ther.* (2011) 2:23. doi: 10.1186/scrt64
19. Wang LT, Ting CH, Yen ML, Liu KJ, Sytwu HK, Wu KK, et al. Human mesenchymal stem cells (MSCs) for treatment towards immune- and inflammation-mediated diseases: review of current clinical trials. *J Biomed Sci.* (2016) 23:76. doi: 10.1186/s12929-016-0289-5
20. Li JF, Yin HL, Shuboy A, Duan HF, Lou JY Li J, et al. Differentiation of hUC-MSC into dopaminergic-like cells after transduction with hepatocyte growth factor. *Mol Cell Biochem.* (2013) 381:183–90. doi: 10.1007/s11010-013-1701-z
21. Zappia E, Casazza S, Pedemonte E, Benvenuto F, Bonanni I, Gerdoni E, et al. Mesenchymal stem cells ameliorate experimental autoimmune encephalomyelitis inducing T-cell anergy. *Blood.* (2005) 106:1755–61. doi: 10.1182/blood-2005-04-1496
22. Gerdoni E, Gallo B, Casazza S, Musio S, Bonanni I, Pedemonte E, et al. Mesenchymal stem cells effectively modulate pathogenic immune response in experimental autoimmune encephalomyelitis. *Ann Neurol.* (2007) 61:219–27. doi: 10.1002/ana.21076
23. Liu R, Zhang Z, Lu Z, Borlongan C, Pan J, Chen J, et al. Human umbilical cord stem cells ameliorate experimental autoimmune encephalomyelitis by regulating immunoinflammation and remyelination. *Stem Cells Dev.* (2013) 22:1053–62. doi: 10.1089/scd.2012.0463
24. Fu Y, Yan Y, Qi Y, Yang L, Li T, Zhang N, et al. Impact of autologous mesenchymal stem cell infusion on neuromyelitis optica spectrum disorder: a pilot, 2-year observational study. *CNS Neurosci Ther.* (2016) 22:677–85. doi: 10.1111/cns.12559
25. Abbaspanah B, Reyhani S, Mousavi SH. Applications of umbilical cord derived mesenchymal stem cells in autoimmune and immunological disorders: from literature to clinical practice. *Curr Stem Cell Res Ther.* (2021) 16:454–64. doi: 10.2174/1574888X16999201124153000
26. Wingerchuk DM, Banwell B, Bennett JL, Cabre P, Carroll W, Chitnis T, et al. International panel for NMO diagnosis. International consensus diagnostic criteria for neuromyelitis optica spectrum disorders. *Neurology.* (2015) 85:177–89. doi: 10.1212/WNL.0000000000001729
27. Kitley J, Leite MI, Nakashima I, Waters P, McNeillis B, Brown R, et al. Prognostic factors and disease course in aquaporin-4 antibody-positive patients with neuromyelitis optica spectrum disorder from the United Kingdom and Japan. *Brain.* (2012) 135:1834–49. doi: 10.1093/brain/aws109
28. Lam CL, Tse EY, Gandek B, Fong DY. The SF-36 summary scales were valid, reliable, and equivalent in a Chinese population. *J Clin Epidemiol.* (2005) 58:815–22. doi: 10.1016/j.jclinepi.2004.12.008
29. Koda M, Hanaoka H, Sato T, Fujii Y, Hanawa M, Takahashi S, et al. Study protocol for the G-SPIRIT trial: a randomised, placebo-controlled, double-blinded phase III trial of granulocyte colony-stimulating factor-mediated neuroprotection for acute spinal cord injury. *BMJ Open.* (2018) 8:e019083. doi: 10.1136/bmjopen-2017-019083
30. Chen L, Xi H, Huang H, Zhang F, Liu Y, Chen D, et al. Multiple cell transplantation based on an intraparenchymal approach for patients with chronic phase stroke. *Cell Transplant.* (2013) 22(Suppl 1):S83–91. doi: 10.3727/096368913X672154
31. Liu J, Han D, Wang Z, Xue M, Zhu L, Yan H, et al. Clinical analysis of the treatment of spinal cord injury with umbilical cord mesenchymal stem cells. *Cytotherapy.* (2013) 15:185–91. doi: 10.1016/j.jcyt.2012.09.005
32. Zhao Y, Tang F, Xiao Z, Han G, Wang N, Yin N, et al. Clinical study of neuroregen scaffold combined with human mesenchymal stem cells for the repair of chronic complete spinal cord injury. *Cell Transplant.* (2017) 26:891–900. doi: 10.3727/096368917X695038
33. Jin JL, Liu Z, Lu ZJ, Guan DN, Wang C, Chen ZB, et al. Safety and efficacy of umbilical cord mesenchymal stem cell therapy in hereditary spinocerebellar ataxia. *Curr Neurovasc Res.* (2013) 10:11–20. doi: 10.2174/156720213804805936
34. Dongmei H, Jing L, Mei X, Ling Z, Hongmin Y, Zhidong W, et al. Clinical analysis of the treatment of spinocerebellar ataxia and multiple system atrophy-cerebellar type with umbilical cord mesenchymal stromal cells. *Cytotherapy.* (2011) 13:913–7. doi: 10.3109/14653249.2011.579958
35. Li JF, Zhang DJ, Geng T, Chen L, Huang H, Yin HL, et al. The potential of human umbilical cord-derived mesenchymal stem cells as a novel cellular therapy for multiple sclerosis. *Cell Transplant.* (2014) 23(Suppl 1):S113–22. doi: 10.3727/096368914X685005

36. Can A, Celikkan FT, Cinar O. Umbilical cord mesenchymal stromal cell transplantations: a systemic analysis of clinical trials. *Cytotherapy*. (2017) 19:1351–82. doi: 10.1016/j.jcyt.2017.08.004
37. Lu Z, Ye D, Qian L, Zhu L, Wang C, Guan D, et al. Human umbilical cord mesenchymal stem cell therapy on neuromyelitis optica. *Curr Neurovasc Res*. (2012) 9:250–5. doi: 10.2174/156720212803530708
38. Mohyeddin Bonab M, Mohajeri M, Sahraian MA, Yazdanifar M, Aghsaie A, Farazmand A, et al. Evaluation of cytokines in multiple sclerosis patients treated with mesenchymal stem cells. *Arch Med Res*. (2013) 44:266–72. doi: 10.1016/j.arcmed.2013.03.007
39. Meamar R, Nematollahi S, Dehghani L, Mirmosayyeb O, Shayegannejad V, Basiri K, et al. The role of stem cell therapy in multiple sclerosis: an overview of the current status of the clinical studies. *Adv Biomed Res*. (2016) 5:46. doi: 10.4103/2277-9175.178791
40. Barati S, Tahmasebi F, Faghihi F. Effects of mesenchymal stem cells transplantation on multiple sclerosis patients. *Neuropeptides*. (2020) 84:102095. doi: 10.1016/j.npep.2020.102095

Conflict of Interest: The authors declare that the research was conducted in the absence of any commercial or financial relationships that could be construed as a potential conflict of interest.

frontiers | Frontiers in Neurology

CASE REPORT
published: 13 May 2022
doi: 10.3389/fneur.2022.863151

Chronic Cognitive Impairment in AQP4+ NMOSD With Improvement in Cognition on Eculizumab: A Report of Two Cases

Georges Saab[1,2], *David G. Munoz*[1,2] *and Dalia L. Rotstein*[1,2]*

[1] Department of Medicine, University of Toronto, Toronto, ON, Canada, [2] St. Michael's Hospital, Toronto, ON, Canada

Cognitive impairment may be associated with aquaporin-4 antibody positive (AQP4+) NMOSD, particularly where there is prominent cerebral, corpus callosum, or thalamic involvement. It is unclear to what extent this phenomenon may be treatable after months to years. We describe two cases of AQP4+ NMOSD with cognitive impairment persisting over more than 6 months, where cognition improved after eculizumab was initiated. In the first case, a 51-year-old woman presented with a 2-month history of cognitive decline and ataxia, and diffuse involvement of the corpus callosum on MRI. AQP4 antibody testing returned positive. Cognitive impairment persisted on therapy with mycophenolate, then rituximab. She was switched to eculizumab from rituximab 18 months after disease onset because of breakthrough optic neuritis; memory and cognitive function improved on eculizumab. In the second case, a 26-year-old woman initially presented with visual, auditory and tactile hallucinations, and impairment in activities of daily living, and was given a diagnosis of schizophrenia. Nine months later she was hospitalized for increasing confusion. MRI showed leukoencephalopathy and diffuse involvement of the corpus callosum with multiple enhancing callosal lesions. AQP4 antibody testing was positive and CSF testing for other antibodies of autoimmune encephalitis was negative. She had some improvement in cognition with high dose corticosteroids but remained significantly impaired. On follow-up, her repeat MRI showed a small new right inferomedial frontal enhancing lesion although she did not complain of any new cognitive issues, her MOCA score was 21/30, and she was started on eculizumab. Two months after eculizumab initiation she and her family reported cognitive improvement and MOCA score was 25/30. Common features of these two cases included extensive callosal involvement and an element of ongoing gadolinium enhancement on MRI. Our experience suggests the possibility that cognitive impairment may be amenable to immunotherapy in certain cases of NMOSD.

Keywords: Neuromyelitis Optica Spectrum Disorder (NMOSD), aquaporin-4 (AQP4), cognitive impairment, eculizumab, corpus callosum

OPEN ACCESS

Edited by:
Yu Cai,
University of Nebraska Medical Center, United States

Reviewed by:
Yoshiki Takai,
Tohoku University Hospital, Japan
Yanhan Ren,
Rosalind Franklin University of Medicine and Science, United States

***Correspondence:**
Dalia L. Rotstein
dalia.rotstein@unityhealth.to

Specialty section:
This article was submitted to Multiple Sclerosis and Neuroimmunology, a section of the journal Frontiers in Neurology

Received: *26 January 2022*
Accepted: *19 April 2022*
Published: *13 May 2022*

Citation:
Saab G, Munoz DG and Rotstein DL (2022) Chronic Cognitive Impairment in AQP4+ NMOSD With Improvement in Cognition on Eculizumab: A Report of Two Cases. Front. Neurol. 13:863151. doi: 10.3389/fneur.2022.863151

INTRODUCTION

Neuromyelitis Optica Spectrum Disorder (NMOSD) is an inflammatory disorder of the central nervous system (CNS) that is characterized most commonly by optic neuritis and myelitis. Detection of serum antibodies to aquaporin-4 (AQP4), a water channel on the foot processes of astrocytes, distinguishes NMOSD from other CNS inflammatory diseases. Cognitive Impairment (CI) has been well established in multiple sclerosis, the most common demyelinating disease of the CNS, but it remains controversial to what extent CI is associated with NMOSD (1, 2). CI in NMOSD may be pronounced in the presence of specific brain lesions including cerebral, corpus callosum, or thalamic involvement, but also has been reported even in absence of such lesions (3). It is unclear whether CI in AQP4+ NMOSD may be treatable, particularly after months to years. Here we present two cases of patients with AQP4+ NMOSD presenting with chronic CI along with diffuse corpus callosum lesions who experienced significant improvement in cognition after starting eculizumab therapy.

CASE 1

A 51-year-old woman presented with a 2-month history of cognitive decline and ataxia. She complained of progressively worsening short term memory and impairment in her activities of daily living, including ability to bathe and dress herself. On neurologic exam, she was oriented to person and place, but not to time. There was evidence of truncal ataxia, bilateral intention hand tremors, and left sided dysmetria. She had an MRI of the brain that showed diffuse involvement of the corpus callosum, particularly the splenium, with diffusion restriction and patchy enhancement (**Figures 1A–C**), and a lesion in the right superior cerebellar peduncle. CTA of the head did not reveal any vascular abnormalities. She also had an MRI of the spinal cord, which showed a lesion in the high thoracic cord centered on the left side from T1 through T3 (**Figure 1D**). Cerebrospinal fluid (CSF) demonstrated 10 white blood cells/mm^3 and protein was mildly elevated. Oligoclonal bands and culture were negative. Serum serologies for various autoimmune conditions including ANA, anti-DNA, RF, and ANCA were all negative as well. CT of the chest did not show any abnormality including hilar lymphadenopathy.

She was treated with a course of high dose IV corticosteroids followed by IVIG with mild improvement in cognition and ataxia but worsened again when steroids were tapered. Subsequently she underwent a biopsy of her brain lesions which at the time was reported to show non-specific findings of inflammation, with infiltration of macrophages and destruction of myelin and axons. She was then empirically started on mycophenolate mofetil for an inflammatory process of unknown etiology. She had gradual improvement in her ADLs and was able to resume functions including dressing and bathing herself. MRI of the brain showed an improvement in the lesions with a resolution of the enhancement (**Figures 1E,F**).

One year after her initial presentation she developed blurry vision in her right eye, followed by complete vision loss in her left eye several days later. Exam showed no light perception in the left eye and she was only able to count fingers in her right eye. MRI of the brain and orbits revealed enhancement of both optic nerves in their orbital portions. She was treated with a course of high dose IV steroids followed by IVIG with an improvement in her right eye vision. A serum cell-based AQP4 antibody test was sent and returned positive, confirming a diagnosis of AQP4+ NMOSD. Her former biopsy slides were obtained and reviewed again; there was extensive loss of AQP4+ and GFAP+ astrocytes supporting the diagnosis of NMOSD (**Figures 2A–D**). In addition, sparse AQP4+ and GFAP+ astrocytes were observed in clusters around blood vessels, perhaps suggesting an early repair phenomenon (**Figures 2E–H**).

The patient's maintenance immunotherapy was switched to rituximab because of the breakthrough relapse. After 2 cycles of rituximab she was found to have worsening vision in her right eye from 20/80 to 20/160 along with new enhancement along the intraorbital portions of the optic nerves consistent with a bilateral optic neuritis (**Figures 1G,H**). She had remained cognitively impaired on rituximab with short-term memory issues and inability to take care of independent activities of daily living such as meal preparation and banking. She was switched to eculizumab. Repeat MRI brain showed no new lesion and resolution of the enhancement in the optic nerves (**Figures 1I–L**). The patient reported a progressive improvement in her memory and cognition, and ability to newly take on household organization, journal writing, and some banking. On follow-up 1 year after starting eculizumab, her MOCA score was 26/30.

CASE 2

A 26-year-old woman was initially seen by psychiatry 1 year prior to neurologic consultation because of paranoid visual, auditory, and tactile hallucinations. She was diagnosed with schizophrenia and started on multiple antipsychotics including aripriprazole, ziprasidone, and risperidone, but found to have an increase in her compulsions and severe nausea and vomiting. She was switched to risperidone with resolution of the nausea and vomiting. Six months later she became more acutely confused and complained of severe headaches. She was admitted to hospital and neurology was consulted. On exam she was drowsy, had stuttering and hesitant speech and evidence of psychomotor retardation. However, she was alert to person, place and time. Fundoscopy was unremarkable. She had some mild give-way weakness in all limbs without a clear pyramidal distribution.

MRI of the brain revealed T2 hyperintensities in the left frontal lobe, left insula, bilateral basal ganglia, corpus callosum, bilateral mesial temporal lobes, bilateral inferior frontal lobes, and bilateral pons and midbrain (**Figures 3A–C**). Lesions were fairly symmetric although there was more extensive involvement of the left frontal lobe. There were discrete enhancing lesions visualized in several places in the corpus callosum (**Figure 3D**). Her CSF revealed 34 white blood cells/mm^3, 50% neutrophils, protein 1.16 g/L, and glucose 2.4 mmol/L. ANA was positive

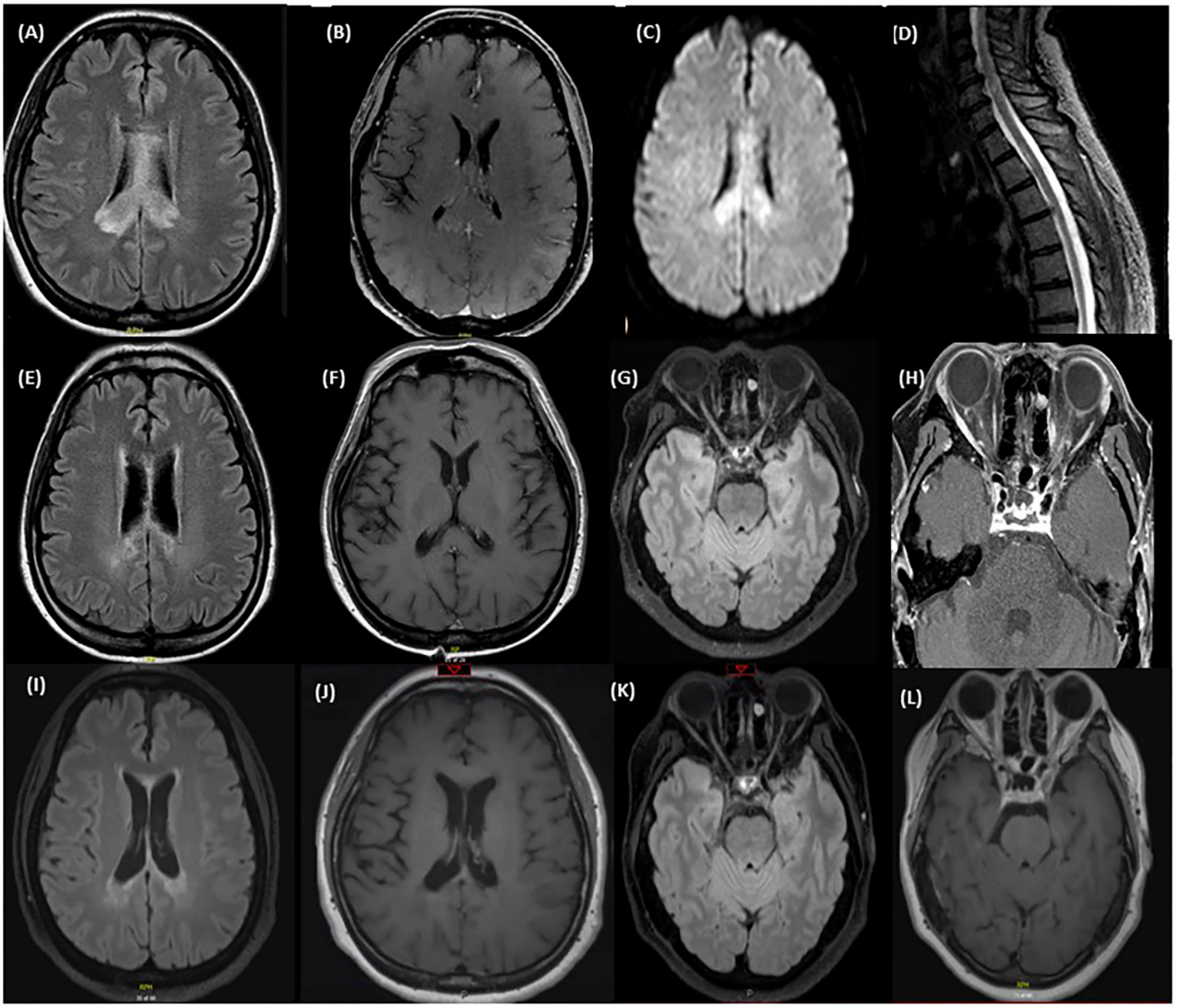

FIGURE 1 | MRI at time of first relapse: **(A)** Axial T2 FLAIR sequence of the brain showing diffuse corpus callosum involvement. **(B)** Axial T1 with gadolinum showing patchy enhancement of the lesion in the right splenium of the corpus callosum. **(C)** Axial DWI sequence of the brain showing diffusion restriction. **(D)** T2 STIR sequence of the lower cervical spine and thoracic spine showing a central hyperintensity extending from the level of T1-T3. MRI after treatment of first relapse with corticosteroids: **(E)** Axial T2 FLAIR sequence of the brain showing an improvement of the corpus callosum lesions after the steroid course. **(F)** Axial T1 with gadolinium showing a resolution of the patchy enhancement after the steroid course. MRI immediately prior to eculizumab: **(G)** Axial T2 FLAIR sequence of the brain showing an increased T2 signal in the right optic nerve in the mid intraorbital course with focal atrophy of the left optic nerve. **(H)** Axial T1 with Gadolinium sequence of the orbits before starting eculizumab showing mild enhancement of both optic nerves. MRI after eculizumab: **(I)** Axial T2 FLAIR sequence of the brain showing stable deep periventricular lesions without any new lesions identified. **(J)** Axial T1 with gadolinium showing no enhancing lesions. **(K)** Axial T2 FLAIR sequence of the brain showing a decrease in the intensity of the T2 signal in the right optic nerve. **(L)** Axial T1 with gadolinium shows resolution of the previously enhancing optic nerve lesions.

at 1:80 and SSA was positive as well. A CSF autoimmune encephalitis panel including NMDA receptor antibody testing and CSF cytology were negative. Serum syphilis, HIV, Lyme disease, West Nile virus, Influenza, and COVID-19 serologies, and MOG antibody were all negative. Her serum AQP4 cell-based antibody test returned strongly positive. She was initially treated with antivirals and antibiotics for a presumed encephalitis, then later with a course of high dose steroids with improvement in alertness and concentration, although she remained significantly cognitively impaired and unable to perform independent activities of daily living. She was not treated with an oral prednisone taper because of her psychiatric history.

On follow-up, repeat MRI showed a small, 7 mm, new right inferomedial frontal lesion with patchy enhancement, although she did not complain of any new cognitive issues (**Figures 3E–H**). Her MOCA score was 21/30. Eculizumab therapy was initiated. Two months after eculizumab initiation she and her family

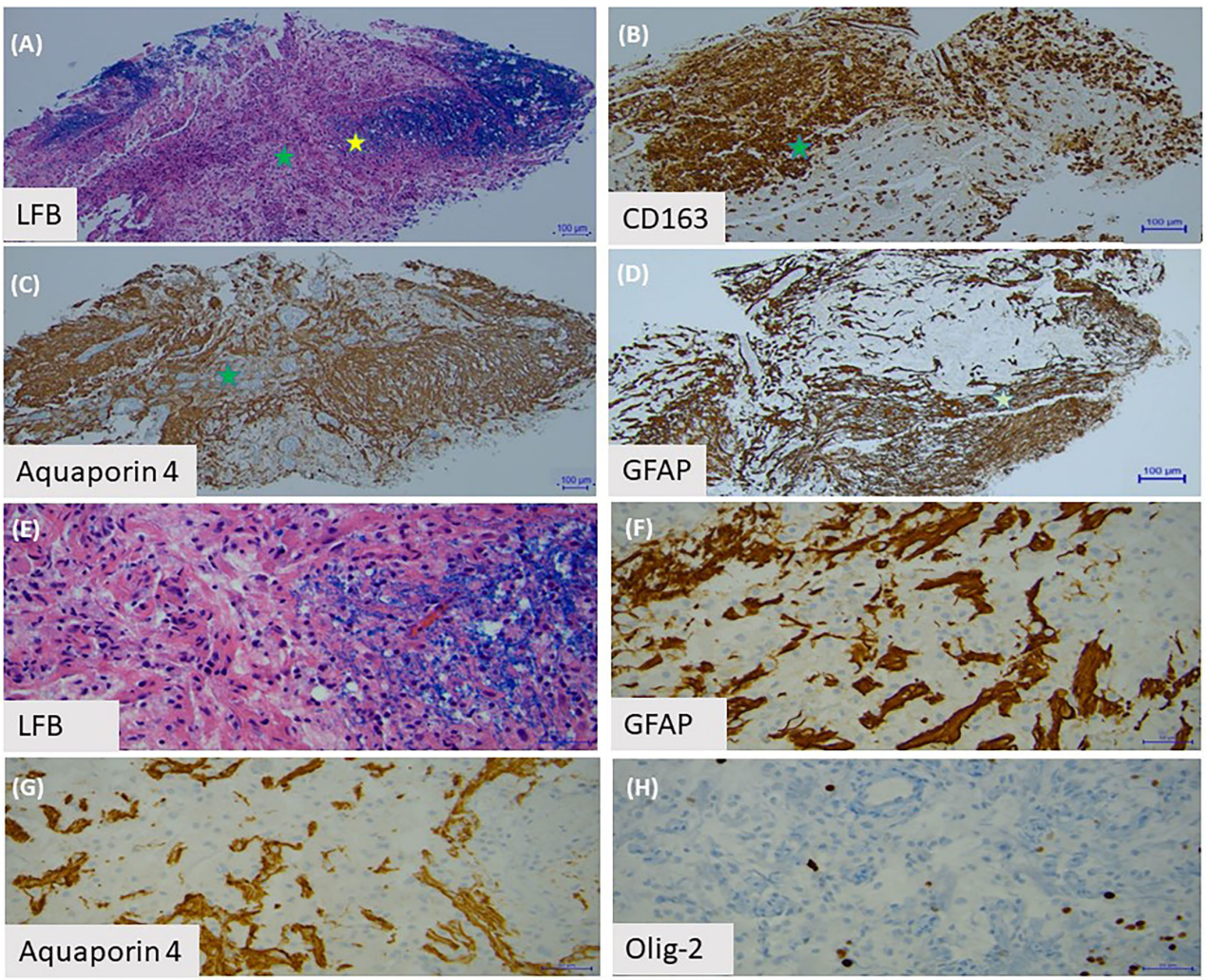

FIGURE 2 | Brain biopsy with **(A)** Luxol Fast Blue staining of myelin shows a sharply demarcated area of myelin loss. **(B)** This area is infiltrated by lipid-laden macrophages, labeled by CD163. **(C)** The area with the green star demonstrates partial loss of aquaporin-4 astrocytes. **(D)** There is also depletion of GFAP positive astrocytes in this area. **(E)** Under high power (yellow star area on first slide), we observed the edge of the demyelinated lesion. **(F)** There are sparse GFAP positive astrocytes and **(G)** aquaporin-4 positive astrocytes present around blood vessels. **(H)** Olig-2 stain shows loss of oligodendrocytes.

reported cognitive improvement and her MOCA score was 25/30. However, due to persistent hallucinations, she remained unable to work. MRI of the brain showed stable lesions with a resolution of the enhancement (**Figures 3I–L**).

DISCUSSION

Cognitive and psychiatric presentations of NMOSD are relatively rare but may be underrecognized. In one Korean series, 10% of patients with NMOSD presented with an encephalopathic syndrome and diagnosis was often delayed until subsequent presentation with optic neuritis (4). Psychiatric symptoms reported in association with NMOSD have included hallucinations and confusion as were observed in our second patient (5). Catatonia has also been reported (6). Cognitive and psychiatric presentations of NMOSD may lead to permanent disability due to delayed recognition and misdiagnosis. Common localization for cognitive and psychiatric relapses in AQP4+ NMOSD have included lesions in the cerebral hemispheres (4), diencephalon (5), and corpus callosum (7), and both of our cases demonstrated prominent involvement of the latter. There have been reported cases of autoimmune encephalitis, in particular NMDA receptor antibody positive encephalitis, co-existing with AQP4+ NMOSD (8, 9). This was considered in our second case because of the patient's psychiatric symptoms and confusion, but autoimmune encephalitis panel was negative. To summarize, NMOSD should be considered in the differential diagnosis of subacute onset of cognitive and psychiatric symptoms where imaging is suggestive of an inflammatory cause, and serologic testing for the AQP4 antibody testing should be performed so as not to delay diagnosis.

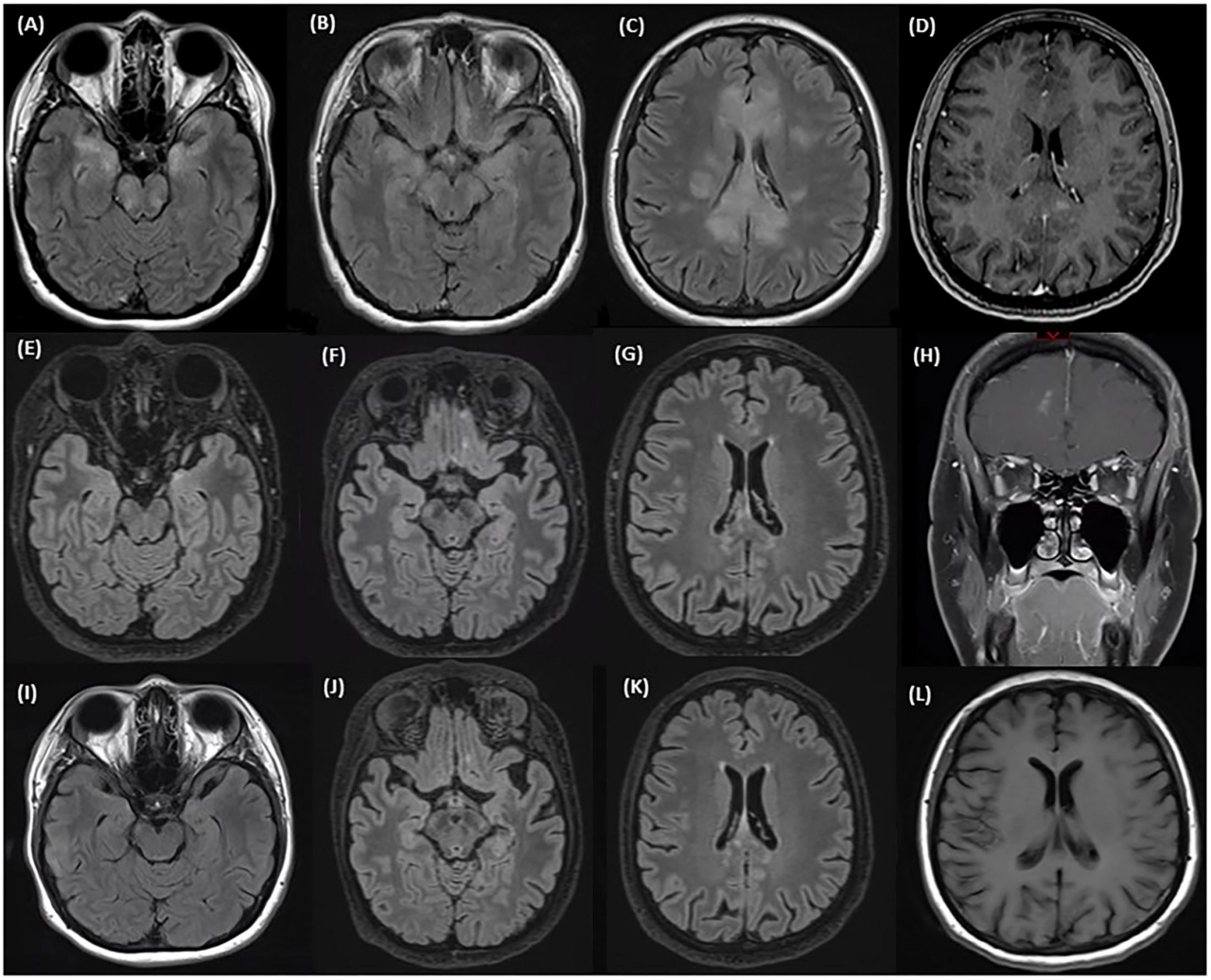

FIGURE 3 | MRI at time of first relapse: **(A–C)** Axial T2 FLAIR sequence of the brain showing involvement of the corpus callosum, bilateral mesial temporal lobes, bilateral inferior frontal lobes, and bilateral pons and midbrain. **(D)** Axial sequence of the brain with gadolinium showing discrete enhancing lesions in the corpus callosum. MRI after treatment of first relapse with corticosteroids and prior to eculizumab: **(E–G)** Axial T2 FLAIR sequences of the brain showing an improvement in the mesial temporal lobe and corpus callosum lesions after a course of steroids. **(H)** Coronal T1 sequences with gadolinium showing a new small right inferomedial frontal lesion with patchy enhancement. MRI after eculizumab: **(I–K)** Axial T2 FLAIR sequences of the brain showing stable inferior frontal and temporal lobe and corpus callosum lesions after starting eculizumab. **(L)** Axial T1 sequences with gadolinium showing no enhancement.

Corpus callosal lesions are relatively common in NMOSD; recent cohorts suggest a prevalence of up to 20% (10, 11). Such lesions have a distinct appearance from corpus callosal lesions in multiple sclerosis (MS), as they are often diffuse, cystic, oriented along the axis of the corpus callosum, and may demonstrate heterogenous signal intensity and blurred margins (12, 13). Enhancement patterns are frequently heterogenous as well. "Bridge arch" lesions of the corpus callosum have been reported, particularly in the splenium, and this appearance can sometimes be confused for a neoplastic process such as lymphoma or "butterfly" glioma (12, 13). Differential diagnosis of corpus callosum syndromes includes inflammatory causes such as MOGAD, Susac syndrome, and neurosarcoidosis in addition to NMOSD; ischemia; hereditary leukoencephalopathy; Marchiafava-Bignami disease; as well as neoplastic causes. The corpus callosum lesions seen in both our patients were more suggestive of NMOSD than MS given diffuse involvement of the corpus callosum and heterogeneous blurred margins.

Corpus callosal damage has been associated with cognitive impairment in multiple diseases including MS and Alzheimer's disease (14, 15), and was likely a major contributor to cognitive impairment in our two patients. However, cognitive deficits may occur in AQP4+ NMOSD even in the absence of a history of cognitive relapse and/or brain lesions. Recent observational studies suggest a wide range of 30–70% of NMOSD participants with CI (2, 3, 16, 17). In a cross-sectional study, no association was observed between frequency of brain lesions or overall brain T2 lesion load between cognitively preserved and cognitively

impaired patients with NMOSD (18). A pathological study of NMOSD brains found evidence of diffuse cortical neuronal loss despite absence of cortical demyelinating lesions (1). The authors suggested that loss of astrocytes may be implicated in release of excitotoxic and neurotoxic factors affecting cortical neurons (1). CI in NMOSD may involve multiple cognitive domains including memory, attention, and speed of information processing (3). Neural correlates of the cognitive impairment in NMOSD have been attributed to focal reductions in white matter volume and integrity in some studies (19, 20). Other studies have suggested that focal hippocampal or thalamic volume loss may be critical to CI in NMOSD (18, 21). Further study of CI in AQP4+ NMOSD is necessary to clarify prevalence, localization, evolution, and pathologic basis of this process.

Moreover, it is unclear whether chronic CI in AQP4+ NMOSD may be amenable to immunotherapy, and to what extent such a response may depend on the duration of CI and associated MRI features including localization of lesions and the presence of gadolinium enhancing lesions. Acute cognitive and psychiatric relapses of NMOSD have been reported to improve with immunotherapy including high dose corticosteroids and IVIG (5). To our knowledge, these are the first reported cases of chronic CI in AQP4+ NMOSD with improvement on escalation of immunotherapy. The response to eculizumab in our cases supports the importance of the complement pathway in the underlying pathophysiology of AQP4+ NMOSD (22). Common features to our two cases include diffuse involvement of the corpus callosum and on-going gadolinium enhancement on MRI. Both patients demonstrated significant improvement in cognitive function after starting eculizumab, and our first patient reported an improvement in her quality of life with ability to participate in activities like meal preparation, journal writing, and banking which she had not performed for the preceding 2 years since onset of her NMOSD. Neither patient returned to her cognitive baseline however, and neither was able to return to work.

It is possible that the cognitive improvement observed in our two cases was due to suboptimal treatment of active inflammation given ongoing gadolinium enhancement on MRI. On the other hand, there was only minor change on MRIs compared before and after institution of eculizumab, and, for Case 1, the enhancement was in the optic nerves, not in a region associated with cognition. A recent histopathologic study of autopsied AQP4+ NMOSD brain specimens showed that while complement deposition is most marked at the time of relapse, there was deposition of a complement degradation product, C3d, in fibrous gliosis, a chronic stage of NMOSD lesions (23). This finding may support the possibility of chronic pathology as a therapeutic target in AQP4+ NMOSD, although this needs to be further explored. The presence of subclinical disease activity in AQP4+ NMOSD—and its potential contribution to chronic NMOSD symptoms like fatigue and CI—remains controversial. Biomarkers like serum glial fibrillary acid protein (sGFAP) levels are under investigation, as elevated levels may predict the risk of future attacks as was observed in participants in the N-MOmentum trial (24). Symptom burden was increased in N-MOmentum participants with higher sGFAP levels as well even in the absence of an adjudicated attack.

Our two cases suggest that eculizumab should be considered as a therapy in AQP4+ NMOSD patients with CI, even when CI has been present for up to 1–2 years, and particularly if there is on-going gadolinium enhancement on MRI. Taking a broader perspective, and given the prevalence of cognitive deficits in NMOSD, we wonder if regular cognitive assessments may allow for better evaluation of disease severity, functional impact, response to therapy, and more timely escalation in therapy, where chronic impairment or decline is observed. The possibility of cognitive improvement in response to certain therapies such as eculizumab in AQP4+ NMOSD warrants further consideration. This question could potentially be answered by a multi-center, observational study with formal cognitive assessments and imaging before and after initiating specific long-term therapies.

DATA AVAILABILITY STATEMENT

The original contributions presented in the study are included in the article/supplementary material, further inquiries can be directed to the corresponding authors.

ETHICS STATEMENT

Written informed consent was obtained from the individual(s) for the publication of any potentially identifiable images or data included in this article.

AUTHOR CONTRIBUTIONS

GS drafted the manuscript. DM analyzed the biopsy specimen and reviewed the manuscript. DR drafted the manuscript and reviewed it. All authors contributed to the article and approved the submitted version.

REFERENCES

1. Saji E, ArakawaM, Yanagawa K, Toyoshima Y, Yokoseki A, Okamoto K, et al. Cognitive impairment and cortical degeneration in neuromyelitis optica. *Ann Neurol.* (2013) 73:65–76. doi: 10.1002/ana.23721
2. Kim S-H, Kwak K, Jeong IH, Hyun J-W, Jo H-J, Joung A, et al. Cognitive impairment differs between neuromyelitis optica spectrum disorder and multiple sclerosis. *Mult Scler.* (2016) 22:1850–8. doi: 10.1177/1352458516636246
3. Oertel FC, Schließeit J, Brandt AU, Paul F. Cognitive impairment in neuromyelitis optica spectrum disorders: a review of clinical and neuroradiological features. *Front Neurol.* (2019) 10:608. doi: 10.3389/fneur.2019.00608
4. Kim W, Kim SH, Lee SH, Li XF, Kim HJ. Brain abnormalities as an initial manifestation of neuromyelitis optica spectrum disorder. *Mult Scler.* (2011) 17:1107–12. doi: 10.1177/1352458511404917
5. Tang H, Wang L, Zhou H, Hao X. Psychiatric symptoms as initial manifestation in neuromyelitis optica spectrum disorder without

cortical lesions: a report of two cases. *J Neuroimmunol.* (2021) 359:577693. doi: 10.1016/j.jneuroim.2021.577693
6. Alam A, Patel R, Locicero B, Rivera N. Neuromyelitis optica presenting with psychiatric symptoms and catatonia: a case report. *Gen Hosp Psychiatry*. (2015) 37:274.e271–2. doi: 10.1016/j.genhosppsych.2015.02.007
7. Camera V, Messina S, Elhadd KT, Sanpera-Iglesias J, Mariano R, Hacohen Y, et al. Early predictors of disability of paediatric-onset AQP4-IgG-seropositive neuromyelitis optica spectrum disorders. *J Neurol Neurosurg Psychiatry*. (2022) 93:101–11. doi: 10.1136/jnnp-2021-327206
8. Sinani AA, Maawali SA, Alshekaili J, Kindi MA, Ramadhani KA, Khabouri JA, et al. Overlapping demyelinating syndrome (Neuromyelitis optica spectrum disorders NMOSD with anti-NMDA receptor encephalitis); A case report. *Multiple Sclerosis Relat Disord*. (2020) 42:102153. doi: 10.1016/j.msard.2020.102153
9. Tao S, Zhang Y, Ye H, Guo D. AQP4-IgG-seropositive neuromyelitis optica spectrum disorder (NMOSD) coexisting with anti-N-methyl-D-aspartate receptor (NMDAR) encephalitis: a case report and literature review. *Multiple Sclerosis Relat Disord*. (2019) 35:185–92. doi: 10.1016/j.msard.2019.07.008
10. Makino T, Ito S, Mori M, Yonezu T, Ogawa Y, Kuwabara S. Diffuse and heterogeneous T2-hyperintense lesions in the splenium are characteristic of neuromyelitis optica. *Mult Scler.* (2013) 19:308–15. doi: 10.1177/1352458512454772
11. Carnero Contentti E, Daccach Marques V, Soto de Castillo I, Tkachuk V, Antunes Barreira A, Armas E, et al. Frequency of brain MRI abnormalities in neuromyelitis optica spectrum disorder at presentation: a cohort of Latin American patients. *Mult Scler Relat Disord.* (2018) 19:73–8. doi: 10.1016/j.msard.2017.11.004
12. Clarke L, Arnett S, Bukhari W, Khalilidehkordi E, Jimenez Sanchez S, O'Gorman C, et al. MRI patterns distinguish AQP4 antibody positive neuromyelitis optica spectrum disorder from multiple sclerosis. *Front Neurol.* (2021) 12:722237. doi: 10.3389/fneur.2021.722237
13. Nakamura M, Misu T, Fujihara K, Miyazawa I, Nakashima I, Takahashi T, et al. Occurrence of acute large and edematous callosal lesions in neuromyelitis optica. *Mult Scler.* (2009) 15:695–700. doi: 10.1177/1352458509103301
14. Granberg T, Martola J, Bergendal G, Shams S, Damangir S, Aspelin P, et al. Corpus callosum atrophy is strongly associated with cognitive impairment in multiple sclerosis: results of a 17-year longitudinal study. *Mult Scler.* (2015) 21:1151–8. doi: 10.1177/1352458514560928
15. Hamphel H, Teipel SJ, Alexander GE, Horwitz B, Teichberg D, Schapiro MB, et al. Corpus callosum atrophy is a possible indicator of region- and cell type-specific neuronal degeneration in Alzheimer disease: a magnetic resonance imaging analysis. *Arch Neurol.* (1998) 55:193–8. doi: 10.1001/archneur.55.2.193
16. Moore P, Methley A, Pollard C, Mutch K, Hamid S, Elsone L, et al. Cognitive and psychiatric comorbidities in neuromyelitis optica. *J Neurol Sci.* (2016) 360:4–9. doi: 10.1016/j.jns.2015.11.031
17. Meng H, Xu J, Pan C, Cheng J, Hu Y, Hong Y, et al. Cognitive dysfunction in adult patients with neuromyelitis optica: a systematic review and metaanalysis. *J Neurol.* (2017) 264:1549–58. doi: 10.1007/s00415-016-8345-3
18. Liu Y, Fu Y, Schoonheim MM, Zhang N, Fan M, Su L, et al. Structural MRI substrates of cognitive impairment in neuromyelitis optica. *Neurology*. (2015) 85:1491–9. doi: 10.1212/WNL.0000000000002067
19. He D, Wu Q, Chen X, Zhao D, Gong Q, Zhou H. Cognitive impairment and whole brain diffusion in patients with neuromyelitis optica after acute relapse. *Brain Cogn.* (2011) 77:80–8. doi: 10.1016/j.bandc.2011.05.007
20. Blanc F, Noblet V, Jung B, Rousseau F, Renard F, Bourre B, et al. White matter atrophy and cognitive dysfunctions in neuromyelitis optica. *PLoS ONE.* (2012) 7:e33878. doi: 10.1371/journal.pone.0033878
21. Wang Q, Zhang N, Yu C, Li Y, Fu Y, Li T, et al. Gray matter volume reduction is associated with cognitive impairment in neuromyelitis optica. *Am J Neuroradiol*. (2015) 36:1822–29. doi: 10.3174/ajnr.A4403
22. Pittock SJ, Berthele A, Fujihara K, Kim HJ, Levy M, Palace J, et al. Eculizumab in aquaporin-4-positive neuromyelitis optica spectrum disorder. *N Engl J Med.* (2019) 381:614–25. doi: 10.1056/NEJMoa1900866
23. Takai Y, Misu T, Suzuki H, Takahashi T, Okada H, Tanaka S, et al. Staging of astrocytopathy and complement activation in neuromyelitis optica spectrum disorders. *Brain*. (2021) 144:2401–15. doi: 10.1093/brain/awab102
24. Aktas O, Smith MA, Rees WA, Bennett JL, She D, Katz E, et al. Serum glial fibrillary acidic protein: a neuromyelitis optica spectrum disorder biomarker. *Ann Neurol*. (2021) 89:895–910. doi: 10.1002/ana.26067

Conflict of Interest: DR has received research support from the MS Society of Canada, Consortium of Multiple Sclerosis Centers and Roche. She has received speaker or consultant fees from Alexion, Biogen, EMD Serono, Novartis, Roche, and Sanofi Aventis.

The remaining authors declare that the research was conducted in the absence of any commercial or financial relationships that could be construed as a potential conflict of interest.

Publisher's Note: All claims expressed in this article are solely those of the authors and do not necessarily represent those of their affiliated organizations, or those of the publisher, the editors and the reviewers. Any product that may be evaluated in this article, or claim that may be made by its manufacturer, is not guaranteed or endorsed by the publisher.

frontiers | Frontiers in Immunology

CASE REPORT
published: 19 May 2022
doi: 10.3389/fimmu.2022.864664

Case Report: Neuromyelitis Optica Spectrum Disorder With Progressive Elevation of Cerebrospinal Fluid Cell Count and Protein Level Mimicking Infectious Meningomyelitis: A Diagnostic Challenge

Yin-Xi Zhang[1†], *Meng-Ting Cai*[1†], *Ming-Xia He*[2], *Yu-Qiang Lu*[3], *Xiao Luo*[4] *and Tian-Yi Zhang*[3*]

[1] Department of Neurology, Second Affiliated Hospital, School of Medicine, Zhejiang University, Hangzhou, China, [2] Department of Hematology, Tongde Hospital of Zhejiang Province, Hangzhou, China, [3] Department of Neurology, Tongde Hospital of Zhejiang Province, Hangzhou, China, [4] Department of Radiology, Second Affiliated Hospital, School of Medicine, Zhejiang University, Hangzhou, China

OPEN ACCESS

Edited by:
Wei Qiu,
Third Affiliated Hospital of Sun Yat-sen University, China

Reviewed by:
Eun-Jae Lee,
University of Ulsan, South Korea
Yasutaka Tajima,
Sapporo City General Hospital, Japan
Mang Suo Zhao,
Tsinghua University Yuquan Hospital, China

***Correspondence:**
Tian-Yi Zhang
21718237@zju.edu.cn

[†]These authors have contributed equally to this work

Specialty section:
This article was submitted to Multiple Sclerosis and Neuroimmunology, a section of the journal Frontiers in Immunology

Received: 28 January 2022
Accepted: 20 April 2022
Published: 19 May 2022

Citation:
Zhang Y-X, Cai M-T, He M-X, Lu Y-Q, Luo X and Zhang T-Y (2022) Case Report: Neuromyelitis Optica Spectrum Disorder With Progressive Elevation of Cerebrospinal Fluid Cell Count and Protein Level Mimicking Infectious Meningomyelitis: A Diagnostic Challenge. Front. Immunol. 13:864664. doi: 10.3389/fimmu.2022.864664

Neuromyelitis optica spectrum disorder (NMOSD) is an autoimmune-mediated idiopathic inflammatory demyelinating disease with a typical clinical presentation of optic neuritis, acute myelitis, and area postrema syndrome. Most NMOSD patients are seropositive for disease-specific and pathogenic aquaporin-4 (AQP4) antibodies, which are key markers for the NMOSD diagnosis. Herein, we report an atypical case of a 41-year-old man who complained of intractable hiccups and vomiting at disease onset, followed by fever, headache, back pain, progressive paresthesia, and weakness of extremities later on. Magnetic resonance imaging revealed longitudinally extensive transverse myelitis. Cerebrospinal fluid analysis showed progressive increases in the white blood cell count and the protein level, which were accompanied by the deterioration of clinical manifestations. The patient was initially suspected of infectious meningomyelitis but was finally diagnosed with NMOSD. This case with distinct cerebrospinal fluid findings broadens the phenotypic spectrum of NMOSD. Furthermore, it also highlights the clinical value of AQP4 antibody test for early definitive diagnosis and proper treatment.

Keywords: neuromyelitis optica spectrum disorder, aquaporin-4 antibody, infectious meningomyelitis, cerebrospinal fluid, longitudinally extensive transverse myelitis, area postrema syndrome

INTRODUCTION

Neuromyelitis optica (NMO) is an autoimmune-mediated idiopathic inflammatory demyelinating disease that predominantly affects the optic nerve and spinal cord. The 2015 International Panel for NMO Diagnosis introduced neuromyelitis optica spectrum disorder (NMOSD) to include a broader spectrum and established its diagnostic criteria (1). NMOSD is characterized by recurrent attacks of

optic neuritis, transverse myelitis, and area postrema syndrome (APS). Typical neuroradiological findings include long-segment involvement of the optic nerve (particularly when simultaneous bilateral and extending posteriorly into the optic chiasm), longitudinally extensive transverse myelitis (LETM), and lesions of the dorsal medulla (especially the area postrema) (2). The majority of patients with NMOSD are seropositive for disease-specific and pathogenic aquaporin-4 (AQP4) antibodies, which are key markers for its diagnosis (1, 3). The wide application of AQP4 antibody test expands the phenotype of uncommon clinical manifestations of this disease. Here, we present an atypical case of NMOSD with fever, headache, back pain, progressive paresthesia, weakness of the extremities, and continuously elevating white blood cell (WBC) count, and protein level in the cerebrospinal fluid (CSF). These misdirecting manifestations seemed to all lead to infectious meningomyelitis in this case; however, the patient was finally diagnosed with NMOSD.

CASE DESCRIPTION

A 41-year-old previously healthy man was sent to the hospital with a 1-month history of intractable hiccups and vomiting and a 1-week history of headache, back pain, and ascending paresthesia. Neurological examination on admission showed intact cranial nerves, neck rigidity, hypoesthesia below the T6 level, vibration hypoesthesia, bilateral positive Babinski signs, and normal muscle strength. Routine workup including complete blood cell count, basic metabolic panel, tumor markers, and rheumatology panel was normal. Chest computerized tomography (CT), abdominal ultrasound, and brain magnetic resonance imaging (MRI) were unremarkable. Spinal MRI demonstrated longitudinally extensive T2 hyperintensities from C2 to T8 without enhancement (**Figure 1**). Spinal contrast-enhanced MR angiography showed no abnormalities. Initial lumbar puncture revealed a CSF opening pressure of 140 mmH_2O, a WBC count of 120/μl (93% lymphocytes), a protein level of 48 mg/dl, and a normal glucose level (**Figure 2**). No intrathecal oligoclonal bands were found.

Three days later, the patient developed progressive weakness of lower extremities (Medical Research Council, grade 3) with dysuria and constipation and fever up to 38°C, while all serum infectious indicators (e.g., leukocytes, procalcitonin test, C-reactive protein, and cultures), and urinalysis/urine culture were negative. Therefore, a reexamination of the lumbar puncture was performed, revealing an increased WBC count (520/μl) and protein level (255.5 mg/dl). CSF next-generation sequencing (NGS) for bacteria, viruses, fungi, and parasites with known genome sequences and cultures for bacteria and fungi were negative. Moreover, the CSF cytology was suspicious for tumor cells. Fluorodeoxyglucose positron emission tomography/CT showed increased metabolism in multiple segments of the cervical and thoracic regions and no evidence of systemic tumors.

In the following 2 days, the weakness progressed to all extremities (Medical Research Council, grade 0) and anesthesia arose to the C3 level, accompanied by hoarseness, dysphagia, dysuria, dyspnea, and a peak temperature of 38.8°C. The reexamination of serum and urine showed no evidence of infection. Based on the evaluation, neither tumor nor infection of the central nervous system could be ruled out. A third lumbar puncture was performed, which showed a WBC count of 1,250/μl (97% lymphocytes) and a protein level of 864.4 mg/dl. Flow

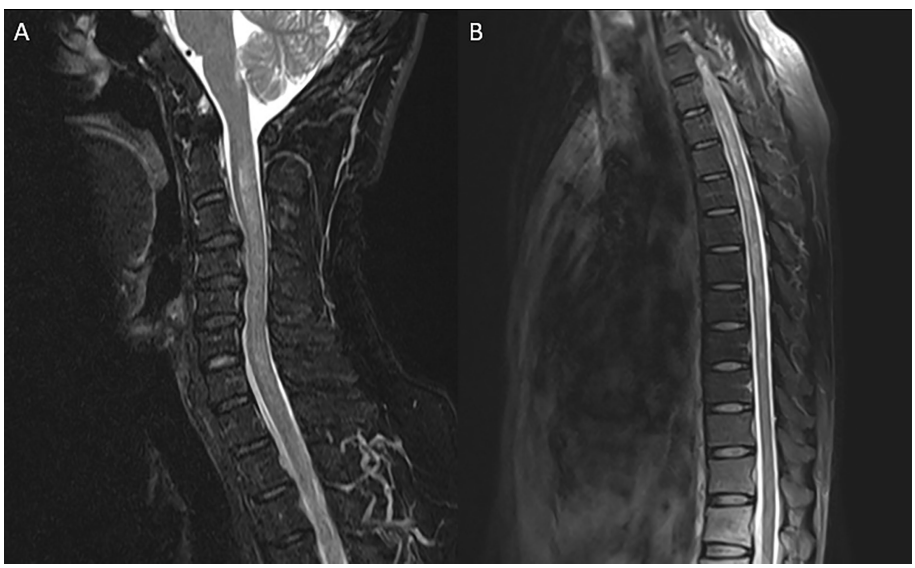

FIGURE 1 | Magnetic resonance imaging of the cervical **(A)** and thoracic **(B)** spinal cord. Sagittal T2-weighted imaging showed longitudinally extensive hyperintense lesion extending from C2 to T8.

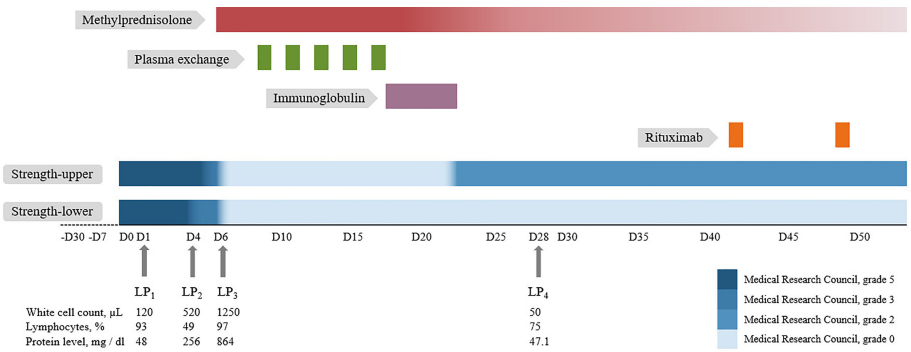

FIGURE 2 | Timeline depicting muscle strength change, immunotherapy, and cerebrospinal fluid analysis of the patient. For further details, refer to the main text. LP, lumbar puncture.

cytometry and repeated NGS analysis in CSF were unrevealing. The results of the AQP4 antibody test at admission returned, demonstrating positivity in both the serum (titer, 1:100) and the CSF (titer, 1:3.2) using cell-based assay. The final diagnosis of NMOSD was made.

The patient was then treated with intravenous methylprednisolone (500 mg/day for 5 days, followed by a tapering scheme) combined with plasma exchange (5 cycles, every other day) and intravenous immunoglobulin (0.4 g/kg per day for 5 days) (**Figure 2**). After the first-line treatment, muscle strength of the upper extremities recovered to grade 2 and anesthesia decreased to the level of T4. The symptoms of hiccup and vomiting disappeared completely. A reexamination of the lumbar puncture revealed that the CSF WBC count and protein level decreased significantly. The reexamined serum AQP4 antibody titer was 1:10. Rituximab (500 mg, twice) was administered for sequential therapy. In the follow-up 3 months after discharge, the patient could lift both upper extremities but suffered from pain all over the body. The movement of the lower extremities and the tactile sensation below the xiphoid process were still poor.

DISCUSSION

Here, we report an NMOSD patient who successively presented with hiccups, vomiting, headache, back pain, fever, paresthesia, and weakness of the extremities. In addition, the CSF tests also showed progressive increases in the WBC count and the protein level consistently with the aggravation of myelitis symptoms, which has not been reported before. Although the patient had infectious meningomyelitis-like symptoms, the repeated tests showed no evidence of infection. Nevertheless, the involvement of infection was difficult to completely exclude, leading to a diagnostic challenge. However, the detection of AQP4 antibodies in both serum and CSF with the clinical manifestations of APS and acute myelitis, according to the 2015 diagnostic criteria, makes the definite diagnosis of NMOSD. Furthermore, the fact that the patient's symptoms improved after immunotherapy, rather than anti-infective treatment, also supported this diagnosis.

The intractable hiccups and vomiting that the patient suffered initially were ignored at the time, while those symptoms met the definition of APS, which is considered to be one of the typical clinical features of NMOSD with great diagnostic value (4). This patient also developed LETM, which is also a characteristic of NMOSD. A previous study confirmed that when a longitudinally extensive spinal cord lesion extends to the area postrema and happens simultaneously with intractable nausea and vomiting, it is highly specific for AQP4 antibody-seropositive NMOSD (5). Thus, the typical presentation and neuroimaging of APS and LETM require more attention clinically.

We reviewed the previous literature and summarized the characteristics of the reported cases of NMOSD with seropositive AQP4 antibodies who presented with meningitis/meningomyelitis-like symptoms in the first attack (**Table 1**) (6–8). All patients had infection-like manifestations such as fever or headache in their early stages, along or subsequent with core symptoms of NMOSD. Brain MRI revealed that some of the cases have multiple T2 hyperintense lesions and meningeal enhancement. These symptoms were so similar to those of infectious meningomyelitis that left the diagnosis process in dilemma. However, previous reports showed that the lack of improvement in empiric antibiotic or anti-tuberculosis therapy favored the NMOSD attack (6, 8). Some patients were not correctly diagnosed at the first hospitalization but were further diagnosed when they relapsed during the follow-up (6). Most patients had relapses or disabilities. In comparison, our patient presented not only infectious meningomyelitis-like symptoms, which were similar to cases discussed above, but also APS in the earlier stage. Thanks to the timely AQP4 antibody test, the diagnosis successfully locked down on NMOSD, and the treatments focusing on NMOSD proved to be effective for our patient. Although meningitis/meningomyelitis-like phenotype is rare, it should have an attached importance, since delayed diagnosis and treatment may result in a poor prognosis.

Furthermore, in our case, the progressive elevation of the CSF WBC count and the protein level was accompanied by the exacerbation of symptoms. In previous studies, CSF pleocytosis is present in around 50%–65% of samples (9, 10). A study

TABLE 1 | Clinical, MRI, and CSF characteristics of AQP4 antibody-seropositive NMOSD patients with meningitis/meningomyelitis-like symptoms at first attack.

Case report	Age, years/ sex	Initial symptoms	Other symptoms during the courses of disease	Meningeal irritation	MRI		CSF		
					T2WI	Contrast enhancement	Cell count (/μl)	Protein level (mg/dl)	Other details
1. Wang et al. (6)	40/M	Headache	Fever, consciousness change	Kernig's sign and nuchal rigidity	T2WI hyperintense in the right periventricular regions, corpus callosum, hypothalamus, cerebral peduncle, midbrain, and upper pons	Irregular parenchymal and meningeal gadolinium enhancement	606 (95% L)	285	310 mmH_2O, 30.24 mg/dl glucose, normal chloride
2. Wang et al. (6)	38/F	Headache	Fever, APS, symptomatic narcolepsy, apathy	Kernig's sign and nuchal rigidity	T2WI hyperintense lesions around the third ventricle, in the corpus callosum, bilateral periventricular parenchyma, temporal lobes, thalamus, cerebellum, and cerebellar peduncle	Irregular parenchymal, meningeal and bilateral ependymal gadolinium enhancement	625 (34.9% N)	102	200 mmH_2O, normal glucose and chloride
3. Benedetti et al. (7)	45/F	Paresthesia	Fever, headache, ON, consciousness change, hyponatremia	Neck rigidity	T2WI hyperintense in the frontal lobes, optic tracts, optic chiasm, midbrain, anteroinferior region of basal ganglia, internal capsule, and hypothalamus, with swelling of the cerebral parenchyma	No enhancement	Pleocytosis (80 lymphocytes/ mm^3)	200	Absent OB
4. Shi et al. (8)	28/F	Fever, headache, acute myelitis	–	NA	NA	Cerebral meninge, spinal meninge enhancement	280 (33% N)	368	220 mmH_2O, 12.06 mg/dl glucose, 113 mmol/l chloride
5. Shi et al. (8)	34/F	Fever, headache, acute myelitis	–	NA	NA	Spinal cord, spinal meninge enhancement	1,200 (60% N)	215.15	160 mmH_2O, 32.4 mg/dl glucose, 121.4 mmol/l chloride
6. Shi et al. (8)	29/F	Fever, headache, acute myelitis	ON	NA	NA	Spinal cord, spinal meninge enhancement	1,131 (83% N)	158.67	220 mmH_2O, 39.6 mg/dl glucose, 122.4 mmol/l chloride
7. (Index)	41/M	APS	Fever, headache, acute myelitis	Neck rigidity	T2WI hyperintensities from C2 to T8	No enhancement	1,250 (97% L)	864.4	180 mmH_2O, normal glucose and chloride

APS, area postrema syndrome; AQP4, aquaporin-4; CSF, cerebrospinal fluid; F, female; L, lymphocyte; M, male; MRI, magnetic resonance imaging; N, neutrophil; NA, not available; NMOSD, neuromyelitis optica spectrum disorder; ON, optic neuritis; T2WI, T2-weighted imaging; WBC, white blood cell.

including 211 AQP4 antibody-positive samples found that marked pleocytosis (CSF WBC ≥100/μl) was observed only in 6%, while protein levels exceeding 100 mg/dl were observed in about 29%, and CSF protein levels were correlated with the length of the spinal cord lesions indicated by a study (10). Previous research suggests CSF leukocyte counts as an inflammation indicator and protein concentrations as a blood–brain barrier (BBB) disruption indicator (11). In our case, the patient suffered progressively ascending CSF leukocyte counts and protein levels, which respectively indicate inflammation and the BBB disruption, and could further explain the progress severity of the patient's symptoms. Our case suggested that the progressive growth in the CSF leukocyte count and the protein level cannot completely rule out the diagnosis of NMOSD.

The clinical symptoms of our patient improved with immunotherapy alone, also supporting the diagnosis of NMOSD. Unfortunately, the short-term therapeutic effect of this case was not satisfactory. The delayed diagnosis and treatment might be the critical factors. Previous studies found that tetraparesis and long spinal cord lesions were associated with long-term disability (12, 13). Since our case presented with these poor prognostic factors, follow-up is required to define the long-term prognosis.

In conclusion, we report a meningomyelitis-like case with distinct CSF findings that expands the phenotypic spectrum of

NMOSD. To our knowledge, this is the first report that showed progressive elevation of the CSF WBC count and the protein level along with the aggravation of clinical symptoms. It may also lead to delayed diagnosis or even misdiagnosis. Although atypical symptoms exist, APS and LETM are still highly suggestive of the diagnosis of NMOSD. Testing for AQP4 antibody in this scenario is recommended, since it helps definite diagnosis and initiating therapy of this treatable disease in the early stage.

DATA AVAILABILITY STATEMENT

The original contributions presented in the study are included in the article/supplementary material. Further inquiries can be directed to the corresponding author.

ETHICS STATEMENT

Written informed consent was obtained from the individual for the publication of any potentially identifiable images or data included in this article.

AUTHOR CONTRIBUTIONS

Y-XZ and T-YZ contributed to the concept and design of the study. All authors contributed to the acquisition and analysis of the data. Y-XZ and M-TC contributed to drafting the initial article. T-YZ contributed to revising the article for intellectual content. All authors read and approved the final version before submission.

REFERENCES

1. Wingerchuk DM, Banwell B, Bennett JL, Cabre P, Carroll W, Chitnis T, et al. International Consensus Diagnostic Criteria for Neuromyelitis Optica Spectrum Disorders. *Neurology* (2015) 85:177–89. doi: 10.1212/WNL.0000000000001729
2. Kim HJ, Paul F, Lana-Peixoto MA, Tenembaum S, Asgari N, Palace J, et al. MRI Characteristics of Neuromyelitis Optica Spectrum Disorder: An International Update. *Neurology* (2015) 84:1165–73. doi: 10.1212/WNL.0000000000001367
3. Li L, Fang GL, Zheng Y, Zhang YX. Late-Onset Neuromyelitis Optica Spectrum Disorder Mimicking Stroke in an Elderly Chinese Man: Case Report. *J Spinal Cord Med* (2020)45:148–50. doi: 10.1080/10790268.2020.1749475
4. Camara-Lemarroy CR, Burton JM. Area Postrema Syndrome: A Short History of a Pearl in Demyelinating Diseases. *Mult Scler* (2019) 25:325–9. doi: 10.1177/1352458518813105
5. Dubey D, Pittock SJ, Krecke KN, Flanagan EP. Association of Extension of Cervical Cord Lesion and Area Postrema Syndrome With Neuromyelitis Optica Spectrum Disorder. *JAMA Neurol* (2017) 74:359–61. doi: 10.1001/jamaneurol.2016.5441
6. Wang JY, Wang K, Chen XW, Wang JW, Zhang K, Xu MW, et al. Meningoencephalitis as an Initial Manifestation of Neuromyelitis Optica Spectrum Disorder. *Mult Scler* (2013) 19:639–43. doi: 10.1177/1352458512459785
7. Benedetti L, Franciotta D, Beronio A, Delucchi S, Capellini C, Del Sette M. Meningoencephalitis-Like Onset of Post-Infectious AQP4-IgG-Positive Optic Neuritis Complicated by GM1-IgG-Positive Acute Polyneuropathy. *Mult Scler* (2015) 21:246–8. doi: 10.1177/1352458514524294
8. Shi B, Jiang W, He M, Sun H, Sun X, Yang Y, et al. Aseptic Meningitis as an Atypical Manifestation of Neuromyelitis Optica Spectrum Disorder Flare. *Mult Scler Relat Disord* (2020) 41:102013. doi: 10.1016/j.msard.2020.102013
9. Jarius S, Ruprecht K, Wildemann B, Kuempfel T, Ringelstein M, Geis C, et al. Contrasting Disease Patterns in Seropositive and Seronegative Neuromyelitis Optica: A Multicentre Study of 175 Patients. *J Neuroinflamm* (2012) 9:14. doi: 10.1186/1742-2094-9-14
10. Jarius S, Paul F, Franciotta D, Ruprecht K, Ringelstein M, Bergamaschi R, et al. Cerebrospinal Fluid Findings in Aquaporin-4 Antibody Positive Neuromyelitis Optica: Results From 211 Lumbar Punctures. *J Neurol Sci* (2011) 306:82–90. doi: 10.1016/j.jns.2011.03.038
11. Deisenhammer F, Zetterberg H, Fitzner B, Zettl UK. The Cerebrospinal Fluid in Multiple Sclerosis. *Front Immunol* (2019) 10:726. doi: 10.3389/fimmu.2019.00726
12. Jarius S, Paul F, Weinshenker BG, Levy M, Kim HJ, Wildemann B. Neuromyelitis Optica. *Nat Rev Dis Primers* (2020) 6:85. doi: 10.1038/s41572-020-0214-9
13. Cortese R, Giorgio A, Severa G, De Stefano N. MRI Prognostic Factors in Multiple Sclerosis, Neuromyelitis Optica Spectrum Disorder, and Myelin Oligodendrocyte Antibody Disease. *Front Neurol* (2021) 12:679881. doi: 10.3389/fneur.2021.679881

Conflict of Interest: The authors declare that the research was conducted in the absence of any commercial or financial relationships that could be construed as a potential conflict of interest.

frontiers | Frontiers in Immunology

ORIGINAL RESEARCH
published: 14 June 2022
doi: 10.3389/fimmu.2022.897959

Transformer-Based Deep-Learning Algorithm for Discriminating Demyelinating Diseases of the Central Nervous System With Neuroimaging

Chuxin Huang[1,2], Weidao Chen[3], Baiyun Liu[3], Ruize Yu[3], Xiqian Chen[2], Fei Tang[1], Jun Liu[1,4] and Wei Lu[2]**

[1] Department of Radiology, The Second Xiangya Hospital of Central South University, Changsha, China, [2] Department of Neurology, The Second Xiangya Hospital of Central South University, Changsha, China, [3] Infervision Medical Technology Co., Ltd., Ocean International Center, Beijing, China, [4] Clinical Research Center for Medical Imaging in Hunan Province, Changsha, China

OPEN ACCESS

Edited by:
Wei Qiu,
Third Affiliated Hospital of Sun Yat-sen University, China

Reviewed by:
Eun-Jae Lee,
University of Ulsan, South Korea
Omar Al-Louzi,
Cedars Sinai Medical Center, United States

***Correspondence:**
Jun Liu
junliu123@csu.edu.cn
Wei Lu
luwei0338@csu.edu.cn

Specialty section:
This article was submitted to Multiple Sclerosis and Neuroimmunology, a section of the journal Frontiers in Immunology

Received: *16 March 2022*
Accepted: *18 May 2022*
Published: *14 June 2022*

Citation:
Huang C, Chen W, Liu B, Yu R, Chen X, Tang F, Liu J and Lu W (2022) Transformer-Based Deep-Learning Algorithm for Discriminating Demyelinating Diseases of the Central Nervous System With Neuroimaging. Front. Immunol. 13:897959. doi: 10.3389/fimmu.2022.897959

Background: Differential diagnosis of demyelinating diseases of the central nervous system is a challenging task that is prone to errors and inconsistent reading, requiring expertise and additional examination approaches. Advancements in deep-learning-based image interpretations allow for prompt and automated analyses of conventional magnetic resonance imaging (MRI), which can be utilized in classifying multi-sequence MRI, and thus may help in subsequent treatment referral.

Methods: Imaging and clinical data from 290 patients diagnosed with demyelinating diseases from August 2013 to October 2021 were included for analysis, including 67 patients with multiple sclerosis (MS), 162 patients with aquaporin 4 antibody-positive (AQP4+) neuromyelitis optica spectrum disorder (NMOSD), and 61 patients with myelin oligodendrocyte glycoprotein antibody-associated disease (MOGAD). Considering the heterogeneous nature of lesion size and distribution in demyelinating diseases, multi-modal MRI of brain and/or spinal cord were utilized to build the deep-learning model. This novel transformer-based deep-learning model architecture was designed to be versatile in handling with multiple image sequences (coronal T2-weighted and sagittal T2-fluid attenuation inversion recovery) and scanning locations (brain and spinal cord) for differentiating among MS, NMOSD, and MOGAD. Model performances were evaluated using the area under the receiver operating curve (AUC) and the confusion matrices measurements. The classification accuracy between the fusion model and the neuroradiological raters was also compared.

Results: The fusion model that was trained with combined brain and spinal cord MRI achieved an overall improved performance, with the AUC of 0.933 (95%CI: 0.848, 0.991), 0.942 (95%CI: 0.879, 0.987) and 0.803 (95%CI: 0.629, 0.949) for MS, AQP4+ NMOSD, and MOGAD, respectively. This exceeded the performance using the brain or spinal cord MRI alone for the identification of the AQP4+ NMOSD (AUC of 0.940, brain only and 0.689, spinal cord only) and MOGAD (0.782, brain only and 0.714, spinal cord only). In the

multi-category classification, the fusion model had an accuracy of 81.4%, which was significantly higher compared to rater 1 (64.4%, p=0.04<0.05) and comparable to rater 2 (74.6%, p=0.388).

Conclusion: The proposed novel transformer-based model showed desirable performance in the differentiation of MS, AQP4+ NMOSD, and MOGAD on brain and spinal cord MRI, which is comparable to that of neuroradiologists. Our model is thus applicable for interpretating conventional MRI in the differential diagnosis of demyelinating diseases with overlapping lesions.

Keywords: deep learning, demyelinating disease, differential diagnosis, MRI, multiple sclerosis, myelin oligodendrocyte glycoprotein antibody-associated disease, neuromyelitis optica spectrum disorder, transformer

1 INTRODUCTION

Inflammatory demyelinating diseases of the central nervous system (CNS) are important causes of nontraumatic neurological disabilities (1, 2). Multiple sclerosis (MS), neuromyelitis optica spectrum disorder (NMOSD), and myelin oligodendrocyte glycoprotein antibody-associated disease (MOGAD) are major disease entities in this field (3, 4). Increasing evidence indicates that NMOSD is an independent disorder associated with the expression of anti-aquaporin-4 (AQP4) antibodies rather than a variant of MS (5, 6). With the discovery of antibodies targeting myelin oligodendrocyte glycoprotein (MOG) in AQP4 antibody-negative NMOSD, MOGAD is now recognized as a unique immunological entity that is distinct from both MS and NMOSD (4, 7).

Indeed, MS, NMOSD and MOGAD exhibit divergent pathogeneses, treatment options for relapse prevention, and prognoses (8), and their diagnosis is mainly based on combined results involving clinical findings, radiological manifestations, and cerebrospinal fluid and serological tests. In conventional magnetic resonance imaging (MRI), bilateral periventricular white matter and cortical lesions are often considered typical features of MS (9), whereas longitudinally extensive transverse myelitis and posterior long-segment optic nerve lesions are more specific to NMOSD (10). MOGAD is considered to exhibit intermediate MRI features between those of MS and NMOSD (11). However, the MRI manifestations in some cases are indistinguishable among these conditions. Owing to the presence of overlapping clinical and radiological findings among these disorders, differential diagnosis can be challenging.

Autoantibody tests normally confer high sensitivity, but are invasive and time-consuming to obtain results, and conversion to an antibody-negative status may occur during the disease course (12). An improper choice of treatment may lead to disease deterioration. For example, disease-modifying therapies such as interferon beta and dimethyl fumarate are recommended as the standard treatment for MS but may exacerbate NMOSD and increase relapse rates (13, 14). Immunosuppressive agents such as azathioprine and mycophenolate mofetil are the first-line therapies for NMOSD and MOGAD. Moreover, several emerging therapies have shown different efficacies in controlling disease recurrence in patients with AQP4+ NMOSD and MOGAD (15). Thus, to reduce the delay from disease onset to appropriate treatment, thereby improving clinical benefits, there is an urgent need to develop an effective non-invasive approach for a rapid and precise differential diagnosis.

Many researchers have explored imaging differences among the three diseases using multi-model MRI sequences, indicating that the classification of MR image features can be helpful in the diagnosis of these diseases. Duan et al. (16) compared brain structural alterations on MRI, and demonstrated cortical and subcortical atrophy without severe white matter rarefaction in MOGAD in comparison with MS and AQP4+ NMOSD, whereas diffusion MRI measurements showed lower fractional anisotropy and higher mean diffusivity in MS. Moreover, Banks et al. (17) retrospectively compared the involvement of the brainstem or cerebellar region in CNS inflammatory demyelination diseases, and revealed that diffuse middle cerebellar peduncle MRI lesions favored a diagnosis of MOGAD over MS and AQP4+ NMOSD. They further showed that diffuse medulla, pons, or midbrain MRI lesions occasionally occurred in MOGAD and AQP4-IgG-NMOSD but never in MS. Although these findings have revealed image-dependent differentiation, few studies have been conducted using conventional MRI and its possible integration with the deep learning technique into the clinical workflow.

Recent advances in artificial intelligence have prompted the development of deep learning-based algorithms designed for the automatic classification of demyelinating diseases based on conventional MRI (11, 18–20). For example, Kim et al. (18) constructed a three-dimensional convolutional neural network (CNN) deep-learning-based model using brain MRI and clinical information to differentiate NMOSD from MS, achieving a moderate accuracy of 71.1%, sensitivity of 87.8%, and specificity of 61.6%. Rocca et al. (20) also applied a deep-learning algorithm based on CNN using brain MRI to discriminate between MS and its mimics, including NMOSD, revealing the highest accuracy (98.8%) and specificity (98.4%), and the lowest false positive rate (4.4%) for MS.

Notably, these aforementioned studies mostly used brain MRI with or without incorporation of clinical information for image-based classification using a traditional CNN. There has been minimal exploration of integrated MRI sequences and multi-site consideration of neuroimaging protocols. To address this gap, we here proposed a novel deep-learning algorithm, according to Co-

scale conv-attentional image Transformers (CoaT)-based network (21), which was trained on multi-sequence (coronal T2-weighted and sagittal T2-FLAIR) and multi-location (brain, cervicothoracic and thoracolumbar spinal cord) MRI. The combined image sequences represent a better reflection of a realistic clinical setting and may contribute to increased classification accuracy.

2 MATERIALS AND METHODS

2.1 Ethics

This study was approved by the Ethics Committee of the Second Xiangya Hospital of Central South University, and the requirement for written informed consent was waived due to the retrospective nature of the study.

2.2 Participants

MR images and clinical data of patients with a CNS inflammatory demyelinating disease treated at the neurological department of our hospital between August 2013 and October 2021 were retrospectively reviewed for inclusion. The inclusion criteria were as follows: (a) confirmed diagnosis of MS, AQP4+ NMOSD, or MOGAD according to the 2017 McDonald diagnostic criteria (9), 2015 NMOSD criteria (10), and 2018 MOGAD diagnostic criteria (22), respectively; (b) at least one clinical demyelinating episode of the CNS (myelitis, optic neuritis, or encephalopathy); (c) AQP4 antibody and MOG antibody were tested using a cell-based assay method; and (d) all participants underwent MRI scanning of the brain and/or spinal cord. The exclusion criteria were: (a) both AQP4 and MOG antibody positivity; (b) incomplete clinical assessment; (c) a history of other neurological diseases, including stroke, epilepsy, traumatic brain injury, or psychiatric problems and (d) excessive artifacts in MR images.

Notably, images acquired during acute presentation of first attack or relapses were selected for inclusion in the analysis, whereas patients in their remission phase were not included. Clinical information on sex, age, Expanded Disability Status Scale (EDSS) score, onset times, and disease duration (calculated from the first symptom onset to the scan date) were also recorded.

2.3 MRI Acquisition

All brain and/or spinal cord imaging was sequences were performed on 1.5T (Magnetom Avanto, Siemens Healthcare, Erlangen, Germany; uMR 588, Shanghai United Imaging Healthcare, Shanghai, China; GE Sigma Twin speed, GE Healthcare, Milwaukee, WI, USA) or 3.0T (Magnetom Skyra, Siemens Healthcare, Erlangen, Germany; Philips Achieva 3.0T X-Series, Phillips Healthcare, the Netherlands; uMR 790, Shanghai United Imaging Healthcare, Shanghai, China) MRI scanners in the Second Xiangya Hospital of Central South University. The MRI data included brain imaging with axial T2-weighted and coronal T2-FLAIR sequences, and spinal cord imaging with sagittal T2-weighted sequences. It is worth mentioning that when patients suspected with demyelinating diseases, a standard scanning protocol of routine brain and spinal MRI were always performed in our hospital regardless of the presence of neurological deficits. However, a small proportion of patients who met the aforementioned inclusion criteria were found with only brain or spinal cord MRI and also included in this analysis. This may be attributed to the fact that these patients only performed MRI scans of a single location according to the presence of relevant neurological deficits. There have been some variations in the acquisition parameter over the years. Detailed parameters of the brain and spinal cord MRI sequences were shown in **Table S1 in the Supplemental Material**.

2.4 Reference Standard and Image Interpretations

Two neuroradiologists (CXH and FT, with 4 and 6 years of working experience, respectively) and a neurologist (WL) with 28 years of working experience were involved in visual assessment of the brain lesions and differential classification of MS, AQP4+ NMSDO, and MOGAD patients. Images were reviewed using RadiAnt Dicom Viewer software (Version 2021.2, Medixant, Poland).

The assessment was based on T1WI, T2WI and T2-FLAIR MRI sequences of the brain, spinal cord, and optic nerve, along with clinical data (e.g., age, sex, disease duration, EDSS score, and laboratory testing results). In the diagnosis of clinically confirmed demyelinating disease, each specialist reviewed all relevant data in detail and made diagnostic decisions in accordance with the 2017 McDonald diagnostic criteria (9), 2015 NMOSD criteria (10), and 2018 MOGAD diagnostic criteria (22), respectively; in the case of any discrepancy, the data were jointly reviewed until an agreement was reached. The diagnosis based on these medical records was considered as the reference standard of this research.

2.5 Deep-Learning Model

Given most patients suspected with autoimmune demyelinating diseases had undergone MRI scans of both brain and spinal cord, the goal of the study is to develop a model that can handle the combination of brain and spinal cord MRI data for diagnosis, which is closer to the current clinical scenario. In the current analysis, we have developed the data pool consist of multimodal MRI data, which included brain T2WI, brain T2-FLAIR, cervicothoracic T2WI, and thoracolumbar T2WI; each patient had one or more types of these sequences. Moreover, MRI imaging manifestations of the lesions showed broad heterogeneity in terms of size, distribution and locations. To address this challenge, we used the state-of-art transformer network as the basic structure to build our multimodal model combined with weak-label multiple instance learning (MIL) strategy. This novel deep-learning model were designed to be versatile in handling with images of multiple sequences and scanning locations for differentiating among MS, NMOSD, and MOGAD from conventional MRI data.

2.5.1 Data Preprocessing

The dataset was randomly split into a development set and a testing set at a ratio of 4:1. We first applied intensity

normalization by z-score transformation within the non-zero region of the MR images. The normalized intensities of all voxels were set to have a mean of 0 and standard deviation (SD) of 1 for each MRI sequence. We then adjusted the intensity of these voxels and other outliers by clipping them to the range [1st percentile of the image to 99th percentile of the image]. We then performed background removal, where all voxels from the background regions outside of the non-zero region were set to −9 to ensure a uniform background intensity.

2.5.2 Multiple Instance Learning Strategy

To address the challenge of weakly labeled data (i.e., patient-level prediction without lesion/region-level annotation), we introduced a former-established MIL strategy (23). MIL is a typical weakly supervised learning paradigm that was proposed to tackle the problem of abnormalities in various locations to complement the diagnosis of tuberculosis or chronic obstructive pulmonary disease (24, 25). Specifically, MIL used slice as the model input, which leads to increased size of data in the training stage. Together with the slice-level data augmentation, such as cropping, rotation, flip, lightness and other data enhancements, we were able to mitigate the issue of imbalanced samples between brain and spinal cord MRI scans. Therefore, the bag-level MixUp on the data had the same amount of training samples in each category (26, 27). Detailed illustration of MIL-CoaT Transformer Framework was shown in **Figure S1 in the Supplemental Material**.

2.5.3 CoaT-Based Transformer Network

Transformer-based algorithms are state-of-the-art deep-learning algorithms for image recognition, including MRI (28, 29). In this study, the Siamese CoaT-based transformer network (21) was adopted as the basic network for feature extraction. By using shared parameters, the CoaT network can extract features from all instances in the same "bag," and the attention pooling block is used to fuse extracted class tokens of all instances. Finally, the fully connected layer and softmax activation function were applied to obtain the bag-level prediction probability of the three categories. The detailed network architecture and descriptions can be found **Figures S2 and S3 in the Supplemental Material**.

2.5.4 Implementation

To train the proposed MIL-CoaT model, we used Adam optimization with a batch size of 16 and learning rate of $5 \times 10^{-4} \times \frac{global\ \ batch\ \ size}{512}$. In the training phase, the Siamese CoaT-based network was initialized using the pre-trained parameters of ImageNet (30), and cross-entropy loss was used. To address the problem of sample imbalance, the number of samples in each category was guaranteed to be consistent in each training iteration cycle. Therefore, the samples of the categories with smaller sample size were transformed and reused through data augmentation technique which can be treated as the new samples in iterative cycles. To test the deep learning model, we selected the middle slice from each sub-part as an instance in the MIL setting to construct the input sample. During the training and testing process, our deep-learning model was implemented using the popular open-source PyTorch framework and was run on four Nvidia GTX 1080Ti GPUs. The code of the model in this study have been uploaded to GitHub and are available at https://github.com/TXVision/Demyelinating_Diseases_Classification_MRI.

2.6 Reader Experiment

To assess the performance of our proposed deep learning model in the classification of demyelinating diseases, we recruited two neuroradiologist SNC and HYL (with 7 and 13 years of working experience, respectively) in the reader experiment. Briefly, the raters who were blinded to the patients' clinical status independently reviewed all cases in the test dataset and were asked to classify subtypes of the demyelinating diseases with an assigned confidence score (0%-100%) for each class. The sum of the scores should equal to 100% (e.g., MS: 70%; NMOSD: 20%, MOGAD: 10%).

2.7 Statistical Analysis

Statistical analyses were performed using SPSS software (version 26.0; SPSS Inc., Chicago, IL, USA). Descriptive statistics are presented as frequencies and percentages for categorical variables and as means and SD for continuous variables. Differences in categorical variables between groups were analyzed using the Pearson chi-square test or Fisher's exact test, as appropriate. Differences in continuous variables were analyzed using the Mann-Whitney U test. The diagnostic performance of the proposed model was assessed using the receiver operating curve (AUC) with the 95% confidence interval (CI). The optimal cut-off value was chosen using the Youden index (sensitivity + specificity -1), as previously in Huang et al. (31). Thus, sensitivity, specificity; accuracy, positive predictive value (PPV), negative predictive value (NPV), and F1 score were calculated accordingly.

For performance evaluation in multi-category classification of the raters, the category with the highest probability value among the rater's output was regarded as the differential diagnosis of the disease. Thereafter, confusion matrices were drawn and overall accuracy were compared between the fusion model and the raters using the McNemar test, with p-value < 0.05 indicating the statistically significant difference. Confusion matrix deriving Matthew's correlation coefficient (MCC) and Cohen's kappa coefficient (Kappa) were also recorded and compared.

3 RESULTS

3.1 Demographic and Clinical Characteristics

A total of 290 patients with CNS inflammatory demyelinating diseases, including 67 with MS, 162 with AQP4+ NMOSD, and 61 with MOGAD, were included for analysis. **Figure 1** shows a flowchart of the selection process of the included patients. All patients were randomly assigned to the development set (composed of training and validation sets), including 231 patients (53 with MS, 129 with AQP4+ NMOSD, and 49 with MOGAD) and the testing set, including 59 patients (14 with MS, 33 with AQP4+ NMOSD, and 12 with MOGAD) at a ratio of 4:1.

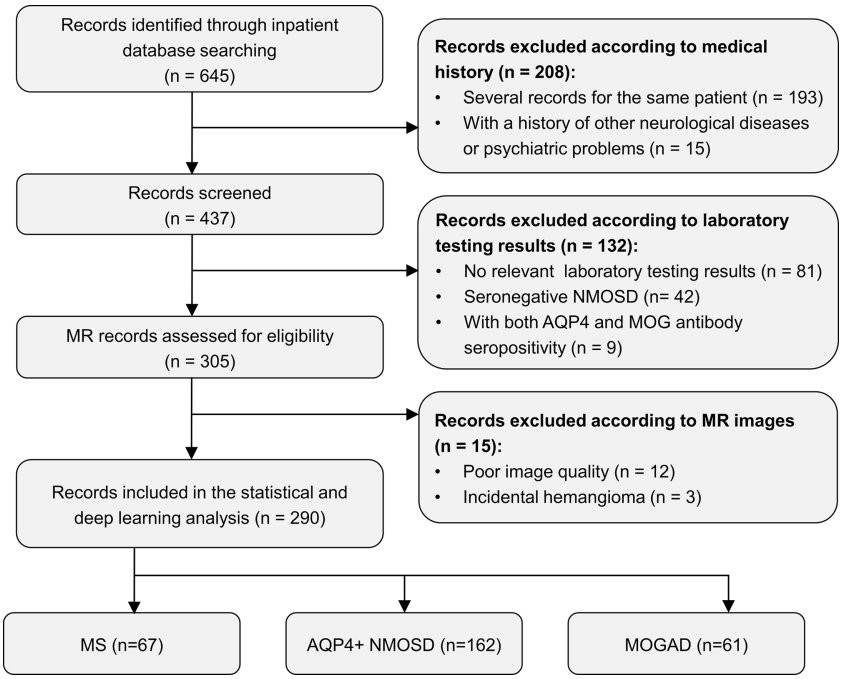

FIGURE 1 | Flow chart of the selection process of included participants. AQP4+ NMOSD, aquaporin 4 positive neuromyelitis optica spectrum disorders; MOGAD, myelin oligodendrocyte glycoprotein antibody associated disease; MR, magnetic resonance; MS, multiple sclerosis.

The demographic and clinical characteristics of all patients are summarized in **Table 1**. There were no significant differences in age, sex, disease duration, onset times, EDSS score, and the presence of visual disturbance for the MS, AQP4+ NMOSD, and MOGAD groups, respectively, between the development and testing datasets.

All patients underwent MRI scanning of the brain and/or spinal cord, and a total of 953 sequences were analyzed. Among the 290 patients included in the study, a total of 211 patients (72.8%) who have undergone both brain and spinal cord MRI scans. Among 250 (86.2%) patients with brain MRI and 251 (86.6%) patients with spinal cord MRI, there were 188/250 (75.2%) patients and 214/251 (85.3%) patients containing abnormal lesions, respectively. MR images of 14 (4.8%) patients from the AQP4+ NMOSD or MOGAD group showed no visible lesions in both the brain and spinal cord.

3.2 Diagnostic Performance of the MIL-Transformer Network Using Single- or Multi- Site MRI

We chose the Youden index as the optimal cut-off value to retrieve the variety of measurements including accuracy, sensitivity, specificity, PPV, NPV, and F1 score, which was shown in **Table 2**.

For AQP4+ NMOSD, the ROC curves (**Figure 2**) showed that deep-learning models trained with individual brain and spinal cord MRI had AUCs of 0.940 (95%CI: 0.870, 0.986) and 0.689 (95%CI: 0.520, 0.833) respectively. In comparison, the deep-learning fusion model provided better diagnostic performance with AUC of 0.942 (95%CI: 0.879, 0.987) for AQP4+ NMOSD.

When identifying MOGAD, the AUCs of the models trained with individual brain and spinal cord MRI were 0.782 (95% CI: 0.606, 0.938) and 0.714 (95% CI: 0.494, 0.919), respectively. In comparison, the deep-learning fusion model exhibited superior diagnostic performance with AUC of 0.803 (95%CI: 0.629, 0.949) for MOGAD.

The deep-learning model based on the spinal cord MRI had AUC of 0.724 (95%CI: 0.539, 0.897) for MS, which was small than that of the model trained with the brain MRI with AUC of 0.936 (95%CI: 0.855, 0.990) and the combined sequences (the fusion model) with AUC of 0.933 (95%CI: 0.848, 0.991). The AUC of the fusion model was marginally smaller than that of the model trained with brain MRI for MS.

3.3 Multi-Category Classification Comparison of the Deep-Learning Model Against Neuroradiologists

Multi-category classification using the proposed MIL-transformer network also exhibited better performance in the fusion model. Among the models trained with MRI on individual and combined locations, the fusion model exhibited better performance with an accuracy of 81.4% (Kappa 0.666, MCC 0.682). On the contrary, the model using individual brain or spinal cord MRI as input had an accuracy of 75.9% (Kappa 0.605, MCC 0.623) and 62.7% (Kappa 0.202, MCC 0.215), respectively.

We also compared the classification performance obtained with the proposed models versus that of human raters. In the same test dataset of 59 patients, the overall accuracy of the deep-

TABLE 1 | Demographic and clinical characteristics in patients with MS, AQP4+ NMOSD, and MOGAD.

	Development Set (n = 231)			Testing Set (n = 59)			
	MS	AQP4+ NMOSD	MOGAD	MS	AQP4+ NMOSD	MOGAD	p value*
Clinical characteristics							
No. of patients, n	53	129	49	14	33	12	–
Age, mean ± SD, years	33.11 ± 12.83	44.21 ± 14.10	23.31 ± 18.09	34.50 ± 14.03	42.12 ± 15.30	27.33 ± 15.74	> 0.05
Adults (≥18 years), n (%)	50 (94.34%)	126 (97.67%)	22 (44.90%)	14 (100%)	31 (93.94%)	7 (58.33%)	–
Sex (male/female)	28/25	10/119	20/29	8/6	3/30	6/6	> 0.05
Disease duration, mean ± SD, months	31.74 ± 50.41	26.76 ± 51.80	14.15 ± 37.74	46.96 ± 48.99	38.50 ± 79.02	10.33 ± 24.11	> 0.05
Onset times, mean ± SD	1.96 ± 0.88	1.90 ± 1.34	1.47 ± 0.92	2.14 ± 0.66	1.73 ± 1.21	1.17 ± 0.39	> 0.05
First attack, n (%)	18 (33.96%)	66 (51.16%)	36 (73.47%)	2 (14.29%)	20 (60.61%)	10 (83.33%)	–
Second attack, n (%)	22 (41.51%)	35 (27.13%)	6 (12.24%)	8 (57.14%)	7 (21.21%)	2 (16.67%)	–
≥3 attacks, n (%)	13 (24.53%)	28 (21.71%)	7 (14.29%)	4 (28.57%)	6 (18.18%)	0 (0)	–
EDSS score at the time of MRI, mean ± SD	3.53 ± 1.87	5.70 ± 2.22	2.45 ± 1.28	4.14 ± 1.62	4.86 ± 1.99	2.54 ± 1.66	> 0.05
Visual disturbance, n (%)	21 (39.62%)	48 (37.21%)	27 (55.10%)	4 (28.57%)	9 (27.27%)	5 (41.67%)	> 0.05
MRI scanning information							
No. of MRI sequences	178	411	166	45	112	41	–
Brain + spinal cord, n (%)	39 (73.58%)	91 (70.54%)	36 (73.47%)	10 (71.43%)	26 (78.79%)	9 (75.00%)	–
Brain only, n (%)	13 (24.53%)	6 (4.65%)	12 (24.49%)	4 (28.57%)	1 (3.03%)	3 (25.00%)	–
Cervicothoracic and/or thoracolumbar spinal cord only, n (%)	1 (1.89%)	32 (24.81%)	1 (2.04%)	0 (0)	6 (18.18%)	0 (0)	–
MR scanner field strength							
3.0 T scanners	12	50	28	2	13	3	–
1.5 T scanners	41	79	21	12	20	9	–

**Significant difference (p < 0.05) of each clinical variable in the MS, AQP4+ NMOSD, and MOGAD groups, respectively, between the development and testing datasets.*
AQP4+ NMOSD, aquaporin 4 positive neuromyelitis optica spectrum disorders; EDSS, expanded disability status scale; MOGAD, myelin oligodendrocyte glycoprotein antibody associated disease; MRI, magnetic resonance imaging; MS, multiple sclerosis; SD, standard deviation.

TABLE 2 | Diagnostic performance of our proposed MIL-CoaT transformer model based on different inputs in classification of MS, AQP4+ NMOSD and MOGAD.

One-vs.-rest classification	ROC_AUC (95% CI)	Accuracy (%)	Sensitivity (%)	Specificity (%)	PPV (%)	NPV (%)	F1
Brain MRI as model inputs							
MS vs. others	0.936 (0.855, 0.990)	88.9	78.6	92.5	78.6	92.5	0.786
AQP4+ NMOSD vs. others	0.940 (0.870, 0.986)	87.0	78.6	96.2	95.7	80.6	0.863
MOGAD vs. others	0.782 (0.606, 0.938)	85.2	58.3	92.9	70.0	88.6	0.636
Spinal cord MRI as model inputs							
MS vs. others	0.724 (0.539, 0.897)	74.5	70.0	75.6	41.2	91.2	0.519
AQP4+ NMOSD vs. others	0.689 (0.520, 0.833)	70.6	71.9	68.4	79.3	59.1	0.780
MOGAD vs. others	0.714 (0.494, 0.919)	82.4	55.6	88.1	50.0	90.2	0.526
Combined brain and spinal cord MRI as model inputs							
MS vs. others	0.933 (0.848, 0.991)	84.7	92.9	82.2	61.9	97.4	0.743
AQP4+ NMOSD vs. others	0.942 (0.879, 0.987)	88.1	87.9	88.5	90.6	85.2	0.892
MOGAD vs. others	0.803 (0.629, 0.949)	72.9	83.3	70.2	41.7	94.3	0.556

AQP4+ NMOSD, aquaporin 4 positive neuromyelitis optica spectrum disorders; AUC, area under curve; CI, confidence interval; MOGAD, myelin oligodendrocyte glycoprotein antibody associated disease; MS, multiple sclerosis; ROC, receiver operating characteristic curve.

learning model was higher than that of rater 1 and comparable to rater 2 (81.4% vs. 64.4% for rater 1, p = 0.04 < 0.05 and 81.4% vs. 74.6% for rater 2, p = 0.388 > 0.05). Meanwhile, as shown in **Figure 3**, the confusion matrix of the fusion model exhibited a higher Kappa of 0.666, MCC of 0.682 than that of human raters, who had a Kappa of 0.426, MCC of 0.431 for rater1 and Kappa of 0.576, MCC of 0.578 for rater 2.

3.4 Visual Explanation of the Deep-Learning Model

The lack of transparency in deep learning can be overcome by applying gradient-weighted class activation (Grad-CAM) to visualize feature extraction using an activation heatmap (32). As shown in **Figure 4**, lesions in the brain and spinal cord manifested as relatively dark color in the Grad-CAM results. Insights generated from Grad-CAM were compared with manual annotations, and the results indicated that the model focuses on these lesions when distinguishing demyelinating diseases. This can help us to gain an understanding of the regions within the MR images that are responsible for network predictions.

4 DISCUSSION

In this study, we proposed transformer-based deep-learning model to differentiate among MS, AQP4+ NMOSD and

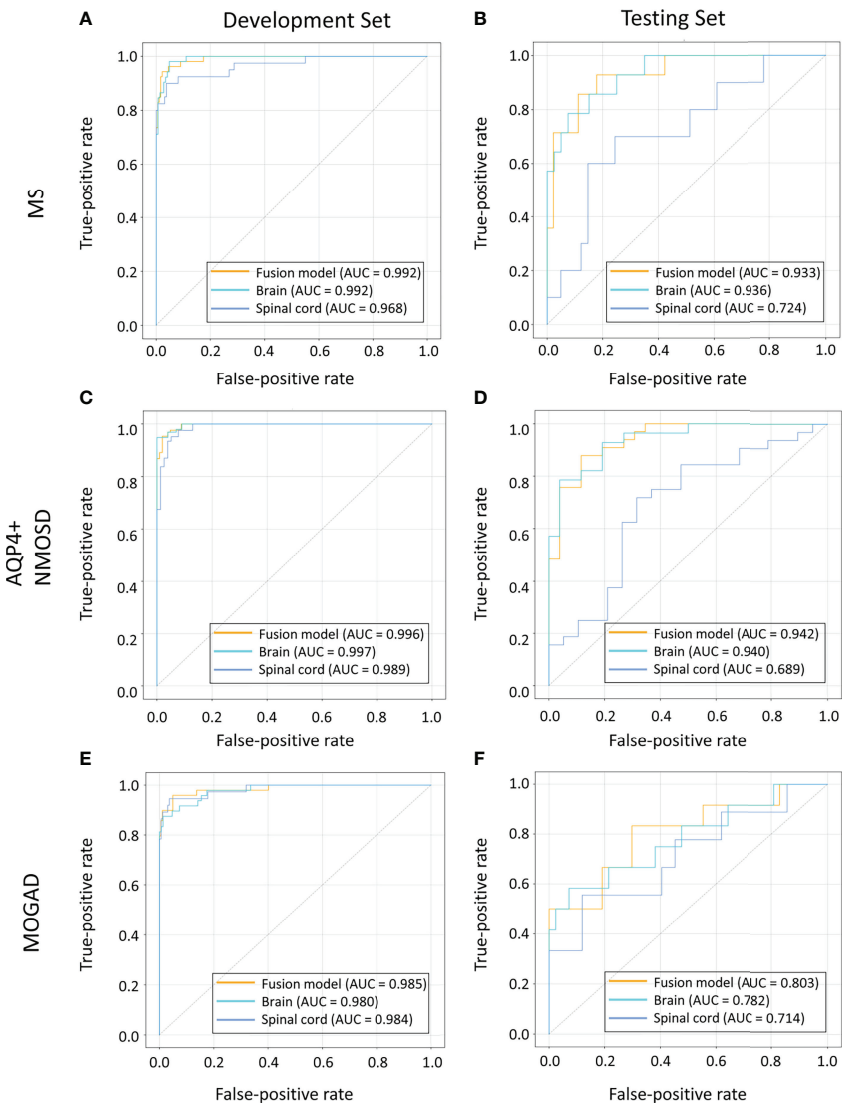

FIGURE 2 | ROC curves of the models based on brain, spinal cord, and combined MRI sequences in the cohorts of patients with MS **(A, B)**, AQP4+ NMOSD **(C, D)** and MOGAD **(E, F)**. AQP4+ NMOSD, aquaporin 4 positive neuromyelitis optica spectrum disorders; MOGAD, myelin oligodendrocyte glycoprotein antibody associated disease; MRI, magnetic resonance imaging; MS, multiple sclerosis; ROC, receiver operating characteristic.

MOGAD based on conventional brain and spinal cord MRI. This novel transformer-based model architecture was designed to be versatile in handling with images of multiple sequences and scanning locations whichever were available at clinical practice, for differentiating among MS, NMOSD, and MOGAD at a high accuracy. The fusion model using images of combined locations exhibited significantly higher accuracy than the models trained with a single location MRI as well as two experienced radiologists, which referred to possible alternative tool in assisting clinical decisions for a fast and accurate treatment referral.

To our knowledge, this is the first study to use an ensemble-location approach in the task of multi-category classification to improve the differential diagnosis of CNS inflammatory demyelinating diseases. Given patients suspected with demyelinating disease may undergo brain and/or spinal cord MRI scans, the model was developed to handle with the data in the single- or multi- location manner on conventional MR images. When MR images at one location were taken, our results showed that taking brain images as model inputs had a relative higher accuracy in classifying these three conditions than using spinal cord images only (pooled accuracy: 75.9% vs. 62.7%). Moreover, when multi-location MR images were available, the fusion model demonstrated an improved accuracy of 81.4%, which was comparable compared to the performance of two neuroradiologists (accuracy: 64.4% for rater 1 and 74.6% for rater 2). Meanwhile, the fusion model exhibited higher Kappa and MCC than that of human raters.

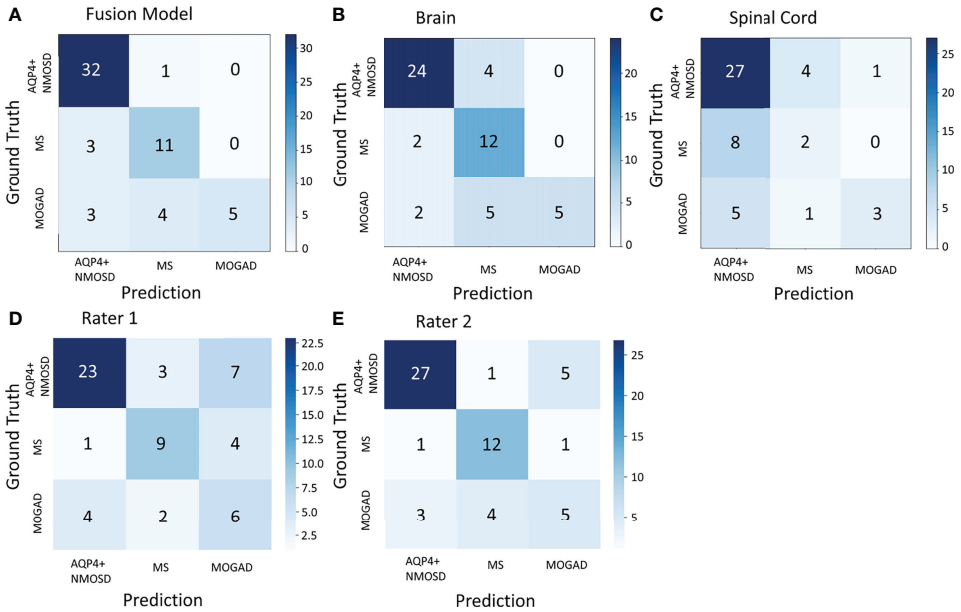

FIGURE 3 | The confusion matrix of the fusion model in the test dataset of 59 patients **(A)**, the model based on the brain MRI **(B)**, the model based on the spinal cord MRI **(C)**, and human rater 1 and 2 **(D, E)**. AQP4+ NMOSD, aquaporin 4 positive neuromyelitis optica spectrum disorders; MOGAD, myelin oligodendrocyte glycoprotein antibody associated disease; MS, multiple sclerosis.

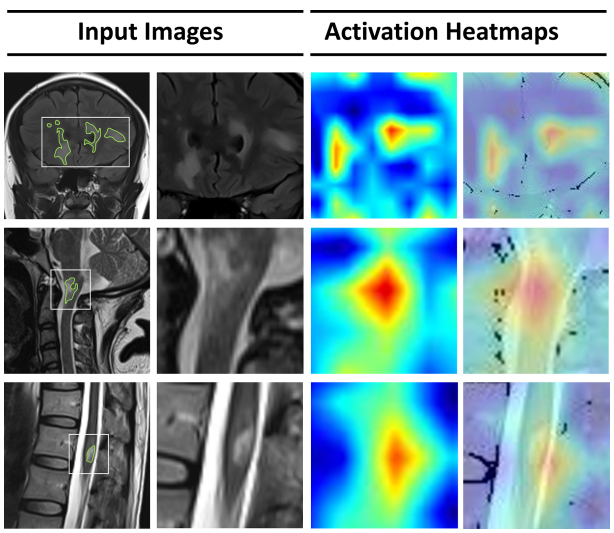

FIGURE 4 | Visualization of features extracted by the deep-learning model from the input images. From the left, the first column represents the original MRI slices with manual annotations of lesions in the brain, cervical spinal cord, and thoracic spinal cord. In the second column, a smaller patch is cropped around the lesions. The third column represents the activation heatmaps. The color depth of the heatmaps represents the possibility of predicted lesions by the model. The fourth column overlaps the activation mapping with the original MRI for better visual reference.

Previous studies have used only brain or spinal cord images (11, 20), along with accompanying clinical variables (18, 33) for prediction. Among these studies, Rocca et al. (20) used CNN and achieved an accuracy of 98.8% for the differential diagnosis of MS from NMOSD. However, it shall be noted that this high diagnostic performance of these models may be attributed to obvious differences in lesion volume and distribution, which may lead to over-estimated classification accuracy of the models. This potential bias was addressed in our study by enrolling images from patients whose MRI were taken at multi-location and the features extracted broad heterogeneity in lesion distribution were regarded as shared manifestations among target demyelinated disease.

Deep-learning algorithms are an active area of research in medical image processing. These algorithms can extract information from conventional MR images, including features that cannot be recognized by the human eye, and help to make a more accurate diagnosis (34), prognosis evaluation (35) and therapeutic guidance (36). Our proposed multimodal MIL-CoaT deep-learning network can perform multicategory classification using hybrid MRI sequences. This model was developed based on an MIL strategy and incorporated the CoaT transformer as the basic network structure. Specifically, the MIL strategy used slice as the model input, which leads to increased size of data in the training stage. Together with the slice-level data augmentation, we were able to mitigate the issue of imbalanced samples between brain and spinal cord MRI scans. Furthermore, during the training stage, each epoch has the same amount of training sample at each group. The samples of the categories with smaller sample size were transformed and reused through data augmentation technique which can be treated as the new samples in iterative cycles. Moreover, the CoaT-based

transformer structure has the characteristics of dynamic attention and global context fusion, which are not available with a traditional CNN. Thus, by combining the extracted features and subsequent instance-wise feature fusion using attention pooling, we obtained a model with improved generalization ability.

We reviewed misclassified cases to determine their imaging characteristics and speculate possible reasons. We found that the cases misclassified as AQP4+ NMOSD can exhibit certain characteristics such as the presence of brain lesions adjacent to the fourth ventricle, and multiple short segment lesions that fused into long segment lesions in the spinal cord, which may resemble the appearance of AQP4+ NMOSD. Moreover, the presence of severe brain atrophy, and involvement of cortical or juxtacortical regions may be a possible cause of being misdiagnosed as MS.

This study indeed had some limitations. First, optic nerve lesions may exist in CNS demyelinating diseases, whereas the limited imaging data of optic nerve MRI were not suitable for inclusion in big data analysis. Second, the lack of thin-section MRI data due to time-cost issues may have resulted in lower image resolution and less precise information. However, it shall be mentioned that in most hospitals in China, the conventional MRI protocol with thick slices was utilized for the diagnosis of patients suspected with demyelinated diseases. This is attributed to larger number of patients and longer waiting times compared to western countries. Under this condition, we focused on research-quality MR images and developed the deep learning model that could be used to classify major types of demyelinated disease with high accuracy. Third, the loss of accuracy with the fusion model including spinal cord MRI in MS cases may have been attributed to the limited sample size and the fact that some MS patients did not have lesions in the spinal cord. This would be an important feature for co-learning to ensure reliability in applying the model to clinical practice.

5 CONCLUSION

Overall, our results provide evidence that deep-learning networks may be used for differential diagnosis based on brain and spinal cord MRI for patients with MS, AQP4+ NMOSD, and MOGAD. To our knowledge, this is the first study to apply the newly proposed MIL-CoaT transformer-based deep-learning algorithm to conventional MRI of multiple locations and sequences in attempt to solve the clinical challenge of diagnosing CNS demyelinating diseases. This evidence is also expected to motivate future research for delving into the clinical and radiological basis of deep-learning networks, as well as to validate the findings with a prospective study design.

DATA AVAILABILITY STATEMENT

The original contributions presented in the study are included in the article/**Supplementary Material**. Further inquiries can be directed to the corresponding authors.

ETHICS STATEMENT

The studies involving human participants were reviewed and approved by the Ethics Committee of the Second Xiangya Hospital of Central South University. Written informed consent from the participants' legal guardian/next of kin was not required to participate in this study in accordance with the national legislation and the institutional requirements.

AUTHOR CONTRIBUTIONS

JL and WL conceived and designed the study. XC collected imaging and clinical data. CH, FT, and WL reviewed the data. BL, WC, and RY analyzed and interpreted the data. CH drafted the manuscript. All authors contributed to the article and approved the final version.

FUNDING

This work was supported by the Clinical Research Center for Medical Imaging in Hunan Province (2020SK4001). Leading talents of scientific and technological innovation in Hunan Province in 2021 (2021RC4016). The accurate localization study of mild traumatic brain injury based on deep learning through multimodal image and neural network (2021gfcx05).

SUPPLEMENTARY MATERIAL

The Supplementary Material for this article can be found online at: https://www.frontiersin.org/articles/10.3389/fimmu.2022.897959/full#supplementary-material

REFERENCES

1. Papp V, Magyari M, Aktas O, Berger T, Broadley SA, Cabre P, et al. Worldwide Incidence and Prevalence of Neuromyelitis Optica: A Systematic Review. *Neurology* (2021) 96:59–77. doi: 10.1212/WNL.0000000000011153
2. Walton C, King R, Rechtman L, Kaye W, Leray E, Marrie RA, et al. Rising Prevalence of Multiple Sclerosis Worldwide: Insights From the Atlas of MS, Third Edition. *Mult Scler* (2020) 26:1816–21. doi: 10.1177/1352458520970841
3. Lucchinetti CF, Mandler RN, McGavern D, Bruck W, Gleich G, Ransohoff RM, et al. A Role for Humoral Mechanisms in the Pathogenesis of Devic's Neuromyelitis Optica. *Brain* (2002) 125:1450–61. doi: 10.1093/brain/awf151
4. Leite MI, Sato DK. MOG-Antibody-Associated Disease is Different From MS and NMOSD and Should be Considered as a Distinct Disease Entity - Yes. *Mult Scler* (2020) 26:272–4. doi: 10.1177/1352458519868796
5. Jarius S, Wildemann B. The History of Neuromyelitis Optica. *J Neuroinflammat* (2013) 10:8. doi: 10.1186/1742-2094-10-8

6. Wingerchuk DM, Lennon VA, Lucchinetti CF, Pittock SJ, Weinshenker BG. The Spectrum of Neuromyelitis Optica. *Lancet Neurol* (2007) 6:805–15. doi: 10.1016/S1474-4422(07)70216-8
7. Fujihara K, Cook LJ. Neuromyelitis Optica Spectrum Disorders and Myelin Oligodendrocyte Glycoprotein Antibody-Associated Disease: Current Topics. *Curr Opin Neurol* (2020) 33:300–8. doi: 10.1097/WCO.0000000000000828
8. Fujihara K. Neuromyelitis Optica Spectrum Disorders: Still Evolving and Broadening. *Curr Opin Neurol* (2019) 32:385–94. doi: 10.1097/WCO.0000000000000694
9. Thompson AJ, Banwell BL, Barkhof F, Carroll WM, Coetzee T, Comi G, et al. Diagnosis of Multiple Sclerosis: 2017 Revisions of the McDonald Criteria. *Lancet Neurol* (2018) 17:162–73. doi: 10.1016/S1474-4422(17)30470-2
10. Wingerchuk DM, Banwell B, Bennett JL, Cabre P, Carroll W, Chitnis T, et al. International Consensus Diagnostic Criteria for Neuromyelitis Optica Spectrum Disorders. *Neurology* (2015) 85:177–89. doi: 10.1212/WNL.0000000000001729
11. Cacciaguerra L, Storelli L, Radaelli M, Mesaros S, Moiola L, Drulovic J, et al. Application of Deep-Learning to the Seronegative Side of the NMO Spectrum. *J Neurol* (2021) 269:1546–56. doi: 10.1007/s00415-021-10727-y
12. Borisow N, Mori M, Kuwabara S, Scheel M, Paul F. Diagnosis and Treatment of NMO Spectrum Disorder and MOG-Encephalomyelitis. *Front Neurol* (2018) 9:888. doi: 10.3389/fneur.2018.00888
13. Palace J, Leite MI, Nairne A, Vincent A. Interferon Beta Treatment in Neuromyelitis Optica: Increase in Relapses and Aquaporin 4 Antibody Titers. *Arch Neurol* (2010) 67:1016–7. doi: 10.1001/archneurol.2010.188
14. Popiel M, Psujek M, Bartosik-Psujek H. Severe Disease Exacerbation in a Patient With Neuromyelitis Optica Spectrum Disorder During Treatment With Dimethyl Fumarate. *Mult Scler Relat Disord* (2018) 26:204–6. doi: 10.1016/j.msard.2018.09.011
15. Durozard P, Rico A, Boutiere C, Maarouf A, Lacroix R, Cointe S, et al. Comparison of the Response to Rituximab Between Myelin Oligodendrocyte Glycoprotein and Aquaporin-4 Antibody Diseases. *Ann Neurol* (2020) 87:256–66. doi: 10.1002/ana.25648
16. Duan Y, Zhuo Z, Li H, Tian DC, Li Y, Yang L, et al. Brain Structural Alterations in MOG Antibody Diseases: A Comparative Study With AQP4 Seropositive NMOSD and MS. *J Neurol Neurosurg Psychiatry* (2021) 92:709–16. doi: 10.1136/jnnp-2020-324826
17. Banks SA, Morris PP, Chen JJ, Pittock SJ, Sechi E, Kunchok A, et al. Brainstem and Cerebellar Involvement in MOG-IgG-Associated Disorder Versus Aquaporin-4-IgG and MS. *J Neurol Neurosurg Psychiatry* (2020). doi: 10.1136/jnnp-2020-325121
18. Kim H, Lee Y, Kim YH, Lim YM, Lee JS, Woo J, et al. Deep Learning-Based Method to Differentiate Neuromyelitis Optica Spectrum Disorder From Multiple Sclerosis. *Front Neurol* (2020) 11:599042. doi: 10.3389/fneur.2020.599042
19. Wang Z, Yu Z, Wang Y, Zhang H, Luo Y, Shi L, et al. 3d Compressed Convolutional Neural Network Differentiates Neuromyelitis Optical Spectrum Disorders From Multiple Sclerosis Using Automated White Matter Hyperintensities Segmentations. *Front Physiol* (2020) 11:612928. doi: 10.3389/fphys.2020.612928
20. Rocca MA, Anzalone N, Storelli L, Del Poggio A, Cacciaguerra L, Manfredi AA, et al. Deep Learning on Conventional Magnetic Resonance Imaging Improves the Diagnosis of Multiple Sclerosis Mimics. *Invest Radiol* (2021) 56:252–60. doi: 10.1097/RLI.0000000000000735
21. Xu W, Xu Y, Chang T, Tu Z. Co-Scale Conv-Attentional Image Transformers. *ArXiv E-print* (2021), 9981–90. doi: 10.48550/arXiv.2104.06399
22. Jarius S, Paul F, Aktas O, Asgari N, Dale RC, de Seze J, et al. MOG Encephalomyelitis: International Recommendations on Diagnosis and Antibody Testing. *J Neuroinflammat* (2018) 15:134. doi: 10.1186/s12974-018-1144-2
23. Ilse M, Tomczak JM, Welling M. Attention-Based Deep Multiple Instance Learning. *Proc 35 Th Int Conf Mach Learn* (2018) 80:2127–36. doi: 10.48550/arXiv.1802.04712
24. Lopes UK, Valiati JF. Pre-Trained Convolutional Neural Networks as Feature Extractors for Tuberculosis Detection. *Comput Biol Med* (2017) 89:135–43. doi: 10.1016/j.compbiomed.2017.08.001
25. Xu C, Qi S, Feng J, Xia S, Kang Y, Yao Y, et al. DCT-MIL: Deep CNN Transferred Multiple Instance Learning for COPD Identification Using CT Images. *Phys Med Biol* (2020) 65:145011. doi: 10.1088/1361-6560/ab857d
26. Zhang H, Cisse M, Dauphin YN, Lopez-Paz D. Mixup: Beyond Empirical Risk Minimization. *ArXiv E-print* (2018). doi: 10.48550/arXiv.1710.09412
27. Yun S, Han D, Oh SJ, Chun S, Choe J, Yoo Y. CutMix: Regularization Strategy to Train Strong Classifiers With Localizable Features. *Proc IEEE/CVF Int Conf Comput Vision (ICCV), ArXiv E-print* (2019), 6023–32. doi: 10.48550/arXiv.1905.04899
28. Hering A, Kuckertz S, Heldmann S, Heinrich MP. Memory-Efficient 2.5D Convolutional Transformer Networks for Multi-Modal Deformable Registration With Weak Label Supervision Applied to Whole-Heart CT and MRI Scans. *Int J Comput Assist Radiol Surg* (2019) 14:1901–12. doi: 10.1007/s11548-019-02068-z
29. Santhirasekaram A, Pinto K, Winkler M, Aboagye E, Glocker B, Rockall A. Multi-Scale Hybrid Transformer Networks: Application to Prostate Disease Classification. In: *International Workshop on Multimodal Learning for Clinical Decision Support Lecture Notes in Computer Science* (2021). p. 13050. doi: 10.1007/978-3-030-89847-2_2
30. Russakovsky O, Deng J, Su H, Krause J, Satheesh S, Ma S, et al. ImageNet Large Scale Visual Recognition Challenge. *Int J Comput Vision* (2015) 115:211–52. doi: 10.1007/s11263-015-0816-y
31. Huang Z, Liu D, Chen X, He D, Yu P, Liu B, et al. Deep Convolutional Neural Network Based on Computed Tomography Images for the Preoperative Diagnosis of Occult Peritoneal Metastasis in Advanced Gastric Cancer. *Front Oncol* (2020) 10:601869. doi: 10.3389/fonc.2020.601869
32. Selvaraju RR, Cogswell M, Das A, Vedantam R, Parikh D, Batra D. Grad-CAM: Visual Explanations From Deep Networks *via* Gradient-Based Localization. *Int J Comput Vision* (2020) 128:336–59. doi: 10.1007/s11263-019-01228-7
33. Liu Y, Dong D, Zhang L, Zang Y, Duan Y, Qiu X, et al. Radiomics in Multiple Sclerosis and Neuromyelitis Optica Spectrum Disorder. *Eur Radiol* (2019) 29:4670–7. doi: 10.1007/s00330-019-06026-w
34. Zaharchuk G, Gong E, Wintermark M, Rubin D, Langlotz CP. Deep Learning in Neuroradiology. *AJNR Am J Neuroradiol* (2018) 39:1776–84. doi: 10.3174/ajnr.A5543
35. She Y, Jin Z, Wu J, Deng J, Zhang L, Su H, et al. Development and Validation of a Deep Learning Model for Non-Small Cell Lung Cancer Survival. *JAMA Netw Open* (2020) 3:e205842. doi: 10.1001/jamanetworkopen.2020.5842
36. Burgos N, Bottani S, Faouzi J, Thibeau-Sutre E, Colliot O. Deep Learning for Brain Disorders: From Data Processing to Disease Treatment. *Brief Bioinform* (2021) 22:1560–76. doi: 10.1093/bib/bbaa310

Conflict of Interest: Authors BL, WC, and RY were employed by Infervision Medical Technology Co., Ltd.

The remaining authors declare that the research was conducted in the absence of any commercial or financial relationships that could be construed as a potential conflict of interest.

frontiers | Frontiers in Neurology

REVIEW
published: 17 June 2022
doi: 10.3389/fneur.2022.885218

Myelin Oligodendrocyte Glycoprotein Antibody-Associated Disease (MOGAD): A Review of Clinical and MRI Features, Diagnosis, and Management

Elia Sechi[1], *Laura Cacciaguerra*[2,3], *John J. Chen*[3,4], *Sara Mariotto*[5], *Giulia Fadda*[6], *Alessandro Dinoto*[5], *A. Sebastian Lopez-Chiriboga*[7], *Sean J. Pittock*[3,8] *and Eoin P. Flanagan*[3,8]*

[1] Neurology Unit, Department of Medical, Surgical and Experimental Sciences, University of Sassari, Sassari, Italy, [2] Neuroimaging Research Unit, Division of Neuroscience, IRCCS San Raffaele Scientific Institute and Vita-Salute San Raffaele University, Milan, Italy, [3] Department of Neurology and Center for Multiple Sclerosis and Autoimmune Neurology Mayo Clinic, Rochester, MN, United States, [4] Department of Ophthalmology, Mayo Clinic, Rochester, MN, United States, [5] Neurology Unit, Department of Neurosciences, Biomedicine, and Movement Sciences, University of Verona, Verona, Italy, [6] Department of Neurology and Neurosurgery, McGill University, Montreal, QC, Canada, [7] Department of Neurology, Mayo Clinic, Jacksonville, FL, United States, [8] Department of Laboratory Medicine and Pathology, Mayo Clinic, Rochester, MN, United States

OPEN ACCESS

Edited by:
Jodie Burton,
University of Calgary, Canada

Reviewed by:
Scott Douglas Newsome,
Johns Hopkins Medicine,
United States
Florian Deisenhammer,
Innsbruck Medical University, Austria

***Correspondence:**
Eoin P. Flanagan
flanagan.eoin@mayo.edu

Specialty section:
This article was submitted to Multiple Sclerosis and Neuroimmunology, a section of the journal Frontiers in Neurology

Received: *27 February 2022*
Accepted: *06 May 2022*
Published: *17 June 2022*

Citation:
Sechi E, Cacciaguerra L, Chen JJ, Mariotto S, Fadda G, Dinoto A, Lopez-Chiriboga AS, Pittock SJ and Flanagan EP (2022) Myelin Oligodendrocyte Glycoprotein Antibody-Associated Disease (MOGAD): A Review of Clinical and MRI Features, Diagnosis, and Management. Front. Neurol. 13:885218. doi: 10.3389/fneur.2022.885218

Myelin oligodendrocyte glycoprotein (MOG) antibody-associated disease (MOGAD) is the most recently defined inflammatory demyelinating disease of the central nervous system (CNS). Over the last decade, several studies have helped delineate the characteristic clinical-MRI phenotypes of the disease, allowing distinction from aquaporin-4 (AQP4)-IgG-positive neuromyelitis optica spectrum disorder (AQP4-IgG+NMOSD) and multiple sclerosis (MS). The clinical manifestations of MOGAD are heterogeneous, ranging from isolated optic neuritis or myelitis to multifocal CNS demyelination often in the form of acute disseminated encephalomyelitis (ADEM), or cortical encephalitis. A relapsing course is observed in approximately 50% of patients. Characteristic MRI features have been described that increase the diagnostic suspicion (e.g., perineural optic nerve enhancement, spinal cord H-sign, T2-lesion resolution over time) and help discriminate from MS and AQP4+NMOSD, despite some overlap. The detection of MOG-IgG in the serum (and sometimes CSF) confirms the diagnosis in patients with compatible clinical-MRI phenotypes, but false positive results are occasionally encountered, especially with indiscriminate testing of large unselected populations. The type of cell-based assay used to evaluate for MOG-IgG (fixed vs. live) and antibody end-titer (low vs. high) can influence the likelihood of MOGAD diagnosis. International consensus diagnostic criteria for MOGAD are currently being compiled and will assist in clinical diagnosis and be useful for enrolment in clinical trials. Although randomized controlled trials are lacking, MOGAD acute attacks appear to be very responsive to high dose steroids and plasma exchange may be considered in refractory cases. Attack-prevention treatments also lack class-I data and empiric maintenance treatment is generally reserved for relapsing cases or patients with severe residual disability after the presenting attack. A variety of empiric steroid-sparing immunosuppressants can be

considered and may be efficacious based on retrospective or prospective observational studies but prospective randomized placebo-controlled trials are needed to better guide treatment. In summary, this article will review our rapidly evolving understanding of MOGAD diagnosis and management.

Keywords: MOG, NMOSD, neuromyelitis optica, multiple sclerosis, demyelinating diseases, false positive, differential diagnosis

INTRODUCTION

During the last 15 years, the global concept of inflammatory demyelinating disorders of the central nervous system (CNS) has radically changed with the identification of specific autoantibody-associated conditions distinct from multiple sclerosis (MS), namely aquaporin-4 (AQP4)-IgG-positive neuromyelitis optica spectrum disorder (AQP4-IgG+NMOSD) and myelin oligodendrocyte glycoprotein (MOG)-IgG-associated disease (MOGAD) (1–4). Consensual refinements in the clinical-MRI characterization of these three disease entities has increased diagnostic precision, and allowed identification of important differences in pathophysiology, treatment response, and outcomes. Awareness of the specific features that define each demyelinating disorder is crucial for a correct diagnosis and timely initiation of an appropriate treatment (4).

In this review article we will summarize our current understanding of MOGAD, the most recently characterized demyelinating CNS disorder, and provide guidance for diagnosis and management. Although not representing the focus of this work, AQP4-IgG+NMOSD and MS will be discussed as comparison groups to highlight differences and similarities with MOGAD.

History and Definitions: The Concept of NMOSD and MOGAD

There is often confusion among clinicians since both the terms NMOSD and MOGAD have been used in the literature to refer to the CNS demyelinating disorder associated with MOG-IgG. The term neuromyelitis optica (NMO) was first used in 1894 by Eugene Devic and his student Fernand Gault to describe a syndrome characterized by the simultaneous occurrence of bilateral optic neuritis (ON) and acute myelitis. Devic and Gault reviewed the literature at the time for similar cases and proposed the disease as a distinct entity, although the syndrome was regarded for decades by many as a more severe variant of MS, sometimes with different names worldwide (e.g., optic-spinal MS in Asia) (5). In 2004, Vanda Lennon and Brian Weinshenker published on a novel autoantibody that they identified in a cohort of patients with NMO but not in patients with MS, which they initially named NMO-IgG (1). The antibody was later found to target AQP4, the main water-channel protein in the CNS mostly expressed on astrocytic end-feet, and the name was changed to AQP4-IgG (6). It soon became clear that the spectrum of clinical-MRI manifestations related to AQP4-IgG extended beyond the exclusive involvement of optic nerves and spinal cord. Brain involvement was in fact recognized in a significant proportion of patients (7, 8), with area postrema syndrome (i.e., intractable nausea, vomiting, and hiccups) being one of the cardinal manifestations of the disease (9). Patients with AQP4-IgG could also present with partial forms of isolated myelitis or optic neuritis that did not meet the former NMO criteria. As a consequence, the definition of NMO spectrum disorders (NMOSD) was created to include the different clinical-MRI syndromes associated with the novel antibody (10). In 2015, NMOSD diagnostic criteria were published by a panel of experts (11). In addition to the main diagnosis based on AQP4-IgG detection, these criteria introduced the concept of seronegative NMOSD defined by more stringent clinical-MRI requirements based on the core clinical-MRI manifestations observed in patients with AQP4-IgG. However, the actual identification of patients meeting these criteria despite testing negative for AQP4-IgG raised the possibility that other autoantibodies could account for similar syndromes, which was later found to be true for MOG-IgG.

The historical scientific interest for the MOG protein dates back to the 1980's when it was first identified as a major potential autoantibody target of CNS myelin in models of experimental autoimmune encephalomyelitis (12). In 2003, MOG-IgM detected by Western Blot was proposed as a biomarker to predict conversion from clinically isolated syndrome to definite MS (13). However, a number of subsequent studies conducted with similar testing assays using denaturated MOG proteins (e.g., ELISA) showed that MOG-IgG was not disease-specific, being detectable with similar frequency in patients with MS, other demyelinating CNS disorders, and unaffected controls (14, 15). In 2007, a seminal study by O'Connor et al. showed that laboratory assays expressing MOG in its tridimensional conformational form (rather than linear epitopes targeted on denaturated proteins as with other assays) identified a sub-set of conformation-sensitive MOG-IgG in patients with acute disseminated encephalomyelitis (ADEM) or optic neuritis, but not in patients with MS (2). Subsequent studies using cell-based assays expressing human full length MOG on mammalian cells confirmed the detection of MOG-IgG in patients with non-MS demyelinating CNS disorders (16, 17), including 30–70% of patients with seronegative NMOSD (18–21). The spectrum of clinical-MRI manifestations associated with MOG-IgG is now recognized to extend beyond the NMOSD phenotype and the disease is referred to as MOGAD (22–24).

To avoid confusion and overlaps between clinical-MRI phenotypes (e.g., NMOSD, ADEM), an antibody-based nomenclature is preferred. As an example, the disease associated with MOG-IgG (i.e., MOGAD) can manifest with different

clinical-MRI phenotypes, such as optic neuritis, myelitis, encephalitis, ADEM, NMOSD, or combinations thereof. On the contrary, an NMOSD phenotype can be seen in patients with AQP4-IgG, MOG-IgG, or rare double seronegative cases. In this review article, we will refer to the spectrum of clinical-MRI phenotypes associated with AQP4-IgG and MOG-IgG as AQP4-IgG+NMOSD and MOGAD, respectively.

Pathology and Pathophysiology

The MOG protein is selectively expressed in the CNS where it represents approximately 0.05% of the total myelin proteins. Its location on the outermost myelin sheath layers and oligodendrocyte cell surface makes it directly accessible to MOG-IgG, although the exact role of MOG-IgG in the pathophysiology of MOGAD remains unclear (3, 25, 26).

The neuropathological hallmarks of MOGAD include perivenous and confluent white matter demyelination, MOG-dominant myelin loss, intracortical demyelination, predominant CD4+ T-cell and granulocytic inflammation, complement deposition within active white matter lesions, partial axonal preservation, and reactive gliosis (27–29). Most of these features resemble the pathology of ADEM, which is characterized by perivenous and confluent diffuse inflammation and demyelination, and is now known to be associated with MOG-IgG in about 50% of cases (30).

These aspects are also partially overlapping with the neuropathological characteristics of MS, and in particular are reminiscent of "MS pattern II," with IgG and activated complement deposits in active demyelinating lesions (28, 31–33). However, the predominant intracortical location of cortical demyelinating lesions, together with predominant CD4+ rather than CD8+ T-cells/B cells inflammatory infiltrates help distinguish MOGAD from MS. In addition, slowly expanding demyelinated plaques, which are a common feature in MS, are usually absent in MOGAD. In MOGAD pathology, AQP4 is well-preserved and associated with hypertrophic reactive astrocytes with no evidence of complement deposition in sites of AQP4 expression and relative preservation of oligodendrocyte, which are aspects that clearly distinguishes MOGAD and AQP4-IgG+NMOSD (27, 29, 34, 35). These pathologic features of MOGAD are also observed in fulminant cases, where, in addition, superimposed ischemic damage, necrosis, astrocyte and axonal damage can be observed (36).

Of note, the same neuropathological features observed in MOGAD seropositive cases are detected in rare seronegative patients with exclusive intrathecal MOG-Abs synthesis (CSF MOG-IgG positive patients who are seronegative for MOG-IgG), where confluent demyelination with perivascular accentuation, gliosis, relative axonal sparing, and complement deposition are observed. These cases also show an almost equal presence of T- and B-cells, possibly representing a specific feature of CSF MOG-Abs synthesis (37, 38). Altogether, these neuropathological characteristics suggest that humoral mechanisms are involved in the pathogenesis of the disease, through processes of antibody/complement mediated demyelination. After binding of the antibodies to the surface of myelin, the damage might be induced by complement (activated by the IgG1 subclass of MOG-Abs) or antibody-dependent cellular cytotoxicity supported by activated innate effector cells, but the specific pathogenesis is still being elucidated (33, 39, 40).

Epidemiology

There are limited population-based data on the epidemiology of MOGAD in relation to different geographical areas and ethnicities. Two major limitations for a robust assessment of MOG-IgG seroprevalence in a population include: (1) MOG-IgG titer may drop to undetectable after disease attacks (i.e., MOGAD patients tested during remission may result negative and erroneously be excluded from a study); and (2) screening of large populations for epidemiology purposes increases the risk of false positive results (see also "*Atypical clinical-MRI phenotypes and risk of false positivity*" below). Similar problems are not encountered with AQP4-IgG+NMOSD for which antibody positivity persists over time and the risk of false positive results using cell-based assay technique is negligible (19).

MOGAD has a female-to-male ratio of approximately 1:1, which is different from the female predominance typically observed in other autoimmune/immune-mediated disorders including AQP4-IgG+NMOSD (9:1) (41), and MS (3:1) (42). The relative frequency of MOGAD among demyelinating CNS disorders seems higher in children (<18 years of age) than in adults, although any age can potentially be affected. A study by de Mol et al. found a 7% frequency of MOG-IgG positivity among 1,414 samples (1,277 patients) sent to the central reference laboratory in the Netherlands between February 2014 and December 2017 for routine diagnostics. In the same study, the estimated annual incidence was 1.6/million person-years (children, 3.1/million; adults, 1.3/million). Overall, this is similar to that of AQP4-IgG+NMOSD (0.4–7.3/million) (41, 43), and markedly lower than that of MS (7–144/million) (42, 44), accepting a wide geographical variability. While no clear ethnic preponderance has been demonstrated for MOGAD, its frequency in Caucasian populations seems two to three-fold higher compared to that of AQP4-IgG+NMOSD (45, 46), while the latter might be more represented than MOGAD among African-Americans or Afro-caribbeans (41, 43, 47). In Asia, AQP4-IgG+NMOSD is more prevalent compared to the Caucasian populations although the frequency of MOGAD might be even higher. One study assessing the frequency of autoantibodies among 726 serum samples consecutively referred to the National Hospital of Sri Lanka for suspected demyelinating CNS disorder, found the frequency of MOG-IgG (17%) was 3.5 times higher than that of AQP4-IgG (5%) (46). The increased relative frequency of antibody-mediated demyelinating CNS disorders in Asia is counterbalanced by a lower MS prevalence compared to Caucasians (48, 49).

The expected frequency of MOG-IgG positivity in clinical practice also varies based on the presenting clinical phenotype. In a population based-study of patients with new-onset ON conducted in Olmsted County (Minnesota, United States), the frequency of MOGAD and AQP4-IgG+NMOSD ON were 5 and 3%, respectively; with MS (57%) and idiopathic ON (29%) being the most common final diagnoses (50). Another

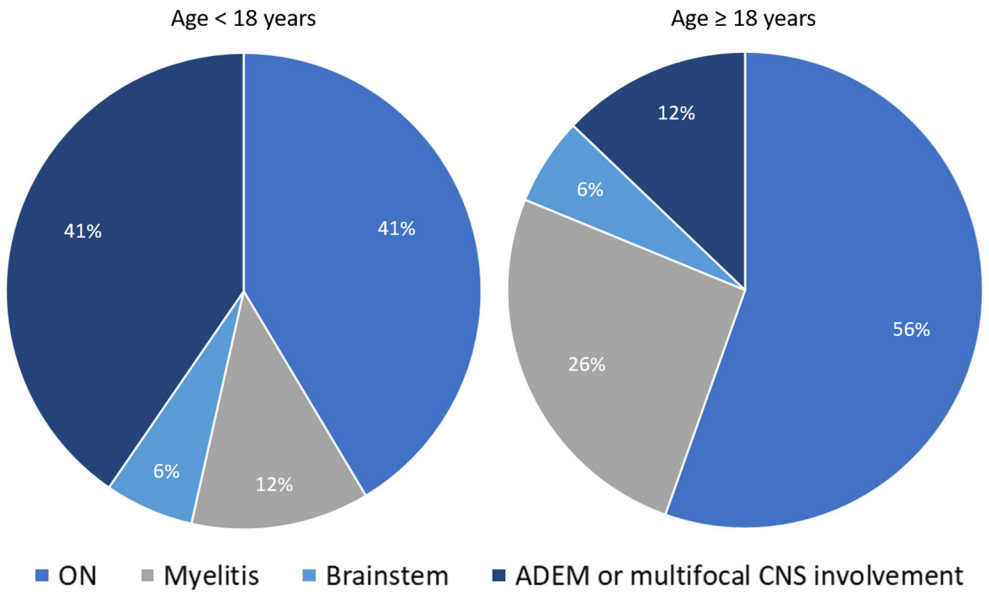

FIGURE 1 | Distribution of different disease phenotypes at MOGAD presentation stratified by age. The two pie-charts show the relative frequency of different disease phenotypes at MOGAD onset in patients below 18 years of age and older: ON (optic neuritis, unilateral or bilateral); myelitis; brainstem syndromes; ADEM (acute disseminated encephalomyelitis), or multifocal central nervous system involvement without encephalopathy. Note that the frequency of ADEM is significantly higher in younger patients. The reported frequencies are abstracted from Cobo-Calvo et al. (52).

population-based study in Olmsted County on patients with isolated idiopathic transverse myelitis (based on 2002 ITM diagnostic criteria) found AQP4-IgG-related myelitis to be twice as common as MOG-IgG-related myelitis, although both antibody-positive etiologies accounted for only 14% of total incident cases (51). This frequency increased to 50% when only cases with longitudinally extensive transverse myelitis were considered (51). Lastly, in patients with ADEM the overall frequency of MOG-IgG positivity far exceeds that of AQP4-IgG positivity, observed in approximately 50% and 5% of cases, respectively, with an important age-related variability of disease phenotypes (23, 30). In particular, ADEM or multifocal CNS involvement are four times less common in adults compared to pediatric MOGAD patients (in whom they represent the most common disease phenotype along with ON). **Figure 1** shows the relative frequency of different disease phenotypes at MOGAD presentation stratified by age (52).

CLINICAL-MRI ATTRIBUTES

The spectrum of clinical-MRI manifestations of MOGAD is more heterogeneous when compared to other CNS demyelinating disorders, and important differences exist when the disease is studied during or after acute attacks (see also "*Attack-related manifestations*" and "*Post-attack MRI characteristics, disease course, and outcomes*" below). In general, MOGAD is characterized by severe clinical attacks accompanied by large or longitudinally extensive T2-lesions on brain, spine, or orbit MRI, sometimes described as "fluffy" due to the often poorly defined margins particularly compared to lesions in approximately MS that are well circumscribed (53, 54). Acute gadolinium enhancement of at least one lesion (generally considered an indirect hallmark of active inflammation on MRI) is seen in 50–75% of patients with brain and myelitis attacks, while with MS it is more consistently evident (55). In contrast, optic nerve enhancement is seen during almost all ON attacks and can characteristically involve the optic nerve sheath or peribulbar fat, which has been termed perineural enhancement (56, 57). Notably, the initial brain or spinal cord MRI in MOGAD can be normal in up to 10% of cases despite severe acute disability (58–60). In these patients, somatosensory evoked potentials or repeat MRI within days may help confirm involvement of the affected CNS region (59). **Table 1** summarizes and compares the main clinical, laboratory, and MRI features generally observed in patients with MOGAD, AQP4-IgG+NMOSD, and MS; while examples of typical MRI abnormalities seen in MOGAD patients with ON, brain, and myelitis attacks compared to AQP4-IgG+NMOSD and MS are shown in **Figures 2–4**, respectively (61, 62).

Attack-Related Manifestations

The different clinical-MRI phenotypes seen in patients with MOGAD attacks can occur in isolation or in various combinations, with variable frequency in children and adults (30, 52, 63). For example, ADEM is more common in children while optic neuritis is the most common manifestation of MOGAD in adults (**Figure 1**).

- Optic neuritis is the most common manifestation in MOGAD and frequently occurs in isolation. It is recurrent or

TABLE 1 | Comparison of demographics, clinical, laboratory and MRI characteristics in MOGAD compared to AQP4-IgG+NMOSD, and MS.

	MOGAD	AQP4-IgG-NMOSD	MS
Demographics			
Most commonly affected age	0–40	30–50	20–40
Sex (F:M)	1:1	9:1	2–3:1
Ethnicity	No clear racial predominance	Any, African-American and Asian at higher risk	Any, mostly Caucasian
Clinical features			
Antecedent infection/immunization	Common	Rare	Rare
Disease course	Relapsing (50%) or monophasic (50%); a progressive course is rare	Generally relapsing; a progressive course is extremely rare	Relapsing (85%) or progressive from onset (15%)
Optic neuritis	+++	+++	++
Myelitis	++	+++	+++
Area postrema syndrome	Rare	++	Rare
Encephalopathy	++	Rare	Rare
Seizures	+	Rare	Rare
CSF			
Oligoclonal bands	<20% (transient)	<20% (transient)	>85% (persistent)
White cell count >50/μl	35%	13–35%	Rare
MRI			
Acute attacks			
Optic nerve	Uni-/bilateral, long lesions (>50%), mainly anterior segments, perineural enhancement	Uni-/bilateral, mainly posterior segments including chiasm	Generally unilateral, short lesions, mainly along the intraorbital tract
Spinal cord	Longitudinally extensive (60%), generally >1 lesion, conus involved, H-sign axially, enhancement in 50%	Longitudinally extensive (85%), single lesion. Central/diffuse on axial images. Elongated ring or patchy enhancement	Multiple short lesions; periphery of cord. Ring or nodular enhancement
Brain	ADEM-like, "fluffy" lesions in both white and deep gray matter; extensive involvement of cerebellar peduncles. Cortical hyperintensity may occur	Often non-specific; area postrema, peri-3rd/4th ventricle, corticospinal tracts, sometimes extensive white matter lesions	Ovoid periventricular, infratentorial, juxtacortical. Central vein sign. Ring enhancement
Initially normal MRI	Up to 10%	Rare	Rare
Post-attack MRI			
T2-lesion resolution	50–80%	Rare	Rare
New asymptomatic T2-lesions occurrence	Rare	Rare	Common
Residual T1-hypointensity	Rare	Common	Common
Persistent acute gadolinium enhancement >6 months	Rare	Rare	Rare
Treatment			
Acute	IVMP; PLEX if severe episode; IVIg possible alternative, especially for children	IVMP; low threshold to follow with PLEX	IVMP; PLEX reserved for the rare very severe attacks
Recovery	Generally good despite severe attacks	Often incomplete	Generally good
Maintenance	No proven treatments with class 1 evidence. Common empiric options include mycophenolate, rituximab, periodic IVIg, tocilizumab, oral steroids	Class 1 evidence for: eculizumab, inebilizumab, rituximab and satralizumab; other: azathioprine, mycophenolate, oral steroids, tocilizumab	Large variety of MS medications proven to be effective in class 1 studies

ADEM, acute disseminated encephalomyelitis; AQP4-IgG+NMOSD, aquaporin-4-IgG-positive neuromyelitis optica spectrum disorder; CSF, cerebrospinal fluid; IVIg, intravenous immunoglobulins; IVMP, intravenous methyl-prednisone; MOGAD, myelin oligodendrocyte glycoprotein antibody-associated disease MS, multiple sclerosis; PLEX, plasma exchange.

bilateral/simultaneous in approximately 50% of cases (57), and sometimes is steroid-dependent with a chronic relapsing inflammatory optic neuropathy (CRION)-like phenotype (64). Patients typically present with pain with extraocular movements and/or optic disc oedema (85%) on fundoscopic examination that may be severe and sometimes accompanied by hemorrhages. The visual deficit at nadir is usually severe (count fingers in most cases), but fortunately recovery is usually good leading to significantly better visual outcomes than AQP4-IgG+NMOSD (57). Up to 50% of patients

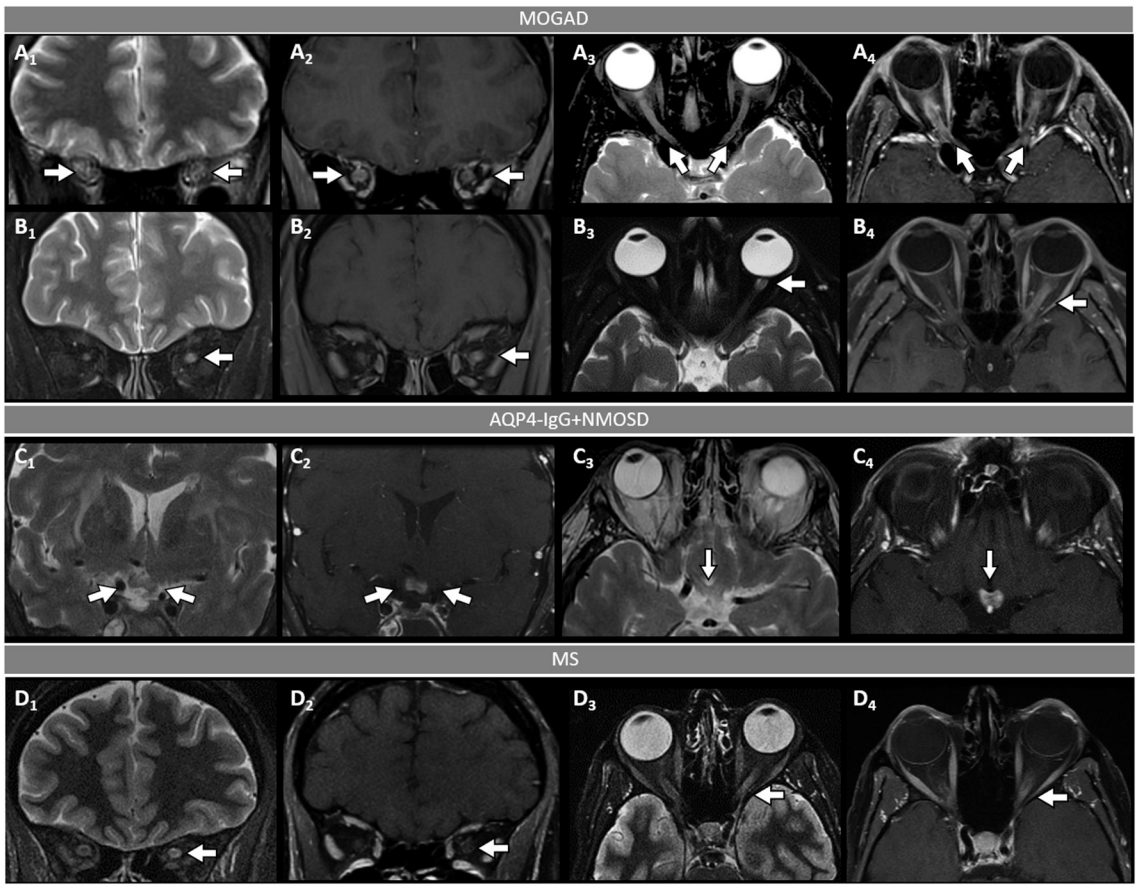

FIGURE 2 | Orbital fat-saturated MRI in optic neuritis with MOGAD, AQP4-IgG+NMOSD, and MS. [**(A,B)**: MOGAD] Bilateral optic nerve sheath thickening (A_1, coronal view, arrows) and optic nerve T2-hyperintensity (A_3, axial view, arrows) on T2-weighted images, and corresponding longitudinally extensive optic nerve and sheath enhancement on T1-post gadolinium images (A_2, coronal view, arrows, and A_4, axial view, arrows). Unilateral left optic nerve T2-hyperintensity on T2-weighted images (B_1, coronal view, arrow, and B_3, axial view, arrow) and longitudinally extensive enhancement of the left optic nerve on T1-post-gadolinium images (B_2, coronal view, arrow, and B_4, axial view, arrow). [**(C)**: AQP4-IgG+NMOSD] Bilateral optic chiasm T2-hyperintensity on T2-weighted images (C_1, coronal view, arrows, and C_3, axial view, arrow) and optic chiasm enhancement on T1-post-gadolinium images (C_2 coronal views, arrow, and C_4, axial view, arrow). [**(D)**: MS] Unilateral left optic nerve T2-hyperintensity on T2-weighted images (D_1, coronal view, arrow, and D_3, axial view, arrow), with a corresponding short segment of gadolinium-enhancement on T1-post-gadolinium images (D_2, coronal view, arrow, and D_4, axial view, arrow). MOGAD, myelin oligodendrocyte glycoprotein antibody-associated disease; AQP4-IgG+NMOSD, aquaporin-4-IgG seropositive neuromyelitis optica spectrum disorder; MS, multiple sclerosis. Definitions: Longitudinally extensive gadolinium enhancement= enhancement involving >50% the length of the optic nerve. Short-segment gadolinium enhancement= enhancement involving<50% the length of the optic nerve.

complain of a new-onset, often severe periorbital and fronto-temporal headache a few days before the visual deficit (65). On MRI, an extensive involvement of the optic nerve for most of its length on T2 or post-gadolinium T1-weighted images is characteristic (∼85% of patients), with enhancement of the optic nerve sheath (perineural enhancement) often extending to the surrounding orbital tissue observed in 50% of cases (**Figure 2**) (57). Involvement of the optic chiasm, originally considered characteristic of AQP4-IgG+NMOSD, can be seen in a minority of MOGAD patients but rarely in isolation, and generally accompanied by extensive involvement of the optic nerves (66, 67). Bilateral longitudinally extensive enhancement of the optic nerve not involving the chiasm is suggestive of MOGAD (56).

- An ADEM or ADEM-like phenotype with multifocal CNS involvement are more common in children but can occur at any age (**Figure 1**) (52, 68). Patients may present with encephalopathy, focal deficits referable to the brain, or have asymptomatic brain abnormalities in the context of other MOGAD manifestations (e.g., ON or myelitis). The severity of episodes can be such that patients require ventilatory support with cerebral attacks in up to 3% (69). Brain MRI usually shows multiple large T2-abnormalities variably affecting the supratentorial white matter, the cortex, and/or the deep gray nuclei; unilateral or bilateral thalamic and basal ganglia signal abnormalities are common (**Figure 3**) (54). Confluence of large symmetrical lesions bilaterally may sometimes occur and mimic a leukodystrophy, especially in pediatric patients (70). On

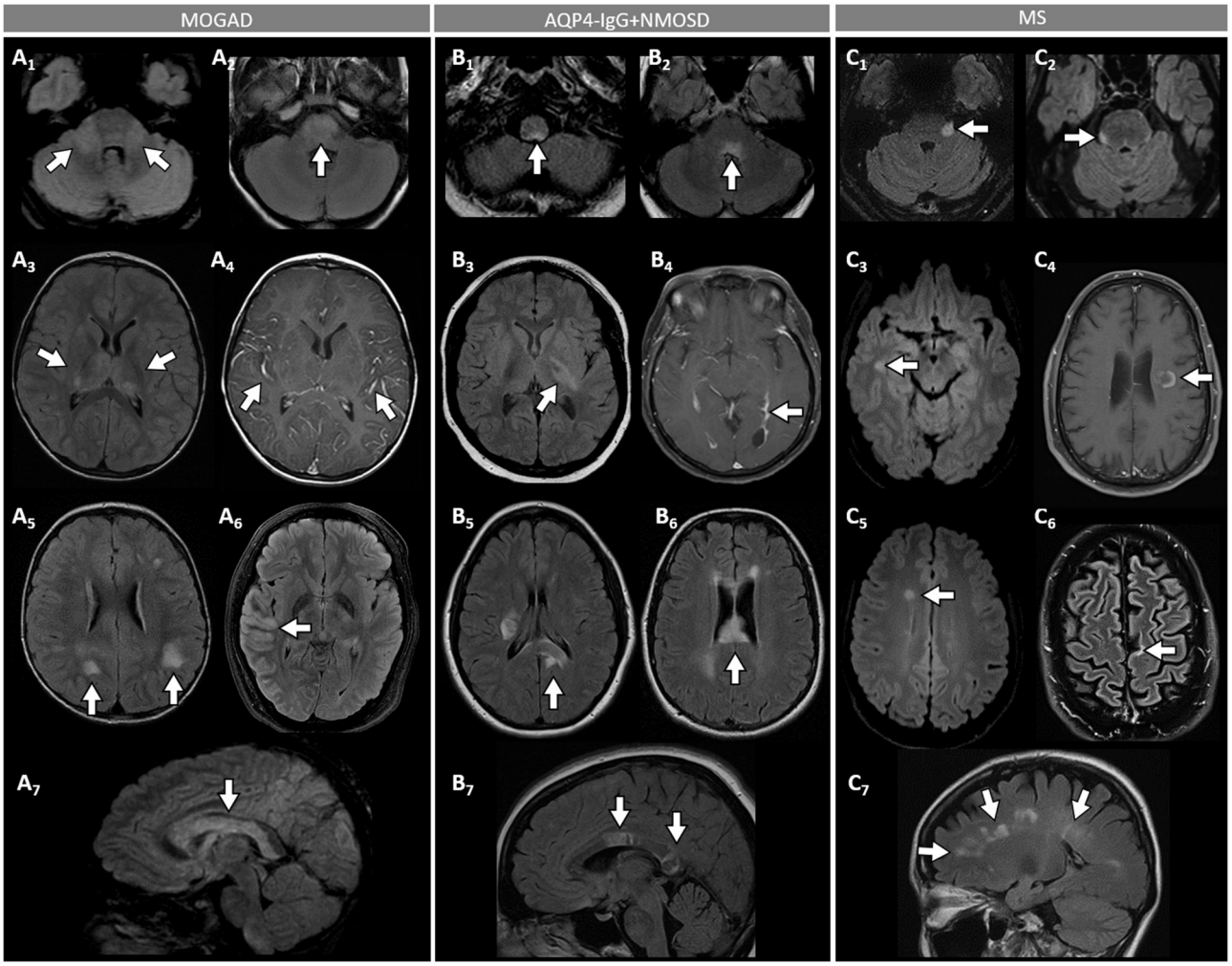

FIGURE 3 | Brain MRI features in patients with MOGAD, AQP4-IgG+NMOSD, and MS. [**(A)**: MOGAD] T2-hyperintense lesions on axial FLAIR images diffusely involving the middle cerebellar peduncles bilaterally (A_1, arrows), pons (A_2, arrow), and bilateral thalami (A_3, arrows); while extensive leptomeningeal enhancement is noted on axial T1-post gadolinium images (A_4, arrows); axial FLAIR images reveal T2-hyperintensities that are poorly marginated or "fluffy" in the hemispheric white matter (A_5, arrows), with thickening of the right temporal-parietal cortex (A_6, arrow), and diffuse involvement of the corpus callosum on sagittal view (A_7, arrow). [**(B)**: AQP4-IgG+NMOSD] Axial FLAIR images show T2-hyperintense lesions in the area postrema (B_1, arrow), dorsal pons adjacent to the 4th ventricle (B_2, arrow), and left corticospinal tract at level of the internal capsule (B_3, arrow); axial T1-post gadolinium image reveals linear ependymal enhancement in the posterior horn of the left lateral ventricle (B_4, arrow); FLAIR images reveal T2-hyperintense lesions involving the splenium of the corpus callosum (B_5, arrow, axial view) and a diffuse "marble pattern" hyperintensity of the corpus callosum (B_6, axial view, arrow, and B_7, sagittal view, arrows). [**(C)**: MS] Axial FLAIR images reveal small foci of T2-hyperintensity involving the pons at the emergence of the left trigeminal nerve (C_1, arrow), and on its ventral-right surface (C_2, arrow); axial FLAIR images reveal periventricular T2-hyperintense lesions in the inferior temporal pole (C3, arrow) and frontal horn with an ovoid appearance (C5, arrow); on axial T1-post gadolinium images an incomplete ring enhancing white matter lesion is shown (C_4, arrow); FLAIR images reveal a juxtacortical T2-hyperintense lesion (C_6, axial view, arrow) and Dawson's fingers T2-hyperintense lesions (C_7, sagittal view, arrows). MOGAD, myelin oligodendrocyte glycoprotein antibody-associated disease; AQP4-IgG+NMOSD, aquaporin-4-IgG seropositive neuromyelitis optica spectrum disorder; MS, multiple sclerosis; FLAIR, fluid attenuated inversion recovery.

the contrary, solitary brain lesions are less common (54). The corticospinal tracts are often affected at the internal capsule or midbrain peduncle level, sometimes bilaterally mimicking Behcet's disease or genetic/metabolic disorders (71). The central vein sign, a highly specific finding in MS brain lesions (72), is uncommon in MOGAD and AQP4-IgG+NMOSD (73). When present, gadolinium enhancement of lesions is generally nonspecific (e.g., the ring or open-ring enhancement typically seen in MS lesions is uncommon in MOGAD) (62).

- Brainstem involvement rarely occurs in isolation and can be asymptomatic in up to 40% of cases (**Figure 1**) (74). Diffuse midbrain, pons or medulla T2-hyperintense lesions are seen in approximately 20% of cases, which are different from the short focal T2-lesions in MS. Unilateral or bilateral large poorly demarcated middle cerebellar peduncle lesions

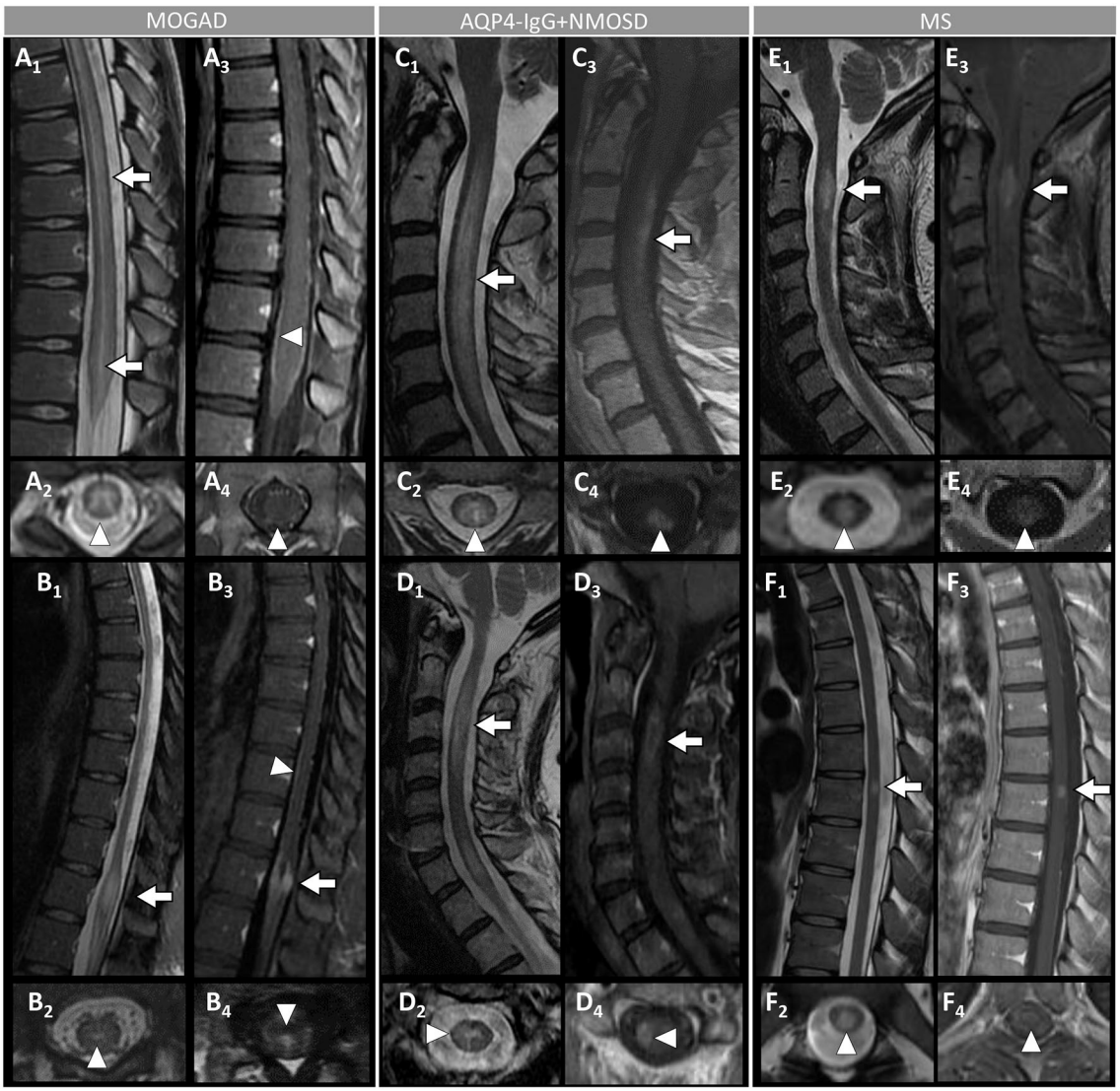

FIGURE 4 | Spinal cord MRI features in patients with MOGAD, AQP4-IgG+NMOSD, and MS. [**(A,B)**: MOGAD] A longitudinally-extensive T2-hyperintense lesion involving the conus medullaris on sagittal images (A_1, arrows), with T2-hyperintensity restricted to the gray matter forming a H-sign on the axial view (A_2), accompanied by leptomeningeal enhancement but no spinal cord parenchymal enhancement on T1-post-gadolinium images (A_3, sagittal view, arrowhead, and A_4, axial view, arrowhead); a sagittal short T2-hyperintense lesion involving the conus (B_1, arrow), centrally located on axial images (B_2, arrowhead), with corresponding gadolinium-enhancement (B_3, arrow) and leptomeningeal enhancement on T1-post-gadolinium images (B_3, sagittal view, arrowhead, and B_4, axial view, arrowhead). [**(C,D)**: AQP4-IgG+NMOSD] A sagittal longitudinally-extensive T2-hyperintense cervical cord lesion with spinal cord swelling (C_1, arrow), gray matter involvement and T2-"bright spotty sign" on axial view (C_2, arrowhead), and gadolinium-enhancement on T1-post-gadolinium images (C_3, sagittal view, arrow, and C_4, axial view, arrowhead); a sagittal longitudinally extensive T2-hyperintense cervical cord lesion (D_1, arrow), predominantly involving the right hemi-cord on axial view (D_2, arrowhead), accompanied by ring enhancement (D_3, arrow; D_4, arrowhead) on T1-post-gadolinium images. [**(E,F)**: MS] A sagittal short T2-hyperintense cervical cord lesion (E_1, arrow) involving central spinal cord (E_2, arrowhead), showing homogeneous gadolinium-enhancement on T1-post-gadolinium images (E_3, sagittal view, arrow, and E_4, axial view, arrowhead); a sagittal short T2-hyperintens thoracic spinal cord lesion (F_1, arrow), involving the gray matter and the dorsal white matter tracts (F_2, arrowhead), with homogeneous enhancement on T1-post-gadolinium images (F_3, sagittal view, arrow, and F_4, axial view, arrowhead). MOGAD, myelin oligodendrocyte glycoprotein antibody-associated disease; AQP4-IgG+NMOSD, aquaporin-4-IgG seropositive neuromyelitis optica spectrum disorder; MS, multiple sclerosis. Definitions: Longitudinally extensive spinal cord lesion= lesion involving ≥3 vertebral segments. Short spinal cord lesion= lesion involving <3 vertebral segments.

are often seen in MOGAD and help discriminate from AQP4-IgG+NMOSD or MS (**Figure 3**) (74). Rarely, patients may present clinically with intractable nausea, vomiting, or hiccups characteristic of the area postrema syndrome accompanied by T2-lesions in the region of the area postrema (a finding more typical of AQP4-IgG+NMOSD). More frequently, nausea and vomiting in MOGAD occur in the setting of ADEM and multifocal brain lesions,

rather than in association with discrete area postrema lesions (75).

- Spinal cord involvement in MOGAD is frequently severe with paraparesis requiring a gait aid, and/or bladder dysfunction requiring catheterization at myelitis nadir. On MRI, spinal cord T2-lesions are typically longitudinally extensive spanning ≥3 contiguous vertebral body segments, although shorter lesions may coexist (as opposed to patients with AQP4-IgG+NMOSD, in whom a single longitudinally extensive lesion is noted in the majority of patients). Single or multiple short lesions can occur in MOGAD but are uncommon and should always raise the suspicion for a false MOG-IgG positivity in the context of MS, particularly when the lesions are peripherally located on axial spinal cord MRI (60, 76, 77). The conus medullaris is more frequently involved in MOGAD compared to AQP4-IgG+NMOSD (53). MOGAD myelitis T2-lesions often predominantly affect the ventral part of the spinal cord on sagittal images ("ventral sagittal line"), and/or the central gray matter on axial images ("H-sign") in about a third (**Figure 4**) (53). Although highly suggestive of MOGAD, these signs are not 100% specific and can be seen in other myelopathies (*e.g.*, acute flaccid myelitis, viral myelitis, idiopathic myelitis) (60, 78). Similar to brain lesions, acute gadolinium enhancement is often nonspecific, differing from other myelitis for which characteristic enhancement patterns have been described (e.g., "elongated ring" in AQP4-IgG+NMOSD, dorsal subpial enhancement and "trident sign" in spinal cord sarcoidosis) (78–81). Leptomeningeal enhancement accompanying the myelitis can occur, and may be more common in children (60).
- Cerebral cortical encephalitis is a less common phenotype, also known as FLAMES (unilateral cortical FLAIR-hyperintense Lesions in Anti-MOG-associated Encephalitis with Seizures), characterized by encephalopathy, seizures, headache, marked CSF pleocytosis, and cortical hyperintensity on FLAIR images (82, 83). The seizures may evolve into status epilepticus and require ventilatory support (69). The cortical hyperintensity is generally unilateral but can be bilateral and accompanied by leptomeningeal enhancement in the affected brain region (**Figure 3**). The cortical hyperintensity can be the only MRI abnormality or occur in association with other brain and/or spinal cord lesions typical of MOGAD (84). Unilateral leptomeningeal enhancement has also been reported in patients with encephalitis and normal cortical signal on FLAIR images (85). The main differential of the FLAMES phenotype on MRI is with meningitis, subarachnoid hemorrhage, and CNS vasculitis (84, 86).
- Patients with MOGAD may rarely present with concomitant peripheral nervous system involvement and sometimes fulfill the criteria for combined central and peripheral demyelination (87). The peripheral neuropathy in these cases remains of unclear significance given the exclusive presence of MOG in the CNS in humans, although MOG mRNA transcripts have been detected in the peripheral nerves of rodents and primates (87, 88). Cranial nerve involvement beyond the optic nerve has also been reported (89).

Post-attack MRI Characteristics, Disease Course, and Outcomes

After the presenting attack, approximately 40%-50% of MOGAD patients maintain a monophasic course while 50–60% of cases experience disease relapses (22, 23, 63, 90). The persistence of MOG-IgG serum positivity after the first attack increases the likelihood of subsequent relapses, although relapses can also be observed in a minority of patients who become seronegative. In addition, many patients that are persistently positive can remain monophasic and therefore an exact prediction of the disease course at presentation is not possible based on MOG-IgG titers (23, 30, 91–94). An important characteristic of MOGAD MRI lesions is the tendency to resolve completely after the acute attacks, resulting in a complete normalization of the brain and/or spine MRI in 50–80% of cases (30, 55, 60). This represents a major difference from AQP4-IgG+NMOSD and MS where complete lesion resolution is extremely rare (**Figures 5**, **6**). Similarly, the occurrence of new asymptomatic T2-lesions is rare in MOGAD (approximately 3% of cases), suggesting absence of disease activity between attacks (95, 96). This also suggests that serial MRI using conventional sequences in MOGAD is of limited utility for monitoring of disease activity in both clinical trials and clinical practice. This further differentiates the disease from MS where serial MRI have high yield of capturing silent disease activity between attacks, although is less common in the era of high efficacy MS disease modifying treatments. A few studies using nonconventional MRI sequences at sites of T2-lesion resolution show values of fractional anisotropy, mean diffusivity, and magnetization transfer ratio comparable to those of unaffected controls, suggesting absence of residual structural damage (97–99). However, reduction in gray matter volumes (cortex, deep gray nuclei, and spinal central gray matter) has been reported in patients with relapsing disease or persistent T2-abnormalities, highlighting the importance of preventing relapses in MOGAD (98, 99). Diffusion tensor imaging in non-lesional white matter in MOGAD do not show structural abnormalities (99).

Available data on the long-term clinical outcomes in MOGAD patients are in keeping with the above-mentioned MRI findings, showing complete or nearly complete recovery from attacks in most cases (82, 84, 100). However, residual cognitive deficits may occur even in children, and a minority of MOGAD patients have an unfavorable functional outcome (101–104). In one series of 29 patients followed for a median of 14 (range, 9–31) years, the median EDSS at last clinical follow-up was 2, with only two cases (7%) having an EDSS of ≥6 (100, 101). Another study on 61 patients followed for a median of 15 (range, 8–55) years, reported a median EDSS at last follow-up of 1 (range, 0–7.5) with 12.5% of cases having an EDSS of ≥6. In the same study, 16% of patients remained blind in at least one eye (105). In most patients with MOGAD ON, recovery of visual acuity is generally very good, although irreversible visual loss and blindness may occur in a minority of cases

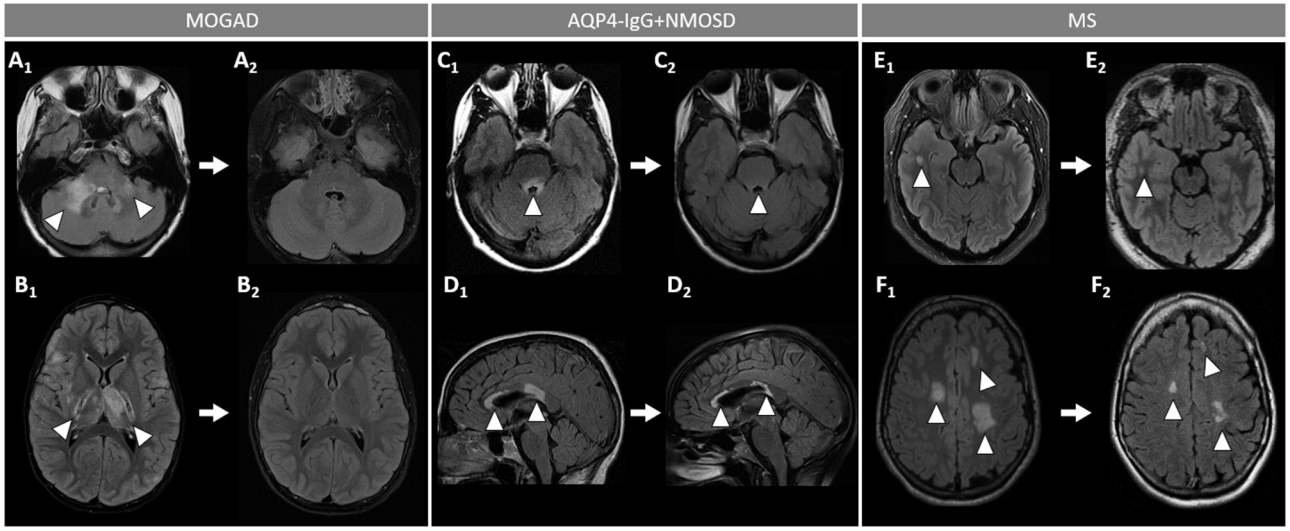

FIGURE 5 | Brain MRI lesion evolution in patients with MOGAD, AQP4-IgG+NMOSD, and MS on FLAIR images. [**(A,B)**: MOGAD] Acute bilateral large T2-hyperintensities of middle cerebellar peduncles (right > left) (A_1, arrowheads), and in the thalamus and cortico-spinal tract bilaterally (B_1, arrowheads). All T2-lesions had resolved completely by the time of follow-up MRI (A_2, B_2). [**(C D)**: AQP4-IgG+NMOSD] Acute T2-hyperintense lesion around the 4th ventricle (C_1, arrowhead), resolving to nearly undetectable at follow-up MRI (C_2, arrowhead); and lesions involving the corpus callosum (D_1, arrowheads), undergoing reduction in size without resolution on follow-up MRI (D_2, arrowheads). [**(E,F)**: MS] Acute T2-hyperintense white matter lesions (E_1, F_1, arrowheads), reduced in size but still visible on follow-up MRI (E_2, F_2, arrowheads). MOGAD, myelin oligodendrocyte glycoprotein antibody-associated disease; AQP4-IgG+NMOSD, aquaporin-4-IgG seropositive neuromyelitis optica spectrum disorder; MS, multiple sclerosis. FLAIR, fluid attenuated inversion recovery.

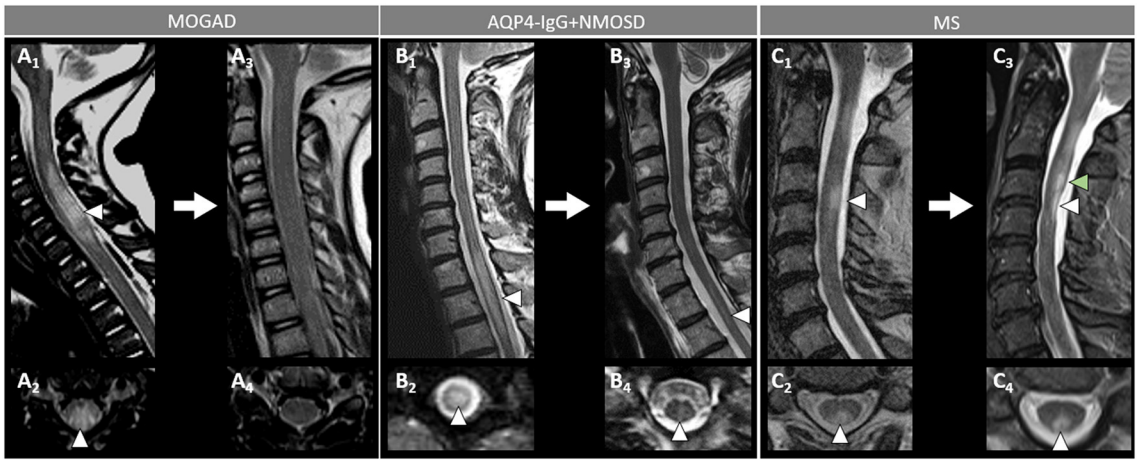

FIGURE 6 | Spinal cord MRI lesion evolution in patients with MOGAD, AQP4-IgG+NMOSD, and MS on T2-images. [**(A)**: MOGAD) A longitudinally extensive T2-hyperintense spinal cord lesion with accompanying spinal cord swelling (A_1, arrowhead) and gray matter involvement (A_2, arrowhead), with complete resolution at follow-up (A_3, sagittal, and A_4, axial view). [**(B)**: AQP4-IgG+NMOSD] A longitudinally extensive T2-hyperintense (B_1, arrowhead), centrally located thoracic spinal cord lesion (B_2, arrowhead). The T2-lesion has substantially reduced in size at follow-up (B_3, arrowhead), with only a mild residual hyperintensity still visible on sagittal view (B_3, arrowhead) and axial view (B_4, arrowhead). [**(C)**: MS] A short T2-hyperintense cervical cord lesion with accompanying spinal cord swelling (C_1, arrowhead) and involving the posterior white matter tracts (C_2, arrowhead), with residual T2-hyperintensity and local atrophy at follow-up (C_3, sagittal view, white arrowhead, and C_4, axial view, arrowhead). At follow-up, the patient also developed a new interval lesion (C_3, green arrowhead). MOGAD, myelin oligodendrocyte glycoprotein antibody-associated disease; AQP4-IgG+NMOSD, aquaporin-4-IgG seropositive neuromyelitis optica spectrum disorder; MS, multiple sclerosis.

(100, 105, 106). Despite the severity of acute MOGAD attacks being similar to AQP4-IgG+NMOSD, the complete or nearly complete recovery observed in the majority of MOGAD cases is more similar to MS. In contrast to MS, however, a secondary progressive disease course is extremely rare in both AQP4-IgG+NMOSD and MOGAD and should prompt considering alternative etiologies (see also "*Atypical clinical-MRI phenotypes and risk of false positivity*" below) (100).

Cerebrospinal Fluid Findings

Lumbar puncture during MOGAD attacks reveals CSF pleocytosis (>5 white blood cells/mm^3) in >50% of patients, with important variability based on the specific attack phenotype (isolated optic neuritis, 16%; isolated myelitis, 74%; isolated brain/brainstem attacks, 72%; multifocal CNS involvement, 50–80%) (107–109). The pleocytosis is marked (>50 white blood-cells/mm^3) in approximately 30% of patients acutely, a very uncommon finding in MS but that can be similarly seen in AQP4-IgG+NMOSD (108, 109). Also similar to AQP4-IgG+NMOSD, CSF-restricted oligoclonal bands (OCB) are rare and found in only approximately 15% of cases and may be transient. This is very different from MS where OCB are found in approximately 85% of cases and persist over time, except for some specific circumstances (110).

The cytokine profile in MOGAD during acute attacks is similar to that of AQP4-IgG+NMOSD, with predominant representation of Th17-related cytokines (e.g., IL-6, IL-8, IL-17) that may also serve as potential therapeutic targets (111). This differs from the Th1-related cytokines mainly observed in MS (112). CSF and serum levels of glial fibrillary acidic protein (GFAP), a marker of astrocytic damage, are generally lower in MOGAD compared to AQP4-IgG+NMOSD, which is in line with the different antibody cell target (oligodendrocyte vs. astrocyte) (113, 114). In all these three diseases, however, CSF levels of neurofilament light chains (a marker of neuroaxonal damage) increase during attacks, in particular at onset, and can also be detected in serum by using ultra-sensitive techniques, suggesting indirect neuronal damage in both conditions (115–118).

Coexisting Autoimmunity

Other neural autoantibodies can rarely be detected in association with MOG-IgG. In these patients, the clinical-MRI phenotype seems predominantly driven by the accompanying autoantibody, although some features may overlap with MOGAD (119). Antibodies against the N-methyl-D-Aspartate receptor (NMDA-R-IgG) are the most commonly encountered in association with MOG-IgG, and patients typically present with encephalopathy, seizures, and leptomeningeal enhancement (119, 120). A double positivity for AQP4-IgG and MOG-IgG is extremely rare (0.06% of cases tested by live cell based assay [CBA]), with MOG-IgG generally at low titer, and patients typically following a AQP4-IgG+NMOSD phenotype (45).

Systemic non-organ and organ specific autoantibodies are generally not observed in patients with MOGAD, which is different from AQP4-IgG+NMOSD where the association with systemic autoantibodies is stronger (121, 122). Nonspecific positivity for autoantibodies that are relatively common in the general population (e.g., low titer glutamic acid decarboxylase (GAD)-65-IgG) can rarely be detected due to passive transfer after administration of hemoderivates (*e.g.*, intravenous immune-globulins) (123).

Optical Coherence Tomography

Optical coherence tomography (OCT) is an essential part of the diagnostic evaluation of optic neuritis and this imaging diagnostic test can be useful for confirming an optic neuropathy as well as potentially discriminating between MOGAD, AQP4-IgG+NMOSD and MS (124–128). In the acute setting of MOGAD optic neuritis, the peripapillary retinal nerve fiber layer (pRNFL) is often significantly thickened, and indeed the median thickness was greater in MOGAD at 164 μm vs. MS at 103 μm in one study (129). Over 3–6 months after optic neuritis, there is progressive thinning of the pRNFL and the macular ganglion cell and inner plexiform layer (mGCIPL); the thinning of the mGCIPL tends to occur earlier and within a few weeks of the attack while the pRNFL thinning takes longer to develop possibly due to the slowly resolving optic nerve head edema (130). Severe thinning of these layers often occurs in MOGAD optic neuritis from recurrent attacks, while AQP4-IgG+NMOSD tends to cause significant thinning after single attacks (**Figure 7**). One of the initial large studies on OCT in optic neuritis demonstrate that thinning of the pRNFL below 75 μm was associated with worse visual outcomes (131), however some patients can have significant pRNFL and mGCIPL thinning and retain good visual function (132), especially in MOGAD patients (133–135). While optic neuritis from AQP4-IgG+NMOSD is known to cause more severe vision loss, some studies have shown similar amounts of thinning of the pRNFL and mGCIPL despite this discordant visual outcome (125, 135). The cause of the discrepancy between the detected structural abnormalities and different functional impairment in the two diseases remains unclear, and has been speculated to be related to the pathophysiology of AQP4-IgG+NMOSD being an astrocytopathy with potential for more severe retinal dysfunction (135). Another possibility is that the pRNFL and mGCIPL becomes "bottomed out" at around 50-60 μm and therefore OCT may not capture the greater extent of optic nerve damage that may occur in AQP4-IgG+NMOSD optic neuritis compare to MOGAD.

DIAGNOSIS

A correct diagnosis of MOGAD requires: (1) detection of MOG-IgG in serum and/or CSF with a reliable laboratory assay; and (2) presence of a clinical-MRI phenotype compatible with MOGAD (23, 136). Positivity for MOG-IgG in patients with atypical phenotypes should raise the suspicion for a false positive result, which may have important treatment implications (137). As MOG-IgG titer can decrease to undetectable in 30–40% of cases (and MRI abnormalities resolve completely) after acute attacks (23, 30, 55), the diagnosis of MOGAD is sometimes not possible outside of the acute setting. In similar cases, testing MOG-IgG on stored serum and/or CSF samples obtained at the time of the attack (when available) is useful.

MOG-IgG Testing

Demonstration of MOG-IgG positivity with a reliable assay is crucial for a correct MOGAD diagnosis and to reduce the risk of false positive results. Live cell-based assays (CBA) using full-length human MOG are optimal, and typically include: (1) a fluorescence activated cell sorting (FACS) assay providing a quantitative fluorescence ratio between MOG transfected vs

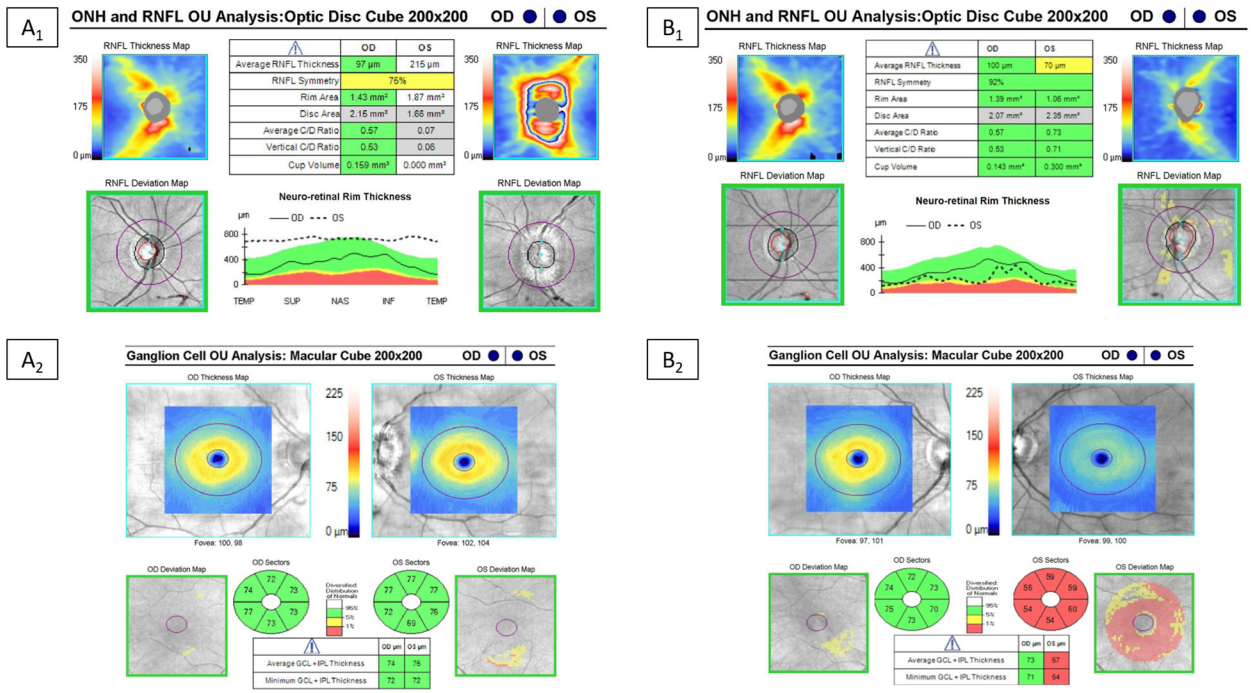

FIGURE 7 | Example of optical coherence tomography alterations in patients with MOGAD ON. Optical coherence tomography in a MOGAD patient with optic neuritis in the left eye. Left images **(A1,A2)** are the OCT images at the time of the acute optic neuritis, which shows significant peripapillary retinal nerve fiber layer thickening (RNFL) in the left eye and a normal ganglion cell-inner plexiform layer (GC-IPL) thickness. Images on the right **(B1,B2)** are the repeat OCT 1 year after the optic neuritis attack, which shows thinning of the peripapillary RNFL and macular GC-IPL in the left eye despite recovery back to a visual acuity of 20/20.

non-transfected cells; or (2) a visual assessment of transfected cells using a fluorescence microscope (138, 139). While these assays have consistently shown a very high (≈99%) specificity for typical MOGAD phenotypes in multicentre comparative studies, a correct assessment of their sensitivity is limited by the lack of a reference diagnostic gold-standard for comparison. A slightly lower specificity (≈98%) is reported for the commercially available cell-based assay using fixed transfected cells (Euroimmun), where the natural spatial conformation of the MOG protein can be altered by the fixation process hampering its recognition by MOG-IgG (138, 139). The sensitivity of fixed CBA is also lower when compared to the live CBA. However, a fixed CBA is still significantly superior to other non-CBAs, such as ELISA, which cannot reliably identify MOG-IgG.

Testing for MOG-IgG is generally recommended in serum, especially initially during the diagnostic work-up in patients suspected of having MOGAD. Concomitant serum and CSF positivity is not uncommon. Isolated CSF positivity for MOG-IgG is a rare but recognized possibility (37, 140–143). Therefore, CSF testing should be considered in patients with clinical-MRI features suggestive of MOGAD but negative results on serum testing. However, similar to the occurrence of serum MOG-IgG false positives, rare CSF false positive results have been encountered in other diseases such as MS and thus a positive result always needs to be interpreted within the context of the clinical and MRI phenotype (see also "*Atypical clinical-MRI phenotypes and risk of false positivity*" below).

Atypical Clinical-MRI Phenotypes and Risk of False Positivity

Importantly, antibody positivity is not always sufficient to guarantee a correct diagnosis of MOGAD (144). Despite the high specificity of CBAs for MOG-IgG, false positive results may occur, especially when the test is performed indiscriminately in large unselected populations (137, 145). When MOG-IgG testing is ordered, a thorough phenotypical assessment is mandatory to determine the pre-test probability. Patients with clinical-MRI phenotypes typically recognized to be associated with MOGAD (see also "*Clinical-MRI attributes*" above) are considered to have a high pre-test probability and a low risk of false positive results (137). On the other hand, patients presenting with clinical-MRI features that are generally not seen in MOGAD or that are more suggestive of an alternative diagnosis (low pre-test probability) have a significantly higher risk of false positive results. One study on 1,260 patients consecutively tested for MOG-IgG over 2 years at Mayo Clinic found a rate of false positive results of 28% (26/92 positive results) by using FACS CBA, corresponding to a positive predictive value of 72% despite a specificity of 98% (137). The positive predictive value was significantly higher after stratification for pre-test probability (high, 85%; low, 12%) and

TABLE 2 | Major red flags for false MOG-IgG positivity in patients with suspected CNS demyelinating syndromes.

Clinical features and disease course	- Progressive disease course, either from onset (primary progressive course) or after an initial period of relapsing disease activity (secondary progressive course). Consider MS, spinal cord sarcoidosis, metabolic, or genetic etiologies (e.g., B12 deficiency, adrenoleukodystrophy). - Hyperacute severe presentation (<12 h). Consider stroke/ischemic damage (e.g., spinal cord infarction, ischemic optic neuropathy). - Concomitant peripheral neuropathy. Can rarely be found in patients with MOGAD but its significance is unclear. Consider other causes of myeloneuropathy or encephalomyeloneuropathy (e.g., other autoimmune/paraneoplastic neurologic disorders, metabolic or genetic conditions).
CSF findings	- Oligoclonal bands or elevated IgG-Index. Consider MS or sarcoidosis.
MRI	- Brain abnormalities typical of MS: Ovoid periventricular lesions in the hemispheric white matter (perpendicularly oriented to the main ventricle axis), brainstem, or cerebellar hemispheres; linear or S-shaped juxtacortical lesions. Ring or open-ring enhancement. - Spinal cord abnormalities typical of MS: Multiple, short (< 3 contiguous vertebral body segments) lesions peripherally located on axial images (commonly along the dorsal-lateral columns), often accompanied by focal atrophy. Ring or open-ring enhancement. - Lesion persistence, or development of new asymptomatic brain/spine lesions over time. Consider MS. - Central vein sign. Consider MS.
Serology	- Borderline or low MOG-IgG titer. These should be interpreted based on the clinical-MRI phenotype. Consider repeat testing, preferably with a more accurate assay (e.g., live vs. fixed CBA). Consider CSF testing when the diagnostic suspicion is high.* - Coexistence of neural autoantibodies other than MOG-IgG. In these patients the contribution of MOG-IgG to the neurological syndrome is generally poor and the clinical-MRI phenotype is mostly driven by the accompanying antibody.
Other	- Other clinical-MRI findings suggestive of alternative diagnosis (e.g., blood or microhemorrhages on MRI, positive screening for infections on serum and/or CSF).

*CBA, cell-based assays; CSF, cerebrospinal fluid; MOGAD, myelin oligodendrocyte glycoprotein-IgG associated disease; MS, multiple sclerosis. *The validity of CSF-exclusive MOG-IgG positivity in conferring a diagnosis of MOGAD is still pending validation.*

antibody titer (≥1:1,000, 100%; 1:100, 82%; 1:20 or 1:40, 51%), highlighting the importance of a correct phenotypical assessment before testing. In another study assessing MOG-IgG in all neurology patients admitted to hospital regardless of diagnosis, MOG-IgG was detected in approximately 1% of patients with other neurologic diseases and generally at low titer (145).

Interestingly, false MOG-IgG positivity may occur in patients with various alternative neurologic disorders (e.g., neoplastic, genetic, metabolic, vascular) but seems rare in subjects without known neurologic diseases. This might suggest MOG-IgG production may increase in the context of epitope spreading from neurologic damage due to other etiologies, or cross-reactivity with autoantibodies directed against alternative targets. In patients with false MOG-IgG positivity, MS is generally the most common alternative diagnosis. This is due to the higher frequency of MS among demyelinating CNS disorders compared to MOGAD (approximately 40-50 times higher), and the common tendency among physicians to routinely test MS patients for MOG-IgG in order to exclude other diagnostic possibilities. Although patients with MS phenotype and MOG-IgG positivity are sometimes regarded as having "atypical manifestations of MOGAD that can mimic MS," their clinical characteristics (e.g., presence of CSF-restricted OCB, persistence of T2-abnormalities over time, development of progressive disability) and response to MS-targeted disease modifying treatments are more suggestive of a false positive (or true positive but clinically irrelevant) result (146). This is also in line with rare cases of MOG-IgG coexisting with other autoantibodies (e.g., AQP4-IgG, NMDAR-IgG) where the clinical-MRI phenotype is typically predicted by the accompanying antibody, although overlapping features may occur (see also "*Coexisting autoimmunity*" above) (45, 147). In conclusion, routine MOG-IgG testing should strongly be avoided in patients with clinical-MRI features typical of MS. Other major red flags that should prompt considering MOG-IgG positivity as a false positive are listed in **Table 2**.

Special Settings Potentially at Higher Risk of Neurological Autoimmunity

A number of emerging settings putting patients potentially at higher risk for development of neurological autoimmunity have recently been reported, and some are applicable to MOGAD:

1. Neurological immune-mediated disorders of any type (including CNS demyelination) are a well-established complication of treatment with immune-checkpoint inhibitors (148, 149). Despite a number of different neural antibodies having been described in patients treated with these drugs, the association with MOG-IgG seems particularly scarce and deserves further dedicated investigations.
2. Cases of MOGAD have recently been reported following both SARS-CoV-2 infection and vaccination (150, 151). Although prodromal episodes of infection or vaccination are known to occur in up to one third of MOGAD patients (53), the overall risk of developing MOGAD or a MOGAD relapse after SARS-CoV-2 infection/vaccination appears to be extremely low (152), given the extremely high prevalence of the infection and vaccination without an associated observed large increase in MOGAD cases (153). Thus, most experts believe the benefits of COVID-19 vaccination far outweigh this extremely rare possibility.
3. Treatment with TNF-inhibitors has been associated with an increased risk of CNS demyelination (154). Although this association seems particularly true for MS and antibody-negative CNS demyelinating disorders, onset of MOGAD in patients exposed to TNF-inhibitors seems rare (155).

4. Neurological autoimmunity has been reported in post-transplant patients and patients treated with alemtuzumab (156, 157). In both cases, imbalance between B- and T-cell reconstitution after aggressive immunosuppression may rarely result in autoimmunity, including MOGAD (156).
5. Little is known about the risk of MOGAD relapses during pregnancy and post-partum. Small case series suggest a reduction in relapse rate during pregnancy compared to the pre-pregnancy period similar to other autoimmune conditions. The frequency of relapses increases again in the post-partum period and is lower in those receiving immunosuppressive treatment (158, 159).
6. In contrast to other neural antibodies, MOG-IgG does not have a strong paraneoplastic association and therefore MOGAD patients should not be routinely screened for cancer. However, cases of paraneoplastic MOGAD have seldomly been reported with evidence of MOG expression in the neoplastic tissue (160).

MANAGEMENT

There are no randomized controlled trials available in MOGAD and existing recommendations for treatment are mostly empirical, derived from existing data on AQP4-IgG+NMOSD, and/or based on retrospective studies. Interestingly, some drugs that are typically very effective in AQP4-IgG+NMOSD, such as rituximab, seem less effective in MOGAD, further highlighting the need for dedicated randomized controlled trials.

Treatment of Disease Attacks

Similar to other demyelinating and non-demyelinating inflammatory disorders, disease flares in MOGAD are generally treated with high dose corticosteroids and most patients respond briskly to this. A retrospective study including both AQP4-IgG+NMOSD and MOGAD suggested that earlier treatment may lead to better outcomes (161). In patients with severe attacks and high disability at attack nadir, early initiation of a combination of intravenous corticosteroids and PLEX is reasonable. The efficacy of PLEX in patients with severe demyelinating attacks who fail to recover after intravenous corticosteroids was first proven in 1999 with a seminal randomized, sham-controlled, double-masked trial (162). Data on the use of IVIg for MOGAD attacks are limited so that IVIg may represent a reasonable treatment option after PLEX in very severe/refractory cases. Testing for MOG-IgG and other antibodies on serum is preferred before treatment initiation as acute immunotherapy may reduce MOG-IgG titer to undetectable (23, 30). After samples of serum have been obtained, acute treatment should promptly be initiated while waiting for antibody test results.

Commonly used dosages and types of acute treatment include:

- Corticosteroids - Intravenous methylprednisolone (IVMP) 1,000 mg once daily for 5 days is the standard treatment for a MOGAD attack. Oral prednisone 1250 mg (25 × 50 mg tablets) once daily for 5 days is an alternative and equivalent to the 1,000 mg IVMP dose but swallowing 25 tablets daily can sometimes pose a challenge for some patients. Common side effects include hyperglycaemia (more relevant in diabetic patients) and steroid-induced psychosis. A slow taper with oral prednisone over 6–8 weeks is sometimes considered to prevent early relapse but needs to be balanced by the risk of side effects and further studies are needed to evaluate this approach (25, 90).
- IVIg – Typically 0.4 g/Kg/day for 5 days. In some studies, IVIg have been associated with hyperviscosity and an increased risk of thromboembolic events, especially in patients at risk (163). Renal failure and aseptic meningitis may also rarely occur, but are generally preventable with sufficient hydration and slow infusion rate (163). Serum IgA levels should be obtained before the first administration to prevent IgA deficiency-related anaphylactic reactions (163).
- PLEX – Typically 5–7 exchanges every other day. PLEX is generally well-tolerated and safe, although often requires a central line and rare cases of severe vascular hypotension and cardiac arrythmias have been reported (164). PLEX-associated infections have also been reported rarely and may be severe (potentially related to both the central line placed and the treatment-associated immunosuppressive effect) (165).

In rare cases refractory to the conventional acute treatments, a more aggressive immunosuppression with cyclophosphamide, rituximab or tocilizumab can be considered.

Maintenance Treatment

Given the high frequency of patients with a monophasic course (40–50%), and the generally good recovery from disease attacks, the decision of initiating a long-term immunosuppressive treatment in MOGAD should carefully be discussed on a patient-by-patient basis. In general, maintenance attack-prevention immunotherapy is offered to those that have had two or more attacks, but not initiated after the first attack (including in those persistently positive for MOG-IgG) to avoid over treatment of monophasic disease. However, exceptions are considered in cases of severe residual deficits following the presenting attack, to prevent further disability (e.g., preserve vision in patients with residual monocular blindness after the initial attack).

Common long-term treatment options include:

- Maintenance IVIg – Maintenance infusions of IVIg (loading dose of 0.4 g/Kg/day for 5 consecutive days, followed by treatment every 4 weeks with a dose of 0.4 g/kg to 2 g/kg) can be considered, especially in pediatric patients or in patients with higher risk of infections, in whom avoiding long-term immunosuppression might be preferrable. In one retrospective series of 70 MOGAD patients, the relapse rate in those receiving periodic IVIg infusions (20%) was significantly lower compared to patients receiving azathioprine (59%), rituximab (61%), and mycophenolate mofetil (74%) (166). Another retrospective study on 59 adult patients with MOGAD (58 with relapsing disease) found a significant reduction in annualized relapse rate during treatment with IVIg compared to the pre-IVIg period. The results were similar in patients receiving IVIg as first-line treatment and those who

initiated IVIg after failure of other immunotherapies. The risk of relapse was lower in those treated with higher IVIG doses or more frequently (e.g., 0.4 g/kg every week, or 2 g/kg every 4 weeks). Two patients (3%) experienced worsening disability (EDSS score) during IVIG treatment (167). The high costs and restricted availability are the main elements that limit the use of this treatment in a larger scale. Subcutaneous Ig has recently been reported to be safe and effective in preventing relapses in a series of six MOGAD patients, and may represent an advantageous treatment option due to the better tolerability; subcutaneous immune globulin is self-administered and IVIg can also often be given at home when home infusion services are available (168).

- Rituximab (anti-CD20 monoclonal antibody) – Despite its high utility in preventing relapses in AQP4-IgG+NMOSD, the efficacy of rituximab in patients with MOGAD seems less (169), with up to one third of patients or more expected to experience relapses despite full B-cell depletion (170). Nonetheless, rituximab remains a potential treatment option for MOGAD, with higher efficacy reported when the drug is administered as first-line maintenance therapy (166, 170). In adults, rituximab is typically administered in one of the following two regimens: 1) 375 mg/m^2 of body surface area weekly for four consecutive weeks (induction), followed by 375 mg/m^2 weekly for 2–4 weeks at the time of reinfusion; or 2) 1 g/week repeated after 2 weeks (induction), followed by reinfusions (generally 1 g x 2 doses separated by 2 weeks, single 1 g reinfusion, or 375 mg/m^2/week for two consecutive weeks). Since the B-cells usually start to repopulate 8–12 months after rituximab administration, the timing of reinfusions can either be predetermined (generally at fixed 6 months intervals), or guided by periodic monitoring of blood CD19+ B-cells (every 6–8 weeks) until their value re-increases over 1% of total mononuclear cells (171). Since some cases with NMOSD experience relapses despite CD19+ cell-depletion, monitoring of CD27+ memory B-cells has been proposed (although not commercially available) (172). Rare cases of prolonged B-cell depletion after rituximab have been reported (173). Rituximab is generally well tolerated and safe. The most common adverse events include infusion-related reactions and increased risk of infections long-term (with a higher risk in patients with prior history of immunosuppression, lymphopenia or hypogammaglobulinemia) (174, 175). Rituximab treatment seems to increase the risk of severe COVID-19 infections and reduce the effect of COVID-19 vaccines, although an increased mortality was only observed in patients with NMOSD and comorbid conditions (176–178).
- Azathioprine (generally administered at the dose of 2–3 mg/Kg/day) and mycophenolate mofetil (generally administered at the dose of 600 mg/m^2 or 2 g daily in divided doses) can also be considered for long-term immunosuppression in MOGAD (166, 179, 180). Advantages of these medications include the oral route of administration, their availability and lower costs compared to the other treatment options. A disadvantage of these drugs is the long time (usually several months) from treatment initiation to action. During this time, oral prednisone can be continued and later tapered, but this can increase the side effect burden. These medications are associated with an increased risk of infection and long-term use can be associated with an increased risk of hematologic and skin malignancies.
- IL-6 targeting treatments (e.g., tocilizumab, satralizumab) – Small case series suggest tocilizumab might be highly effective in patients with MOGAD refractory to other immunosuppressive treatments (181, 182). The drug is generally administered at a dose of 8 mg/Kg monthly, for a maximum recommended dose of 800 mg/month in adults. A multicenter randomized controlled trial is currently underway to evaluate the efficacy of satralizumab in MOGAD.
- Future treatment directions: (1) B-cell depleting monoclonal antibodies other than rituximab have poorly been studied in MOGAD. These include other anti-CD20 agents (e.g., ocrelizumab, ofatumumab) and anti-CD19 agents (e.g., inebilizumab) (183, 184). These drugs can reasonably be considered alternatives to rituximab in MOGAD due to the similar mechanisms of action. In AQP4-IgG+NMOSD, inebilizumab was shown to be effective in reducing relapses in a randomized clinical trial (185). (2) Eculizumab (anti-C5) has been proven very effective for relapse prevention in AQP4-IgG+NMOSD in a recent randomized trial (186), but very little data exist on its potential utility in MOGAD, and complement has not been definitively proven to be integral to the pathogenesis of MOGAD. This drug might be considered as a second-line agent for very refractory cases (33, 39), but there are no published case series reporting its treatment in MOGAD to date. (3) Rozanolixizumab (anti-neonatal Fc receptor) – Blocking of the neonatal Fc receptors favors degradation of pathogenic autoantibodies. This mechanism has been proven to be effective in patients with myasthenia gravis and antibodies against the acetylcholine receptor (187), and a randomized placebo controlled clinical trial is underway in MOGAD.

Quality of Life and Supportive Treatment

Chronic pain and depression have been reported in up to 51 and 42% of patients with MOGAD, respectively, and have a significant impact on quality of life (188). Pain can be neuropathic, spasticity-associated, and/or secondary to painful tonic spasms (i.e., episodes of intense pain that accompany tonic postures of one or more limbs lasting 30–60 s). Given the strong correlation between pain and depression in these patients, effective treatment of pain can indirectly have a beneficial effect on depression, and vice versa (188, 189). In the absence of dedicated trials, common pain medications include non-opioid analgesics, antidepressants (e.g., duloxetine), and antiepileptic agents (e.g., gabapentin, pregabalin). Painful tonic spasms in particular generally respond well to low dose carbamazepine (200–300 mg/day) although are more common with AQP4-IgG+NMOSD than MOGAD (190). Initiation of immunosuppressive treatment has also been reported to improve pain (188, 189). Muscle relaxants (e.g., baclofen, benzodiazepines) and physical rehabilitation should be offered for spasticity. A more detailed description of the different

treatment options in MOGAD is beyond the scope of this review article but has been summarized elsewhere (191).

CONCLUSIONS

MOGAD is now recognized to be a distinct demyelinating CNS disorder, different from MS and AQP4-IgG+NMOSD. Awareness of the clinical-MRI characteristics of MOGAD is fundamental for prompt diagnosis and treatment. The disease is defined by MOG-IgG which is a highly specific biomarker, but caution is needed with the interpretation of low titers and atypical phenotypes, as false positives can occur. Although the prognosis is generally favorable, severe residual disability can occur in MOGAD, highlighting the importance of attack prevention in patients with relapsing disease. Major unmet needs for future studies include early identification of patients at higher risk of relapsing disease and/or permanent disability, and identification of effective acute and long-term treatments through dedicated randomized clinical trials.

AUTHOR CONTRIBUTIONS

ES and EF study concept, design, and drafted the manuscript and figures. LC and JC drafted the figures and revised the manuscript for intellectual content. SM, GF, AD, AL-C, and SP revised the manuscript for intellectual content. All authors contributed to the article and approved the submitted version.

FUNDING

EF has received funding from the NIH (R01NS113828).

REFERENCES

1. Lennon VA, Wingerchuk DM, Kryzer TJ, Pittock SJ, Lucchinetti CF, Fujihara K, et al. A serum autoantibody marker of neuromyelitis optica: distinction from multiple sclerosis. *Lancet.* (2004) 364:2106–12. doi: 10.1016/S0140-6736(04)17551-X
2. O'Connor KC, McLaughlin KA, De Jager PL, Chitnis T, Bettelli E, Xu C, et al. Self-antigen tetramers discriminate between myelin autoantibodies to native or denatured protein. *Nat Med.* (2007) 13:211–7. doi: 10.1038/nm1488
3. Reindl M, Waters P. Myelin oligodendrocyte glycoprotein antibodies in neurological disease. *Nat Rev Neurol.* (2019) 15:89–102. doi: 10.1038/s41582-018-0112-x
4. Flanagan EP. Neuromyelitis optica spectrum disorder and other non-multiple sclerosis central nervous system inflammatory diseases. *Continuum (Minneap Minn).* (2019) 25:815–44. doi: 10.1212/CON.0000000000000742
5. Jarius S, Wildemann B. The history of neuromyelitis optica. *J Neuroinflammation.* (2013) 10:8. doi: 10.1186/1742-2094-10-8
6. Lennon VA, Kryzer TJ, Pittock SJ, Verkman AS, Hinson SR. IgG marker of optic-spinal multiple sclerosis binds to the aquaporin-4 water channel. *J Exp Med.* (2005) 202:473–7. doi: 10.1084/jem.20050304
7. Pittock SJ, Weinshenker BG, Lucchinetti CF, Wingerchuk DM, Corboy JR, Lennon VA. Neuromyelitis optica brain lesions localized at sites of high aquaporin 4 expression. *Arch Neurol.* (2006) 63:964–8. doi: 10.1001/archneur.63.7.964
8. Sechi E, Addis A, Batzu L, Mariotto S, Ferrari S, Conti M, et al. Late presentation of NMOSD as rapidly progressive leukoencephalopathy with atypical clinical and radiological findings. *Mult Scler.* (2018) 24:685–8. doi: 10.1177/1352458517721661
9. Popescu BF, Lennon VA, Parisi JE, Howe CL, Weigand SD, Cabrera-Gomez JA, et al. Neuromyelitis optica unique area postrema lesions: nausea, vomiting, and pathogenic implications. *Neurology.* (2011) 76:1229–37. doi: 10.1212/WNL.0b013e318214332c
10. Wingerchuk DM, Lennon VA, Lucchinetti CF, Pittock SJ, Weinshenker BG. The spectrum of neuromyelitis optica. *Lancet Neurol.* (2007) 6:805–15. doi: 10.1016/S1474-4422(07)70216-8
11. Wingerchuk DM, Banwell B, Bennett JL, Cabre P, Carroll W, Chitnis T, et al. International consensus diagnostic criteria for neuromyelitis optica spectrum disorders. *Neurology.* (2015) 85:177–89. doi: 10.1212/WNL.0000000000001729
12. Lebar R, Lubetzki C, Vincent C, Lombrail P, Boutry JM. The M2 autoantigen of central nervous system myelin, a glycoprotein present in oligodendrocyte membrane. *Clin Exp Immunol.* (1986) 66:423–34.
13. Berger T, Rubner P, Schautzer F, Egg R, Ulmer H, Mayringer I, et al. Antimyelin antibodies as a predictor of clinically definite multiple sclerosis after a first demyelinating event. *N Engl J Med.* (2003) 349:139–45. doi: 10.1056/NEJMoa022328
14. Kuhle J, Pohl C, Mehling M, Edan G, Freedman MS, Hartung HP, et al. Lack of association between antimyelin antibodies and progression to multiple sclerosis. *N Engl J Med.* (2007) 356:371–8. doi: 10.1056/NEJMoa063602
15. Lampasona V, Franciotta D, Furlan R, Zanaboni S, Fazio R, Bonifacio E, et al. Similar low frequency of anti-MOG IgG and IgM in MS patients and healthy subjects. *Neurology.* (2004) 62:2092–4. doi: 10.1212/01.WNL.0000127615.15768.AE
16. Chan A, Decard BF, Franke C, Grummel V, Zhou D, Schottstedt V, et al. Serum antibodies to conformational and linear epitopes of myelin oligodendrocyte glycoprotein are not elevated in the preclinical phase of multiple sclerosis. *Mult Scler.* (2010) 16:1189–92. doi: 10.1177/1352458510376406
17. Ketelslegers IA, Van Pelt DE, Bryde S, Neuteboom RF, Catsman-Berrevoets CE, Hamann D, et al. Anti-MOG antibodies plead against MS diagnosis in an Acquired Demyelinating Syndromes cohort. *Mult Scler.* (2015) 21:1513–20. doi: 10.1177/1352458514566666
18. Kim SM, Woodhall MR, Kim JS, Kim SJ, Park KS, Vincent A, et al. Antibodies to MOG in adults with inflammatory demyelinating disease of the CNS. *Neurol Neuroimmunol Neuroinflamm.* (2015) 2:e163. doi: 10.1212/NXI.0000000000000163
19. Redenbaugh V, Montalvo M, Sechi E, Buciuc M, Fryer JP, McKeon A, et al. Diagnostic value of aquaporin-4-IgG live cell based assay in neuromyelitis optica spectrum disorders. *Mult Scler J Exp Transl Clin.* (2021) 7:20552173211052656. doi: 10.1177/20552173211052656
20. Sato DK, Callegaro D, Lana-Peixoto MA, Waters PJ, de Haidar Jorge FM, Takahashi T, et al. Distinction between MOG antibody-positive and AQP4 antibody-positive NMO spectrum disorders. *Neurology.* (2014) 82:474–81. doi: 10.1212/WNL.0000000000000101
21. Carnero Contentti E, Lopez PA, Pettinicchi JP, Pappolla A, Miguez J, Patrucco L, et al. What percentage of AQP4-ab-negative NMOSD patients are MOG-ab positive? A study from the Argentinean multiple sclerosis registry (RelevarEM). *Mult Scler Relat Disord.* (2021) 49:102742. doi: 10.1016/j.msard.2021.102742
22. Cobo-Calvo A, Ruiz A, Maillart E, Audoin B, Zephir H, Bourre B, et al. Clinical spectrum and prognostic value of CNS MOG autoimmunity in adults: the MOGADOR study. *Neurology.* (2018) 90:e1858–e69. doi: 10.1212/WNL.0000000000005560
23. Lopez-Chiriboga AS, Majed M, Fryer J, Dubey D, McKeon A, Flanagan EP, et al. Association of MOG-IgG serostatus with relapse after acute disseminated encephalomyelitis and proposed diagnostic criteria for MOG-IgG-associated disorders. *JAMA Neurol.* (2018) 75:1355–63. doi: 10.1001/jamaneurol.2018.1814
24. Kunchok A, Chen JJ, Saadeh RS, Wingerchuk DM, Weinshenker BG, Flanagan EP, et al. Application of 2015 seronegative neuromyelitis optica spectrum disorder diagnostic criteria for patients with myelin

oligodendrocyte glycoprotein IgG-associated disorders. *JAMA Neurol.* (2020) 77:1572–5. doi: 10.1001/jamaneurol.2020.2743
25. Marignier R, Hacohen Y, Cobo-Calvo A, Probstel AK, Aktas O, Alexopoulos H, et al. Myelin-oligodendrocyte glycoprotein antibody-associated disease. *Lancet Neurol.* (2021) 20:762–72. doi: 10.1016/S1474-4422(21)00218-0
26. Fadda G, Armangue T, Hacohen Y, Chitnis T, Banwell B. Paediatric multiple sclerosis and antibody-associated demyelination: clinical, imaging, and biological considerations for diagnosis and care. *Lancet Neurol.* (2021) 20:136–49. doi: 10.1016/S1474-4422(20)30432-4
27. Hoftberger R, Guo Y, Flanagan EP, Lopez-Chiriboga AS, Endmayr V, Hochmeister S, et al. The pathology of central nervous system inflammatory demyelinating disease accompanying myelin oligodendrocyte glycoprotein autoantibody. *Acta Neuropathol.* (2020) 139:875–92. doi: 10.1007/s00401-020-02132-y
28. Spadaro M, Gerdes LA, Mayer MC, Ertl-Wagner B, Laurent S, Krumbholz M, et al. Histopathology and clinical course of MOG-antibody-associated encephalomyelitis. *Ann Clin Transl Neurol.* (2015) 2:295–301. doi: 10.1002/acn3.164
29. Takai Y, Misu T, Kaneko K, Chihara N, Narikawa K, Tsuchida S, et al. Myelin oligodendrocyte glycoprotein antibody-associated disease: an immunopathological study. *Brain.* (2020) 143:1431–46. doi: 10.1093/brain/awaa102
30. Waters P, Fadda G, Woodhall M, O'Mahony J, Brown RA, Castro DA, et al. Serial anti-myelin oligodendrocyte glycoprotein antibody analyses and outcomes in children with demyelinating syndromes. *JAMA Neurol.* (2020) 77:82–93. doi: 10.1001/jamaneurol.2019.2940
31. Jarius S, Metz I, Konig FB, Ruprecht K, Reindl M, Paul F, et al. Screening for MOG-IgG and 27 other anti-glial and anti-neuronal autoantibodies in 'pattern II multiple sclerosis' and brain biopsy findings in a MOG-IgG-positive case. *Mult Scler.* (2016) 22:1541–9. doi: 10.1177/1352458515622986
32. Di Pauli F, Hoftberger R, Reindl M, Beer R, Rhomberg P, Schanda K, et al. Fulminant demyelinating encephalomyelitis: Insights from antibody studies and neuropathology. *Neurol Neuroimmunol Neuroinflamm.* (2015) 2:e175. doi: 10.1212/NXI.0000000000000175
33. Keller CW, Lopez JA, Wendel EM, Ramanathan S, Gross CC, Klotz L, et al. Complement Activation Is a Prominent Feature of MOGAD. *Ann Neurol.* (2021) 90:976–82. doi: 10.1002/ana.26226
34. Zhou L, Huang Y, Li H, Fan J, Zhangbao J, Yu H, et al. MOG-antibody associated demyelinating disease of the CNS: A clinical and pathological study in Chinese Han patients. *J Neuroimmunol.* (2017) 305:19–28. doi: 10.1016/j.jneuroim.2017.01.007
35. Papathanasiou A, Tanasescu R, Davis J, Rocha MF, Singhal S, O'Donoghue MF, et al. MOG-IgG-associated demyelination: focus on atypical features, brain histopathology and concomitant autoimmunity. *J Neurol.* (2020) 267:359–68. doi: 10.1007/s00415-019-09586-5
36. Hochmeister S, Gattringer T, Asslaber M, Stangl V, Haindl MT, Enzinger C, et al. A fulminant case of demyelinating encephalitis with extensive cortical involvement associated with anti-MOG antibodies. *Front Neurol.* (2020) 11:31. doi: 10.3389/fneur.2020.00031
37. Carta S, Hoftberger R, Bolzan A, Bozzetti S, Bonetti B, Scarpelli M, et al. Antibodies to MOG in CSF only: pathological findings support the diagnostic value. *Acta Neuropathol.* (2021) 141:801–4. doi: 10.1007/s00401-021-02286-3
38. Kortvelyessy P, Breu M, Pawlitzki M, Metz I, Heinze HJ, Matzke M, et al. ADEM-like presentation, anti-MOG antibodies, and MS pathology: TWO case reports. *Neurol Neuroimmunol Neuroinflamm.* (2017) 4:e335. doi: 10.1212/NXI.0000000000000335
39. McCombe JA, Flanagan EP, Chen JJ, Zekeridou A, Lucchinetti CF, Pittock SJ. Investigating the Immunopathogenic Mechanisms Underlying MOGAD. *Ann Neurol.* (2022) 91:299–300. doi: 10.1002/ana.26279
40. Pache F, Ringelstein M, Aktas O, Kleiter I, Jarius S, Siebert N, et al. C3 and C4 complement levels in AQP4-IgG-positive NMOSD and in MOGAD. *J Neuroimmunol.* (2021) 360:577699. doi: 10.1016/j.jneuroim.2021.577699
41. Flanagan EP, Cabre P, Weinshenker BG, Sauver JS, Jacobson DJ, Majed M, et al. Epidemiology of aquaporin-4 autoimmunity and neuromyelitis optica spectrum. *Ann Neurol.* (2016) 79:775–83. doi: 10.1002/ana.24617
42. Kingwell E, Marriott JJ, Jette N, Pringsheim T, Makhani N, Morrow SA, et al. Incidence and prevalence of multiple sclerosis in Europe: a systematic review. *BMC Neurol.* (2013) 13:128. doi: 10.1186/1471-2377-13-128
43. Papp V, Magyari M, Aktas O, Berger T, Broadley SA, Cabre P, et al. Worldwide incidence and prevalence of neuromyelitis optica: a systematic review. *Neurology.* (2021) 96:59–77.
44. Willumsen JS, Aarseth JH, Myhr KM, Midgard R. High incidence and prevalence of MS in More and Romsdal County, Norway, 1950-2018. *Neurol Neuroimmunol Neuroinflamm.* (2020) 7:e858. doi: 10.1212/NXI.0000000000000713
45. Kunchok A, Chen JJ, McKeon A, Mills JR, Flanagan EP, Pittock SJ. Coexistence of Myelin Oligodendrocyte Glycoprotein and Aquaporin-4 Antibodies in adult and pediatric patients. *JAMA Neurol.* (2020) 77:257–9. doi: 10.1001/jamaneurol.2019.3656
46. Senanayake B, Jitprapaikulsan J, Aravinthan M, Wijesekera JC, Ranawaka UK, Riffsy MT, et al. Seroprevalence and clinical phenotype of MOG-IgG-associated disorders in Sri Lanka. *J Neurol Neurosurg Psychiatry.* (2019) 90:1381–3. doi: 10.1136/jnnp-2018-320243
47. Papais-Alvarenga RM, Neri VC, de Araujo EAACR, da Silva EB, Alvarenga MP, Pereira A, et al. Lower frequency of antibodies to MOG in Brazilian patients with demyelinating diseases: an ethnicity influence? *Mult Scler Relat Disord.* (2018) 25:87–94. doi: 10.1016/j.msard.2018.07.026
48. Tian DC, Li Z, Yuan M, Zhang C, Gu H, Wang Y, et al. Incidence of neuromyelitis optica spectrum disorder (NMOSD) in China: a national population-based study. *Lancet Reg Health West Pac.* (2020) 2:100021. doi: 10.1016/j.lanwpc.2020.100021
49. Tian DC, Zhang C, Yuan M, Yang X, Gu H, Li Z, et al. Incidence of multiple sclerosis in China: a nationwide hospital-based study. *Lancet Reg Health West Pac.* (2020) 1:100010. doi: 10.1016/j.lanwpc.2020.100010
50. Hassan MB, Stern C, Flanagan EP, Pittock SJ, Kunchok A, Foster RC, et al. Population-based incidence of optic neuritis in the era of aquaporin-4 and myelin oligodendrocyte glycoprotein antibodies. *Am J Ophthalmol.* (2020) 220:110–4. doi: 10.1016/j.ajo.2020.07.014
51. Sechi E, Shosha E, Williams JP, Pittock SJ, Weinshenker BG, Keegan BM, et al. Aquaporin-4 and MOG autoantibody discovery in idiopathic transverse myelitis epidemiology. *Neurology.* (2019) 93:e414–e20. doi: 10.1212/WNL.0000000000007828
52. Cobo-Calvo A, Ruiz A, Rollot F, Arrambide G, Deschamps R, Maillart E, et al. Clinical features and risk of relapse in children and adults with myelin oligodendrocyte glycoprotein antibody-associated disease. *Ann Neurol.* (2021) 89:30–41. doi: 10.1002/ana.25909
53. Dubey D, Pittock SJ, Krecke KN, Morris PP, Sechi E, Zalewski NL, et al. Clinical, Radiologic, and Prognostic Features of Myelitis Associated With Myelin Oligodendrocyte Glycoprotein Autoantibody. *JAMA Neurol.* (2019) 76:301–9. doi: 10.1001/jamaneurol.2018.4053
54. Jurynczyk M, Geraldes R, Probert F, Woodhall MR, Waters P, Tackley G, et al. Distinct brain imaging characteristics of autoantibody-mediated CNS conditions and multiple sclerosis. *Brain.* (2017) 140:617–27. doi: 10.1093/brain/aww350
55. Sechi E, Krecke KN, Messina SA, Buciuc M, Pittock SJ, Chen JJ, et al. Comparison of MRI lesion evolution in different central nervous system demyelinating disorders. *Neurology.* (2021) 97:e1097–e109. doi: 10.1212/WNL.0000000000012467
56. Akaishi T, Sato DK, Nakashima I, Takeshita T, Takahashi T, Doi H, et al. MRI and retinal abnormalities in isolated optic neuritis with myelin oligodendrocyte glycoprotein and aquaporin-4 antibodies: a comparative study. *J Neurol Neurosurg Psychiatry.* (2016) 87:446–8. doi: 10.1136/jnnp-2014-310206
57. Chen JJ, Flanagan EP, Jitprapaikulsan J, Lopez-Chiriboga ASS, Fryer JP, Leavitt JA, et al. Myelin oligodendrocyte glycoprotein antibody-positive optic neuritis: clinical characteristics, radiologic clues, and outcome. *Am J Ophthalmol.* (2018) 195:8–15. doi: 10.1016/j.ajo.2018.07.020
58. Armangue T, Olive-Cirera G, Martinez-Hernandez E, Sepulveda M, Ruiz-Garcia R, Munoz-Batista M, et al. Associations of paediatric demyelinating and encephalitic syndromes with myelin oligodendrocyte glycoprotein antibodies: a multicentre observational study. *Lancet Neurol.* (2020) 19:234–46. doi: 10.1016/S1474-4422(19)30488-0
59. Sechi E, Krecke KN, Pittock SJ, Dubey D, Lopez-Chiriboga AS, Kunchok A, et al. Frequency and characteristics of MRI-negative myelitis associated with MOG autoantibodies. *Mult Scler.* (2021) 27:303–8. doi: 10.1177/1352458520907900
60. Fadda G, Alves CA, O'Mahony J, Castro DA, Yeh EA, Marrie RA, et al. Comparison of spinal cord magnetic resonance imaging features

among children with acquired demyelinating syndromes. *JAMA Netw Open.* (2021) 4:e2128871. doi: 10.1001/jamanetworkopen.2021.28871
61. Cacciaguerra L, Meani A, Mesaros S, Radaelli M, Palace J, Dujmovic-Basuroski I, et al. Brain and cord imaging features in neuromyelitis optica spectrum disorders. *Ann Neurol.* (2019) 85:371–84. doi: 10.1002/ana.25411
62. Filippi M, Preziosa P, Banwell BL, Barkhof F, Ciccarelli O, De Stefano N, et al. Assessment of lesions on magnetic resonance imaging in multiple sclerosis: practical guidelines. *Brain.* (2019) 142:1858–75. doi: 10.1093/brain/awz144
63. Jurynczyk M, Messina S, Woodhall MR, Raza N, Everett R, Roca-Fernandez A, et al. Clinical presentation and prognosis in MOG-antibody disease: a UK study. *Brain.* (2017) 140:3128–38. doi: 10.1093/brain/awx276
64. Lee HJ, Kim B, Waters P, Woodhall M, Irani S, Ahn S, et al. Chronic relapsing inflammatory optic neuropathy (CRION): a manifestation of myelin oligodendrocyte glycoprotein antibodies. *J Neuroinflammation.* (2018) 15:302. doi: 10.1186/s12974-018-1335-x
65. Asseyer S, Hamblin J, Messina S, Mariano R, Siebert N, Everett R, et al. Prodromal headache in MOG-antibody positive optic neuritis. *Mult Scler Relat Disord.* (2020) 40:101965. doi: 10.1016/j.msard.2020.101965
66. Tajfirouz D, Padungkiatsagul T, Beres S, Moss HE, Pittock S, Flanagan E, et al. Optic chiasm involvement in AQP-4 antibody-positive NMO and MOG antibody-associated disorder. *Mult Scler.* (2021) 28:149–153. 13524585211011450. doi: 10.1177/13524585211011450
67. Carnero Contentti E, Lopez PA, Criniti J, Pettinicchi JP, Cristiano E, Patrucco L, et al. Chiasmatic lesions on conventional magnetic resonance imaging during the first event of optic neuritis in patients with neuromyelitis optica spectrum disorder and myelin oligodendrocyte glycoprotein-associated disease in a Latin American cohort. *Eur J Neurol.* (2021) 29:802–809. doi: 10.1111/ene.15178
68. Mariotto S, Monaco S, Peschl P, Coledan I, Mazzi R, Hoftberger R, et al. MOG antibody seropositivity in a patient with encephalitis: beyond the classical syndrome. *BMC Neurol.* (2017) 17:190. doi: 10.1186/s12883-017-0971-6
69. Zhao-Fleming HH, Valencia Sanchez C, Sechi E, Inbarasu J, Wijdicks EF, Pittock SJ, et al. CNS demyelinating attacks requiring ventilatory support with myelin oligodendrocyte glycoprotein or aquaporin-4 antibodies. *Neurology.* (2021) 97:e1351–e8. doi: 10.1212/WNL.0000000000012599
70. Hacohen Y, Rossor T, Mankad K, Chong W, Lux A, Wassmer E, et al. 'Leukodystrophy-like' phenotype in children with myelin oligodendrocyte glycoprotein antibody-associated disease. *Dev Med Child Neurol.* (2018) 60:417–23. doi: 10.1111/dmcn.13649
71. Mastrangelo V, Asioli GM, Foschi M, Padroni M, Pavolucci L, Cenni P, et al. Bilateral extensive corticospinal tract lesions in MOG antibody-associated disease. *Neurology.* (2020) 95:648–9. doi: 10.1212/WNL.0000000000010662
72. Maggi P, Absinta M, Grammatico M, Vuolo L, Emmi G, Carlucci G, et al. Central vein sign differentiates Multiple Sclerosis from central nervous system inflammatory vasculopathies. *Ann Neurol.* (2018) 83:283–94. doi: 10.1002/ana.25146
73. Ciotti JR, Eby NS, Brier MR, Wu GF, Chahin S, Cross AH, et al. Central vein sign and other radiographic features distinguishing myelin oligodendrocyte glycoprotein antibody disease from multiple sclerosis and aquaporin-4 antibody-positive neuromyelitis optica. *Mult Scler.* (2022) 28:49–60. doi: 10.1177/13524585211007086
74. Banks SA, Morris PP, Chen JJ, Pittock SJ, Sechi E, Kunchok A, et al. Brainstem and cerebellar involvement in MOG-IgG-associated disorder versus aquaporin-4-IgG and MS. *J Neurol Neurosurg Psychiatry.* (2020). doi: 10.1136/jnnp-2020-325121 [Epub ahead of print].
75. Kunchok A, Krecke KN, Flanagan EP, Jitprapaikulsan J, Lopez-Chiriboga AS, Chen JJ, et al. Does area postrema syndrome occur in myelin oligodendrocyte glycoprotein-IgG-associated disorders (MOGAD)? *Neurology.* (2020) 94:85–8. doi: 10.1212/WNL.0000000000008786
76. Mariotto S, Ferrari S, Monaco S, Benedetti MD, Schanda K, Alberti D, et al. Clinical spectrum and IgG subclass analysis of anti-myelin oligodendrocyte glycoprotein antibody-associated syndromes: a multicenter study. *J Neurol.* (2017) 264:2420–30. doi: 10.1007/s00415-017-8635-4
77. Asnafi S, Morris PP, Sechi E, Pittock SJ, Weinshenker BG, Palace J, et al. The frequency of longitudinally extensive transverse myelitis in MS: a population-based study. *Mult Scler Relat Disord.* (2020) 37:101487. doi: 10.1016/j.msard.2019.101487
78. Sechi E, Flanagan EP. Evaluation and Management of acute myelopathy. *Semin Neurol.* (2021) 41:511–29. doi: 10.1055/s-0041-1733792
79. Mustafa R, Passe TJ, Lopez-Chiriboga AS, Weinshenker BG, Krecke KN, Zalewski NL, et al. Utility of MRI Enhancement Pattern in Myelopathies With Longitudinally Extensive T2 Lesions. *Neurol Clin Pract.* (2021) 11:e601–e11. doi: 10.1212/CPJ.0000000000001036
80. Zalewski NL, Krecke KN, Weinshenker BG, Aksamit AJ, Conway BL, McKeon A, et al. Central canal enhancement and the trident sign in spinal cord sarcoidosis. *Neurology.* (2016) 87:743–4. doi: 10.1212/WNL.0000000000002992
81. Zalewski NL, Morris PP, Weinshenker BG, Lucchinetti CF, Guo Y, Pittock SJ, et al. Ring-enhancing spinal cord lesions in neuromyelitis optica spectrum disorders. *J Neurol Neurosurg Psychiatry.* (2017) 88:218–25. doi: 10.1136/jnnp-2016-314738
82. Budhram A, Mirian A, Le C, Hosseini-Moghaddam SM, Sharma M, Nicolle MW. Unilateral cortical FLAIR-hyperintense Lesions in Anti-MOG-associated Encephalitis with Seizures (FLAMES): characterization of a distinct clinico-radiographic syndrome. *J Neurol.* (2019) 266:2481–7. doi: 10.1007/s00415-019-09440-8
83. Ogawa R, Nakashima I, Takahashi T, Kaneko K, Akaishi T, Takai Y, et al. MOG antibody-positive, benign, unilateral, cerebral cortical encephalitis with epilepsy. *Neurol Neuroimmunol Neuroinflamm.* (2017) 4:e322. doi: 10.1212/NXI.0000000000000322
84. Wang W, Yin J, Fan Z, Kang J, Wei J, Yin X, et al. Case report: four cases of cortical/brainstem encephalitis positive for myelin oligodendrocyte glycoprotein immunoglobulin G. *Front Neurol.* (2021) 12:775181. doi: 10.3389/fneur.2021.775181
85. Budhram A, Kunchok AC, Flanagan EP. Unilateral Leptomeningeal Enhancement in Myelin Oligodendrocyte Glycoprotein Immunoglobulin G-Associated Disease. *JAMA Neurol.* (2020) 77:648–9. doi: 10.1001/jamaneurol.2020.0001
86. Boulouis G, de Boysson H, Zuber M, Guillevin L, Meary E, Costalat V, et al. Primary angiitis of the central nervous system: magnetic resonance imaging spectrum of parenchymal, meningeal, and vascular lesions at baseline. *Stroke.* (2017) 48:1248–55. doi: 10.1161/STROKEAHA.116.016194
87. Rinaldi S, Davies A, Fehmi J, Beadnall HN, Wang J, Hardy TA, et al. Overlapping central and peripheral nervous system syndromes in MOG antibody-associated disorders. *Neurol Neuroimmunol Neuroinflamm.* (2021) 8:e924. doi: 10.1212/NXI.0000000000000924
88. Vazquez Do Campo R, Stephens A, Marin Collazo IV, Rubin DI, MOG. antibodies in combined central and peripheral demyelination syndromes. *Neurol Neuroimmunol Neuroinflamm.* (2018) 5:e503. doi: 10.1212/NXI.0000000000000503
89. Cobo-Calvo A, Ayrignac X, Kerschen P, Horellou P, Cotton F, Labauge P, et al. Cranial nerve involvement in patients with MOG antibody-associated disease. *Neurol Neuroimmunol Neuroinflamm.* (2019) 6:e543. doi: 10.1212/NXI.0000000000000543
90. Ramanathan S, Mohammad S, Tantsis E, Nguyen TK, Merheb V, Fung VSC, et al. Clinical course, therapeutic responses and outcomes in relapsing MOG antibody-associated demyelination. *J Neurol Neurosurg Psychiatry.* (2018) 89:127–37. doi: 10.1136/jnnp-2017-316880
91. Oliveira LM, Apostolos-Pereira SL, Pitombeira MS, Bruel Torretta PH, Callegaro D, Sato DK. Persistent MOG-IgG positivity is a predictor of recurrence in MOG-IgG-associated optic neuritis, encephalitis and myelitis. *Mult Scler.* (2019) 25:1907–14. doi: 10.1177/1352458518811597
92. Epstein SE, Levin S, Onomichi K, Langston C, Yeshokumar A, Fabian M, et al. Myelin oligodendrocyte glycoprotein (MOG) antibody-mediated disease: the difficulty of predicting relapses. *Mult Scler Relat Disord.* (2021) 56:103229. doi: 10.1016/j.msard.2021.103229
93. Cobo-Calvo A, Sepulveda M. d'Indy H, Armangue T, Ruiz A, Maillart E, et al. Usefulness of MOG-antibody titres at first episode to predict the future clinical course in adults. *J Neurol.* (2019) 266:806–15. doi: 10.1007/s00415-018-9160-9
94. Hennes EM, Baumann M, Schanda K, Anlar B, Bajer-Kornek B, Blaschek A, et al. Prognostic relevance of MOG antibodies in children with an acquired demyelinating syndrome. *Neurology.* (2017) 89:900–8. doi: 10.1212/WNL.0000000000004312

95. Camera V, Holm-Mercer L, Ali AAH, Messina S, Horvat T, Kuker W, et al. Frequency of New Silent MRI Lesions in Myelin Oligodendrocyte Glycoprotein Antibody Disease and Aquaporin-4 Antibody Neuromyelitis Optica Spectrum Disorder. *JAMA Netw Open.* (2021) 4:e2137833. doi: 10.1001/jamanetworkopen.2021.37833
96. Fadda G, Banwell B, Waters P, Marrie RA, Yeh EA, O'Mahony J, et al. Silent new brain MRI lesions in children with MOG-antibody associated disease. *Ann Neurol.* (2021) 89:408–13. doi: 10.1002/ana.25957
97. Mariano R, Messina S, Roca-Fernandez A, Leite MI, Kong Y, Palace JA. Quantitative spinal cord MRI in MOG-antibody disease, neuromyelitis optica and multiple sclerosis. *Brain.* (2021) 144:198–212. doi: 10.1093/brain/awaa347
98. Duan Y, Zhuo Z, Li H, Tian DC Li Y, Yang L, et al. Brain structural alterations in MOG antibody diseases: a comparative study with AQP4 seropositive NMOSD and MS. *J Neurol Neurosurg Psychiatry.* (2021) 92:709–16. doi: 10.1136/jnnp-2020-324826
99. Messina S, Mariano R, Roca-Fernandez A, Cavey A, Jurynczyk M, Leite MI, et al. Contrasting the brain imaging features of MOG-antibody disease, with AQP4-antibody NMOSD and multiple sclerosis. *Mult Scler.* (2021) 28:217–227. 13524585211018987. doi: 10.1101/2020.09.22.20198978
100. Lopez-Chiriboga AS, Sechi E, Buciuc M, Chen JJ, Pittock SJ, Lucchinetti CF, et al. Long-term outcomes in patients with myelin oligodendrocyte glycoprotein immunoglobulin G-associated disorder. *JAMA Neurol.* (2020) 77:1575–7. doi: 10.1001/jamaneurol.2020.3115
101. Buciuc M, Sechi E, Flanagan EP, Lopez-Chiriboga AS. Unfavorable outcome in highly relapsing MOGAD encephalitis. *J Neurol Sci.* (2020) 418:117088. doi: 10.1016/j.jns.2020.117088
102. Wang J, Qiu Z, Li D, Yang X, Ding Y, Gao L, et al. Clinical and imaging features of patients with encephalitic symptoms and myelin oligodendrocyte glycoprotein antibodies. *Front Immunol.* (2021) 12:722404. doi: 10.3389/fimmu.2021.722404
103. Mariano R, Messina S, Kumar K, Kuker W, Leite MI, Palace J. Comparison of Clinical outcomes of transverse myelitis among adults with myelin oligodendrocyte glycoprotein antibody vs aquaporin-4 antibody disease. *JAMA Netw Open.* (2019) 2:e1912732. doi: 10.1001/jamanetworkopen.2019.12732
104. Fabri TL, O'Mahony J, Fadda G, Gur RE, Gur RC, Yeh EA, et al. Cognitive function in pediatric-onset relapsing myelin oligodendrocyte glycoprotein antibody-associated disease (MOGAD). *Mult Scler Relat Disord.* (2022) 59:103689. doi: 10.1016/j.msard.2022.103689
105. Deschamps R, Pique J, Ayrignac X, Collongues N, Audoin B, Zephir H, et al. The long-term outcome of MOGAD: An observational national cohort study of 61 patients. *Eur J Neurol.* (2021) 28:1659–64. doi: 10.1111/ene.14746
106. Akaishi T, Himori N, Takeshita T, Misu T, Takahashi T, Takai Y, et al. Five-year visual outcomes after optic neuritis in anti-MOG antibody-associated disease. *Mult Scler Relat Disord.* (2021) 56:103222. doi: 10.1016/j.msard.2021.103222
107. Jarius S, Lechner C, Wendel EM, Baumann M, Breu M, Schimmel M, et al. Cerebrospinal fluid findings in patients with myelin oligodendrocyte glycoprotein (MOG) antibodies. Part 2: Results from 108 lumbar punctures in 80 pediatric patients. *J Neuroinflammation.* (2020) 17:262. doi: 10.1186/s12974-020-01825-1
108. Jarius S, Pellkofer H, Siebert N, Korporal-Kuhnke M, Hummert MW, Ringelstein M, et al. Cerebrospinal fluid findings in patients with myelin oligodendrocyte glycoprotein (MOG) antibodies. Part 1: results from 163 lumbar punctures in 100 adult patients. *J Neuroinflammation.* (2020) 17:261. doi: 10.1186/s12974-020-01824-2
109. Sechi E, Buciuc M, Flanagan EP, Pittock SJ, Banks SA, Lopez-Chiriboga AS, et al. Variability of cerebrospinal fluid findings by attack phenotype in myelin oligodendrocyte glycoprotein-IgG-associated disorder. *Mult Scler Relat Disord.* (2021) 47:102638. doi: 10.1016/j.msard.2020.102638
110. Dobson R, Ramagopalan S, Davis A, Giovannoni G. Cerebrospinal fluid oligoclonal bands in multiple sclerosis and clinically isolated syndromes: a meta-analysis of prevalence, prognosis and effect of latitude. *J Neurol Neurosurg Psychiatry.* (2013) 84:909–14. doi: 10.1136/jnnp-2012-304695
111. Kaneko K, Sato DK, Nakashima I, Ogawa R, Akaishi T, Takai Y, et al. CSF cytokine profile in MOG-IgG+ neurological disease is similar to AQP4-IgG+ NMOSD but distinct from MS: a cross-sectional study and potential therapeutic implications. *J Neurol Neurosurg Psychiatry.* (2018) 89:927–36. doi: 10.1136/jnnp-2018-317969
112. Hofer LS, Mariotto S, Wurth S, Ferrari S, Mancinelli CR, Delogu R, et al. Distinct serum and cerebrospinal fluid cytokine and chemokine profiles in autoantibody-associated demyelinating diseases. *Mult Scler J Exp Transl Clin.* (2019) 5:2055217319848463. doi: 10.1177/2055217319848463
113. Chang X, Huang W, Wang L, ZhangBao J, Zhou L, Lu C, et al. Serum neurofilament light and GFAP are associated with disease severity in inflammatory disorders with aquaporin-4 or myelin oligodendrocyte glycoprotein antibodies. *Front Immunol.* (2021) 12:647618. doi: 10.3389/fimmu.2021.647618
114. Kim H, Lee EJ, Kim S, Choi LK, Kim K, Kim HW, et al. Serum biomarkers in myelin oligodendrocyte glycoprotein antibody-associated disease. *Neurol Neuroimmunol Neuroinflamm.* (2020) 7:e708. doi: 10.1212/NXI.0000000000000708
115. Mariotto S, Ferrari S, Gastaldi M, Franciotta D, Sechi E, Capra R, et al. Neurofilament light chain serum levels reflect disease severity in MOG-Ab associated disorders. *J Neurol Neurosurg Psychiatry.* (2019) 90:1293–6. doi: 10.1136/jnnp-2018-320287
116. Mariotto S, Sechi E, Ferrari S. Serum neurofilament light chain studies in neurological disorders, hints for interpretation. *J Neurol Sci.* (2020) 416:116986. doi: 10.1016/j.jns.2020.116986
117. Sechi E, Mariotto S, McKeon A, Krecke KN, Pittock SJ, Ferrari S, et al. Serum neurofilament to magnetic resonance imaging lesion area ratio differentiates spinal cord infarction from acute myelitis. *Stroke.* (2021) 52:645–54. doi: 10.1161/STROKEAHA.120.031482
118. Mariotto S, Gastaldi M, Grazian L, Mancinelli C, Capra R, Marignier R, et al. NfL levels predominantly increase at disease onset in MOG-Abs-associated disorders. *Mult Scler Relat Disord.* (2021) 50:102833. doi: 10.1016/j.msard.2021.102833
119. Kunchok A, Flanagan EP, Krecke KN, Chen JJ, Caceres JA, Dominick J, et al. MOG-IgG1 and co-existence of neuronal autoantibodies. *Mult Scler.* (2021) 27:1175–86. doi: 10.1177/1352458520951046
120. Titulaer MJ, Hoftberger R, Iizuka T, Leypoldt F, McCracken L, Cellucci T, et al. Overlapping demyelinating syndromes and anti-N-methyl-D-aspartate receptor encephalitis. *Ann Neurol.* (2014) 75:411–28. doi: 10.1002/ana.24117
121. Kunchok A, Flanagan EP, Snyder M, Saadeh R, Chen JJ, Weinshenker BG, et al. Coexisting systemic and organ-specific autoimmunity in MOG-IgG1-associated disorders versus AQP4-IgG+ NMOSD. *Mult Scler.* (2021) 27:630–5. doi: 10.1177/1352458520933884
122. Guerra H, Pittock SJ, Moder KG, Fryer JP, Gadoth A, Flanagan EP. Frequency of aquaporin-4 immunoglobulin g in longitudinally extensive transverse myelitis with antiphospholipid antibodies. *Mayo Clin Proc.* (2018) 93:1299–304. doi: 10.1016/j.mayocp.2018.02.006
123. Dimitriadou MM, Alexopoulos H, Akrivou S, Gola E, Dalakas MC. Anti-Neuronal antibodies within the IVIg preparations: importance in clinical practice. *Neurotherapeutics.* (2020) 17:235–42. doi: 10.1007/s13311-019-00796-3
124. Bartels F, Lu A, Oertel FC, Finke C, Paul F, Chien C. Clinical and neuroimaging findings in MOGAD-MRI and OCT. *Clin Exp Immunol.* (2021) 206:266–81. doi: 10.1111/cei.13641
125. Filippatou AG, Mukharesh L, Saidha S, Calabresi PA, Sotirchos ES. AQP4-IgG and MOG-IgG related optic neuritis-prevalence, optical coherence tomography findings, and visual outcomes: a systematic review and meta-analysis. *Front Neurol.* (2020) 11:540156. doi: 10.3389/fneur.2020.540156
126. Deschamps R, Philibert M, Lamirel C, Lambert J, Vasseur V, Gueguen A, et al. Visual field loss and structure-function relationships in optic neuritis associated with myelin oligodendrocyte glycoprotein antibody. *Mult Scler.* (2021) 27:855–63. doi: 10.1177/1352458520937281
127. Oertel FC, Outteryck O, Knier B, Zimmermann H, Borisow N, Bellmann-Strobl J, et al. Optical coherence tomography in myelin-oligodendrocyte-glycoprotein antibody-seropositive patients: a longitudinal study. *J Neuroinflammation.* (2019) 16:154. doi: 10.1186/s12974-019-1521-5
128. Martinez-Lapiscina EH, Sepulveda M, Torres-Torres R, Alba-Arbalat S, Llufriu S, Blanco Y, et al. Usefulness of optical coherence tomography to distinguish optic neuritis associated with AQP4 or MOG in neuromyelitis

optica spectrum disorders. *Ther Adv Neurol Disord.* (2016) 9:436–40. doi: 10.1177/1756285616655264
129. Chen JJ, Sotirchos ES, Henderson AD, Vasileiou ES, Flanagan EP, Bhatti MT, et al. OCT retinal nerve fiber layer thickness differentiates acute optic neuritis from MOG antibody-associated disease and Multiple Sclerosis: RNFL thickening in acute optic neuritis from MOGAD vs MS. *Mult Scler Relat Disord.* (2022) 58:103525. doi: 10.1016/j.msard.2022.103525
130. Costello F, Pan YI, Yeh EA, Hodge W, Burton JM, Kardon R. The temporal evolution of structural and functional measures after acute optic neuritis. *J Neurol Neurosurg Psychiatry.* (2015) 86:1369–73. doi: 10.1136/jnnp-2014-309704
131. Costello F, Coupland S, Hodge W, Lorello GR, Koroluk J, Pan YI, et al. Quantifying axonal loss after optic neuritis with optical coherence tomography. *Ann Neurol.* (2006) 59:963–9. doi: 10.1002/ana.20851
132. Brandt AU, Specovius S, Oberwahrenbrock T, Zimmermann HG, Paul F, Costello F. Frequent retinal ganglion cell damage after acute optic neuritis. *Mult Scler Relat Disord.* (2018) 22:141–7. doi: 10.1016/j.msard.2018.04.006
133. Roca-Fernandez A, Camera V, Loncarevic-Whitaker G, Messina S, Mariano R, Vincent A, et al. The use of OCT in good visual acuity MOGAD and AQP4-NMOSD patients; with and without optic neuritis. *Mult Scler J Exp Transl Clin.* (2021) 7:20552173211066446. doi: 10.1177/20552173211066446
134. Narayan RN, McCreary M, Conger D, Wang C, Greenberg BM. Unique characteristics of optical coherence tomography (OCT) results and visual acuity testing in myelin oligodendrocyte glycoprotein (MOG) antibody positive pediatric patients. *Mult Scler Relat Disord.* (2019) 28:86–90. doi: 10.1016/j.msard.2018.11.026
135. Sotirchos ES, Filippatou A, Fitzgerald KC, Salama S, Pardo S, Wang J, et al. Aquaporin-4 IgG seropositivity is associated with worse visual outcomes after optic neuritis than MOG-IgG seropositivity and multiple sclerosis, independent of macular ganglion cell layer thinning. *Mult Scler.* (2020) 26:1360–71. doi: 10.1177/1352458519864928
136. Jarius S, Paul F, Aktas O, Asgari N, Dale RC, de Seze J, et al. MOG encephalomyelitis: international recommendations on diagnosis and antibody testing. *J Neuroinflammation.* (2018) 15:134. doi: 10.1186/s12974-018-1144-2
137. Sechi E, Buciuc M, Pittock SJ, Chen JJ, Fryer JP, Jenkins SM, et al. Positive predictive value of myelin oligodendrocyte glycoprotein autoantibody testing. *JAMA Neurol.* (2021) 78:741–6. doi: 10.1001/jamaneurol.2021.0912
138. Reindl M, Schanda K, Woodhall M, Tea F, Ramanathan S, Sagen J, et al. International multicenter examination of MOG antibody assays. *Neurol Neuroimmunol Neuroinflamm.* (2020) 7:e674. doi: 10.1212/NXI.0000000000000674
139. Waters PJ, Komorowski L, Woodhall M, Lederer S, Majed M, Fryer J, et al. A multicenter comparison of MOG-IgG cell-based assays. *Neurology.* (2019) 92:e1250–e5. doi: 10.1212/WNL.0000000000007096
140. Mariotto S, Gajofatto A, Batzu L, Delogu R, Sechi G, Leoni S, et al. Relevance of antibodies to myelin oligodendrocyte glycoprotein in CSF of seronegative cases. *Neurology.* (2019) 93:e1867–e72. doi: 10.1212/WNL.0000000000008479
141. Akaishi T, Takahashi T, Misu T, Kaneko K, Takai Y, Nishiyama S, et al. Difference in the source of anti-AQP4-IgG and Anti-MOG-IgG antibodies in CSF in patients with neuromyelitis optica spectrum disorder. *Neurology.* (2021) 97:e1–e12. doi: 10.1212/WNL.0000000000012175
142. Kwon YN, Kim B, Kim JS, Mo H, Choi K, Oh SI, et al. Myelin oligodendrocyte glycoprotein-immunoglobulin G in the CSF: clinical implication of testing and association with disability. *Neurol Neuroimmunol Neuroinflamm.* (2022) 28:e1095. doi: 10.1212/NXI.0000000000001095
143. Pace S, Orrell M, Woodhall M, Palace J, Leite MI, Irani SR, et al. Frequency of MOG-IgG in cerebrospinal fluid versus serum. *J Neurol Neurosurg Psychiatry.* (2021) 93:334–335. doi: 10.1136/jnnp-2021-326779
144. Sechi E, Flanagan EP. Antibody-Mediated Autoimmune Diseases of the CNS: challenges and approaches to diagnosis and management. *Front Neurol.* (2021) 12:673339. doi: 10.3389/fneur.2021.673339
145. Held F, Kalluri SR, Berthele A, Klein AK, Reindl M, Hemmer B. Frequency of myelin oligodendrocyte glycoprotein antibodies in a large cohort of neurological patients. *Mult Scler J Exp Transl Clin.* (2021) 7:20552173211022767. doi: 10.1177/20552173211022767
146. Zara P, Floris V, Flanagan EP, Lopez-Chiriboga AS, Weinshenker BG, Solla P, et al. Clinical significance of myelin oligodendrocyte glycoprotein autoantibodies in patients with typical MS lesions on MRI. *Mult Scler J Exp Transl Clin.* (2021) 7:20552173211048761. doi: 10.1177/20552173211048761
147. Nan D, Zhang Y, Han J, Jin T. Clinical features and management of coexisting anti-N-methyl-D-aspartate receptor encephalitis and myelin oligodendrocyte glycoprotein antibody-associated encephalomyelitis: a case report and review of the literature. *Neurol Sci.* (2021) 42:847–55. doi: 10.1007/s10072-020-04942-0
148. Sechi E, Markovic SN, McKeon A, Dubey D, Liewluck T, Lennon VA, et al. Neurologic autoimmunity and immune checkpoint inhibitors: autoantibody profiles and outcomes. *Neurology.* (2020) 95:e2442–e52. doi: 10.1212/WNL.0000000000010632
149. Sechi E, Zekeridou A. Neurologic Complications of Immune Checkpoint Inhibitors in Thoracic Malignancies. *J Thorac Oncol.* (2021) 16:381–94. doi: 10.1016/j.jtho.2020.11.005
150. Dams L, Kraemer M, Becker J. MOG-antibody-associated longitudinal extensive myelitis after ChAdOx1 nCoV-19 vaccination. *Mult Scler.* (2021) 13524585211057512. doi: 10.1177/13524585211057512 [Epub ahead of print].
151. Dias da Costa M, Leal Rato M, Cruz D, Valadas A, Antunes AP, Albuquerque L. Longitudinally extensive transverse myelitis with anti-myelin oligodendrocyte glycoprotein antibodies following SARS-CoV-2 infection. *J Neuroimmunol.* (2021) 361:577739. doi: 10.1016/j.jneuroim.2021.577739
152. Dinoto AS E, Ferrari S, Gajofatto A, Orlandi R, Solla P, Maccabeo A, et al. Risk of disease relapse following COVID-19 vaccination in patients with AQP4-IgG-positive NMOSD and MOGAD. *Mult Scler Relat Disord.* (2022). doi: 10.1016/j.msard.2021.103424 [Epub ahead of print].
153. Lotan I, Romanow G, Levy M. Patient-reported safety and tolerability of the COVID-19 vaccines in persons with rare neuroimmunological diseases. *Mult Scler Relat Disord.* (2021) 55:103189. doi: 10.1016/j.msard.2021.103189
154. Kunchok A, Aksamit AJ Jr, Davis JM 3rd, Kantarci OH, Keegan BM, Pittock SJ, et al. Association Between Tumor Necrosis Factor Inhibitor Exposure and Inflammatory Central Nervous System Events. *JAMA Neurol.* (2020) 77:937–46. doi: 10.1001/jamaneurol.2020.1162
155. Redenbaugh V, Flanagan EP, Floris V, Zara P, Bhatti MT, Sanchez F, et al. Exposure to TNF inhibitors is rare at MOGAD presentation. *J Neurol Sci.* (2022) 432:120044. doi: 10.1016/j.jns.2021.120044
156. Cohen DA, Lopez-Chiriboga AS, Pittock SJ, Gadoth A, Zekeridou A, Boilson BA, et al. Posttransplant autoimmune encephalitis. *Neurol Neuroimmunol Neuroinflamm.* (2018) 5:e497. doi: 10.1212/NXI.0000000000000497
157. Maniscalco GT, Mariotto S, Hoftberger R, Capra R, Servillo G, Manzo V, et al. GABAA receptor autoimmunity after alemtuzumab treatment for multiple sclerosis. *Neurology.* (2020) 95:399–401. doi: 10.1212/WNL.0000000000010310
158. Collongues N, Alves Do Rego C, Bourre B, Biotti D, Marignier R, da Silva AM, et al. Pregnancy in Patients With AQP4-Ab, MOG-Ab, or Double-Negative Neuromyelitis Optica Disorder. *Neurology.* (2021) 96:e2006–e15. doi: 10.1212/WNL.0000000000011744
159. Jarius S, Ruprecht K, Kleiter I, Borisow N, Asgari N, Pitarokoili K, et al. MOG-IgG in NMO and related disorders: a multicenter study of 50 patients. Part 2: Epidemiology, clinical presentation, radiological and laboratory features, treatment responses, and long-term outcome. *J Neuroinflammation.* (2016) 13:280. doi: 10.1186/s12974-016-0718-0
160. Wildemann B, Jarius S, Franz J, Ruprecht K, Reindl M, Stadelmann C. MOG-expressing teratoma followed by MOG-IgG-positive optic neuritis. *Acta Neuropathol.* (2021) 141:127–31. doi: 10.1007/s00401-020-02236-5
161. Stiebel-Kalish H, Hellmann MA, Mimouni M, Paul F, Bialer O, Bach M, et al. Does time equal vision in the acute treatment of a cohort of AQP4 and MOG optic neuritis? *Neurol Neuroimmunol Neuroinflamm.* (2019) 6:e572. doi: 10.1212/NXI.0000000000000572
162. Weinshenker BG, O'Brien PC, Petterson TM, Noseworthy JH, Lucchinetti CF, Dodick DW, et al. A randomized trial of plasma exchange in acute central nervous system inflammatory demyelinating disease. *Ann Neurol.* (1999) 46:878–86. doi: 10.1002/1531-8249(199912)46:6<878::aid-ana10>3.0.co;2-q
163. Katz U, Achiron A, Sherer Y, Shoenfeld Y. Safety of intravenous immunoglobulin (IVIG) therapy. *Autoimmun Rev.* (2007) 6:257–9. doi: 10.1016/j.autrev.2006.08.011

164. Rodnitzky RL, Goeken JA. Complications of plasma exchange in neurological patients. *Arch Neurol.* (1982) 39:350–4. doi: 10.1001/archneur.1982.00510180028007
165. Singer DR, Roberts B, Cohen J. Infective complications of plasma exchange: a prospective study. *Arthritis Rheum.* (1987) 30:443–7. doi: 10.1002/art.1780300413
166. Chen JJ, Flanagan EP, Bhatti MT, Jitprapaikulsan J, Dubey D, Lopez Chiriboga ASS, et al. Steroid-sparing maintenance immunotherapy for MOG-IgG associated disorder. *Neurology.* (2020) 95:e111–e20. doi: 10.1212/WNL.0000000000009758
167. Chen JJ, Huda S, Hacohen Y, Levy M, Lotan I, Wilf-Yarkoni A, et al. Association of maintenance intravenous immunoglobulin with prevention of relapse in adult myelin oligodendrocyte glycoprotein antibody-associated disease. *JAMA Neurol.* (2022). doi: 10.1001/jamaneurol.2022.0489
168. Sotirchos ES, Vasileiou ES, Salky R, Huda S, Mariotto S, Chen JJ, et al. Treatment of myelin oligodendrocyte glycoprotein antibody associated disease with subcutaneous immune globulin. *Mult Scler Relat Disord.* (2021) 57:103462. doi: 10.1016/j.msard.2021.103462
169. Durozard P, Rico A, Boutiere C, Maarouf A, Lacroix R, Cointe S, et al. Comparison of the Response to Rituximab between Myelin Oligodendrocyte Glycoprotein and Aquaporin-4 Antibody Diseases. *Ann Neurol.* (2020) 87:256–66. doi: 10.1002/ana.25648
170. Whittam DH, Cobo-Calvo A, Lopez-Chiriboga AS, Pardo S, Gornall M, Cicconi S, et al. Treatment of MOG-IgG-associated disorder with rituximab: an international study of 121 patients. *Mult Scler Relat Disord.* (2020) 44:102251. doi: 10.1016/j.msard.2020.102251
171. Ellwardt E, Ellwardt L, Bittner S, Zipp F. Monitoring B-cell repopulation after depletion therapy in neurologic patients. *Neurol Neuroimmunol Neuroinflamm.* (2018) 5:e463. doi: 10.1212/NXI.0000000000000463
172. Lebrun C, Cohen M, Rosenthal-Allieri MA, Bresch S, Benzaken S, Marignier R, et al. Only follow-up of memory b cells helps monitor rituximab administration to patients with neuromyelitis optica spectrum disorders. *Neurol Ther.* (2018) 7:373–83. doi: 10.1007/s40120-018-0101-4
173. Sechi E, Zarbo R, Biancu MA, Chessa P, Idda ML, Orru V, et al. Prolonged B-cell depletion after rituximab in AQP4-IgG-positive neuromyelitis optica spectrum disorder. *J Neuroimmunol.* (2021) 358:577666. doi: 10.1016/j.jneuroim.2021.577666
174. Damato V, Evoli A, Iorio R. Efficacy and safety of rituximab therapy in neuromyelitis optica spectrum disorders: a systematic review and meta-analysis. *JAMA Neurol.* (2016) 73:1342–8. doi: 10.1001/jamaneurol.2016.1637
175. Vollmer BL, Wallach AI, Corboy JR, Dubovskaya K, Alvarez E, Kister I. Serious safety events in rituximab-treated multiple sclerosis and related disorders. *Ann Clin Transl Neurol.* (2020) 7:1477–87. doi: 10.1002/acn3.51136
176. Januel E, De Seze J, Vermersch P, Maillart E, Bourre B, Pique J, et al. Post-vaccine COVID-19 in patients with multiple sclerosis or neuromyelitis optica. *Mult Scler.* (2021) 13524585211049737. doi: 10.1177/13524585211049737 [Epub ahead of print].
177. Newsome SD, Cross AH, Fox RJ, Halper J, Kanellis P, Bebo B, et al. COVID-19 in Patients With Neuromyelitis Optica Spectrum Disorders and Myelin Oligodendrocyte Glycoprotein Antibody Disease in North America: From the COViMS Registry. *Neurol Neuroimmunol Neuroinflamm.* (2021) 8:e1057. doi: 10.1212/NXI.0000000000001057
178. Bock H, Juretzek T, Handreka R, Ruhnau J, Lobel M, Reuner K, et al. Humoral and cellular immune responses to SARS CoV-2 vaccination in People with Multiple Sclerosis and NMOSD patients receiving immunomodulatory treatments. *Mult Scler Relat Disord.* (2022) 59:103554. doi: 10.1016/j.msard.2022.103554
179. Wang M, Zeng P, Du C, Xue H, Cui Z, Zhang H, et al. Differential efficacy of mycophenolate mofetil in adults with relapsing myelin oligodendrocyte glycoprotein antibody-associated disorders. *Mult Scler Relat Disord.* (2021) 53:103035. doi: 10.1016/j.msard.2021.103035
180. Whittam DH, Karthikeayan V, Gibbons E, Kneen R, Chandratre S, Ciccarelli O, et al. Treatment of MOG antibody associated disorders: results of an international survey. *J Neurol.* (2020) 267:3565–77. doi: 10.1007/s00415-020-10026-y
181. Elsbernd PM, Hoffman WR, Carter JL, Wingerchuk DM. Interleukin-6 inhibition with tocilizumab for relapsing MOG-IgG associated disorder (MOGAD): a case-series and review. *Mult Scler Relat Disord.* (2021) 48:102696. doi: 10.1016/j.msard.2020.102696
182. Ringelstein M, Ayzenberg I, Lindenblatt G, Fischer K, Gahlen A, Novi G, et al. Interleukin-6 Receptor Blockade in Treatment-Refractory MOG-IgG-Associated Disease and Neuromyelitis Optica Spectrum Disorders. *Neurol Neuroimmunol Neuroinflamm.* (2022) 9:e1100. doi: 10.1212/NXI.0000000000001100
183. Graf J, Mares J, Barnett M, Aktas O, Albrecht P, Zamvil SS, et al. Targeting B cells to modify MS, NMOSD, and MOGAD: part 2. *Neurol Neuroimmunol Neuroinflamm.* (2021) 8:e919. doi: 10.1212/NXI.0000000000000919
184. Graf J, Mares J, Barnett M, Aktas O, Albrecht P, Zamvil SS, et al. Targeting B Cells to Modify MS, NMOSD, and MOGAD: Part 1. *Neurol Neuroimmunol Neuroinflamm.* (2021) 8:e918. doi: 10.1212/NXI.0000000000000918
185. Cree BAC, Bennett JL, Kim HJ, Weinshenker BG, Pittock SJ, Wingerchuk DM, et al. Inebilizumab for the treatment of neuromyelitis optica spectrum disorder (N-MOmentum): a double-blind, randomised placebo-controlled phase 2/3 trial. *Lancet.* (2019) 394:1352–63. doi: 10.1016/S0140-6736(19)31817-3
186. Pittock SJ, Berthele A, Fujihara K, Kim HJ, Levy M, Palace J, et al. Eculizumab in Aquaporin-4-Positive Neuromyelitis Optica Spectrum Disorder. *N Engl J Med.* (2019) 381:614–25. doi: 10.1056/NEJMoa1900866
187. Howard JF Jr, Bril V, Vu T, Karam C, Peric S, Margania T, et al. Safety, efficacy, and tolerability of efgartigimod in patients with generalised myasthenia gravis (ADAPT): a multicentre, randomised, placebo-controlled, phase 3 trial. *Lancet Neurol.* (2021) 20:526–36. doi: 10.1016/S1474-4422(21)00159-9
188. Asseyer S, Henke E, Trebst C, Hummert MW, Wildemann B, Jarius S, et al. Pain, depression, and quality of life in adults with MOG-antibody-associated disease. *Eur J Neurol.* (2021) 28:1645–58. doi: 10.1111/ene.14729
189. Ayzenberg I, Richter D, Henke E, Asseyer S, Paul F, Trebst C, et al. Pain, Depression, and quality of life in neuromyelitis optica spectrum disorder: a cross-sectional study of 166 AQP4 antibody-seropositive patients. *Neurol Neuroimmunol Neuroinflamm.* (2021) 8:e985. doi: 10.1212/NXI.0000000000000985
190. Kim SM, Go MJ, Sung JJ, Park KS, Lee KW. Painful tonic spasm in neuromyelitis optica: incidence, diagnostic utility, and clinical characteristics. *Arch Neurol.* (2012) 69:1026–31. doi: 10.1001/archneurol.2012.112
191. Lai QL, Zhang YX, Cai MT, Zheng Y, Qiao S, Fang GL, et al. Efficacy and safety of immunosuppressive therapy in myelin oligodendrocyte glycoprotein antibody-associated disease: a systematic review and meta-analysis. *Ther Adv Neurol Disord.* (2021) 14:17562864211054157. doi: 10.1177/17562864211054157

Conflict of Interest: The authors declare that the research was conducted in the absence of any commercial or financial relationships that could be construed as a potential conflict of interest.

frontiers | Frontiers in Immunology

ORIGINAL RESEARCH
published: 11 July 2022
doi: 10.3389/fimmu.2022.853891

Plasma Complement 3 and Complement 4 Are Promising Biomarkers for Distinguishing NMOSD From MOGAD and Are Associated With the Blood-Brain-Barrier Disruption in NMOSD

Liuyu Lin, Yuqing Wu, Hailun Hang, Jie Lu and Yuanliang Ding*

Department of Neurology, The Affiliated Brain Hospital of Nanjing Medical University, Nanjing, China

OPEN ACCESS

Edited by:
Yu Cai,
University of Nebraska Medical Center, United States

Reviewed by:
Shuhei Nishiyama,
Massachusetts General Hospital and Harvard Medical School, United States
Petra Nytrová,
Charles University, Czechia

****Correspondence:***
Jie Lu
lujieyx@126.com

Specialty section:
This article was submitted to Multiple Sclerosis and Neuroimmunology, a section of the journal Frontiers in Immunology

Received: *13 January 2022*
Accepted: *14 June 2022*
Published: *11 July 2022*

Citation:
Lin L, Wu Y, Hang H, Lu J and Ding Y (2022) Plasma Complement 3 and Complement 4 Are Promising Biomarkers for Distinguishing NMOSD From MOGAD and Are Associated With the Blood-Brain-Barrier Disruption in NMOSD. Front. Immunol. 13:853891. doi: 10.3389/fimmu.2022.853891

Background and Objective: Neuromyelitis optica spectrum disorders (NMOSD) and myelin oligodendrocyte glycoprotein antibody (MOG-IgG) associated disease (MOGAD) are autoimmune inflammatory demyelinating diseases of the central nervous system (CNS). As the clinical features of NMOSD are similar to MOGAD, diagnostic confusion exists between the two diseases. To better discriminate NMOSD from MOGAD, we investigated whether the plasma levels of complement 3 (C3) and complement 4 (C4) are different in NMOSD and MOGAD during the acute attacks of the diseases. We sought to determine whether C3 or C4 has an influence on the features of NMOSD.

Methods: In this observational study, data from 73 aquaporin-4 antibodies (AQP4-IgG) positive NMOSD patients and 22 MOG-IgG positive MOGAD patients were collected retrospectively. Demographics, clinical characteristics, plasma parameters, and cerebrospinal fluid (CSF) findings will be analyzed for comparability between the two groups. Immunoglobulin-G (IgG) and albumin were measured in both plasma and CSF. Plasma levels of C3 and C4 were measured and compared between the NMOSD, MOGAD, and 42 healthy controls (HC). The correlations between plasma C3, C4, and NMOSD clinical parameters were analyzed.

Results: The ages of onset were later in the AQP4-IgG positive NMOSD group and females predominated, which differed from the MOGAD group, whose ages were younger and with a slight male preponderance. The AQP4-IgG positive NMOSD patients presented with the clinical symptoms of optic neuritis (ON) and transverse myelitis (TM), whereas encephalitis symptoms were more prevalent in MOGAD patients. CSF analysis shows that slight but not significantly higher white cell count (WCC) and protein were observed in the MOGAD group than in the AQP4-IgG positive NMOSD group. The plasma levels of IgG in MOGAD patients are significantly lower (p = 0.027) than in NMOSD patients. On the contrary, the plasma levels of albumin in MOGAD were higher than in NMOSD, which reached statistical significance (p = 0.039). Both the plasma C3 and C4

levels in the NMOSD group were significantly lower than in MOGAD and HC. The receiver operating characteristic (ROC) curve of the prediction model comprises C3 and C4 to distinguish NMOSD from MOGAD [area under the curve (AUC): 0.731, 0.645], which are considered to have discriminatory values. The results of Spearman's analysis revealed that there was a significant positive correlation between the plasma C3 and the CSF WCC ($r = 0.383$, $p = 0.040$). There was an inverse correlation between plasma C4 and plasma IgG ($r = -0.244$, $p = 0.038$). Plasma C3 or C4 was significantly positively correlated with CSF albumin and Q-Alb, which is considered a measure of blood-brain barrier (BBB) disruption.

Conclusion: During the acute phase of NMOSD and MOGAD, plasma C3 and C4 may become potential biomarkers for distinguishing the two diseases and reflecting the NMOSD BBB damage.

Keywords: neuromyelitis optica spectrum disorder, myelin oligodendrocyte glycoprotein antibody-associated disease, complement 3, complement 4, blood brain barrier (BBB)

INTRODUCTION

Neuromyelitis optica spectrum disorders (NMOSD) is a chronic, severe autoimmune demyelinating disease of the central nervous system (CNS) with the optic nerves and the spinal cord as primary target sites (1). It is widely accepted that the antibody target for the water channel aquaporin-4 (AQP4) is a pathogenic marker of NMOSD (2). Most NMOSD patients are seropositive for AQP4-IgG, but a proportion of NMOSD patients remain negative despite the use of cell-based assays (CBA) (3). In AQP4-IgG seronegative NMOSD, approximately 15% to 40% of myelin oligodendrocyte glycoprotein (MOG) antibody (MOG-IgG) are present (4, 5). Using the CBA, MOG-IgG was also detected in acute disseminated encephalomyelitis (ADEM), encephalitis, optic neuritis (ON), and myelitis (6). MOG-IgG-associated disease (MOGAD) has distinct biomarker, clinical, and radiologic characteristics from NMOSD and is considered an independent disease entity.

Experimental studies have indicated that AQP4-IgG primarily attacks the water channels of the astrocytes through antibody-dependent cellular cytotoxicity (ADCC) (7) or complement-dependent cytotoxicity (CDC) (8). The pathogenic mechanisms mediated by the complement system in MOGAD may be distinct from those in NMOSD (9). Since the activation of complement 3 (C3) and complement 4 (C4) is the core of complement activation, C3 and C4 are indispensable parts of the complement system (10). Previous studies showed plasma C3 (11) or C4 (12) was significantly lower in NMOSD compared to multiple sclerosis. Less focus has been given to the different levels of C3 and C4 in NMOSD and MOGAD. Therefore, the plasma C3, C4 levels be measured in AQP4-IgG positive NMOSD, MOGAD, and healthy controls (HC) to determine if there are any differences in AQP4-IgG or MOG-IgG associated effector mechanisms. Our study is also required to determine if there is a relationship between C3, C4 and the clinical features of NMOSD.

METHODS

Samples

Patients who were recruited from the affiliated brain hospital of Nanjing Medical University between 2012 and 2021 were included in this single-center, retrospective observational study. Inclusion criteria are as follows: (1) be 18 years of age or older, and (2) be seropositive for AQP4-IgG by commercial CBA, meeting the IPND 2015 criteria (1) for NMOSD; (3) be seropositive for MOG-IgG by commercial CBA, meeting the Jarius et al. criteria (6) for MOGAD; (4) all plasma and CSF samples from NMOSD and MOGAD patients were in the acute phase of the diseases. Exclusion criteria included being seronegative for AQP4-IgG and MOG-IgG, having a disease that affects the complement system, or having missing clinical data. Overall, 73 NMOSD patients and 22 MOGAD patients met the inclusion and exclusion criteria and were included in this study. 42 healthy controls (HC) were recruited from the surrounding community. HC subjects suffering from neurological diseases or systemic autoimmune diseases were excluded. All patients will be included in this study after signing the informed consent. The study has been approved by the ethics committee of the affiliated Brain hospital of Nanjing Medical University.

Data Collection

The demographic information, including gender and age at onset, was recorded. The clinical and paraclinical data were obtained from the electronic medical records and were compared between NMOSD and MOGAD. The clinical data included annual relapse rate (ARR), Expanded Disability Status Scale (EDSS) at sampling, clinical symptoms, and pharmacological treatments. The paraclinical data recorded included IgG and albumin, both in plasma and cerebrospinal fluid (CSF). CSF white cell count (WCC), CSF protein, oligoclonal bands, IgG index, CSF/plasma albumin ratio (Q-Alb), and plasma levels of C3, C4 were collected and analyzed. To

assess the integrity of the blood-brain barrier (BBB), the CSF/plasma albumin ratio (Q-Alb) was considered a marker, and the detection of the IgG index was used as an indicator of intrathecal IgG synthesis. Plasma and CSF samples were obtained from NMOSD and MOGAD patients at the time of disease attack before hormone shock therapy. AQP4-IgG and MOG-IgG are also important indicators to distinguish NMOSD from MOGAD. The serum AQP4-IgG and MOG-IgG were all detected by a standardized immunohistochemical cell-based assay (CBA) according to the manufacturer's protocol (Euroimmun, Germany) and using HEK293 cells transfected with human AQP4-M23 as a target to determine the titers. Plasma C3 and C4 were measured by immunofluorescence. Plasma levels of C3 (reference range, 0.90-1.80g/L) and C4 (reference range, 0.10-0.40g/L) were compared between AQP4-IgG-positive NMOSD, MOGAD and HC.

Statistical Analysis

All statistical analysis was conducted in SPSS (version 24) software (SPSS, Inc., Chicago, IL) and GraphPad Prism 8.0 (GraphPad Software, Inc., San Diego, CA, USA). Differences in quantitative variables were compared using the student *t* statistics or Mann-Whitney U tests, while the chi-square test or Fisher exact probability methods were used for comparison of categorical variables. Comparisons between three groups (NMOSD group, MOGAD group, and HC group) were performed using a nonparametric Kruskal-Wallis-test. The corrected p-values using the Bonferroni correction to avoid type I errors. Receiver operating characteristics (ROC) curve analysis was used to calculate the area under the ROC curve (AUC) and evaluate the diagnostic value of plasma C3, C4 for differentiating NMOSD from MOGAD. To analyze correlations between plasma C3, C4 and EDSS, CSF findings, albumin and IgG both in plasma and CSF, IgG index, and Q-Alb, the Spearman correlation was used for correlation analysis.

RESULTS

Demographic, Clinical Features, and Treatment in NMOSD and MOGAD Patients

A total of 73 AQP4-IgG positive NMOSD patients, 22 MOG-IgG positive MOGAD patients, and 42 HC were enrolled in this study. **Table 1** shows the demographics, ARR, disease duration, EDSS, clinical symptoms, and immunotherapy treatment in the NMOSD and MOGAD groups. Compared to MOGAD, there was a female gender dominance of the NMOSD participants (94.52% *vs.* 27.27%, $p<0.001$). The age at onset in the NMOSD group is slightly older than in the MOGAD group, but has not reached statistical significance. There was no significant difference between NMOSD and MOGAD regarding ARR, disease duration, or EDSS. Significance differences were found between the NMOSD and MOGAD groups regarding the clinical symptoms. In summary, more optic neuritis (ON, 57.53% *vs.* 31.82%, $p = 0.034$) and transverse myelitis (TM, 75.34% *vs.* 31.82%, $p<0.001$) present in NMOSD, whereas acute disseminated encephalomyelitis (ADEM, 9.59% *vs.* 50%, $p<0.001$) is common in MOGAD.

In our cohort, receipt of a high dose of corticoid medication was found in all NMOSD and MOGAD patients during the acute-phase. Most NMOSD (97.21%) and MOGAD (95.45%) patients were started at a dose of 500mg/d and gradually tapered, maintaining a dose of 10–15 mg/d in remission. In addition to hormone shock therapy, some patients use intravenous immunoglobulins (IVIg) or plasma exchange (PLEX) during the acute phase to improve treatment efficacy. The use of immunosuppressants is associated with slow disease progression and reduced relapse in patients who have had CNS demyelinating diseases. In our cohort, mycophenolate mofetil was the most frequently used immunosuppressant in remission, followed by azathioprine. Eleven NMOSD patients and one MOGAD patient had been treated with Azathioprine. The other two NMOSD patients in the study had received cyclosporine and rituximab, respectively.

Comparison of Plasma and CSF Detailed Findings Among Patients With NMOSD and MOGAD Patients

Detection of antibodies by the CBA test allowed quantitative measurements of AQP4-IgG and MOG-IgG serum titers. The median AQP4-IgG titer is 1:100 (IQR: 1:32-1:320) and the MOG-IgG titer is 1:10 (IQR: 1:10-1:100). **Table 2** summarizes the plasma and CSF detailed findings of the study subjects. In this study, the CSF samples of 29 NMOSD and 17 MOGAD patients were collected and analyzed before any treatment. In terms of findings of WCC, protein, and oligoclonal bands positivity in CSF, no significant difference could be detected between patients with NMOSD and MOGAD groups. Significant differences were also not observed in the comparison of the two groups regarding Q-Alb and the IgG index. Regardless of the slight differences in levels of IgG and albumin in CSF, there were significant differences in plasma ($p = 0.027$ and $p = 0.039$, respectively). The NMOSD group plasma level of C3, C4 was lower in the HC and MODAD groups, where the difference reached statistical significance. There were no significant differences in plasma levels of C3, C4 in MOGAD and HC. The differences in levels of plasma C3, C4 in HC, NMOSD, and MOGAD groups were presented as scatter dot plots, which had medians and interquartile ranges (IQR) (**Figure 1A, B**). Receiver-operating characteristic (ROC) analysis indicated that plasma C3, C4 dramatically distinguished NMOSD from MOGAD (**Figure 2**). The models to differentiate between NMOSD and MOGAD were evaluated by area under curve (AUC). Plasma C3 and C4 had AUCs of 0.731 and 0.645, respectively, which was considered moderately predictive.

Correlations Between Plasma C3, C4 and Clinical Features of NMOSD Patients

Spearman's correlation was used to analyze the correlation between plasma C3, C4, and EDSS, the plasma level of IgG, and albumin. The correlation between the plasma C3, C4, and CSF findings (WCC, protein, IgG, and albumin), Q-Alb, and IgG index were also examined by Spearman correlation analysis. Negative

TABLE 1 | The detailed findings of Demographic, clinical features, and treatment in NMOSD and MOGAD patients.

	HC	NMOSD (AQP4-IgG positive)	MOGAD (MOG-IgG positive)	p^a	p^b	p^c
Patients number	42	73	22			
Female, n (%)	28, (66.67)	69, (94.52)	6, (27.27)	0.003*	0.002*	<0.001*
Age at onset (mean ± SD)	42.07 ± 9.42	41.86 ± 14.27	37.91 ± 17.26	0.925	0.302	0.336
ARR, median, (IQR)	–	0.8, (0.16-1.32)	0.83, (0.43-1.21)	–	–	0.876
Disease duration, years, median, (IQR)	–	4, (1-9)	2, (1-2)	–	–	0.175
EDSS, median, (IQR)	–	3.0, (2.0-4.0)	3.0, (2.0-4.0)	–	–	0.775
Clinical symptom, n (%)						
ON	–	42, (57.53)	7, (31.82)	–	–	**0.034**
TM	–	55, (75.34)	7, (31.82)	–	–	**<0.001**
Encephalopathy	–	7, (9.59)	11, (50)	–	–	**<0.001**
Acute treatment, n (%)						
IVMP	–	71, (97.26)	21, (95.45)	–	–	0.551
IVIg	–	24, (32.88)	6, (27.27)	–	–	0.795
PLEX	–	1, (1.37)	0, (0)	–	–	1.000
Maintenance treatment, n (%)						
Mycophenolate mofetil		26, (35.62)	9, (40.91)	–	–	0.801
Azathioprine		11, (15.07)	1, (4.55)	–	–	0.284
Cyclosporine		1, (1.37)	0, (0)	–	–	1.000
rituximab		1, (1.37)	0, (0)	–	–	1.000

HC, healthy control; AQP4-IgG, aquaporin-4 immunoglobulin-G; NMOSD, neuromyelitis optica spectrum disorders; MOG-IgG, myelin oligodendrocyte glycoprotein immunoglobulin-G; MOGAD, MOG-IgG-associated disease; ARR, annual relapse rate; EDSS, Expanded Disability Status Scale; SD, standard deviation; IQR, interquartile range; ON, optic neuritis; TM, transverse myelitis; IVMP, intravenous methylprednisolone; IVIg, intravenous immunoglobulins; PLEX, plasma exchange.

[a]*AQP4-IgG positive NMOSD versus HC.*

[b]*MOGAD versus HC.*

[c]*AQP4-IgG positive NMOSD versus MOGAD.*

*bold: p<0.05; *: Bonferoni-adjusted p<0.05.*

correlations were much less common than positive correlations. The results of the Spearman correlation analysis are shown in **Table 3**. Plasma C3 and C4 do not correlate with EDSS (**Figures 3A, J**, respectively), CSF-protein (**Figures 3C, L**, respectively), CSF-IgG (**Figures 3D, M**, respectively), plasma albumin (Figures 3G, P, respectively), and IgG index (**Figures 3I, R**, respectively). Similar unmeaningful results were attained when the correlation between Plasma C4 and CSF-WCC was examined (**Figure 3K**). A significant association between plasma C3 and CSF-WCC was found (r = 0.383, p = 0.040, **Figure 3B**). However, no significant association was found between plasma C3 and plasma-IgG (**Figure 3F**). The results of the analysis show a correlation between plasma C4 and plasma IgG (r = -0.244, p = 0.038, **Figure 3O**). Plasma C3 significantly correlates with CSF

TABLE 2 | Plasma and CSF detailed findings among patients with NMOSD and MOGAD patients.

	HC	NMOSD (AQP4-IgG positive)	MOGAD (MOG-IgG positive)	p^a	p^b	p^c
AQP4-IgG titer, median, (IQR)	–	1:100(1:32-1:320)	–	–	–	–
MOG-IgG titer, median, (IQR)	–	–	1:10(1:10-1:100)	–	–	–
CSF findings		n=29	n=17			
WCC, cell/μL, median, (IQR)	–	8, (4-20),	15, (6-108),	–	–	0.056
Protein, mg/dL, median, (range)	–	59, (42-77)	64, (44-74)	–	–	0.724
Oligoclonal bands positivity, n (%)	–	0, (0)	1, (4.55)	–	–	0.232
CSF IgG, (mg/L) median, (IQR)		49.1, (30-74)	37, (30.7-84.5)			0.937
CSF albumin, median, (IQR)	–	257, (174-385)	310, (264-405)			0.125
Plasma IgG, (mg/L) median, (IQR)	–	11.9, (8.95-14.2)	9.26, (7.81-11.75)			**0.027**
Plasma albumin, median, (IQR)	–	39.4, (37-42.2)	41.4, (39.2-43.5)			**0.039**
IgG index	–	0.62, (0.44-0.82)	0.62, (0.57-0.68)			0.794
Q-Alb, median, (IQR),	–	7.18, (4.38-9.62)	7.16, (5.99-10.17)			0.393
C3(g/L), median, (IQR)	1.08, (1.03-1.20)	0.96, (0.84-1.08)	1.21, (1.06-1.26)	0.002*	1.000	0.001*
C4(g/L), median, (IQR)	0.20, (0.17-0.26)	0.17, (0.13-0.19)	0.19, (0.15-0.23)	<0.001*	0.948	0.046*

HC, healthy control; AQP4-IgG, aquaporin-4 immunoglobulin-G; NMOSD, neuromyelitis optica spectrum disorders; MOG-IgG, myelin oligodendrocyte glycoprotein immunoglobulin-G; MOGAD, MOG-IgG-associated disease; CSF, cerebrospinal fluid; WCC, white cell count; IgG, immunoglobulin-G; IQR, interquartile range; Q-Alb, CSF/plasma albumin ratio; C3, complement 3; C4, complement 4.

[a]*AQP4-IgG positive NMOSD versus HC.*

[b]*MOGAD versus HC.*

[c]*AQP4-IgG positive NMOSD versus MOGAD.*

*bold: p<0.05; *: Bonferroni-adjusted p<0.05.*

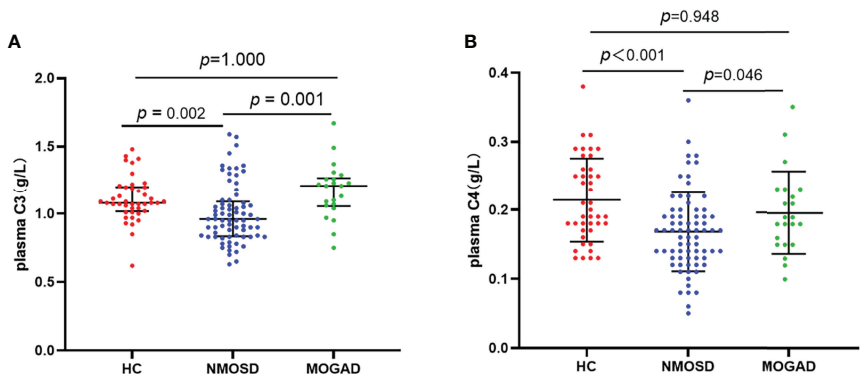

FIGURE 1 | Plasma levels of C3 **(A)** and C4 **(B)** in heathy control, AQP4-IgG positive NMOSD, and MOGAD. Results are presented as scatter plots with the median and interquartile range (IQR). The statistically significant differences were analyzed using the Kruskal-Wallis-test and the corrected p-values using the Bonferroni. C3, complement 3; C4, complement 4; HC, healthy control; NMOSD, neuromyelitis optica spectrum disorders; MOGAD, myelin oligodendrocyte glycoprotein antibody associated disease.

albumin (r = 0.448, p = 0.015, **Figure 3E**), and Q-Alb (r = 0.500, p = 0.006, **Figure 3H**). Similarly, it was found that good correlations exist between plasma C4 and CSF albumin (r = 0.412, p = 0.026, **Figure 3N**), and Q-Alb (r = 0.377, p = 0.043, **Figure 3Q**).

DISCUSSION

Our study also provides evidence that NMOSD and MOGAD are two distinct diseases, as reflected by demographic, clinical, and molecular data. In our cohort, female patients account for 94.5% of all NMOSD patients, while female patients only account for 27.3% of all MOGAD. Discrepancies in the male to female incidence ratio in the MOGAD group from the previous study are likely due to the low sample size (13). The age onset was not compatible among the NMOSD and MOGAD groups. We saw a preference for AQP4-IgG positive NMOSD in the ON and TM, while ADEM was more likely observed in MOGAD, which is in line with previous research (14).

Compared to the plasma median of the MOG-IgG titer, the AQP4-IgG titer is higher, these discrepancies could be due to different sensitivity of assay methods. In a multicenter study, although the CBA detect the MOG-IgG showed excellent

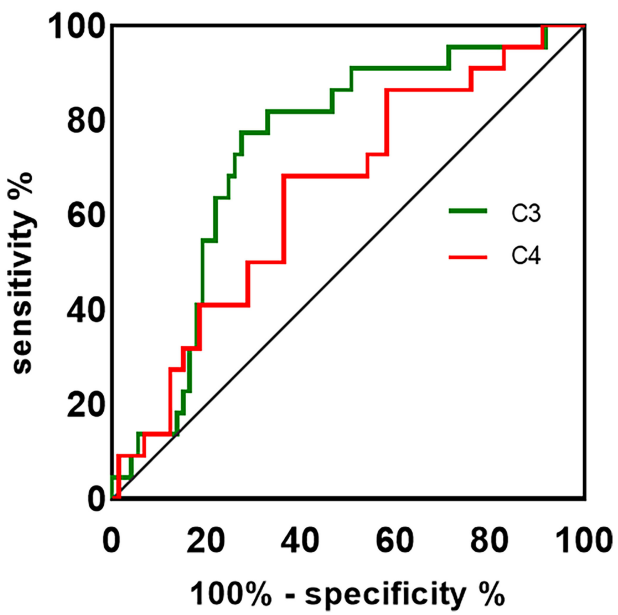

FIGURE 2 | The ROC curve is used to assess the discriminating ability of plasma C3, C4 in NMOSD and MOGAD. The AUC values showed the predictive power of the C3 (0.731) and C4 (0.645). ROC, receiver-operating characteristic; AUC, area under curve; C3, complement 3; C4, complement 4.

TABLE 3 | Correlations between plasma C3, C4, and EDSS, immunological findings of NMOSD patients.

Clinical findings	C3		C4	
	Correlation coefficient	*p*-value	Correlation coefficient	*p*-value
EDSS	0.093	0.433	0.158	0.183
CSF-WCC	0.383	**0.040**	0.073	0.704
CSF protein	0.311	0.100	0.249	0.192
CSF-IgG	0.147	0.445	0.049	0.803
CSF albumin	0.448	**0.015**	0.412	**0.026**
plasma IgG	-0.096	0.421	-0.244	**0.038**
plasma albumin	0.009	0.943	0.033	0.783
Q-Alb	0.500	**0.006**	0.377	**0.043**
IgG index	-0.063	0.742	-0.121	0.532

C3, complement 3; C4, complement 4; EDSS, Expanded Disability Status Scale; CSF, cerebrospinal fluid; WCC, white cell count; IgG, immunoglobulin-G; Q-Alb, CSF/plasma albumin ratio; bold: p<0.05.

agreement with other assays for both highly positive and negative samples, the low positive remained (15). NMOSD patients show significantly higher plasma immunoglobulin (IgG) than MOGAD patients (p = 0.027), which may reflect the different molecular mechanisms that exist in the two diseases. *In vitro in vivo* findings have shown that when reaching serum AQP4-IgG titers in experimental animals comparable with NMOSD patients, they are sufficient to trigger immune cascade reactions (16), while only the affinity-purified MOG-IgG extracted from MOGAD has the potential to cause pathogenicity (17). Therefore, we speculated that the CNS is more susceptible to inflammatory attack by AQP4-IgG than MOG-IgG. In our cohort study, plasma levels of albumin in NMOSD were significantly lower than in MOGAD. Yao et al. (18) reported that the low level of plasma albumin is associated with more disease severity in NMOSD. A possible explanation for our result as follows: Albumin has the potential to regulate immunology, anti-inflammatory function, and its decrease has also been described as associated with increased systemic inflammatory load (19). This implies a more vigorous inflammatory load produced by NMOSD.

Compelling evidence also shows that different underlying autoimmune-driven mechanisms exist in the NMOSD and MOGAD, in which the complement system plays an important role (20, 21). There is substantial evidence that complement analytes have been proved to distinguish MS from NMOSD (22). However, there are comparatively few studies on whether the levels of the complement components are different in NMOSD and MOGAD. C3, C4 are the central component of complement, and C3 is the convergent point of all the complement activation pathways (classical pathway, lectin pathway, or alternative pathway). C3,C4 are key complement factor in the complement activation pathway and reacts with C5, C6, C7, C8, and C9, participate in the formation of membrane attack complex (MAC, C5b-9), which acts as a permeability pore to cause astrocyte injury, followed by the BBB disruption, myelin loss, gliosis, and neuronal death in NMOSD (23). Our results indicated that the plasma levels of C3, C4 in AQP4-IgG positive NMOSD patients were lower than MOGAD and reached statistical significance, these results tallied with previous studies (12, 24). No statistical difference was observed in the C3, C4 between the MOGAD and HC. From the ROC curve analysis, conclusions can be drawn regarding C3, C4, which can become discriminating factors for NMOSD and MOGAD. Perhaps our findings can be explained by the subtle consumption of C3, C4 in NMOSD rather than MOGAD. MOG-IgG targeted the oligodendrocytes (MOG expressed on the myelin sheath) to activate the complement system, resulting in myelin loss but relative axonal and astrocyte preservation (9). The specific mechanism of complement system mediated-injury in MOGAD needs to be studied and further elucidated.

Our results show that plasma C4 is negatively correlated with plasma-IgG, maybe the more IgG is produced, in particular AQP4-IgG, the more plasma C4 consumption. The negative correlation between C3 and plasma IgG may indicate that C3 was consumed in the synthesis of IgG (maybe AQP4-IgG). However, the relationship between C3-the convergent point of all the complement activation pathways and plasma IgG is not simply linear or nonlinear. When C3 is cleaved, it releases C3a, C3b and C3d and binds to CR1 and CR2, which are expressed in the B cells. CR1 binds C3b with high affinity to inhibit B cell receptors (BCR), which mediate B cell activation, proliferation, and antibody production. The inhibitory effects of CR2 and C3d binding on the initial steps of peripheral B cell activation play a significant role in the maintenance of peripheral B cells (25). This suggests that C3 may have a natural feedback mechanism to keep activated B cells from producing too many antibodies. Most NMOSD are seropositive for IgG1 autoantibodies against AQP4 (26), followed by the binding of AQP4 to activate CDC and ADCC mediated astrocyte injury (27). In NMOSD, there may be IgG subclass that is similar to MOGAD (MOG-IgG 1,2,3,4) (28). The IgG4 subclass in NMOSD may have limited ability to mobilize CDC and ADCC and blocks the ligand-receptor interaction of the target antigen (29). Therefore, the relationship between C3 and plasma IgG in NMOSD is complicated, and further experiments will be necessary to clarify the mechanisms involved.

Both C3 and C4 significantly correlate with CSF albumin and Q-Alb. The Q-Alb is considered a common indicator for the evaluation of the destruction of the BBB. Abundant evidence supports a pathogenesis mechanism for AQP4-IgG positive NMOSD in which AQP4-IgG binds to the astrocyte endfoot of AQP4 to activate CDC *via* the classical pathway by binding to C1q, which is followed by C3 convertase enzymes converting C3 into C3a and C3b (20). Once cleaved, C3a sends signals and binding to its receptor C3aR, which is expressed by the vascular endothelial cells in the brain (30), resulting in the altered vascular

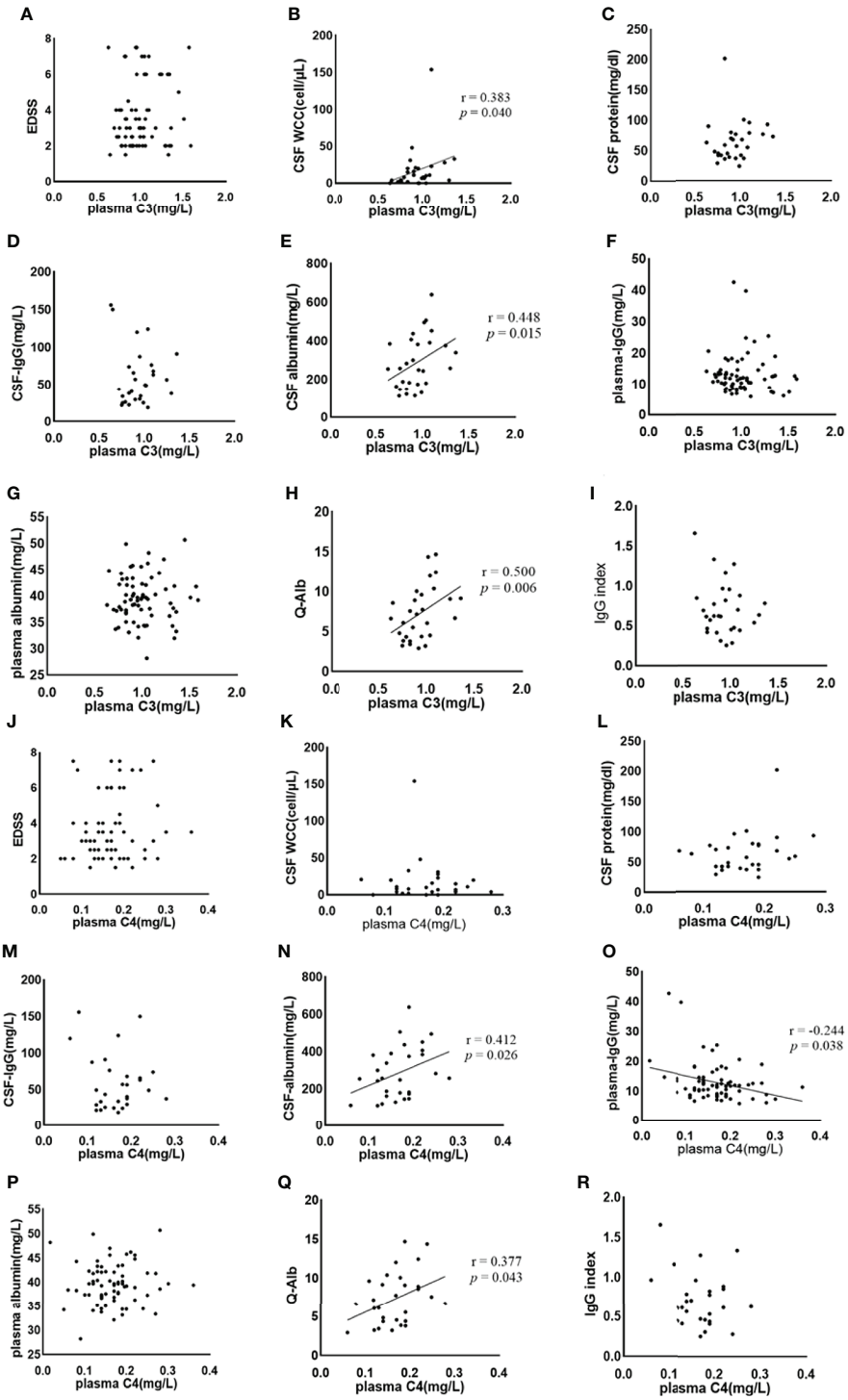

FIGURE 3 | The association between plasma C3, C4 and NMOSD features was analysed by Spearman's correlation. C3, complement 3; C4, complement 4; EDSS, Expanded Disability Status Scale; CSF, cerebrospinal fluid; WCC, white cell count; IgG: immunoglobulin-G; Q-Alb, CSF/plasma albumin ratio. The **(A–I)** shows the Spearman results of serum complement C3 and EDSS **(A)**, CSF WCC **(B)**, CSF protein **(C)**, CSF-IgG **(D)**, CSF albumin **(E)**, plasma IgG **(F)**, plasma albumin **(G)**, Q-Alb **(H)**, and IgG index **(I)**, respectively. There is a significant association between plasma CSF WCC, CSF albumin, and Q-Alb. The **(J–R)** shows the Spearman results of serum complement C4 and EDSS **(J)**, CSF WCC **(K)**, CSF protein **(L)**, CSF-IgG **(M)**, CSF albumin **(N)**, plasma IgG **(O)**, plasma albumin **(P)**, Q-Alb **(Q)**, and IgG index **(R)**, respectively. Positive associations exist between plasma C4 and CSF albumin, and Q-Alb respectively. A negative association exists between plasma C4 and plasma IgG.

morphology and increased BBB permeability (31). Therefore, we propose that C3 indirectly affects the BBB through the C3aR binding to C3a, which is elevated in the plasma of NMOSD (32). Increased permeability of the BBB caused by complement activation can also explain the massive infiltration of leucocytes in CSF (33). There is also evidence from a recent study that C3 is elevated in NMOSD CSF compared to controls (22), implying blood-cerebrospinal fluid barrier dysfunction, which leads to C3 entering into CSF and then affecting the immune environment and leukocytes in CSF. Plasma C3 positively correlates with the CSF-WCC, proposing the view that C3 has an impact on the CSF-WCC through increased blood-cerebrospinal fluid and BBB permeability. The regulation mechanism of C4 in the BBB of NMOSD patients remains elusive. C4a, is released from complement component C4 upon activation of the complement system's classical and lectin pathways. C4a-induced activation of the protease-activated receptors 1 and 4 (PAR1, PAR4) has an impact on the stability of endothelial cells, thereby increasing the BBB permeability (34). Although the elevated C4 in CSF of NMOSD (22), it may be that the levels of plasma C4 entering the CNS through the blood-cerebrospinal fluid barrier and the plasma C4 are not enough to cause the change in WCC.

It is important to note that there are differences in the effects of C3, and C4 in SLE. In SLE, low complement (C3, C4) is an important serological manifestation. According to a previous study, C3 has a negative relationship with IFN- and IL-18, which have the highest positive likelihood ratios for active SLE (35). Durcan et al. (36) found there is a strong relationship between low C3 and lupus nephriand that is associated with poor renal outcomes (glomerular filtration rate (GFR) <50 and chronic proteinuria). C4 did not seem to affect disease activity and lupus nephritis. The discrepancy between C3 and C4 is, we propose, a more important marker due to the C3's central role in the complement cascade, and the fact that complement components or complement activator molecules are released and play different roles in autoimmune diseases.

The present study suffers from several limitations. The MOGAD group sample size was small compared to the NMOSD group, which might have yielded statistical bias. In addition, they may be prone to recall bias because of the retrospective nature of the study. Moreover, all the participants are ethnically Chinese, so our results may yield different results and may not apply to other countries. Although the plasma levels of C3, C4 are found to be lower in NMOSD than in MOGAD, the mechanics of these factors were explored less deeply during the study. Further studies about the complement system in the pathogenesis of mediated tissue injury in CNS inflammatory demyelinating disorders need to be performed and to elaborate on the specific mechanisms more deeply and accurately.

CONCLUSION

Our study reveals that there seems to be more plasma C3, C4 consumption in the NMOSD, further implying that the plasma C3, C4 can be able to distinguish the NMOSD from MOGAD. Plasma C3 or C4 may become potential biomarkers reflecting BBB disruption in NMOSD.

DATA AVAILABILITY STATEMENT

The original contributions presented in the study are included in the article/supplementary material. Further inquiries can be directed to the corresponding author.

ETHICS STATEMENT

The studies involving human participants were reviewed and approved by The Ethics Committee of the Affiliated Brain Hospital of Nanjing Medical University. Written informed consent to participate in this study was provided by the participants' legal guardian/next of kin. Written informed consent was obtained from the individual(s), and minor(s)' legal guardian/next of kin, for the publication of any potentially identifiable images or data included in this article.

AUTHOR CONTRIBUTIONS

LL participated in the conceptualization, collected and analyzed the data, and wrote the original manuscript. YW proofread the data and analyzed the data again. HH visualized the data. JL and YD reviewed and suggested the manuscript and provided financial support. All authors approved the final manuscript before submission.

FUNDING

The research is financially sponsored by the National Natural Science Research Foundation of China (81500969).

REFERENCES

1. Wingerchuk DM, Banwell B, Bennett JL, Cabre P, Carroll W, Chitnis T, et al. International Consensus Diagnostic Criteria for Neuromyelitis Optica Spectrum Disorders. *Neurology* (2015) 85:177–89. doi: 10.1212/WNL.0000000000001729
2. Jarius S, Wildemann B. AQP4 Antibodies in Neuromyelitis Optica: Diagnostic and Pathogenetic Relevance. *Nat Rev Neurol* (2010) 6:383–92. doi: 10.1038/nrneurol.2010.72
3. Jarius S, Probst C, Borowski K, Franciotta D, Wildemann B, Stoecker W, et al. Standardized Method for the Detection of Antibodies to Aquaporin-4 Based on a Highly Sensitive Immunofluorescence Assay Employing Recombinant

Target Antigen. *J Neurological Sci* (2010) 291:52–6. doi: 10.1016/j.jns.2010.01.002
4. Hamid SHM, Whittam D, Mutch K, Linaker S, Solomon T, Das K, et al. What Proportion of AQP4-Igg-Negative NMO Spectrum Disorder Patients are MOG-Igg Positive? *A Cross Sectional Stud 132 Patients J Neurol* (2017) 264:2088–94. doi: 10.1007/s00415-017-8596-7
5. Mao Z, Lu Z, Hu X. Distinction Between MOG Antibody-Positive and AQP4 Antibody-Positive NMO Spectrum Disorders. *Neurology* (2014) 83:1122. doi: 10.1212/WNL.0000000000000830
6. Jarius S, Paul F, Aktas O, Asgari N, Dale RC, de Seze J, et al. MOG Encephalomyelitis: International Recommendations on Diagnosis and Antibody Testing. *J Neuroinflamm* (2018) 15:134. doi: 10.1186/s12974-018-1144-2
7. Ratelade J, Asavapanumas N, Ritchie AM, Wemlinger S, Bennett JL, Verkman AS. Involvement of Antibody-Dependent Cell-Mediated Cytotoxicity in Inflammatory Demyelination in a Mouse Model of Neuromyelitis Optica. *Acta neuropathologica* (2013) 126:699–709. doi: 10.1007/s00401-013-1172-z
8. Yick LW, Ma OK, Ng RC, Kwan JS, Chan KH. Aquaporin-4 Autoantibodies From Neuromyelitis Optica Spectrum Disorder Patients Induce Complement-Independent Immunopathologies in Mice. *Front Immunol* (2018) 9:1438. doi: 10.3389/fimmu.2018.01438
9. Fang L, Kang X, Wang Z, Wang S, Wang J, Zhou Y, et al. Myelin Oligodendrocyte Glycoprotein-Igg Contributes to Oligodendrocytopathy in the Presence of Complement, Distinct From Astrocytopathy Induced by AQP4-Igg. *Neurosci Bull* (2019) 35:853–66. doi: 10.1007/s12264-019-00375-8
10. Romano R, Giardino G, Cirillo E, Prencipe R, Pignata C. Complement System Network in Cell Physiology and in Human Diseases. *Int Rev Immunol* (2021) 40:159–70. doi: 10.1080/08830185.2020.1833877
11. Hakobyan S, Luppe S, Evans DR, Harding K, Loveless S, Robertson NP, et al. Plasma Complement Biomarkers Distinguish Multiple Sclerosis and Neuromyelitis Optica Spectrum Disorder. *Multiple Sclerosis (Houndmills Basingstoke England)* (2017) 23:946–55. doi: 10.1177/1352458516669002
12. Pache F, Ringelstein M, Aktas O, Kleiter I, Jarius S, Siebert N, et al. C3 and C4 Complement Levels in AQP4-Igg-Positive NMOSD and in MOGAD. *J Neuroimmunol* (2021) 360:577699. doi: 10.1016/j.jneuroim.2021.577699
13. Chen JJ, Bhatti MT. Clinical Phenotype, Radiological Features, and Treatment of Myelin Oligodendrocyte Glycoprotein-Immunoglobulin G (MOG-Igg) Optic Neuritis. *Curr Opin Neurol* (2020) 33:47–54. doi: 10.1097/WCO.0000000000000766
14. Shahriari M, Sotirchos ES, Newsome SD, Yousem DM. MOGAD: How it Differs From and Resembles Other Neuroinflammatory Disorders. *AJR. Am J Roentgenol* (2021) 216:1031–9. doi: 10.2214/AJR.20.24061
15. Reindl M, Schanda K, Woodhall M, Tea F, Ramanathan S, Sagen J, et al. International Multicenter Examination of MOG Antibody Assays. *Neurology(R) Neuroimmunol Neuroinflamm 7* (2020). doi: 10.1212/NXI.0000000000000674
16. Bradl M, Misu T, Takahashi T, Watanabe M, Mader S, Reindl M, et al. Neuromyelitis Optica: Pathogenicity of Patient Immunoglobulin *In Vivo*. *Ann Neurol* (2009) 66:630–43. doi: 10.1002/ana.21837
17. Spadaro M, Winklmeier S, Beltrán E, Macrini C, Höftberger R, Schuh E, et al. Pathogenicity of Human Antibodies Against Myelin Oligodendrocyte Glycoprotein. *Ann Neurol* (2018) 84:315–28. doi: 10.1002/ana.25291
18. Yao XY, Wu YF, Gao MC, Hong RH, Ding J, Hao Y, et al. Serum Albumin Level is Associated With the Severity of Neurological Dysfunction of NMOSD Patients. *Multiple Sclerosis Related Disord* (2020) 43:102130. doi: 10.1016/j.msard.2020.102130
19. Xu M, Cen M, Chen X, Chen H, Liu X, Cao Q. Correlation Between Serological Biomarkers and Disease Activity in Patients With Inflammatory Bowel Disease. *BioMed Res Int* (2019) 2019:6517549. doi: 10.1155/2019/6517549
20. Asavapanumas N, Tradtrantip L, Verkman AS. Targeting the Complement System in Neuromyelitis Optica Spectrum Disorder. *Expert Opin Biol Ther* (2021) 21:1073–86. doi: 10.1080/14712598.2021.1884223
21. Carpanini SM, Torvell M, Morgan BP. Therapeutic Inhibition of the Complement System in Diseases of the Central Nervous System. *Front Immunol* (2019) 10:362. doi: 10.3389/fimmu.2019.00362
22. Zelek WM, Fathalla D, Morgan A, Touchard S, Loveless S, Tallantyre E, et al. Cerebrospinal Fluid Complement System Biomarkers in Demyelinating Disease. *Multiple Sclerosis (Houndmills Basingstoke England)* (2020) 26:1929–37. doi: 10.1177/1352458519887905
23. Dalakas MC, Alexopoulos H, Spaeth PJ. Complement in Neurological Disorders and Emerging Complement-Targeted Therapeutics. *Nat Rev Neurol* (2020) 16:601–17. doi: 10.1038/s41582-020-0400-0
24. Qin C, Chen B, Tao R, Chen M, Ma X, Shang K, et al. The Clinical Value of Complement Proteins in Differentiating AQP4-Igg-Positive From MOG-Igg-Positive Neuromyelitis Optica Spectrum Disorders. *Multiple Sclerosis Related Disord* (2019) 35:1–4. doi: 10.1016/j.msard.2019.06.035
25. Erdei A, Kovacs KG, Nagy-Balo Z, Lukacsi S, Macsik-Valent B, Kurucz I, et al. New Aspects in the Regulation of Human B Cell Functions by Complement Receptors CR1, CR2, CR3 and CR4. *Immunol Lett* (2021) 237:42–57. doi: 10.1016/j.imlet.2021.06.006
26. Lennon VA, Kryzer TJ, Pittock SJ, Verkman AS, Hinson SR. Igg Marker of Optic-Spinal Multiple Sclerosis Binds to the Aquaporin-4 Water Channel. *J Exp Med* (2005) 202:473–7. doi: 10.1084/jem.20050304
27. Wu Y, Zhong L, Geng J. Neuromyelitis Optica Spectrum Disorder: Pathogenesis, Treatment, and Experimental Models. *Multiple Sclerosis Related Disord* (2019) 27:412–8. doi: 10.1016/j.msard.2018.12.002
28. Mariotto S, Ferrari S, Monaco S, Benedetti MD, Schanda K, Alberti D, et al. Clinical Spectrum and Igg Subclass Analysis of Anti-Myelin Oligodendrocyte Glycoprotein Antibody-Associated Syndromes: A Multicenter Study. *J Neurol* (2017) 264:2420–30. doi: 10.1007/s00415-017-8635-4
29. Zografou C, Vakrakou AG, Stathopoulos P. Short- and Long-Lived Autoantibody-Secreting Cells in Autoimmune Neurological Disorders. *Front Immunol* (2021) 12:686466. doi: 10.3389/fimmu.2021.686466
30. Schraufstatter IU, Trieu K, Sikora L, Sriramarao P, DiScipio R. Complement C3a and C5a Induce Different Signal Transduction Cascades in Endothelial Cells. *J Immunol (Baltimore Md: 1950)* (2002) 169:2102–10. doi: 10.4049/jimmunol.169.4.2102
31. Propson NE, Roy ER, Litvinchuk A, Köhl J, Zheng H. Endothelial C3a Receptor Mediates Vascular Inflammation and Blood-Brain Barrier Permeability During Aging. *J Clin Invest 131* (2021). doi: 10.1172/JCI140966
32. Nytrova P, Potlukova E, Kemlink D, Woodhall M, Horakova D, Waters P, et al. Complement Activation in Patients With Neuromyelitis Optica. *J Neuroimmunol* (2014) 274:185–91. doi: 10.1016/j.jneuroim.2014.07.001
33. Wingerchuk DM, Lennon VA, Lucchinetti CF, Pittock SJ, Weinshenker BG. The Spectrum of Neuromyelitis Optica. *Lancet Neurol* (2007) 6:805–15. doi: 10.1016/S1474-4422(07)70216-8
34. Wang H, Ricklin D, Lambris JD. Complement-Activation Fragment C4a Mediates Effector Functions by Binding as Untethered Agonist to Protease-Activated Receptors 1 and 4. *Proc Natl Acad Sci United States America* (2017) 114:10948–53. doi: 10.1073/pnas.1707364114
35. Ruchakorn N, Ngamjanyaporn P, Suangtamai T, Kafaksom T, Polpanumas C, Petpisit V, et al. Performance of Cytokine Models in Predicting SLE Activity. *Arthritis Res Ther* (2019) 21:287. doi: 10.1186/s13075-019-2029-1
36. Durcan L, Petri M. The Clinical and Serological Associations of Hypocomplementemia in a Longitudinal Sle Cohort. *Semin Arthritis Rheumatism* (2020) 50:1081–6. doi: 10.1016/j.semarthrit.2020.06.009

Conflict of Interest: The authors declare that the research was conducted in the absence of any commercial or financial relationships that could be construed as a potential conflict of interest.

Advantages of publishing in Frontiers

OPEN ACCESS
Articles are free to read for greatest visibility and readership

FAST PUBLICATION
Around 90 days from submission to decision

HIGH QUALITY PEER-REVIEW
Rigorous, collaborative, and constructive peer-review

TRANSPARENT PEER-REVIEW
Editors and reviewers acknowledged by name on published articles

Frontiers
Avenue du Tribunal-Fédéral 34
1005 Lausanne | Switzerland

Visit us: www.frontiersin.org
Contact us: frontiersin.org/about/contact

REPRODUCIBILITY OF RESEARCH
Support open data and methods to enhance research reproducibility

DIGITAL PUBLISHING
Articles designed for optimal readership across devices

FOLLOW US
@frontiersin

IMPACT METRICS
Advanced article metrics track visibility across digital media

EXTENSIVE PROMOTION
Marketing and promotion of impactful research

LOOP RESEARCH NETWORK
Our network increases your article's readership